

**TAXONOMIC STUDY ON THE ELAPID SNAKES OF MIZORAM,
INDIA (REPTILIA: SERPENTES: ELAPIDAE)**

**A THESIS SUBMITTED IN PARTIAL FULFILLMENT OF THE
REQUIREMENTS FOR THE DEGREE OF DOCTOR OF PHILOSOPHY**

LALBIAKZUALA

MZU REGN NO.: 2189 OF 2012

PH.D REGN NO.: MZU/PH.D./1384 OF 16.03.2020



DEPARTMENT OF ZOOLOGY

SCHOOL OF LIFE SCIENCES

NOVEMBER, 2024

Taxonomic study on the elapid snakes of Mizoram, India
(Reptilia: Serpentes: Elapidae)

BY

LALBIAKZUALA

Department of Zoology

Name of Supervisor

Professor H.T. Lalremsanga

Submitted

In partial fulfillment of the requirement of the Degree of Doctor of Philosophy in
Zoology of Mizoram University, Aizawl.

SUPERVISOR'S CERTIFICATE

This is to certify that Taxonomic study on the elapid snakes of Mizoram, India (Reptilia: Serpentes: Elapidae) written by Lalbiakzuala has been written under my supervision.

He has fulfilled all the required norms laid down within the Ph.D regulations of Mizoram University. The thesis is the result of his own investigation. Neither the thesis as a whole nor part of it was ever submitted by any other University for any degree.

(Prof. H.T. LALREMSANGA)

Supervisor/Professor

Department of Zoology

Mizoram University

DECLARATION

**Mizoram University
November, 2024**

I Lalbiakzuala, hereby declare that the subject matter of this thesis is the record of work done by me, that the contents of this thesis did not form basis of the award of any previous degree to me or to do the best of my knowledge to anybody else, and that the thesis has not been submitted by me for any research degree in any other University/Institute.

This is being submitted to the Mizoram University for the degree of Doctor of Philosophy in Zoology.

(LALBIAKZUALA)

**(Prof. H.T. LALREMSANGA)
Head
Department of Zoology
Mizoram University
Aizawl-796004**

**(Prof. H.T. LALREMSANGA)
Supervisor
Department of Zoology
Mizoram University
Aizawl-796004**

ACKNOWLEDGEMENTS

In the first place, I thank the Creator God Jesus Christ [Yeshua] for His unceasing Divine guidance and blessings.

I express my deep and sincere gratitude to my supervisor, Prof. H.T. Lalremsanga, for his continuous support, persistent guidance and encouragement throughout this research work.

Furthermore, I thank Dr. Zothansiana and Dr. Amit Kumar Trivedi, members of Research Advisory Committee for their insightful comments and constructive suggestions.

I am grateful to Prof. G. Gurusubramanian, Dean, School of Life Sciences; and Prof. H.T. Lalremsanga, Head, Department of Zoology for providing the facilities necessary for this work.

I offer my special thanks to Dr. M. Vabeiryureilai (Assistant Professor, Dept. of Zoology), Dr. Andrew Vanlallawma (Department of Biotechnology), and my fellow lab mates in the Developmental Biology & Herpetology Laboratory, Mizoram University for their valuable help and support in every part of this work.

I would like to extend my heartfelt thanks to the faculty members Dr. Esther Lalhmingliani, Dr. Vikas Kumar Roy, Dr. Kiran R. Kharat; and the non-teaching staff and research scholars in the Department of Zoology, Mizoram University for their warm encouragement, inspiration and motivation during my research work.

I am deeply grateful to the International and National collaborators in this works: Dr. Anita Malhotra (Bangor University, UK), Dr. Gernot Vogel (Germany), Mr. Zeeshan A. Mirza (Max Planck Institute, Germany), Dr. Shantanu Kundu (Pukyong National University, South Korea), Dr. A.A. Thasun Amarasinghe (Universitas Indonesia, Indonesia), Mr. Vishal Santra (CONCERN, West Bengal), Col. Yashpal Singh Rathee (Meghalaya), Dr. Jayaditya Purkayastha (Help Earth, Assam), and Mr. Girish Choure (Maharashtra).

In conclusion, I give my warmest appreciation and thanks to my late grandmother, my wife, and my family as a whole for their continuous support and prayer during the course of my study.

LALBIAKZUALA

TABLE OF CONTENTS

Contents		Page No.
General Introduction		i–v
Chapter 1 <i>Bungarus fasciatus</i> (Schneider, 1801)	Review of Literature	1–2
	Materials and methods	2–10
	Results	11–35
	Discussion	36–39
Chapter 2 <i>Bungarus niger</i> Wall, 1908	Review of Literature	40–42
	Materials and methods	42–49
	Results	49–81
	Discussion	82–84
Chapter 3 <i>Naja kaouthia</i> Lesson, 1831	Review of Literature	85–87
	Materials and methods	87–96
	Results	97–136
	Discussion	137–138
Chapter 4 <i>Ophiophagus hannah</i> (Cantor, 1836)	Review of Literature	139–140
	Materials and methods	140–150
	Results	151–182
	Discussion	183–184
Chapter 5 <i>Sinomicrurus maccllellandi</i> (Reinhardt, 1844)	Review of Literature	185–187
	Materials and methods	188–199
	Results	200–243
	Discussion	244–248
Summary		249–253
References		254–287
Brief Bio-data of the candidate		288
Certificate on plagiarism check		289
Plagiarism verification certificate and copy of the reports		290–292
Publications & paper presentation		294–316
Particulars of the candidate		317

LIST OF TABLES

Table No.	Legends	Page No.
1.1	Information on PCR thermal conditions used in the amplification of four mitochondrial genes utilized in this chapter.	5
1.2	Information on the specimen vouchers, locations, GenBank accession numbers, and references of the DNA sequences of <i>Bungarus fasciatus</i> (BF) with <i>B. caeruleus</i> (BCR), <i>B. candidus</i> (BC), <i>B. multicinctus</i> (BM), <i>B. niger</i> (BN), <i>B. ceylonicus</i> (BCY), <i>B. sindanus</i> (BS), and <i>B. bungaroides</i> (BB) as outgroups. The sequences generated in this study are shown in bold.	6–7
1.3	Information on partitioning schemes and nucleotide substitution models used in the concatenated Bayesian Inference (BI) and Maximum Likelihood (ML) phylogenetic analyses.	11
1.4	Uncorrected p-distance (pairwise sequence divergence) estimated using the mitochondrial <i>cytb</i> (1047 bp) gene of <i>Bungarus fasciatus</i> (BF) with <i>B. caeruleus</i> (BCR), <i>B. candidus</i> (BC), <i>B. multicinctus</i> (BM), <i>B. niger</i> (BN), <i>B. ceylonicus</i> (BCY), <i>B. sindanus</i> (BS), and <i>B. bungaroides</i> (BB) as outgroups. Abbreviations of country and state/province names are: ID: Indonesia, JW/J: Java; MM: Myanmar, AY: Ayeyarwady; IN: India, WB: West Bengal, MZ: Mizoram, AS: Assam; VN: Vietnam, VC: Vinh Phuc; CN: China, GZ: Guizhou, GX: Guangxi, GD: Guangdong, YN: Yunnan; TH: Thailand.	14–15
1.5	Morphometry (in mm) and scalation data of <i>Bungarus fasciatus</i> examined from Mizoram, India. Damaged body parts are indicated in asterisk (*), and the character	20

	that is unable to determined are shown as octothorp (#).	
1.6	Evaluation on the meristic and mensural characters measured for 38 <i>Bungarus fasciatus</i> individuals from Java (JV), Mizoram (MZ), and West Bengal (WB), including mean, standard deviation, minimum and maximum values. The characters tested for inter-population difference across the three populations are indicated by asterisk (*). Characters tested using the alternative Brown-Forsythe test was indicated by octothorp (#). Significant values at the alpha level of 0.05 are given in bold.	21
1.7	Correlation matrix across the standardized variables utilized for PCA ordination.	22
1.8	Information on Principal Component Analysis (PCA) and loadings for <i>Bungarus fasciatus</i> in east India, northeastern India and Great Sunda Islands. Principal components (PC) 1 and 2 collectively explained 84% of variation.	22
1.9	Some comparative morphological data of <i>Bungarus fasciatus</i> sensu lato in each biogeographic region, based on this study and published data.	30
1.10	Detailed locality records of <i>Bungarus fasciatus</i> sensu stricto specimens based on the combined data of this study and Lalbiakzuala (2019) in Mizoram, India. New records from this work are indicated with bold.	33–34
2.1	Information on specimen vouchers, locations, GenBank accession numbers, and references of the DNA sequences used in this study. The sequences generated in this study are shown in bold. Taxon's name abbreviations: <i>Bungarus niger</i> (BN), <i>B. candidus</i> (BC), <i>B. multicinctus</i> (BM), <i>B. wanghaotingi</i> (BW), <i>B.</i>	44–45

	<i>suzhenae</i> (BSZ), <i>B. lividus</i> (BL), <i>B. fasciatus</i> (BF), <i>B. caeruleus</i> (BCR), <i>B. slowinski</i> (BSL), <i>B. ceylonicus</i> (BCY), <i>B. sindanus</i> (BS), <i>B. bungaroides</i> (BB), <i>B. flaviceps</i> (BFL), and <i>Naja naja</i> (NN).	
2.2	Nucleotide substitution models selected for the concatenated dataset of mitochondrial <i>16s</i> , <i>cox1</i> , and <i>cytb</i> genes.	50
2.3	Uncorrected p-distance estimated using the mitochondrial 16S rRNA (536 bp) sequence of <i>Bungarus niger</i> (BN), <i>B. fasciatus</i> (BF), <i>B. suzhenae</i> (BSZ), <i>B. caeruleus</i> (BCR), <i>B. candidus</i> (BC), <i>B. multicinctus</i> (BM), <i>B. ceylonicus</i> (BCY), and <i>Naja naja</i> (NN) as outgroup.	60
2.4	Uncorrected p-distance (pairwise sequence divergence) estimated using the mitochondrial NADH Dehydrogenase subunit 4 (871 bp) sequence of <i>Bungarus niger</i> (BN), <i>B. fasciatus</i> (BF), <i>B. ceylonicus</i> (BCY), <i>B. bungaroides</i> (BB), <i>B. sindanus</i> (BS), <i>B. slowinskii</i> (BSL), <i>B. flaviceps</i> (BFL), <i>B. caeruleus</i> (BCR), <i>B. multicinctus</i> (BM), <i>B. wanghaotingi</i> (BW), <i>B. suzhenae</i> (BSZ), and <i>Naja naja</i> (NN) as outgroups.	61
2.5	Uncorrected p-distance (pairwise sequence divergence) estimated using the mitochondrial cytochrome b (1,131 bp) sequence of <i>Bungarus niger</i> (BN), <i>B. lividus</i> (BL), <i>B. fasciatus</i> (BF), <i>B. caeruleus</i> (BCR), <i>B. candidus</i> (BC), <i>B. multicinctus</i> (BM), <i>B. slowinskii</i> (BSL), <i>B. ceylonicus</i> (BCY), <i>B. sindanus</i> (BS), <i>B. bungaroides</i> (BB), <i>B. wanghaotingi</i> (BW), <i>B. suzhenae</i> (BSZ), <i>B. flaviceps</i> (BFL), and <i>Naja naja</i> (NN) as outgroup.	62–63
2.6	Morphometry and meristics of <i>B. niger</i> from Mizoram. Damaged/missing characters are indicated by asterisk	67–74

	(*).	
2.7	Screening of sexual dimorphism using the meristic and mensural characters obtained from 46 adult <i>Bungarus niger</i> (37 males and 9 females) from Mizoram, Northeast India. Standardized meristic data were analyzed through one-way ANOVA with sex as a factor. Allometric adjusted mensural data were analysed through one-way ANCOVA using SVL as a covariate and sex as a factor. The characters with statistically significant variations at the alpha level of 0.05 are shown in boldface, and marginally significance in octothorp (#).	74
2.8	Detailed collection data of <i>Bungarus niger</i> based on the combined data of this study and Lalbiakzuala (2019) in Mizoram, India. New records from this work are indicated with bold.	77–78
3.1	Details of three mitochondrial genes utilized in this study. Abbreviations for species names: <i>Naja kaouthia</i> (NK), <i>N. atra</i> (NA), <i>N. annulata</i> (NAN), <i>N. sumatrana</i> (NS), <i>N. naja</i> (NN), <i>N. oxiana</i> (NO), <i>N. haje</i> (NH), <i>N. annulifera</i> (NAF), <i>N. nivea</i> (NNV), <i>N. ashei</i> (NAS), <i>N. mossambica</i> (NMO), <i>N. mandalayensis</i> (NMA), <i>N. philippinensis</i> (NP), <i>N. sputatrix</i> (NSX), <i>N. savannula</i> (NSV), <i>N. siamensis</i> (NSM), and <i>Bungarus fasciatus</i> (BF).	89–92
3.2	Nucleotide substitution model selected for the BI and ML phylogenetic analyses.	97
3.3	Uncorrected p-distance estimate among the different haplotypes recovered in <i>cytb</i> dataset.	103
3.4	Uncorrected p-distance estimate among the different haplotypes recovered in <i>cox1</i> dataset.	104

3.5	Uncorrected p-distance estimate among the different haplotypes recovered in <i>16s</i> dataset.	105
3.6	Uncorrected p-distance estimate between the two clades of <i>Naja kaouthia</i> along with other congeneric sequences based on <i>cytb</i> dataset. The mean of within group distance for each clade are given under the column marked with “#”.	106
3.7	Morphometry (in mm) and scalation data of <i>Naja kaouthia</i> examined from Mizoram, India. Damaged character is shown as asterisk (*), and the characters that are not feasible to examine in life individuals are shown in dash (-). Life individuals examined are indicated by their respective locality.	113–118
3.8	Comparative meristic data of <i>Naja kaouthia</i> originated from this study, published and unpublished data from Indo-Myanmar region.	119
3.9	Test for sexual dimorphism on the meristic and mensural characters using 44 (14 adult males; 15 females; 13 juvenile males; 3 juvenile females) <i>Naja kaouthia</i> individuals from Mizoram, Northeast India, including mean, standard deviation, minimum and maximum values. Standardized meristic data were analysed through one-way ANOVA with sex as a factor. Adjusted mensural data were analysed through one-way ANCOVA using SVL as a covariate and sex as a factor. The characters with statistically significant variations at the alpha level of 0.05 are shown in boldface. After removal of specimens with high number of missing data, a total of 13 adult males, 10 adult females are retained, while all the juvenile specimens are retained because the estimated percentage of missing	120–122

	value is <30%.	
3.10	Information on Principal Component Analysis (PCA) and loadings for <i>Naja kaouthia</i> population in Mizoram, northeastern India between the adult male and female specimens.	123
3.11	Test for intra-population difference on the meristic and mensural characters using 44 (14 adult males; 15 adult females; 13 juvenile males; 3 juvenile females) <i>Naja kaouthia</i> individuals from Mizoram, Northeast India, including mean, standard deviation, minimum and maximum values. Standardized meristic data were analysed through one-way ANOVA with phenotypic group as a factor. Adjusted mensural data were analysed through one-way ANCOVA using SVL as a covariate and phenotypic group as a factor. The characters with statistically significant variations at the alpha level of 0.05 are shown in boldface. After removal of adult specimens with high number of missing data, typical group contains eight adult males, six adult females, seven juvenile males, and two juvenile females; in the variant group, a total of five adult males, four adult females, six juvenile males, and one juvenile female are retained for the test. Since there is a single female in the variant juvenile group, the test for juveniles is performed only for either male (for sexually dimorphic characters) or sex pooled.	127–130
3.12	Information on Principal Component Analysis (PCA) and loadings for <i>Naja kaouthia</i> population in Mizoram, northeastern India between the phenotypic groups.	131
3.13	Detailed distributional records of <i>Naja kaouthia</i> documented in this study from Mizoram, India.	134–135

4.1	Details of three mitochondrial genes utilized for <i>Ophiophagus hannah</i> (OH) with <i>Sinomicrurus peinani</i> (SP) and <i>S. kelloggi</i> (SK) as outgroups.	142–145
4.2	Nucleotide substitution model selected for the BI and ML phylogenetic analyses.	152
4.3	Uncorrected p-distance (pairwise sequence divergence) estimated using the mitochondrial 16S rRNA (<i>16s</i>) sequences of <i>Ophiophagus hannah</i> (OH) with GenBank sequences of <i>Sinomicrurus peinani</i> (SP) and <i>S. kelloggi</i> (SK) as outgroups. DNA sequences generated from Mizoram samples in this study are indicated by bold, while other sequences of Mizoram samples from published work are indicated by asterisk.	157–159
4.4	Uncorrected p-distance (pairwise sequence divergence) estimated using the mitochondrial cytochrome c oxidase subunit 1 (<i>cox1</i>) sequences of <i>Ophiophagus hannah</i> (OH) with GenBank sequences of <i>Sinomicrurus peinani</i> (SP) and <i>S. kelloggi</i> (SK) as outgroups. DNA sequences generated from Mizoram samples in this study are indicated by bold.	160
4.5	Uncorrected p-distance (pairwise sequence divergence) estimated using the mitochondrial cytochrome b (<i>cytb</i>) sequences of <i>Ophiophagus hannah</i> (OH) with GenBank sequences of <i>Sinomicrurus peinani</i> (SP) and <i>S. kelloggi</i> (SK) as outgroups. DNA sequences generated from Mizoram samples in this study are indicated by bold, while other sequences of Mizoram samples from published work are indicated by asterisk.	161–163
4.6	Uncorrected p-distance estimate among the different lineages in <i>16s</i> dataset.	164
4.7	Uncorrected p-distance estimate among the different	164

	lineages in <i>cytb</i> dataset.	
4.8	Morphometry (in mm) and scalation data of <i>Ophiophagus hannah</i> examined from Mizoram, India. Damaged character is shown as asterisk (*), and the missing characters or that are not feasible to examine in life individuals are shown in dash (-). Live individuals examined are indicated by their respective locality.	167–171
4.9	Information on Principal Component Analysis (PCA) and loadings for <i>Ophiophagus hannah</i> population in Mizoram, northeastern India between the adult male and female specimens.	172
4.10	Test for intraspecific difference (sex pooled) on the standardized meristics of <i>O. hannah</i> through one-way ANOVA with population/lineage as the factor. Analysis was performed for Mizoram population against the pre-defined four distinct lineages recovered by Shankar et al. (2021). Significant variations at the alpha level of 0.05 are shown in boldface. Characters tested using Brown-Forsythe test is indicated with octothorpe (#).	176
4.11	Bonferroni Post hoc test between Mizoram population and the four lineages recovered by Shankar et al. (2021).	176
4.12	Information on Principal Component Analysis (PCA) and loadings across populations of <i>O. hannah</i> using the characters <i>Ve</i> , <i>Sc</i> and <i>ADSR</i> .	176
4.13	Details of the king cobra nests documented in this study from Mizoram, Northeast India. Abbreviations used: CRF - Community Reserved Forest; RF - Reserved Forest; RRA - Riverine Reserved Area; WLS - Wildlife Sanctuary.	180
5.1	Detailed information on the primer pairs and PCR	194

	thermal conditions used in the amplification of four mitochondrial genes and one nuclear gene of <i>Sinomicrurus</i> species.	
5.2	Details of three mitochondrial genes utilized for <i>Ophiophagus hannah</i> (OH) with <i>Sinomicrurus peinani</i> (SP) and <i>S. kelloggi</i> (SK) as outgroups.	195–199
5.3	The best partitioning schemes and nucleotide substitution models selected for the partitioned concatenated matrix, Bayesian Poisson Tree Processes species delimitation, and multispecies coalescent tree in the present study.	202
5.4	Morphometry (in mm) and scalation data of <i>Sinomicrurus</i> species examined from Mizoram, India. Damaged character that are not feasible to examine is shown in dash (-).	208–213
5.5	Descriptive statistics for sexual dimorphism and difference between <i>Sinomicrurus macclellandi</i> var. <i>typica</i> and <i>S. gorei</i> comb. nov. based on the examined specimens from the populations of Mizoram, Meghalaya, Arunachal Pradesh, and other published meristic data from Assam, Bangladesh, and Cambodia. Meristics data are analyzed using two-way ANOVA using sex and variety as the factors, or Brown-Forsythe test (indicated in octothorp '#') for meristics; while two-way ANCOVA using sex and variety as the factors with SVL as covariate was used for the mensurals. Statistical significance at the level of alpha 0.05 is indicated by bold. Measurements are given in millimetre.	214–216
5.6	Principal Component (PCA) loadings for <i>Sinomicrurus macclellandi</i> var. <i>typica</i> and <i>Sinomicrurus</i> var. <i>gorei</i> based on the standardized meristics and adjusted	219

	mensurals of the examined specimens from the populations of Mizoram, Meghalaya, Arunachal Pradesh, and other published meristic data from Assam, Bangladesh, and Cambodia. Principal components (PC) 1 and 2 collectively explained 82% of variations.	
5.7	Comparative meristic data between <i>Sinomicrurus gorei</i> comb. nov. and <i>S. macclellandi</i> var. <i>typica</i> from this study and published data.	231
5.8	Comparative morphometric ratios between <i>Sinomicrurus gorei</i> comb. nov. and <i>S. macclellandi</i> var. <i>typica</i> examined in this study. Interspecific difference in the ratios are analyzed using one-way ANOVA using taxa as the factor, and Brown-Forsythe test (indicated in octothorp '#'). Statistical significance at the level of alpha 0.05 is indicated by bold.	232
5.9	Detailed specimens collected and/or examined or documented for <i>Sinomicrurus</i> species from Mizoram in this work. Voucher acronym: Departmental Museum of Zoology, Mizoram University, India (MZMU). New sampling sites from this work are indicated with bold.	234–236
5.10	Detailed specimens collected and/or examined or documented for <i>Sinomicrurus</i> species from outside Mizoram. Voucher acronyms: Arunachal Pradesh Regional Centre, Zoological Survey of India (APRC); Collection of Yashpal Singh Rathee (YSR). New sampling sites from this work are indicated with bold.	237
5.11	Neonate biometric data (measurements in mm; weights in g) of <i>Sinomicrurus gorei</i> comb. nov. (MZMU2590) from Mizoram, Northeast India.	242

LIST OF FIGURES

Figure No.	Legends	Page No.
i	Elapid snake species found in Mizoram, India. Photo credit: H.T. Lalremsanga.	v
1.1	Description of head morphometrics used in this chapter: (top) maximum width of head (HW), width of snout at level of nostril (SW); (below) length of head from tip of snout to angle of jaw (HL), horizontal eye diameter (ED), eye to snout distance (E-S), eye to nostril distance (E-N); and the meristics nuchal band width in scale (NBW) is also depicted.	10
1.2	Bayesian inference (BI) phylogenetic tree based on concatenated mitochondrial <i>16s</i> , <i>cox1</i> , <i>nd4</i> and <i>cytb</i> genes; lineage partitions recovered from CYTB-based PTP analyses are presented besides the BI tree (only the <i>cytb</i> dataset was utilized for PTP analyses because it contains more representative samples from the three clades compared to the other genes). Values at each node represent Bayesian posterior probabilities (PP) and Ultrafast Bootstrap (UFB) values from the Maximum Likelihood (ML) analysis (PP/UFB). Abbreviations of country and state/province names are: ID: Indonesia, JW/J: Java; MM: Myanmar, AY: Ayeyarwady; IN: India, WB: West Bengal, MZ: Mizoram, AS: Assam; VN: Vietnam, VC: Vinh Phuc; CN: China, GZ: Guizhou, GX: Guangxi, GD: Guangdong, YN: Yunnan; TH: Thailand.	12
1.3	Ordination of <i>Bungarus fasciatus</i> specimens in a Principal Coordinate Analysis of standardized p-distance of mitochondrial 16S rRNA (<i>16s</i>), cytochrome c oxidase subunit 1 (<i>cox1</i>), cytochrome b (<i>cytb</i>) and	16

	NADH dehydrogenase subunit 4 (<i>nd4</i>) genes. Red dots represent the samples of Indo-Myanmar lineage and green squares denotes samples of Eastern Asian lineage. A total percentage of variance captured by the first and second Principal coordinates are given in each axis.	
1.4	Mitochondrial gene-based (<i>16s</i> , <i>cox1</i> , <i>cytb</i> and <i>nd4</i>) Median-joining haplotype network among populations of <i>Bungarus fasciatus</i> . The number of samples present in each haplotype corresponds to the relative size of the circles. Hatch marks at the branch represent mutational steps found between haplotypes, and a black dot at the branch is an inferred median.	18
1.5	(A) Ordination of <i>Bungarus fasciatus</i> populations from Mizoram, West Bengal and Java along the first two principal components based on a PCA of the characters Ve, BB, BT, and NBW. Total variance associated with the PC1 and PC2 are 64% and 20%, respectively. (B) PCA loading plot showing the distribution of the analysed variables along the first two principal components.	23
1.6	<i>Bungarus fasciatus</i> sensu stricto (MZMU1883) from Northeast India: (A) dorsal view of full body, (B) ventral view of full body, (C) dorsal view of head, (D) lateral view of the left side of head, and (E) ventral view of head.	27
1.7	Live individuals of <i>Bungarus fasciatus</i> sensu stricto (A) from Khamrang village, Mizoram, India, and (B) a juvenile with creamish dorsum coloration from Saikhawthlir village, Mizoram, India.	28
1.8	Sulcal (left) and asulcal (right) views of the right hemipenis of <i>Bungarus fasciatus</i> sensu stricto	29

	(MZMU2935) from Mizoram, India. The organ is single and subcylindrical, relatively short, robust, and capitate with a complex ornamentation of retiform ridges.	
1.9	Digital elevation map showing the distributional records of <i>Bungarus fasciatus</i> in Mizoram. The previous records fide Lalbiakzuala (2019) are given in blue triangles, and the new records from this work are given in red circles: 1. Vairengte; 2. Bukpui; 3. North Hlimen; 4. Luangmual; 5. Thingsulthliah; 6. Sateek; 7. New Khawlek.	31
1.10	Map showing the distribution range of <i>Bungarus fasciatus</i> sensu lato, based on the latest species map provided by the World Health Organization (2022); the coloration corresponds to the three distinct evolutionary lineages recovered in the phylogenetic analyses. The type locality of <i>Bungarus fasciatus</i> sensu stricto is indicated by a black star. Localities of specimens used in the morphological and DNA analyses are indicated by black filled circles, while locations for the specimens used for only DNA analysis and morphology only are shown in white and grey circles, respectively. Abbreviations for countries are: IN: India, NP: Nepal, BT: Bhutan, BD: Bangladesh, LK: Sri Lanka, CN: China, MM: Myanmar, LA: Laos, TH: Thailand, VN: Vietnam, KH: Cambodia, MY: Malaysia, BN: Brunei Darussalam, ID: Indonesia (KA: Kalimantan, SM: Sumatra, JW: Java).	32
1.11	(A) <i>Bungarus fasciatus</i> fatally run over by vehicles while swallowing its prey <i>Trimeresurus erythrurus</i> ; (B) The anterior half of the swallowed prey poked out from the oesophagus of <i>B. fasciatus</i> ; (C) Hemipenis of the	35

	road-kill <i>B. fasciatus</i> ; (D) The habitat of <i>B. fasciatus</i> showing the exact spot of the incidence (pointed in red arrow) locating close to a brook at New Khawlek, Mizoram, India. Photo credit: Malsawmtluanga.	
2.1	Description of head morphometrics used in <i>Bungarus niger</i> : (top) maximum width of head (HW), width of rostral (RW), snout to nostril distance (S-N), length of internarial (INL), width of internarial (INW), internarial space (INS), length of prefrontal (PFL), width of prefrontal (PFW), length of frontal (FL), width of frontal (FW), length of parietal (PL), width of parietal (PW); (below) length of head from tip of snout to angle of jaw (HL), depth of head (HD), horizontal eye diameter (ED), eye to snout distance (E-S), eye to nostril distance (E-N), rostral height (RH); and the meristics nuchal band width in scale (NBW) is also depicted.	43
2.2	Concatenated Bayesian Inference (BI) phylogenetic tree of <i>Bungarus</i> species using the mitochondrial <i>16s</i> , <i>nd4</i> and <i>cytb</i> genes. The Bayesian posterior probability (PP) supports are shown at each branch.	51
2.3	Concatenated Maximum Likelihood (ML) phylogenetic tree of <i>Bungarus</i> species using the mitochondrial <i>16s</i> , <i>nd4</i> and <i>cytb</i> genes. The Ultrafast bootstrap support (UFB) are shown at each branch.	52
2.4	Species delimitation by Assemble Species by Automatic Partitioning (ASAP) using <i>16s</i> (top) and <i>nd4</i> (bottom) gene fragments of the genus <i>Bungarus</i> . The Neighbour-joining cladogram (right) concorded to the ASAP partitions (left). Species abbreviations: <i>B. niger</i> (BN), <i>B. fasciatus</i> (BF), <i>B. suzhenae</i> (BSZ), <i>B. caeruleus</i> (BCR),	54

	<i>B. candidus</i> (BC), <i>B. bungaroides</i> (BB), <i>B. wanghaotingi</i> (BW), <i>B. multicinctus</i> (BM), <i>B. sindanus</i> (BS), <i>B. slowinskii</i> (BSL), <i>B. flaviceps</i> (BFL), <i>B. ceylonicus</i> (BCY), and <i>Naja naja</i> (NN) as outgroup.	
2.5	Species delimitation by Assemble Species by Automatic Partitioning (ASAP) using <i>cytb</i> gene fragments of the genus <i>Bungarus</i> . The Neighbour-joining cladogram (right) concorded to the ASAP partitions (left). Species abbreviations: <i>B. niger</i> (BN), <i>B. lividus</i> (BL), <i>B. fasciatus</i> (BF), <i>B. caeruleus</i> (BCR), <i>B. candidus</i> (BC), <i>B. multicinctus</i> (BM), <i>B. slowinskii</i> (BSL), <i>B. ceylonicus</i> (BCY), <i>B. sindanus</i> (BS), <i>B. bungaroides</i> (BB), <i>B. wanghaotingi</i> (BW), <i>B. suzhenae</i> (BSZ), <i>B. flaviceps</i> (BFL), and <i>Naja naja</i> (NN) as outgroup.	55
2.6	Mitochondrial gene-based (<i>16s</i> , and <i>nd4</i>) Median-joining haplotype network among <i>Bungarus</i> species. The number of samples present in each haplotype corresponds to the relative size of the circles. Hatch marks at the branch represent mutational steps found between haplotypes, and a black dot at the branch is an inferred median.	57
2.7	Mitochondrial gene-based (<i>cytb</i>) Median-joining haplotype network among <i>Bungarus</i> species. The number of samples present in each haplotype corresponds to the relative size of the circles. Hatch marks at the branch represent mutational steps found between haplotypes, and a black dot at the branch is an inferred median.	58
2.8	Ordination of <i>Bungarus</i> species in a Principal Coordinate Analysis of standardized p-distance of mitochondrial 16S rRNA (<i>16s</i>) NADH Dehydrogenase	64

	subunit 4 (<i>nd4</i>), and Cytochrome b (<i>cytb</i>) genes. A total percentage of variance captured by the first and second Principal coordinates are given in the x and y axes, respectively. Species abbreviations: <i>B. niger</i> (BN), <i>B. lividus</i> (BL), <i>B. fasciatus</i> (BF), <i>B. caeruleus</i> (BCR), <i>B. candidus</i> (BC), <i>B. multinctus</i> (BM), <i>B. slowinskii</i> (BSL), <i>B. ceylonicus</i> (BCY), <i>B. sindanus</i> (BS), <i>B. bungaroides</i> (BB), <i>B. wanghaotingi</i> (BW), <i>B. suzhenae</i> (BSZ), and <i>B. flaviceps</i> (BFL).	
2.9	A juvenile <i>Bungarus niger</i> (MZMU 1809) from Tanhril, Mizoram. Inset showing a dorso-lateral view of the head. Photo credit: Romalsawma.	65
2.10	Live adult <i>Bungarus niger</i> from Mizoram, India. Photo credit: H.T. Lalremsanga	66
2.11	<i>Bungarus niger</i> . (A–C) Lateral, dorsal and ventral views of the head; (D) Sulcate, and (E) asulcate view of the everted hemipenis. The organ is cylindrical with ill-defined demarcation between calyculate and spinose region. Photo credits: Melvin Selvan (A–C); Jayaditya Purkayastha (D & E).	66
2.12	Box plot showing median, interquartile range, range (minimum to maximum), and outliers for the adjusted (adj) mensurals such as internarial length (INL), prefrontal length (PFL), and inter-orbital space (IOS) between male and female specimens of <i>Bungarus niger</i> population from Mizoram, Northeast India. Significance at the alpha level of 0.05 are given at each plot.	75
2.13	Digital elevation map showing the distributional records of <i>Bungarus niger</i> in Mizoram. The previous records fide Lalbiakzuala (2019) are given in blue triangles, and	79

	the new records from this work are given in red circles: 1. Bilkhawthlir; 2. NE Bualpui; 3. Dampa Tiger Reserve; 4. Samtlang; 5. Lungphunlian; 6. Kanhmun; 7. Lungsai; 8. Lamchhip; 9. Paikhai road; 10. Darzo.	
2.14	Distributional records of <i>Bungarus niger</i> (in red diamond and red shaded) and <i>Bungarus lividus</i> (in blue dots). Distribution in Chin and Rakhine States in Myanmar is based on Leviton et al. (2008), and Mizoram (Mz) State in India is based on this study and Lalbiakzuala (2019). Abbreviations: India (IN), Mizoram state (Mz); Bangladesh (BD); Myanmar (MM), Rakhine state (Rk), Chin state (Ch); Nepal (NP); Bhutan (BT); China (CN).	80
2.15	Adult male <i>B. niger</i> preying on adult <i>Smithophis atemporalis</i> at Paikai road, Mizoram, NE India. Photo credit: Roluahpuia.	81
3.1	Description of head morphometrics used in <i>Naja kaouthia</i> : (top) width of head (HW), width of rostral (RW), snout to nostril distance (S-N), length of internarial (INL), width of internarial (INW), internarial space (INS), length of prefrontal (PFL), width of prefrontal (PFW), length of frontal (FL), width of frontal (FW), length of parietal (PL), width of parietal (PW); (below) length of head from tip of snout to angle of jaw (HL), depth of head (HD), horizontal eye diameter (ED), eye to snout distance (E-S), eye to nostril distance (E-N), and rostral height (RH).	88
3.2	Bayesian Inference (left) and Maximum likelihood (right) phylogenetic trees of <i>Naja</i> species inferred based on the concatenated <i>16s</i> , <i>cox1</i> and <i>cytb</i> genes. For the nodal supports, Bayesian posterior probabilities > 0.50	98

	from the BI analysis and ultrafast bootstrap values >50 from the ML analysis are shown.	
3.3	Bayesian inference (BI) phylogenetic tree based on concatenated mitochondrial <i>16s</i> , <i>cox1</i> and <i>cytb</i> genes. Values at each node represent Bayesian posterior probabilities (PP).	99
3.4	Species delimitation by Assemble Species by Automatic Partitioning (ASAP) using <i>16s</i> (top) and <i>cox1</i> (bottom) gene fragments of the genus <i>Naja</i> with <i>Bungarus fasciatus</i> as outgroup. The Neighbour-joining cladogram (right) concorded to the ASAP partitions (left).	101
3.5	Species delimitation by Assemble Species by Automatic Partitioning (ASAP) using <i>cytb</i> gene fragments of the genus <i>Naja</i> with <i>Bungarus fasciatus</i> as outgroup. The Neighbour-joining cladogram (right) concorded to the ASAP partitions (left).	102
3.6	Mitochondrial gene-based (<i>16s</i> , <i>cox1</i> and <i>cytb</i>) Median-joining haplotype network among populations of <i>Naja kaouthia</i> . The number of samples present in each haplotype corresponds to the relative size of the circles. Numbers at the branch represent mutational steps found between haplotypes, and a black dot at the branch is an inferred median.	107
3.7	Ordination of <i>Naja</i> species in a Principal Coordinate Analysis of standardized p-distance of mitochondrial 16S rRNA (<i>16s</i>) cytochrome c oxidase subunit 1 (<i>cox1</i>), and Cytochrome b (<i>cytb</i>) genes. A total percentage of variance captured by the first and second Principal coordinates are given in the x and y axes, respectively.	108
3.8	<i>Naja kaouthia</i> specimens from Mizoram, Northeast India in life (A) and preserved specimens. (B–D) The	111

	dorsal views of the hood with typical monocellate mark in adult. (E) Preserved juvenile specimen with the typical monocellate hood mark. (F–I) The dorsal views of adult anterior body showing a broken monocellate mark either at the anterior end (F, H, I) or at both anterior and posterior sides (G). (J) Preserved juvenile with a prominent dot present within the left lateral side of the marking. (K) Complete absence of hood mark. (L) The monocellate extended at the lateral flanks to form a mask-like marking. (M) The monocellate widely opens at the anterior end forming a spectacle-like marking, this particular specimen was killed by local people in the Northern part of Mizoram not far from Assam boundary, and was recovered for museum specimen. Phot credits: H.T. Lalremsanga (B–D, F–I, K), anonymous (M).	
3.9	Live adult <i>Naja kaouthia</i> from Mizoram. Photo credit: H.T. Lalremsanga.	112
3.10	Hemipenis showing the asulcate (left) and sulcate (right) views of <i>Naja kaouthia</i> . The organ is bilobed with small spines throughout that were slightly larger at the basal region. Photo credit: Lalmuansanga	112
3.11	Box plot showing median, interquartile range, range (minimum to maximum), and outliers for standardised (Z score) meristic and adjusted (adj) mensurals such as number of ventrals (Ve), subcaudals (Sc), tail length (TaL), eye diameter (ED), snout to eye distance (S-E), head length (HL), and nostril diameter (ND) between male and female specimens of <i>Naja kaouthia</i> population from Mizoram, Northeast India. Significance at the alpha level of 0.05 is given as asterisk in each plot.	124
3.12	(A) Ordination of <i>Naja kaouthia</i> population from	125

	Mizoram along the first two principal components based on a PCA of the standardised ventrals (Ve), subcaudals (Sc), and adjusted tail length (TaL), snout to eye distance (S-E) and eye diameter (ED) of adult specimens. Total variance associated with the PC1 and PC2 are 52% and 26%, respectively. (B) PCA loading plot showing the distribution of the analysed variables along the first two principal components.	
3.13	Box plot showing median, interquartile range, range (minimum to maximum), and outliers for adult's standardised (Z score) ventrals (Ve) in males, adjusted (adj) mensurals such as tail length (TaL) in females, sex pooled adult's head width (HW), head depth (HD), snout to nostril distance (S-N), rostril height (RH), internarial space (INS), internarial width (INW), prefrontal length (PFL), prefrontal width (PFW), frontal length (FL), HL in juvenile males, and rostral width (RW) in sex pooled juveniles between the phenotypic groups of <i>Naja kaouthia</i> population from Mizoram, Northeast India. Significance at the alpha level of 0.05 is given as asterisk in each plot.	132
3.14	(A) Ordination of <i>Naja kaouthia</i> population from Mizoram along the first two principal components based on a PCA of the allometric adjusted head width (HW), head depth (HD), snout to nostril distance (S-N), rostril width (RH), internarial space (IOS), internarial width (INW), prefrontal length (PFL), prefrontal width (PFW), and frontal length (FL) of adult specimens. Total variance associated with the PC1 and PC2 are 67% and 12%, respectively. (B) PCA loading plot showing the distribution of the analysed variables along the first two	133

	principal components.	
3.15	Digital elevation map showing the distributional records of <i>Naja kaouthia</i> in Mizoram (red circles): 1. Kawnpui; 2. Sawleng; 3. Lungdai; 4–35 Aizawl city area; 36. Thiak; 37. Hmuifang; 38. Thenzawl (see also Table 3.13).	135
3.16	Map showing the known distribution range of <i>Naja kaouthia</i> , based on the distributional range provided in published; the colour shadings correspond to the distinct clades recovered in the phylogenetic analyses.	136
4.1	Live adult male <i>Ophiophagus hannah</i> at Mizoram University campus.	141
4.2	Description of head morphometrics used in this chapter: (top) maximum width of head (HW), width of snout at level of nostril (SW), distance between the nostrils i.e., internarial space (INS), length of internarial scale (INL), width of internarial scale (INW), length of prefrontal scale (PFL), width of prefrontal scale (PFW), length of frontal scale (FL), width of frontal scale (FW), length of parietal scale (PL), width of parietal scale (PW), height of rostral scale (RH), width of rostral scale (RW), width of white inter-band on head at level of supraocular in measurement (WBH); (below) length of head from tip of snout to angle of jaw (HL), depth of head (HD), horizontal eye diameter (ED), maximum nostril diameter (ND), eye to snout distance (E-S), eye to nostril distance (E-N). Photo credit: H.T. Lalremsanga.	150
4.3	Bayesian inference (BI) phylogenetic tree based on concatenated mitochondrial <i>16s</i> , <i>cox1</i> , and <i>cytb</i> genes of <i>Ophiophagus hannah</i> ; lineage partitions recovered from CYTB-based PTP analyses are presented besides the BI	152

	tree. Values at each node represent Bayesian posterior probabilities (PP).	
4.4	Maximum Likelihood (ML) phylogenetic tree based on concatenated mitochondrial <i>16s</i> , <i>cox1</i> , and <i>cytb</i> genes of <i>Ophiophagus hannah</i> ; lineage partitions recovered from CYTB-based PTP analyses are presented besides the ML tree. Values at each node represent Ultrafast Bootstrap values (UFB).	153
4.5	Mitochondrial gene-based (<i>16s</i> , <i>cox1</i> , and <i>cytb</i>) Median-joining haplotype network among populations of <i>Ophiophagus hannah</i> . The number of samples present in each haplotype corresponds to the relative size of the circles. Hatch marks at the branch represent mutational steps found between haplotypes, and a black dot at the branch is an inferred median.	155
4.6	Ordination of <i>Bungarus</i> species in a Principal Coordinate Analysis of standardized p-distance of mitochondrial 16S rRNA (<i>16s</i>) cytochrome c oxidase subunit 1 (<i>cox1</i>), and Cytochrome b (<i>cytb</i>) genes. A total percentage of variance captured by the first and second Principal coordinates are given in the x and y axes, respectively.	165
4.7	Sulcate (left) and asulcate views of the hemipenis of <i>Ophiophagus hannah</i> . Hemipenes elongated and deeply bifurcated with two forks with the spines prominently present around the basal area of the organ.	166
4.8	Box plot showing the median, interquartile range, range (minimum to maximum), and outliers of the standardised (Z score) meristic and adjusted (adj) mensurals that differed between sexes of <i>O. hannah</i> population in Mizoram. Significance at the alpha level	173

	of 0.05 are given at each plot.	
4.9	(A) Ordination of male and female specimens of <i>O. hannah</i> population from Mizoram along the first two principal components based on a PCA of the standardised meristics (ventrals, undivided subcaudals, subcaudals) and allometric adjusted mensurals (tail length, head length, head width, head depth, nostril diameter, internarial space, frontal width, parietal width). (B) PCA loading plot showing the distribution of the analysed variables along the first two principal components.	174
4.10	Box plot showing the median, interquartile range, range (minimum to maximum), and outliers of the standardised (Z score) Ve (A), Sc (B), and ADSR (C) that differed among <i>O. hannah</i> populations/lineages. Significance at the alpha level of 0.05 are given at each plot.	177
4.11	(A) Ordination of <i>O. hannah</i> populations to see the clustering of Mizoram samples with respect to the pre-defined four lineages (Indo-Chinese, Western Ghats, Indo-Malayan and Luzon Island) along the first two principal components based on a PCA of the standardised meristics (ventrals, subcaudals, anterior dorsal scale rows). (B) PCA loading plot showing the distribution of the analysed variables along the first two principal components.	178
4.12	Map showing king cobra nesting sites in Mizoram, north-east India from both previous studies and the current conservation programme (red stars, some red stars refer to more than one nesting site) - 1. Hualngo, 2. Tanhril, 3. Muthi, 4. Dampa Tiger Reserve, 5.	181

	Chhingchhip, 6. Samlukhai, 7. Sailam, 8. Thenzawl I–IV, 9. Chhipphir, 10. Khawzawl I, 11. Khawzawl II, 12. N. Khawbung, 13. Tlangsam, 14. Zote I, 15. Zote II.	
4.13	<i>Ophiophagus hannah</i> in Mizoram, north-east India: A. Deserted nest at Thenzawl IV, B. Deserted hatchlings uncovered inside the nest at Chhingchhip, C. Completely destroyed nest and eggs with the freshly killed female from Tlangsam, D. Female coiling above its nest in Dampa Tiger Reserve, E. Hatching of the incubated eggs, F. Releasing hatchlings at Zongaw Reserved Forests. Photo credits: H.T. Lalremsanga (A & B, E–F), Zakhuma (D), anonymous (C).	182
5.1	Description of head morphometrics used in this chapter: (a) maximum width of head (HW), width of head at level of eye (HWE), width of snout at level of nostril (SW), distance between the nostrils i.e., internarial space (INS), distance between the orbits i.e., interorbital space (IOS), width of internarial scale (INW), width of prefrontal scale (PFW), length of frontal scale (FL), length of parietal scale (PL), width of white inter-band on head at level of supraocular in measurement (WBH); (b) length of head from tip of snout to angle of jaw (HL), depth of head (HD), horizontal eye diameter (ED), eye to snout distance (E-S), eye to nostril distance (E-N); and the meristics nuchal band width in scale (NBW) is also depicted where the NBW is one in this case.	193
5.2	Bayesian inference phylogenetic tree constructed using partitioned concatenated sequences of <i>16s</i> , <i>cox1</i> , <i>cytb</i> , <i>nd4</i> and <i>nt3</i> of <i>Sinomicrurus</i> species with <i>Micrurus fulvius</i> as outgroup. Numbers at the nodes indicate	203

	Bayesian posterior probability and values <0.50 are not shown. The specimens of <i>S. macclellandi</i> var. <i>typica</i> are shaded in red box, <i>S. gorei</i> comb. nov. in blue box, and <i>S. macclellandi</i> sensu stricto fide Smart et al. (2021) are indicated in vertical dark-greyish box.	
5.3	Maximum likelihood phylogenetic tree constructed using partitioned concatenated sequences of <i>16s</i> , <i>cox1</i> , <i>cytb</i> , <i>nd4</i> and <i>nt3</i> of <i>Sinomicrurus</i> species with <i>Micrurus fulvius</i> as outgroup. Numbers at the nodes indicate ultrafast bootstrap values.	204
5.4	Ordination of standardized p-distance estimated from the concatenated mitochondrial 16S, COI, CYTB, ND4 (a) and nuclear NT3 (b) among <i>Sinomicrurus</i> species along the first and second principal coordinate (PCo) axes. The total variance captured by PCo1 and PCo2 are given at the x and y axes, respectively.	205
5.5	DensiTree showing different topologies in the sets of mitochondrial gene trees with posterior probability values at the nodes, and the sets of consensus trees are given in black colour (a), and the species tree of <i>Sinomicrurus</i> species summarized using maximum clade credibility (b).	206
5.6	Box plot showing median, interquartile range, range (minimum to maximum), and outliers for the statistically significant sexually dimorphic characters among the adult specimens of <i>Sinomicrurus macclellandi</i> (in pooling the two varieties) population from Northeast India. The depicted characters are the standardised (Z score) ventrals (Ve) and subcaudals (Sc), and the allometric adjusted (Adj) tail length (TaL) and snout to eye distance (S-E). Significant level (p	217

	values) at the alpha level of 0.05 are given at each plot.	
5.7	(a) PCA score plot of <i>Sinomicrurus macclellandi</i> populations from Northeast India along the first two principal components based on a PCA of the standardised meristics such as nuchal band width (NBW), black bands on body (BB), black spots on body (BS), and black bands on tail (BT); and allometric adjusted mensurals such as head length (HL) head width (HW), head depth (HD), interorbital space (IOS), and horizontal eye diameter (ED). Total variance associated with the PC1 and PC2 are 63% and 19%, respectively; (b) PCA loading plot showing the distribution of the analysed variables along the first two principal components.	218
5.8	(a) Live specimens of <i>Sinomicrurus macclellandi</i> var. <i>typica</i> (YSR006) from the type locality in Shillong, Northeast India, photo by Jayaditya Purkayastha; (b) <i>S. macclellandi</i> var. <i>typica</i> (MZMU2588) from Mizoram, Northeast India in life; (c) <i>S. gorei</i> comb. nov. (MZMU2589) from Mizoram, Northeast India, photo by Vivek Sharma; (d) Unvouchered live specimen of <i>S. gorei</i> comb. nov. flattens its posterior body dorsoventrally and elevating the coiled tail, and inset showing its flatten body and tail display in different view from Mizoram, Northeast India.	221
5.9	Head of <i>Sinomicrurus gorei</i> comb. nov. (MZMU2910): (a) dorsal, (b) ventral, and (c) lateral views. Head of <i>S. macclellandi</i> var. <i>typica</i> (MZMU2588): (d) dorsal, (e) ventral, and (f) lateral views.	227
5.10	Ventral view of the head in <i>Sinomicrurus gorei</i> comb. nov.: (a) MZMU831, (b) MZMU840, (c) MZMU945,	228

	(d) MZMU1157, (e) MZMU1911, (f) MZMU2910; in <i>S. macclellandi</i> var. <i>typica</i> : (g) MZMU2588, (h) APRC/R/91/A. Photo credit: Lalmuansanga (a–e).	
5.11	MicroCT scans of the head of <i>Sinomicrurus gorei</i> comb. nov. (a–c) and <i>S. macclellandi</i> var. <i>typica</i> (d–f); head dorsal view (a & d), head lateral view (b & e). and ventral view of head (c & f). Scale bar 1mm.	230
5.12	Sulcate view (left) and asulcate view (right) of the hemipenis: (a) <i>S. gorei</i> comb. nov. (MZMU2341); (b) <i>S. macclellandi</i> var. <i>typica</i> (YSR006). The organs are slightly forked with two distinctly pointed apical lobes in both species. Main body of hemipenis moderately enlarged with spines 19–22 around main body in <i>S. gorei</i> comb. nov. while it is highly enlarged with 27 spines around the main body in <i>S. macclellandi</i> . Photo credit: Jayaditya Purkayastha.	230
5.13	Digital elevation map showing the distributional records of <i>Sinomicrurus macclellandi</i> var. <i>typica</i> and <i>S. gorei</i> comb. nov. in Mizoram. The locality numbers are corresponds to the serial number as given in Table 5.9.	238
5.14	Map showing the studied populations of <i>Sinomicrurus macclellandi</i> from Northeast India: type locality of <i>S. macclellandi</i> from Shillong, Meghalaya (formerly Assam) (in red star); studied populations of <i>S. macclellandi</i> var. <i>typica</i> from Meghalaya and Mizoram with DNA+ morphological data (in red diamond with dot), and Arunachal Pradesh with morphological data (in red diamond); type locality of <i>S. gorei</i> comb. nov. from Dibrugarh, Assam (in blue star); studied population of <i>S. gorei</i> comb. nov. from Mizoram with DNA+morphological data shown in blue circle with dot	239

	and with only morphological data shown in blue circle. See the detailed global distributional records of <i>Sinomicrurus</i> species in Smart et al. (2021).	
5.15	(a) Newly hatched neonates of <i>Sinomicrurus gorei</i> comb. nov. (MZMU2590) from Mizoram, Northeast India; (b) neonate which was prematurely hatched along with the egg shell.	243
5.16	(a) Ordination of the standardized meristic characters of body band (BB), tail band (BT), and width of nuchal band (NBW) between <i>Sinomicrurus macclellandi</i> var. <i>typica</i> and <i>S. gorei</i> comb. nov. based on the phenotypic dataset adopted from Smart et al. (2021). Total variance associated with the PC1 and PC2 are 67% and 21%, respectively. Box plot showing median, interquartile range, range (minimum to maximum), and outliers for the statistically significant difference in the standardized ventral (Ve) among male (b) and female (c) specimens between <i>S. macclellandi</i> var. <i>typica</i> and <i>S. gorei</i> comb. nov. Significant level (p values) at the alpha level of 0.05 given at each plot.	246
6.0	Digital elevation map showing the overall distributional records of elapid snakes documented in this study from Mizoram, Northeast India.	253

General introduction

Species is the fundamental unit in biology (Hohenegger 2014), thereupon species recognition and accurate taxonomic treatment is crucial in various disciplines in biological sciences like ecology, evolutionary biology, population biology, biodiversity, agriculture, etc. (Savage 1995; Hohenegger 2014). Various operational criteria have been implemented for species recognition as determined by the type of species concepts that is being followed (de Queiroz 2007). For instances, reproductive isolation has been used as the operational criteria under the biological species concept (Mayr 1942; Coyne 1994); reciprocal monophyly under the phylogenetic species concept (Baum & Shaw 1995); and the morphology-based taxonomy which mainly enticed to the phenetic species concept, and this approach practically remained the key framework in species identification (Sokal & Crovello 1970; Luo et al. 2018). However, during the past few decades, the growing availability of molecular methods for species identification that largely appealed to the phylogenetic species concept contributed a valuable compliment to the morphological-based taxonomy (Luo et al. 2018). Moreover, the molecular species delimitation methods have been employed either as an autonomous method or part of an integrative taxonomical method (Hotaling et al. 2016; Mason et al. 2016).

Evolution is basically driven by selection acting upon variation in morphological, behavioural, or physiological traits (Bolnick et al. 2011; Kaliontzopoulou et al. 2018). When this variation is further fortified by a divergence of population, interspecific variations will be the outcome of the gradually developing reproductive isolation within species (Turelli et al. 2001). Moreover, conspecific variation is a widely studied topic because it provides a raw material for natural selection, a focal point of evolutionary theory (Bolnick et al. 2011); for instance, among mammals (Tarrowx et al. 2012), birds (Westerberg et al. 2019), fish (Kekäläinen et al. 2010), amphibians (Gascon et al. 1996), and reptiles (Miles et al. 2001). Owing to the advancement of genetic methods for species delimitation (Luo et al. 2018), various studies have revealed cryptic diversity within the widespread vertebrate species from tropical and sub-tropical Asia. For example, Pisces (Dwivedi et al. 2017; Halasan et al. 2021), Amphibia (Nishikawa et al. 2012; Ramesh et al.

2020; Stuart et al. 2006), Aves (Lohman et al. 2010; Outlaw & Voelker 2008; Rheindt et al. 2022), and Mammalia (Chattopadhyay et al. 2021; Chen et al. 2020; Nater et al. 2017). Moreover, recent studies have rectified our interpretation and perception of cryptic speciation across or within biogeographical boundaries and regions (Pfenninger & Schwenk 2007; Voda et al. 2014); and reptiles were also specifically nominated as potential biogeographic indicators (Bauer 1989; Camargo et al. 2010). Recent works particularly on the widespread members of Reptilia have also determined the existence of previously unknown cryptic diversity, including among lizards (Gowande et al. 2021; Guo et al. 2015; Wagner et al. 2021; Zug et al. 2007) and snakes (Alfaro et al. 2004; Malhotra et al. 2011; Mallik et al. 2020; Shankar et al. 2021; Thorpe et al. 2007; Wuster 1996; Wuster & Thorpe 1994; Wuster et al. 1992).

This study focuses on the snake family Elapidae Boie, 1827, one of the several families accommodating under the caenophidian snake lineage. Species of this family are having a well-developed venom delivery system with a non-movable pair of venom delivering fangs at the anterior end of the upper dentition except the genus *Emydocephalus* Krefft, 1869, the only known non-venomous elapid snake genus (Voris 1966). Elapid snakes are estimated to emerged less than 40 million years ago and showed high rates of diversification among reptiles (Sanders & Lee 2008). The family accommodates over 60 genera (more than 300 nominal species) distributing worldwide in the tropical and subtropical regions including the terrestrial genera like *Bungarus* Daudin, 1803 (Kraits), *Elapsoidea* Bocage, 1866 (African garter snakes), *Micrurus* Wagler, 1824 (American coral snakes), *Naja* Laurenti, 1768 (Cobras), *Ophiophagus* Gunther, 1864 (King cobra), *Pseudonaja* Gunther, 1858 (Brown snakes), *Sinomicrurus* Slowinski, Boundy & Lawson, 2001 (Asian coral snakes), *Oxyuranus* Kinghorn, 1923 (Taipans) etc.; arboreal genera like *Pseudohaje* Gunther, 1858 (tree cobras or forest cobras), *Dendroaspis* Schlegel, 1848 (Mambas) etc.; and the marine genera like *Laticauda* Laurenti, 1768 (Sea kraits), *Hydrophis* Sonnini & Latreille, 1801 (Sea snakes) (see Uetz et al. 2023; Wallach et al. 2014). In India, a total of 43 elapid snake species have been recorded (Mohapatra et al. 2024).

From the study area in Mizoram state of northeastern India, the existing literature have recognized a total of five elapid snake species namely *B. fasciatus* (Schneider, 1801), *B. niger* Wall, 1908, *N. kaouthia* Lesson, 1831, *O. hannah* (Cantor, 1836), and *S. macclellandi* (Reinhardt, 1844) (see Mathew 2007; Laltanpuia et al. 2008; Lalremsanga et al. 2011). Because these five elapid taxa are predominantly widespread taxa globally, various workers have also reassessed their systematics and taxonomy (e.g., McCarthy 1985; Wuster 1996; Wuster & Thorpe 1992; Slowinski & Keogh 2000; Slowinski & Wüster 2000; Castoe et al. 2007; Peng et al. 2018; Mirza et al. 2020; Chen et al. 2021; Shi et al. 2022), biogeography (e.g., Keogh 1998; Wüster et al. 2007; Kelly et al. 2009; Kazemi et al. 2020), evolutionary biology (e.g., Daltry et al. 1996; Lee et al. 2016; Raveendran et al. 2017; Kazandjian et al. 2021; van Thiel et al. 2022), venomics (e.g., Fry et al. 2003; Harrison et al. 2003; Tan et al. 2016; Hia et al. 2020; Deka et al. 2023; Talukdar et al. 2023), ecology (e.g., Hrima et al. 2014; Dolia 2018; Knierim et al. 2019; Marshall et al. 2018; Jones 2020; Koirala & Tshering 2021; Jones et al. 2022), etc. Even so, the aforementioned existing literature underrepresented elapid specimens in their studies, and limited data is available at morphological and molecular level from Mizoram particularly for *O. hannah* (Shanker et al. 2021), *S. macclellandi* (Lalremsanga & Zothansiam 2015; Smart et al. 2021), *B. fasciatus* and *B. niger* (Lalbiakzuala 2019); while there is no existing taxonomic or systematic framework for *N. kaouthia* from the area so far. Except for *S. macclellandi*, the target elapid species are confirmed deadly venomous species that are capable of inflicting severe clinical or even lethal envenomation upon humans; but, the distribution and other status of the deadly venomous snakes beyond the “Big Four” are poorly known across pan India (Whitaker & Martin 2014). Correspondingly, not only the lethal dose and lethality period of snake venoms differed across species (Ahmed et al. 2008), but ecological and environmental factors are also known to have suggested variation in venom composition across populations of a similar species (Tan et al. 2016; Laxme et al. 2021). Due to this intraspecies venom variability, the efficacy of snakebite treatment can be compromised because anti snake venom (ASV) prepared against the venom of a particular snake population may fail to neutralize the envenomation from disparate snake population (Laxme et al. 2021). In fact, cryptic diversity occurs in most animal

species groups (Pfenninger & Schwenk 2007), and the failure to determine cryptic diversity can result to imprecise estimation of the true degrees of biodiversity (Vodă et al. 2014). So, accurate determination of intra-specific variations and inter-specific boundaries among the deadly venomous elapid snakes will be critical for accurate biodiversity assessment as well as for developing efficient snakebite management particularly in Mizoram as well as for the whole Northeast Indian region. This study aims to establish taxonomic framework for the elapid snakes in Mizoram for the better understanding of their respective species distribution and the true diversity of the family in the area.

Henceforth, by implementing the combination of descriptive morphology, morphometrics and molecular analyses, the following objectives were proposed for this study:

1. To survey and document the distribution of species belonging to the family Elapidae in Mizoram.
2. To analyze the morphological and meristic variations among different species of the family Elapidae.
3. To analyze the genetic data and phylogenetic status of different species under the family Elapidae using mitochondrial *16s*, *cox1*, and *cytb*.

Systematic position of Elapidae

Kingdom: Animalia

Phylum: Chordata

Class: Reptilia

Order: Squamata

Family: Elapidae Boie, 1827



Figure (i). Elapid snake species found in Mizoram, India. Photo credit: H.T. Lalremsanga

CHAPTER 1

Bungarus fasciatus (Schneider, 1801)

Review of literature

Bungarus, collectively called as kraits are considered deadly venomous, and they are found in the Asian subcontinent (Midtgaard 2022; Uetz et al. 2024). Despite the fact that majority of the extant *Bungarus* species are understudied, modern studies that particularly dealt with the elapid origin and evolution have suggested that kraits diversification took place roughly 30–25 million years ago, and are also regarded to have a very close relationship with the other Australasian elapid genera and sea snakes (Lee et al. 2016). The banded krait, *B. fasciatus* is nocturnal in activity, it is a large-sized krait species that can reaches up to 2,250 mm in total length, and is phenotypically distinguishable by its yellowish (or sometimes creamish) and black banded body (Ahmed et al. 2009). It inhabits various types of niches like primary forests, agricultural areas, domestic gardens in the vicinity of human settlements at the altitudes of up to 2,300 m above sea level (Ahmed et al. 2009; Knierim et al. 2019). This species has been recorded so far from eastern India, Nepal, Bhutan, Bangladesh, Myanmar, Thailand, Malaysia, Singapore through the Indonesian archipelago, Laos, Vietnam, and China (Stuart et al. 2013; Wallach et al. 2014; Uetz et al. 2024). The species is currently listed as a Least Concern (LC) species in the IUCN Red List (Stuart et al. 2013) and Schedule II under the Wildlife (Protection) Amendment Act (2022) in India. Although it is a widely distributed species, most of the existing studies have hitherto dealt onto its possible medical significance (Pe et al. 1997), ecology (Ahsan & Rahman 2017; Tongpoo et al. 2018), or venomics (Lo & Lu 1978; Lu et al. 2008; Rusmili et al. 2014; Tan & Ponnudurai 1990; Tsai et al. 2007; Ziganshin et al. 2015).

Although the molecular systematics of *B. fasciatus* has never been deeply studied, several previous DNA barcoding research have dictated the existence of intra-specific or geographical variations (Kundu et al. 2020a; Laopichienpong et al. 2016; Supikamolseni et al. 2015). Moreover, some authors proposed that variations in venom composition can be useful in taxonomical aspects (Goncalves & Deutsch 1956; Tu et al. 1965), while some argued that venom variation is not a good indicator

of taxonomic status due to intraspecific venom variability (Sato et al. 1988). However, establishment of accurate species boundary is critical in considering this variability in snake venom composition (Chippaux et al. 1991) and its possible consequence to the antivenom effectiveness (Harrison et al. 2003). Most of the published literature on *Bungarus* taxonomy and systematics have apparently underestimated the diversity of *B. fasciatus* at the intraspecies level (Abtin et al. 2014; Ashraf et al. 2019; Chen et al. 2021; Keogh 1998; Kuch & Mebs 2007; Kuch et al. 2005; Slowinski 1994; Slowinski & Keogh 2000). This chapter attempt to enhance the inherent knowledge insufficiency for the species through comparative morphological analyses and molecular phylogenetic inferences using mitochondrial genes.

Materials and methods

Sampling

Field surveys were conducted during the day and night employing visual encounter surveys (Flint and Harris 2005). All the specimen collection were undertaken after obtaining specimen collection permit from the Environment, Forests and Climate Change Department, Government of Mizoram (Permit No. B.19060/5/2020-CWLW/20-26). A total of 15 specimens are examined from Mizoram, where 12 specimens are preserved specimens housed in the collections of the Departmental Museum of Zoology, Mizoram University (MZMU), and three are life individuals captured during this work. The three life specimens collected (MZMU1421, MZMU1562, MZMU1883) were euthanized with MS-222 following the standard procedure (Conroy et al. 2009) complying to the American Veterinary Medical Association (AMVA) guidelines and approved by the Institutional Animal Ethics Committee (IAEC) (Permission No. MZU-IAEC/2018/12). The specimens were stored in 70% ethanol at MZMU. The liver tissues were dissected and preserved for DNA analysis in 95% ethanol, and were stored at -20°C . The distribution map was prepared using QGIS v3.16.2 and the digital elevation model (DEM) was downloaded from Open Topography (<https://opentopography.org/>).

DNA extraction and PCR amplification

Liver tissue was used for isolation of genomic DNA using DNeasy (Qiagen™) blood and tissue kits following the manufacturer's instructions (DNeasy® Blood & Tissue Handbook 2023). The fragments of four mitochondrial gene markers such as 16S rRNA (*16s*), cytochrome c oxidase subunit 1 (*cox1*), cytochrome b (*cytb*) and NADH dehydrogenase subunit 4 (*nd4*) were amplified using Polymerase Chain Reaction (Mullis et al. 1986). The PCR reaction was carried out in a 20 µL reaction volume, containing 1X DreamTaq PCR Buffer, 2.5 mM MgCl₂, 0.25 mM dNTPs, 0.2 pM of each gene primer pair, approximately 3.0 ng of extracted DNA, and 1 U of Taq polymerase. A negative control with reagent grade water instead of DNA template was always included. Target mt gene sequences were amplified using the thermal conditions and primer pairs as listed in Table 1.1. PCR products were checked using gel electrophoresis on a 1.5% agarose gel containing ethidium bromide. The PCR products were cleaned using ThermoFisher ExoSAP-IT PCR product cleanup reagent and sequenced using the Sanger dideoxy method using the ABI 3730xl DNA Analyzer at Barcode BioSciences, Bangalore, India.

Phylogenetic analyses

The generated partial gene sequences were deposited on the NCBI repository with the GenBank accession numbers as given in Table 1.2. In this study, a total of one *cox1*, six *16s*, six *nd4*, and nine *cytb* sequences were generated and were combined with published sequences of *B. fasciatus* obtained from the NCBI database; database sequences of *B. caeruleus*, *B. candidus*, *B. ceylonicus*, *B. sindanus*, and *B. multicolor* were used as outgroups. The four gene alignments were concatenated in SequenceMatrix (Vaidya et al. 2011). Using the *cytb* dataset, the uncorrected p-distance was estimated in MEGA 11 using the complete deletion option for the treatment of gaps/missing data (Tamura et al. 2021). PartitionFinder v2.1 (Lanfear et al. 2017) was employed for searching the best partitioning schemes and the best fitting nucleotide evolutionary model through Bayesian Information Criterion (BIC). Bayesian phylogeny (BI) was reconstructed in Mr.Bayes v3.2.5 (Ronquist et al. 2012) by implementing the best partitions and models selected by PartitionFinder v2.1 (Lanfear et al. 2017). The MCMC was run with four chains (one

cold and three hot chains) for 20 million generations and sampled every 5000 generations. The convergence of likelihood and the burn-in cut-off was checked in Tracer v1.7 (Rambaut et al. 2018). The BI tree was further illustrated using web-based tree annotator iTOL software v5 (Letunic & Bork 2021). The Maximum Likelihood (ML) tree was reconstructed in IQ-TREE (Nguyen et al. 2015) using 10,000 Ultrafast Bootstrap (UFB) (Minh et al. 2013), by allowing FreeRate heterogeneity (Yang 1995; Soubrier et al. 2012), and by implementing the best partitioning schemes selected by PartitionFinder v2.1 (Lanfear et al. 2017) model selected by ModelFinder (Kalyaanamoorthy et al. 2017) integrated in IQ-TREE (Nguyen et al. 2015).

Species delimitation

The *cytb* dataset, partitioned by codon, was utilized for performing BI and ML based Poisson Tree Processes (PTP) species delineation analyses (Zhang et al. 2013) implemented in iTaxoTools v0.1 (Vences et al. 2021). For the input file of PTP, a non-ultrametric tree was produced in IQ-TREE (Nguyen et al. 2015) with 10,000 UFB replicates (Minh et al. 2013) using the models selected for *cytb* partitions. Only the *cytb* dataset was utilized for the species delimitation analysis as it contains a suitable number of samples from different geographical regions compared to the other three genes. The standardized p-distances were further utilized for Principal Coordinate Analysis (PCoA) (Gower 1966) to visualize the genetic differentiation among the target taxa in PAST 4.13 (Hammer et al. 2001).

Matrilineal haplotype networks

The four mitochondrial DNA sequences were separately analysed for haplotype diversity (Hd) and reconstruction of haplotype networks. The four aligned datasets were processed in DnaSP v.6 (Rozas et al. 2017) for estimating haplotype diversity, and the trait matrix corresponding to the locality of the samples was inserted in the output file. The haplotype networks were plotted in PopArt v.1.7 (Leigh and Bryant 2015) using the Median-Joining method, which is a useful statistical approach for intra-species haplotype networks (Bandelt et al. 1999).

Table 1.1. Information on PCR thermal conditions used in the amplification of four mitochondrial genes utilized in this chapter.

Target genes	Primer pairs	Primer references	Initial denaturation	Repeated steps (35 cycles)			Final extension	Cooling
				Denaturation	Annealing	Extension		
<i>16s</i>	L02510 (Forward); H03063 (Reverse)	Palumbi 1996; Rassmann 1997	95°C for 5 min	95°C for 1 min	50.3°C for 30 sec	72°C for 1 min	72°C for 5 min	4°C for 15 min
<i>cox1</i>	LCO (Forward); HCO (Reverse)	Folmer et al. 1994	94°C for 3 min	94°C for 30 sec	50°C for 40 sec	72°C for 45 sec	72°C for 5 min	
<i>nd4</i>	ND4 (Forward); ND4 LEU (Reverse)	Arévalo et al. 1994	94°C for 3 min	94°C for 30 sec	52°C for 45 sec	72°C for 1 min	72°C for 5 min	
<i>cytb</i>	L14910 (Forward); H16064 (Reverse)	Burbrink et al. 2000	94°C for 3 min	94°C for 30 sec	49°C for 40 sec	72°C for 30 sec	72°C for 5 min	

Table 1.2. Information on the specimen vouchers, locations, GenBank accession numbers, and references of the DNA sequences of *Bungarus fasciatus* (BF) with *B. caeruleus* (BCR), *B. candidus* (BC), *B. multicinctus* (BM), *B. niger* (BN), *B. ceylonicus* (BCY), *B. sindanus* (BS), and *B. bungaroides* (BB) as outgroups. The sequences generated in this study are shown in bold.

Species	GenBank Accession Numbers				Specimen vouchers	Locality	References
	<i>16s</i>	<i>cox1</i>	<i>nd4</i>	<i>cytb</i>			
BF	OQ256169	OQ256190	-	OQ266796	MZMU1883	Mizoram, India	This study
BF	-	-	-	OQ266797	MZMU1421	Mizoram, India	This study
BF	-	-	-	OQ266798	MZMU1562	Mizoram, India	This study
BF	OQ256170	-	OQ266805	OQ266799	15.v26	Mizoram, India	This study
BF	OQ256171	-	OQ266806	OQ266800	14.36	West Bengal, India	Biakzuala et al. 2023
BF	-	-	OQ266807	OQ266801	14.37	West Bengal, India	Biakzuala et al. 2023
BF	OQ256172	-	OQ266808	OQ266802	15.69	West Bengal, India	Biakzuala et al. 2023
BF	OQ256173	-	OQ266809	OQ266803	15.v11	West Bengal, India	Biakzuala et al. 2023
BF	OQ256174	-	OQ266810	OQ266804	15.v12	West Bengal, India	Biakzuala et al. 2023
BF	-	-	-	MW596475	MZMU978	Mizoram, India	This study
BF	-	-	-	MN853157	MZMU1314	Mizoram, India	This study
BF	XXXXXX	-	-	XXXXXX	CESS246	Assam, India	Malhotra et al. unpublished
BF	XXXXXX	-	-	XXXXXX	CESS346	Assam, India	Malhotra et al. unpublished
BF	-	-	-	AF217830	No voucher	Ayeyarwadi, Myanmar	Slowinski and Keogh 2000
BF	-	AB920189	-	AB920243	BFA1	Thailand	Supikamolteni et al. 2015
BF	-	AB920190	-	AB920244	BFA2	Thailand	Supikamolteni et al. 2015
BF	-	AB920191	-	AB920245	BFA3	Thailand	Supikamolteni et al. 2015
BF	-	-	AJ830224	AJ749347	BfasT	Thailand	Kuch 2007
BF	JN687935	-	-	-	No voucher	Thailand	Suntrarachun et al. 2011
BF	-	-	-	AJ749349	UKH9	Java (Indonesia)	Kuch 2007
BF	-	-	AJ830244	AJ749350	UKB24	Java (Indonesia)	Kuch 2007
BF	-	-	KX130763	-	Ophi-3576	Java (Indonesia)	Brown et al. 2018
BF	MK194029	MK064719	-	MK201379	CHS285	Yunnan, China	Li et al. 2020

BF	MK194175	MK064841	-	MK201490	CHS727	Yunnan, China	Li et al. 2020
BF	MK194121	MK064798	-	MK201451	CHS647	Guangdong, China	Li et al. 2020
BF	-	-	-	KY952772	GP915	Guizhou, China	Xie et al. 2017
BF	-	MF099659	-	-	JHS01	Hubei, China	Chen et al. 2017
BF	-	MF099660	-	-	JHS02	Hubei, China	Chen et al. 2017
BF	-	JN833615	-	-	BF1	Guangxi, China	Chao and Liao 2011
BF	-	JN833616	-	-	BF2	Guangxi, China	Chao and Liao 2011
BF	-	JF700190	-	-	AS57MT01	Guangxi, China	Zhang et al. 2011
BF	-	KF698923	-	-	S117	Guangxi, China	Cao et al. 2016
BF	EU579523	EU579523	EU579523	EU579523	CIB093922	China	Chen et al. 2008
BF	-	KY769763	-	-	MVZ224274	Vietnam	Nguyen et al. 2017
BF	-	KY769764	-	-	MVZ224275	Vietnam	Nguyen et al. 2017
BF	-	KY769765	-	-	MVZ226609	Vietnam	Nguyen et al. 2017
BF	-	KY769766	-	-	MVZ226610	Vietnam	Nguyen et al. 2017
BF	-	KY769767	-	-	MVZ226611	Vietnam	Nguyen et al. 2017
BF	-	-	-	JN709990	No voucher	Vietnam	Dang et al. 2011
BF	EU547184	-	EU547037	EU547086	ABTC85504	Not specified	Sanders et al. 2008
BF	JF357944	-	-	-	No voucher	Not specified	Lukoschek et al. 2012
BC	JN687933	-	AJ830246	AJ749328	No voucher	Thailand	Kuch 2007; Suntrarachun et al. 2011
BCR	MT573970	-	-	MK941838	BC2 (16S)/ ZMUVAS11 (CYTB)	Punjab, Pakistan	Ashraf et al. 2019; Ali et al. 2018
BCR	-	-	AJ830220	AJ749305	UKH7	Pakistan	Kuch 2007
BS	-	-	AJ830242	AJ749346	Bsin1	Pakistan	Kuch 2007
BCY	KC347350	-	KC347501	KC347457	RS-135	Sri Lanka	Pyron et al. 2013a
BM	EU579522	EU579522	EU579522	EU579522	No voucher	China	Chen et al. 2008

Morphology

The morphological (mensural and meristic) data of *B. fasciatus* were obtained for Mizoram (MZ), West Bengal (WB; examined by Vishal Santra), Java (JV; examined by A.A. Thasun Amarasinghe), and published literature (Chen et al. 2021; Smith 1943; Yang and Rao 2008; Leviton et al. 2008). The following characters were measured to the nearest millimetre with a Mitutoyo digital calliper and dissecting microscopes: eye diameter, ED; eye–nostril length, E-N; eye to snout distance, E-S; head length, HL; head width, HW; snout–vent length, SVL; tail length, TaL. Meristic characters were taken as follows: supralabials, SL; supralabials touching the eye, SLe; infralabials, IL; infralabial touching the sublabial, ILSl; temporals, Tem; preoculars, PrO; postoculars, PoO; dorsal scale rows, DSR (counted on one head length behind neck, at midbody and at one head length prior to cloacal plate); the ventral scales (Ve) were counted following Dowling (1951). The terminal scute is excluded when counting subcaudal scales (Sc). Sex of the specimens was identified by examining everted hemipenes or by ventral tail dissection. The relative size of the nuchal band the number of the black cross bands of each individual were evaluated. The number of cross bands on the body (BB) were counted from the first band posterior to the nuchal band on the nape up to the level of cloaca, the count on the tail from the level of cloaca to the tip of tail (BT), and number of vertebral scales covering the nuchal band (NBW) as depicted in Fig. 1.1. In addition, the number of vertebral scales covering the first cross band is also considered a reliable character for adult individuals. Values for bilateral head characters are given in left/right order. Keogh (1999) was followed for hemipenial terminology, and the extent of inverted hemipenis was expressed in terms of percentage of subcaudal scales (HpR).

Statistical analyses

Before performing any further analyses, the meristic data were standardized to zero mean and unit standard deviation to avoid potential bias due to difference in the range of measurement among variables; for mensural data, the combination of characters with the highest R-squared score obtained through linear regression was selected as the best log transformation model to make linear relationship with body size. Since there is no gender information from the WB population, the meristics of

the remaining populations (JV and MZ) were first tested using separate one-way analysis of variance (ANOVA) using sex and locality as factors along with Levene's test (Levene 1961) to test the homogeneity of variances; if the assumption of homoscedasticity was violated, Brown-Forsythe test (Brown and Forsythe 1974) was utilised as an alternative approach. For mensurals (TaL, HL, and HW), a two-way analysis of covariance (ANCOVA) was carried out with snout-vent length (SVL) as a covariate. The meristic variables identified without sexual dimorphism were used for multiple comparison among the three populations by pooling sexes using one-way ANOVA using locality as a factor, and post-hoc test was performed with applying Bonferroni correction. In addition, a potential observer difference was screened by repeating measurements on the same specimens and then tested using one-way ANCOVA. The variable characters among lineages identified through the univariate analyses were utilized further for Principal Component Analysis (PCA) to visualize the clustering of the different populations. The correlation matrices between all pairs of the morphological variables, variance explained by each eigenvalue as well as the correlations of each variable to the first two components are explored. Specimens with missing characters were excluded in the multivariate analysis. All statistical analyses and graphical representations were performed using free access statistical packages viz. PAST 4.13 (Hammer et al. 2001) and PSCP v.1.6.2 (GNU Project 2015).

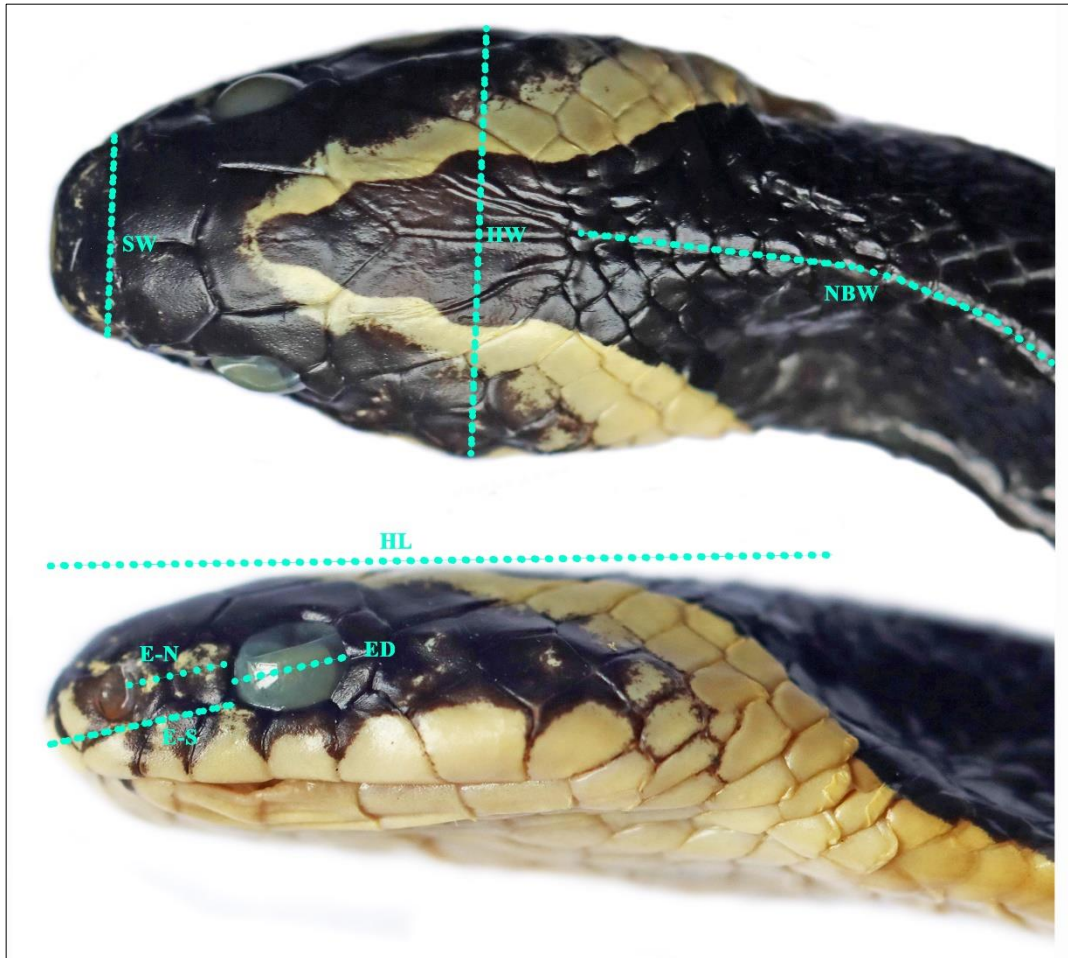


Figure. 1.1. Description of head morphometrics used in this chapter: (top) maximum width of head (HW), width of snout at level of nostril (SW); (below) length of head from tip of snout to angle of jaw (HL), horizontal eye diameter (ED), eye to snout distance (E-S), eye to nostril distance (E-N); and the meristic nuchal band width in scale (NBW) is also depicted.

Results

Phylogenetic relationships

The best partitioning schemes and nucleotide evolutionary models selected for the two types of phylogenetic inferences were provided in (Table 1.3). The first 25% of trees from the BI analysis were discarded as burn-in, and the standard deviation of split frequencies were < 0.005 when analyses terminated. The estimates sample size was < 200 . The inferred concatenated trees from BI and ML analyses were congruent with each other. The BI tree, created using Mr.Bayes v3.2.5 (Ronquist et al. 2012) and further illustrated using iTOL software v5 (Letunic and Bork 2021), is show in Fig. 1.2, with Bayesian posterior probabilities from the BI analysis and UFB values from the ML analysis. The *cytb* dataset consisted of a total of 1047 aligned characters, with 97 variablesites (excluding outgroups).

Molecular phylogenetic based on the concatenated aligned matrix for four mitochondrial genes (*16s*, *cox1*, *cytb*, and *nd4*; 2850 bp in length), recovered a monophyletic clade consisting of three lineages within Asia. Both the phylogenetic analyses and the single-locus-based PTP species delineation approach significantly support these three distinct clades which is describe as (i) *B. fasciatus* from the Sundaic region, especially from Greater Sunda islands which represent the Sundaic lineage (Clade I; Fig. 1.2); (ii) *B. fasciatus* from Indo-Myanmar (Clade II; Fig. 1.2), and (iii) *B. fasciatus* from mainland Sundaland including southern China which represent east Asian lineage (Clade III; Fig. 1.2).

Table 1.3. Information on partitioning schemes and nucleotide substitution models used in the concatenated Bayesian Inference (BI) and Maximum Likelihood (ML) phylogenetic analyses.

Partitions	Sites	BI tree (PartitionFinder)	ML tree (ModelFinder)
I	<i>16s</i> , <i>cytb</i> pos1, <i>nd4</i> pos1	TRN+G	TIM2+F+G4
II	<i>cytb</i> pos2, <i>nd4</i> pos2, <i>cox1</i> pos2	HKY+I	HKY+F+I
III	<i>cytb</i> pos3, <i>nd4</i> pos3, <i>cox1</i> pos3	TRN+G	TIM2+F
IV	<i>cox1</i> pos1	TRNEF	TNe

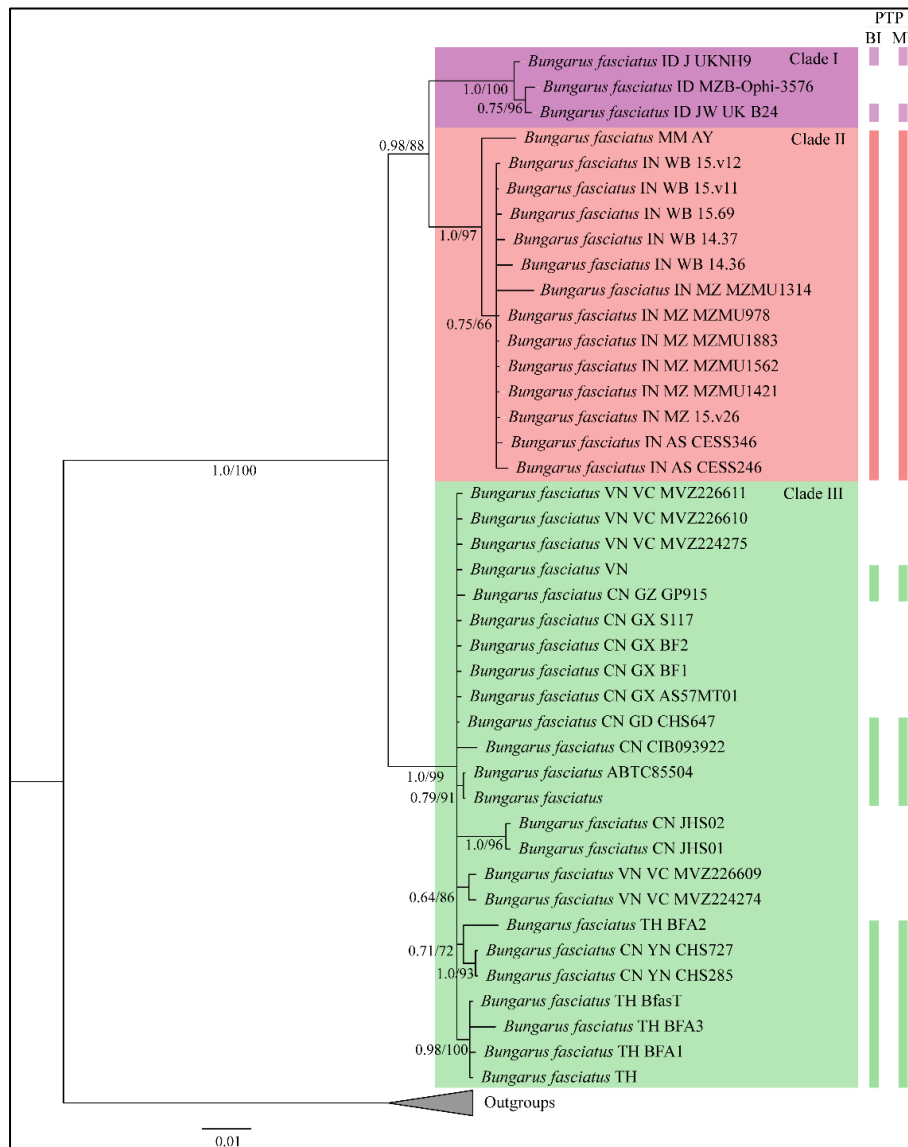


Figure 1.2. Bayesian inference (BI) phylogenetic tree based on concatenated mitochondrial *16s*, *cox1*, *nd4* and *cytb* genes; lineage partitions recovered from CYTB-based PTP analyses are presented besides the BI tree (only the *cytb* dataset was utilized for PTP analyses because it contains more representative samples from the three clades compared to the other genes). Values at each node represent Bayesian posterior probabilities (PP) and Ultrafast Bootstrap (UFB) values from the Maximum Likelihood (ML) analysis (PP/UFB). Abbreviations of country and state/province names are: ID: Indonesia, JW/J: Java; MM: Myanmar, AY: Ayeyarwady; IN: India, WB: West Bengal, MZ: Mizoram, AS: Assam; VN: Vietnam, VC: Vinh Phuc; CN: China, GZ: Guizhou, GX: Guangxi, GD: Guangdong, YN: Yunnan; TH: Thailand.

Genetic divergence

The overall mean intra-specific divergence across all lineages of *B. fasciatus* (uncorrected p-distance) was 3.5%. Furthermore, 0.4% intra-clade genetic divergence was observed within Clade I (between two locations in JV), 0.0%–1.3% within Clade II (between India and Myanmar), and 0.0%–6.5% within Clade III (among China, Vietnam, Thailand, and an unknown locality). The mean inter-clade genetic divergence is 5.0% between Clade I (Sundaic) and Clade II (Indo-Myanmar), 5.3% between Clade II (Indo-Myanmar) and III (east Asia); 5.7% between Clade I (Sundaic) and III (east Asia). Combined *B. fasciatus* (Clades I + II + III) shows the least interspecific genetic divergence (19.5%–19.8%) with *B. candidus*, while inter-specific distances among other species (*B. sindanus*, *B. caeruleus*, *B. candidus*, *B. ceylonicus*, and *B. multicinctus*) range from 3.0% (between *B. candidus* and *B. multicinctus*) to 19.0% (between these two species and *B. ceylonicus*) (Table 1.4). The PCoA ordinations of genetic divergence in the four genes also dictated the discrete clustering of the three distinct clades recovered in the phylogenetic inferences (Fig. 1.3).

Table 1.4. Uncorrected p-distance (pairwise sequence divergence) estimated using the mitochondrial *cytb* (1047 bp) gene of *Bungarus fasciatus* (BF) with *B. caeruleus* (BCR), *B. candidus* (BC), *B. multicinctus* (BM), *B. niger* (BN), *B. ceylonicus* (BCY), *B. sindanus* (BS), and *B. bungaroides* (BB) as outgroups. Abbreviations of country and state/province names are: ID: Indonesia, JW/J: Java; MM: Myanmar, AY: Ayeyarwady; IN: India, WB: West Bengal, MZ: Mizoram, AS: Assam; VN: Vietnam, VC: Vinh Phuc; CN: China, GZ: Guizhou, GX: Guangxi, GD: Guangdong, YN: Yunnan; TH: Thailand.

Species	1	2	3	4	5	6	7	8	9	10	11	12	13	14	15	16	17	
1 BF IN MZ MZMU978																		
2 BF IN MZ MZMU1314	0.000																	
3 BF IN MZ MZMU1421	0.000	0.000																
4 BF IN MZ MZMU1562	0.000	0.000	0.000															
5 BF IN MZ MZMU1883	0.000	0.000	0.000	0.000														
6 BF IN MZ 15.v26	0.000	0.000	0.000	0.000	0.000													
7 BF IN WB 14.36	0.000	0.000	0.000	0.000	0.000	0.000												
8 BF IN WB 15.v11	0.000	0.000	0.000	0.000	0.000	0.000	0.000											
9 BF IN WB 15.v12	0.000	0.000	0.000	0.000	0.000	0.000	0.000	0.000										
10 BF IN WB 15.69	0.000	0.000	0.000	0.000	0.000	0.000	0.000	0.000	0.000									
11 BF IN AS CESS346	0.000	0.000	0.000	0.000	0.000	0.000	0.000	0.000	0.000	0.000								
12 BF IN AS CESS246	0.007	0.007	0.007	0.007	0.007	0.007	0.007	0.007	0.007	0.007	0.007							
13 BF MM AY	0.013	0.013	0.013	0.013	0.013	0.013	0.013	0.013	0.013	0.013	0.013	0.013	0.020					
14 BF	0.033	0.033	0.033	0.033	0.033	0.033	0.033	0.033	0.033	0.033	0.033	0.033	0.039	0.033				
15 BF ABTC85504	0.033	0.033	0.033	0.033	0.033	0.033	0.033	0.033	0.033	0.033	0.033	0.033	0.039	0.033	0.000			
16 BF TH BFA1	0.033	0.033	0.033	0.033	0.033	0.033	0.033	0.033	0.033	0.033	0.033	0.033	0.039	0.033	0.013	0.013		
17 BF TH BFA2	0.039	0.039	0.039	0.039	0.039	0.039	0.039	0.039	0.039	0.039	0.039	0.039	0.046	0.039	0.020	0.020	0.033	
18 BF VN	0.033	0.033	0.033	0.033	0.033	0.033	0.033	0.033	0.033	0.033	0.033	0.033	0.039	0.033	0.000	0.000	0.013	0.020

Table 1.4. Continued.

Species	18	19	20	21	22	23	24	25	26	27	28	29	30	31	32	33	34	35
19 BF CN GD CHS647	0.000																	
20 BF CN CIB093922	0.000	0.000																
21 BF CN GZ GP915	0.000	0.000	0.000															
22 BF CN YN CHS285	0.020	0.020	0.020	0.020														
23 BF CN YN CHS727	0.020	0.020	0.020	0.020	0.000													
24 BF TH BfasT	0.013	0.013	0.013	0.013	0.033	0.033												
25 BF TH	0.013	0.013	0.013	0.013	0.033	0.033	0.000											
26 BF TH BFA3	0.046	0.046	0.046	0.046	0.059	0.059	0.033	0.033										
27 BF ID J UKNH9	0.033	0.033	0.033	0.033	0.052	0.052	0.046	0.046	0.078									
28 BF ID JW UK B24	0.033	0.033	0.033	0.033	0.039	0.039	0.046	0.046	0.078	0.013								
29 BM CN	0.176	0.176	0.176	0.176	0.196	0.196	0.176	0.176	0.190	0.183	0.183							
30 BCR PK UKH7	0.163	0.163	0.163	0.163	0.157	0.157	0.176	0.176	0.196	0.183	0.170	0.144						
31 BN NP	0.144	0.144	0.144	0.144	0.150	0.150	0.131	0.131	0.144	0.137	0.137	0.124	0.183					
32 BB CN XZ KIZ98R0186	0.203	0.203	0.203	0.203	0.209	0.209	0.216	0.216	0.242	0.190	0.183	0.229	0.196	0.209				
33 BC TH	0.163	0.163	0.163	0.163	0.183	0.183	0.163	0.163	0.176	0.170	0.170	0.013	0.137	0.111	0.216			
34 BS PK	0.131	0.131	0.131	0.131	0.150	0.150	0.144	0.144	0.176	0.137	0.137	0.150	0.137	0.163	0.183	0.137		
35 BCR PK PB ZMUVAS11	0.163	0.163	0.163	0.163	0.157	0.157	0.176	0.176	0.196	0.183	0.170	0.144	0.000	0.183	0.196	0.137	0.137	
36 BCY LK RS135	0.170	0.170	0.170	0.170	0.176	0.176	0.183	0.183	0.203	0.190	0.176	0.157	0.085	0.196	0.229	0.150	0.163	0.085

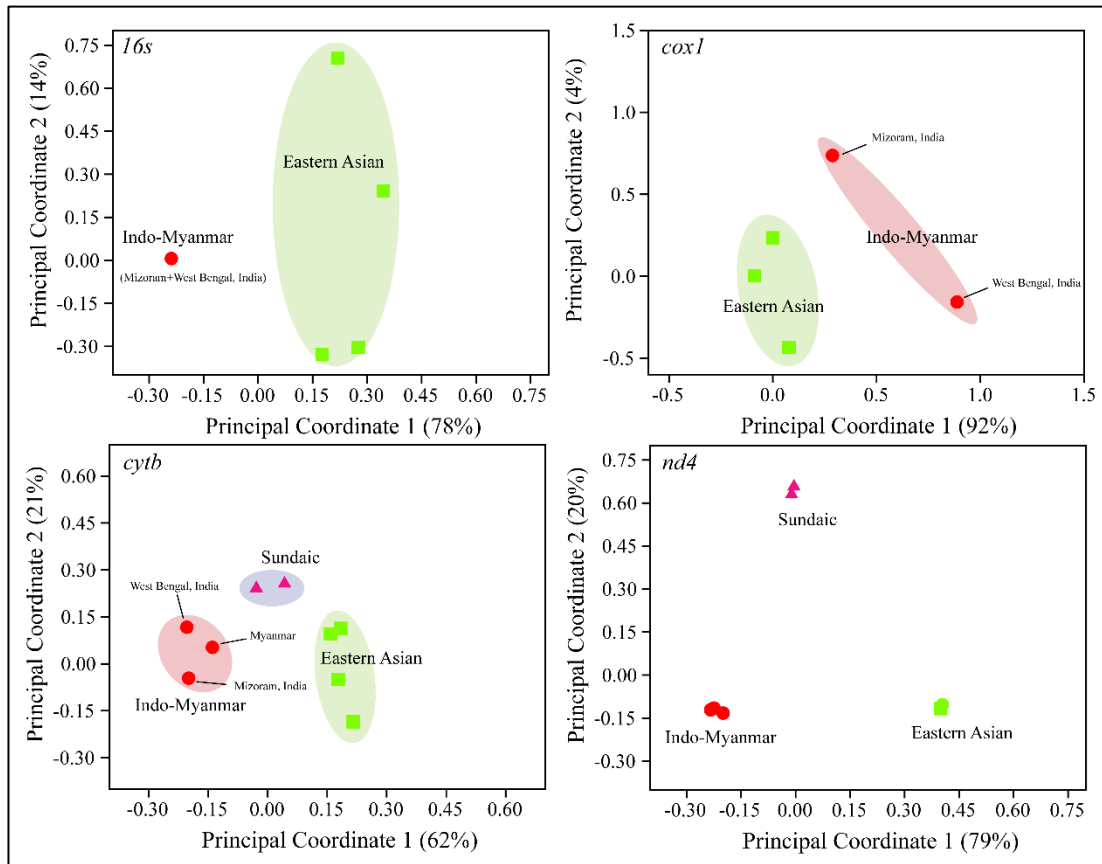


Figure 1.3. Ordination of *Bungarus fasciatus* specimens in a Principal Coordinate Analysis of standardized p-distance of mitochondrial 16S rRNA (*16s*), cytochrome c oxidase subunit 1 (*coxI*), cytochrome b (*cytb*) and NADH dehydrogenase subunit 4 (*nd4*) genes. Red dots represent the samples of Indo-Myanmar lineage and green squares denotes samples of Eastern Asian lineage. A total percentage of variance captured by the first and second Principal coordinates are given in each axis.

Matrilineal haplotype

The gene wise estimation of haplotype diversity (Hd) and reconstruction of haplotype networks was conducted based on the four mitochondrial genes. In *16s*, a total of five distinct haplotypes (Hap) with Hd=0.6952 are recovered: Hap 1 [ABTC85504 (Thailand)], Hap 2 [CIB093922 (China)], Hap 3 [CHS647, CHS285, CHS727 (China)], Hap 4 [CESS246, CESS346 (Assam, India); 15.v26, MZMU1883 (Mizoram, India); 14.36, 15.69, 15.v11, 15.v12 (West Bengal, India)], and Hap 5 [unvouchered (Thailand)]. In *coxI*, a total of five distinct haplotypes with Hd=0.4421

are recovered: Hap 1 [CIB093922, AS57MT01, BF1, BF2, S117, JHS01, JHS02, CHS285, CHS647, CHS727 (China); MVZ224274, MVZ224275, MVZ226609, MVZ226610, MVZ226611 (Vietnam)], Hap 2 [MZMU1883 (Mizoram, India)], Hap 3 [CFSLK-Bf01 (West Bengal, India)], Hap 4 [BFA1, BFA3 (Thailand)], and Hap 5 [BFA2 (Thailand)]. In *cytb*, a total of 10 distinct haplotypes with Hd=0.8042 are recovered: Hap 1 [unvouchered, ABTC85504 (unknown locality); CHS647, CIB093922, GP915 (China); unvouchered (Vietnam)], Hap 2 [unvouchered, BFA1, BfasT (Thailand)], Hap 3 [BFA2 (Thailand)], Hap 4 [BFA3 (Thailand)], Hap 5 [CHS285, CHS727 (China)], Hap 6 [B24 (Java, Indonesia)], Hap 7 [CESS246 (Assam, India)], Hap 8 [CESS346 (Assam, India); 15.v26, MZMU978, MZMU1314, MZMU1421, MZMU1562, MZMU1883, (Mizoram, India); 14.36, 15.69, 15.v11, 15.v12 (West Bengal, India)], Hap 9 [unvouchered (Myanmar)], and Hap 10 [UKNH9 (Java, Indonesia)]. In *nd4*, a total of 10 distinct haplotypes with Hd=0.9487 are recovered: Hap 1 [unvouchered, ABTC85504 (unknown locality)], Hap 2 [CIB093922 (China)], Hap 3 [B24 (Java, Indonesia)], Hap 4 [Ophi-3576 (Java, Indonesia)], Hap 5 [CESS246 (Assam, India)], Hap 6 [15.v26 (Mizoram, India)], Hap 7 [14.36 (West Bengal, India)], Hap 8 [14.37, 15.v11, 15.v12 (West Bengal, India)], Hap 9 [15.69 (West Bengal, India)], and Hap 10 [unvouchered (Thailand)]. In *I6s*, Indo-Myanmar lineage accommodates in a single haplotype, while Eastern Asian lineage dispersed into four distinct haplotypes. In *cox1*, the Indo-Myanmar, Eastern Asian lineages dispersed into two and three distinct haplotypes, respectively. In *cytb*, the Indo-Myanmar, Eastern Asian, and Sundaic lineages dispersed into three, five, and two haplotypes, respectively. In *nd4*, the Indo-Myanmar, Eastern Asian, and Sundaic lineages dispersed into five, three, and two distinct haplotypes, respectively (Fig. 1.4).

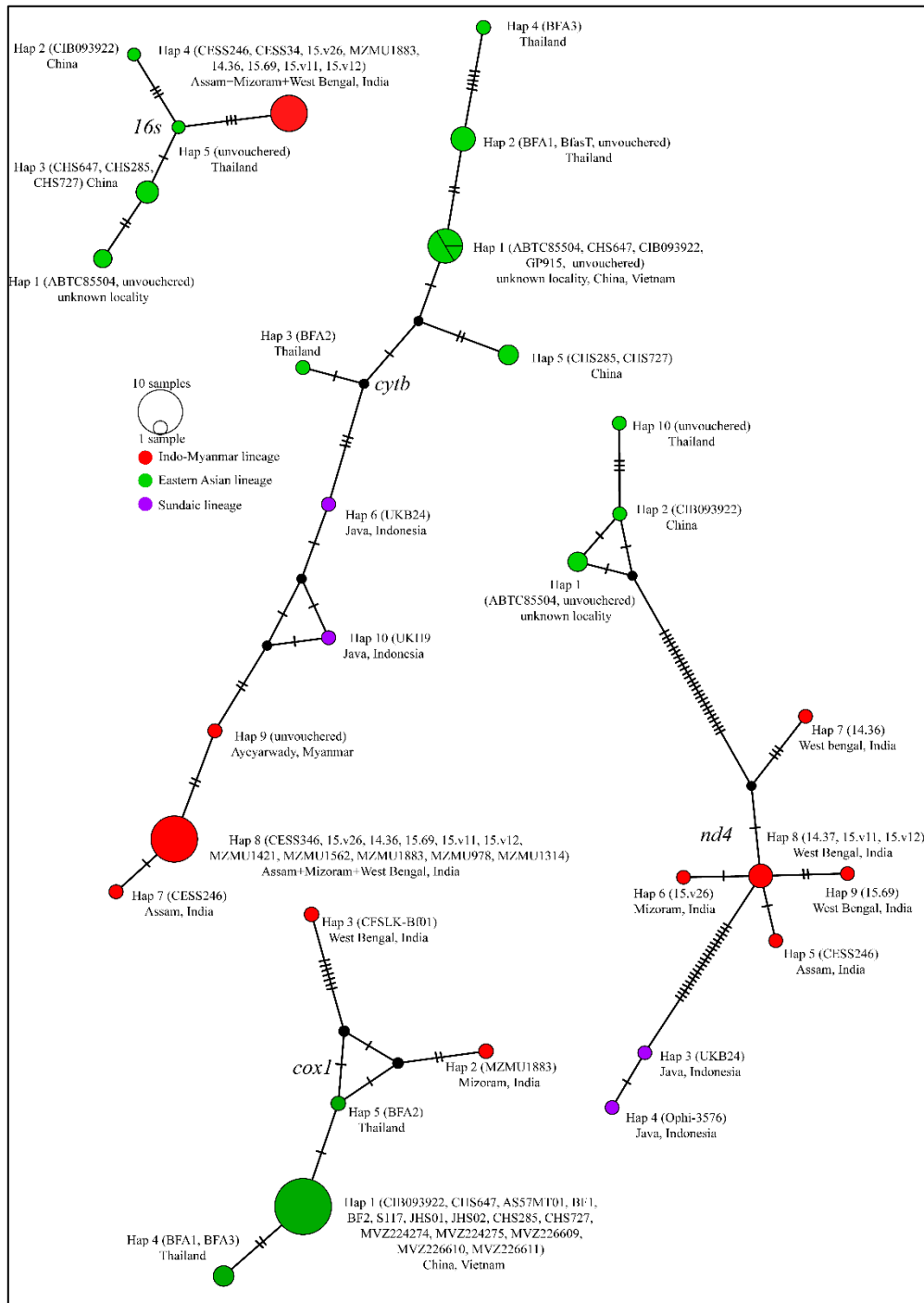


Figure 1.4. Mitochondrial gene-based (*16s*, *cox1*, *cytb* and *nd4*) Median-joining haplotype network among populations of *Bungarus faciatus*. The number of samples present in each haplotype corresponds to the relative size of the circles. Hatch marks at the branch represent mutational steps found between haplotypes, and a black dot at the branch is an inferred median.

Morphometric analyses

Analyses on the morphological characters were performed to identify taxonomically informative features among the examined populations of MZ (n=15), WB (n=8), and JV (n=15) (Table 1.5). Only the mensurals such as TaL ($p<0.001$), HW ($p<0.05$) and HL ($p<0.05$) showed significant dimorphism between males and females within JV and MZ populations. For meristic characters, inter-population differences were statistically significant ($p<0.001$) for Ve (MZ vs. JV), BB, BT, and NBW (the latter three characters are tested among three populations), all of which showed a higher number in the MZ population; for mensural characters, inter-population differences were also statistically significant for TaL ($p<0.05$) and HL ($p<0.001$) (Table 1.6). Post-hoc tests conducted among the three populations for BB, BT, and NBW showed that, except for BT between MZ and WB populations ($p>0.05$), significant differences are seen for all characters: BB ($p<0.001$ across all the populations), NBW ($p<0.001$ in MZ vs. WB, and JV vs. WB; $p<0.05$ in MZ vs. JV), and BT ($p<0.001$ in MZ vs. JV; $p<0.01$ in JV vs. WB). Comparison was also made based on the identified variable meristic characters among the three populations using a PCA. The correlation matrix showed weak correlations between pairs of variables ($r<0.7$) (Table 1.7); thus, all variables were retained for this analysis. The first two components accounted for 84% of the total variation of the data, with PC1, PC2 and PC3 representing 64%, 20% and 11%, respectively. The loadings of all variables are high on the first axis, while only Ve loads considerably highly on the second axis, with Ve having less effect on PC1 than PC2. The representation of the first two components depicts substantial separation of the Javanese and the Indian populations on the first axis (PC1), and marginal separation of the WB and MZ populations on the second axis (PC2) (Table 1.8; Fig. 1.5). Given that the samples from the three populations (WB, MZ and JV) were examined by different recorders, we also tested for potential recorder bias between the East Indian and northeast Indian specimens; however, no significant differences were seen after re-examination of the same specimens ($p>0.05$).

Table 1.5. Morphometry (in mm) and scalation data of *Bungarus fasciatus* examined from Mizoram, India. Damaged body parts are indicated in asterisk (*), and the character that is unable to determined are shown as octothorp (#).

Characters	MZMU 933	MZMU 934	MZMU 1314	MZMU 1319	MZMU 1320	MZMU 1321	MZMU 1417	MZMU 1421	MZMU 1550	MZMU 1562	MZMU 1561	MZMU 1548	MZMU 1572	MZMU 1883	MZMU 2481
Sex	M	F	M	F	M	F	M	M	F	F	F	F	F	M	F
ED	4.20	2.9	2.00	3.56	4.14	4.80	5.10	5.18	2.92	3.19	3.10	4.40	4.29	2.72	3.18
E-N	5.70	*	3.44	4.20	5.76	5.66	6.04	6.36	3.26	4.10	3.24	4.44	4.48	5.02	4.52
E-S	7.4	*	4.8	6.62	9.14	8.04	7.98	7.91	4.63	5.47	4.85	6.64	6.14	6.12	6.78
SW	7.90	*	4.24	7.30	9.00	8.00	8.62	8.21	5.65	5.61	5.53	9.06	8.26	6.64	9.48
HL	26.60	*	12.80	18.40	22.80	22.14	26.46	24.54	15.74	16.68	16.49	23.54	25.54	16.42	29.68
HW	22.10	10.4	10.66	15.20	19.20	20.40	22.46	20.12	12.46	12.80	13.04	19.70	18.34	12.18	22.76
SVL	1075	914	444	862	1019	935	1093	1220	700	835	767	1120	1180	470	1186
TaL	123	96	47	100	116	103	131	133	76	82	89	118	119	56	100*
TaL/TL	0.103	0.095	0.096	0.104	0.102	0.099	0.107	0.098	0.098	0.089	0.104	0.095	0.092	0.106	*
Ve	227	229	228	229	226	230	222	227	224	231	228	230	231	226	230
Sc	35	33	36	34	35	32	36	36	33	33	36	34	35	37	30*
DSR	15:15:15	15:15:15	15:15:15	15:15:15	15:15:15	15:15:15	15:15:15	15:15:15	15:15:15	15:15:15	15:15:15	15:15:15	15:15:15	15:15:15	15:15:15
ILSI	4 th -6 th	4 th -6 th	4 th -6 th	4 th -6 th	4 th -6 th	4 th -6 th	4 th -6 th	4 th -6 th	4 th -6 th	4 th -6 th	4 th -6 th	4 th -6 th	4 th -6 th	4 th -6 th	4 th -6 th
SL	7/7	7/7	7/7	7/7	7/7	7/7	7/7	7/7	7/7	7/7	7/7	7/7	7/7	7/7	7/7
SLe	3-4 th	3-4 th	3 rd -4 th	3 rd -4 th	3 rd -4 th	3 rd -4 th	3 rd -4 th	3 rd -4 th	3 rd -4 th	3 rd -4 th	3 rd -4 th	3 rd -4 th	3 rd -4 th	3 rd -4 th	3 rd -4 th
IL	7/7	7/7	7/7	7/7	7/7	7/7	7/7	7/7	7/7	7/7	7/7	7/7	7/7	7/7	7/7
Tem	1+2/1+2	1+2/1+2	1+2/1+2	1+2/1+2	1+2/1+ 2	1+2/2+2	1+2/1+2	1+2/1+2	1+2/1+ 2	1+2/1+2	1+2/1+ 2	1+2/1+2	1+2/1+2	1+2/1+2	1+2/1+2
PoO	2/2	2/2	2/2	2/2	2/2	3/2	2/2	2/2	2/2	2/2	2/2	2/2	2/2	2/2	2/2
PrO	1/1	1/1	1/1	1/1	1/1	1/1	1/1	1/1	1/1	1/1	1/1	1/1	1/1	1/1	1/1
BB	26	22	27	27	25	26	23	23	25	26	25	23	25	22	26
BT	5	4	5	5	5	4	5	5	5	4	4	4	4	5	4
NBW	18	18	18	18	18	19	*	19	17	15	15	20	19	18	18
HpR (approx.)	7 Sc (22.50) 20%		#		7 Sc (31.60) 20%		7 Sc (28.20) 19.4%	4 Sc (20.10) 11.1%						#	

Table 1.6. Evaluation on the meristic and mensural characters measured for 38 *Bungarus fasciatus* individuals from Java (JV), Mizoram (MZ), and West Bengal (WB), including mean, standard deviation, minimum and maximum values. The characters tested for inter-population difference across the three populations are indicated by asterisk (*). Characters tested using the alternative Brown-Forsythe test was indicated by octothorp (#). Significant values at the alpha level of 0.05 are given in bold.

Characters	Sex	Java (n=15)		Mizoram (n=15)		West Bengal (n=8) unsexed		Sexual dimorphism		Inter-population difference	
		Mean±SD	Range	Mean±SD	Range	Mean±SD	Range				
Ve	Male	205.44±3.43	199–210	226±2.10	222–228	217.63±3.12	212–222	$F_{1,28} = 1.35$	$p = 0.256$	$F_{1,28} = 469.80$	$p < \mathbf{0.001}$
	Female	206.83±1.94	205–210	229.11±2.15	224–231						
Sc	Male	34.43±0.98	33–36	35.83±0.75	35–37	34.63±1.49	31–36	$F_{1,25} = 2.44$	$p = 0.131$	$F_{1,25} = 1.30$	$p = 0.266$
	Female	31.17±1.60	30–34	33.75±1.28	32–36						
BB	Male	22.67±1.12	21–25	24.33±1.97	22–27	28.38±1.73	26–31	$F_{1,28} = 0.44$	$p = 0.511$	$F_{2,35} = 39.78^*$	$p < \mathbf{0.001}^*$
	Female	21.83±1.17	20–23	25.00±1.58	23–27						
BT	Male	3.22±0.67	2–4	5.00±0.00	5	5.25±1.09	4–7	$F_{1,21} = 0.12^\#$	$p = 0.728^\#$	$F_{2,12} = 17.86^{*\#}$	$p < \mathbf{0.001}^{*\#}$
	Female	3.17±0.41	3–4	4.22±0.44	4–5						
NBW	Male	19.00±1.00	18–20	18.20±0.45	18–19	15.63±1.11	14–17	$F_{1,27} = 0.40$	$p = 0.533$	$F_{2,34} = 22.16^*$	$p < \mathbf{0.001}^*$
	Female	19.00±0.63	18–20	17.67±1.73	15–20						
TaL	Male	120.74±20.01	90–145	101±38.92	47–133	-	-	$F_{1,24} = 18.96$	$p < \mathbf{0.001}$	$F_{1,24} = 6.01$	$p = \mathbf{0.022}$
	Female	107.86±23.43	85–145	97.88±15.56	76–119						
HL	Male	35.06±4.97	27.10–40.90	21.60±5.71	12.80–26.60	-	-	$F_{1,24} = 4.37$	$p = \mathbf{0.047}$	$F_{1,24} = 79.38$	$p < \mathbf{0.001}$
	Female	34.81±6.19	25.90–44.50	21.03±5.03	15.74–29.68						
HW	Male	20.88±4.03	13.80– 25.70	17.79±5.10	12.18–22.46	-	-	$F_{1,25} = 4.33$	$p = \mathbf{0.048}$	$F_{1,25} = 0.97$	$p = 0.334$
	Female	20.70±3.13	16.40– 26.20	16.12±4.30	10.40–22.76						

Table 1.7. Correlation matrix across the standardized variables utilized for PCA ordination.

Correlations	Zscore(BB)	Zscore(BT)	Zscore(NBW)	Zscore(Ve)
Zscore(BB)	1.000	0.698	-0.711	0.430
Zscore(BT)	0.698	1.000	-0.498	0.491
Zscore(NBW)	-0.711	-0.498	1.000	-0.268
Zscore(Ve)	0.430	0.491	-0.268	1.000

Table 1.8. Information on Principal Component Analysis (PCA) and loadings for *Bungarus fasciatus* in east India, northeastern India and Great Sunda Islands. Principal components (PC) 1 and 2 collectively explained 84% of variation.

Variables	PC1 (64%)	PC2 (20%)	PC3 (11%)
BB	0.906	-0.195	0.04
BT	0.85	0.109	0.48
NBW	-0.786	0.475	0.332
Ve	0.645	0.709	-0.285

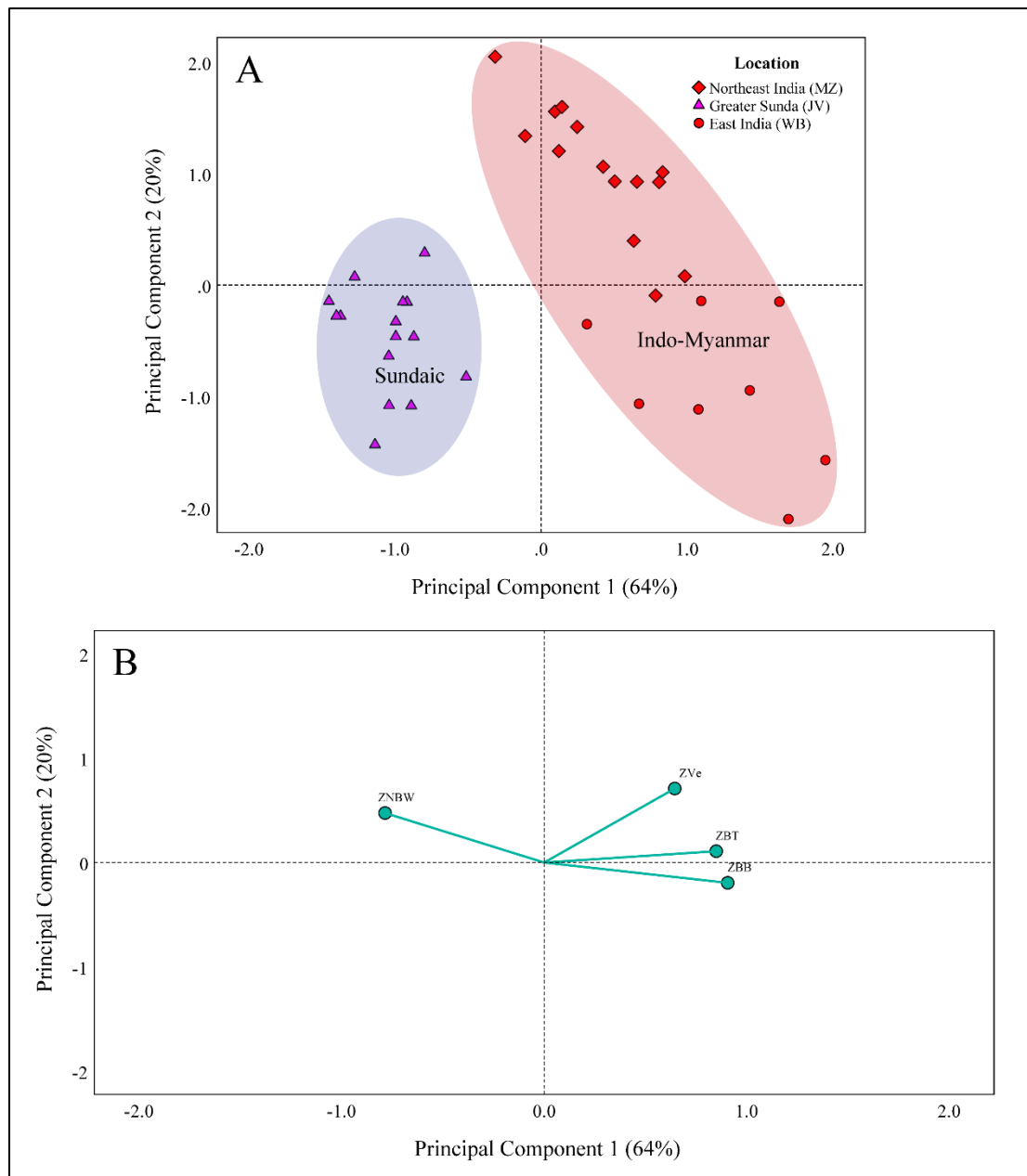


Figure 1.5. (A) Ordination of *Bungarus fasciatus* populations from Mizoram, West Bengal and Java along the first two principal components based on a PCA of the characters Ve, BB, BT, and NBW. Total variance associated with the PC1 and PC2 are 64% and 20%, respectively. (B) PCA loading plot showing the distribution of the analysed variables along the first two principal components.

Taxonomy

The examined specimens of *B. fasciatus* from India are morphologically distinguishable from the Sundaic population (Table 1.9). Based on the present study, the existence of at least three different taxonomic entities was postulated within the nomen *B. fasciatus*, and also confirm that populations in eastern India (e.g. Odisha, West Bengal, etc.) and northeastern India (e.g. Mizoram, Assam, etc.) are conspecific. Based on the original description of *Pseudoboa fasciata*, minimum three specimens were available or referable to Schneider (1801); hence syntypes. Among these syntypes two specimens (ZMB 2771, 2772) have been deposited at ZMB from the collection of Marcus Bloch (fide Bauer 2021). In addition, one of syntypes was depicted in Russell (1796) (page 3, plate 3) as the “Bungarum Pamah”, an adult from “Mansoor Cottah” (now Gopalpur, Odisha (Orissa), India), specimen is now lost (fide Bauer (2015)). So far, the only existing name-bearing type specimens are the two syntypes in the collection of Berlin Zoological Museum (ZMB 2771–72) originating from “Indien” (=India) fide ZMB catalogue (Wallach et al. 2014). It was affirmed that the specimen used by Russell (1796) for his illustration is the same specimen (syntype) housed in the ZMB, thus, the type locality adhered to that given by Russell (1796). Therefore, the Indo-Myanmar population (Clade II) was postulated as *B. fasciatus* sensu stricto, while considering the populations from Sundaic region, especially from Greater Sunda Islands (Clade I) and mainland Sundaland including southern China (Clade III) as *B. fasciatus* sensu lato. Consequently, *B. fasciatus* sensu stricto was redescribed in this chapter, including hemipenis morphology, based on MZ population, from where a large number of samples are available.

***Bungarus fasciatus* (Schneider, 1801) sensu stricto**

(Figs. 1.6–1.8; 1.11A–C)

[English: Banded krait; Bengali: Sankhamuti/Sankhini/Chamorkasa; Mizo: Chawnglei/Tiangsir]

Pseudoboa fasciata Schneider, 1801

Bungarus annularis Daudin, 1803.

Bungarus fasciatus bifasciatus Mell, 1929.

Bungarus fasciatus insularis Mell, 1930.

Redescription of *B. fasciatus sensu stricto*. Based on the overall examined MZ materials with combined sexes, adults SVL 444.0–1220.0 mm, tail length 47.0–133.0 mm; head elongate (HL 2.0–3.5% of SVL), wide (HW 71.8–92.1% of HL), slightly flattened, indistinct from neck; snout elongate (ES 22.8–40.1% of HL), moderate, flat in dorsal view, rounded in lateral profile, rather depressed. Rostral shield large, flat, slightly visible from above, pointed posteriorly; interorbital width broad; internasals subtriangular; nostrils rather large, nasals large, divided, and elongated, in anterior contact with rostral, and internasal and prefrontal dorsally, 1st and 2nd supralabial ventrally, preocular posteriorly; no loreal; prefrontal rather large, broader than long, and pentagonal; frontal large, hexagonal, short, slightly longer than width; supraoculars narrow, elongate, subrectangular, posteriorly wider; parietals large, elongate, butterfly wing-like in shape, bordered by supraoculars, frontal, upper postocular anteriorly, anterior and upper posterior temporals, and five or six nuchal scales posteriorly; one preocular, vertically slightly elongated, hexagonal, in contact with prefrontal and posterior nasal anteriorly, supraocular dorsally, and 2nd and 3rd supralabials ventrally; eye moderate (ED 10.7–21.7% of HL), round, about half of the size of snout length (ED 41.7–69.9% of ES), pupil rounded; two PoO, subequal or upper one larger, pentagonal, upper postocular in broad contact with supraocular, parietal and anterior temporal, lower PoO in contact with anterior Tem and 5th SL; Tem 1+2, large, slightly elongated, subrectangular or pentagonal; anterior Tem larger than the posterior, in contact with parietal and both PoO dorsally, and 5th and 6th SL ventrally; lower posterior Tem in contact with 6th and 7th SL ventrally. SL seven (on both sides), 5th–7th largest in size; 1st SL in contact with rostral anteriorly, nasals dorsally, 2nd with posterior nasal and preocular dorsally, 3rd with preocular and orbit dorsally, 4th with orbit; 5th with orbit, lower PoO, and anterior Tem dorsally, and 6th with anterior and lower posterior Tem dorsally, 7th with lower posterior Tem dorsally and scales of the neck posteriorly.

Mental large, triangular, blunt posteriorly; first IL pair larger than mental plate and in broad contact with each other, in contact with anterior chin shields

posteriorly; seven IL, 1st–4th in contact with anterior chin shields, 4th IL largest in size in contact with both anterior and posterior chin shields; 4th–7th IL in contact with gular scales; two larger anterior chin shields, and two slightly smaller posterior chin shields; anterior chin shields in broad contact between them; posterior chin shields bordered posteriorly by seven gular scales.

Body robust, elongate and subcylindrical; DSR in 15 midbody rows, all smooth and pointed posteriorly; 222–228 Ve in males and 224–231 in females; cloacal plate divided. Tail comparatively short, TaL 8.9–10.4% of total length in males and 13.5–17.1% of total length in males, robust and thick; Sc 35–37 in males and 32–36 in females, divided.

Coloration. In preservative, dorsum and venter white or yellow; 22–27 black cross bands along the body and 4 or 6 on the tail; cross bands complete laterally, and reaching the Ve except the nuchal band; the bands on the tail distinct; the nuchal band on the nape anteriorly inverted V-shaped covering 15–20 vertebral scales; nuchal band starts from mid frontal; snout, anterior head, and lateral head black making remaining the white dorsal color an inverted V-shaped marking; first black band on the body covering 6 or 7 vertebral scales; inter-band width covers with 3–5 vertebral scales; lower parts of the SL white; ventral head white until the first black band; tail tip black dorsally, white ventrally (Fig. 1.6).

In life (Fig. 1.7A), same color as in preservative, but the white body color may vary from white, cream, pale yellow to bright yellow. One juvenile with cream and black body bands was encountered in Saikhawthlir, MZ (Fig. 1.7B), but the snake escaped before recording morphological data.

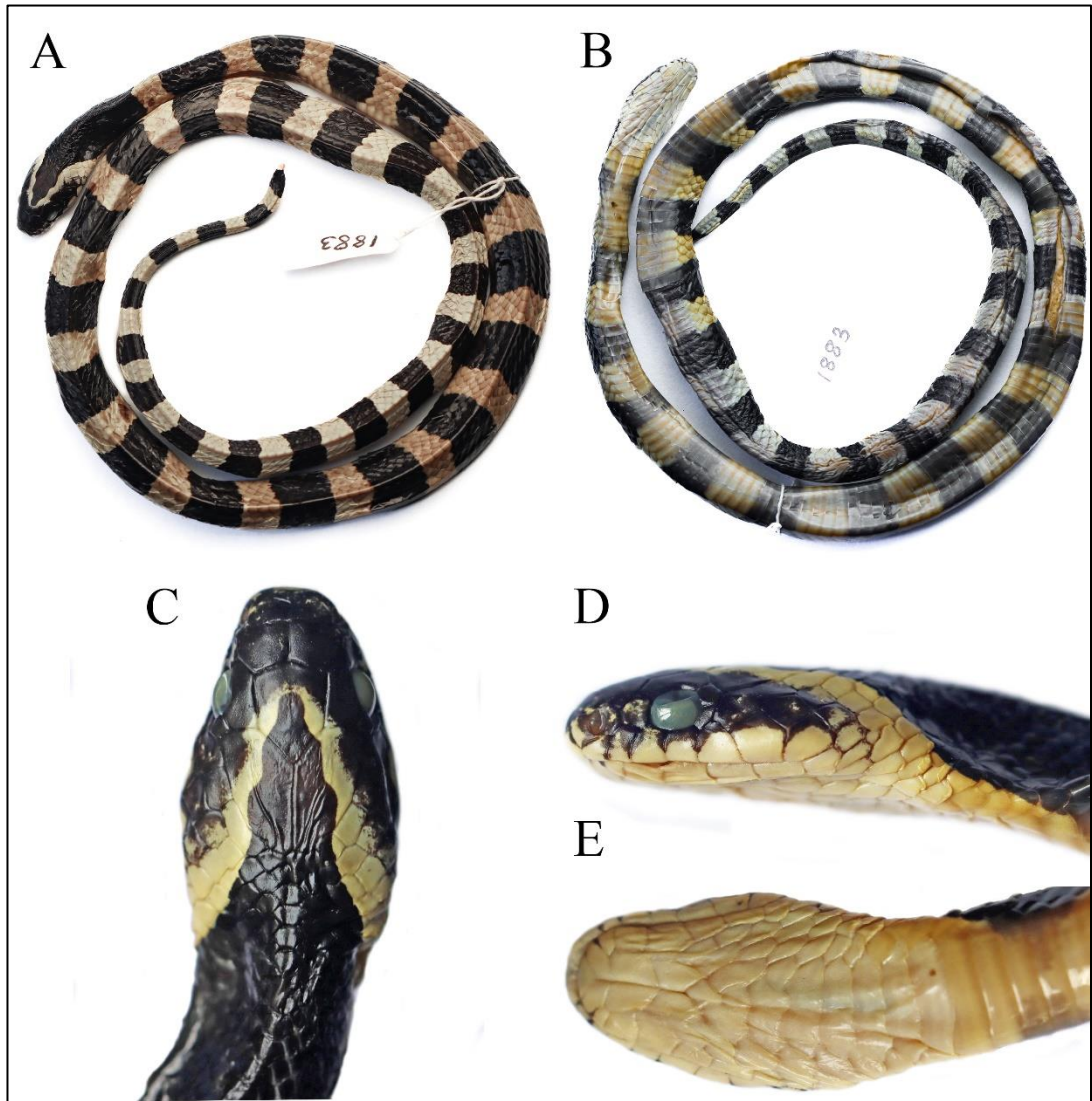


Figure 1.6. *Bungarus fasciatus* sensu stricto (MZMU1883) from Northeast India: (A) dorsal view of full body, (B) ventral view of full body, (C) dorsal view of head, (D) lateral view of the left side of head, and (E) ventral view of head.

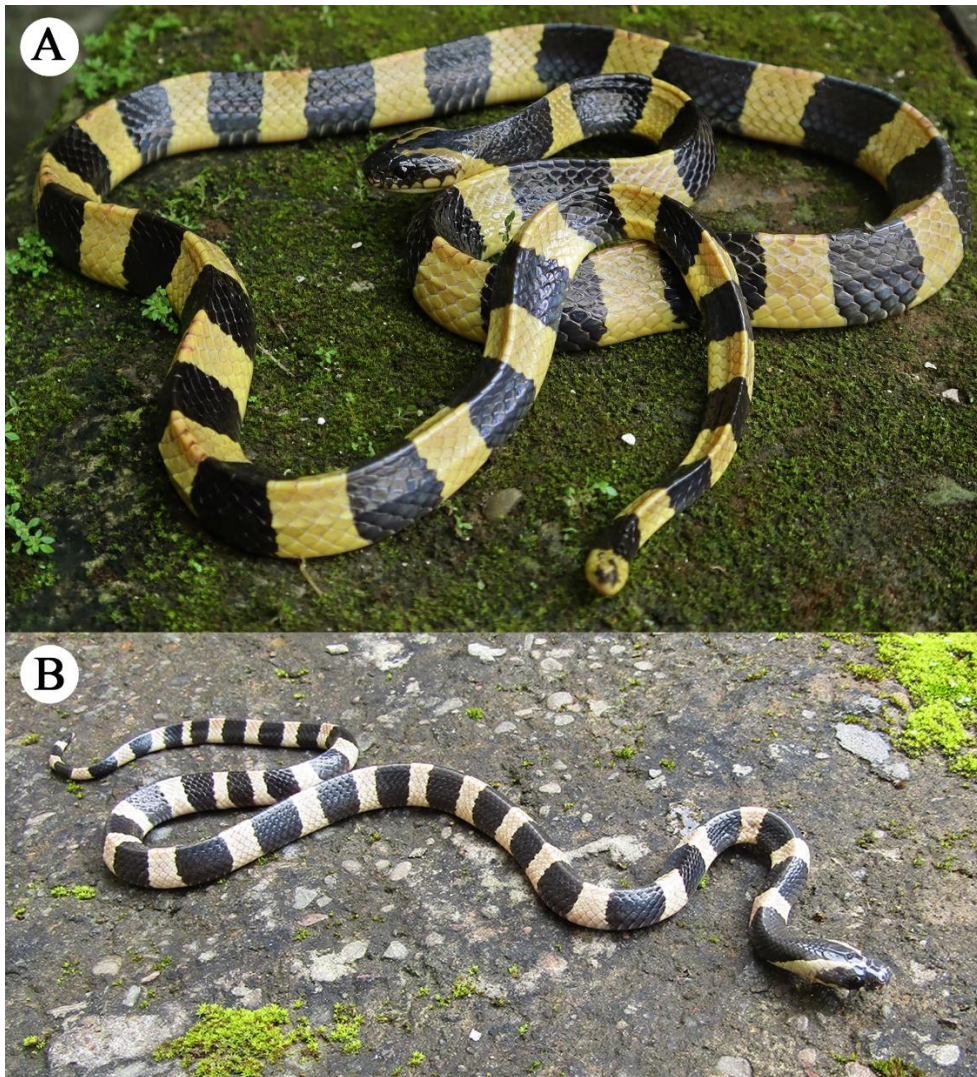


Figure 1.7. Live individuals of *Bungarus fasciatus* sensu stricto (A) from Khamrang village, Mizoram, India, and (B) a juvenile with creamish dorsum coloration from Saikhawthlir village, Mizoram, India.

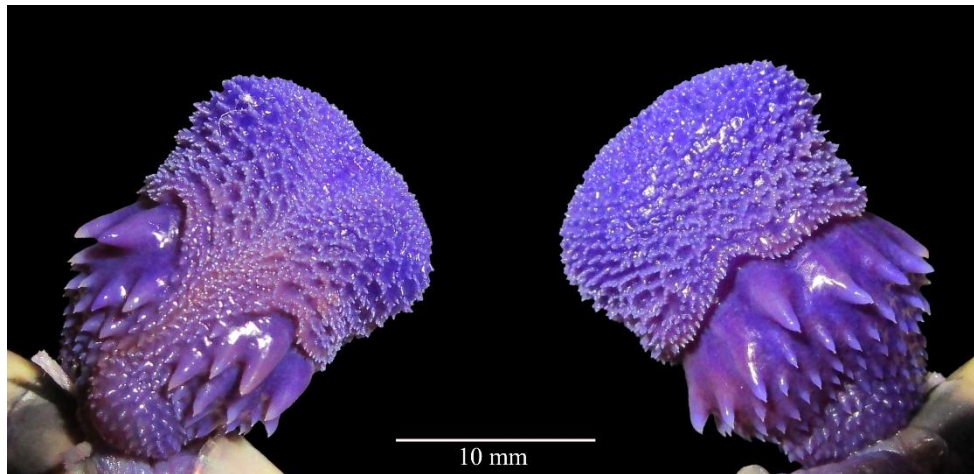


Figure 1.8. Sulcal (left) and asulcal (right) views of the right hemipenis of *Bungarus fasciatus* sensu stricto (MZMU2935) from Mizoram, India. The organ is single and subcylindrical, relatively short, robust, and capitate with a complex ornamentation of retiform ridges.

Variation. Except the anomalous specimen (MZMU1321) which had three postoculars on left and two on right, and temporals 1 + 2 on the left and 2 + 2 on the right, all other meristic and morphometric characters obtained so far did not show any significant variation between the examined populations, and also correspond to the conventional taxonomical characters provided in previously published literature (Leviton et al. 2003; Smith 1911; Whitaker and Captain 2008).

Hemipenis. Based on MZMU2935, the organ is single and subcylindrical, relatively short, robust, and capitate; inverted hemipenis extends to 4th–7th subcaudal level (i.e. 11.1–20% from the total number of Sc); sulcus spermaticus bifurcate below the crotch, shallow and centripetal; apical lobe less evident with only slight apical flaring; calyculate organ with a complex ornamentation of retiform ridges, papillate flounces, and spines; spines on the upper basal areas enlarged and decreasing the size towards the proximal portion; apical region sharply separated from the basal portion by a well-defined demarcation, so the apex is free and the apical part of the hemipenis is richly capitate (Fig. 1.8).

Table 1.9. Some comparative morphological data of *Bungarus fasciatus* sensu lato in each biogeographic region, based on this study and published data.

Character	Population / clade		
	Indo-Myanmar (n=23)	East Asia (n=11)	Greater Sunda (n=15)
Ve	200–234	217–237	199–210
Sc	23–39	33–41	30–36
NBW	22–31	19–21	20–25
BT	4–7	?	2–4
BB	14–20	?	18–20
Background body colour	Yellow / cream	Yellow	Yellow / cream
Source	Smith (1943) This study	Yang and Rao (2008); Chen et al. (2021); Leviton et al. (2003)	Thasun Amarasinghe (Unpubl. data)

Distribution

The distributional records for *B. fasciatus* sensu stricto are provided herein based on 47 localities from Mizoram, India. Out of which a total of 40 localities are based on Lalbiakzuala (2019) and the remaining seven localities represent the new records documented in this work (Table 1.10; Fig. 1.9). The new localities are confined within three Districts viz. Aizawl (Sateek, Luangmual and Thingsulthliah), Kolasib (Vairengte, Bukpui and North Hlimen), and Lunglei (New Khawlek) at the elevational range of 240–1,020 m a.s.l. So far, the lowest elevation record for the species is 4 m a.s.l. at Chitrasali in Hooghly District, WB (Vishal Santra pers. obs.). Based on the published records, the elevation range was between 40 and 2,300 m a.s.l. (Ahmed et al. 2009; Knierim et al. 2019). Additionally, an estimated distribution range of the species depicting the estimated range for the different lineages was plotted (Fig. 1.10) following WHO's range estimation for *B. fasciatus* (World Health Organization 2022).

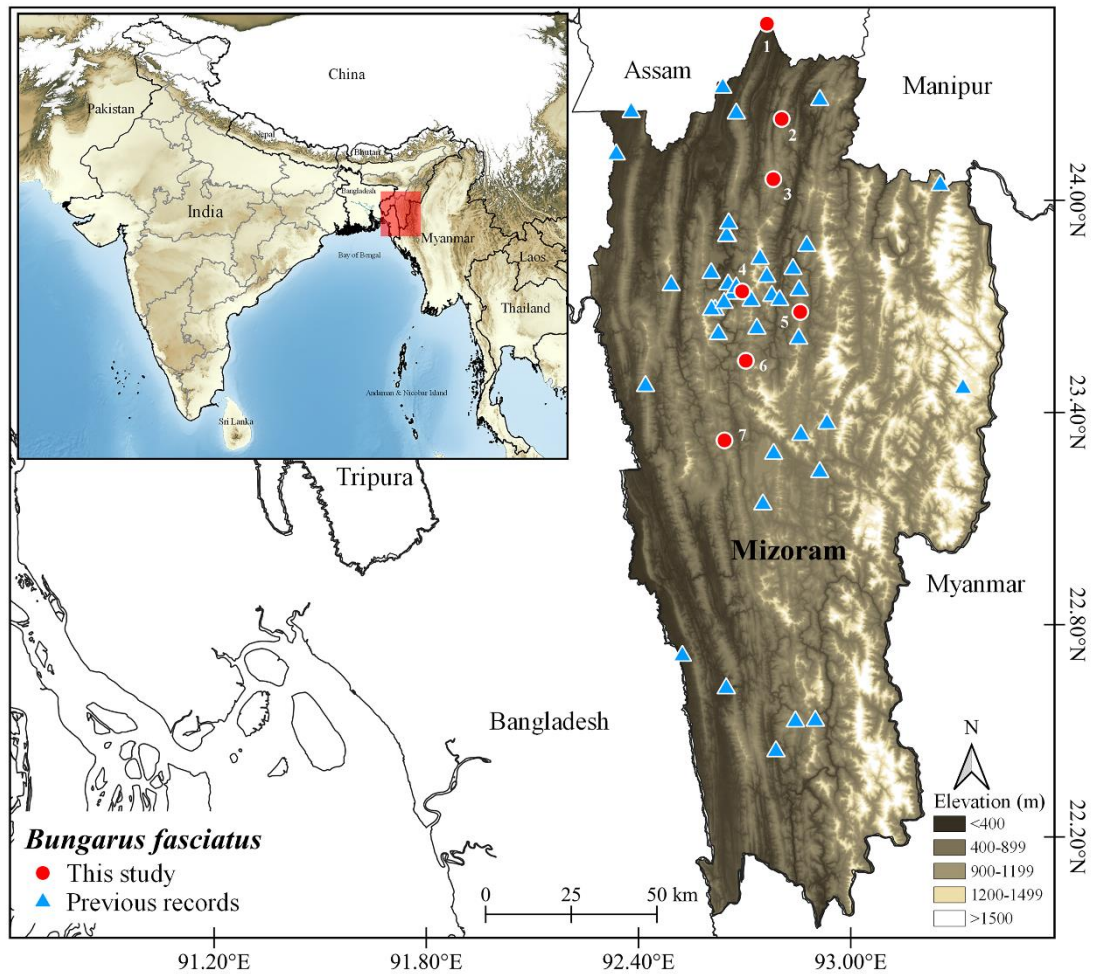


Figure 1.9. Digital elevation map showing the distributional records of *Bungarus fasciatus* in Mizoram. The previous records fide Lalbiakzuala (2019) are given in blue triangles, and the new records from this work are given in red circles: 1. Vairengte; 2. Bukpui; 3. North Hlimen; 4. Luangmual; 5. Thingsulthlah; 6. Sateek; 7. New Khawlek.

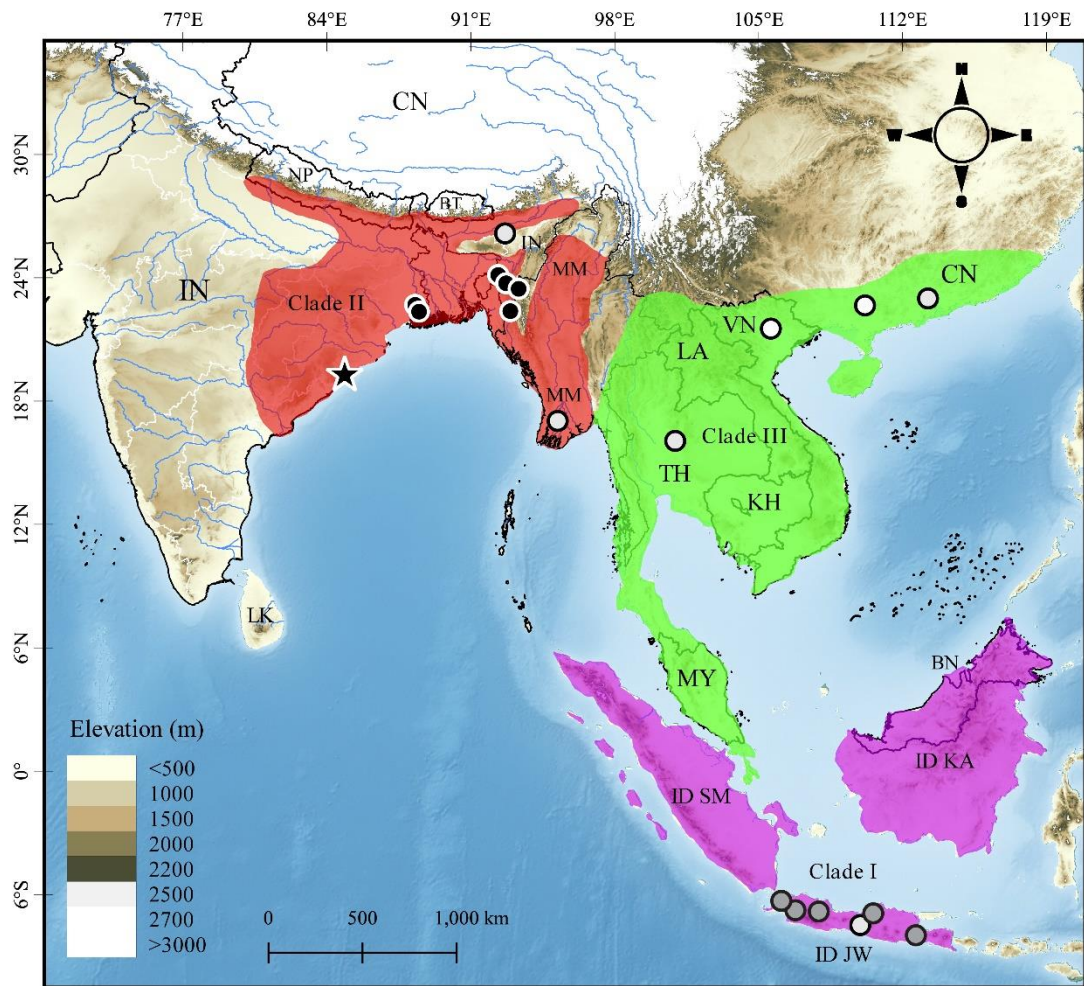


Figure 1.10. Map showing the distribution range of *Bungarus fasciatus* sensu lato, based on the latest species map provided by the World Health Organization (2022); the coloration corresponds to the three distinct evolutionary lineages recovered in the phylogenetic analyses. The type locality of *Bungarus fasciatus* sensu stricto is indicated by a black star. Localities of specimens used in the morphological and DNA analyses are indicated by black filled circles, while locations for the specimens used for only DNA analysis and morphology only are shown in white and grey circles, respectively. Abbreviations for countries are: IN: India, NP: Nepal, BT: Bhutan, BD: Bangladesh, LK: Sri Lanka, CN: China, MM: Myanmar, LA: Laos, TH: Thailand, VN: Vietnam, KH: Cambodia, MY: Malaysia, BN: Brunei Darussalam, ID: Indonesia (KA: Kalimantan, SM: Sumatra, JW: Java).

Table 1.10. Detailed locality records of *Bungarus fasciatus* sensu stricto specimens based on the combined data of this study and Lalbiakzuala (2019) in Mizoram, India. New records from this work are indicated with bold.

Sl. No.	Locality	District	Geo-coordinates	Elevation
1	Ailawng	Mamit	23.690138°N; 92.617108°E	1172 m
2	Buhchang	Kolasib	24.318141°N; 92.638588°E	49 m
3	Champhai Jail veng	Champhai	23.468161°N; 93.317772°E	1426 m
4	Chawngte	Lawngtlai	22.620006°N; 92.648507°E	81 m
5	CTI Sesawng	Aizawl	23.745833°N; 92.854751°E	814 m
6	Dapchhuah	Mamit	23.759784°N; 92.492873°E	447 m
7	Durlui A	Aizawl	23.899000°N; 92.652129°E	95 m
8	Durlui B	Aizawl	23.899191°N; 92.649556°E	88 m
9	Khamrang	Kolasib	23.934774°N; 92.655455°E	232 m
10	Khawrihnim	Mamit	23.621382°N; 92.626148°E	1057 m
11	Khawruhlian	Aizawl	23.870982°N; 92.876104°E	924 m
12	Kolasib Saidan	Kolasib	24.245402°N; 92.676890°E	613 m
13	Lengte road	Mamit	23.794119°N; 92.605881°E	296 m
14	Lawngtlai	Lawngtlai	22.528505°N; 92.900511°E	721 m
15	Mampui	Lawngtlai	22.526439°N; 92.844184°E	1056 m
16	Mission veng	Aizawl	23.716264°N; 92.718944°E	1084 m
17	Mualmam	Aizawl	23.805626°N; 92.837221°E	554 m
18	Muthi park	Aizawl	23.783832°N; 92.763273°E	1054 m
19	MZU campus	Aizawl	23.736143°N; 92.667240°E	848 m
20	Neihbawih Sihphir	Aizawl	23.834704°N; 92.744017°E	1323 m
21	New Lato	Saiha	23.368595°N; 92.933221°E	428 m
22	Ngengpui WLS	Lawngtlai	22.441958°N; 92.788998°E	208 m
23	Paikhai road	Aizawl	23.637089°N; 92.735141°E	745 m
24	Palsang	Aizawl	24.283545°N; 92.913105°E	758 m
25	Phuldungsei	Mamit	23.474677°N; 92.420315°E	898 m
26	Reiek	Mamit	23.690327°N; 92.606771°E	1280 m
27	Sakawrtuichhun	Aizawl	23.762003°N; 92.653885°E	477 m
28	Sekhum	Lunglei	23.140123°N; 92.752131°E	851 m
29	Serchhip	Serchhip	23.336536°N; 92.859369°E	982 m
30	Thenzawl	Serchhip	23.283152°N; 92.782637°E	773 m
31	Thinghlun	Mamit	24.249253°N; 92.379732°E	78 m
32	Tlungvel	Aizawl	23.608755°N; 92.853249°E	1058 m
33	Tuivai	Aizawl	24.042688°N; 93.253722°E	449 m
34	Near Tuirial	Aizawl	23.729786°N; 92.777452°E	666 m
35	Tuirial	Aizawl	23.717744°N; 92.799631°E	171 m
36	Tuivamit	Aizawl	23.753556°N; 92.676859°E	800 m
37	Vaipuanpho	Mamit	23.709914°N; 92.642254°E	441 m
38	Zawlnuam	Mamit	24.129764°N; 92.337398°E	76 m
39	Keitum	Serchhip	23.231403°N; 92.912985°E	630 m
40	Borapansury	Lawngtlai	22.711888°N; 92.524362°E	55 m
41	Sateek	Aizawl	23.546317°N; 92.703869°E	916 m
42	Luangmual	Aizawl	23.742444°N; 92.693421°E	926 m
43	Thingsulthliah	Aizawl	23.684339°N; 92.857785°E	940 m
44	Vairengte	Kolasib	24.499249°N; 92.763463°E	240 m
45	Bukpui	Kolasib	24.059838°N; 92.781644°E	1020 m

46	North Hlimen	Kolasib	24.229943°N; 92.805232°E	670 m
47	New Khawlek	Lunglei	23.321111°N; 92.643597°E	715 m

Natural history

On 16 June 2021, at 2105 h, a freshly road-kill adult male *B. fasciatus* (TL=1,460 mm) lying on a newly constructed tarmac road (width of road= ca. 5.8 m) at New Khawlek, Lunglei District, Mizoram, India (23°19'16.00"N, 92°38'36.95"E; elev. 715 m asl) was encountered by Malsawmtluanga. It seems the krait remained vulnerably exposed on the motorway while subduing the Redtail Pit-viper *Trimeresurus erythrurus* (TL=488 mm), and fatally run over while busy swallowing more than half length of the prey (Fig. 1.11A) probably a few minutes prior to our arrival at the site (at ca. 2050 h). So, obviously the vehicles badly trampled upon the snakes, even causing the anterior half of the swallowed Redtail Pit-viper poking out from the oesophagus of the krait (Fig. 1.11B), and the hemipenis can be easily pressed out for determining the sex (Fig. 1.11C). After taking photographs, the carcass was relocated and left in the nearby forest. Earlier, another individual of foraging *B. fasciatus* was also seen to emerge out from a brook locating close to the current spot (Fig. 1.11D), but the snake was unfortunately killed by the local people while wandering in the open; however, the brook was known to be inhabited by various anuran species particularly during monsoon period (Malsawmtluanga pers. obs.).

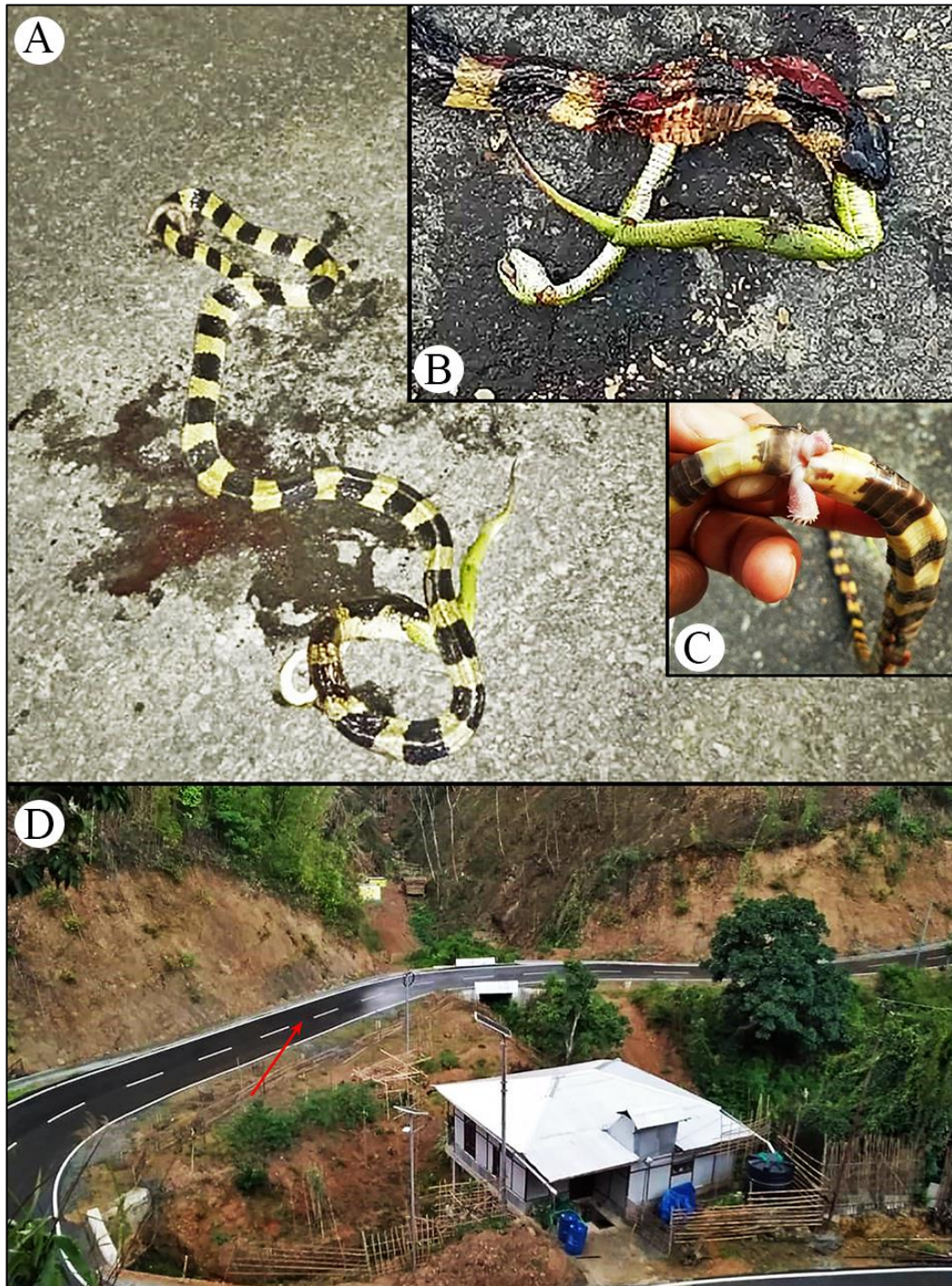


Figure 1.11. (A) *Bungarus fasciatus* fatally run over by vehicles while swallowing its prey *Trimeresurus erythrurus*; (B) The anterior half of the swallowed prey poked out from the oesophagus of *B. fasciatus*; (C) Hemipenis of the road-kill *B. fasciatus*; (D) The habitat of *B. fasciatus* showing the exact spot of the incidence (pointed in red arrow) locating close to a brook at New Khawlek, Mizoram, India. Photo credit: Malsawmtluanga.

Discussion

Distribution. By taking account of the systematic reassessment in this work, the distributional range of *B. fasciatus* sensu stricto can be regarded to confined in India and Myanmar, and possibly including the populations from Bangladesh, Nepal and Bhutan until further confirmatory work. Within India, the distributional range includes Uttar Pradesh (Gorakhpur, fide Masson (1930); also see Anwar (2012) and Das et al. (2012) in the north, central Maharashtra in the west (Bhandarkar et al. 2012; Deshmukh et al. 2020; Joshi et al. 2017) and extending across Telangana (Hyderabad, fide Kinnear (1913), Andhra Pradesh (Srinivasulu et al. 2009), Chhattisgarh (Chandra et al. 2013; Ingle 2011), Jharkhand (Koderma, fide Smith (1911); also see Husain (2020), Bihar (Wall 1912), Odisha (Mahanadi valley, fide Wall (1912); also see Boruah et al. (2016), and northern part of West Bengal (Sharma 2007) to northeastern India, including Arunachal Pradesh (Borang et al. 2005; Das 2018), Assam (Wall 1912; Mathew 1983; Purkayastha et al. 2011), Meghalaya (Mathew 1995), Mizoram (Lalremsanga et al. 2011; Pawar & Birand 2001), Tripura (Majumder et al. 2012), Manipur (Singh 1995; also see Das 2018) and Nagaland (Dasgupta & Raha 2006). A few unverified records are available from Madhya Pradesh (Wallach et al. 2014), Uttarakhand (Stuart et al. 2013), and southern peninsular India in Tamil Nadu, Karnataka and Kerala (Hussain 2020; Padmakumar and Murugan 2022).

Natural history. During this work, despite *B. fasciatus* crossing a motorway was rarely found, *T. erythrurus* was one of the most commonly encountered species on road especially during a showering night time. It has been noted that road mortality significantly contributes to mortality in animal and became a major problem in concerning for several taxa's conservational issues (Hobbs et al. 1990). A vulnerable natural area, but inhabited by threatened populations of unique or rare biota are often arrayed with unmitigated road systems which are lacking fences or wildlife crossing structures (Sodhi & Brook 2006; Laurance et al. 2009). There have rather been limited studies evaluating the potential impacts of vehicle roads on amphibian and reptile populations (Rytwinski & Fahrig 2015). But few studies suggested that amphibians and reptiles were containing more species at risk to road mortality

compared to other animal taxa like mammals or bird; herptile species are further speculated to be susceptible especially to road-kill in the vicinity of their natural habitats (see Rytwinski & Fahrig 2015; Heigl et al. 2017).

In addition to the previous record of road-kill *B. fasciatus* exposing its semi-digested prey *B. ochracea* from Buichali bridge, Sairang road, Aizawl District, Mizoram (Biakzuala et al. 2019). The present documentation constitutes the second case of road-kill *B. fasciatus* from the State, as well as contributes a new venomous species (*T. erythrurus*) in its diet. Given the vast range of distribution, the species was documented to preyed upon various species of non-venomous snakes like *Boiga ochracea* (Biakzuala et al. 2019), *B. trigonata*, *Fowlea piscator*, *Ptyas mucosa*, *P. korros*, *Amphiesma stolatum*, *Xenopeltis unicolor*, *Enhydris enhydris*, and *Indotyphlops braminus* in captivity (H.T. Lalremsanga pers. obs.); and venomous species like *Daboia russelii*, *Cylindrophis ruffus* (Daniels 2002), even including the congeneric species like *B. caeruleus* (Bharos 2013), *B. walli* and *B. lividus* (Subba et al. 2023). Eggs of snakes and other non-ophiophagic diet like skinks and fish are also recorded in the prey items (Daniels 2002).

Systematics. Evidence from this study, based on morphology and molecular data, defines three distinct clades of *B. fasciatus* with non-overlapping distribution clusters. The high genetic divergence among lineages also suggests distinct species-level groups within *B. fasciatus* as currently conceived. Our morphometric data analysis also provides evidence of their morphological distinctiveness between Clade I and II. Moreover, the lineage from east Asia is basal to the other two lineages but, if these clades were to be accepted as full species, the name-bearing lineage is Clade II. Thus, according to the newly presented evidence, and partly according to Russell (1796), the distribution range of *Bungarus fasciatus* sensu stricto (Indo-Myanmar clade) comprises east and northeast India extending towards Myanmar (Figs. 1.2, 1.10).

This study elucidated the presence of three independent lineages within *B. fasciatus*, which is crucial for future nomenclatural revision. In the *cytb* gene, while negligible intra-clade genetic divergence was observed within Clade I (0.4%;

between two locations in JV) and Clade II (0.0–1.3%; Myanmar, east and northeast India), a wide range of intra-clade genetic divergence (0.0–6.5%) was evident within Clade III (China, Vietnam, Thailand). Consequently, it was speculated that there might still be cryptic diversity within the east Asian lineage (Clade III). Moreover, for robust delimitation of the *B. fasciatus* complex, it is necessary to establish whether these lineages have undergone some degree of extrinsic or intrinsic reproductive isolation to be evolving separately (Hillis 2019). For instance, due to the high evolutionary rate of hemipenial traits compared to the other morphological traits (Gilman et al. 2018; Klaczko et al. 2015), the organ has commonly been used to provide a picture of sexual barrier even among cryptic species (Arnold 1986; Myers & McDowell 2014; Nunes et al. 2012).

Although it has been previously stressed that delimiting the taxonomic status of geographically diversified populations of venomous snakes alone cannot necessarily predict patterns of venom variation, it can play a pivotal role in overcoming the consequential variability of venoms (Daltry et al. 1996; Fry et al. 2003; Williams et al. 2019). Fry et al. (2003) further indicated that the medical importance of *B. fasciatus* has been overestimated. Moreover, the possible existence of undiscovered cryptic species accompanied by more venom diversity with uncharacterized components had been pointed out (Chatrath 2011). Siqueira-Silva et al. (2021) observed that more productive environments favour more complex venom, with more toxins in similar proportions. Based on the verbal autopsy conducted so far within Mizoram, there are three cases of fatal envenomation potentially from the bite of banded krait. Therefore, analyzing the venom compositions in different populations in each biogeographically isolated clade will be crucial.

The combination of multivariate morphometric analysis and mitochondrial gene-based phylogeography has been applied successfully for species delineation (Malhotra et al. 2011; Wüster and Broadley 2003; Wüster and Broadley 2007) as well as for testing species boundaries (Puerto et al. 2001). Aside from its taxonomical importance, recognition and ascertainment of independently evolving lineages is crucial for understanding the evolutionary processes affecting the origin

of population structure and species diversification (Jirsová et al. 2019). Consequently, the potential species-level diversity across different *B. fasciatus* populations depicted in this study cannot be overlooked, and a thorough comprehension of *B. fasciatus* systematics is still a fundamental challenge.

CHAPTER 2

Bungarus niger Wall, 1908

Review of literature

Kraits (*Bungarus*) are one of the most medically important snake species which are widely distributed in Asia from Iran through the Indian subcontinent to eastwards in China and south-eastwards up to Indonesia (Slowinski 1994; Kuch et al. 2005; Abtin et al. 2014; Ahsan and Rahman 2017; Chen et al. 2021; Midtgaard 2022). Kraits are showing secretive behaviour and not readily bite although they are generally having highly lethal venom (Tan & Ponnudurai 1989). Amongst the extant *Bungarus* species, the black-and-white banded species are known to be taxonomically intriguing to identify due to their overlapping taxonomical attributes, and they are mostly diagnosed based on the number of cross bands on the body and tail (Chen et al. 2021). Furthermore, among kraits of Northeast India, the two poorly studied species of black kraits *B. niger* (Greater black krait) and *B. lividus* Cantor, 1839 (Lesser black krait) that having overlapping distributional range and shared most of the morphological characters also warrant systematic attention. These two black krait species were considered to be closely related to each other according to the morpho-based phylogenetic analysis of the genus (Slowinski 1994). The global distributional range of *B. niger* includes India, Bangladesh, Nepal, and Bhutan (Uetz et al. 2023; Wallach et al. 2014) with the type locality in Tindharia, Darjeeling District of West Bengal in India (Wall 1908); while *B. lividus* is known so far from Northeastern India, Nepal, and Bangladesh with the type locality in Assam, India (Wallach et al. 2014). Currently, both the two black kraits are listed as Least Concern (LC) species in the IUCN Red List (Das et al. 2022; Limbu et al. 2022), and Schedule II under the Wildlife (Protection) Amendment Act (2022) in India.

Slowinski (1994) used six parameters in his morpho-based phylogenetic analysis such as the relative size of the vertebral scales, postzygapophysial processes, osteology, subcaudals, hemipenial morphology, and colouration. According to his model, *B. lividus* and *B. niger* were phenotypically hypothesized as sister taxon in having five common traits out of the six traits considered for his study. Both the

species differed from each other only in the relative size of the vertebral scales: *B. niger* has vertebral scales which are strongly enlarged compared to other dorsal scales, whereas in *B. lividus* the posterior vertebral scales are only slightly enlarged. Both the species together were placed as the sister group to a clade comprising *B. andamanensis*, *B. caeruleus*, *B. candidus*, *B. ceylonicus*, *B. magnimaculatus*, *B. multicinctus* and *B. sindanus*. Although morpho-taxonomical approach practically remained the key framework in species identification (Sokal and Crovello 1970; Luo et al. 2018), advancement in molecular methods for species identification contributed a valuable compliment to the morpho-taxonomy (Luo et al. 2018). Moreover, recent integrated taxonomical studies particularly on the widespread snake species have also determined the existence of previously undetected cryptic diversity (e.g., Thorpe et al. 2007; Wüster 1996; Wüster and Thorpe 1992). So, the use of molecular tools will assist in species identification, assuring their evolutionary trends, diversification, and other genomic features to discriminate the population (Burbrink and Lawson 2007; Castoe et al. 2012). Prior this study, Lalbiakzuala (2019) briefly presented systematic data of the species, and Biakzuala et al. (2021) have also addressed the systematics of the taxon along with the morphologically alike *B. lividus*. Even so, limited study and data is still available for the species especially from Mizoram, and there even exist insubstantial number of genetic data across its range that are accessible in the public access genetic data repository like GenBank (Benson et al. 2017), and the only available data were also originated from Nepal (Kuch 2007) and unspecified locality from India (Ghosh et al. 2018). Considering the fact that the species can be medically important due to its venom lethality and few existing records of deadly envenomation (Faiz et al. 2010; Pandey et al. 2016), appraising the regional and overall distributional records of this species will be crucial for mapping and better understanding of the taxon's geographical range. Based on an integrated taxonomic approach, this chapter attempts to reinvestigate the systematic status of the species among the congeneric species especially with respect to the morphologically alike species *B. lividus* as well as the other congeneric species based on a greater number of specimens, genetic markers with more robust genetic analytical approaches as well as morphological parameters and analyses. Thus, this chapter will be important for enriching the knowledge paucity, particularly on the

morpho-taxonomy, molecular systematics and distribution of this poorly studied deadly venomous species.

Materials and methods

Sampling

During this study, a total of 46 adults and 3 juvenile specimens housed in the collections of the Departmental Museum of Zoology, Mizoram University (MZMU) were examined. For molecular analysis, the liver tissues were dissected from a total of six road-killed/human persecuted specimens collected during this study (MZMU2030, MZMU1809, MZMU1792, MZMU1791, MZMU1549, MZMU975), and the tissues were stored in 95% ethanol at -20°C for DNA extraction. Genetic data bearing specimens and few other fresh road-killed/human persecuted specimens were stored in 70% ethanol, while the other examined individuals were preserved specimens stored in 10% formalin at the MZMU. All the specimen collection were undertaken after obtaining sample collection permit from the Environment, Forests and Climate Change Department, Government of Mizoram (Permit No. B.19060/5/2020-CWLW/20-26).

DNA extraction and PCR amplification

Liver tissues were used to extract the genomic DNA using DNeasy (Qiagen™) blood and tissue kits following the manufacturer's instructions (DNeasy® Blood & Tissue Handbook 2023). Fragments of three mitochondrial markers such as 16S rRNA (*16s*), cytochrome c oxidase subunit 1 (*cox1*) and cytochrome b (*cytb*) were amplified through Polymerase Chain Reaction (Mullis et al. 1986). The PCR reaction was carried out in a 20 µL reaction volume, containing 1X DreamTaq PCR Buffer, 2.5 mM MgCl₂, 0.25 mM dNTPs, 0.2 pM of primer pairs, approximately 3.0 ng of extracted DNA, and 1U of Taq polymerase using the thermal profiles and primers as given in Chapter 1 (Table 1.1). Gel electrophoresis was utilized to the quality of the PCR products using 1.5% agarose gel containing ethidium bromide. The PCR products were purified using ThermoFisher ExoSAP-IT PCR product clean up reagent, sequencing was subsequently performed using Sanger's dideoxy method using the ABI 3730xl DNA Analyzer at Barcode

BioSciences, Bangalore, India. For this study, the fragments of *16s* (n=3), and *cytb* (n=5) genes were amplified originating from six individuals of *B. niger* (MZMU 975, MZMU 1549, MZMU 1791, MZMU1792, MZMU1809, MZMU2030) with the GenBank accession numbers as given in Table 2.1. The *cox1* gene is not generated in this study due to limited comparative data from published works and database. The newly generated sequences were combined with published sequences of *Bungarus* species obtained from NCBI database with the sequence of *Naja naja* as the outgroup (Table 2.1).

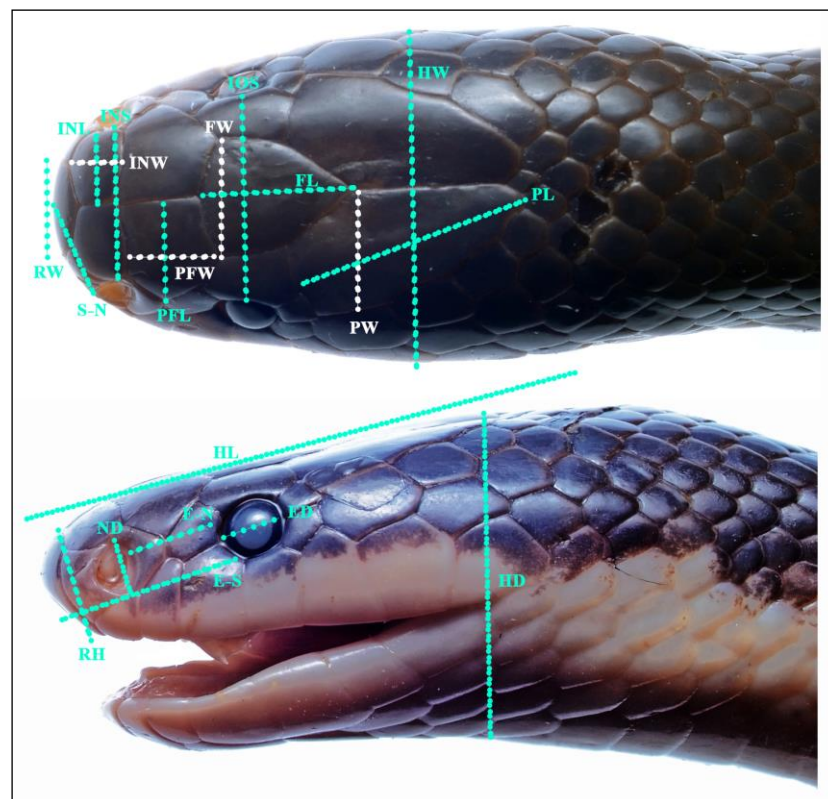


Figure 2.1. Description of head morphometrics used in *Bungarus niger*: (top) maximum width of head (HW), width of rostral (RW), snout to nostril distance (S-N), length of internarial (INL), width of internarial (INW), internarial space (INS), length of prefrontal (PFL), width of prefrontal (PFW), length of frontal (FL), width of frontal (FW), length of parietal (PL), width of parietal (PW); (below) length of head from tip of snout to angle of jaw (HL), depth of head (HD), horizontal eye diameter (ED), eye to snout distance (E-S), eye to nostril distance (E-N), rostral height (RH); and the meristics nuchal band width in scale (NBW) is also depicted.

Table 2.1. Information on specimen vouchers, locations, GenBank accession numbers, and references of the DNA sequences used in this study. The sequences generated in this study are shown in bold. Taxon's name abbreviations: *Bungarus niger* (BN), *B. candidus* (BC), *B. multicinctus* (BM), *B. wanghaotingi* (BW), *B. suzhenae* (BSZ), *B. lividus* (BL), *B. fasciatus* (BF), *B. caeruleus* (BCR), *B. slowinski* (BSL), *B. ceylonicus* (BCY), *B. sindanus* (BS), *B. bungaroides* (BB), *B. flaviceps* (BFL), and *Naja naja* (NN).

Species	Voucher	<i>16s</i>	<i>nd4</i>	<i>cytb</i>	Locality	References
BN	MZMU1809	OR593343	-	MW596474	Mizoram, India	This study
BN	MZMU1792	OR593345	-	OR601489	Mizoram, India	This study
BN	MZMU1791	OR593344	-	OR601488	Mizoram, India	This study
BN	MZMU2030	-	-	OR601487	Mizoram, India	This study
BN	MZMU975	-	-	MW596473	Mizoram, India	This study
BN	DDBRVp	-	-	MH423773	India	Ghosh et al. 2018
BN	Bnig	-	AJ830241	AJ749304	Nepal	Kuch 2007
BM	CHS666	MK194133	-	MK201459	China	Li et al. 2020
BM	CHS648	MK194122	-	MK201452	China	Li et al.2020
BM	Bm1	-	-	AJ749344	China	Kuch 2007
BM	CIB104228	-	-	MN165137	China	Chen et al. 2021
BM	SYNU R180305	-	MN165163	MN165135	China	Chen et al. 2021
BC	UK B39	-	-	AJ749329	Java (Indonesia)	Kuch 2007
BC	Bcba	-	-	AJ749339	Bali (Indonesia)	Kuch 2007
BC	UK B21	-	-	AJ749341	Java (Indonesia)	Kuch 2007
BC	-	JN687933	-	AJ565001	Thailand	Kuch 2007; Suntrarachun et al. 2011
BW	ROM 35250	-	-	AJ749308	Vietnam	Kuch 2007
BW	CIB MLMY20170801	-	MN165171	MN165144	China	Chen et al. 2021
BW	JK20181101	-	-	MN165146	China	Chen et al. 2021
BSZ	CIB116091	-	MN165170	MN165143	China	Chen et al. 2021
BSZ	CIB116089	-	MN165169	MN165141	China	Chen et al. 2021
BSZ	CIB116088	-	MN165168	MN165140	China	Chen et al. 2021

Table 2.1. Continued.

Species	Voucher	<i>16s</i>	<i>nd4</i>	<i>cytb</i>	Locality	References
BSZ	CAS 221526	-	-	AJ749345	Myanmar	Kuch 2007
BFL	JAM 1946	-	AJ830251	AJ749351	Malaysia	Kuch 2007
BCY	RS-135	KC347350	KC347501	KC347457	Sri Lanka	Pyron et al. 2013a
BS	Bsin1	-	AJ830242	AJ749346	Pakistan	Kuch 2007
BSL	IEBR 1172	-	AJ830250	AJ749306	Vietnam	Kuch et al. 2005
BB	KIZ 98R0186	-	AJ830218	AY973270	India	Kuch et al. 2005
BF	MZMU1421	OR593341	-	OQ266797	Mizoram, India	This study
BF	MZMU1562	OR593342	-	OQ266798	Mizoram, India	This study
BF	MZMU1883	OQ256169	-	OQ266796	Mizoram, India	This study
BF	MZMU978	-	-	MW596475	Mizoram, India	This study
BF	15.v26	OQ256170	OQ266805	OQ266799	Mizoram, India	This study
BCR	UK H7	-	AJ830220	AJ749305	Pakistan	Kuch 2007
BCR	BC11	MT573968	-	-	Pakistan	Ashraf et al. 2019
BCR	BC1	MT573969	-	-	Pakistan	Ashraf et al. 2019
BL	YSR187	-	-	MW596472	Meghalaya, India	Biakzuala et al. 2021
NN	-	NC010225	NC010225	NC010225	-	Yan et al. 2008

Phylogenetic analyses

Nucleotide sequences were aligned using MUSCLE algorithm (Edgar 2004) under complete deletion option for the treatment of gaps/missing data in MEGA 11 (Tamura et al. 2021). Although the fragment of *cox1* gene sequence (GenBank Accession No. MN722643) was generated, this gene was excluded in the present phylogenetics and other analyses due to insufficient comparable data; instead, the database sequences of mitochondrial NADH Dehydrogenase subunit 4 (*nd4*) gene was utilized for the phylogenetic analyses. Hence, for the phylogenetic trees, the three mitochondrial gene alignments (*16s*, *nd4*, and *cytb*) were concatenated in SequenceMatrix (Vaidya et al. 2011), and were partitioned by gene and codon positions. The uncorrected p-distances were estimated in MEGA 11 (Tamura et al. 2021). The optimal partitioning schemes and nucleotide evolutionary model were screened through PartitionFinder v2.1 (Lanfear et al. 2017) under the Bayesian Information Criterion (BIC). Bayesian inference (BI) phylogeny was inferred in Mr.Bayes v3.2.5 (Ronquist et al. 2012) by applying the optimal partitioning schemes and nucleotide evolutionary models selected by PartitionFinder v2.1 (Lanfear et al. 2017). The MCMC was run with four chains comprised of one cold and three hot chains for 20 million generations with sampling every 5000 generations. Tracer v1.7 (Rambaut et al. 2018) was utilized for checking the burn-in cut-off and likelihood convergence. Maximum likelihood (ML) phylogenetic tree was inferred in IQ-TREE webserver (Nguyen et al. 2015) by using FreeRate heterogeneity (Soubrier et al. 2012; Yang 1995) at 10,000 iteration and Ultrafast Bootstrap (UFB) replicates (Minh et al. 2013). For ML inference tree, the optimal partitioning schemes selected by PartitionFinder v2.1 (Lanfear et al. 2017) was utilized, while the best models selected under BIC scores in ModelFinder (Kalyaanamoorthy et al. 2017) integrated in the IQ-TREE webserver (Nguyen et al. 2015). Both BI and ML phylogenetic trees were annotated in the web-based tree annotator iTOL software v5 (Letunic and Bork 2021). The equality of nucleotide evolutionary rate was also analysed between the lineages of *B. niger* and *B. lividus* in Tajima's relative rate test (Tajima 1993).

Mitochondrial haplotype networks

The four mitochondrial DNA sequences were utilized to screen the matrilineal relationships among populations through mtDNA-based haplotype estimation. The aligned dataset was utilized for generating haplotypes in DnaSP v.6 (Rozas et al. 2017), and the trait matrix corresponding to the locality of the samples was inserted in the output file. Median-Joining method (Bandelt et al. 1999) integrated in PopArt v.1.7 (Leigh and Bryant 2015) was used for plotting the mitochondrial haplotype networks.

Species delimitation

The three gene datasets, partitioned by codon positions were also utilized for performing a single locus-based Assemble Species by Automatic Partitioning (ASAP) (Puillandre et al. 2021). This approach assembles species partitions based on the probabilities and barcode gap width; these two metrics are combined into a single ASAP-score for ranking the partitions, the lower the ASAP-score, the better the partition. The standardized p-distances were further utilized for Principal Coordinate Analysis (PCoA) (Gower 1966) to visualize the genetic differentiation among the target taxa in PAST 4.13 (Hammer et al. 2001).

Morphology

Mensural and meristic data were obtained from the 46 adult individuals of *B. niger* population of Mizoram. The following mensural characters were measured to the nearest millimetre with a Mitutoyo digital calliper (Fig. 2.1): snout–vent length (SVL, measured from tip of snout to anterior margin of vent); tail length (TaL, measured from anterior margin of vent to tail tip); eye diameter (ED, horizontal diameter of orbit); nostril diameter (ND, largest diameter of nostril); eye–nostril length (E-N, distance between posteriormost point of nostril and anteriormost point of eye); eye–snout length (E-S, distance between anteriormost point of eye and tip of snout); snout–nostril length (S-N, distance between tip of snout and anteriormost point of nostril); head length (HL, distance between posterior edge of mandible and tip of snout); head width (HW, maximum width of head); head depth (HD, maximum depth of head); height of rostrum (RH, the height of rostral scale); width of rostrum (RW, the width of rostral scale); internarial space (INS, distance between the

nostrils); interorbital space (IOS, distance between the orbits); internarial length (INL, length of internarial scale); internarial width (INW, width of internarial scale); prefrontal length (INL, length of internarial scale); frontal length (FL, length of frontal scale); prefrontal length (PFL, length of frontal scale); prefrontal width (PFW, width of frontal scale); parietal length (PL, length of parietal scale); parietal width (PW, width of parietal scale). Meristic characters were taken as follows: supralabials (SL) and infralabials (IL) (first labial scale to last labial scale bordering gape); dorsal scale rows (DSR, counted around the body from one side of ventrals to the other in three positions, on one head length behind the neck, at midbody and at one head length before cloacal plate); when counting the number of ventral scales (Ve), the values were scored following Dowling (1951). Subcaudal scales (Sc) were counted from the first subcaudal scale meeting its opposite to the scale before the tip of the tail excluding the terminal scute. The sex of the specimens was identified by examining everted hemipenes or by ventral tail dissection. Values for bilateral head characters are given in left/right order. Keogh (1999) was followed for hemipenis terminology.

Statistical analyses

The morphological information was obtained from various localities in Mizoram state, India. Prior to conducting any further statistical analyses, missing values for the variables were calculated. Only the adult specimens (n=46) were utilized for statistical analyses to avoid the effect of life stages. The meristic data were standardized first to their zero mean and standard deviation. For mensural data, the best allometric adjustment model was determined based on the best linear regression model which gives the highest within-group correlation to make a linear relationship with body size to avoid the effect of allometric growth (Thorpe 1975). Firstly, the meristics (Ve and Sc) were tested for sexual dimorphism utilizing a separate one-way analysis of variance (ANOVA) for both life stages using sex as a factor along with Levene's test (Levene 1961) for testing homogeneity of variances. Brown-Forsythe test (Brown and Forsythe 1974) was also tested as an alternative approach in case the assumption of homoscedasticity was violated. For mensural (TaL, HL, HW, HD, ED, ND, E-S, N-S, E-N, RH, RW, INS, IOS, INL, INW, PFL,

PFW, FL, FW, PL, and PW), one-way analysis of covariance (ANCOVA) was carried out with snout-vent length (SVL) as a covariate and sex as a factor. All statistical analyses and graphical representations were performed using free access statistical packages viz. PAST 4.13 (Hammer et al. 2001) and PSPP v.1.6.2 (GNU Project 2015).

Results

Phylogenetic relationships

The best partitioning schemes and nucleotide evolutionary models selected for the two types of phylogenetic inferences were provided in (Table 2.2). The concatenated BI (Fig. 2.2) and ML (Fig. 2.3) phylogenetic analyses largely concurred in their topologies. In both the phylogenetic trees, the samples of *B. niger* from Mizoram were clustered together (PP=0.96; UFB=87) and formed a distinct lineage along with the conspecific samples from Nepal and unspecified locality from India (PP=1.0; UFB=100). Our analyses also clearly nested *B. lividus* among the kraits of Indian subcontinent such as *B. sindanus*, *B. caeruleus* and *B. ceylonicus* with a high branch support (PP=1.0; UFB=100), whereas *B. niger* formed a highly-supported sister lineage to the Southeast Asian endemic kraits such as *B. suzhenae* and *B. multinctus* + *B. candidus* + *B. wanghaotingi* clade (PP=1.0; UFB=94). Furthermore, within the clade of *B. multinctus* + *B. candidus* + *B. wanghaotingi*, distinct sub-clades were formed by the specimens of *B. multinctus* (Bm1, CIB104228, SYNU R180305) (PP=1.0; UFB=95), *B. candidus* (Bcba, unvouchered, UK B21, UK B39) (PP=1.0; UFB=100), while specimens designated as *B. multinctus* (CHS666, CHS648) are forming a sub-clade with the specimens of *B. wanghaotingi* (JK20181101, CIB MLMY20170801, ROM 35250) (PP=1.0; UFB=99). The study population of *B. fasciatus* were also clustered together and formed a well-supported distinct lineage (PP=1.0; UFB=100) basal to the kraits of Indian subcontinent (*B. sindanus*, *B. caeruleus* and *B. ceylonicus*) and Southeast Asia (*B. suzhenae*, *B. multinctus*, *B. candidus*, and *B. wanghaotingi*). The clade formed by the kraits of Indian subcontinent is also basal to the clade of Southeast Asian kraits with a high branch support (PP=1.0; UFB=100). Paraphyly of *B. caeruleus* was also uncovered in both the trees, and polytomy formed by *B. lividus*, *B.*

caeruleus, and *B. ceylonicus* was further evident in the BI tree. The equality of nucleotide evolutionary rate test conducted between the sequences of *B. niger* (MZMU 1809) and *B. lividus* (YSR 187) with *N. naja* as the outgroup in Tajima's relative rate test showed $p > 0.05$ ($\chi^2 = 0.03$; $df = 1$) whereby the null hypothesis of equal rates between lineages is accepted.

Table 2.2. Nucleotide substitution models selected for the concatenated dataset of mitochondrial *16s*, *cox1*, and *cytb* genes.

Partitions	Sites	BI tree (PartitionFinder)	ML tree (ModelFinder)
I	<i>16s</i> , <i>cytb</i> pos1, <i>nd4</i> pos2	GTR+G	TIM2+F+G4
II	<i>cytb</i> pos2, <i>nd4</i> pos3	TRN+I	TN+F+I
III	<i>cytb</i> pos3, <i>nd4</i> pos1	TRN+I+G	TN+F+I+G4

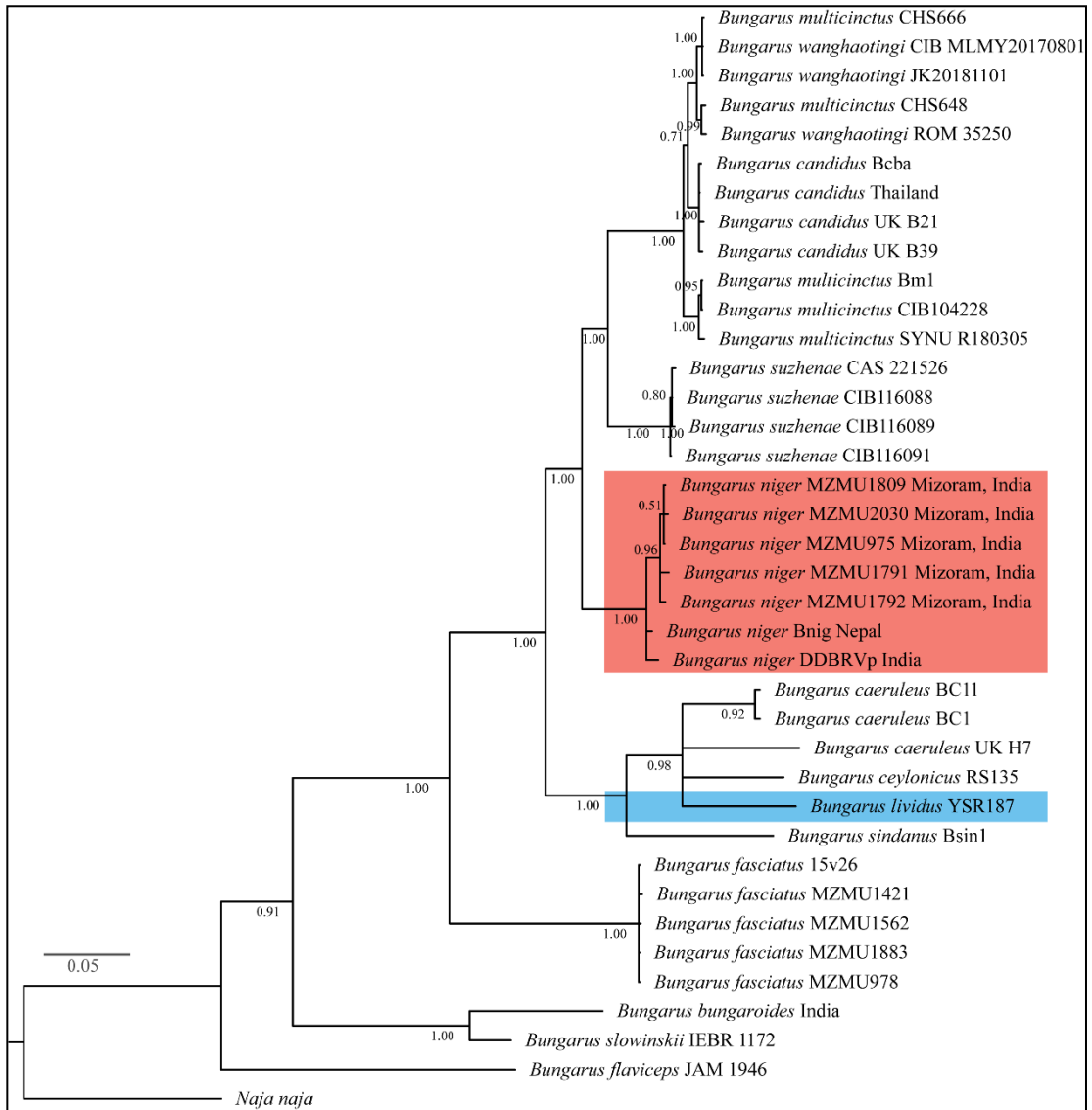


Figure 2.2. Concatenated Bayesian Inference (BI) phylogenetic tree of *Bungarus* species using the mitochondrial *16s*, *nd4* and *cytb* genes. The Bayesian posterior probability (PP) supports are shown at each branch.

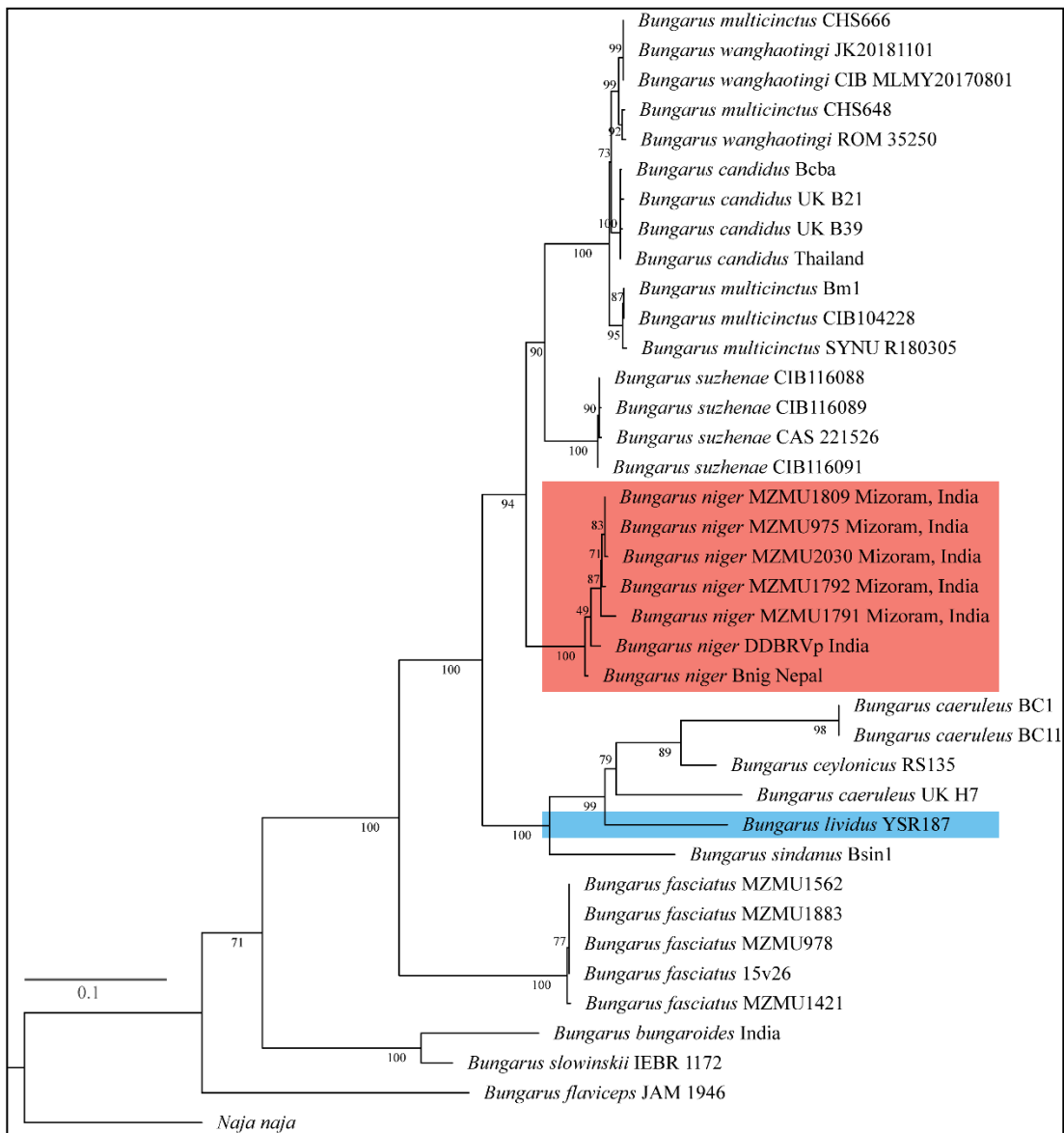


Figure 2.3. Concatenated Maximum Likelihood (ML) phylogenetic tree of *Bungarus* species using the mitochondrial *16s*, *nd4* and *cytb* genes. The Ultrafast bootstrap support (UFB) are shown at each branch.

Species delimitation

The ASAP species delimitation was conducted for the three mitochondrial genes separately and produced 10 distinct species partitions each (Fig. 2.4). In *16s*, the method produced two unidentical optimal partitions (ASAP score=2.0). One of these two partitions (Partition 6) detected *B. niger* as distinct species while detecting *B. multicinctus* (CHS666; CHS648) and *B. candidus* from Thailand (unvouchered) as similar species. On the contrary, the second optimal partition (Partition 5) is more inclusive compared to the previous partition so that all the aforesaid three taxa are detected as single species. But, considering the topology of the phylogenetic inferences, the partition that showing *B. niger* as distinct species was taking into account for species recognition. In *nd4*, the optimal partition (ASAP score=2.0) detected the specimen of *B. niger* as distinct species and all the other included taxa are also detected as distinct species (Fig. 2.4). In *cytb*, the optimal partition (ASAP score=2.0) detected the specimens of *B. niger* from this study (Mizoram, India), unknown locality, and Nepal as single species. Moreover, the *B. multicinctus*+*wanghaotingi* species group was partitioned into four species. The specimens of *B. multicinctus* (CHS666) and *B. wanghaotingi* (CIBMLMY20170801; JK20181101) are detected as single species; *B. multicinctus* (CHS648) and *B. wanghaotingi* (ROM35250) as single species; *B. multicinctus* (Bm1; CIB104228) as single species; and *B. multicinctus* (SYNU R180305) as distinct species (Fig. 2.5).

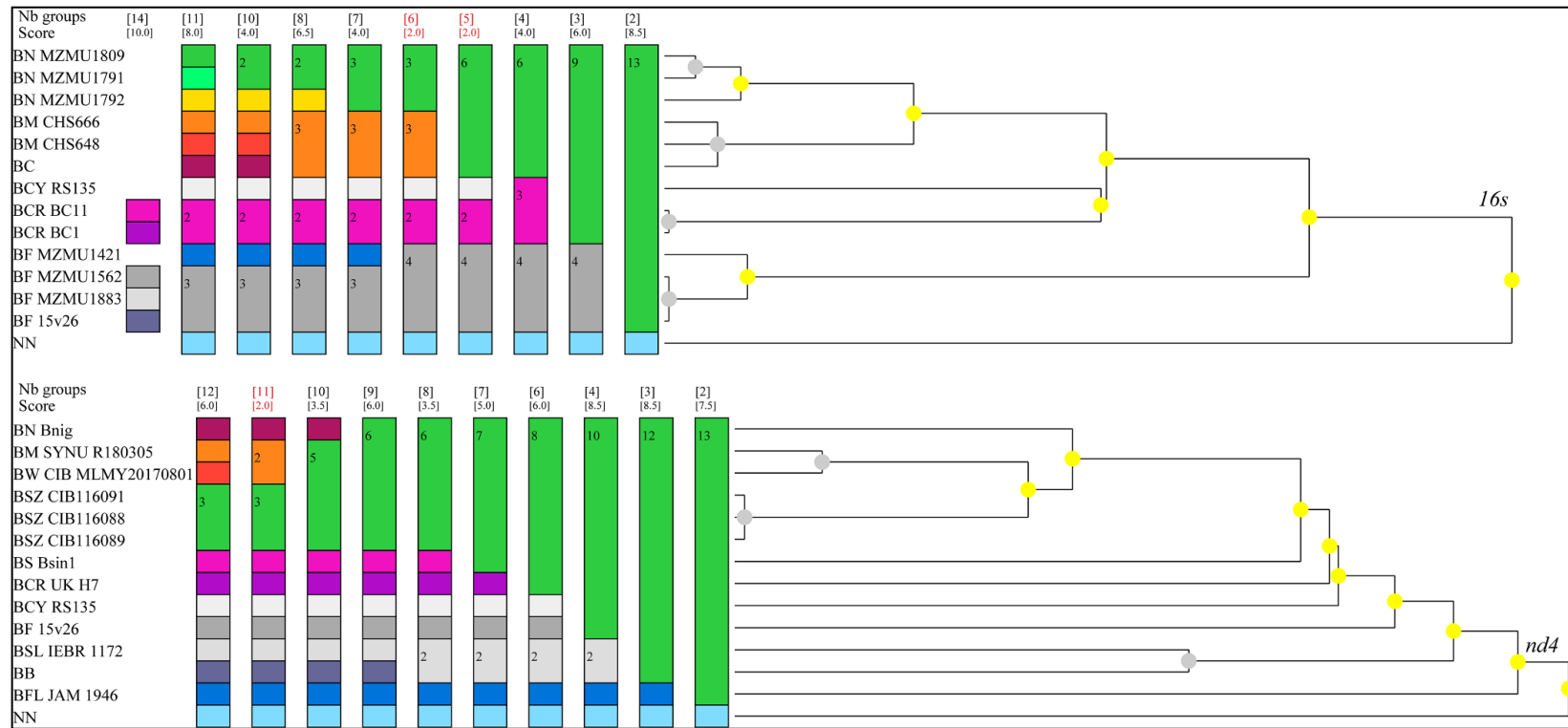


Figure 2.4. Species delimitation by Assemble Species by Automatic Partitioning (ASAP) using *16s* (top) and *nd4* (bottom) gene fragments of the genus *Bungarus*. The Neighbour-joining cladogram (right) concorded to the ASAP partitions (left). Species abbreviations: *B. niger* (BN), *B. fasciatus* (BF), *B. suzhenae* (BSZ), *B. caeruleus* (BCR), *B. candidus* (BC), *B. bungaroides* (BB), *B. wanghaotingi* (BW), *B. multicinctus* (BM), *B. sindanus* (BS), *B. slowinskii* (BSL), *B. flaviceps* (BFL), *B. ceylonicus* (BCY), and *Naja naja* (NN) as outgroup.

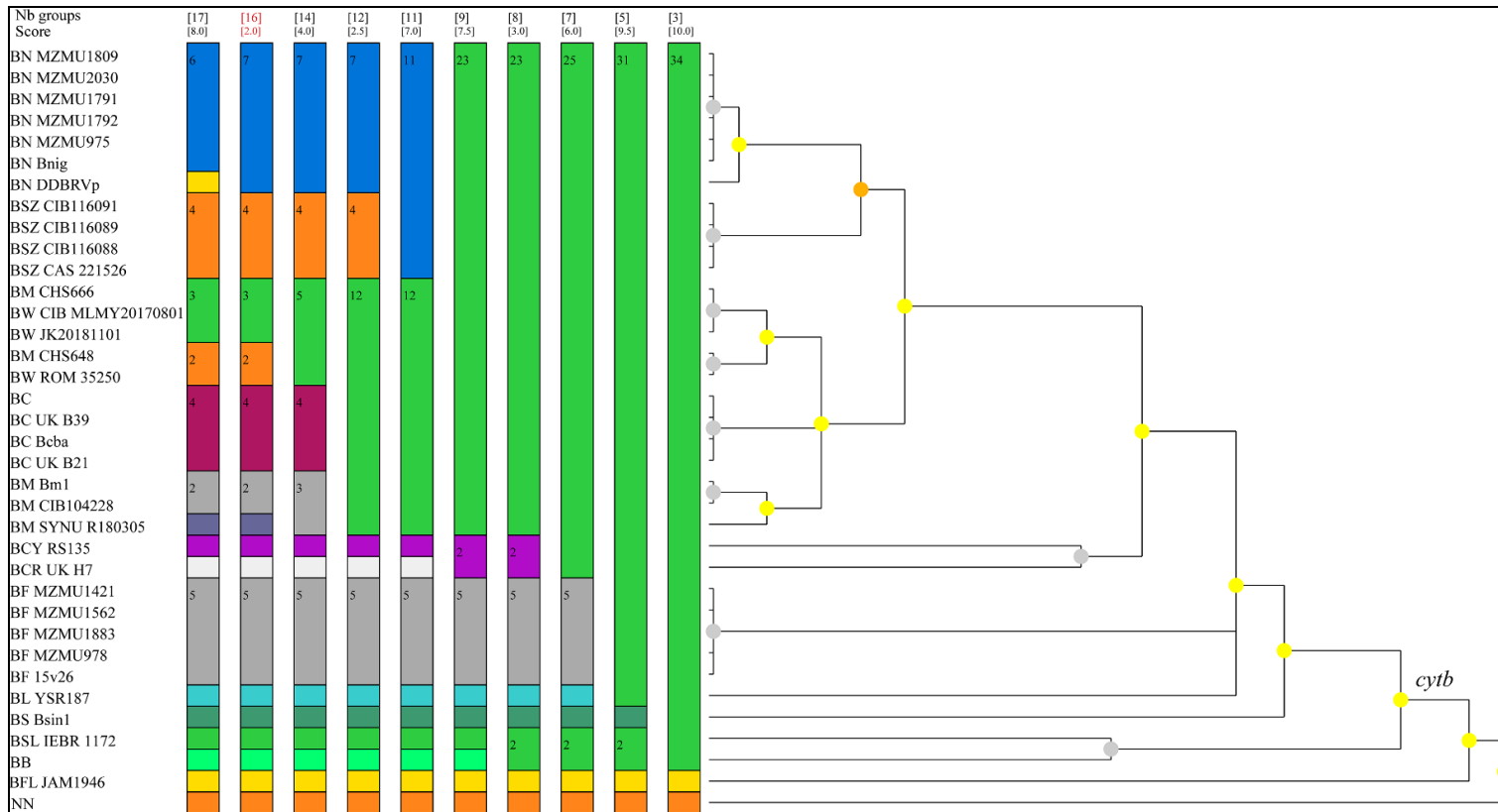


Figure 2.5. Species delimitation by Assemble Species by Automatic Partitioning (ASAP) using *cytb* gene fragments of the genus *Bungarus*. The Neighbour-joining cladogram (right) concorded to the ASAP partitions (left). Species abbreviations: *B. niger* (BN), *B. lividus* (BL), *B. fasciatus* (BF), *B. caeruleus* (BCR), *B. candidus* (BC), *B. multicinctus* (BM), *B. slowinskii* (BSL), *B. ceylonicus* (BCY), *B. sindanus* (BS), *B. bungaroides* (BB), *B. wanghaotingi* (BW), *B. suzhenae* (BSZ), *B. flaviceps* (BFL), and *Naja naja* (NN) as outgroup.

Matrilineal haplotype

The haplotype diversity (Hd) and haplotype networks were inferred among *Bungarus* species using the three mitochondrial genes. In *16s*, a total of nine distinct haplotypes (Hap) with Hd=0.9359 are recovered: Hap 1 [*B. niger* from Mizoram (MZMU1809, MZMU1791)], Hap 2 [*B. niger* from Mizoram (MZMU1792)], Hap 3 [*B. multicinctus* (CHS666)], Hap 4 [*B. multicinctus* (CHS648)]; Hap 5 [*B. candidus* from Thailand (unvouchered)]; Hap 6 [*B. ceylonicus* (RS135)]; Hap 7 [*B. fasciatus* from Mizoram (MZMU1421)]; Hap 8 [*B. fasciatus* from Mizoram (MZMU1562, MZMU1883, 15v26)]; and Hap 9 [*B. caeruleus* (BC1, BC11)] (Fig. 2.6). In *nd4*, a total of 11 distinct haplotypes with Hd=0.9615 are recovered: Hap 1 [*B. niger* from Nepal (Bnig)]; Hap 2 [*B. multicinctus* (SYNU R180305)]; Hap 3 [*B. suzhenae* (CIB116088, CIB116089, CIB116091)]; Hap 4 [*B. wanghaotingi* (CIB MLMY20170801)]; Hap 5 [*B. flaviceps* (JAM 1946)]; Hap 6 [*B. ceylonicus* (RS135)]; Hap 7 [*B. sindanus* (Bsin1)]; Hap 8 [*B. slowinskii* (IEBR 1172)]; Hap 9 [*B. bungaroides* from India (unvouchered)]; Hap 10 [*B. caeruleus* (UK H7)]; and Hap 11 [*B. fasciatus* from Mizoram (15v26)] (Fig. 2.6). In *cytb*, a total of 16 distinct haplotypes with Hd=0.9294 are recovered: Hap 1 [*B. niger* from Mizoram (MZMU975, MZMU1791, MZMU1792, MZMU1809, MZMU2030) and Nepal (Bnig)]; Hap 2 [*B. multicinctus* (CHS666) and *B. wanghaotingi* (CIB MLMY20170801, JK20181101)]; Hap 3 [*B. multicinctus* (CHS648) and *B. wanghaotingi* (ROM 35250)]; Hap 4 [*B. candidus* (unvouchered, Bcba, UK B21, UK B39)]; Hap 5 [*B. multicinctus* (Bm1, CIB104228)]; Hap 6 [B24 (Java, Indonesia)], Hap 7 [CESS246 (Assam, India)], Hap 8 [*B. multicinctus* (SYNU R180305)]; Hap 9 [*B. ceylonicus* (RS135)]; Hap 10 [*B. sindanus* (Bsin1)]; Hap 11 [*B. slowinskii* (IEBR 1172)]; Hap 12 [*B. bungaroides* from India (unvouchered)]; Hap 13 [*B. fasciatus* from Mizoram (MZMU1421, MZMU1562, MZMU1883, MZMU978, 15v26)]; Hap 14 [*B. caeruleus* (UK H7)]; Hap 15 [*B. lividus* from Meghalaya (YSR187)]; and Hap 16 [*B. niger* from India (DDBRVp)]. (Fig. 2.7).

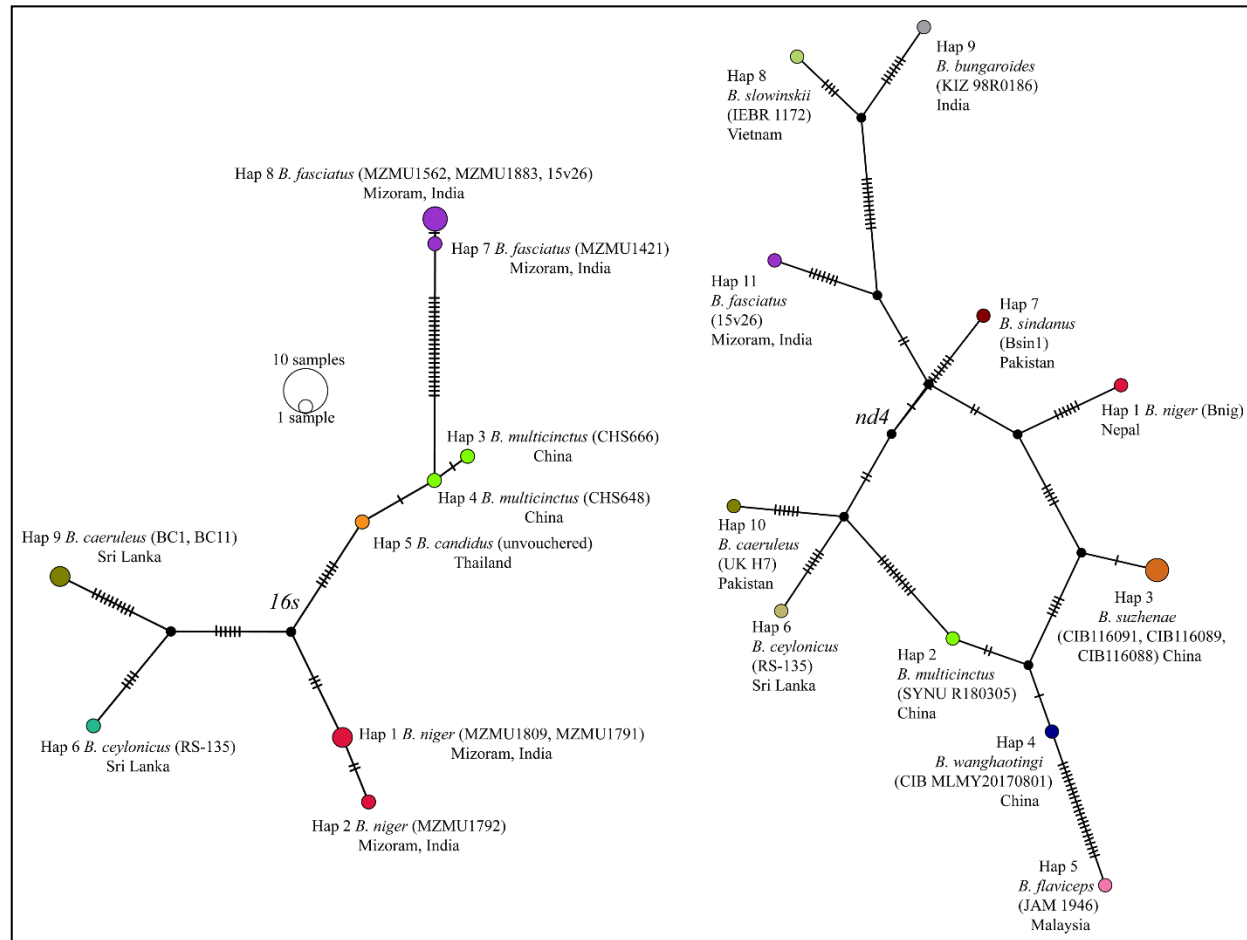


Figure 2.6. Mitochondrial gene-based (*16s*, and *nd4*) Median-joining haplotype network among *Bungarus* species. The number of samples present in each haplotype corresponds to the relative size of the circles. Hatch marks at the branch represent mutational steps found between haplotypes, and a black dot at the branch is an inferred median.

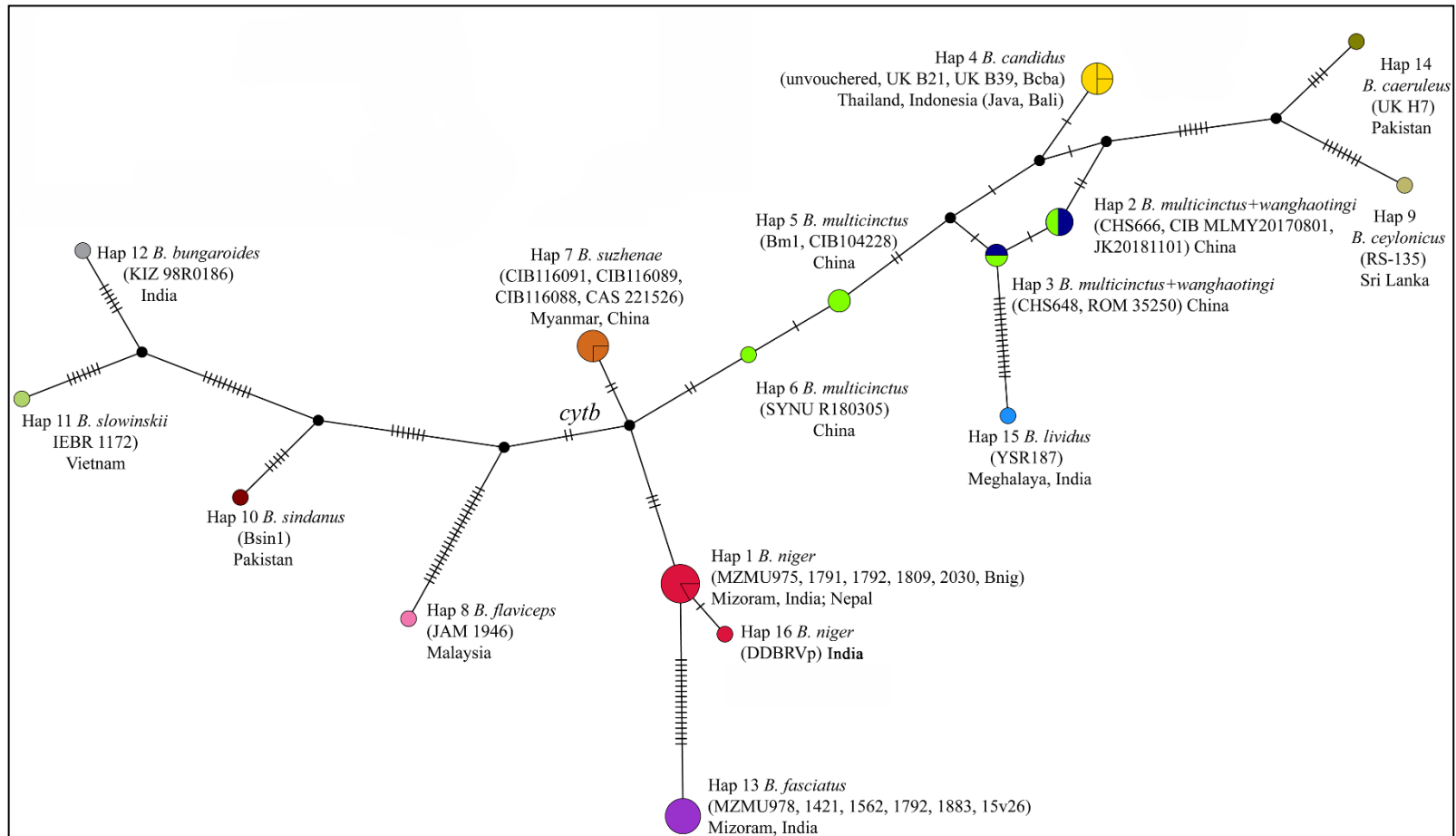


Figure 2.7. Mitochondrial gene-based (*cytb*) Median-joining haplotype network among *Bungarus* species. The number of samples present in each haplotype corresponds to the relative size of the circles. Hatch marks at the branch represent mutational steps found between haplotypes, and a black dot at the branch is an inferred median.

Genetic divergence

The estimated intraspecific genetic divergence within *B. niger* ranged from 0.0% (between MZMU975 and MZMU1809 from Mizoram) to 0.7% (between MZMU1792 to both MZMU1809 and MZMU1791 from Mizoram) in *16s*; while it ranged from 0.0% (between MZMU975 and MZMU1809 from Mizoram) to 3.0% (between MZMU1971 from Mizoram and DDBRVp from India) in *cytb*. The least interspecific genetic divergence from *B. niger* is seen with *B. candidus* from Thailand (2.9%) in *16s* (Table 2.3), *B. suzhenae* (9.4%) in *nd4* (Table 2.4), and *B. wanghaotingi* (ROM 35250) from Vietnam in *cytb* (3.8–6.0%) (Table 2.5). The genetic divergence between the morphologically alike black kraits (*B. niger* and *B. lividus*) also ranged from 14.3–15.8% in *cytb*, while *B. lividus* showed interspecific genetic divergence from 11.3% (with *B. caeruleus* UK H7 and *B. ceylonicus* RS135) to 20.3% (*B. bungaroides*) in *cytb*. The PCoA ordinations of genetic divergence using the three genes separately also dictated the discrete clustering of *B. niger* from the other congeneric species. The total variance captured by the PCo1 and PCo2 are 62% and 29% in *16S*, 56% and 17% in *nd4*, 62% and 17% in *cytb*, respectively. In *16s*, *B. niger* is positioned nearby the marginally overlapping clusters of *B. candidus* and *B. multicinctus*, while *B. fasciatus*, *B. ceylonicus* and *B. caeruleus* are distantly positioned. On the other hand, *B. niger* was distinctly placed from the species group of *B. multicinctus* + *B. candidus* + *B. wanghaotingi* in both the *nd4* and *cytb*. Moreover, specimens of the *B. multicinctus* + *B. candidus* + *B. wanghaotingi* species group are cohesively clustered in the *cytb*, while *B. wanghaotingi*, *B. multicinctus* and *B. suzhenae* formed a non-overlapping clustering in *nd4*. The specimens of *B. lividus* is also positioned very close to *B. ceylonicus* in the *cytb* (Fig. 2.8).

Table 2.3. Uncorrected p-distance estimated using the mitochondrial 16S rRNA (536 bp) sequence of *Bungarus niger* (BN), *B. fasciatus* (BF), *B. suzhenae* (BSZ), *B. caeruleus* (BCR), *B. candidus* (BC), *B. multicinctus* (BM), *B. ceylonicus* (BCY), and *Naja naja* (NN) as outgroup.

Species	1	2	3	4	5	6	7	8	9	10	11	12	13
1 BN MZMU1809													
2 BN MZMU1791	0.000												
3 BN MZMU1792	0.007	0.007											
4 BC Thailand	0.029	0.029	0.036										
5 BM CHS648	0.033	0.033	0.039	0.003									
6 BM CHS666	0.036	0.036	0.042	0.007	0.003								
7 BCY RS135	0.042	0.042	0.049	0.052	0.055	0.059							
8 BF 15v26	0.075	0.075	0.081	0.075	0.072	0.075	0.085						
9 BF MZMU1562	0.075	0.075	0.081	0.075	0.072	0.075	0.085	0.000					
10 BF MZMU1883	0.075	0.075	0.081	0.075	0.072	0.075	0.085	0.000	0.000				
11 BF MZMU1421	0.078	0.078	0.085	0.078	0.075	0.078	0.088	0.003	0.003	0.003			
12 BCR BC1	0.068	0.068	0.075	0.072	0.075	0.078	0.046	0.098	0.098	0.098	0.101		
13 BCR BC11	0.068	0.068	0.075	0.072	0.075	0.078	0.046	0.098	0.098	0.098	0.101	0.000	
14 NN	0.085	0.085	0.091	0.085	0.081	0.085	0.098	0.117	0.117	0.117	0.121	0.101	0.101

Table 2.4. Uncorrected p-distance (pairwise sequence divergence) estimated using the mitochondrial NADH Dehydrogenase subunit 4 (871 bp) sequence of *Bungarus niger* (BN), *B. fasciatus* (BF), *B. ceylonicus* (BCY), *B. bungaroides* (BB), *B. sindanus* (BS), *B. slowinskii* (BSL), *B. flaviceps* (BFL), *B. caeruleus* (BCR), *B. multicinctus* (BM), *B. wanghaotingi* (BW), *B. suzhenae* (BSZ), and *Naja naja* (NN) as outgroups.

Species	1	2	3	4	5	6	7	8	9	10	11	12	13
1 BN Bnig													
2 BSZ CIB116091	0.094												
3 BSZ CIB116089	0.094	0.000											
4 BSZ CIB116088	0.094	0.000	0.000										
5 BM SYNU R180305	0.117	0.063	0.063	0.063									
6 BW CIB MLMY20170801	0.125	0.055	0.055	0.055	0.023								
7 BCR UK H7	0.133	0.133	0.133	0.133	0.133	0.148							
8 BF 15v26	0.133	0.141	0.141	0.141	0.172	0.148	0.164						
9 BS Bsin1	0.141	0.141	0.141	0.141	0.172	0.172	0.133	0.188					
10 BCY RS135	0.141	0.156	0.156	0.156	0.156	0.164	0.094	0.141	0.133				
11 BFL JAM 1946	0.219	0.195	0.195	0.195	0.195	0.180	0.203	0.188	0.250	0.219			
12 BSL IEBR 1172	0.234	0.242	0.242	0.242	0.250	0.242	0.227	0.180	0.211	0.211	0.219		
13 BB	0.234	0.203	0.203	0.203	0.227	0.219	0.219	0.211	0.195	0.234	0.188	0.086	
14 NN	0.195	0.188	0.188	0.188	0.188	0.188	0.227	0.188	0.242	0.242	0.172	0.242	0.250

Table 2.5. Uncorrected p-distance (pairwise sequence divergence) estimated using the mitochondrial cytochrome b (1,131 bp) sequence of *Bungarus niger* (BN), *B. lividus* (BL), *B. fasciatus* (BF), *B. caeruleus* (BCR), *B. candidus* (BC), *B. multicinctus* (BM), *B. slowinskii* (BSL), *B. ceylonicus* (BCY), *B. sindanus* (BS), *B. bungaroides* (BB), *B. wanghaotingi* (BW), *B. suzhenae* (BSZ), *B. flaviceps* (BFL), and *Naja naja* (NN) as outgroup.

Species	1	2	3	4	5	6	7	8	9	10	11	12	13	14	15	16	17
1 BN MZMU975																	
2 BN MZMU1809	0.000																
3 BN MZMU2030	0.002	0.002															
4 BN MZMU1792	0.002	0.002	0.004														
5 BN MZMU1791	0.006	0.006	0.006	0.006													
6 BN Bnig	0.012	0.018	0.012	0.011	0.012												
7 BN DDBRVp	0.015	0.015	0.018	0.013	0.030	0.013											
8 BW ROM 35250	0.093	0.098	0.095	0.096	0.085	0.090	0.100										
9 BW CIB MLMY20170801	0.098	0.102	0.100	0.100	0.093	0.096	0.103	0.009									
10 BW JK20181101	0.100	0.100	0.100	0.101	0.093	0.098	0.103	0.009	0.000								
11 BM Bm1	0.098	0.103	0.103	0.103	0.089	0.095	0.105	0.027	0.025	0.028							
12 BM SYNU R180305	0.099	0.103	0.103	0.102	0.087	0.098	0.105	0.030	0.028	0.031	0.005						
13 BM CIB104228	0.100	0.104	0.103	0.103	0.089	0.097	0.105	0.027	0.025	0.028	0.000	0.005					
14 BM CHS648	0.104	0.104	0.103	0.103	0.090	0.103	0.108	0.005	0.012	0.012	0.031	0.036	0.031				
15 BM CHS666	0.109	0.109	0.108	0.108	0.100	0.104	0.108	0.014	0.000	0.000	0.032	0.038	0.032	0.012			
16 BC Thailand	0.099	0.105	0.102	0.103	0.087	0.096	0.108	0.020	0.020	0.019	0.023	0.025	0.022	0.021	0.022		
17 BC UK B39	0.100	0.106	0.103	0.104	0.087	0.097	0.108	0.022	0.022	0.021	0.025	0.027	0.024	0.021	0.022	0.002	
18 BC Bcba	0.100	0.106	0.103	0.104	0.089	0.097	0.108	0.021	0.021	0.020	0.024	0.026	0.023	0.022	0.024	0.001	0.003

Table 2.5. Continued.

	Species	18	19	20	21	22	23	24	25	26	27	28	29	30	31	32	33	34	35
19	BC UK B21	0.004																	
20	BSZ CIB116091	0.093	0.094																
21	BSZ CIB116089	0.092	0.094	0.003															
22	BSZ CIB116088	0.092	0.094	0.001	0.002														
23	BSZ CAS 221526	0.091	0.093	0.003	0.004	0.002													
24	BS Bsin1	0.134	0.134	0.140	0.140	0.140	0.140												
25	BF MZMU978	0.148	0.148	0.141	0.144	0.142	0.143	0.166											
26	BF MZMU1562	0.149	0.149	0.141	0.144	0.142	0.143	0.167	0.000										
27	BF MZMU1883	0.147	0.147	0.139	0.142	0.140	0.141	0.164	0.000	0.000									
28	BF 15v26	0.151	0.151	0.143	0.146	0.144	0.146	0.169	0.000	0.000	0.000								
29	BF MZMU1421	0.152	0.152	0.143	0.146	0.144	0.146	0.171	0.000	0.000	0.000	0.000							
30	BL YSR187	0.144	0.146	0.138	0.141	0.139	0.140	0.141	0.169	0.169	0.169	0.169	0.171						
31	BCR UK H7	0.144	0.142	0.141	0.142	0.142	0.141	0.135	0.154	0.154	0.154	0.154	0.157	0.113					
32	BCY RS135	0.146	0.147	0.137	0.138	0.138	0.142	0.131	0.176	0.179	0.176	0.183	0.182	0.113	0.108				
33	BSL IEBR 1172	0.185	0.190	0.174	0.175	0.174	0.179	0.190	0.187	0.187	0.187	0.187	0.187	0.200	0.199	0.205			
34	BB India	0.176	0.179	0.184	0.185	0.184	0.191	0.196	0.183	0.184	0.184	0.185	0.185	0.203	0.201	0.199	0.094		
35	BFL JAM 1946	0.184	0.184	0.182	0.184	0.182	0.186	0.202	0.191	0.193	0.191	0.197	0.200	0.195	0.198	0.196	0.193	0.188	
36	NN	0.221	0.223	0.209	0.209	0.209	0.217	0.217	0.203	0.207	0.206	0.205	0.206	0.207	0.192	0.206	0.175	0.196	0.197

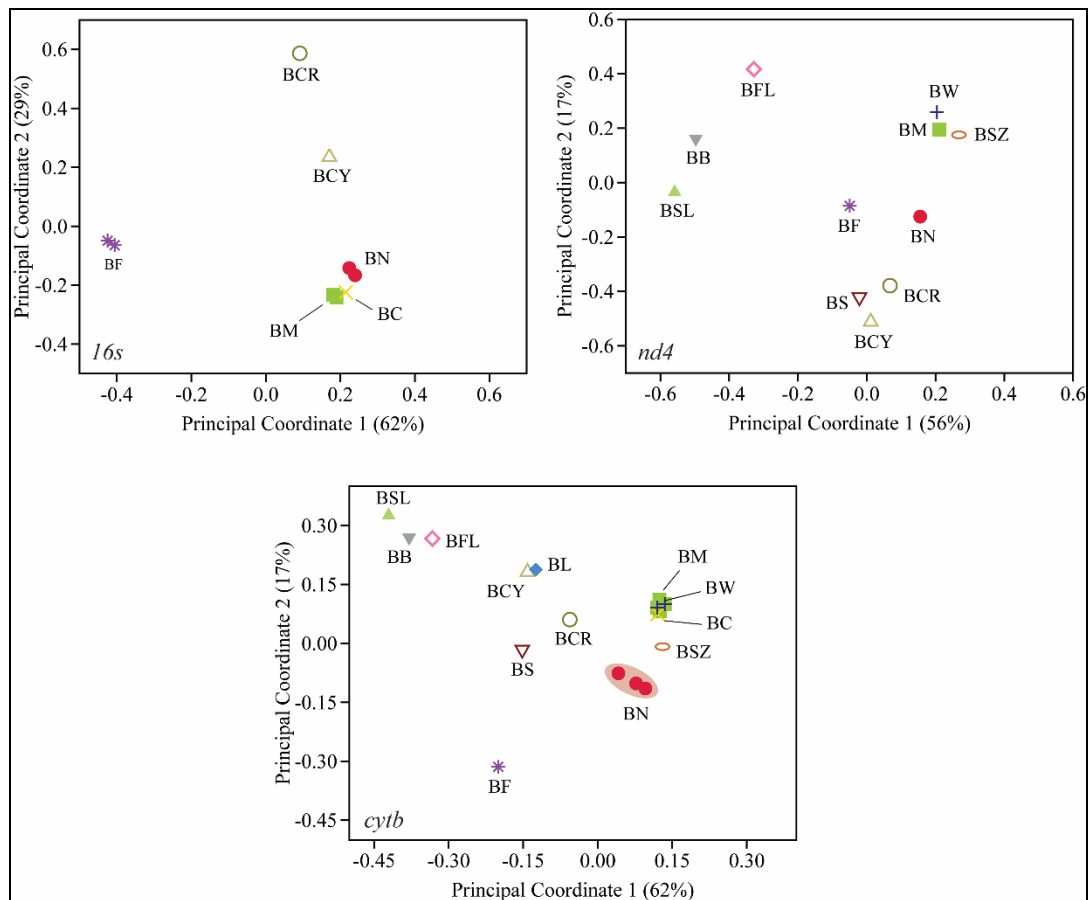


Figure 2.8. Ordination of *Bungarus* species in a Principal Coordinate Analysis of standardized p-distance of mitochondrial 16S rRNA (*16s*) NADH Dehydrogenase subunit 4 (*nd4*), and Cytochrome b (*cytb*) genes. A total percentage of variance captured by the first and second Principal coordinates are given in the x and y axes, respectively. Species abbreviations: *B. niger* (BN), *B. lividus* (BL), *B. fasciatus* (BF), *B. caeruleus* (BCR), *B. candidus* (BC), *B. multicinctus* (BM), *B. slowinskii* (BSL), *B. ceylonicus* (BCY), *B. sindanus* (BS), *B. bungaroides* (BB), *B. wanghaotingi* (BW), *B. suzhenae* (BSZ), and *B. flaviceps* (BFL).

Morphology

This study updated the morphological data based on 46 specimens examined in this study (Male = 37, Female = 9) (Table 2.6). It is a medium-sized snake (SVL max: 1,175 mm), with the head not distinct from the neck, longer than broad. Pupil round; SL and IF 7 in number, 3rd and 4th touching the eyes; PrO 1, and 2 PoO (except MZMU 1418 with single PrO); ATem 1, PTem 2. In males, Ve 214–228 (avg. 221.57 ± 3.56) and Sc 38–57 (avg. 52.14 ± 3.35); in females, Ve 220–226 (avg. 222.56 ± 2.07) and Sc 48–54 (avg. 50.88 ± 2.53). Among the examined specimens, a peculiar nape colouration was observed in a juvenile specimen (MZMU 1809); it was mottled with light patches at both sides from the rim of posterior temporals up to part of the first dorsal scale (Fig. 2.9). Hemipenis extends up to 5–12 Sc (avg. 8), vaguely bilobed; about one-third of the distal is calyculate, followed by spinose from mid region with the size of spines decrease as they approach to the proximal area with ill-defined demarcation between calyculate and spinose region (Fig. 2.11D–E). Based on the statistical analyses, it was uncovered that only the characters of INL and PFL are statistically significant with $p < 0.05$, while IOS is marginally significant with $p = 0.053$ between male and female specimens of the study population (Fig. 2.12). A peculiar male specimen was collected from Thenzawl locality (MZMU2030) which was characterized by the unusual formula of dorsal scale rows with 17:17:15 while the known feature for the species is 15:15:15.



Figure 2.9. A juvenile *Bungarus niger* (MZMU 1809) from Tanhril, Mizoram. Inset showing a dorso-lateral view of the head. Photo credit: Romalsawma.



Figure 2.10. Live adult *Bungarus niger* from Mizoram, India. Photo credit: H.T. Lalremsanga

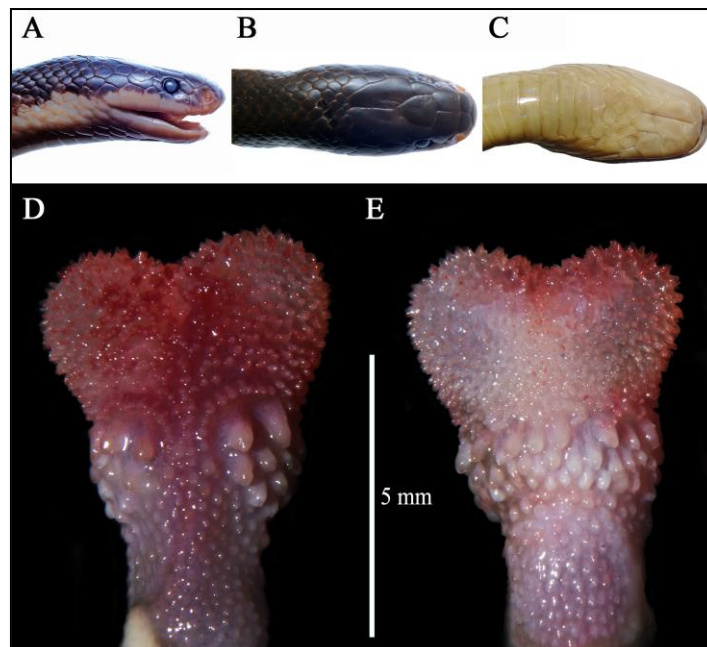


Figure 2.11. *Bungarus niger*. (A–C) Lateral, dorsal and ventral views of the head; (D) Sulcate, and (E) asulcate view of the everted hemipenis. The organ is cylindrical with ill-defined demarcation between calyculate and spinose region. Photo credits: Melvin Selvan (A–C); Jayaditya Purkayastha (D & E).

Table 2.6. Morphometry and meristics of *B. niger* from Mizoram. Damaged/missing characters are indicated by asterisk (*).

Museum number	MZMU 1324	MZMU 978	MZMU 975	MZMU 1315	MZMU 993	MZMU 986	MZMU 1337
Sex	M	M	M	M	M	M	M
HL	21.80	24.22	18.00	16.54	11.10	14.12	22.86
HW	19.56	20.26	12.94	13.28	12.50	11.10	19.82
HD	13.90	12.38	8.34	7.70	*	6.68	13.10
ED	3.04	3.84	2.48	2.37	2.42	2.40	3.12
ND	2.40	1.98	1.44	1.14	0.68	0.92	1.80
S-N	2.82	2.82	1.46	1.40	1.68	1.32	1.34
E-S	7.51	9.97	5.75	5.81	6.20	5.89	7.49
E-N	3.50	5.96	3.10	3.22	3.33	3.38	4.96
RW	7.14	7.16	5.60	5.50	5.66	4.10	8.16
RH	5.04	5.30	3.62	2.92	3.40	2.66	4.84
INS	7.02	7.10	5.64	5.50	5.28	4.50	7.88
IOS	10.24	10.02	7.44	7.98	7.84	6.94	11.00
INL	3.80	4.08	2.88	2.66	2.40	2.34	3.86
INW	3.04	3.32	2.40	2.00	1.98	2.14	2.92
PFL	5.34	5.58	4.16	4.06	4.22	3.74	5.80
PFW	5.33	5.44	3.82	3.80	3.80	3.48	5.54
FL	7.30	7.88	6.14	5.30	5.40	5.22	7.84
FW	5.84	5.88	4.86	4.52	4.64	4.28	6.40
PL	13.38	7.34	9.20	8.94	8.84	7.70	12.22
PW	7.00	7.12	5.58	5.38	4.62	4.30	6.80
SVL	1030	1050	779	684	695	635	1015
TaL	151	171	132	122	123	110	175
Ve	222	219	220	222	223	222	219
SC	50	53	51	54	55	56	53
DSR	15:15:15	15:15:15	15:15:15	15:15:15	15:15:15	15:15:15	15:15:15
SL	7/7	7/7	7/7	7/7	7/7	7/7	7/7
SLE	3-4 th	3-4 th	3 rd -4 th	3 rd -4 th	3 rd -4 th	3 rd -4 th	3 rd -4 th
IF	7/7	7/7	7/7	7/7	7/7	7/7	7/7
Te	1+2	1+2	1+2	1+2	1+2	1+2	1+2
PoO	2	2	2	2	2	2	2
PrO	1	1	1	1	1	1	1
HpR	up to 6 SC (20.45 mm)	up to 6 SC (19.80 mm)	up to 6 SC (19.54 mm)	up to 6 SC (11.12 mm)	up to 6 SC (15.94 mm)	up to 7 SC (17.30 mm)	up to 5 SC (20.54 mm)

Table 2.6. Continued.

Museum number	MZMU 1338	MZMU 1339	MZMU 1340	MZMU 1341	MZMU 1342	MZMU 1343	MZMU 1388
Sex	M	M	M	M	M	M	M
HL	22.02	19.48	9.80	16.52	13.96	21.81	20.66
HW	19.78	15.60	7.26	11.92	13.00	17.58	15.52
HD	12.34	*	*	9.38	7.22	12.42	10.14
ED	3.00	2.23	1.52	2.28	1.44	2.87	2.48
ND	1.92	1.72	*	1.52	1.00	2.06	1.68
S-N	1.40	1.10	0.56	1.20	1.04	1.91	1.50
E-S	7.67	5.67		5.93	5.85	7.60	7.10
E-N	5.08	3.38	1.80	3.54	3.62	4.50	4.41
RW	7.26	6.62	*	5.58	5.00	6.64	6.56
RH	4.32	3.80	*	3.70	3.10	4.58	3.88
INS	6.80	6.42	*	5.44	5.54	7.14	6.30
IOS	9.82	8.76	*	7.40	7.10	11.04	8.60
INL	3.70	3.18	*	2.92	3.30	3.74	3.36
INW	2.94	2.60	*	2.42	1.90	2.96	2.44
PFL	5.58	4.90	*	4.08	3.66	5.80	4.90
PFW	5.00	3.88	*	3.74	3.20	5.48	4.40
FL	8.28	5.64	*	6.18	4.90	7.64	7.30
FW	5.96	5.10	*	4.64	3.84	5.64	5.96
PL	11.44	9.36	*	8.98	7.24	12.20	10.22
PW	6.60	6.10	*	5.00	4.60	5.80	5.62
SVL	887	787	319	742	593	895	1170
TaL	146	129	57	105	106	143	142
Ve	226	223	222	222	222	214	216
SC	54	51	58	49	51	48	52
DSR	15:15:15	15:15:15	15:15:15	15:15:15	15:15:15	15:15:15	15:15:15
SL	7/7	7/7	7/7	7/7	7/7	7/7	7/7
SLE	3 rd -4 th	3 rd -4 th	3 rd -4 th	3 rd -4 th	3 rd -4 th	3 rd -4 th	3 rd -4 th
IF	7/7	7/7	7/7	7/7	7/7	7/7	7/7
Te	1+2	1+2	1+2	1+2	1+2	1+2	1+2
PoO	2	2	2	2	2	2	2
PrO	1	1	1	1	1	1	1
HpR	upto 7 SC (20.64 mm)	upto 7 SC (20.36 mm)	-	upto 7 SC (18.01 mm)	upto 8 SC (17.52 mm)	upto 6 SC (19.74 mm)	-

Table 2.6. Continued.

Museum number	MZMU 1418	MZMU 1416	MZMU 1453	MZMU 1527	MZMU 1085	MZMU 1086	MZMU 1482
Sex	F	M	F	M	F	F	M
HL	17.72	26.44	8.47	21.46	15.5	14.38	20.40
HW	15.09	22.46	6.78	17.28	11.2	11.85	15.38
HD	9.90	*	4.08	13.00	8.36	7.50	9.26
ED	2.46	2.95	1.27	2.95	2.46	2.36	2.72
ND	1.50	1.90	0.50	2.18	1.24	1.02	1.48
S-N	1.12	1.32	0.85	1.30	1.24	1.32	1.62
E-S	6.04	6.95	3.21	7.10	5.87	5.32	6.79
E-N	3.73	4.44	1.40	4.61	3.44	2.81	3.98
RW	5.46	6.70	2.16	7.56	5.18	4.60	6.18
RH	3.80	3.88	1.70	4.74	3.14	2.94	3.54
INS	5.80	6.92	2.86	7.40	5.04	4.50	6.70
IOS	8.92	8.32	3.92	11.00	6.82	6.94	9.32
INL	3.00	3.80	1.78	4.34	2.70	2.36	3.58
INW	2.24	3.14	1.16	3.18	2.26	2.32	2.90
PFL	4.20	5.00	2.36	5.60	3.96	3.56	5.00
PFW	4.10	4.52	2.24	5.92	3.38	3.44	4.36
FL	6.54	6.80	3.36	8.60	5.66	4.64	7.16
FW	4.24	5.60	2.00	6.52	4.96	3.78	4.86
PL	8.54	10.74	5.60	12.00	8.76	8.36	10.20
PW	5.10	5.68	2.80	7.60	5.92	4.82	6.20
SVL	722	934	272	1025	695	690	880
TaL	128	143	46	159	120	110	140
Ve	220	221	228	219	221	225	219
SC	48	52	56	51	52	53	52
DSR	15:15:15	15:15:15	15:15:15	15:15:15	15:15:15	15:15:15	15:15:15
SL	7/7	7/7	7/7	7/7	7/7	7/7	7/7
SLE	3 rd -4 th	3 rd -4 th	3 rd -4 th	3 rd -4 th	3-4 th	3-4 th	3-4 th
IF	7/7	7/7	7/7	7/7	7/7	7/7	7/7
Te	1+2	1+2	1+2	1+2	1+2	1+2	1+2
PoO	1	2	2	2	2	2	2
PrO	1	1	1	1	1	1	1
HpR		up to 6 SC (15.86 mm)		up to 10 SC (32.21 mm)			up to 9 SC (27.40 mm)

Table 2.6. Continued.

Museum number	MZMU 1483	MZMU 1549	MZMU 1528	MZMU 1525	MZMU 1526	MZMU 1570	MZMU 1571
Sex	M	M	M	M	M	M	M
HL	23.80	24.87	19.96	21.96	20.18	15.93	17.02
HW	16.90	19.68	14.57	15.85	13.73	13.36	13.82
HD	11.44	*	11.00	11.90	11.44	*	*
ED	2.82	3.48	2.78	2.61	2.28	2.89	2.26
ND	1.42	*	1.94	1.64	1.66	*	1.52
S-N	1.90	1.99	1.43	1.75	1.92	1.96	1.39
E-S	8.13	8.38	6.51	7.66	6.76	7.27	5.83
E-N	5.04	5.20	3.89	4.72	3.65	4.12	3.25
RW	7.04	*	6.64	6.70	6.78	*	5.54
RH	4.92	*	4.56	4.20	4.00	*	3.16
INS	6.78	*	6.22	7.04	6.44	*	5.56
IOS	10.22	*	9.34	10.10	9.30	*	7.56
INL	4.00	*	3.36	4.78	3.42	*	2.92
INW	3.48	*	2.90	2.96	2.90	*	2.48
PFL	5.40	*	5.22	5.24	5.12	*	4.34
PFW	5.38	*	4.32	4.96	4.66	*	4.16
FL	7.24	*	7.08	7.10	6.00	*	6.00
FW	5.34	*	5.70	5.56	5.06	*	4.22
PL	11.74	*	10.88	11.60	10.58	*	9.26
PW	6.44	*	6.02	5.96	5.48	*	5.00
SVL	1060	1155	925	950	935	775	720
TaL	152	170	152	140	142	140	122
Ve	222	221	223	228	228	216	217
SC	51	49	55	50	52	56	51
DSR	15:15:15	15:15:15	15:15:15	15:15:15	7/7	7/7	7/7
SL	7/7	7/7	7/7	7/7	3-4 th	3-4 th	3-4 th
SLE	3-4 th	3-4 th	3-4 th	3-4 th	7/7	7/7	7/7
IF	7/7	7/7	7/7	7/7	1+2	1+2	1+2
Te	1+2	1+2	1+2	1+2	2	2	2
PoO	2	2	2	2	1	1	1
PrO	1	1	1	1	7/7	7/7	7/7
HpR	up to 10 SC (29.82 mm)	up to 12 SC (46.09 mm)	up to 9 SC (26.0 mm)	up to 8 SC (27.13 mm)	up to 10 SC (29.27 mm)	up to 10 SC (20.88 mm)	up to 11 SC (25.39 mm)

Table 2.6. Continued.

Museum number	MZMU 1585	MZMU 1584	MZMU 1594	MZMU 1595	MZMU 2980	MZMU 2937	MZMU 2030
Sex	F	F	M	M	M	F	M
HL	11.39	17.7	14.81	17.87	18.52	16.04	27.50
HW	8.18	11.8	11.80	14.46	13.00	10.00	20.04
HD	*	8.74	8.00	9.78	9.60	7.32	15.10
ED	1.54	2.68	2.18	2.54	2.70	2.42	3.00
ND	0.86	1.72	1.36	1.60	1.70	1.40	2.10
S-N	0.63	1.43	1.35	1.31	2.44	2.10	3.26
E-S	4.15	6.67	5.50	6.59	6.32	5.84	9.22
E-N	2.33	4.05	2.96	4.09	3.08	2.96	4.90
RW	3.38	5.28	5.06	6.18	5.70	5.24	7.74
RH	1.70	3.16	3.00	3.42	3.40	3.18	5.40
INS	3.48	5.50	5.10	6.26	5.76	5.86	8.06
IOS	4.60	6.46	7.14	9.06	8.16	6.50	11.12
INL	2.00	3.00	2.84	3.46	3.32	2.60	4.18
INW	1.34	2.42	2.00	2.86	2.74	2.00	3.60
PFL	2.80	4.40	3.80	5.12	4.54	4.04	6.06
PFW	2.50	4.00	2.98	4.92	3.92	3.58	6.36
FL	3.70	5.70	5.44	7.06	5.94	4.88	7.14
FW	3.00	4.72	4.20	4.92	4.44	4.38	5.62
PL	5.76	9.56	8.42	10.10	9.54	7.68	13.64
PW	3.50	5.00	4.90	5.48	5.70	4.54	7.22
SVL	415	790	625	825	850	640	1175
TaL	68	130	105	126	132	108	138
Ve	223	221	224	219	223	224	227
SC	48	54	54	46(tip broken)	54	53	38
DSR	15:15:15	15:15:15	15:15:15	15:15:15	15	15	15
SL	7/7	7/7	7/7	7/7	7/7	7/7	7/7
SLE	3-4 th	3-4 th	3-4 th	3-4 th	3-4 th	3-4 th	3-4 th
IF	7/7	7/7	7/7	7/7	7/7	7/7	7/7
Te	1+2	1+2	1+2	1+2	1+2	1+2	1+2
PoO	2	2	2	2	2	2	2
PrO	1	1	1	1	1	1	1
HpR	-	-	up to 9 SC (19.50 mm)	up to 10 SC (20.38 mm)	-	-	-

Table 2.6. Continued.

Museum number	MZMU 2036	MZMU 2510	MZMU 2509	MZMU 2624	MZMU 2837	MZMU 223	MZMU 2991
Sex	M	F	M	M	F	M Juv	M
HL	14.76	21.10	21.76	16.62	21.06	10.74	20.88
HW	10.04	15.56	16.30	12.94	14.70	7.08	15.30
HD	7.36	10.70	10.90	8.00	8.10	4.60	8.80
ED	2.08	2.40	2.88	2.40	2.68	1.74	2.90
ND	1.20	1.24	1.74	1.52	*	0.66	1.66
S-N	1.66	2.04	2.40	1.90	*	0.84	1.42
E-S	5.18	8.08	8.00	6.26	7.22	3.28	6.44
E-N	2.40	4.02	3.94	3.44	*	1.76	3.44
RW	4.80	6.72	6.70	5.80	*	2.80	6.32
RH	2.90	3.86	4.84	3.00	*	1.84	3.88
INS	4.90	6.20	7.20	5.78	*	2.62	5.52
IOS	6.50	9.52	9.96	7.92	8.46	4.10	8.90
INL	2.64	3.16	3.84	3.18	*	1.60	3.90
INW	1.94	2.78	3.06	2.44	2.70	1.00	2.72
PFL	3.32	4.80	5.42	4.16	4.40	2.70	4.68
PFW	2.96	4.46	4.64	3.88	4.30	2.46	4.36
FL	4.84	7.00	6.70	5.12	6.42	3.90	6.20
FW	3.62	5.52	5.50	4.38	5.06	2.98	5.18
PL	7.54	10.70	11.12	9.06	10.14	5.88	9.98
PW	4.26	6.50	6.16	5.00	5.56	3.38	6.50
SVL	574	940	1033	645	775	310	980
TaL	76	*	160	120	130	58	150
Ve	224	221	225	219	222	223	222
SC	48	*	55	53	48	59	55
DSR	15	15	15	15	15	15	15
SL	7/7	7/7	7/7	7/7	7/7	7/7	7/7
SLE	3-4 th	3-4 th	3-4 th	3-4 th	3-4 th	3-4 th	3-4 th
IF	7/7	7/7	7/7	7/7	7/7	7/7	7/7
Te	1+2	1+2	1+2	1+1/1+1	1+2	1+2	1+2
PoO	2	2	2	2	2	2	2
PrO	1	1	1	1	1	1	1
HpR	-	-	-	-	-	-	-

Table 2.6. Continued.

Museum number	MZMU 1992	MZMU 1993	MZMU 1994	MZMU 1995	MZMU 1996	MZMU 1997	MZMU 1998
Sex	F	M	M	M	M	M	M
HL	19.80	18.00	19.18	*	16.50	19.44	12.06
HW	13.28	11.58	13.94	*	13.00	12.76	8.00
HD	8.48	7.56	10.88	*	8.00	8.60	5.42
ED	2.54	2.24	2.34	*	1.82	2.56	1.68
ND	1.22	1.16	1.56	*	1.00	1.30	0.72
S-N	1.70	1.46	1.74	*	1.50	1.66	1.18
E-S	7.64	5.90	5.34	*	5.94	7.12	4.66
E-N	4.12	3.82	3.38	*	3.32	3.64	2.36
RW	6.36	5.62	5.38	*	5.08	5.86	3.96
RH	3.70	3.20	3.94	*	3.18	3.44	1.96
INS	5.70	5.66	5.58	*	3.90	5.98	3.90
IOS	8.84	7.44	8.00	*	7.16	7.72	5.76
INL	3.26	3.00	2.96	*	3.22	3.34	2.20
INW	2.84	2.38	2.20	*	2.36	2.52	1.84
PFL	3.84	4.30	4.12	*	4.62	4.84	3.10
PFW	4.00	4.00	3.96	*	3.92	4.40	2.84
FL	6.92	5.78	5.44	*	5.36	6.26	4.10
FW	3.30	4.32	4.00	*	4.32	4.50	3.20
PL	9.80	9.00	10.02	*	8.42	9.18	6.64
PW	4.64	4.80	5.84	*	5.52	5.00	3.82
SVL	900	720	940	1145	675	815	442
TaL	152	118	160	170	115	140	76
Ve	226	225	217	226	219	217	227
SC	51	53	54	52	52	56	57
DSR	15	15	15	15	15	15	15
SL	7/7	7/7	7/7	7/7	7/7	7/7	7/7
SLE	3-4 th	3-4 th	3-4 th	3-4 th	3-4 th	3-4 th	3-4 th
IF	7/7	7/7	7/7	7/7	7/7	7/7	7/7
Te	1+2	1+1/1+1	1+1/1+2	1+2	1+2	1+2	1+2
PoO	2	2	2	2	2	2	2
PrO	1	1	1	1	1	1	1
HpR	-	-	-	-	-	-	-

Table 2.7. Screening of sexual dimorphism using the meristic and mensural characters obtained from 46 adult *Bungarus niger* (37 males and 9 females) from Mizoram, Northeast India. Standardized meristic data were analyzed through one-way ANOVA with sex as a factor. Allometric adjusted mensural data were analysed through one-way ANCOVA using SVL as a covariate and sex as a factor. The characters with statistically significant variations at the alpha level of 0.05 are shown in boldface, and marginally significance in octothorp (#).

Characters	Male (n=37)		Female (n=9)		Sexual dimorphism	
	Mean±SD	Range	Mean±SD	Range		
Ve	221.57±3.56	214–228	222.56±2.07	220–226	$F_{1,44} = 0.63$	$p = 0.431$
Sc	52.54±2.34	48–57	50.88±2.53	48–54	$F_{1,41} = 3.21$	$p = 0.081$
TaL	135.08±24.16	76–175	118.25±24.53	68–152	$F_{1,41} = 0.06$	$p = 0.810$
HL	19.25±3.85	11.10–27.50	17.19±3.23	11.39–21.10	$F_{1,42} = 0.08$	$p = 0.777$
HW	14.97±3.29	8.00–22.46	12.41±2.47	8.18–15.56	$F_{1,42} = 1.94$	$p = 0.171$
HD	9.99±2.38	5.42–15.10	8.64±1.15	7.32–10.70	$F_{1,35} = 1.34$	$p = 0.255$
ED	2.58±0.47	1.44–3.84	2.39±0.34	1.54–2.68	$F_{1,42} = 0.66$	$p = 0.421$
ND	1.55±0.41	0.68–2.40	1.28±0.27	0.86–1.72	$F_{1,33} = 3.72$	$p = 0.063$
S-N	1.69±0.51	1.04–3.26	1.45±0.49	0.63–2.10	$F_{1,40} = 0.001$	$p = 0.974$
E-S	6.73±1.14	4.66–9.97	6.31±1.22	4.15–8.08	$F_{1,42} = 0.37$	$p = 0.545$
E-N	3.88±0.81	2.36–5.96	3.43±0.67	2.33–4.12	$F_{1,41} = 0.004$	$p = 0.950$
RH	3.82±0.82	1.96–5.40	3.19±0.69	1.70–3.86	$F_{1,39} = 1.05$	$p = 0.311$
RW	6.13±0.99	3.96–8.16	5.28±1.03	3.38–6.72	$F_{1,39} = 2.82$	$p = 0.101$
INS	6.09±1.02	3.90–8.06	5.26±0.89	3.48–6.20	$F_{1,39} = 1.40$	$p = 0.243$
IOS	8.65±1.44	5.76–11.12	7.45±1.58	4.60–9.52	$F_{1,40} = 3.96$	$p = 0.053^{\#}$
INL	3.37±0.59	2.20–4.78	2.76±0.43	2.00–3.26	$F_{1,39} = 5.82$	$p < \mathbf{0.05}$
INW	2.64±0.47	1.84–3.60	2.32±0.46	1.34–2.84	$F_{1,40} = 0.72$	$p = 0.401$
PFL	4.73±0.75	3.10–6.06	4.00±0.58	2.80–4.80	$F_{1,40} = 5.49$	$p < \mathbf{0.05}$
PFW	4.36±0.86	2.84–6.36	3.75±0.60	2.50–4.46	$F_{1,40} = 1.05$	$p = 0.312$
FL	6.36±1.09	4.10–8.60	5.72±1.13	3.70–7.00	$F_{1,40} = 0.23$	$p = 0.635$
FW	4.96±0.81	3.20–6.52	4.33±0.84	3.00–5.52	$F_{1,40} = 1.43$	$p = 0.239$
PL	9.90±1.73	6.64–13.64	8.81±1.49	5.76–10.70	$F_{1,40} = 0.63$	$p = 0.433$
PW	5.68±0.91	3.82–7.60	5.06±0.87	3.50–6.50	$F_{1,40} = 0.57$	$p = 0.453$

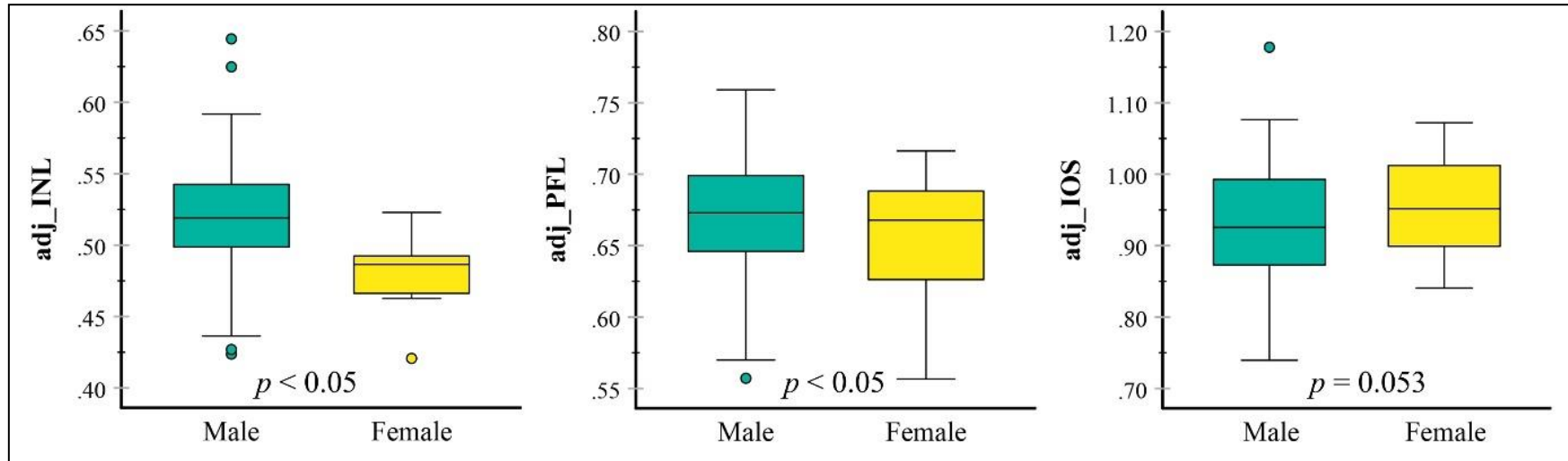


Figure 2.12. Box plot showing median, interquartile range, range (minimum to maximum), and outliers for the adjusted (adj) mensurals such as internarial length (INL), prefrontal length (PFL), and inter-orbital space (IOS) between male and female specimens of *Bungarus niger* population from Mizoram, Northeast India. Significance at the alpha level of 0.05 are given at each plot.

Distribution

In this study, *B. niger* was recorded from a total of 10 localities such as Samtlang village, Paikhai road, NE Bualpui village, and Lungsai village from Aizawl District; Dampa Tiger Reserve, Lungphunlian village, and Kanghmun village from Mamit District; Rullam village in Serchhip District; and Darzo village in Lunglei District at the elevations ranging from 260 m asl. (Dampa Tiger Reserve) to 1,433 m asl. (Rullam) (Fig. 2.13; Table 2.8).

In addition, the published distributional records are reviewed and compiled for mapping the overall distributional range of the two morphologically alike black kraits (*B. niger* and *B. lividus*). For *B. niger*: Bangladesh (Chittagong Division—Chandanaish, Khagrachhari, Fatikchhari, Dighinala, Chittagong University, Dudpukuria-Dhopachari WS, Teknaf WS, Baraiyadhala NP, Bandarban, Rangamati, Kaptai NP, Cox's Bazar; Mymensingh Division—Sherpur, Jamalpur; Sylhet Division—Habiganj, Moulvibazar, Lawachara NP; Dhaka Division—Savar. Bhutan: Chukha District—Phuntsholing); India (Assam—Dibrugarh, Margherita, Sadiya, Sivasagar, Guwahati, Nameri NP, Nambor WS, Borail WS, Maruacherra, Silkuri, Assam University campus; Tripura—Damcherra; Arunachal Pradesh—NERIST campus, Itanagar, Mehao WS, Pakke Khellong in Eaglenest WS; Changlang, Namdapha NP; Meghalaya—Garo Hill, Selbelgiri, Balpakram; Mizoram—Ngengpui WLS, Aizawl, Kolasib, Mamit and Siaha, Buhchangphai and Champhai Vengsang; Uttarakhand—Bungapani; West Bengal—Tindharia, Jalpaiguri; Nagaland with no locality record available); Nepal (Province No. 1—Golbasti, Ilam municipality; Gandaki Pradesh—Naudana, and in Kaski District); and Myanmar (Chin and Rakhine States) (Wall 1908; Wall 1924; Smith 1943; Bauer & Günther 1992; Pawar & Birand 2001; Tillack & Grossmann 2001; Grosselet et al. 2004; Khan 2004; Athreya 2005; Borang et al. 2005; Dasgupta & Raha 2006; Leviton et al. 2008; Theophilus et al. 2008; Faiz et al. 2010; Lalremsanga et al. 2011; Sharma et al. 2013; Pandey et al. 2016; Ahsan & Rahman 2017; Das 2018; Biakzuala et al. 2019). In addition to the specimen of *B. lividus* documented from Azara in Assam State, and Baridua in Meghalaya State (Yashpal Singh Rathee pers. obs.). The following distributional records of *B. lividus* are also compiled from published data: India

(Arunachal Pradesh—Pakke; West Bengal—Tindharia, Darjeeling, Jalpaiguri (Raikatpara Area; Assam—Dibrugarh, near Tezpur, Guwahati; Bangladesh (Rangpur Division—Rangpur, Carmichael University College campus, Dinajpur; Mymensingh division—Mymensingh district; Chittagong Division—Feni District; Barisal Division—Pirojpur; Khulna Division—Bagerhat; Nepal (Province No. 1—Beldangi I Refugee Camp near Damak in Jhapa District; Province No. 2—Amlekhganj and Bhata-Hattisar in Parsa NP; and Bhutan (Langthel in Jigme Singye Wangchuck NP) (Wall, 1908; Wall, F. 1924; Smith 1943; Khan 1992; Sharma et al. 2003; Kuch et al. 2011; Ahsan and Rahman 2017, Bhattarai et al. 2018; Das 2018; Tshewang and Letro, 2018; Ray and Pandey, 2020) (Fig. 2.14).

Table 2.8. Detailed collection data of *Bungarus niger* based on the combined data of this study and Lalbiakzuala (2019) in Mizoram, India. New records from this work are indicated with bold.

Sl. No.	Locality	District	Geo-coordinates	Elevation
1	Bethlehem	Aizawl	23.727222°N; 92.723056°E	966 m
2	Durtlang Gosen	Aizawl	23.795278°N; 92.733611°E	1,107 m
3	Durtlang ICFAI	Aizawl	23.798889°N; 92.728056°E	1,273 m
4	Durtlang Mualveng	Aizawl	23.783333°N; 92.725556°E	1,211 m
5	Falkawn	Aizawl	23.626389°N; 92.724444°E	763 m
6	Hunthar	Aizawl	23.744444°N; 92.713889°E	833 m
7	Melriat	Aizawl	23.647778°N; 92.725833°E	858 m
8	Mission Veng	Aizawl	23.713611°N; 92.710833°E	1,066 m
9	Mission Vengthlang	Aizawl	23.711667°N; 92.706944°E	984 m
10	Model Veng	Aizawl	23.712778°N; 92.713611°E	957 m
11	MZU campus	Aizawl	23.736111°N; 92.665278°E	836 m
12	Phunchawng	Aizawl	23.761111°N; 92.682222°E	561 m
13	Suangpuilawn	Aizawl	23.958889°N; 93.040833°E	1,043 m
14	Thingsulthliah	Aizawl	23.693333°N; 92.860556°E	892 m
15	Tlangnuam	Aizawl	23.699722°N; 92.716389°E	1,008 m
16	Tlungvel	Aizawl	23.607500°N; 92.851667°E	1,110 m
17	Tuivamit	Aizawl	23.749167°N; 92.677500°E	861 m
18	Paikhai road	Aizawl	23.560556°N; 92.832222°E	806 m
19	World Bank road	Aizawl	23.730556°N; 92.732778°E	752 m
20	Zohnuai	Aizawl	23.744722°N; 92.696111°E	949 m
21	Lungleng	Aizawl	23.662222°N; 92.664722°E	1,009 m
22	Selesih	Aizawl	23.805278°N; 92.733333°E	1,134 m
23	Durtlang M Suaka Veng	Aizawl	23.781944°N; 92.724167°E	1,123 m
24	Luangmual	Aizawl	23.738889°N; 92.700556°E	943 m
25	Kepran	Aizawl	23.943056°N; 92.932500°E	1,272 m
26	Darlawn	Aizawl	24.016111°N; 92.927778°E	1,050 m
27	Samtlang	Aizawl	23.658889°N; 92.706667°E	867 m

28	Lamchhip	Aizawl	23.436389°N; 92.779722°E	1,320 m
29	Lungsai	Aizawl	23.501389°N; 92.700556°E	868 m
30	NE Bualpui	Aizawl	24.094167°N; 92.683333°E	916 m
31	Saihapui K	Kolasib	24.279722°N; 92.641389°E	50 m
32	Phainuam	Kolasib	24.468056°N; 92.781944°E	64 m
33	Thingdawl	Kolasib	24.160556°N; 92.693056°E	652 m
34	Bilkhawthlir	Kolasib	24.340556°N; 92.718333°E	360 m
35	Vairengte	Kolasib	24.493889°N; 92.759167°E	236 m
36	Kawnpui Hmarveng	Kolasib	24.048889°N; 92.673056°E	854 m
37	Buhchangphai	Kolasib	24.334716°N; 92.656246°E	42 m
38	Khawzawl	Khawzawl	23.527500°N; 93.187500°E	1,137 m
39	New Chalrang	Khawzawl	23.380000°N; 93.133333°E	1,276 m
40	Tlabung	Lawngtlai	22.915000°N; 92.475278°E	183 m
41	Tlabung Chawnpui	Lawngtlai	22.903611°N; 92.485278°E	236 m
42	Chawngte	Lawngtlai	22.626111°N; 92.642500°E	76 m
43	Mamit	Mamit	23.933333°N; 92.493333°E	722 m
44	Reiek	Mamit	23.693611°N; 92.606389°E	1,220 m
45	Vaipuanpho	Mamit	92.606389°N; 92.642500°E	451 m
46	Rawpuichhip	Mamit	23.784167°N; 92.558611°E	804 m
47	Lengte road	Mamit	23.816944°N; 92.603889°E	480 m
48	Lungphunlian	Mamit	23.590278°N; 92.604167°E	1,000 m
49	Kanghmun	Mamit	23.556752°N; 92.575564°E	970 m
50	Dampa Tiger Reserve	Mamit	23.701944°N; 92.446111°E	260 m
51	Champhai Vengsang	Champhai	23.480273°N; 93.311896°E	1,646 m
52	N. Vanlaiphai	Serchhip	23.123889°N; 93.060278°E	1,351 m
53	Rullam	Serchhip	23.444444°N; 92.999722°E	1,433 m
54	Thenzawl Vengthlang	Serchhip	23.283056°N; 92.774444°E	757 m
55	Chhiahtlang	Serchhip	23.379722°N; 92.846111°E	971 m
56	Tawipui South	Lunglei	22.673889°N; 92.845833°E	975 m
57	Serkawn	Lunglei	22.908889°N; 92.761111°E	1,142 m
58	Darzo	Lunglei	22.832778°N; 92.957222°E	1,366 m

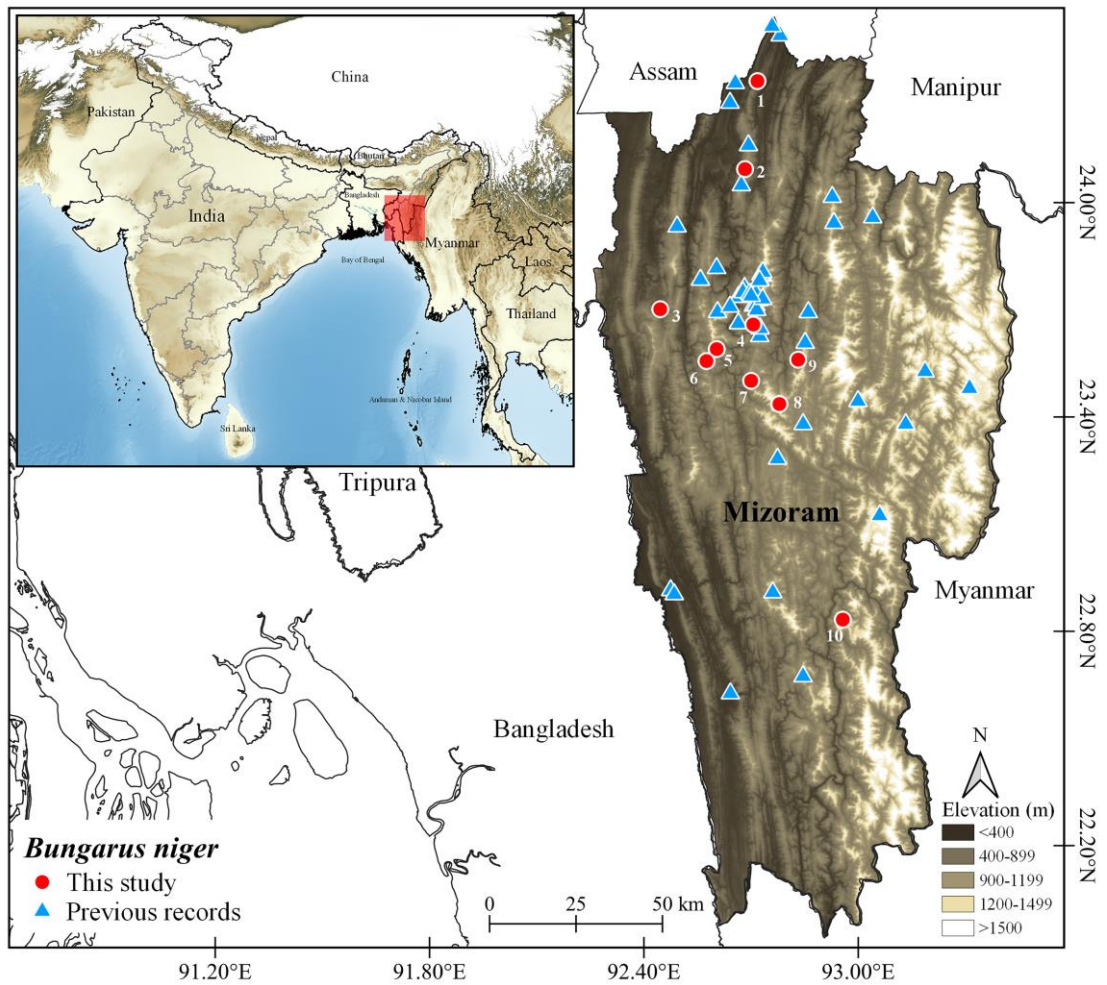


Figure 2.13. Digital elevation map showing the distributional records of *Bungarus niger* in Mizoram. The previous records fide Lalbiakzuala (2019) are given in blue triangles, and the new records from this work are given in red circles: 1. Bilkhawthlir; 2. NE Bualpui; 3. Dampa Tiger Reserve; 4. Samtlang; 5. Lungphunlian; 6. Kanghmun; 7. Lung sai; 8. Lamchhip; 9. Paikhai road; 10. Darzo.

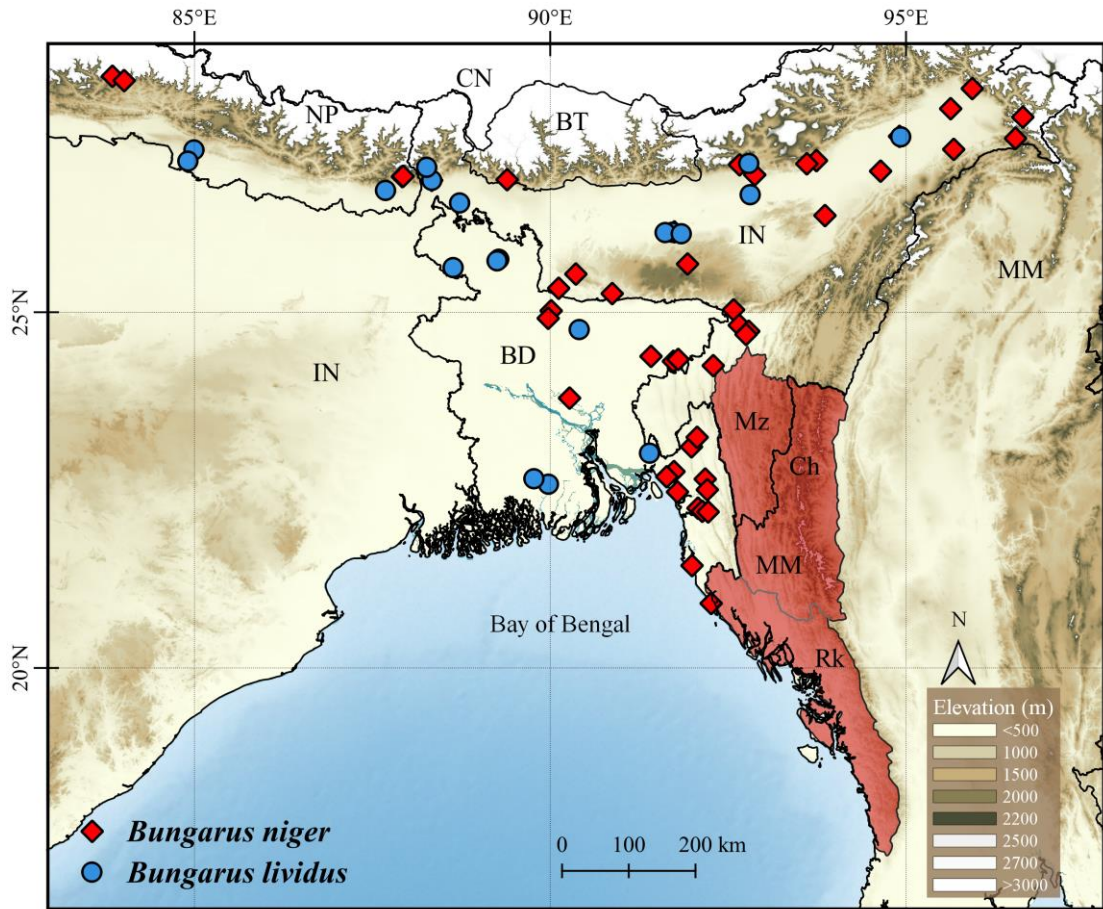


Figure 2.14. Distributional records of *Bungarus niger* (in red diamond and red shaded) and *Bungarus lividus* (in blue dots). Distribution in Chin and Rakhine States in Myanmar is based on Leviton et al. (2008), and Mizoram (Mz) State in India is based on this study and Lalbiakzuala (2019). Abbreviations: India (IN), Mizoram state (Mz); Bangladesh (BD); Myanmar (MM), Rakhine state (Rk), Chin state (Ch); Nepal (NP); Bhutan (BT); China (CN).

Natural History

B. niger is known to be an ophiophagus and nocturnal snake. During this study, the species was usually encountered between ca. 18:00 hrs and 02:00 hrs, and rarely during the daytime. In wild, a male individual was observed preying on adult *Smithophis atemporalis* on 23 September 2020 at ca. 22:00 hrs on a tarmac road at Paikhai road, Mizoram, India (23.560556° N, 92.832222° E; ca. 806 m asl.; Fig. 2.15). In captivity, the species was observed feeding on *Argyrophis diardi*, adult *Psammodynastes pulverulentus*, sub-adult *Trimeresurus erythrurus* and *Oligodon albocinctus*. For the first time, the species was also observed feeding on Indian Forest Skink (*Sphenomorphus indicus*; MZMU2990; SVL 756 mm), a non-ophiophagic diet on 1st September 2022 at 2336 h on the roadside within Synod Hospital Campus, Durtlang, Mizoram, India (23.77422° N, 92.73127° E; 1,244 m asl.).

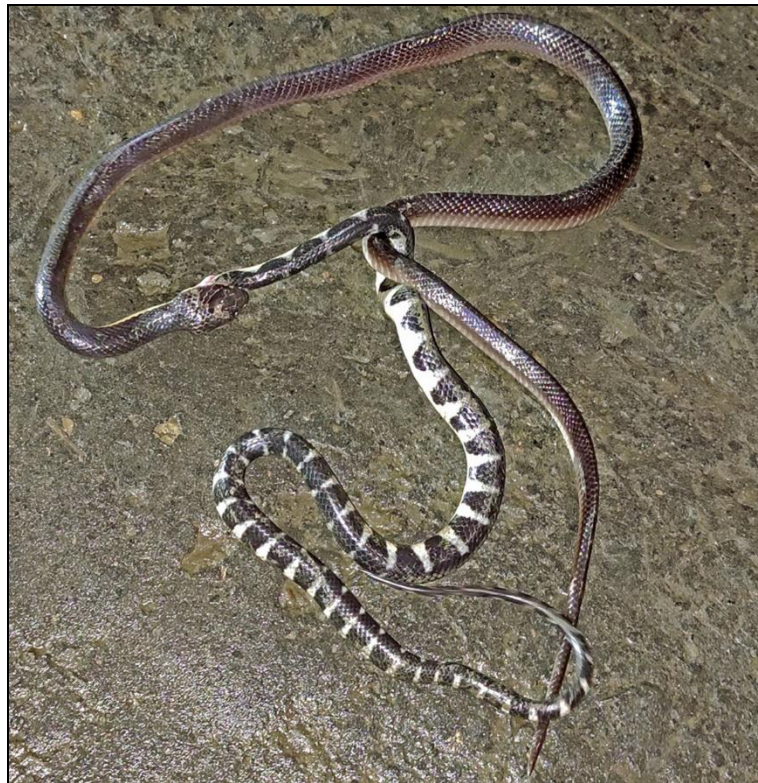


Figure 2.15. Adult male *B. niger* preying on adult *Smithophis atemporalis* at Paikai road, Mizoram, NE India. Photo credit: Roluahpuia.

Discussion

Systematics. *B. niger* commonly known as Greater black krait, is a species morphologically similar to its sister species *B. lividus*, and were even assumed as a sister species according to morpho-based phylogenetic inference (Slowinski 1994). But, from the recent work by Biakzuala et al. (2021) and the present molecular phylogenetic evidences suggested that these two species are not actually sister taxa because they constitute distant lineages where *B. niger* is showing close phylogenetic relationship with the least inter-specific genetic divergence from the Southeast Asian kraits such as *B. suzhenae* (9.4% in *nd4*), *B. candidus* (2.9–3.6% in *16s*), and *B. wanghaotingi* (8.5–10% in *cytb*); while *B. lividus* is showing close phylogenetic relationship with the least inter-specific genetic divergence (in *cytb*) from the kraits of Indian subcontinent such as *B. caeruleus* (11.3%), and *B. ceylonicus* (11.3%). The phylogenetic trees from Biakzuala et al. (2021), this thesis work and the tree from the recent publication from the genus *Bungarus* (Aksornneam et al. 2024) depicted the distant relationship between *B. niger* and *B. lividus*, all of which contradicted with the morphology-based phylogeny of the genus proposed by Slowinski (1994) particularly on the phylogenetic position of *B. niger* and *B. lividus*. However, the phylogenetic tree from Aksornneam et al. (2024) showed unresolved relationships with evidence of polytomy particularly between the kraits of Indian subcontinent and Southeast Asia which is likely due to insufficient genetic information. Concerning this, the phylogenetic relationship between these two lineages (Indian subcontinent and Southeast Asian) is regarded as resolved to a considerable degree in this chapter (UFB=100; PP=1.0).

Nevertheless, *B. niger*, a species originally described from Tindharia, Darjeeling District of West Bengal in India is diagnosable from *B. lividus* in the vertebral row of dorsal scales, where they were much enlarged and were broader than long (vs. vertebral row of dorsal scales feebly enlarged and not broader than long in *B. lividus*); greater number of Ve (214–231 vs. 209–221 in *B. lividus*) and Sc (48–56 vs. 35–43 in *B. lividus*) and larger body size i.e 1,200 mm in *B. niger* vs. 1,020 mm in *B. lividus* (Smith 1943). The meristics on *B. niger* reveal a new lower limit in the Ve range i.e 214–228 vs. 216–231 (Smith 1943). Moreover, the anomalous specimen

(MZMU2030) recorded in this work not only represents the longest specimen among the examined specimens, but also divulged a new record of total length for the species i.e 1313 mm (SVL=1175 mm, TaL=138 mm) vs. 1200 mm fide Smith (1943).

Distribution and natural history. *Bungarus niger* is known to inhabit evergreen and moist deciduous forests, grasslands, plantations, and human habitation (Ahmed et al. 2009) at the elevation range up to 42–1,646 m asl. (Biakzuala et al. 2019). Based on the present survey in Mizoram, it was further speculated that female *B. niger* are seemingly to be more secretive than the males, as only around 20.4% of our randomly collected specimens during this study period plus the specimens housed in the Departmental Museum of Zoology, Mizoram University collected during ca. 2009 to 2023 were female. The present distributional records documented at the elevations of 260–1,433 m a.s.l. further enlarge the existing distributional data of *B. niger* from Mizoram, NE India and were fall within the elevation range previously recorded (Biakzuala et al. 2019). On the other hand, *B. lividus* can also be regarded as a night-active species occurring at the elevations up to 340 m a.s.l. (Wallach et al. 2014). All the individuals of the species were encountered between 19:00 hrs and 23:00 hrs. In one instance, an individual bit itself on its lower lip and soon after died potentially due to self-inflicting envenomation (Purkayastha et al. in press).

Although the two black kraits are existed sympatrically in some parts of their distribution range especially in Bangladesh, Nepal, and the northern part of Northeast India (Assam, Arunachal Pradesh and Meghalaya), no single specimen or even photographic evidence were obtained for *B. lividus* in Mizoram so far, while *B. niger* can be regarded as a commonly found species throughout the State. Apart from the diet reported in this work, it was also reported to feed on *Coelognathus radiatus* in wild (Biakzuala et al. 2019), and *Trachischium tenuiceps* (Wall, 1923). Biogeographically, populations of *B. niger* were known to occupy Rakhine and Chin States in Myanmar and expanded throughout Northeast India to Bangladesh and up to Nepal; on the other hand, populations of *B. lividus* inhabits Nepal, Bangladesh, some part of Bhutan and in the northern part of Northeast India; while Brahmaputra River seemingly act as a Biogeographic barrier for the population dynamics of *B.*

lividus for their migration further towards south in Northeast India. This chapter altogether provides new insights on the systematics, natural history and distribution of *B. niger*, a poorly studied deadly venomous species which will further aid in the integrated snakebite management standpoint (Mukherji and Mackessy 2021), and for future planning of an effective conservation strategy of the species.

CHAPTER 3

Naja kaouthia Lesson, 1831

Review of literature

The elapid snake genus *Naja* (true cobras) comprises 34 currently recognized species (Uetz et al. 2024; Shi et al. 2022). Earlier, the Asian cobras were regarded as solely represented by a single species *N. naja* sensu lato until the systematics reassessment (Wüster 1996; Wüster et al. 2007, 2018) and nomenclatural re-allocations of the extant true cobras (Wallach et al. 2009) that partitioned them under four subgenera, including 11 species of Asiatic cobras in the subgenus *Naja*, namely *N. naja* (type species); *N. oxiana*; *N. kaouthia*; *N. sagittifera*; *N. atra*; *N. mandalyensis*; *N. siamensis*; *N. sumatrana*; *N. philippinensis*; *N. samarensis*; and *N. sputatrix*. In India, four species of *Naja* (*N. oxiana*, *N. naja*, *N. sagittifera*, and *N. kaouthia*) have been recorded so far (Wüster 1996; Aengals et al. 2018), and the existing records of *Naja* in the study region (Mizoram, Northeast India) are solely represented by *N. kaouthia* (Lalremsanga et al. 2011).

Nomenclatural problems for Asiatic cobras have been stressed that majority of the systematic uncertainty is likely explained by extreme phenotypic plasticity even within populations which often causes problematic identification of species. Consequently, the taxon *N. kaouthia* has also been misidentified in some older literature as *N. naja leucodira*, *N. kaouthia suphanensis* in Thailand, or as *N. naja sputatrix* in Vietnam; while the taxa *N. siamensis*, *N. sagittifera* from Andamans, *N. sumatrana* from northern Malaysia were wrongly considered either as *N. kaouthia* or *N. naja kaouthia*; also, *N. naja siamensis* in some toxinological literature were more likely *N. kaouthia* (sensu Wüster 1996).

The name-bearing type material of *N. kaouthia* is a 2,475 mm specimen which was lost fide Wallach et al. (2014). The type locality was mentioned as “Inde continentale” (=Indian subcontinent) (Wallach et al. 2014); also listed as Bengal, India (Uetz et al. 2024). In India, *N. kaouthia* is found throughout Northeast Indian states, westward through the Indian states of West Bengal, Odhisa, Chhatisgarh, Bihar, Jharkhand, and up to Haryana which likely represents the westernmost range

in the country, and also towards the north from Uttar Pradesh and Uttarakhand (Wallach et al. 2014; Wüster 1996; Stuart and Wogan 2012). Within its known range, the species is found at elevations of 40–1,500 m a.s.l. (Lalremsanga et al. 2011) occupying a wide range of habitat types such as natural to artificial environments including paddy fields, swamps, mangroves, grasslands, shrublands, forests, and even human settlements (Stuart and Wogan 2012). *Naja kaouthia* is presently categorized as Least Concern (LC) species in the IUCN Red List (Stuart and Wogan 2012), and Schedule I under the Wildlife (Protection) Amendment Act (2022) in India.

Even though *N. kaouthia* have been included in the multiple phylogenetic studies of elapid snakes (Slowinski and Wüster 2000; Wüster et al. 2007; Wallach et al. 2009; Pyron et al. 2013b), only a few studies on venomics (Ryabinin et al. 2019) and systematic studies (Kundu et al. 2020a; Ratnarathorn et al. 2019) suggested intra-specific or geographical variability among *N. kaouthia* populations. Also, in the recent most study of the Asian cobras, *N. fuxi* Shi, Vogel, Ding, Rao, Liu, Zhang, Wu, and Chen, 2022 was erected from the populations of China which were previously identified as *N. kaouthia*, thereby a total of 12 Asiatic cobra species are recognized under the subgenus *Naja* so far (Wallach et al. 2009; Shi et al. 2022). Although multilocus-based phylogeographic approaches have been increasingly utilized for a robust systematic study, especially among cryptic taxa (Wüster et al. 2018); mitochondrial DNA has also been implemented as a preliminary test for detecting putative cryptic species (Niemiller et al. 2022); the combination of morphological and mitochondrial DNA data has also been successfully implemented for testing species boundaries and species delineation (Wüster et al. 2007; Malhotra et al. 2011). Moreover, mitochondrial genes are considered to evolve under neutral (or nearly-neutral) selection (Ballard and Kreitman 1995); consequently, they have been widely used in intra-population genetic studies (Consuegra et al. 2015). Although Shi et al. (2022) proposed two distinct clades of *N. kaouthia* based on *cox1* gene which is partly based on the DNA sequences generated in this work from Mizoram viz. the South Asian clade which is represented by populations from Northeast India (based on Mizoram specimens), Nepal, Bhutan, Tibet (China), and Bangladesh; while the

Southeastern Asian clade is represented by the populations from Southern Myanmar, central and southern part of Thailand, Cambodia, central and southern part of Laos, southern part of Vietnam, and the Malay Peninsula. Furthermore, in the recent review by Wüster & Kaiser (2023), it was stressed that formal recognition and description of new species will require sufficient evidences that show the proposed species is distinct evolutionary lineage based on extensive morphological and molecular works. Prompted by the limited availability of biological samples and systematic studies of *N. kaouthia* populations from Northeast (NE) India especially from Mizoram, this chapter aims to reassess the systematic status of *N. kaouthia* population from Mizoram, NE India.

Materials and methods

Sampling

In this study, a total of 28 adult and 16 juvenile specimens were examined. Of these, 33 are preserved specimens housed in the collections of the Departmental Museum of Zoology, Mizoram University (MZMU). From the dead specimens (n=8) which are killed by local people (MZMU982, MZMU998, MZMU1163, MZMU1170, MZMU1195, MZMU1426, MZMU2044, MZMU2415), liver tissue was dissected and stored it in 95% ethanol at -20°C for molecular analyses. Then, the specimens were initially fixed overnight in 10% formalin and later stored in 70% ethanol. In addition to preserved specimens, a total of 11 live individuals were examined which were subsequently released after taking morphological data.

DNA extraction and PCR amplification

Genomic DNA was extracted from liver using DNeasy (Qiagen™) blood and tissue kits following the manufacturer's instructions (DNeasy® Blood & Tissue Handbook 2023). Fragments of three mitochondrial markers, 16S rRNA (*16s*), cytochrome c oxidase subunit 1 (*cox1*), and cytochrome b (*cytb*) were amplified through Polymerase Chain Reaction (Mullis et al. 1986). Target gene sequences were amplified in a 20 µL reaction volume, containing 1X DreamTaq PCR Buffer, 2.5 mM MgCl₂, 0.25 mM dNTPs, 0.2 pM of each gene primer pair, approximately 3.0 ng of extracted DNA, and 1U of Taq polymerase using the thermal profiles and primers

given in Table 1.1 in Chapter 1. PCR products were checked using gel electrophoresis on a 1.5% agarose gel containing ethidium bromide. The PCR products were cleaned using ThermoFisher ExoSAP-IT PCR product cleanup reagent and subsequently sequenced using Sanger's dideoxy method using the ABI 3730xl DNA Analyzer at Barcode BioSciences, Bangalore, India. The newly generated partial gene sequences were then screened through nucleotide BLAST (<https://blast.ncbi.nlm.nih.gov/>) and ORF finder (<https://www.ncbi.nlm.nih.gov/orffinder/>), and then deposited in the NCBI repository and are available in GenBank via the accession numbers given in Table 3.1. In this work, a total of three *16s*, one *cox1* and three *cytb* sequences were generated and were combined with published sequences of *Naja* species obtained from GenBank; the sequence of *Bungarus fasciatus* (MZMU1883) was used as the outgroup.

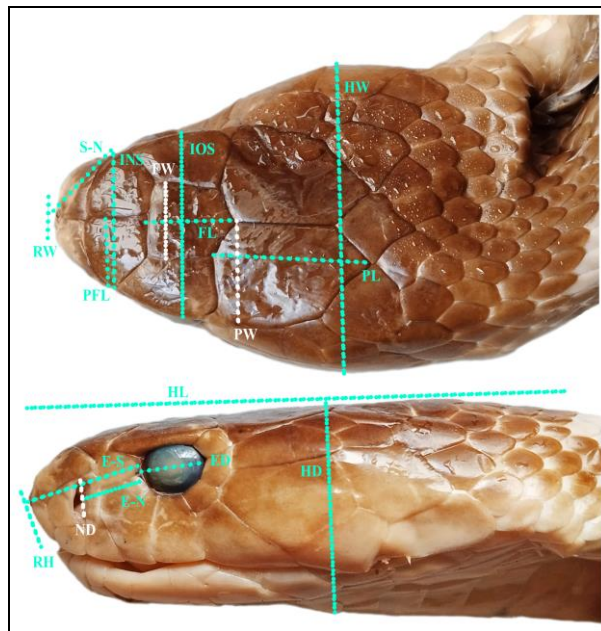


Figure 3.1. Description of head morphometrics used in *Naja kaouthia*: (top) width of head (HW), width of rostral (RW), snout to nostril distance (S-N), length of internarial (INL), width of internarial (INW), internarial space (INS), length of prefrontal (PFL), width of prefrontal (PFW), length of frontal (FL), width of frontal (FW), length of parietal (PL), width of parietal (PW); (below) length of head from tip of snout to angle of jaw (HL), depth of head (HD), horizontal eye diameter (ED), eye to snout distance (E-S), eye to nostril distance (E-N), and rostral height (RH).

Table 3.1. Details of three mitochondrial genes utilized in this study. Abbreviations for species names: *Naja kaouthia* (NK), *N. atra* (NA), *N. annulata* (NAN), *N. sumatrana* (NS), *N. naja* (NN), *N. oxiana* (NO), *N. haje* (NH), *N. annulifera* (NAF), *N. nivea* (NNV), *N. ashei* (NAS), *N. mossambica* (NMO), *N. mandalayensis* (NMA), *N. philippinensis* (NP), *N. sputatrix* (NSX), *N. savannula* (NSV), *N. siamensis* (NSM), and *Bungarus fasciatus* (BF).

Species	Voucher	<i>16s</i>	<i>cox1</i>	<i>cytb</i>	Locality	References
NK	MZMU2415	PP152337	-	PP162903	Mizoram,India	This study
NK	MZMU2044	OP068310	-	PP162902	Mizoram,India	This study
NK	MZMU1426	PP152338	MT348389	PP162904	Mizoram,India	This study
NK	MZMU1195	-	MT348390	-	Mizoram,India	This study
NK	MZMU1170	-	MT348387	-	Mizoram,India	This study
NK	MZMU1163	-	MT348385	-	Mizoram,India	This study
NK	MZMU998	-	MT348388	-	Mizoram,India	This study
NK	MZMU982	-	MT348386	-	Mizoram,India	This study
NK	CHS726	MK194174	MK064840	MK201489	China	Li et al. 2020
NK	CHS026	MK193893	MK064598	MK201244	China	Li et al. 2020
NK	NA	KX277260	-	-	-	Simoese et al. 2016
NK	NA	JF357948	-	-	-	Lukoschek et al. 2012
NK	NA	JN687925	-	-	Thailand	Suntrarachun et al. 2011
NK	Isolate WW585	GQ359757	-	GQ359507	Chumphon Province, Thailand	Pook et al. 2009
NK	KIZYPX18216	MW019917	-	MW111477	China	Xu et al. 2020
NK	NA	LC431744	LC431744	LC431744	Thailand	Singchat et al. 2019
NK	Isolate 839	-	-	MT346708	Myanmar	Kazandjian et al. 2021

Table 3.1. Continued.

Species	Voucher	<i>16s</i>	<i>cox1</i>	<i>cytb</i>	Locality	References
NK	Isolate 818	-	-	MT346707	Thailand	Kazandjian et al. 2021
NK	Isolate 813	-	-	MT346706	Vietnam	Kazandjian et al. 2021
NK	Isolate 812	-	-	MT346705	Vietnam	Kazandjian et al. 2021
NK	-	-	-	FR693728	-	Melaun and Kuch 2010
NK	HS16001	-	-	KU527540	China	Yang et al. 2016
NK	BDS81	-	KM521202	-	Bangladesh	Rahman et al. 2014
NA	CIB093930	EU913475	EU913475	EU913475	China	Chen and Fu 2008
NA	CHS781	MK194217	-	MK201524	China	Li et al. 2020
NA	CHS607	MK194091	MK064771	MK201431	China	Li et al. 2020
NAN	NA	AY188049	-	AY188010	-	Nagy et al. 2003
NAN	Isolate 1305	-	-	MT346699	Congo	Kazandjian et al. 2021
NAN	Isolate 2717	-	-	MT346700	Congo	Kazandjian et al. 2021
NS	Isolate 1827	-	-	MT346738	Philippines	Kazandjian et al. 2021
NS	Isolate 188	-	-	MT346732	Malaysia	Kazandjian et al. 2021
NN	NA	NC_010225	NC_010225	NC_010225	-	Yan et al. 2008
NN	Isolate 595	-	-	DQ897733	Nepal	Wuster et al. 2007
NN	Isolate 580	-	-	MH337569	Sri Lanka	Wuster et al. 2007
NN	Isolate 579	GQ359756	-	GQ359506	Nepal	Pook et al. 2009
NN	ABTC:32465	EU547137	-	-	-	Sanders et al. 2008
NN	Isolate GM5	MN548731	-	-	Punjab: India	Santra et al. 2019
NN	ZMUVAS21	-	MK941841	-	Pakistan	Ali et al. 2019

Table 3.1. Continued.

Species	Voucher	<i>16s</i>	<i>cox1</i>	<i>cytb</i>	Locality	References
NN	BDS80	-	KM521201	-	Bangladesh	Rahman et al. 2014
NN	DUZM S052.1	-	MT215095	-	Dhaka: Bangladesh	Islam et al. 2020
NO	Isolate 838	-	-	MT346714	-	Kazandjian et al. 2021
NO	Isolate 832/WW832	MN648780	-	MT346713	-	Kazandjian et al. 2021; Santra et al. 2019
NO	Isolate 17.v18	MN548728	-	-	Himachal Pradesh, India	Santra et al. 2019
NH	IPMB J141	AY611811	-	AY611994	-	Nagy et al. 2007
NH	Isolate 1079	GQ359751	-	GQ359502	Mali	Pook et al. 2009
NAF	Isolate 881	GQ359753	-	AF155216	Zimbabwe	Slowinski & Wuster 2000
NAF	Isolate 193	-	-	MT346743	South Africa	Kazandjian et al. 2021
NNV	Isolate 1295	GQ359755	-	AF217827	-	Slowinski & Keogh 2000
NNV	Isolate 1482	-	-	MT346760	South Africa	Kazandjian et al. 2021
NAS	Isolate 1430	GQ359742	-	GQ359493	Kenya	Pook et al. 2009
NAS	Isolate 1394	-	-	MT346647	Kenya	Kazandjian et al. 2021
NMO	Isolate 190	GQ359744	-	GQ359495	Mozambique	Pook et al. 2009
NMA	Isolate 593	-	-	MT346710	Myanmar	Kazandjian et al. 2021
NMA	Isolate 592	-	-	MT346709	Myanmar	Kazandjian et al. 2021
NP	Isolate 1828	-	-	MT346719	Philippines	Kazandjian et al. 2021
NP	Isolate 1800	-	-	MT346715	Philippines	Kazandjian et al. 2021
NSX	Isolate 584	-	-	MT346730	Indonesia	Kazandjian et al. 2021
NSX	Isolate 583	-	-	MT346729	Indonesia	Kazandjian et al. 2021
NSV	Isolate 2495	-	-	MH337602	Senegal	Wuster et al. 2018

Table 3.1 Continued.

Species	Voucher	<i>16s</i>	<i>cox1</i>	<i>cytb</i>	Locality	References
NSV	Isolate 1085	-	-	MH337597	Ghana	Wuster et al. 2018
NSM	Isolate 811	-	-	MT346728	Vietnam	Kazandjian et al. 2021
NSM	Isolate 810	-	-	MT346727	Vietnam	Kazandjian et al. 2021
BF	MZMU1883	OQ256169	OQ256190	OQ266796	Mizoram,India	This study

Molecular phylogenetics

DNA sequences were aligned with the default parameter settings of MUSCLE algorithm (Edgar 2004) in MEGA 11 (Tamura et al. 2021); for the *16s* dataset, the ambiguously aligned sites were removed under heuristic method in trimAL software (Capella-Gutiérrez et al. 2009). The three mitochondrial gene alignments were concatenated, and were partitioned by gene and codon positions. Uncorrected p-distances were estimated in MEGA 11 (Tamura et al. 2021) using the complete deletion option for the treatment of gaps/missing data. PartitionFinder v2.1 (Lanfear et al. 2017) was utilized to search for the optimal partitioning schemes and nucleotide evolutionary models through Bayesian Information Criterion (BIC). A Bayesian inference (BI) phylogeny was reconstructed by applying the best partitioning schemes and nucleotide evolutionary models in Mr.Bayes v3.2.5 (Ronquist et al. 2012). The MCMC was run with four chains (one cold and three hot chains) for 20 million generations and sampled every 5000 generations. Tracer v1.7 (Rambaut et al. 2018) was used to check the convergence of likelihood and the burn-in cut-off. Maximum likelihood (ML) phylogenetic tree was inferred using the IQ-TREE webserver (Nguyen et al. 2015) by selecting FreeRate heterogeneity (Soubrier et al. 2012) and 10,000 Ultrafast Bootstrap (UFB) replicates (Minh et al. 2013) using the partitions identified by PartitionFinder v2.1 (Lanfear et al. 2017), and the models selected based on BIC values by ModelFinder (Kalyaanamoorthy et al. 2017) integrated into the IQ-TREE (Nguyen et al. 2015). The phylogenetic trees were viewed and illustrated using web-based tree annotator iTOL software v5 (Letunic and Bork 2021).

Matrilineal haplotype networks

The three mitochondrial DNA sequences were utilized to screen the matrilineal genealogy among populations through mitochondrial DNA-based haplotype estimation. The three datasets were imported to MEGA 11 (Tamura et al. 2021), and the sequences were trimmed to the same length at 465 bp for *16s*, 561 bp for *cytb* and 621 bp for *cox1* datasets. The aligned datasets were utilized for generating haplotypes in DnaSP v.6 (Rozas et al. 2017), and the trait matrix corresponding to the locality of the samples was inserted in the output file. The

haplotype networks were plotted in PopArt v.1.7 (Leigh and Bryant 2015) using the Median-Joining method, which is a useful statistical approach for intra-species haplotype networks (Bandelt et al. 1999). Because *N. fuxi* was only erected as a new species during the processing of this work, they are included in the haplotype estimation to further corroborate the identity of the aforesaid taxon.

Species delimitation

The three gene datasets, partitioned by codon positions were also utilized for performing a single locus-based Assemble Species by Automatic Partitioning (ASAP) (Puillandre et al. 2021). This approach assembles species partitions based on the probabilities and barcode gap width; these two metrics are combined into a single ASAP-score for ranking the partitions, the lower the ASAP-score, the better the partition. The standardized p-distances were further utilized for Principal Coordinate Analysis (PCoA) (Gower 1966) to visualize the genetic differentiation among the target taxa in PAST 4.13 (Hammer et al. 2001).

Morphology

Morphometric (mensural and meristic) data were obtained from the 44 individuals examined from the *N. kaouthia* population of Mizoram. Except snout–vent length (SVL, measured from tip of snout to anterior margin of vent) and tail length (TaL, measured from anterior margin of vent to tail tip) which were measured with a measuring tape, the following mensural characters were measured to the nearest millimetre with a Mitutoyo digital caliper (Fig. 3.1): eye diameter (ED, horizontal diameter of orbit); nostril diameter (ND, largest diameter of nostril); eye–nostril length (E-N, distance between posteriormost point of nostril and anteriormost point of eye); eye–snout length (E-S, distance between anteriormost point of eye and tip of snout); snout–nostril length (S-N, distance between tip of snout and anteriormost point of nostril); head length (HL, distance between posterior edge of mandible and tip of snout); head width (HW, maximum width of head); height of rostrum (RH, the height of rostral scale); width of rostrum (RW, the width of rostral scale); internarial space (INS, distance between the nostrils); interorbital space (IOS, distance between the orbits); internarial length (INL, length of internarial scale); internarial width (INW, width of internarial scale); prefrontal length (INL, length of

internarial scale); frontal length (FL, length of frontal scale); frontal width (FW, width of frontal scale); parietal length (PL, length of parietal scale); parietal width (PW, width of parietal scale). Meristic characters were taken as follows: supralabials (SL); supralabials touching eye (SLe); infralabials (IL) (first labial scale to last labial scale bordering gape); temporals (Tem), postocular (PoO); preocular (PrO); anal scute (As); dorsal scale rows (DSR, counted around the body from one side of ventrals to the other in three positions, on one head length behind the neck, at midbody and at one head length before cloacal plate); when counting the number of ventral scales (Ve), the values were scored following Dowling (1951). Subcaudal scales (Sc) were counted from the first subcaudal scale meeting its opposite to the scale before the tip of the tail excluding the terminal scute. The sex of the specimens was identified by examining everted hemipenes or by ventral tail dissection. Values for bilateral head characters are given in left/right order. Other than the conventional taxonomic characters, relevant morphological parameters which have been utilized by Wüster et al. (1995) were adopted and tested for sexual dimorphism along with intraspecific morphological variation.

Sexual dimorphism

The morphological information was obtained from various localities in Mizoram state, India. Prior to conducting any further statistical analyses, missing values for the variables were calculated and maintained below 30% by removing specimens with high amount of missing data. To avoid the effect of life stages in the analyses, the samples were broadly categorized into two life stage groups: individuals with SVL > 1,000 mm were grouped as adult, while those SVL < 1,000 were grouped as juvenile. The meristic data were standardized first to their zero mean and standard deviation. For mensural data, the best allometric adjustment model was determined based on the best linear regression model which gives the highest within-group correlation to make a linear relationship with body size to avoid the effect of allometric growth (Thorpe 1975). Firstly, the meristics data (Ve and Sc) of adults and juveniles were tested for sexual dimorphism utilizing a separate one-way analysis of variance (ANOVA) for both life stages using sex as a factor along with Levene's test (Levene 1961) for testing homogeneity of variances. Brown-

Forsythe test (Brown and Forsythe 1974) was also tested as an alternative approach in case the assumption of homoscedasticity was violated. For mensural (TaL, HL, HW, HD, ED, ND, E-S, N-S, N-E, RH, RW, INS, IOS, INL, INW, PFL, PFW, FL, FW, PL, and PW), one-way analysis of covariance (ANCOVA) was carried out with snout-vent length (SVL) as a covariate and sex as a factor.

Intraspecific morphological variation

To obtain a statistically operable sample for the test of intraspecific phenotypic variation, the samples with a distinct form of hood markings were pooled. The phenotypic groups were therefore defined *a priori*; individuals with a monocellate mark which may vary in size and shape are grouped as typical, while individuals that have the different forms of hood markings are pooled and defined as a variant. Then, standardized meristic characters (Ve and Sc) were analysed using one-way ANOVA separately for the two life stages (adult and juvenile) using phenotypic grouping as a factor; and Levene's test (Levene 1961) was conducted to test the homogeneity of variances. Brown-Forsythe test (Brown and Forsythe 1974) was also performed to be utilized as an alternative approach in case the assumption of homoscedasticity was violated. For mensural, one-way ANCOVA was performed using the adjusted variables (TaL, HL, HW, HD, ED, ND, E-S, N-S, N-E, RH, RW, INS, IOS, INL, INW, PFL, PFW, FL, FW, PL, and PW) with SVL as a covariate and phenotypic grouping as a factor. To avoid the effect of sexual size differences; the sexually dimorphic characters were analyzed separately for both sexes in the ANOVA and ANCOVA.

Principal component analysis

The sexually dimorphic and intraspecifically different characters identified through the univariate analyses were analysed through Principal component analysis (PCA). The correlation matrices between all pairs of the morphological variables, variance explained by each eigenvalue as well as the correlations of each variable to the first two components are explored. All statistical analyses and graphical representations were performed using free access statistical packages viz. PAST 4.13 (Hammer et al. 2001) and PSPP v.1.6.2 (GNU Project 2015).

Results

Phylogenetic relationships

The best partitioning schemes and nucleotide evolutionary models selected for the two types of phylogenetic inferences were provided in (Table 3.2). The concatenated aligned matrix of *16s*, *cox1*, and *cytb* was 4,198 bp in length; the flanking gaps created by shorter nucleotide sequences were treated as missing data. The BI and ML trees were largely congruent in their topology (Fig. 3.1). The first 25% of trees from the BI analysis were discarded as burn-in, and the average standard deviation of split frequencies among the four Bayesian runs was 0.020811 with the combined values of ESS = 11660.1; the Bayesian posterior probability (PP) values are interpreted as the nodal support in the BI tree (Fig. 3.3). The concatenated three mitochondrial genes based phylogenetic analyses depicted a well-supported (PP=0.99; UFB=93) lineage diversification among *N. kaouthia* populations showing two independent lineages, the South Asian Clade containing populations from Northeast India (Mizoram) and Bangladesh; and the Southeastern Asian Clade which accommodates the populations from Myanmar, China, Vietnam, Thailand, and unknown sample locality. Based on the known range of *N. kaouthia* (Uetz et al. 2023; Wallach et al. 2014; Ratnarathorn et al. 2019; Wüster et al. 1995), our estimated range for the two putative independent lineages of the species recovered in this study is mapped using QGIS 3.16.2.

Table 3.2. Nucleotide substitution model selected for the BI and ML phylogenetic analyses.

Partitions	Sites	BI	ML
I	<i>16s</i>	TRN+I+G	TN+F+G4
II	<i>cox1</i> pos1	TRNEF	TNe
III	<i>cox1</i> pos2, <i>cytb</i> pos2	HKY+I	HKY+F+I
IV	<i>cox1</i> pos3, <i>cytb</i> pos3	TRN+G	TIM3+F+G4
V	<i>cytb</i> pos1	HKY+G	HKY+F+G4

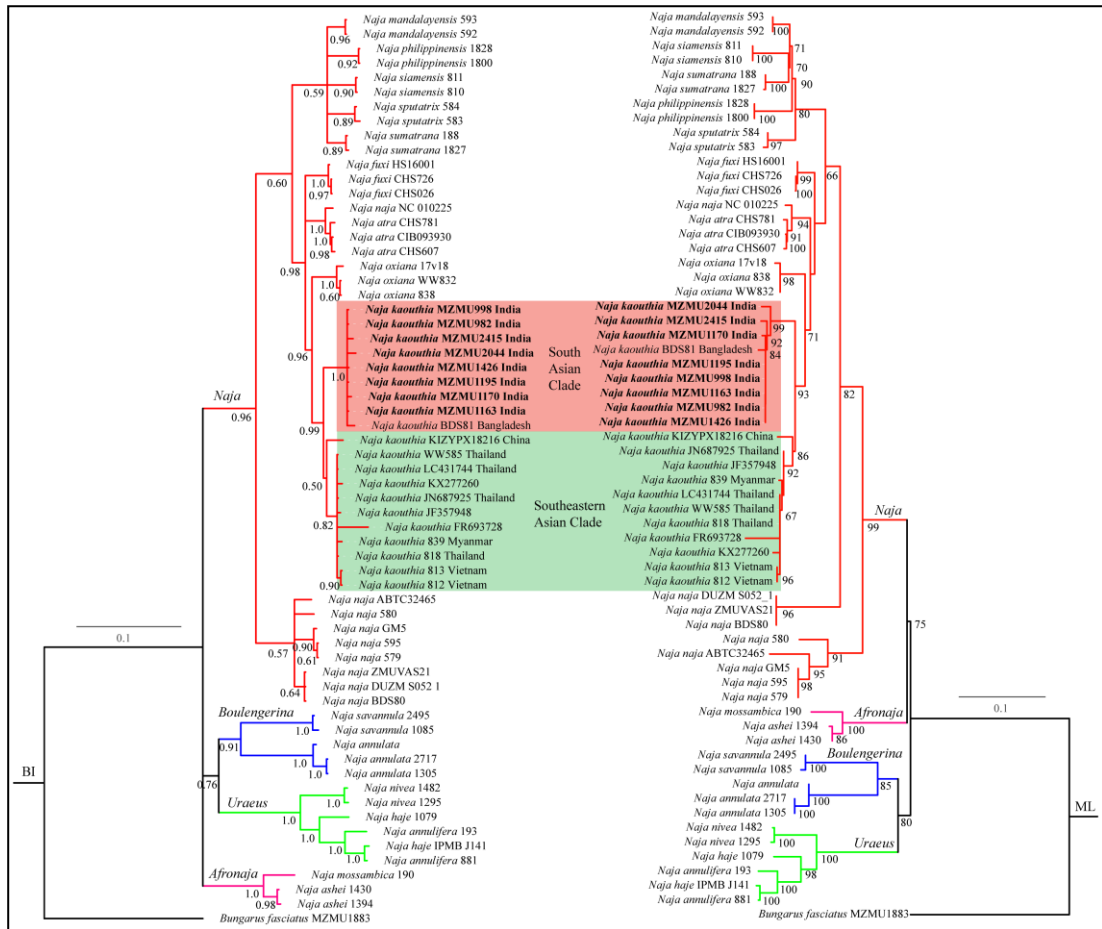


Figure 3.2. Bayesian Inference (left) and Maximum likelihood (right) phylogenetic trees of *Naja* species inferred based on the concatenated *16s*, *cox1* and *cytb* genes. For the nodal supports, Bayesian posterior probabilities >0.50 from the BI analysis and ultrafast bootstrap values >50 from the ML analysis are shown.

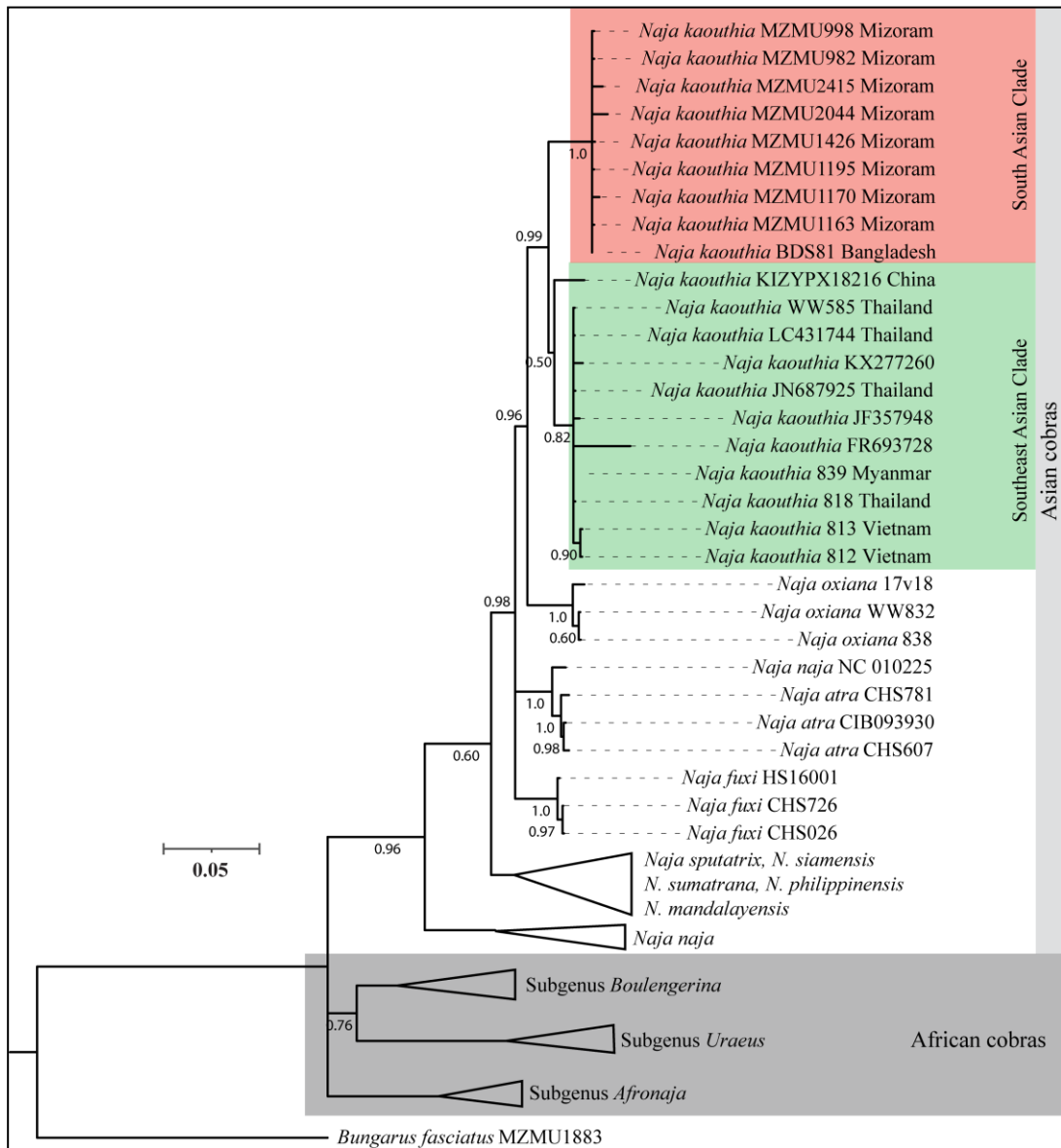


Figure 3.3. Bayesian inference (BI) phylogenetic tree based on concatenated mitochondrial *16s*, *cox1* and *cytb* genes. Values at each node represent Bayesian posterior probabilities (PP).

Species delimitation

The ASAP species delimitation was conducted for the three mitochondrial genes separately and produced 10 distinct species partitions each in *16s* and *cytb*, and 9 distinct partitions in *cox1*. In *16s*, the optimal partitions (Group 1; ASAP score=1.0) detected *N. kaouthia* from Mizoram as distinct species while detecting the conspecific specimens from Thailand (JN687925; LC431744; WW585) and unknown locality (KX277260; JF357948) as single species distinct to Mizoram specimens; while detecting the specimen from China (KIZYPX18216) is detected as distinct to both Mizoram and other populations from Thailand and unknown locality (Fig. 3.4). In *cox1*, the optimal partition (Partition 4; ASAP score=1.0) detected the Mizoram specimens of *N. kaouthia* along with the specimen from Bangladesh (BDS81) as distinct species, while the specimen from Thailand (LC431744) is detected as distinct to the aforementioned specimens (Fig. 3.4). In *cytb*, the optimal partition (Partition 6; ASAP score=1.0) detected the Mizoram specimens of *N. kaouthia* as distinct species to the specimens from Thailand (WW585; LC431744; 818), Vietnam (812; 813), Myanmar (839), and unknown locality (FR693728) as distinct species, while detecting the specimen from China (KIZYPX18216) as distinct to all the aforementioned specimens (Fig. 3.5).

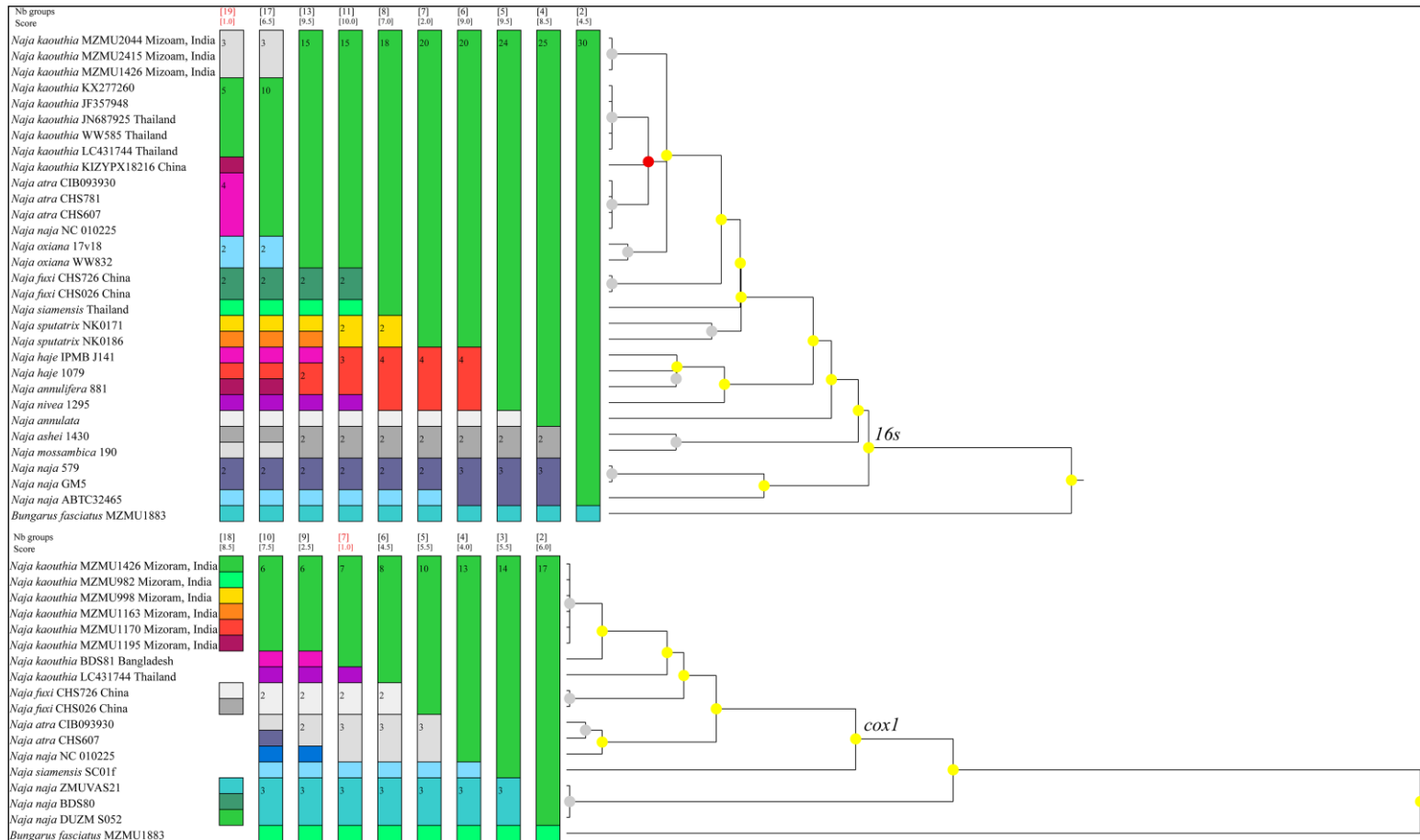


Figure 3.4. Species delimitation by Assemble Species by Automatic Partitioning (ASAP) using *16s* (top) and *cox1* (bottom) gene fragments of the genus *Naja* with *Bungarus fasciatus* as outgroup. The Neighbour-joining cladogram (right) concorded to the ASAP partitions (left).

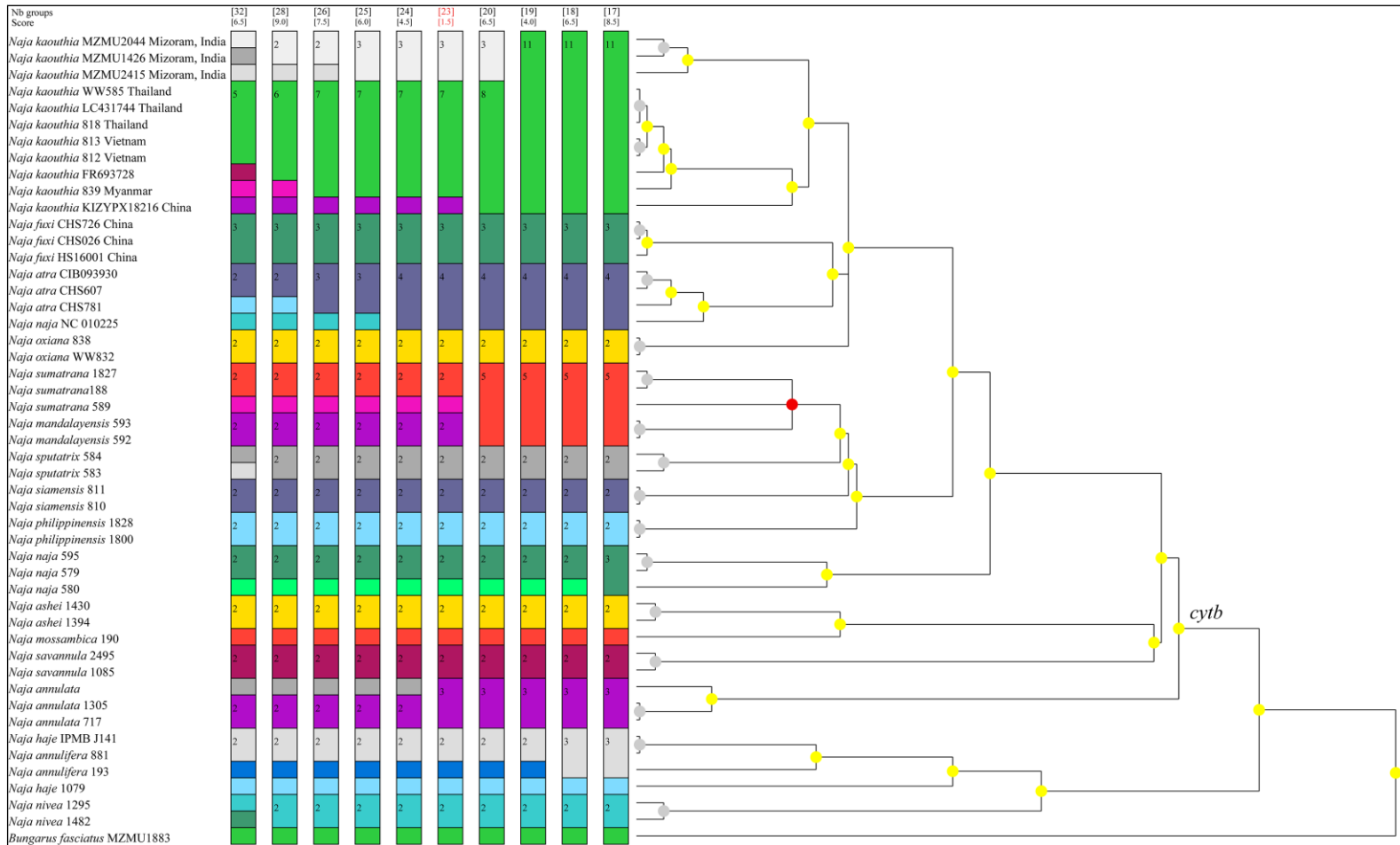


Figure 3.5. Species delimitation by Assemble Species by Automatic Partitioning (ASAP) using *cytb* gene fragments of the genus *Naja* with *Bungarus fasciatus* as outgroup. The Neighbour-joining cladogram (right) concurred to the ASAP partitions (left).

Genetic divergence and haplotype estimation

The gathered dataset of 14 *cytb* sequences identified a total of 65 variable sites with 10 haplotypes (Hap), and haplotype diversity (Hd)=0.9451. The three samples from the studied population (Mizoram) accounted for three distinct Haplotypes (Hap 1–3) separated by 3–6 mutations with genetic divergence of 0.5–1.6% across them (uncorrected p-distance estimated using untrimmed 1,117 bp dataset); Hap 4 is represented by two samples of recently discovered *N. fuxi* from China (CHS026; CHS726) with a genetic divergence of 4.6–5.7% from the studied population (the genetic divergence between the other haplotypes and the studied population is given in parenthesis from this point onwards); Hap 5 comprised of the three samples from Thailand such as 818, WW585, and LC431744 (genetic divergence=3.7–4.8%); Hap 6 is represented by the Chinese sample KIZYPX18216 (genetic divergence=3.9–5.0%); Hap 7 is represented by the Myanmar specimen 839 (genetic divergence=3.7–4.8%); the two Vietnam specimens 812 and 813 formed the Hap 8 (genetic divergence=3.9–5.0%); Hap 9 is the sample from unknown locality (genetic divergence=4.3–5.3%); and Hap 10 is the Chinese sample of *N. fuxi* HS16001 (genetic divergence=4.8–5.9%) (Fig. 3.6; Table 3.3).

Table 3.3. Uncorrected p-distance estimate among the different haplotypes recovered in *cytb* dataset.

Haplotypes	Hap 1	Hap 2	Hap 3	Hap 4	Hap 5	Hap 6	Hap 7	Hap 8	Hap 9
Hap 1									
Hap 2	0.016								
Hap 3	0.005	0.011							
Hap 4	0.052	0.057	0.046						
Hap 5	0.043	0.048	0.037	0.062					
Hap 6	0.045	0.05	0.039	0.068	0.034				
Hap 7	0.043	0.048	0.037	0.066	0.007	0.034			
Hap 8	0.045	0.05	0.039	0.064	0.002	0.036	0.009		
Hap 9	0.048	0.053	0.043	0.068	0.005	0.039	0.012	0.007	
Hap 10	0.053	0.059	0.048	0.002	0.064	0.066	0.068	0.066	0.07

In the scenario of *coxI* dataset (10 sequences), a total of 621 bp remained after trimming to the same length with 26 variable sites, and showing four distinct Hap with Hd=0.6444. The studied population (Mizoram) is accommodated into a single haplotype (Hap 1) with an overall mean genetic divergence of 0.2%. Hap 2 is constituted by the two samples from China CHS026 and CHS726 (genetic divergence=2.6%); Hap 3 is represented by Vietnam sample LC431744 (genetic divergence=1.9%); and Hap 4 is the sample from Bangladesh BDS81 (genetic divergence=0.6%) (Fig. 3.6; Table 3.4).

Table 3.4. Uncorrected p-distance estimate among the different haplotypes recovered in *coxI* dataset.

Haplotypes	Hap 1	Hap 2	Hap 3
Hap 1			
Hap 2	0.023		
Hap 3	0.019	0.029	
Hap 4	0.006	0.029	0.026

In the *I6s* dataset (11 sequences), a total of 465 bp remained after trimming to the same length with 10 variable sites, four distinct Hap and Hd=0.7455. The overall mean genetic divergence is 0.0% within each of the four haplotypes. The studied population (Mizoram) formed the Hap 1; Hap 2 is constituted by the two samples from China CHS026 and CHS726 (genetic divergence=1.7%); Hap 3 consisted of the three Thailand samples LC431744, WW585 and JN687925, and the two samples from unknown locality JF357948 and KX277260 (genetic divergence=0.7%); and Hap 4 is represented by the other sample from China KIZYPX18216 (genetic divergence=1.2%) (Fig. 3.6; Table 3.5).

Table 3.5. Uncorrected p-distance estimate among the different haplotypes recovered in *I6s* dataset.

Haplotypes	Hap 1	Hap 2	Hap 3
Hap 1			
Hap 2	0.017		
Hap 3	0.007	0.015	
Hap 4	0.012	0.020	0.005

The uncorrected p-distance estimated using *cytb* (1,117 bp) dataset (unless indicated for *cox1* and *I6s* in parenthesis) showed overall mean intra-clade genetic divergence of 1.1% (0.2% in COI; 0.0% in *I6s*) within Clade I (Indo-Bangladesh); 1.2% (2.9% in *cox1*; 0.2% in *I6s*) within Clade II (Southeast Asian); and 1.1% (0.0% in *cox1*; 0.0% in *I6s*) within the distantly clustered Chinese samples (CHS026; CHS726; HS16001). The mean genetic distance between Clade I and II is 4.4%. Notably, the Chinese *N. kaouthia* samples (CHS026; CHS726; HS16001) showed the least value of mean genetic distance (5.0%) with the clade of *N. atra* compared to the distances it showed to the *N. kaouthia* Clade I (5.2%) and Clade II (6.5%) (Table 3.6). The PCoA ordinations of genetic divergence in the three genes also showed the discrete clustering of Asian and African cobras in *I6s* and *cytb* while *cox1* is lacking comparable sequence to see the similar clustering of the aforesaid two genes. However, the PCoA ordinations showed the discrete clustering of *N. kaouthia* from Southeast Asia from the other congeneric samples from South Asia, while a single specimen from China is seen distant from both South Asia and Southeast Asian samples (Fig. 3.7).

Table 3.6. Uncorrected p-distance estimate between the two clades of *Naja kaouthia* along with other congeneric sequences based on *cytb* dataset. The mean of within group distance for each clade are given under the column marked with “#”.

Groups	1	2	3	4	#
1 <i>Naja kaouthia</i> South Asian Clade					0.011
2 <i>Naja kaouthia</i> Southeastern Asian Clade	0.044				0.012
3 <i>Naja fuxi</i>	0.052	0.065			0.001
4 <i>Naja atra</i>	0.057	0.057	0.05		0.011
5 <i>Naja oxiana</i>	0.059	0.054	0.047	0.059	0

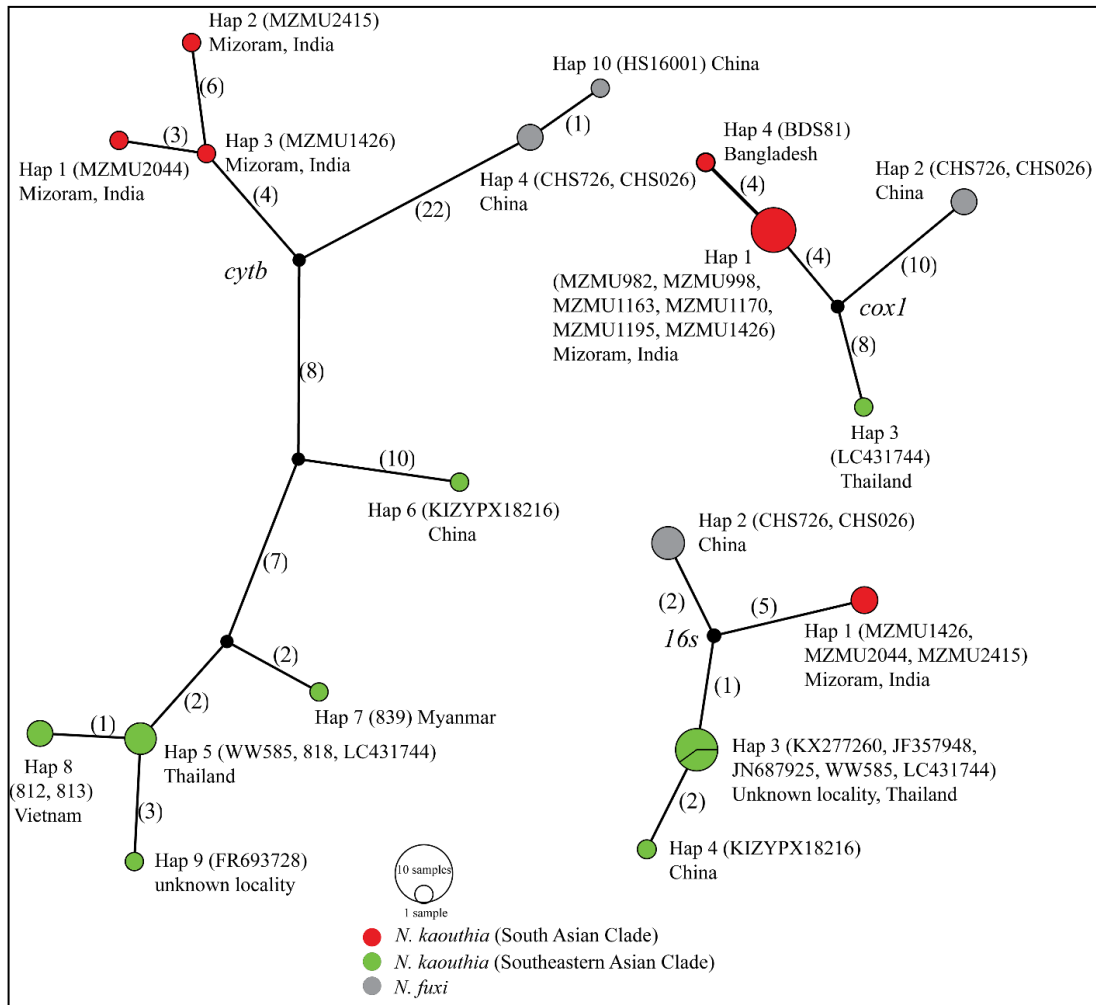


Figure 3.6. Mitochondrial gene-based (*16s*, *cox1* and *cytb*) Median-joining haplotype network among populations of *Naja kaouthia*. The number of samples present in each haplotype corresponds to the relative size of the circles. Numbers at the branch represent mutational steps found between haplotypes, and a black dot at the branch is an inferred median.

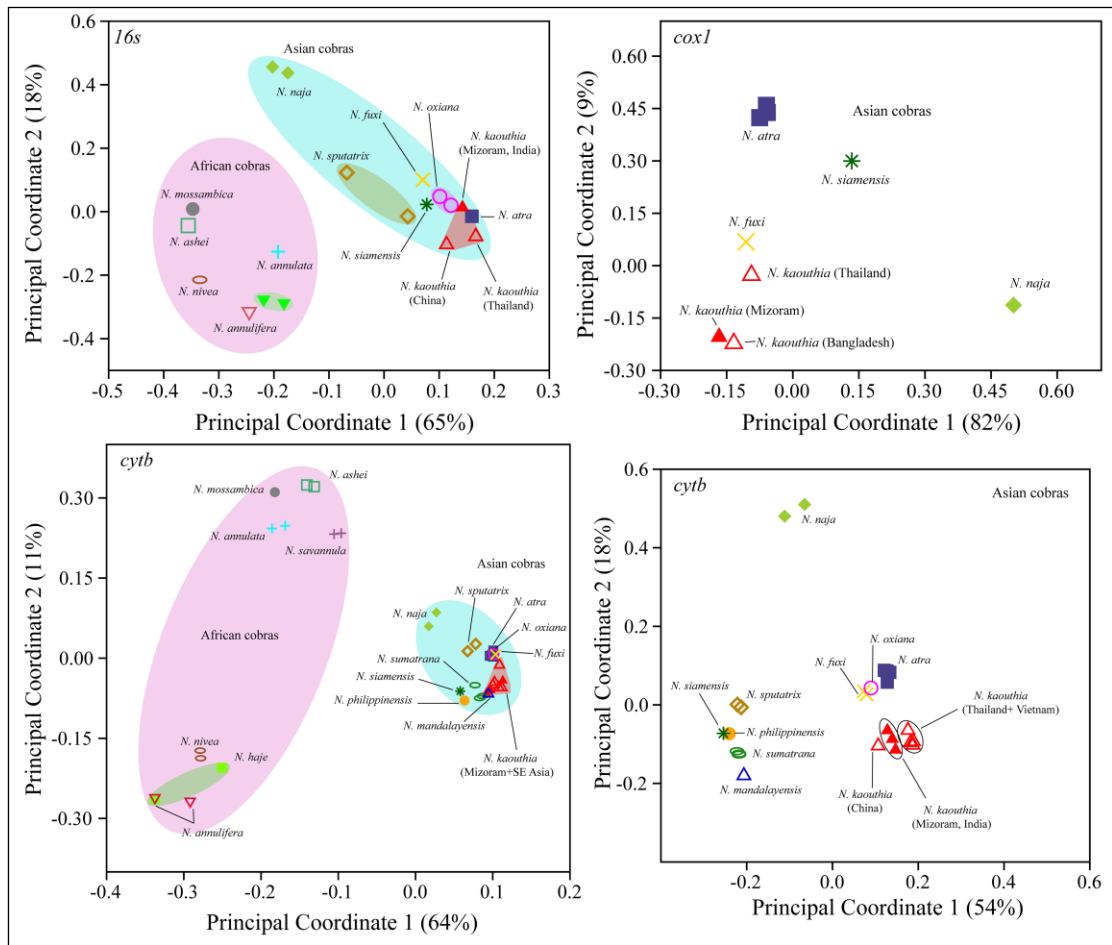


Figure 3.7. Ordination of *Naja* species in a Principal Coordinate Analysis of standardized p-distance of mitochondrial 16S rRNA (*16s*) cytochrome c oxidase subunit 1 (*cox1*), and Cytochrome b (*cytb*) genes. A total percentage of variance captured by the first and second Principal coordinates are given in the x and y axes, respectively.

Morphology

The studied population of *Naja kaouthia* from Mizoram is represented by a total of 33 museum specimens and 11 live individuals. Based on the conventional taxonomical features the species was diagnosed in having oval-shaped smooth dorsal scales with ADSR 23–29, MDSR 19–23, PDSR 13–17; SL 7/7 (rarely 6/7 or 8/7); SLE 3–4/3–4 (rarely 3/3–4 or 3–3/3–3); IL mostly 9/9 or 8/8 (sometimes 8/9, 9/8, 9/10, 10/9, or 10/10); PrO 1/1; PoO 3/3 (rarely 2/3, 2/2, or 1/3); Te mostly 2+3/2+3 (sometimes 2+3/2+4, 2+4/2+3, 2+4/2+4, and rarely 2+3/1+4); As undivided; Ve (sex pooled) 179–200; Sc (sex pooled) 50–61. Inverted hemipenis travels up to 11 to 15 Sc, and the organ is bilobed with small spines throughout that were slightly larger at the basal region of the organ. From the studied specimens, various phenotypic forms of hood markings were observed such as individuals with a typical monocellate mark (either rounded or rhomboid shaped), broken monocellate either at the anterior or both anterior and posterior edges of the mark, rounded monocellate with a prominent dot within the lateral sides (only one side or both) of the marking, a complete absence of hood mark, the mark extended at the lateral flanks to form a mask-like marking, or widely opens at the anterior end forming a spectacle-like mark (Figs. 3.8–3.10). The raw morphological data for the Mizoram specimens are given in Table 3.7. Moreover, comparative meristic data originated from this study along with other populations from published taxonomic literature and unpublished data is given in Table 3.8.

Sexual dimorphism

In the adult, we adjusted the mensural data against SVL using the equation $\text{Character} + (1261 - \text{SVL}) * \text{Regression coefficient}$, where 1261 is the grand mean of adult SVL; while in juveniles, we adjusted the variables using the equation $\text{Character} + (441.63 - \text{SVL}) * \text{Regression coefficient}$, where 441.63 is the grand mean of juvenile SVL. The characters tested between male and female showed significant dimorphism in the following characters: in adult (n=23), Ve ($p < 0.01$), Sc ($p < 0.05$), TaL ($p < 0.01$), ED ($p < 0.01$), S-E ($p < 0.05$); in juvenile (n=16), HL ($p < 0.05$), and ND ($p < 0.05$) (Fig. 3.11; Table 3.9).

For an exploratory analysis (PCA), all of the identified sexually dimorphic characters in adults (Ve, Sc, TaL, ED, and S-E) were utilized; in juveniles, multivariate analysis (PCA) is not conducted because only two variables are identified as sexually dimorphic i.e HL and ND. A total of five components were extracted, from which the first two components accounted for 78% of the total variation of the data, with PC1, PC2 and PC3 representing 52%, 26% and 11%, respectively. The loadings of TaL, ED, and S-E are high on the first axis, while only Ve loaded negatively, with Sc having more effect on PC2 than PC1. The ordination of the first two components depicts evident separation between males and females on the first axis (PC1) (Fig. 3.12; Table 3.10).

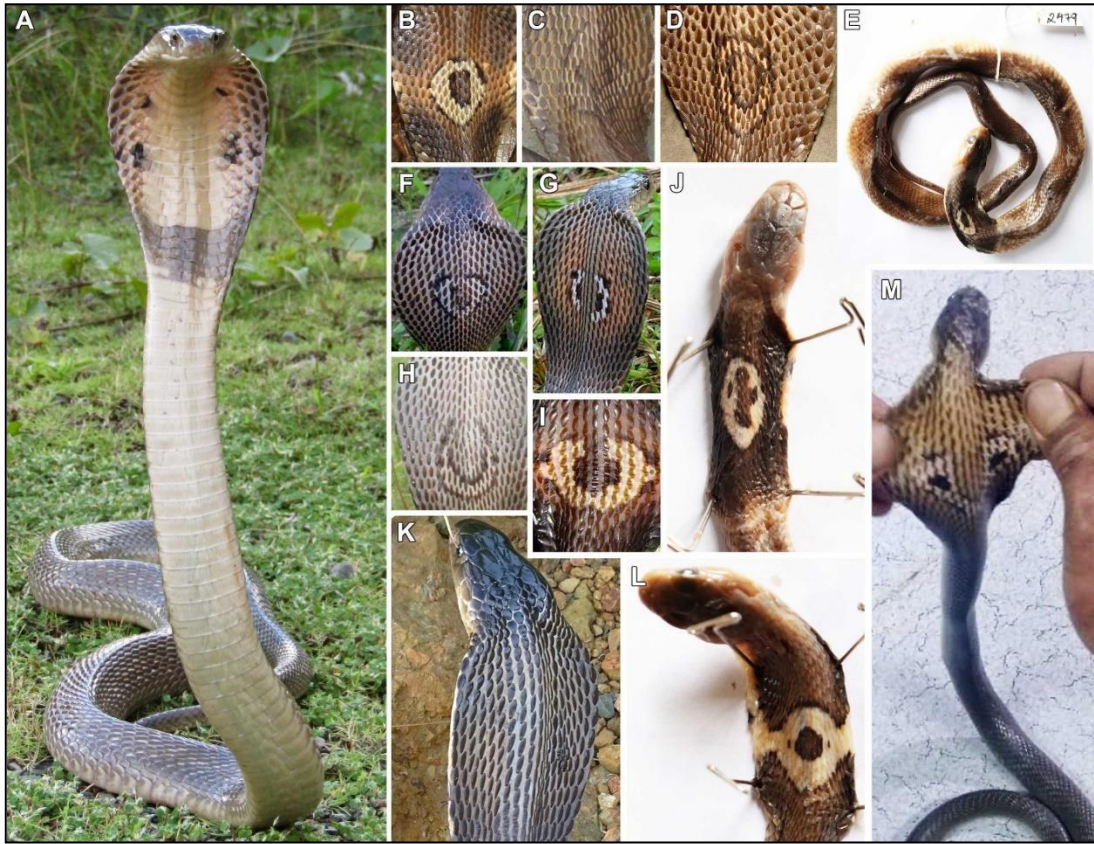


Figure 3.8. *Naja kaouthia* specimens from Mizoram, Northeast India in life (A) and preserved specimens. (B–D) The dorsal views of the hood with typical monocellate mark in adult. (E) Preserved juvenile specimen with the typical monocellate hood mark. (F–I) The dorsal views of adult anterior body showing a broken monocellate mark either at the anterior end (F, H, I) or at both anterior and posterior sides (G). (J) Preserved juvenile with a prominent dot present within the left lateral side of the marking. (K) Complete absence of hood mark. (L) The monocellate extended at the lateral flanks to form a mask-like marking. (M) The monocellate widely opens at the anterior end forming a spectacle-like marking, this particular specimen was killed by local people in the Northern part of Mizoram not far from Assam boundary, and was recovered for museum specimen. Phot credits: H.T. Lalremsanga (B–D, F–I, K), anonymous (M).



Figure 3.9. Live adult *Naja kaouthia* from Mizoram. Photo credit: H.T. Lalremsanga.



Figure 3.10. Hemipenis showing the asulcate (left) and sulcate (right) views of *Naja kaouthia*. The organ is bilobed with small spines throughout that were slightly larger at the basal region. Photo credit: Lalmuansanga

Table 3.7. Morphometry (in mm) and scalation data of *Naja kaouthia* examined from Mizoram, India. Damaged character is shown as asterisk (*), and the characters that are not feasible to examine in life individuals are shown in dash (-). Life individuals examined are indicated by their respective locality.

Characters	MZMU 962B	MZU campus	Mission veng	ITI veng	Dur tlang	Falk land	MZU campus	Kuli kawn	Thiak
Sex	M	M	F	M	F	F	F	M	F
Ve	197	190	194	191	200	193	191	184	194
Sc	*	57	53	52	53	*	54	57	55
SL	8/7	7/7	7/7	7/7	7/7	7/7	7/7	7/7	7/7
SLe	3-4	3-4	3-4	3-4	3-4	3-4	3-4	3-4	3-4
IL	8/9	8/8	8/8	9/9	9/9	8/8	9/9	9/10	9/9
DSR	24:19:14	25:21:15	25:21:15	27:21:15	25:21:15	24:20:15	24:20:15	25:21:15	26:21:15
HL	35.4	51.72	32.90	45.40	51.28	28.22	30.70	33.48	36.14
HW	15.3	32.90	22.82	23.00	25.62	21.46	22.30	22.00	30.28
HD	*	-	-	-	-	-	17.90	15.76	-
ED	7.3	7.18	6.40	5.86	5.80	5.70	4.20	5.72	5.90
ND	*	-	-	-	-	-	-	-	-
S-N	*	-	-	-	-	-	-	-	-
S-E	*	-	-	-	-	-	-	-	-
N-E	5.7	5.60	5.16	5.32	5.10	4.90	4.36	4.60	5.68
RW	*	-	-	-	-	-	-	-	-
RH	*	-	-	-	-	-	-	-	-
INS	*	-	-	-	-	-	-	-	-
IOS	*	-	-	-	-	-	-	-	-
INL	*	-	-	-	-	-	-	-	-
INW	*	-	-	-	-	-	-	-	-
PFL	*	-	-	-	-	-	-	-	-
PFW	*	-	-	-	-	-	-	-	-
FL	*	-	-	-	-	-	-	-	-
FW	*	-	-	-	-	-	-	-	-
PL	*	-	-	-	-	-	-	-	-
PW	*	-	-	-	-	-	-	-	-
SVL	1140	1550	1570	1376	1468	1280	1270	1040	1490
TaL	*	288	246	216	210	*	218	218	222
PrO	1/1	1/1	1/1	1/1	1/1	1/1	1/1	1/1	1/1
PoO	2/3	3/3	3/3	3/3	3/3	3/3	3/3	3/3	3/3
Tem	2+3/2+3	2+3/2+3	2+3/2+3	2+3/2+3	2+3/2+4	2+3/2+3	2+3/2+3	2+3/2+3	2+3/2+3
As	1	1	1	1	1	1	1	1	1
Hood marks	Type V	Type I	Type I	Type II	Type V	Type I	Type I	Type I	Type I

Table 3.7. Continued.

Characters	MZU campus	New Secreta riat	MZU campus	MZMU 110	MZMU 1912	MZMU 1886	MZMU 2459	MZMU 1794	MZMU 2462
Sex	M	F	F	M	M	F	M	F	F
Ve	179	196	195	191	187	191	186	191	194
Sc	55	54	53	53	55	52	56	59	55
SL	7/7	7/7	7/7	7/7	7/7	7/7	7/7	7/7	7/7
SLe	3-4	3-4	3-4	3-4	3-4	3-4	3-4	3-4	3-4
IL	9/9	8/8	9/9	9/9	9/9	9/9	9/9	9/9	10/9
DSR	29:21:17	29:23:15	29:21:15	24:21:15	27:21:15	24:22:15	24:21:15	27:21:15	24:20:15
HL	27.25	30.38	34.04	42.96	39.68	34.72	25.54	33.80	31.50
HW	16.96	26.06	32.20	32.82	30.76	23.46	18.70	24.76	21.32
HD	-	-	-	21.20	18.50	16.16	14.08	15.56	14.38
ED	4.24	5.10	6.0	5.84	6.22	5.60	5.24	4.38	4.94
ND	-	-	-	4.04	3.84	3.34	2.60	2.54	3.30
S-N	-	-	-	4.80	4.22	3.54	4.42	3.68	4.04
S-E	-	-	-	13.80	13.04	10.84	9.50	9.74	9.02
N-E	3.88	4.80	5.20	5.90	5.52	4.66	4.36	4.32	4.64
RW	-	-	-	9.80	9.78	8.52	8.40	8.30	7.54
RH	-	-	-	5.82	5.66	3.88	4.68	4.84	4.60
INS	-	-	-	13.88	12.90	10.30	10.70	10.46	9.48
IOS	-	-	-	17.34	20.26	15.46	13.30	14.82	12.96
INL	-	-	-	8.52	8.48	6.90	5.98	6.72	6.02
INW	-	-	-	7.38	7.20	5.80	5.48	6.28	5.46
PFL	-	-	-	8.00	7.84	6.48	5.72	6.76	5.66
PFW	-	-	-	7.44	7.14	5.70	5.36	6.50	5.44
FL	-	-	-	10.30	9.28	8.40	7.76	7.54	7.48
FW	-	-	-	8.20	8.10	6.68	6.32	6.70	5.56
PL	-	-	-	15.22	10.58	12.36	12.12	12.42	10.72
PW	-	-	-	10.44	8.50	8.20	8.30	8.88	8.04
SVL	900	1244	1365	1400	1480	1294	1010	1250	1016
TaL	150	185	225	242	250	202	174	210	180
PrO	1/1	1/1	1/1	1/1	1/1	1/1	1/1	1/1	1/1
PoO	3/3	3/3	3/3	3/3	3/3	3/3	3/3	3/3	2/2
Tem	2+3/2+3	2+3/2+3	2+3/2+3	2+3/2+3	2+3/2+3	2+4/2+3	2+3/2+3	2+4/2+3	2+3/2+3
As	1	1	1	1	1	1	1	1	1
Hood marks	Type I	Type I	Type I	Type I	Type I	Type V	Type I	Type I	Type I

Table 3.7. Continued.

Characters	MZMU 170	MZM U 2465	MZMU 2466	MZM U 2467	MZM U 1152	MZM U 2468	MZM U 2469	MZM U1159
Sex	M	F	F	M	F	M	M	F
Ve	190	191	191	187	195	191	186	190
Sc	58	54	53	58	55	61	59	52
SL	7/7	7/7	7/7	7/7	7/7	7/7	7/7	7/7
SLe	3-4	3-4	3-4	3-4	3-4	3-4	3-4	3-4
IL	9/9	9/9	10/10	10/9	9/9	9/9	9/9	9/9
DSR	27:21:15	26:21:15	27:21:15	24:21:15	27:21:15	27:21:15	28:20:13	28:21:15
HL	37.38	43.88	43.70	39.75	35.48	39.04	36.20	40.54
HW	27.70	27.94	30.76	35.08	21.52	26.72	22.46	30.60
HD	20.26	22.25	23.16	22.32	15.40	18.34	17.68	21.76
ED	5.16	5.50	5.50	5.52	4.44	5.28	5.58	5.50
ND	3.58	4.12	3.90	4.08	2.36	2.54	2.38	3.48
S-N	4.78	5.68	5.14	5.70	3.27	2.76	4.54	5.08
S-E	11.37	13.12	11.48	12.54	9.04	9.38	10.46	7.74
N-E	5.60	7.22	5.26	6.58	3.84	4.40	5.04	5.70
RW	9.40	10.72	8.97	10.80	7.66	9.50	9.14	9.42
RH	6.36	6.66	7.02	6.36	4.66	4.74	6.04	6.20
INS	12.80	12.98	12.18	12.93	9.06	11.32	11.40	11.60
IOS	17.82	17.82	16.66	18.09	13.32	15.20	15.90	16.72
INL	7.04	8.92	6.88	7.12	6.28	6.96	7.18	7.90
INW	6.48	7.08	6.40	6.84	4.84	6.12	6.38	6.76
PFL	7.20	7.72	7.98	8.41	5.44	6.37	7.24	7.68
PFW	6.36	6.52	7.42	8.12	4.82	6.01	6.92	6.40
FL	8.34	9.92	8.42	9.22	6.68	8.02	7.90	8.96
FW	7.54	8.64	8.10	7.60	5.98	7.10	6.48	7.76
PL	13.70	15.62	13.80	13.12	11.64	11.86	13.24	9.56
PW	10.32	10.64	10.18	9.48	8.06	9.00	9.04	7.92
SVL	1340	1496	1568	1330	1020	1216	1126	1224
TaL	248	234	252	250	176	224	214	228
PrO	1/1	1/1	1/1	1/1	1/1	1/1	1/1	1/1
PoO	3/3	3/3	3/3	3/3	3/3	3/3	3/3	3/3
Tem	2+3/2+4	2+3/2+3	2+3/2+4	2+4/2+4	2+3/2+3	2+3/2+4	2+3/2+4	2+3/2+3
As	1	1	1	1	1	1	1	1
Hood marks	Type I	Type I	Type I	Type I	Type II	Type II	Type I	Type I

Table 3.7. Continued.

Characters	MZMU 2472	MZMU 1252	MZMU 2477	MZMU 2480	MZM U 2484	MZMU 2415	MZMU 2699	MZMU 1426
Sex	M	F	M	M	F	M	M	M
Ve	184	191	191	187	194	189	185	188
Sc	38*	52	57	60	54	57	54	58
SL	7/7	7/7	7/7	7/7	7/7	7/7	7/7	7/7
SLe	3-4	3-4	3-4	3-4	3-4	3-4	3-4	3-4
IL	9/9	9/9	10/10	9/9	9/9	9/9	9/9	9/9
DSR	27:21:15	27:20:15	25:20:13	25:21:15	27:21:15	23:19:15	28:21:15	20:20:13
HL	23.74	17.32	16.90	18.14	30.04	37.36	51.80	44.66
HW	17.60	11.60	12.24	13.00	20.00	22.96	30.52	20.62
HD	12.60	8.34	8.12	7.60	14.72	12.94	18.58	13.94
ED	4.60	3.96	3.76	3.88	5.12	5.06	6.18	5.40
ND	1.74	1.60	1.80	1.60	3.46	2.52	3.26	2.48
S-N	2.98	2.20	2.02	2.18	3.16	3.98	4.94	5.48
S-E	7.80	5.64	5.76	5.48	8.34	9.90	13.60	11.36
N-E	3.94	2.62	2.18	2.04	3.56	4.40	6.60	6.60
RW	7.42	4.54	4.82	4.90	7.94	7.74	9.10	8.38
RH	4.76	2.88	2.40	2.72	4.32	5.24	5.62	4.00
INS	8.16	5.70	5.88	5.00	10.12	8.84	12.20	9.08
IOS	11.84	8.62	9.00	8.52	14.38	13.02	18.70	13.34
INL	5.64	3.90	3.64	3.52	7.04	6.06	8.60	5.82
INW	4.82	3.28	3.12	3.20	5.68	5.60	6.42	4.86
PFL	5.20	3.88	3.68	3.98	5.80	6.20	7.56	6.36
PFW	4.54	3.18	3.36	3.26	5.56	6.06	7.0	5.74
FL	6.32	4.80	5.28	4.70	7.76	7.10	9.54	7.28
FW	5.22	3.82	4.08	3.94	6.92	6.70	7.86	6.82
PL	10.12	7.90	7.66	8.14	12.82	12.44	16.36	13.26
PW	7.38	5.14	5.92	5.10	8.90	9.00	10.62	9.32
SVL	740	432	488	426	1154	1240	1080	1245
TaL	100*	80	90	84	192	242	240	240
PrO	1/1	1/1	1/1	1/1	1/1	1/1	1/1	1/1
PoO	3/3	3/3	3/3	3/3	3/3	3/3	3/3	3/3
Tem	2+3/2+3	2+3/2+3	2+4/2+4	2+2/2+3	2+4/2+4	2+3/2+3	2+3/2+3	2+3/2+3
As	1	1	1	1	1	1	1	1
Hood marks	Type I	Type II	Type II	Type I	Type II	Type IV	Type I	Type

Table 3.7. Continued.

Characters	MZMU 201	MZMU 2460	MZMU 2461	MZMU 2464	MZMU 0009	MZMU 2474
Sex	F (Juvenile)	F (Juvenile)	M (Juvenile)	M (Juvenile)	M (Juvenile)	M (Juvenile)
Ve	188	192	184	189	186	187
Sc	50	54	55	53	54	55
SL	7/7	6/7	7/7	7/7	7/7	7/7
SLe	3-3	3/3-4	3-4	3-4	3-4	3-4
IL	9/9	8/8	9/8	9/9	10/9	9/9
DSR	24:21:15	24:21:15	24:20:15	23:21:14	24:20:15	27:21:15
HL	13.72	19.58	16.00	14.76	14.30	18.60
HW	10.78	14.82	9.36	10.66	11.00	11.56
HD	6.66	10.02	6.92	6.70	6.28	7.92
ED	3.14	4.14	3.50	3.18	3.00	3.84
ND	1.58	2.26	1.06	1.18	1.06	1.30
S-N	1.90	2.38	1.58	1.96	1.82	2.18
S-E	4.62	6.80	4.60	4.56	4.46	5.80
N-E	2.04	3.56	2.20	2.20	2.14	2.92
RW	4.26	6.10	3.96	3.88	3.78	4.52
RH	2.36	3.08	2.04	2.12	2.04	2.82
INS	4.90	7.08	4.70	4.84	4.62	6.02
IOS	7.66	9.90	7.28	7.74	6.60	8.54
INL	3.22	*	2.92	3.14	3.24	3.80
INW	2.94	*	2.58	2.72	2.64	3.10
PFL	3.24	4.80	3.32	3.58	3.15	3.68
PFW	2.84	4.54	3.08	3.06	2.98	3.36
FL	4.76	6.30	4.08	4.40	4.16	4.56
FW	3.66	4.50	3.60	3.30	3.24	3.90
PL	6.50	8.58	6.90	6.68	6.98	7.24
PW	4.64	5.64	4.58	4.54	4.18	4.92
SVL	364	616	350	300	284	470
TaL	62	104	68	58	54	74
PrO	1/1	1/1	1/1	1/1	1/1	1/1
PoO	3/3	3/3	2/3	3/3	3/3	1/3
Tem	2+3/2+4	2+3/1+4	2+3/2+3	2+3/2+3	2+3/2+3	2+3/2+3
As	1	1	1	1	1	1
Hood marks	Type I	Type I	Type I	Type II	Type III	Type VI

Table 3.7. Continued.

Characters	MZMU 2478	MZMU 2479	MZMU 2476	MZMU 1137-B	MZMU 226
Sex	M (Juvenile)	M (Juvenile)	M (Juvenile)	M (Juvenile)	M (Juvenile)
Ve	198	198	184	193	180
Sc	53	54	57	52	51
SL	7/7	7/7	7/7	7/7	7/7
SLe	3-4	3-4	3-4	3-4	3-4
IL	9/9	9/9	9/9	9/9	9/9
DSR	24:21:15	27:21:15	28:21:15	25:21:15	27:21:15
HL	16.46	16.08	15.00	16.30	15.60
HW	9.16	10.90	10.80	10.34	11.10
HD	7.46	6.80	6.88	7.08	7.06
ED	3.70	3.40	3.32	3.28	3.28
ND	1.10	1.12	1.30	1.50	1.26
S-N	1.38	2.04	1.90	1.88	1.80
S-E	4.68	4.70	4.80	4.54	4.24
N-E	2.26	1.92	1.86	1.58	2.06
RW	4.04	4.36	4.16	3.84	4.10
RH	2.38	2.84	2.40	2.54	2.62
INS	4.70	5.44	4.84	4.02	5.20
IOS	7.72	7.68	7.76	7.52	7.16
INL	3.48	2.86	2.84	3.20	3.14
INW	2.84	2.58	2.46	2.86	2.76
PFL	3.38	3.02	3.10	3.30	2.84
PFW	2.84	2.58	2.90	3.16	2.68
FL	4.34	4.80	4.34	4.64	4.76
FW	3.14	3.04	3.38	3.42	3.28
PL	6.70	6.48	6.96	6.62	6.12
PW	4.22	4.46	4.58	4.36	4.60
SVL	394	318	294	332	358
TaL	72	56	56	58	60
PrO	1/1	1/1	1/1	1/1	1/1
PoO	3/3	3/3	3/3	2/3	2/2
Tem	2+3/2+4	2+3/2+3	2+3/2+3	2+3/2+3	2+3/2+4
As	1	1	1	1	1
Hood marks	Type II	Type I	Type I	Type I	Type II

Table 3.8. Comparative meristic data of *Naja kaouthia* originated from this study, published and unpublished data from Indo-Myanmar region.

Populations	Sex	Ve	Sc	ADSR	MDSR	PDSR	Hood mark	Sources
Mizoram (India)	Male (n=26)	179–198	51–61	23–29	19–21	13–17	Typical and variant	This study
	Female (n=18)	188–200	50–59	24–29	20–23	15		
Meghalaya (India)	Male (n=3)	183–191	55	23–25	19–21	13–15	Typical	Yashpal Singh Rathee (unpubl. data)
	Female (n=3)	189–191	52–58	24–25	17–21	14–15		
Sumhpawng Mada, Mahtum, Kajitu, Sumpra (Upper Myanmar)	Male (n=2)	187–188	53–55	25–31	21	15	Typical and variant	Smith (1940)
	Female (n=2)	189–191	54–55+	25–27	21	15		
Indo-Myanmar	Sex pooled	164–196	43–58	25–31	19–21	15–17	Typical	Smith (1943); Leviton et al. (2008)

Table 3.9. Test for sexual dimorphism on the meristic and mensural characters using 44 (14 adult males; 15 females; 13 juvenile males; 3 juvenile females) *Naja kaouthia* individuals from Mizoram, Northeast India, including mean, standard deviation, minimum and maximum values. Standardized meristic data were analysed through one-way ANOVA with sex as a factor. Adjusted mensural data were analysed through one-way ANCOVA using SVL as a covariate and sex as a factor. The characters with statistically significant variations at the alpha level of 0.05 are shown in boldface. After removal of specimens with high number of missing data, a total of 13 adult males, 10 adult females are retained, while all the juvenile specimens are retained because the estimated percentage of missing value is <30%.

Characters	Life stage	Male		Female		Sexual dimorphism	
		Mean±SD	Range	Mean±SD	Range		
Ve	Adult	188.85±3.44	184–197	192.80±3.05	190–200	$F_{1,21} = 8.24$	$p = \mathbf{0.009}$
	Juvenile	187.69±6.01	179–198	190.33±2.08	188–192	$F_{1,14} = 0.54$	$p = 0.475$
Sc	Adult	56.42±2.57	52–61	54.10±2.02	52–59	$F_{1,20} = 5.33$	$p = \mathbf{0.032}$
	Juvenile	54.67±2.46	51–60	52.00±2.00	50–54	$F_{1,13} = 2.97$	$p = 0.108$
TaL	Adult	233.00±27.36	174–288	210.20±23.97	176–252	$F_{1,19} = 12.90$	$p = \mathbf{0.002}$
	Juvenile	73.33±26.84	54–150	82.00±21.07	62–104	$F_{1,12} = 0.10$	$p = 0.761$
HL	Adult	40.05±7.29	25.54–51.80	37.56±7.00	30.04–51.28	$F_{1,20} = 1.72$	$p = 0.205$
	Juvenile	17.63±3.77	14.30–27.25	16.87±2.96	13.72–19.58	$F_{1,13} = 8.36$	$p = \mathbf{0.013}$
HW	Adult	25.11±5.58	15.30–32.90	24.83±3.85	20.00–30.76	$F_{1,20} = 0.22$	$p = 0.642$
	Juvenile	11.90±2.60	9.16–17.60	12.40±2.14	10.78–14.82	$F_{1,13} = 0.003$	$p = 0.955$
HD	Adult	17.13±2.81	12.94–21.20	17.92±3.51	14.38–23.16	$F_{1,16} = 0.09$	$p = 0.767$
	Juvenile	7.62±1.65	6.28–12.60	8.34±1.68	6.66–10.02	$F_{1,12} = 0.53$	$p = 0.481$

Table 3.9. Continued.

Characters	Life stage	Male		Female		Sexual dimorphism	
		Mean±SD	Range	Mean±SD	Range		
ED	Adult	5.85±0.72	5.06–7.30	5.10±0.58	4.20–5.80	$F_{1,20} = 9.07$	$p = \mathbf{0.007}$
	Juvenile	3.61±0.45	3.00–4.60	3.75±0.53	3.14–4.14	$F_{1,13} = 0.11$	$p = 0.741$
ND	Adult	3.03±0.66	2.38–4.04	3.31±0.60	2.36–4.12	$F_{1,14} = 1.15$	$p = 0.302$
	Juvenile	1.34±0.26	1.06–1.80	1.81±0.39	1.58–2.26	$F_{1,12} = 7.30$	$p = \mathbf{0.019}$
S-N	Adult	4.44±0.76	2.76–5.48	4.20±0.97	3.16–5.68	$F_{1,14} = 0.46$	$p = 0.508$
	Juvenile	1.98±0.39	1.38–2.98	2.16±0.24	1.90–2.38	$F_{1,12} = 0.01$	$p = 0.930$
S-E	Adult	11.38±1.74	9.38–13.80	9.92±1.79	7.74–13.12	$F_{1,14} = 5.20$	$p = \mathbf{0.039}$
	Juvenile	5.12±0.99	4.24–7.80	5.69±1.09	4.62–6.80	$F_{1,12} = 0.001$	$p = 0.975$
N-E	Adult	5.36±0.77	4.36–6.60	4.87±1.05	3.56–7.22	$F_{1,20} = 2.57$	$p = 0.125$
	Juvenile	2.40±0.74	1.58–3.94	2.74±0.77	2.04–3.56	$F_{1,13} = 1.09$	$p = 0.315$
RW	Adult	9.03±0.71	7.74–9.80	8.63±1.06	7.54–10.72	$F_{1,14} = 1.82$	$p = 0.199$
	Juvenile	4.48±0.10	3.78–7.42	4.97±0.99	4.26–6.10	$F_{1,12} = 0.09$	$p = 0.770$
RH	Adult	5.35±0.75	4.00–6.36	5.27±1.18	3.88–7.02	$F_{1,14} = 0.10$	$p = 0.754$
	Juvenile	2.64±0.72	2.04–4.76	2.77±0.37	2.36–3.08	$F_{1,12} = 0.70$	$p = 0.419$
INS	Adult	11.46±1.71	8.84–13.88	10.77±1.36	9.06–12.98	$F_{1,14} = 1.64$	$p = 0.221$
	Juvenile	5.29±1.06	4.02–8.16	5.89±1.10	4.90–7.08	$F_{1,12} = 0.02$	$p = 0.903$
IOS	Adult	14.99±3.38	8.70–20.26	15.27±1.72	12.96–17.82	$F_{1,134} = 0.01$	$p = 0.911$
	Juvenile	8.11±1.34	6.60–11.84	8.73±1.12	7.66–9.90	$F_{1,12} = 0.18$	$p = 0.679$

Table 3.9. Continued.

Characters	Life stage	Male		Female		Sexual dimorphism	
		Mean±SD	Range	Mean±SD	Range		
INL	Adult	7.18±1.12	5.82–8.60	7.08±0.93	6.02–8.92	$F_{1,14} = 0.10$	$p = 0.755$
	Juvenile	3.45±0.75	2.84–5.64	3.56±0.48	3.22–3.90	$F_{1,11} = 0.31$	$p = 0.588$
INW	Adult	6.21±0.81	4.86–7.38	6.04±0.73	4.84–7.08	$F_{1,14} = 0.57$	$p = 0.465$
	Juvenile	2.97±0.63	2.46–4.82	3.11±0.24	2.94–3.28	$F_{1,11} = 0.88$	$p = 0.369$
PFL	Adult	6.94±0.80	5.72–8.00	6.69±1.01	5.44–7.98	$F_{1,14} = 1.09$	$p = 0.314$
	Juvenile	3.52±0.62	2.84–5.20	3.97±0.78	3.24–4.80	$F_{1,12} = 0.37$	$p = 0.556$
PFW	Adult	6.45±0.71	5.36–7.44	6.05±0.82	4.82–7.42	$F_{1,14} = 2.78$	$p = 0.118$
	Juvenile	3.15±0.50	2.58–4.54	3.52±0.90	2.84–4.54	$F_{1,12} = 0.14$	$p = 0.716$
FL	Adult	8.39±1.09	7.10–10.30	8.15±1.00	6.68–9.92	$F_{1,14} = 0.47$	$p = 0.504$
	Juvenile	4.70±0.60	4.08–6.32	5.29±0.88	4.76–6.30	$F_{1,12} = 1.48$	$p = 0.247$
FW	Adult	7.24±0.71	6.32–8.20	7.04±1.05	5.56–8.64	$F_{1,14} = 0.92$	$p = 0.354$
	Juvenile	3.63±0.60	3.04–5.22	3.99±0.45	3.66–4.50	$F_{1,12} = 1.12$	$p = 0.734$
PL	Adult	13.20±1.76	10.58–16.36	12.37±1.85	9.56–15.62	$F_{1,14} = 1.01$	$p = 0.332$
	Juvenile	7.22±1.06	6.12–10.12	7.66±1.06	6.50–8.58	$F_{1,12} = 1.10$	$p = 0.752$
PWc	Adult	9.39±0.86	8.30–10.62	8.85±1.04	7.92–10.64	$F_{1,14} = 2.17$	$p = 0.163$
	Juvenile	4.90±0.91	4.18–7.38	5.14±0.50	4.64–5.64	$F_{1,12} = 1.10$	$p = 0.336$

Table 3.10. Information on Principal Component Analysis (PCA) and loadings for *Naja kaouthia* population in Mizoram, northeastern India between the adult male and female specimens.

Variables	PC1	PC2	PC3	PC4	PC5
Zscore (Ve)	-0.864	-0.189	0.102	0.395	0.225
Zscore (Sc)	0.039	0.955	0.203	-0.121	0.173
adj TaL	0.745	0.375	-0.33	0.442	-0.04
adj ED	0.842	-0.4	-0.15	-0.148	0.296
adj S-E	0.765	-0.187	0.587	0.184	-0.05

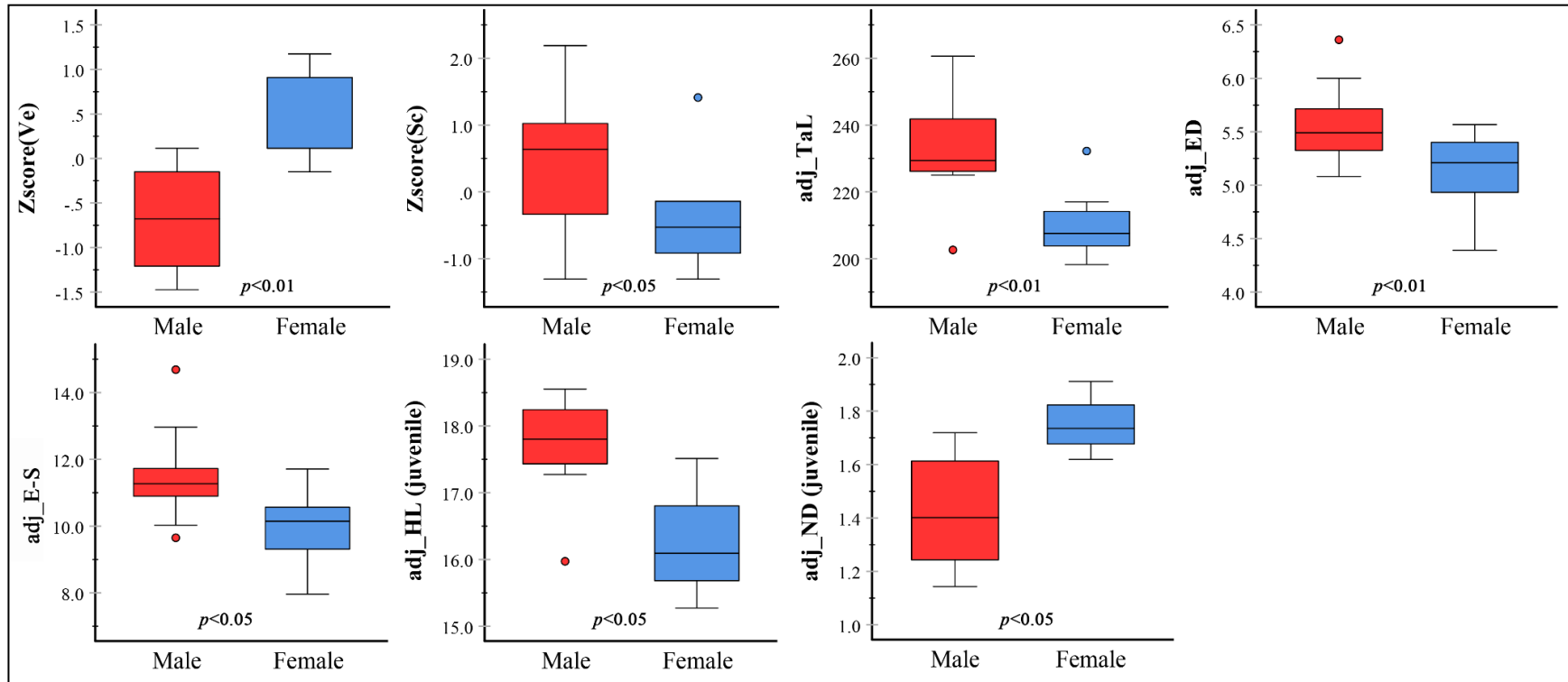


Figure 3.11. Box plot showing median, interquartile range, range (minimum to maximum), and outliers for standardised (Z score) meristic and adjusted (adj) mensurals such as number of ventrals (Ve), subcaudals (Sc), tail length (TaL), eye diameter (ED), snout to eye distance (S-E), head length (HL), and nostril diameter (ND) between male and female specimens of *Naja kaouthia* population from Mizoram, Northeast India. Significance at the alpha level of 0.05 is given as asterisk in each plot.

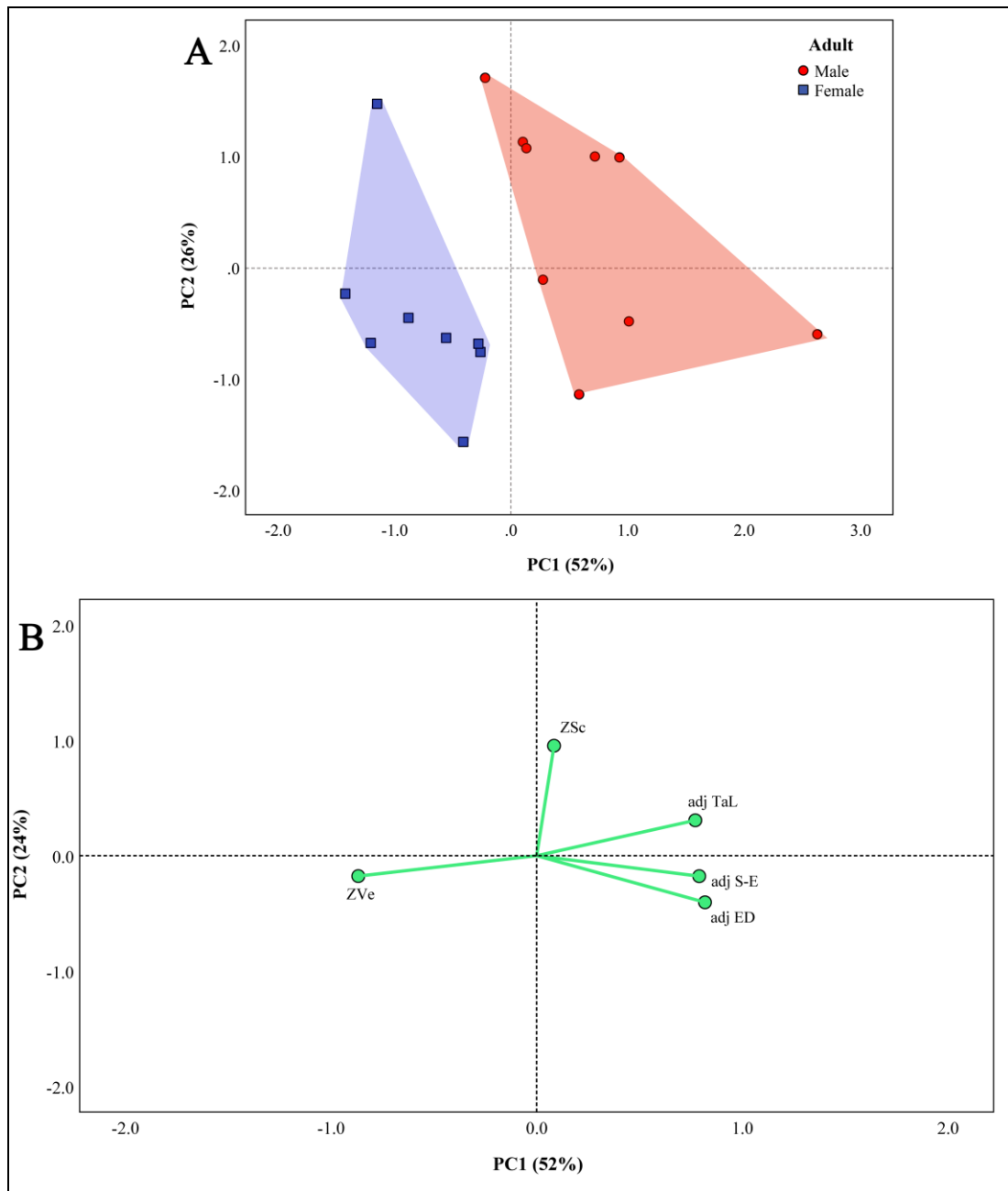


Figure 3.12. (A) Ordination of *Naja kaouthia* population from Mizoram along the first two principal components based on a PCA of the standardised ventrals (Ve), subcaudals (Sc), and adjusted tail length (TaL), snout to eye distance (S-E) and eye diameter (ED) of adult specimens. Total variance associated with the PC1 and PC2 are 52% and 26%, respectively. (B) PCA loading plot showing the distribution of the analysed variables along the first two principal components.

Intraspecific morphological variations

A null hypothesis was established which states that the difference in hood marking within the studied population is just a random accumulation of phenotypic variation; against the alternate hypothesis which states that the intraspecific variations in hood marking is not a single plastic character, but have an effect on the linear morphometry and meristics. Henceforth, the sexually dimorphic characters are tested separately for both sexes while the rest are pooled. Significant differences are seen in the adult's (n=23) HD ($p<0.05$), HW ($p<0.01$), S-N ($p<0.05$), RH ($p<0.01$), INS ($p<0.01$), INW ($p<0.01$), PFL ($p<0.01$), PFW ($p<0.01$), FL ($p<0.05$), Ve in male ($p<0.05$), and TaL in female ($p<0.05$); in juveniles (n=16), significant differences are seen in the RW ($p<0.05$), and HL in males ($p<0.05$) (Fig. 3.13; Table 3.11).

The identified significantly variable characters (HW, HD, S-N, RH, INS, INW, PFL, PFW, and FL) were utilized for PCA; in juvenile, PCA is not conducted because only two variables are identified as sexually dimorphic i.e HL and RW. Among the total of seven components extracted, the first two components accounted for 79% of the total variation of the data, with PC1, PC2 and PC3 representing 67%, 12% and 7%, respectively. All the loadings of the variables are high on the first axis and all are loaded positively. In the second axis, the variables HW, INS, INW, and FL are loaded negatively. The ordination of the first two components depicts marginal separation between the phenotypic groups on the first axis (PC1) (Fig. 3.14; Table 3.12).

Table 3.11. Test for intra-population difference on the meristic and mensural characters using 44 (14 adult males; 15 adult females; 13 juvenile males; 3 juvenile females) *Naja kaouthia* individuals from Mizoram, Northeast India, including mean, standard deviation, minimum and maximum values. Standardized meristic data were analysed through one-way ANOVA with phenotypic group as a factor. Adjusted mensural data were analysed through one-way ANCOVA using SVL as a covariate and phenotypic group as a factor. The characters with statistically significant variations at the alpha level of 0.05 are shown in boldface. After removal of adult specimens with high number of missing data, typical group contains eight adult males, six adult females, seven juvenile males, and two juvenile females; in the variant group, a total of five adult males, four adult females, six juvenile males, and one juvenile female are retained for the test. Since there is a single female in the variant juvenile group, the test for juveniles is performed only for either male (for sexually dimorphic characters) or sex pooled.

Characters	Life stage	Sex	Typical		Variant		Intra-specific difference	
			Mean±SD	Range	Mean±SD	Range		
Ve	Adult	Male	187.38±2.62	184–191	191.20±3.49	188–197	$F_{1,11} = 5.12$	$p = \mathbf{0.045}$
		Female	191.33±1.37	190–194	195.00±3.74	191–200	$F_{1,8} = 5.03$	$p = 0.055$
	Juvenile	Pooled	187.67±5.81	179–198	188.86±5.52	180–198	$F_{1,14} = 0.17$	$p = 0.684$
Sc	Adult	Male	56.13±2.03	53–59	57.00±3.74	52–61	$F_{1,10} = 0.29$	$p = 0.603$
		Female	54.50±2.43	52–59	53.50±1.29	52–55	$F_{1,8} = 0.56$	$p = 0.477$
	Juvenile	Pooled	54.63±3.02	50–60	53.57±1.99	51–57	$F_{1,13} = 0.62$	$p = 0.447$
TaL	Adult	Male	234.25±33.22	174–288	230.50±12.58	216–242	$F_{1,9} = 0.22$	$p = 0.650$
		Female	220.33±24.44	180–252	195.00±14.65	176–210	$F_{1,7} = 9.68$	$p = \mathbf{0.017}$
	Juvenile	Pooled	79.75±32.94	56–150	69.71±13.03	54–90	$F_{1,19} = 0.05$	$p = 0.821$

Table 3.11. Continued.

Characters	Life stage	Sex	Typical		Variant		Intra-specific difference	
			Mean±SD	Range	Mean±SD	Range		
HL	Adult	Pooled	38.78±7.66	25.54–51.80	39.26±6.61	30.04–51.28	$F_{1,20} = 0.30$	$p = 0.592$
	Juvenile	Male	18.93±4.69	15.00–27.25	16.10±1.57	14.30–18.60	$F_{1,10} = 9.43$	$p = \mathbf{0.012}$
HW	Adult	Pooled	26.82±4.78	18.70–32.90	22.13±3.36	15.30–26.72	$F_{1,20} = 8.94$	$p = \mathbf{0.007}$
	Juvenile	Pooled	12.73±3.08	9.36–17.60	11.05±0.98	9.16–12.24	$F_{1,13} = 0.88$	$p = 0.365$
HD	Adult	Pooled	18.54±3.03	14.08–23.16	15.25±1.88	12.94–18.34	$F_{1,16} = 6.70$	$p = \mathbf{0.020}$
	Juvenile	Pooled	8.07±2.13	6.66–12.60	7.41±0.77	6.28–8.34	$F_{1,12} = 0.49$	$p = 0.497$
ED	Adult	Male	5.89±0.65	5.16–7.18	5.78±0.90	5.06–7.30	$F_{1,10} = 0.05$	$p = 0.824$
		Female	5.00±0.60	4.20–5.50	5.24±0.60	4.44–5.80	$F_{1,7} = 1.30$	$p = 0.291$
	Juvenile	Pooled	3.72±0.51	3.14–4.60	3.53±0.37	3.00–3.96	$F_{1,13} = 0.02$	$p = 0.880$
ND	Adult	Pooled	3.37±0.62	2.38–4.12	2.78±0.48	2.36–3.46	$F_{1,14} = 3.13$	$p = 0.099$
	Juvenile	Male	1.52±0.38	1.06–2.26	1.33±0.27	1.06–1.80	$F_{1,12} = 0.83$	$p = 0.380$
S-N	Adult	Pooled	4.67±0.56	3.68–5.68	3.70±0.96	2.76–5.48	$F_{1,14} = 5.51$	$p = \mathbf{0.034}$
	Juvenile	Pooled	2.11±0.42	1.58–2.98	1.91±0.28	1.38–2.20	$F_{1,12} = 0.75$	$p = 0.403$
S-E	Adult	Male	11.96±1.78	9.50–13.80	10.21±1.03	9.38–11.36	$F_{1,6} = 2.80$	$p = 0.145$
		Female	10.22±2.11	7.74–13.12	9.41±1.29	8.34–10.84	$F_{1,5} = 0.09$	$p = 0.783$
	Juvenile	Pooled	5.42±1.23	4.54–7.80	5.02±0.68	4.24–5.80	$F_{1,12} = 0.38$	$p = 0.548$
N-E	Adult	Pooled	5.34±0.87	4.32–7.22	4.84±0.95	3.56–6.60	$F_{1,20} = 1.36$	$p = 0.258$
	Juvenile	Pooled	2.56±0.95	1.58–3.94	2.34±0.31	2.06–2.92	$F_{1,13} = 0.85$	$p = 0.373$

Table 3.11. Continued.

Characters	Life stage	Sex	Typical		Variant		Intra-specific difference	
			Mean±SD	Range	Mean±SD	Range		
RW	Adult	Pooled	9.14±0.86	7.54–10.72	8.29±0.69	7.66–9.50	$F_{1,14} = 3.48$	$p = 0.083$
	Juvenile	Pooled	4.88±1.26	3.84–7.42	4.24±0.39	3.78–4.82	$F_{1,12} = 6.19$	$p = \mathbf{0.029}$
RH	Adult	Pooled	5.77±0.80	4.60–7.02	4.47±0.51	3.88–5.24	$F_{1,14} = 12.72$	$p = \mathbf{0.003}$
	Juvenile	Pooled	2.84±0.84	2.04–4.76	2.47±0.32	2.04–2.88	$F_{1,12} = 1.16$	$p = 0.303$
INS	Adult	Pooled	11.87±1.29	9.48–13.88	9.79±0.96	8.84–11.32	$F_{1,14} = 12.33$	$p = \mathbf{0.003}$
	Juvenile	Pooled	5.52±1.39	4.02–8.16	5.28±0.59	4.62–6.02	$F_{1,12} = 1.12$	$p = 0.736$
IOS	Adult	Pooled	15.66±3.12	8.70–20.26	14.12±1.05	13.02–15.46	$F_{1,14} = 0.51$	$p = 0.487$
	Juvenile	Pooled	8.52±1.58	7.28–11.84	7.91±0.86	6.60–9.00	$F_{1,12} = 1.15$	$p = 0.305$
INL	Adult	Pooled	7.48±1.06	5.98–8.92	6.51±0.52	5.82–7.04	$F_{1,14} = 3.16$	$p = 0.097$
	Juvenile	Pooled	3.46±0.99	2.84–5.64	3.48±0.31	3.14–3.90	$F_{1,11} = 0.69$	$p = 0.424$
INW	Adult	Pooled	6.48±0.62	5.46–7.38	5.48±0.52	4.84–6.12	$F_{1,14} = 12.43$	$p = \mathbf{0.003}$
	Juvenile	Pooled	3.06±0.82	2.46–4.82	2.92±0.24	2.64–3.28	$F_{1,11} = 0.59$	$p = 0.460$
PFL	Adult	Pooled	7.21±0.84	5.66–8.00	6.11±0.40	5.44–6.48	$F_{1,14} = 12.38$	$p = \mathbf{0.003}$
	Juvenile	Pooled	3.75±0.83	3.02–5.20	3.46±0.36	2.84–3.88	$F_{1,12} = 0.51$	$p = 0.490$
PFW	Adult	Pooled	6.59±0.70	5.36–7.44	5.65±0.45	4.82–6.06	$F_{1,14} = 9.34$	$p = \mathbf{0.009}$
	Juvenile	Pooled	3.36±0.76	2.58–4.54	3.07±0.26	2.68–3.36	$F_{1,12} = 0.96$	$p = 0.346$
FL	Adult	Pooled	8.68±0.99	7.48–10.30	7.54±0.64	6.68–8.40	$F_{1,14} = 5.28$	$p = \mathbf{0.038}$
	Juvenile	Pooled	4.99±0.85	4.08–6.32	4.61±0.37	4.16–5.28	$F_{1,12} = 1.38$	$p = 0.262$

Table 3.11. Continued.

Characters	Life stage	Sex	Typical		Variant		Intra-specific difference	
			Mean±SD	Range	Mean±SD	Range		
FW	Adult	Pooled	7.39±0.97	5.56–8.64	6.70±0.39	5.98–7.10	$F_{1,14} = 2.11$	$p = 0.168$
	Juvenile	Pooled	3.85±0.70	3.04–5.22	3.54±0.38	3.14–4.08	$F_{1,12} = 1.89$	$p = 0.194$
PL	Adult	Pooled	13.03±2.20	9.56–16.36	12.40±0.60	11.64–13.26	$F_{1,14} = 0.21$	$p = 0.651$
	Juvenile	Pooled	7.54±1.30	6.48–10.12	7.04±0.61	6.12–7.90	$F_{1,12} = 0.66$	$p = 0.434$
PW	Adult	Pooled	9.35±1.10	7.92–10.64	8.75±0.50	8.06–9.32	$F_{1,14} = 0.83$	$p = 0.378$
	Juvenile	Pooled	5.09±1.01	4.36–7.38	4.79±0.61	4.18–5.92	$F_{1,12} = 0.11$	$p = 0.749$

Table 3.12. Information on Principal Component Analysis (PCA) and loadings for *Naja kaouthia* population in Mizoram, northeastern India between the phenotypic groups.

Variables	PC1	PC2	PC3	PC4	PC5
adj HW	0.838	-0.113	-0.278	-0.371	0.203
adj HD	0.837	0.152	0.185	-0.454	-0.086
adj S-N	0.787	0.415	0.214	0.271	0.281
adj RH	0.749	0.616	0.067	0.021	-0.162
adj INW	0.872	-0.319	0.005	0.205	-0.180
adj PFL	0.963	0.027	-0.199	0.039	0.018
adj PFW	0.839	0.006	-0.470	0.203	-0.051
adj FL	0.819	-0.434	0.272	0.069	0.214
adj INS	0.878	-0.248	0.249	0.021	-0.219

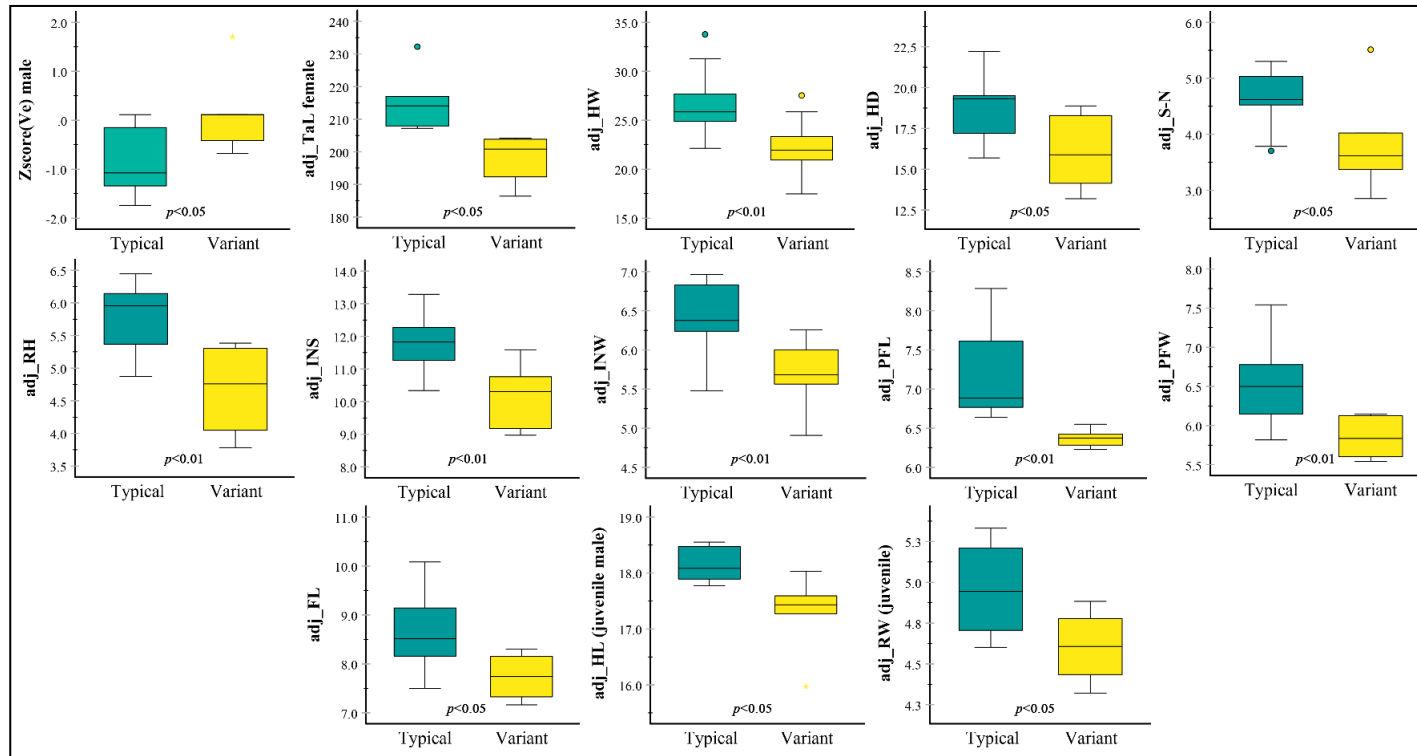


Figure 3.13. Box plot showing median, interquartile range, range (minimum to maximum), and outliers for adult's standardised (Z score) ventrals (Ve) in males, adjusted (adj) mensurals such as tail length (TaL) in females, sex pooled adult's head width (HW), head depth (HD), snout to nostril distance (S-N), rostril height (RH), internarial space (INS), internarial width (INW), prefrontal length (PFL), prefrontal width (PFW), frontal length (FL), HL in juvenile males, and rostral width (RW) in sex pooled juveniles between the phenotypic groups of *Naja kaouthia* population from Mizoram, Northeast India. Significance at the alpha level of 0.05 is given as asterisk in each plot.

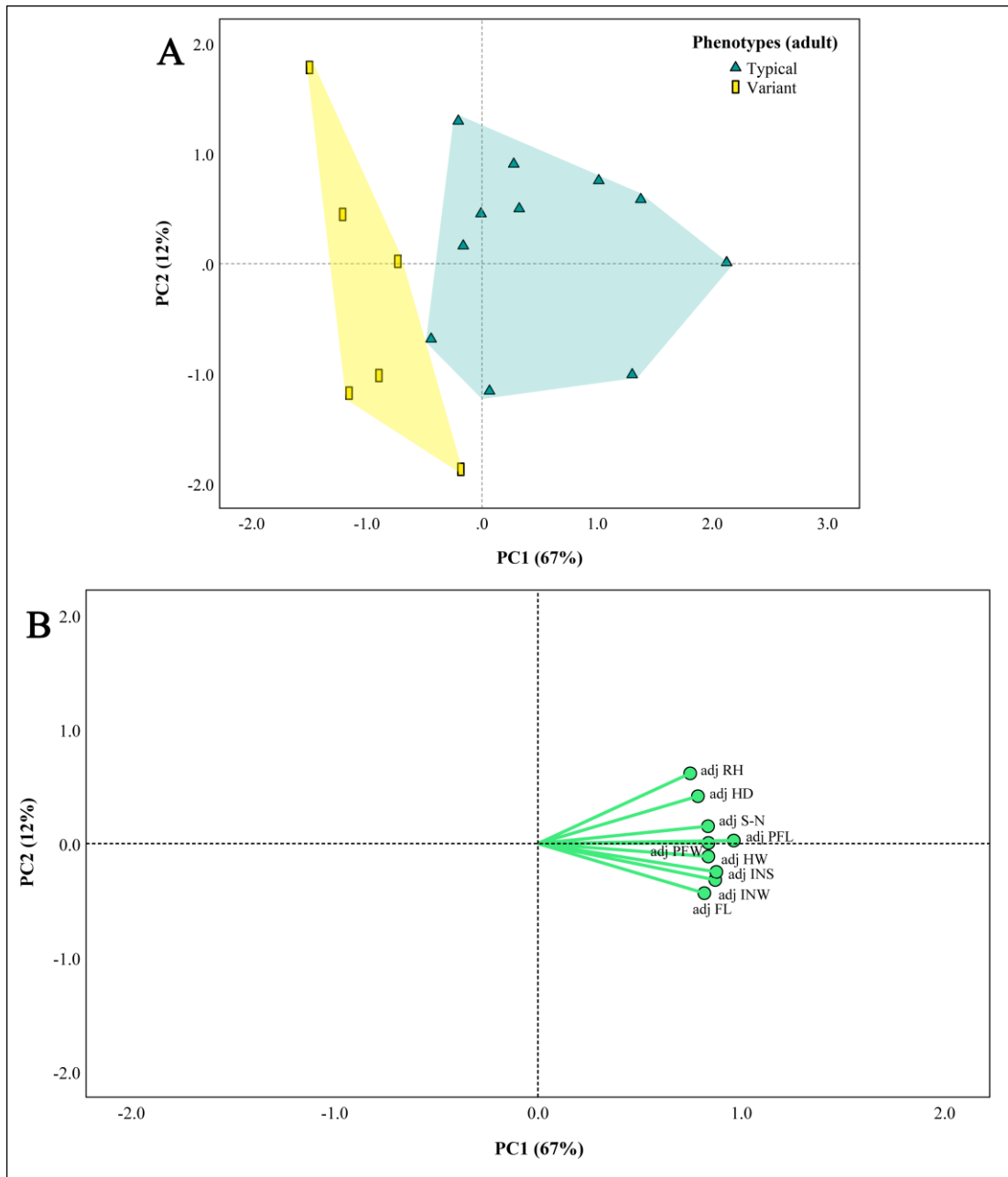


Figure 3.14. (A) Ordination of *Naja kaouthia* population from Mizoram along the first two principal components based on a PCA of the allometric adjusted head width (HW), head depth (HD), snout to nostril distance (S-N), rostril width (RH), internarial space (IOS), internarial width (INW), prefrontal length (PFL), prefrontal width (PFW), and frontal length (FL) of adult specimens. Total variance associated with the PC1 and PC2 are 67% and 12%, respectively. (B) PCA loading plot showing the distribution of the analysed variables along the first two principal components.

Distribution

Naja kaouthia is documented from a total of 48 localities in Mizoram represented by 35 sites from Aizawl District, 4 sites from Kolasib District, 4 sites from Mamit District, 2 sites from Champhai District, 1 site each from Serchhip, Saitual and Lawngtlai Districts, at elevational range of 66– 1,470 m a.s.l (Fig. 3.15; Table 3.13). Moreover, the overall geographical range of the species was plotted based on the range provided in published works and the colour shadings were implemented to correspond the distinct clades recovered in the phylogenetic analyses (Fig. 3.16) (Wallach et al. 2014; Stuart and Wogan 2012; Wüster et al. 1995).

Table 3.13. Detailed distributional records of *Naja kaouthia* documented in this study from Mizoram, India.

Sl. No.	Locality	District	Elevation (m a.s.l.)	Latitude	Longitude
1	Kawnpui	Kolasib	830	24.0460°N	92.6732°E
2	Sawleng	Aizawl	1155	23.980840°N	92.931775°E
3	Lungdai	Kolasib	1189	23.881494°N	92.740626°E
4	Tanhril	Aizawl	952	23.738584°N	92.676006°E
5	Durtlang	Aizawl	1192	23.769065°N	92.742184°E
6	Durtlang North	Aizawl	1107	23.788842°N	92.731065°E
7	Chaltlang	Aizawl	1114	23.7517°N	92.7247°E
8	Chaltlang	Aizawl	1130	23.754022°N	92.724303°E
9	MZU campus	Aizawl	829	23.737694°N	92.665475°E
10	New Secretariat Complex	Aizawl	979	23.726194°N	92.707975°E
11	Mission vengthlang	Aizawl	951	23.712169°N	92.707712°E
12	Mission veng	Aizawl	967	23.714033°N	92.717039°E
13	Lawipu	Aizawl	756	23.723428°N	92.684280°E
14	Bethlehem vengthlang	Aizawl	814	23.730078°N	92.728760°E
15	College veng	Aizawl	810	23.725482°N	92.727310°E
16	Electric veng	Aizawl	939	23.737370°N	92.719981°E
17	Maubawk	Aizawl	954	23.721764°N	92.700134°E
18	Tuivamit	Aizawl	900	23.744663°N	92.683730°E
19	Hunthar	Aizawl	814	23.747806°N	92.715408°E
20	Venglai	Aizawl	1017	23.740862°N	92.723396°E
21	Tlangnuam	Aizawl	945	23.702788°N	92.713338°E
22	ITI veng	Aizawl	827	23.720749°N	92.732250°E
23	Falkland	Aizawl	717	23.730751°N	92.745065°E
24	Kulikawn	Aizawl	844	23.707855°N	92.719994°E
25	Nursery veng	Aizawl	888	23.717384°N	92.705810°E
26	Saikhamakawn	Aizawl	953	23.693702°N	92.718205°E
27	Bawngkawn	Aizawl	961	23.761568°N	92.728524°E

28	Sihphir	Aizawl	1289	23.818031°N	92.734527°E
29	Zemabawk	Aizawl	891	23.736008°E	92.747859°N
30	Luangmual	Aizawl	990	23.738382°N	92.707474°E
31	Zohnuai	Aizawl	941	23.743068°N	92.704262°E
32	Ramrikawn	Aizawl	873	23.746941°N	92.679735°E
33	Mel thum	Aizawl	1008	23.691526°N	92.719161°E
34	Dinthar	Aizawl	956	23.727957°N	92.714849°E
35	Model veng	Aizawl	990	23.7125°N	92.7115°E
36	Thiak	Aizawl	1055	23.471779°N	92.714667°E
37	Hmuifang	Aizawl	1470	23.448744°N	92.759344°E
38	Thenzawl	Serchhip	750	23.284740°N	92.776070°E

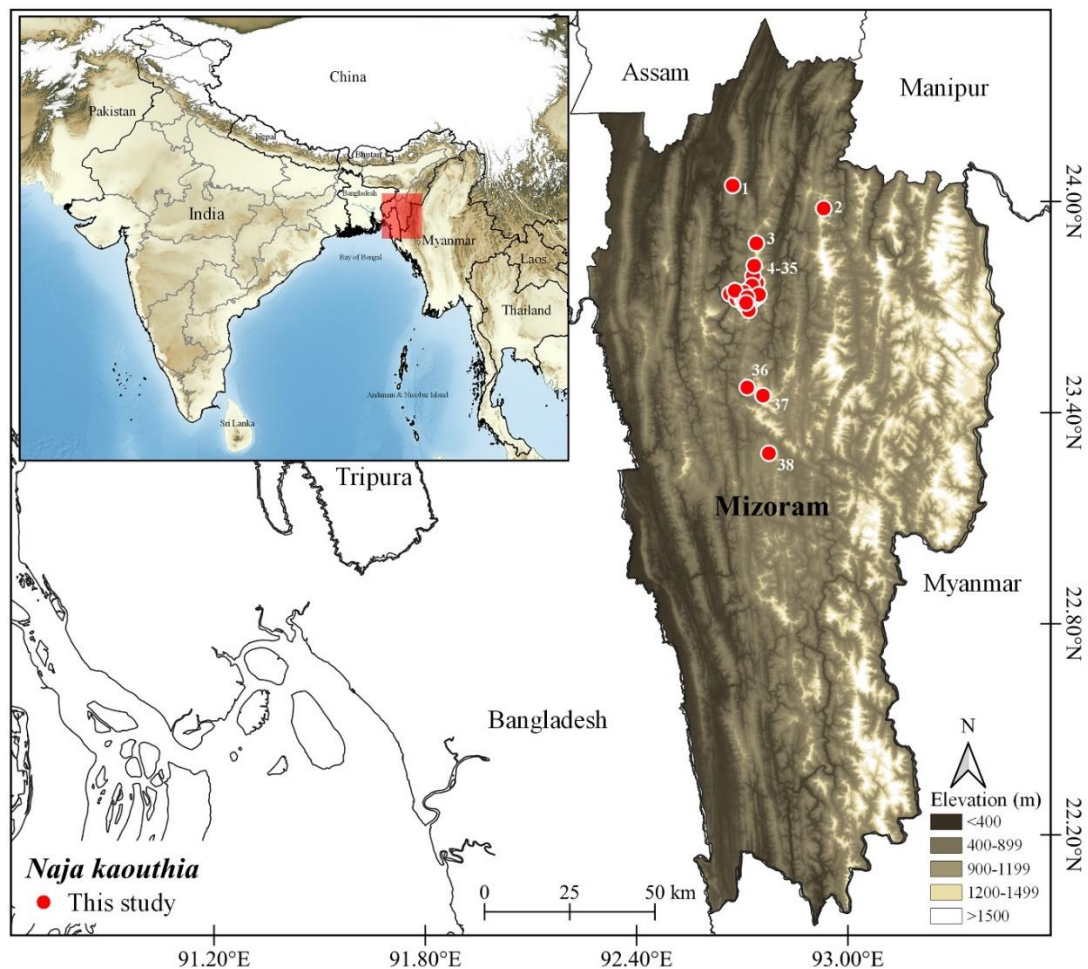


Figure 3.15. Digital elevation map showing the distributional records of *Naja kaouthia* in Mizoram (red circles): 1. Kawnpui; 2. Sawleng; 3. Lungdai; 4–35 Aizawl city area; 36. Thiak; 37. Hmuifang; 38. Thenzawl (see also Table 3.13).

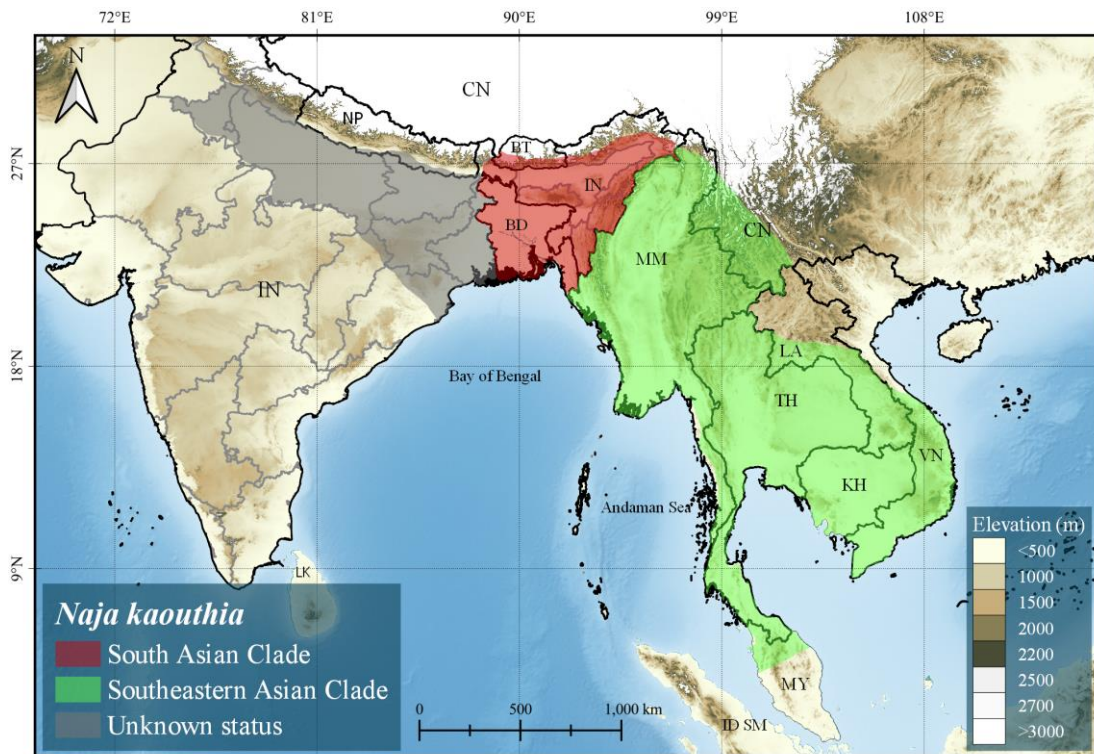


Figure 3.16. Map showing the known distribution range of *Naja kaouthia*, based on the distributional range provided in published works (Wüster et al. 1995; Stuart and Wogan 2012; Wallach et al. 2014); the colour shadings correspond to the distinct clades recovered in the phylogenetic analyses.

Discussion

The documentation of the species based on direct observation or collection during this work along with personal interactions with local people suggested that *N. kaouthia* is not uncommon species in Mizoram, and the rescued individuals or specimens examined were predominantly captured nearby human habitations especially in the urban areas. Moreover, Lalremsanga et al. (2011) considered the species to be found throughout the state. They are commonly encountered from plantation sites, agricultural lands near vicinity of open water sources to human settlements in both urban and rural areas. This work not only corroborated the inter-population genetic variability that has been mentioned in earlier works (Kundu et al. 2020b; Ratnarathorn et al. 2019), but also support the existence two distinct evolutionary lineages namely, South Asian Clade and Southeastern Asian clades as previously proposed by Shi et al. (2022) based on *cox1* gene. In addition, the systematic status of the Chinese specimens of *N. fuxi* (CHS026, CHS726, HS16001) was reaffirmed and they formed a significantly supported sister lineage of *N. atra* in both ML and BI trees (PP=1.00; UFB= 99); they were also detected as distinct species in the ASAP and also separated by a considerably high number of mutational steps in the haplotype networks of *cytb* (22 mutations; Hap 4 and Hap 10) and *cox1* (10 mutations; Hap 2) compared to the separation of other haplotypes within *N. kaouthia*. The outlying sequence of *N. naja* (NC010225) from GenBank also appears to be misidentified specimen of *N. atra* which would need taxonomic confirmation. The present study put forward a taxonomic suggestion to establish a comprehensive reassessment of the species boundaries concerning the distinct clades of *N. kaouthia*. Moreover, the detection of *N. kaouthia* from China (KIZYPX18216) as distinct species from both the representative specimens of South Asian and Southeast Asian Clades in the ASAP analysis warrant further investigation of the taxonomic status of this specimen. Nevertheless, morphological and molecular evidence including data from toptotypical specimens would be imperative for further taxonomic re-evaluation of *N. kaouthia*.

The studied population of *N. kaouthia* is exhibiting sexual dimorphism in the Ve which is significantly higher in adult females, while Sc is significantly higher in

adult males; the TaL, S-E, and ED are significantly higher in adult males; among juveniles, HL is significantly higher in males, while ND is significantly higher in females. We also recognized that among the meristics parameters, only Ve is significantly different between the two groups, and the mean value of variant male's Ve is significantly higher than the typical males; among the mensural parameters, significant intra-population differences are seen in adult female's TaL (higher in typical females); sex pooled adult's HW, HD, S-N, RH, INS, INW, PFL, and PFW (all higher in typical), juvenile male's HL (higher in typical males); sex pooled juvenile's RW (higher in typical). Therefore, we accepted the alternative hypothesis which states that the phenotypic variation of hood marking is having an effect on meristics and morphometrics between the two groups. Owing that *a priori* grouping of the variant accommodated various phenotypic forms; further nesting of significantly different sub-groups within the variant is not unexpected in a larger sampling size.

Genetically, in the *cytb* dataset, three distinct haplotypes were seen within the studied population constituted by the typical (MZMU2044, Hap 1) and variant (MZMU2415, Hap 2; MZMU1425, Hap 3) which suggests that this neutral marker (*cytb*) is a potential candidate marker for further large-scale investigation on the taxon's intra-population genetics. However, ascertainment of the probable correlations between the genetic and phenotypic variations within *N. kaouthia* populations remains a crucial challenge (Orgogozo et al. 2015). Kaliontzopoulou et al. (2018) further expressed the importance of considering the geographical structure of both within-population diversity and among-population divergence for establishing the indirect association between phenotypic, genetic and environmental factors. Based on multiple species delimitation approaches, Kundu et al. (2020b) also suggested cryptic diversity among *N. kaouthia* populations in China, India, Thailand and Bangladesh. Thus, extensive population systematics, precise determination of the species limits across and within different biogeographic boundaries, elucidation of the ecological attributes for the identified sexually dimorphic traits as well as intra-population variations for this genetically and phenotypically complex species are yet to be explored.

CHAPTER 4

Ophiophagus hannah (Cantor, 1836)

Review of literature

King cobra, *Ophiophagus hannah* (Cantor, 1836) is the longest venomous snake reaching up to 5.5 m (Charlton 2018). It is a widespread elapid snake found across East Asia, South Asia, and Southeast Asia (Wallach et al. 2014) at the elevations between 60 to 2,700 m a.s.l. (Ahmed et al. 2009); and occupy various niches of habitat like primary tropical forests, scrubland, cultivated fields as well as suburban areas (Lim et al. 2011; Shankar et al. 2021). King cobra is a Schedule I species under the Wildlife (Protection) Amendment Act (2022) in India, and is currently categorized as Vulnerable under IUCN Red List of Threatened species with its range considered to be declining (Stuart et al. 2012). It is the only snake species where females actively construct a nest from leaf litter or other plant material (Loveridge 1946; Schmidt and Inger 1957; Whitaker et al. 2013; Hrima et al. 2014; Dolia 2018), and can lay up to 14–53 eggs in a single clutch (Das 2012; Hrima et al. 2014; Burchfield 1977). Female snakes are also known to guard the nest, sometimes residing in the nest's upper chamber or coiling on top of the nest (Loveridge 1946; Whitaker et al. 2013; Vanlalchhuana et al. 2016), and subsequently deserting the nest when the neonates hatch (Kannan 1993).

The evidence of many potential biogeographical barriers across the range of the king cobra populations propounded cryptic diversity within the species (Suntrarachun et al. 2014; Shankar et al. 2021). Concerning this, four distinctly evolving lineages representing four candidate species have been detected such as the Indo-Chinese, Western Ghats, Indo-Malayan and Luzon Island lineages where the northeastern Indian populations including samples from Mizoram found to be nested within the foremost lineage (Shankar et al. 2021). The different geographical lineages are also considered to exhibit different phenotypes that suggest divergence in the taxonomy (Shankar et al. 2021) as well as differences in the venom toxicity and antigenicity (Tan et al. 2020). Moreover, biogeographical analyses and niche modeling of the species determined that the distribution of the species across its range is highly influenced by the presence of humid climatic condition (Amat and

Escoriza 2022). Although the occurrence of the species in Mizoram was recorded in earlier faunal inventory works from the state (Pawar and Birand 2001; Mathew 2007; Laltanpuia et al. 2008; Lalremsanga et al. 2011), while other literature on the species from Mizoram predominantly focused on the breeding ecology and natural history (Hrima et al. 2014; Vanlalchhuana et al. 2016). A limited number of specimens from Mizoram has been included in the previous molecular studies, and not much assessment of the morphological data has been done from this population (Kundu et al. 2020b; Shankar et al. 2021). Mizoram king cobra samples were also lacking in the morphological analyses of Shankar et al. (2021). Therefore, this chapter aims to provide additional information on the systematics of king cobra population in Mizoram based on morphological analyses and mitochondrial genes inferences.

Materials and methods

Sampling

A total of 27 adult individuals represented by 14 preserved and 13 live individuals were examined. Liver tissue was dissected from freshly killed six specimens which were persecuted by locals (MZMU1332, MZMU1793, MZMU2046, MZMU2604, MZMU2605, MZMU2411), and the tissue samples were subsequently stored in 95% ethanol at -20°C for molecular analyses. Then, the specimens were preserved in 10% formalin. The live individuals examined were subsequently released after taking morphological data.

DNA extraction and PCR amplification

Genomic DNA was extracted using DNeasy (Qiagen™) blood and tissue kits following the manufacturer's instructions (DNeasy® Blood & Tissue Handbook 2023). Fragments of three mitochondrial markers, 16S rRNA (*16s*), cytochrome c oxidase subunit 1 (*cox1*), and cytochrome b (*cytb*) were amplified through Polymerase Chain Reaction (Mullis et al. 1986). Target mt gene sequences were amplified in a 20 µL reaction volume, containing 1X DreamTaq PCR Buffer, 2.5 mM MgCl₂, 0.25 mM dNTPs, 0.2 pM of each gene primer pair, approximately 3.0 ng of extracted DNA, and 1U of Taq polymerase using the thermal profiles and primers given in Table 1.1 of Chapter 1. PCR products were checked using gel

electrophoresis on a 1.5% agarose gel containing ethidium bromide. The PCR products were cleaned using ThermoFisher ExoSAP-IT PCR product cleanup reagent and subsequently sequenced using Sanger's dideoxy method using the ABI 3730xl DNA Analyzer at Barcode BioSciences, Bangalore, India. The newly generated partial gene sequences were then screened through nucleotide BLAST (<https://blast.ncbi.nlm.nih.gov/>) and ORF finder (<https://www.ncbi.nlm.nih.gov/orffinder/>), and then deposited in the NCBI repository and are available in GenBank via the accession numbers given in Table 4.1. In this work, a total of five *16s*, one *cox1* and six *cytb* sequences were generated and were combined with published conspecific sequences obtained from GenBank; the database sequences of *Sinomicrurus peinani* (CHS643) and *S. kelloggi* (CHS854) were used as the outgroups.



Figure 4.1. Live adult male *Ophiophagus hannah* at Mizoram University campus.

Table 4.1. Details of three mitochondrial genes utilized for *Ophiophagus hannah* (OH) with *Sinomicrurus peinani* (SP) and *S. kelloggi* (SK) as outgroups.

Species	Voucher	<i>16s</i>	<i>cytb</i>	<i>cox1</i>	Locality	Reference
OH	MZMU1793	PP152251	PP162896	PP152256	Mizoram, India	This study
OH	MZMU2046	PP152252	PP162897	-	Mizoram, India	This study
OH	MZMU2604	PP152253	PP162898	-	Mizoram, India	This study
OH	MZMU2605	PP152254	PP162899	-	Mizoram, India	This study
OH	MZMU2411	-	PP162900	-	Mizoram, India	This study
OH	MZMU1332	PP152255	PP162901	-	Mizoram, India	This study
OH	CESS 1001	MZ087825	MZ343879	-	Guddekare, Thirthahalli, Karnataka	Shankar et al. 2021
OH	CESS1003	MZ087829	-	-	Pookode, Wayanad, Kerala	Shankar et al. 2021
OH	CESS1004	MZ087840	-	-	Middle Andamans	Shankar et al. 2021
OH	CESS1013	MZ087842	MZ343880	-	MZU Campus, Mizoram	Shankar et al. 2021
OH	CESS1015	MZ087844	MZ343881	-	Nghalchawm, Mizoram	Shankar et al. 2021
OH	CESS1017	MZ087855	-	-	Darlung, Mizoram	Shankar et al. 2021
OH	CESS1022	MZ087837	MZ343882	-	Bavikere, Megaravalli, Karnataka	Shankar et al. 2021
OH	CESS1030	MZ087834	MZ343883	-	Devachowada, Panshi, Colem, Goa	Shankar et al. 2021
OH	CESS1031	MZ087838	MZ343884	-	Copardem, Valpoi, Goa	Shankar et al. 2021
OH	CESS1033	MZ087830	-	-	Virdi, Dodamarg, Sindhudurga, Maharastra	Shankar et al. 2021
OH	CESS1061	MZ087847	MZ343885	-	Ramagarh, Uttarakhand	Shankar et al. 2021
OH	CESS1081	MZ087850	-	-	Angul, Odisha	Shankar et al. 2021
OH	CESS1082	MZ087854	-	-	Kaziranga, Assam	Shankar et al. 2021
OH	CESS1083	MZ087831	MZ343886	-	Trivandrum, Kerala	Shankar et al. 2021
OH	CESS1086	MZ087851	-	-	Nilgiri, Balasore, Odisha	Shankar et al. 2021

Table 4.1. Continued.

Species	Voucher	<i>16s</i>	<i>cytb</i>	<i>cox1</i>	Locality	Reference
OH	CESS1087	MZ087833	-	-	KMTR, Thirunelveli, Tamilnadu	Shankar et al. 2021
OH	CESS1092	MZ087864	-	-	Bali	Shankar et al. 2021
OH	CESS1097	MZ087871	-	-	Sumatra, Greater Sunda	Shankar et al. 2021
OH	Ohannah502	MZ087836	MZ343874	-	Western Ghats	Shankar et al. 2021
OH	Ohannah500	MZ087843	MZ343872	-	Bitar Kanika, Odhisa	Shankar et al. 2021
OH	Ohannah501	MZ087852	MZ343873	-	Bitar Kanika, Odhisa	Shankar et al. 2021
OH	Ohannah575	MZ087853	MZ343876	-	Bitar Kanika, Odhisa	Shankar et al. 2021
OH	Ohannah577	MZ087841	MZ343877	-	Karawang, Middle Andamans	Shankar et al. 2021
OH	Ohannah588	MZ087863	MT346766	-	Southern Vietnam	Shankar et al. 2021
OH	Ohannah1816	MZ087856	MZ087856	-	Arunachal Pradesh	Shankar et al. 2021
OH	4018		MT346773	-	China	Kazandjian et al. 2020
OH	576	MZ087872	MT346765	-	Singapore Zoo	Kazandjian et al. 2020
OH	1060	MZ087874	MT346767	-	Java	Shankar et al. 2021; Kazandjian et al. 2020
OH	574	-	MZ343875	-	Wandoor, South Andaman	Shankar et al. 2021;
OH	1802	MZ087875	MT346768	-	Puerto Galera, Mindoro, Philippines (Occidental Mindoro)	Shankar et al. 2021; Kazandjian et al. 2020
OH	2922	MZ087873	MT346769	-	Indonesia	Shankar et al. 2021; Kazandjian et al. 2020

Table 4.1. Continued.

Species	Voucher	<i>16s</i>	<i>cytb</i>	<i>cox1</i>	Locality	Reference
OH	2923	MZ087876	MT346770	-	Malaysia	Shankar et al. 2021; Kazandjian et al. 2020
OH	2924	MZ087877	MT346771	-	Malaysia	Shankar et al. 2021; Kazandjian et al. 2020
OH	2925	-	MT346772	-	Indonesia	Kazandjian et al. 2020
OH	187	-	MT346764	-	Sabha	Kazandjian et al. 2020
OH	1820	-	MZ343862	-	Montalban, Rizal, Luzon, Philippines	Shankar et al. 2021
OH	1821	MZ087878	MZ343863	-	Montalban, Rizal, Luzon, Philippines	Shankar et al. 2021
OH	NMNH57	MZ087857	-	-	China	Shankar et al. 2021
OH	NMNH50	MZ087866	-	-	Malaysia (Sarawak)	Shankar et al. 2021
OH	NMNH54	MZ087867	-	-	Malaysia (Sarawak)	Shankar et al. 2021
OH	NMNH49	MZ087865	-	-	Malaysia	Shankar et al. 2021
OH	NMNH55	MZ087868	-	-	Indonesia	Shankar et al. 2021
OH	NMNH56	MZ087869	-	-	Indonesia	Shankar et al. 2021
OH	OH008	MZ087861	-	-	Sakaerat Biospheres Reserves, Thailand	Shankar et al. 2021
OH	OH002	MZ087862	-	-	Sakaerat Biospheres Reserves, Thailand	Shankar et al. 2021
OH	Daknong	JN709991	-	-	Daknong, Vietnam	Dang et al. 2011
OH	06.2008__1	JN709992	-	-	Quang Tri, Vietnam	Dang et al. 2011
OH	Camau	JN709993	-	-	Camau_Vietnam	Dang et al. 2011

Table 4.1. Continued.

Species	Voucher	<i>16s</i>	<i>cytb</i>	<i>cox1</i>	Locality	Reference
OH	SongBe	JN709994	-	-	SongBe, Vietnam	Dang et al. 2011
OH	OHA4		-	LC533892	Thailand	Puinongpo et al. 2020
OH	OHA1	-	AB920234	LC519982	Thailand	Puinongpo et al. 2020; Supikamolteni et al. 2015
OH	SR256	-	-	MH153655	China	Zhou et al. 2022
OH	OH01	-	-	LC075344	Bangkok, Thailand	Laopichienpong et al. 2016
OH	YJWS02	-	-	MF099705	China	Zhou et al. 2022
OH	OHA3	-	AB920236	AB920182	Thailand	Supikamolteni et al. 2015
OH	OHA2	-	AB920235	AB920181	Thailand	Supikamolteni et al. 2015
OH	SR254	-	-	KR046075	China	Gan and Chen 2015
OH	OH2	-	-	JX235708	China	Chao and Liao 2012
SP	CHS643	MK194117	MK201448	MK064794	China	Li et al. 2020
SK	CHS854	MK194268	MK201570	MK064918	China	Li et al. 2020

Molecular phylogenetics

DNA sequences were aligned with the default parameter settings of MUSCLE algorithm (Edgar 2004) in MEGA 11 (Tamura et al. 2021); for the *16s* dataset, the ambiguously aligned sites were removed under heuristic method in trimAL software (Capella-Gutiérrez et al. 2009). The three mitochondrial gene alignments were concatenated, and were partitioned by gene and codon positions. Uncorrected p-distances were estimated in MEGA 11 (Tamura et al. 2021) using the complete deletion option for the treatment of gaps/missing data. PartitionFinder v2.1 (Lanfear et al. 2017) was utilized to search for the optimal partitioning schemes and nucleotide evolutionary models through Bayesian Information Criterion (BIC). A Bayesian inference (BI) phylogeny was reconstructed by applying the best partitioning schemes and nucleotide evolutionary models in Mr.Bayes v3.2.5 (Ronquist et al. 2012). The MCMC was run with four chains (one cold and three hot chains) for 20 million generations and sampled every 5000 generations. Tracer v1.7 (Rambaut et al. 2018) was used to check the convergence of likelihood and the burn-in cut-off. The first 25% of trees from the BI analysis were discarded as burn-in. Maximum likelihood (ML) phylogenetic tree was inferred using the IQ-TREE webserver (Nguyen et al. 2015) by selecting FreeRate heterogeneity (Soubrier et al. 2012) and 10,000 Ultrafast Bootstrap (UFB) replicates (Minh et al. 2013) using the partitions identified by PartitionFinder v2.1 (Lanfear et al. 2017), and the models selected based on BIC values by ModelFinder (Kalyaanamoorthy et al. 2017) integrated into the IQ-TREE (Nguyen et al. 2015). The phylogenetic trees were viewed and illustrated using web-based tree annotator iTOL software v5 (Letunic and Bork 2021).

Matrilineal haplotype networks

The three mitochondrial DNA sequences were utilized to screen the matrilineal genealogy among populations through mtDNA-based haplotype estimation. The three aligned datasets were utilized for generating haplotypes in DnaSP v.6 (Rozas et al. 2017), and the trait matrix corresponding to the locality of the samples was inserted in the output file. The haplotype networks were plotted in

PopArt v.1.7 (Leigh and Bryant 2015) using the Median-Joining method, which is a useful statistical approach for intra-species haplotype networks (Bandelt et al. 1999).

Species delimitation

The *cytb* dataset, partitioned by codon, was utilized for performing BI based Poisson Tree Processes (PTP) species delineation analyses (Zhang et al. 2013) implemented in iTaxoTools v0.1 (Vences et al. 2021). For the input file of PTP, a non-ultrametric tree was produced in IQ-TREE (Nguyen et al. 2015) with 10,000 UFB replicates (Minh et al. 2013) using the models selected for *cytb* partitions. Only the *cytb* dataset was utilized for the species delimitation analysis as it contains suitable number of samples from different geographical regions compared to the other three genes. The standardized p-distances were further utilized for Principal Coordinate Analysis (PCoA) (Gower 1966) to visualize the genetic differentiation among the target taxa. Only the *cytb* dataset was utilized for PTP analyses because it contains more representative samples from the three clades compared to the other genes.

Morphology

Morphometric (mensural and meristic) data were obtained from the 27 adult individuals (15 males + 12 females) examined from the *O. hannah* population of Mizoram. Except snout–vent length (SVL, measured from tip of snout to anterior margin of vent) and tail length (TaL, measured from anterior margin of vent to tail tip) which were measured with a measuring tape, the following mensural characters were measured to the nearest millimetre with a Mitutoyo digital caliper: eye diameter (ED, horizontal diameter of orbit); nostril diameter (ND, largest diameter of nostril); eye–nostril length (E-N, distance between posteriormost point of nostril and anteriormost point of eye); eye–snout length (E-S, distance between anteriormost point of eye and tip of snout); snout–nostril length (S-N, distance between tip of snout and anteriormost point of nostril); head length (HL, distance between posterior edge of mandible and tip of snout); head width (HW, maximum width of head); height of rostrum (RH, the height of rostral scale); width of rostrum (RW, the width of rostral scale); internarial space (INS, distance between the nostrils); interorbital space (IOS, distance between the orbits); internarial length (INL, length of internarial

scale); internarial width (INW, width of internarial scale); prefrontal length (INL, length of internarial scale); frontal length (FL, length of frontal scale); frontal width (FW, width of frontal scale); parietal length (PL, length of parietal scale); parietal width (PW, width of parietal scale) (Fig. 4.1). Meristic characters were taken as follows: supralabials (SL); supralabials touching eye (SLe); infralabials (IL) (first labial scale to last labial scale bordering gape); temporals (Tem), postocular (PoO); preocular (PrO); anal scute (As); dorsal scale rows (DSR, counted around the body from one side of ventrals to the other in three positions, on one head length behind the neck, at midbody and at one head length before cloacal plate); when counting the number of ventral scales (Ve), the values were scored following Dowling (1951). Subcaudal scales (Sc) were counted from the first subcaudal scale meeting its opposite to the scale before the tip of the tail excluding the terminal scute, and the number of undivided subcaudals (USc) are also counted starting from the vent area. The sex of the specimens was identified by examining everted hemipenes or by ventral tail dissection. Values for bilateral head characters are given in left/right order. Other than the conventional taxonomic characters, relevant morphological parameters which have been utilized by Shankar et al. (2021) were adopted and tested for interpopulation morphological variation.

Sexual dimorphism

The meristic data were standardized first to their zero mean and standard deviation. For mensural data, the best allometric adjustment model was determined based on the best linear regression model which gives the highest within-group correlation to make a linear relationship with body size to avoid the effect of allometric growth (Thorpe 1975). Firstly, the meristics data (Ve and Sc) of adults and juveniles were tested for sexual dimorphism utilizing a separate one-way analysis of variance (ANOVA) for both life stages using sex as a factor along with Levene's test (Levene 1961) for testing homogeneity of variances. Brown-Forsythe test (Brown and Forsythe 1974) was also tested as an alternative approach in case the assumption of homoscedasticity was violated. For mensural (TaL, HL, HW, HD, ED, ND, E-S, N-S, N-E, RH, RW, INS, IOS, INL, INW, PFL, PFW, FL, FW, PL, and PW), one-

way analysis of covariance (ANCOVA) was carried out with snout-vent length (SVL) as a covariate and sex as a factor.

Interpopulation difference

The standardized meristic characters such as V_e , S_c and anterior dorsal scale row (ADSR) were analysed using one-way ANOVA by sex pooled using lineage/population as a factor; and Levene's test (Levene 1961) was conducted to test the homogeneity of variances. Brown-Forsythe test (Brown and Forsythe 1974) was also performed to be utilized as an alternative approach in case the assumption of homoscedasticity was violated.

Principal component analysis

The sexually dimorphic and characters differed across different lineage/populations identified through the univariate analyses were further ordinated through Principal component analysis (PCA). The correlation matrices between all pairs of the morphological variables, variance explained by each eigenvalue as well as the correlations of each variable to the first two components are explored. All statistical analyses and graphical representations were performed using free access statistical packages viz. PAST 4.13 (Hammer et al. 2001) and PSPP v.1.6.2 (GNU Project 2015).

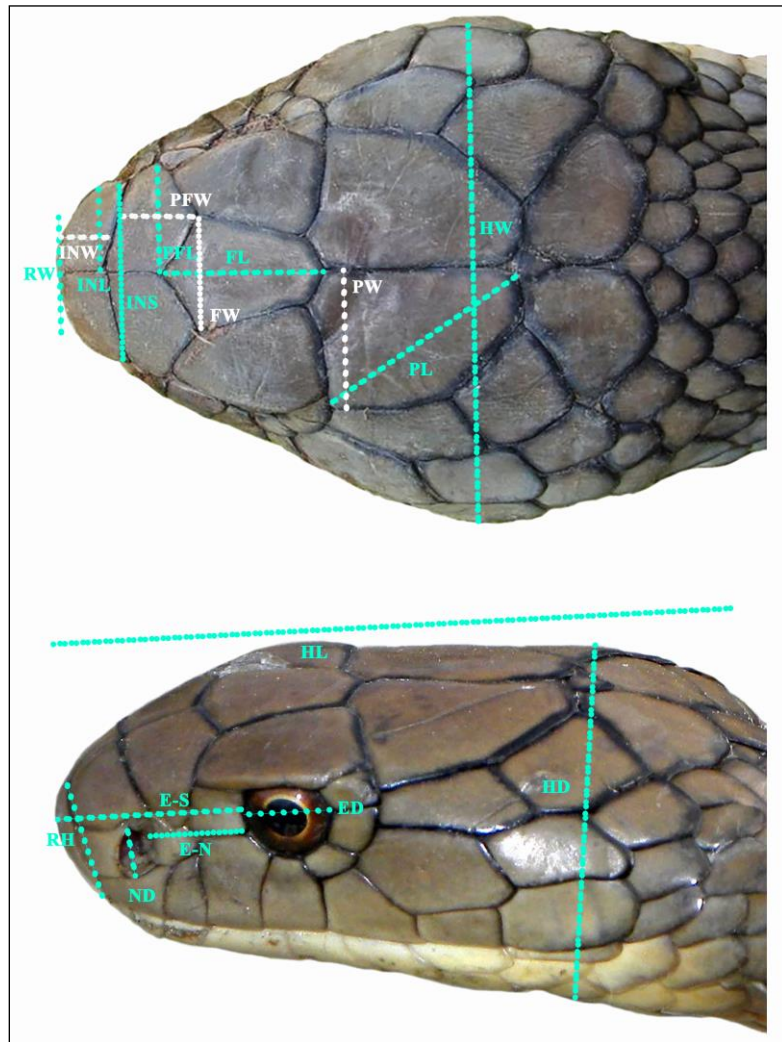


Figure. 4.2. Description of head morphometrics used in this chapter: (top) maximum width of head (HW), width of snout at level of nostril (SW), distance between the nostrils i.e., internarial space (INS), length of internarial scale (INL), width of internarial scale (INW), length of prefrontal scale (PFL), width of prefrontal scale (PFW), length of frontal scale (FL), width of frontal scale (FW), length of parietal scale (PL), width of parietal scale (PW), height of rostral scale (RH), width of rostral scale (RW), width of white inter-band on head at level of supraocular in measurement (WBH); (below) length of head from tip of snout to angle of jaw (HL), depth of head (HD), horizontal eye diameter (ED), maximum nostril diameter (ND), eye to snout distance (E-S), eye to nostril distance (E-N). Photo credit: H.T. Lalremsanga.

Results

Phylogenetic relationships and species delimitation

The best partitioning schemes and nucleotide evolutionary models selected for the two types of phylogenetic inferences were provided in (Table 4.2). The concatenated aligned matrix of *16s*, *cox1*, and *cytb* was 2,293 bp in length; the flanking gaps created by shorter nucleotide sequences were treated as missing data. The BI (Fig. 4.3) and ML (Fig. 4.4) trees were largely congruent in their topology. The average standard deviation of split frequencies among the four Bayesian runs was 0.010458 with the average values of ESS>1,300; the Bayesian posterior probability (PP) values are interpreted as the nodal support in the BI tree. The concatenated three mitochondrial genes based phylogenetic analyses depicted lineage diversification among *O. hannah* populations showing four distinct clades concordant to the pre-defined four independent lineages by Shankar et al. (2021) such as the Indo-Chinese, Western Ghats, Indo-Malayan and Luzon Island lineages. The study population from Mizoram nested within the Indo-Chinese lineage along with the other populations from Northeast India (Arunachal Pradesh, Assam) and other Indian states (Odisha, Uttarakhand, Andaman Islands), Thailand, China, and Vietnam. Moreover, the Indo-Chinese lineage is forming a well-supported sister clade to the Western Ghats lineage (PP=0.94; UFB=91). The clade of Luzon Island lineage is basal to the other three lineages with a well-supported root (PP=1.0; UFB=98); the Indo-Malayan lineage is also forming distinct clade with a well-supported root (PP=0.93; UFB=88) and is forming a moderately supported sister clade to both Western Ghats and Indo-Chinese lineage (PP=0.70; UFB=71); and the clade of Western Ghats lineage is also well-supported (PP=0.93; UFB=97). The bPTP species delimitation detected both Indo-Chinese and Western Ghats lineages as a single putative species, while detecting the other two lineages as distinct species each.

Table 4.2. Nucleotide substitution model selected for the BI and ML phylogenetic analyses.

Partitions	Sites	BI	ML
I	<i>16s</i> , <i>cox1</i> pos 3, <i>cytb</i> pos 3	HKY+I	TN+F+I
II	<i>cox1</i> pos 1	F81+I	F81+F+I+G4
III	<i>cox1</i> pos 2, <i>cytb</i> pos 2	HKY	TN+F
IV	<i>cytb</i> pos 1	HKY	HKY+F

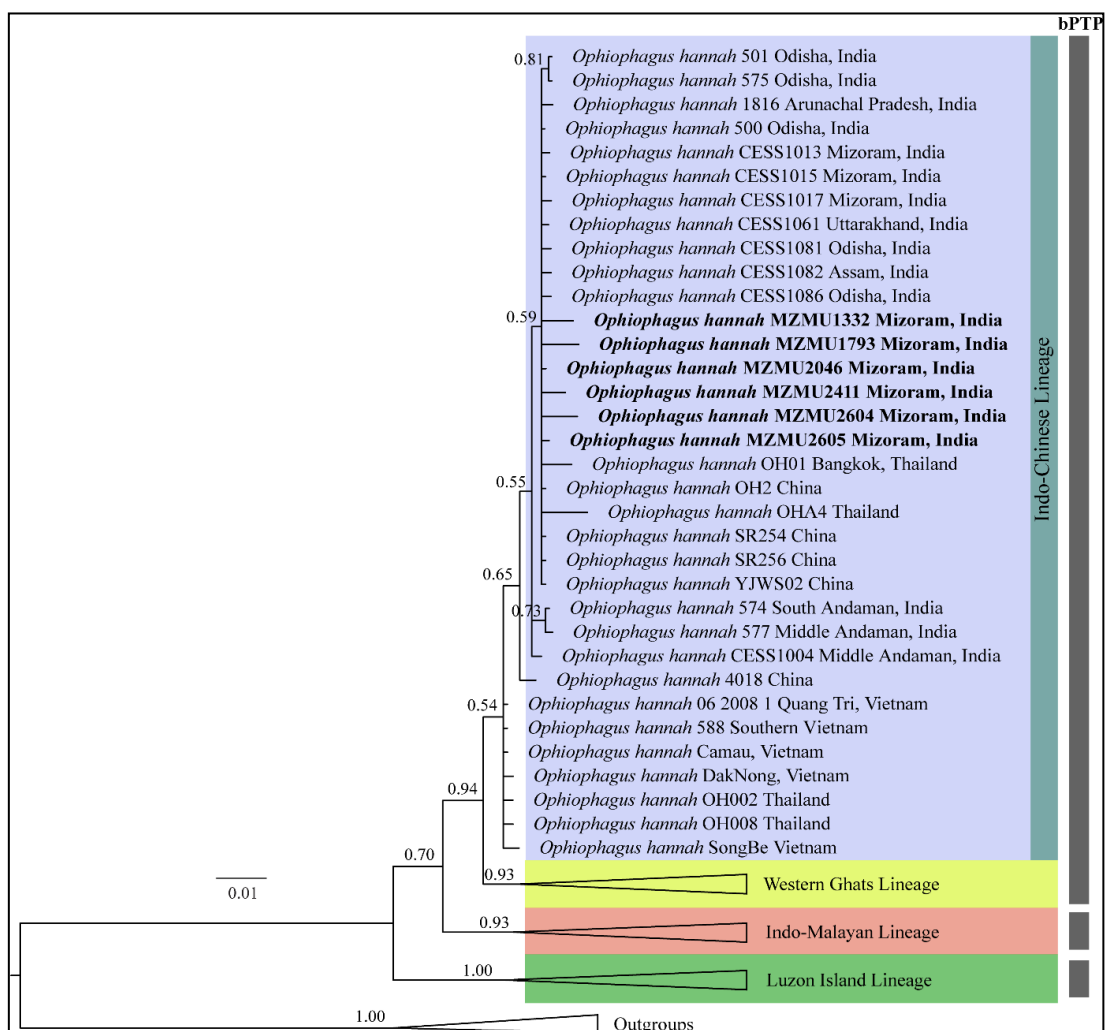


Figure 4.3. Bayesian inference (BI) phylogenetic tree based on concatenated mitochondrial *16s*, *cox1*, and *cytb* genes of *Ophiophagus hannah*; lineage partitions recovered from CYTB-based PTP analyses are presented besides the BI tree. Values at each node represent Bayesian posterior probabilities (PP).

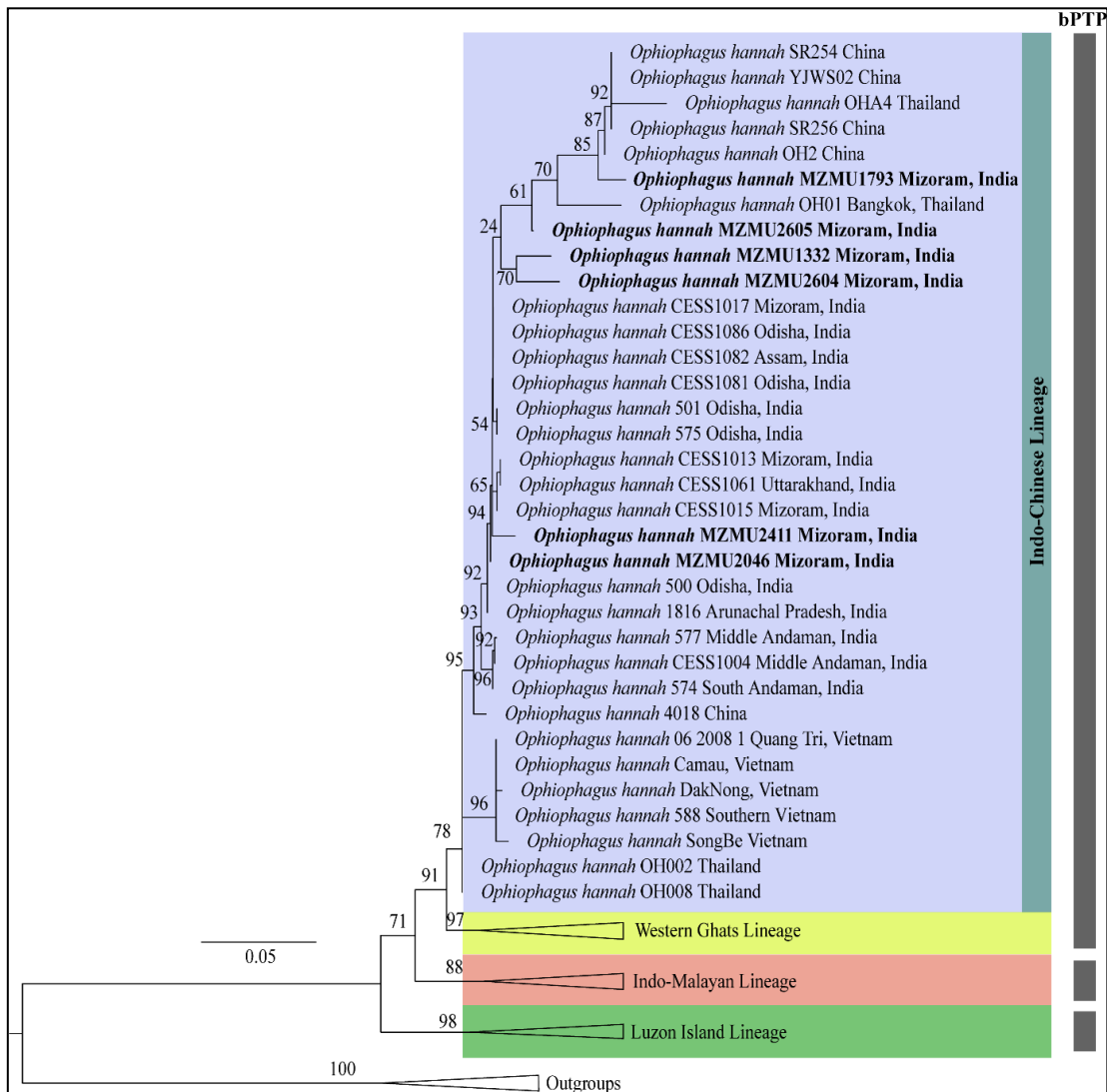


Figure 4.4. Maximum Likelihood (ML) phylogenetic tree based on concatenated mitochondrial *16s*, *cox1*, and *cytb* genes of *Ophiophagus hannah*; lineage partitions recovered from CYTB-based PTP analyses are presented besides the ML tree. Values at each node represent Ultrafast Bootstrap values (UFB).

Matrilineal haplotype

The gene wise estimation of haplotype diversity (H_d) and reconstruction of haplotype networks was conducted based on the three mitochondrial genes. In *16s*, a total of seven distinct haplotypes (Hap) with $H_d=0.7928$ are recovered: Hap 1 [MZMU1793, MZMU2046, MZMU2604, MZMU2605, MZMU1332, CESS1013, CESS1015, CESS1017 (Mizoram, India); CESS1061 (Uttarakhand, India); CESS1081, CESS1086, 500, 501, 575 (Odisha, India); CESS1082 (Assam, India); 1816 (Arunachal Pradesh, India)], Hap 2 [CESS1001, CESS1022 (Karnataka, India); CESS1003, CESS1083 (Kerala, India); CESS1030, CESS1031 (Goa, India); CESS1033 (Maharashtra, India); CESS1087 (Tamil Nadu, India); 502 (Western Ghats, India)], Hap 3 [CESS1004, 577 (Middle Andamans, India)], Hap 4 [CESS1092 (Bali); CESS1097 (Greater Sunda); 576 (Singapore Zoo); 1060 (Java); 2922, NMNH55, NMNH56 (Indonesia)], Hap 5 [588 (Vietnam); OH002, OH008 (Thailand)], Hap 6 [1802 (Philippines); 2923, 2924, NMNH49, NMNH50, NMNH54 (Malaysia)], Hap 7 [1821 (Luzon, Philippines)]. In *cox1*, a total of six distinct haplotypes with $H_d=0.8667$ are recovered: Hap 1 [MZMU1793 (Mizoram, India)], Hap 2 [OHA4 (Thailand)], Hap 3 [OHA1, OHA3 (Thailand)], Hap 4 [SR254, SR256, YJWS02 (China)], Hap 5 [OH01 (Thailand)], and Hap 6 [OH2 (China)]. In *cytb*, a total of 15 distinct haplotypes with $H_d=0.9114$ are recovered: Hap 1 [MZMU1793, MZMU2046, MZMU2605, MZMU2411, CESS1013, CESS1015 (Mizoram, India); CESS1061 (Uttarakhand, India); 500 (Odisha, India), Hap 2 [CESS1001, CESS1022 (Karnataka, India); CESS1030, CESS1031 (Goa, India); CESS1083 (Kerala, India); 502 (Western Ghats, India)], Hap 3 [501, 575 (Odisha, India)], Hap 4 [574, 577 (South and Middle Andamans, India)], Hap 5 [unvouchered, 588 (Daknong, Quang Tri, Camau, Vietnam)], Hap 6 [4018 (China)], Hap 7 [576 (Singapore Zoo)], Hap 8 [1060 (Java); 2922, 2925 (Indonesia); 187 (Sabha)], Hap 9 [1802 (Philippines)], Hap 10 [2923, 2924 (Malaysia)], Hap 11 [1820, 1821 (Luzon, Philippines)], Hap 12 [unvouchered (SongBe, Vietnam)], Hap 13 [OHA1 (Thailand)], Hap 14 [OHA3 (Thailand)], and Hap 15 [OHA2 (Thailand)] (Fig. 4.5).

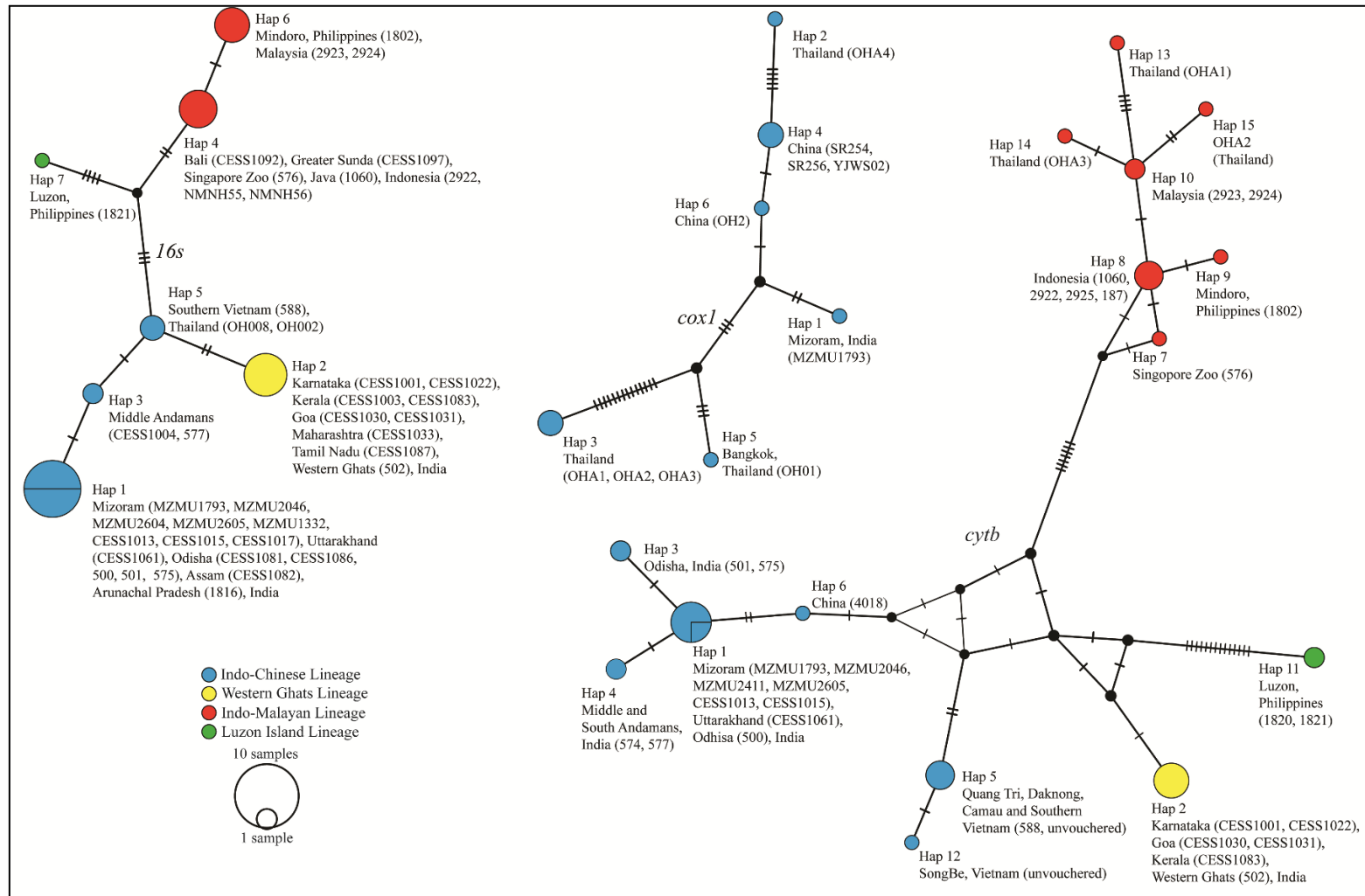


Figure 4.5. Mitochondrial gene-based (*16s*, *cox1*, and *cytb*) Median-joining haplotype network among populations of *Ophiophagus hannah*. The number of samples present in each haplotype corresponds to the relative size of the circles. Hatch marks at the branch represent mutational steps found between haplotypes, and a black dot at the branch is an inferred median.

Genetic divergence

The overall mean intraspecific genetic divergence within *O. hannah* is 1.2% ranging from 0.0 to 2.7% in *I6s* (Table 4.3); overall mean of 2.2% ranging from 0.0 to 4.7% in *coxI* (Table 4.4); overall mean of 4.0% ranging from 0.0 to 10.3% in *cytb* (Table 4.5). Within the study population in Mizoram, the mean intraspecific genetic divergence is 0.0% in *I6s* and 0.6% in *cytb*. Since Mizoram population was previously proposed to be nested in Indo-Chinese lineage based on DNA data, they were pooled in this study with the other Indo-Chinese lineage whereby the mean intra-lineage genetic divergence is 0.2% (*I6s*) and 0.2% (*cytb*) in the Indo-Chinese lineage; 0.5% (*I6s*) and 0.4% (*cytb*) in Indo-Malayan lineage; 0.0% (*I6s*) and 0.0% (*cytb*) in Western Ghats lineage; and 0.0% (*cytb*) in Luzon Island lineage. In *I6s*, inter-lineage genetic divergence is 1.1% (Indo-Chinese vs. Western Ghats); 1.9% (Indo-Chinese vs. Indo-Malayan); 2.6% (Indo-Chinese vs. Luzon Island); 2.0% (Western Ghats vs. Indo-Malayan); 2.1% (Western Ghats vs. Luzon Island); and 1.9% (Indo-Malayan vs. Luzon Island). In *cytb*, inter-lineage genetic divergence is 1.1% (Indo-Chinese vs. Western Ghats), 2.0% (Indo-Chinese vs. Indo-Malayan), 2.5% (Indo-Chinese vs. Luzon Island), 2.1% (Western Ghats vs. Indo-Malayan), 2.1% (Western Ghats vs. Luzon Island), and 1.9% (Indo-Malayan vs. Luzon Island). The total variance captured by the PCo1 and PCo2 are 81% and 13% in *I6s*, 90% and 6% in *coxI*, 66% and 21% in *cytb*, respectively. In *I6s* and *cytb*, the four evolutionary lineages formed a disparate clustering and the Mizoram samples are clustered among the other samples of Indo-Chinese lineage. But low genetic differentiation is seen between Indo-Chinese and the Western Ghats lineage in *cytb* as they clustered adjacently to each other in this gene. On the other hand, the *coxI* comprises solely the samples from Indo-Chinese so that the genetic differentiation across the four lineages is not feasible to conceive using this gene. However, *coxI* plot disclosed the Mizoram (India) samples nested abutting to the Chinese samples, while the other samples from Thailand nested distantly from both the study as well as Chinese samples (Fig. 4.6).

Table 4.3. Uncorrected p-distance (pairwise sequence divergence) estimated using the mitochondrial 16S rRNA (*16s*) sequences of *Ophiophagus hannah* (OH) with GenBank sequences of *Sinomicrurus peinani* (SP) and *S. kelloggi* (SK) as outgroups. DNA sequences generated from Mizoram samples in this study are indicated by bold, while other sequences of Mizoram samples from published work are indicated by asterisk.

Species	1	2	3	4	5	6	7	8	9	10	11	12	13	14	15	16	17
1 OH MZMU1793																	
2 OH MZMU2046	0.000																
3 OH MZMU2604	0.000	0.000															
4 OH MZMU2605	0.000	0.000	0.000														
5 OH MZMU1332	0.000	0.000	0.000	0.000													
6 OH CESS1013*	0.000	0.000	0.000	0.000	0.000												
7 OH CESS1015*	0.000	0.000	0.000	0.000	0.000	0.000											
8 OH CESS1017*	0.000	0.000	0.000	0.000	0.000	0.000	0.000										
9 OH CESS1061	0.000	0.000	0.000	0.000	0.000	0.000	0.000	0.000									
10 OH CESS1081	0.000	0.000	0.000	0.000	0.000	0.000	0.000	0.000	0.000								
11 OH CESS1082	0.000	0.000	0.000	0.000	0.000	0.000	0.000	0.000	0.000	0.000							
12 OH CESS1086	0.000	0.000	0.000	0.000	0.000	0.000	0.000	0.000	0.000	0.000	0.000						
13 OH 500	0.000	0.000	0.000	0.000	0.000	0.000	0.000	0.000	0.000	0.000	0.000	0.000					
14 OH 501	0.000	0.000	0.000	0.000	0.000	0.000	0.000	0.000	0.000	0.000	0.000	0.000	0.000				
15 OH 575	0.000	0.000	0.000	0.000	0.000	0.000	0.000	0.000	0.000	0.000	0.000	0.000	0.000	0.000			
16 OH 1816	0.000	0.000	0.000	0.000	0.000	0.000	0.000	0.000	0.000	0.000	0.000	0.000	0.000	0.000	0.000		
17 OH 577	0.003	0.003	0.003	0.003	0.003	0.003	0.003	0.003	0.003	0.003	0.003	0.003	0.003	0.003	0.003	0.003	
18 OH CESS1004	0.003	0.003	0.003	0.003	0.003	0.003	0.003	0.003	0.003	0.003	0.003	0.003	0.003	0.003	0.003	0.003	0.000

Table 4.3. Continued.

	Species	18	19	20	21	22	23	24	25	26	27	28	29	30	31
19	OH 588	0.003													
20	OH OH002	0.003	0.000												
21	OH OH008	0.003	0.000	0.000											
22	OH CESS1001	0.009	0.006	0.006	0.006										
23	OH CESS1003	0.009	0.006	0.006	0.006	0.000									
24	OH CESS1022	0.009	0.006	0.006	0.006	0.000	0.000								
25	OH CESS1030	0.009	0.006	0.006	0.006	0.000	0.000	0.000							
26	OH CESS1031	0.009	0.006	0.006	0.006	0.000	0.000	0.000	0.000						
27	OH CESS1033	0.009	0.006	0.006	0.006	0.000	0.000	0.000	0.000	0.000					
28	OH CESS1083	0.009	0.006	0.006	0.006	0.000	0.000	0.000	0.000	0.000	0.000				
29	OH CESS1087	0.009	0.006	0.006	0.006	0.000	0.000	0.000	0.000	0.000	0.000	0.000			
30	OH 502	0.009	0.006	0.006	0.006	0.000	0.000	0.000	0.000	0.000	0.000	0.000	0.000		
31	OH NMNH57	0.009	0.006	0.006	0.006	0.012	0.012	0.012	0.012	0.012	0.012	0.012	0.012	0.012	
32	OH CESS1092	0.018	0.015	0.015	0.015	0.021	0.021	0.021	0.021	0.021	0.021	0.021	0.021	0.021	0.015
33	OH CESS1097	0.018	0.015	0.015	0.015	0.021	0.021	0.021	0.021	0.021	0.021	0.021	0.021	0.021	0.015
34	OH 576	0.018	0.015	0.015	0.015	0.021	0.021	0.021	0.021	0.021	0.021	0.021	0.021	0.021	0.015
35	OH 1060	0.018	0.015	0.015	0.015	0.021	0.021	0.021	0.021	0.021	0.021	0.021	0.021	0.021	0.015
36	OH 2922	0.018	0.015	0.015	0.015	0.021	0.021	0.021	0.021	0.021	0.021	0.021	0.021	0.021	0.015
37	OH NMNH55	0.018	0.015	0.015	0.015	0.021	0.021	0.021	0.021	0.021	0.021	0.021	0.021	0.021	0.015
38	OH NMNH56	0.018	0.015	0.015	0.015	0.021	0.021	0.021	0.021	0.021	0.021	0.021	0.021	0.021	0.015

Table 4.3. Continued.

	Species	18	19	20	21	22	23	24	25	26	27	28	29	30	31
39	OH 1802	0.021	0.018	0.018	0.018	0.024	0.024	0.024	0.024	0.024	0.024	0.024	0.024	0.024	0.018
40	OH 2923	0.021	0.018	0.018	0.018	0.024	0.024	0.024	0.024	0.024	0.024	0.024	0.024	0.024	0.018
41	OH 2924	0.021	0.018	0.018	0.018	0.024	0.024	0.024	0.024	0.024	0.024	0.024	0.024	0.024	0.018
42	OH 1821	0.024	0.021	0.021	0.021	0.021	0.021	0.021	0.021	0.021	0.021	0.021	0.021	0.021	0.021
43	OH NMNH50	0.021	0.018	0.018	0.018	0.024	0.024	0.024	0.024	0.024	0.024	0.024	0.024	0.024	0.018
44	OH NMNH54	0.021	0.018	0.018	0.018	0.024	0.024	0.024	0.024	0.024	0.024	0.024	0.024	0.024	0.018
45	OH NMNH49	0.021	0.018	0.018	0.018	0.024	0.024	0.024	0.024	0.024	0.024	0.024	0.024	0.024	0.018
46	SP CHS643	0.109	0.112	0.112	0.112	0.115	0.115	0.115	0.115	0.115	0.115	0.115	0.115	0.115	0.109
47	SK CHS854	0.107	0.109	0.109	0.109	0.112	0.112	0.112	0.112	0.112	0.112	0.112	0.112	0.112	0.109

Table 4.4. Uncorrected p-distance (pairwise sequence divergence) estimated using the mitochondrial cytochrome c oxidase subunit 1 (*cox1*) sequences of *Ophiophagus hannah* (OH) with GenBank sequences of *Sinomicrourus peinani* (SP) and *S. kelloggi* (SK) as outgroups. DNA sequences generated from Mizoram samples in this study are indicated by bold.

Species	1	2	3	4	5	6	7	8	9	10	11
1 OH MZMU1793											
2 OH OH2	0.006										
3 OH SR256	0.008	0.002									
4 OH SR254	0.008	0.002	0.000								
5 OH YJWS02	0.008	0.002	0.000	0.000							
6 OH OH01	0.016	0.014	0.016	0.016	0.016						
7 OH OHA4	0.017	0.012	0.010	0.010	0.010	0.025					
8 OH OHA1	0.037	0.035	0.037	0.037	0.037	0.033	0.047				
9 OH OHA3	0.037	0.035	0.037	0.037	0.037	0.033	0.047	0.000			
10 OH OHA2	0.037	0.035	0.037	0.037	0.037	0.033	0.047	0.000	0.000		
11 SP CHS643	0.151	0.153	0.155	0.155	0.155	0.153	0.159	0.165	0.165	0.165	
12 SK CHS854	0.163	0.169	0.171	0.171	0.171	0.165	0.174	0.159	0.159	0.159	0.126

Table 4.5. Uncorrected p-distance (pairwise sequence divergence) estimated using the mitochondrial cytochrome b (*cytb*) sequences of *Ophiophagus hannah* (OH) with GenBank sequences of *Sinomicrurus peinani* (SP) and *S. kelloggi* (SK) as outgroups. DNA sequences generated from Mizoram samples in this study are indicated by bold, while other sequences of Mizoram samples from published work are indicated by asterisk.

Species	1	2	3	4	5	6	7	8	9	10	11	12	13	14	15	16	17	18	19
1 OH MZMU1793																			
2 OH MZMU2046	0.000																		
3 OH MZMU2411	0.000	0.000																	
4 OH MZMU2605	0.000	0.000	0.000																
5 OH MZMU1332	0.013	0.013	0.013	0.013															
6 OH CESS1013*	0.000	0.000	0.000	0.000	0.013														
7 OH CESS1015*	0.000	0.000	0.000	0.000	0.013	0.000													
8 OH 500	0.000	0.000	0.000	0.000	0.013	0.000	0.000												
9 OH CESS1061	0.000	0.000	0.000	0.000	0.013	0.000	0.000	0.000											
10 OH 501	0.004	0.004	0.004	0.004	0.017	0.004	0.004	0.004	0.004										
11 OH 575	0.004	0.004	0.004	0.004	0.017	0.004	0.004	0.004	0.004	0.000									
12 OH 577	0.004	0.004	0.004	0.004	0.017	0.004	0.004	0.004	0.004	0.009	0.009								
13 OH 574	0.004	0.004	0.004	0.004	0.017	0.004	0.004	0.004	0.004	0.009	0.009	0.000							
14 OH 4018	0.009	0.009	0.009	0.009	0.021	0.009	0.009	0.009	0.009	0.013	0.013	0.013							
15 OH 588	0.026	0.026	0.026	0.026	0.034	0.026	0.026	0.026	0.026	0.030	0.030	0.030	0.017						
16 OH DakNong Vietnam	0.026	0.026	0.026	0.026	0.034	0.026	0.026	0.026	0.026	0.030	0.030	0.030	0.017	0.000					
17 OH Camau Vietnam	0.026	0.026	0.026	0.026	0.034	0.026	0.026	0.026	0.026	0.030	0.030	0.030	0.017	0.000	0.000				
18 OH Quang Tri Vietnam	0.026	0.026	0.026	0.026	0.034	0.026	0.026	0.026	0.026	0.030	0.030	0.030	0.017	0.000	0.000	0.000			
19 OH SongBe Vietnam	0.030	0.030	0.030	0.030	0.039	0.030	0.030	0.030	0.030	0.034	0.034	0.034	0.021	0.004	0.004	0.004	0.004		
20 OH CESS1001	0.030	0.030	0.030	0.030	0.039	0.030	0.030	0.030	0.030	0.034	0.034	0.034	0.021	0.021	0.021	0.021	0.021	0.021	0.026

Table 4.5. Continued.

Species	1	2	3	4	5	6	7	8	9	10	11	12	13	14	15	16	17	18	19
21 OH CESS1022	0.030	0.030	0.030	0.030	0.039	0.030	0.030	0.030	0.030	0.034	0.034	0.034	0.034	0.021	0.021	0.021	0.021	0.021	0.026
22 OH CESS1030	0.030	0.030	0.030	0.030	0.039	0.030	0.030	0.030	0.030	0.034	0.034	0.034	0.034	0.021	0.021	0.021	0.021	0.021	0.026
23 OH CESS1031	0.030	0.030	0.030	0.030	0.039	0.030	0.030	0.030	0.030	0.034	0.034	0.034	0.034	0.021	0.021	0.021	0.021	0.021	0.026
24 OH CESS1083	0.030	0.030	0.030	0.030	0.039	0.030	0.030	0.030	0.030	0.034	0.034	0.034	0.034	0.021	0.021	0.021	0.021	0.021	0.026
25 OH 502	0.030	0.030	0.030	0.030	0.039	0.030	0.030	0.030	0.030	0.034	0.034	0.034	0.034	0.021	0.021	0.021	0.021	0.021	0.026
26 OH 576	0.056	0.056	0.056	0.056	0.064	0.056	0.056	0.056	0.056	0.060	0.060	0.060	0.060	0.047	0.052	0.052	0.052	0.052	0.056
27 OH 1060	0.056	0.056	0.056	0.056	0.064	0.056	0.056	0.056	0.056	0.060	0.060	0.060	0.060	0.047	0.052	0.052	0.052	0.052	0.056
28 OH 2922	0.056	0.056	0.056	0.056	0.064	0.056	0.056	0.056	0.056	0.060	0.060	0.060	0.060	0.047	0.052	0.052	0.052	0.052	0.056
29 OH 2925	0.056	0.056	0.056	0.056	0.064	0.056	0.056	0.056	0.056	0.060	0.060	0.060	0.060	0.047	0.052	0.052	0.052	0.052	0.056
30 OH 187	0.056	0.056	0.056	0.056	0.064	0.056	0.056	0.056	0.056	0.060	0.060	0.060	0.060	0.047	0.052	0.052	0.052	0.052	0.056
31 OH 1802	0.060	0.060	0.060	0.060	0.069	0.060	0.060	0.060	0.060	0.060	0.060	0.064	0.064	0.052	0.056	0.056	0.056	0.056	0.060
32 OH 2923	0.060	0.060	0.060	0.060	0.069	0.060	0.060	0.060	0.060	0.064	0.064	0.064	0.064	0.052	0.056	0.056	0.056	0.056	0.060
33 OH OHA2	0.060	0.060	0.060	0.060	0.069	0.060	0.060	0.060	0.060	0.064	0.064	0.064	0.064	0.052	0.056	0.056	0.056	0.056	0.060
34 OH 2924	0.060	0.060	0.060	0.060	0.069	0.060	0.060	0.060	0.060	0.064	0.064	0.064	0.064	0.052	0.056	0.056	0.056	0.056	0.060
35 OH OHA3	0.064	0.064	0.064	0.064	0.073	0.064	0.064	0.064	0.064	0.069	0.069	0.069	0.069	0.056	0.060	0.060	0.060	0.060	0.064
36 OH 1820	0.077	0.077	0.077	0.077	0.086	0.077	0.077	0.077	0.077	0.082	0.082	0.082	0.082	0.069	0.077	0.077	0.077	0.077	0.077
37 OH 1821	0.077	0.077	0.077	0.077	0.086	0.077	0.077	0.077	0.077	0.082	0.082	0.082	0.082	0.069	0.077	0.077	0.077	0.077	0.077
38 OH OHA1	0.077	0.077	0.077	0.077	0.086	0.077	0.077	0.077	0.077	0.082	0.082	0.082	0.082	0.069	0.073	0.073	0.073	0.073	0.077
39 SP CHS643	0.189	0.189	0.189	0.189	0.189	0.189	0.189	0.189	0.189	0.193	0.193	0.193	0.193	0.197	0.193	0.193	0.193	0.193	0.197
40 SK CHS854	0.180	0.180	0.180	0.180	0.185	0.180	0.180	0.180	0.180	0.185	0.185	0.185	0.185	0.176	0.180	0.180	0.180	0.180	0.185

Table 4.5. Continued.

Species	20	21	22	23	24	25	26	27	28	29	30	31	32	33	34	35	36	37	38	39
21 OH CESS1022	0.000																			
22 OH CESS1030	0.000	0.000																		
23 OH CESS1031	0.000	0.000	0.000																	
24 OH CESS1083	0.000	0.000	0.000	0.000																
25 OH 502	0.000	0.000	0.000	0.000	0.000															
26 OH 576	0.047	0.047	0.047	0.047	0.047	0.047														
27 OH 1060	0.047	0.047	0.047	0.047	0.047	0.047	0.004													
28 OH 2922	0.047	0.047	0.047	0.047	0.047	0.047	0.004	0.000												
29 OH 2925	0.047	0.047	0.047	0.047	0.047	0.047	0.004	0.000	0.000											
30 OH 187	0.047	0.047	0.047	0.047	0.047	0.047	0.004	0.000	0.000	0.000										
31 OH 1802	0.052	0.052	0.052	0.052	0.052	0.052	0.009	0.004	0.004	0.004	0.004									
32 OH 2923	0.052	0.052	0.052	0.052	0.052	0.052	0.009	0.004	0.004	0.004	0.004	0.009								
33 OH OHA2	0.052	0.052	0.052	0.052	0.052	0.052	0.017	0.013	0.013	0.013	0.013	0.017	0.009							
34 OH 2924	0.052	0.052	0.052	0.052	0.052	0.052	0.009	0.004	0.004	0.004	0.004	0.009	0.000	0.009						
35 OH OHA3	0.056	0.056	0.056	0.056	0.056	0.056	0.013	0.009	0.009	0.009	0.009	0.013	0.004	0.013	0.004					
36 OH 1820	0.069	0.069	0.069	0.069	0.069	0.069	0.082	0.082	0.082	0.082	0.082	0.086	0.086	0.086	0.086	0.090				
37 OH 1821	0.069	0.069	0.069	0.069	0.069	0.069	0.082	0.082	0.082	0.082	0.082	0.086	0.086	0.086	0.086	0.090	0.000			
38 OH OHA1	0.069	0.069	0.069	0.069	0.069	0.069	0.026	0.021	0.021	0.021	0.021	0.026	0.017	0.026	0.017	0.021	0.103	0.103		
39 SP CHS643	0.189	0.189	0.189	0.189	0.189	0.189	0.202	0.197	0.197	0.197	0.197	0.202	0.202	0.197	0.202	0.206	0.219	0.219	0.219	
40 SK CHS854	0.180	0.180	0.180	0.180	0.180	0.180	0.185	0.180	0.180	0.180	0.180	0.185	0.180	0.176	0.180	0.185	0.202	0.202	0.197	0.185

Table 4.6. Uncorrected p-distance estimate among the different lineages in *16s* dataset.

Lineages	Indo-Chinese	Western Ghats	Indo-Malayan	Within Group Mean
Indo-Chinese				0.002
Western Ghats	0.011			0.000
Indo-Malayan	0.019	0.020		0.005
Luzon Island	0.026	0.021	0.019	NA

Table 4.7. Uncorrected p-distance estimate among the different lineages in *cytb* dataset.

Lineages	Indo-Chinese	Western Ghats	Indo-Malayan	Within Group Mean
Indo-Chinese				0.002
Western Ghats	0.011			0.000
Indo-Malayan	0.020	0.021		0.004
Luzon Island	0.025	0.021	0.019	0.000

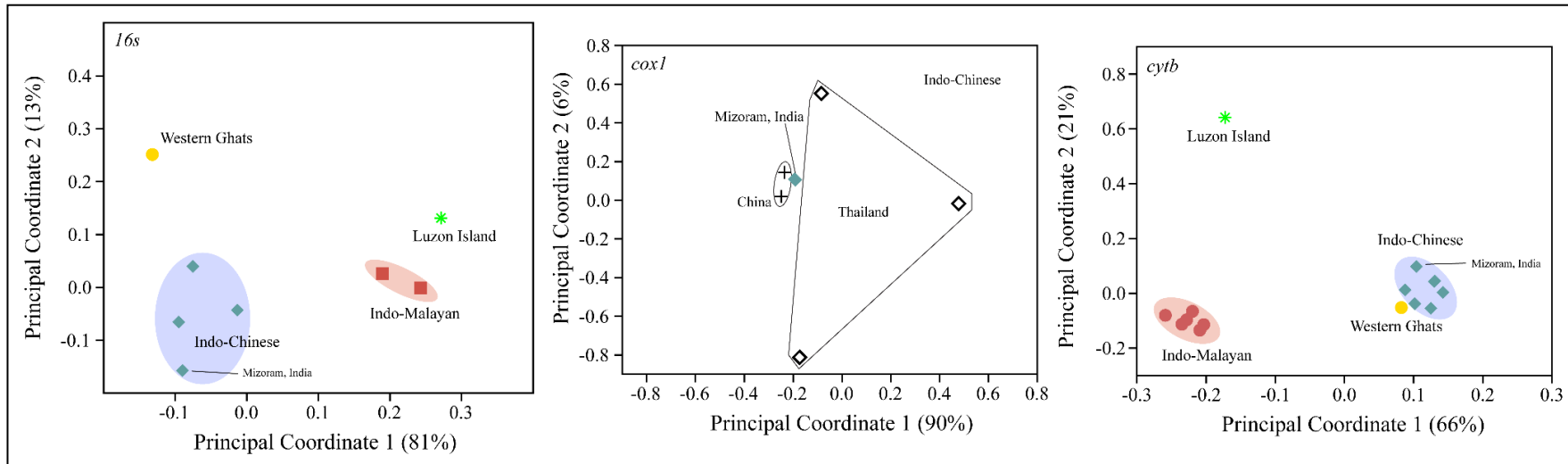


Figure 4.6. Ordination of *Bungarus* species in a Principal Coordinate Analysis of standardized p-distance of mitochondrial 16S rRNA (*16s*) cytochrome c oxidase subunit 1 (*cox1*), and Cytochrome b (*cytb*) genes. A total percentage of variance captured by the first and second Principal coordinates are given in the x and y axes, respectively.

Morphology

The studied population of *O. hannah* from Mizoram is represented by a total of 27 adult individuals comprising 14 preserved specimens and 13 live individuals. The examined specimens are characterized by the following conventional taxonomic features: ADSR 17–19, MDSR 15, PDSR 15; Ve 236–261 in males, 240–258 in females; Sc 80–94 in males, 70–91 in females; USc 5–21 in males, 3–7 in females; SL 7/7 (rarely 6/7 or 8/7); SLE 3–4/3–4; IL 8/8 (rarely 7/8, 8/7, or 9/9); PrO 1/1; PoO 3/3 (rarely 3/2); Tem 2+3/2+3 or 2+2/2+2 (sometimes 2+1/2+1); As undivided. SVL 1245–2960 mm in male, 1626–2225 mm in female; TaL 300–630 mm in males, 308–430 mm in females, and the male specimen MZMU 2410 is the longest among the examined individuals in having 3580 mm (11.8 feet) in total length. Raw morphological data are provided in Table 4.8. Hemipenes elongated and deeply bifurcated with two forks with the spines prominently present around the basal area of the organ (Fig. 4.7).

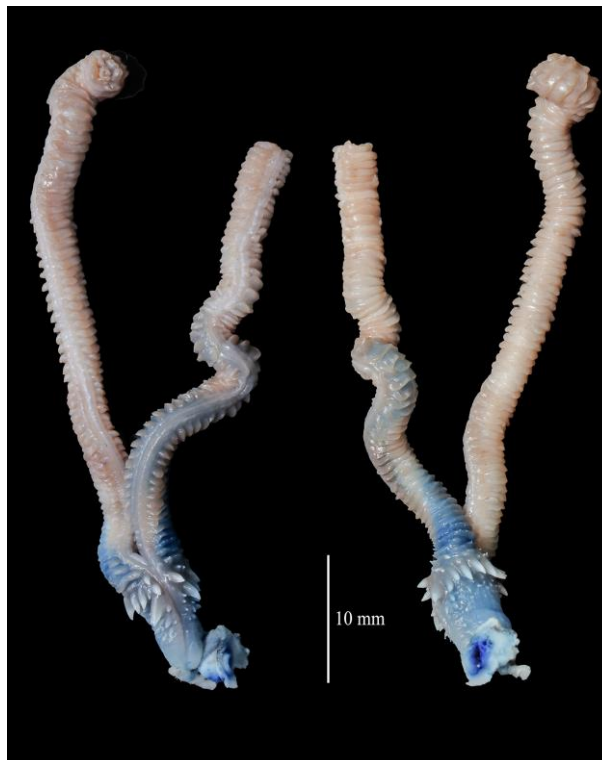


Figure 4.7. Sulcate (left) and asulcate views of the hemipenis of *Ophiophagus hannah*. Hemipenes elongated and deeply bifurcated with two forks with the spines prominently present around the basal area of the organ.

Table 4.8. Morphometry (in mm) and scalation data of *Ophiophagus hannah* examined from Mizoram, India. Damaged character is shown as asterisk (*), and the missing characters or that are not feasible to examine in life individuals are shown in dash (-). Live individuals examined are indicated by their respective locality.

Characters	MZMU 2410	MZMU 2411	MZMU 2436	MZMU 2437	MZMU R118	MZMU 2045	MZMU 1323	MZMU 1793
Sex	M	M	M	M	M	M	M	M
Ve	236	248	245	242	242	243	242	239
Sc	86	94	92	89	94	94	94	45*
USc	13	9	14	9	12	6	21	6
SL	7/7	7/7	7/7	7/7	7/7	7/7	7/7	7/7
SLe	3-4	3-4	3-4	3-4	3-4	3-4	3-4	3-4
IL	8/8	8/8	8/8	8/8	8/8	8/8	8/8	8/8
DSR	17:15:15	19:15:15	19:15:15	19:15:15	17:15:15	17:15:15	19:15:15	19:15:15
HL	76.88	48.48	65.58	83.16	35.50	52.80	32.14	40.00
HW	51.36	29.44	52.12	56.64	22.90	32.24	27.16	21.20
HD	31.84	18.44	30.10	33.74	13.64	20.32	13.10	15.06
ED	8.58	6.30	8.22	8.50	5.00	7.54	5.86	6.48
ND	7.38	3.80	6.28	6.44	2.80	5.36	3.30	2.90
S-N	8.90	5.72	9.14	9.46	4.80	6.88	4.80	4.00
S-E	24.60	9.66	22.64	24.42	11.64	17.24	11.22	11.68
N-E	10.62	6.62	9.90	10.74	5.22	7.46	4.60	5.56
RW	16.60	9.24	15.70	15.88	7.60	6.52	8.06	8.26
RH	9.60	4.96	8.06	6.54	3.44	5.62	3.48	5.60
INS	19.60	12.80	18.12	18.60	14.96	13.24	9.54	10.06
IOS	30.90	20.88	29.00	28.52	14.08	22.90	16.02	17.10
INL	11.82	7.40	10.48	11.20	5.12	8.40	6.00	6.30
INW	9.40	5.74	8.16	8.60	4.38	6.70	4.10	4.24
PFL	13.58	8.12	13.40	12.68	6.04	9.72	6.60	7.30
PFW	9.32	6.74	9.72	9.64	4.90	7.78	5.32	5.90
FL	17.24	11.06	16.26	17.46	10.16	11.86	9.44	10.30
FW	13.00	8.70	11.64	12.48	6.92	9.62	6.90	6.62
PL	25.58	16.38	23.26	23.10	12.26	18.42	13.80	14.76
PW	17.42	11.42	15.86	17.76	8.06	12.48	9.12	9.36
SVL	2950	1880	2680	2960	1410	2180	1370	1245
TaL	630	410	586	592	300	492	316	80*
PrO	1/1	1/1	1/1	1/1	1/1	1/1	1/1	1/1
PoO	3/3	3/3	3/3	3/3	3/3	3/3	3/3	3/3
Tem	2+3/2+3	2+3/2+3	2+3/2+3	2+3/2+3	2+3/2+3	2+3/2+3	2+3/2+3	2+2/2+3
OCL	17.76	10.88	14.90	20.96	8.82	12.40	7.28	8.64
				right absent				
OCW	16.84	9.64	13.20	13.26	6.30	9.34	6.12	6.74
As	1	1	1	1	1	1	1	1

Table 4.8. Continued.

Characters	MZMU 1436	MZMU R117	MZMU 1439	MZMU 2423	MZMU 2046	MZMU 2486	Zohnuai	Lungdai
Sex	M	M	M	F	F	F	M	M
Ve	240	240	241	251	251	258	261	241
Sc	93	90	*	81	88	70	85	82
USc	-	18	*	5	3	-	7	6
SL	7/7	7/7	7/7	7/7	6/7	7/7	7/7	7/7
SLe	3-4	3-4	3-4	3-4	3-4	3-4	3-4	3-4
IL	8/8	8/8	8/8	8/8	7/8	8/8	8/8	8/8
DSR	19:15:15	19:15:15	18:15:15	18:15:15	18:15:15	19:15:15	17:15:15	17:15:15
HL	41.40	47.38	48.08	42.40	34.64	42.60	55.30	80.56
HW	24.64	28.44	31.50	27.20	22.46	24.62	36.70	49.52
HD	14.32	18.50	18.34	19.12	14.84	15.32	18.92	37.70
ED	6.90	6.80	6.62	6.82	6.28	6.40	7.60	10.00
ND	3.72	3.92	3.18	3.70	2.64	2.78	4.80	6.36
S-N	5.16	4.02	4.26	6.10	3.30	3.22	6.92	9.74
S-E	12.02	13.88	13.00	14.14	10.42	12.90	16.34	23.26
N-E	4.88	6.42	7.00	5.62	4.08	6.44	8.42	12.34
RW	9.30	10.04	11.44	10.00	9.10	8.24	11.38	17.70
RH	5.54	6.24	5.84	4.66	4.58	4.90	6.42	9.28
INS	11.12	12.02	12.84	12.70	9.42	10.36	12.00	21.08
IOS	18.10	20.36	20.06	20.60	17.18	19.10	25.38	32.46
INL	6.78	7.70	7.44	6.80	5.38	6.34	8.06	12.60
INW	4.68	5.90	5.60	4.86	4.70	5.38	6.38	9.30
PFL	8.22	9.00	9.00	8.64	6.90	8.90	10.50	17.50
PFW	6.00	6.88	7.54	6.20	5.14	6.40	7.56	11.90
FL	9.52	11.72	11.60	11.00	8.64	10.42	13.84	18.16
FW	7.58	9.50	8.08	8.26	7.00	7.18	9.50	13.00
PL	14.44	15.72	15.38	16.66	13.86	15.78	12.46	25.68
PW	10.22	11.48	11.60	11.60	9.50	11.20	11.66	19.08
SVL	1400	1746	1760	1940	1636	2050	2100	2340
TaL	350	414	*	366	308	330	410	570
PrO	1/1	1/1	1/1	1/1	1/1	1/1	1/1	1/1
PoO	3/3	3/3	3/3	3/3	3/3	3/2	3/3	3/3
Tem	2+2/2+2	2+2/2+2	2+2/2+2	2+3/2+3	2+3/2+3	2+2/2+2	2+2/2+2	2+2/2+2
OCL	9.50	9.50	10.46	11.26	8.42	11.30	14.74	20.34
OCW	8.46	8.46	8.34	9.58	7.22	8.06	12.54	15.34
As	1	1	1	1	1	1	1	1

Table 4.8. Continued.

Characters	Kolasib	MZU campus	Khaw zawl	Khuang thing	Khum tung	Sihphir	Chhip phir	Hualngo
Sex	M	M	F	F	F	F	F	F
Ve	239	244	247	251	249	249	240	246
Sc	80	87	81	82	75	40*	91	83
USc	11	5	5	4	4	7	-	-
SL	7/7	7/7	7/7	7/7	7/7	7/7	7/7	7/7
SLe	3-4	3-4	3-4	3-4	3-4	3-4	3-4	3-4
IL	8/8	8/8	8/7	8/8	8/8	9/9	8/8	8/8
DSR	17:15:15	18:15:15	19:15:15	17:15:15	17:15:15	17:15:15	19:15:15	17:15:15
HL	70.00	70.38	53.44	49.32	51.16	40.46	60.22	49.18
HW	49.80	56.12	33.44	29.50	28.40	26.00	35.06	23.48
HD	31.00	36.32	18.50	18.40	15.54	14.80	22.82	17.64
ED	9.64	9.88	7.70	7.06	7.22	6.70	9.00	8.36
ND	8.80	-	3.40	3.08	3.44	3.16	-	-
S-N	9.97	-	7.48	5.14	5.94	4.36	-	-
S-E	25.80	25.00	16.64	16.24	17.08	12.80	18.76	13.74
N-E	10.81	9.02	7.42	7.34	7.70	6.02	9.00	6.90
RW	13.42	-	11.76	10.94	10.40	9.34	-	-
RH	7.56	-	5.20	5.02	5.80	5.34	-	-
INS	18.04	-	13.70	13.24	12.12	10.50	-	-
IOS	31.10	-	23.18	23.20	22.48	18.20	-	-
INL	10.60	-	8.64	8.58	8.04	6.40	-	-
INW	8.84	-	6.62	6.26	6.18	6.36	-	-
PFL	12.80	-	10.24	9.84	9.36	8.28	-	-
PFW	9.86	-	8.48	7.74	7.96	5.98	-	-
FL	7.90	-	11.98	12.12	11.70	9.86	-	-
FW	12.06	-	8.54	8.92	8.50	7.46	-	-
PL	25.60	-	17.92	18.98	16.74	14.56	-	-
PW	17.15	-	11.40	11.92	10.86	9.62	-	-
SVL	2500	2804	2032	1880	1892	1626	2225	1829
TaL	610	622	406	406	356	178*	430	410
PrO	1/1	1/1	1/1	1/1	1/1	1/1	1/1	1/1
PoO	3/3	3/3	3/3	3/3	3/3	3/3	3/3	3/3
Tem	2+2/2+2	2+3/2+3	2+2/2+2	2+2/2+2	2+2/2+2	2+2/2+2	2+2/2+2	2+3/2+3
OCL	18.46	-	-	12.32	11.92	10.38	-	-
OCW	13.70	-	-	10.72	10.54	10.16	-	-
As	1	1	1	1	1	1	1	1

Table 4.8. Continued.

Characters	Tuivamit	Khaw zawl	N. Khaw bung	Head 1	Head 2	Head 3
Sex	F	F	F	-	-	-
Ve	257	247	250	-	-	-
Sc	70	82	78*	-	-	-
USc	-	5	-	-	-	-
SL	7/7	8/7	7/7	7/7	7/7	7/7
SLe	3-4	3-4	3-4	3-4	3-4	3-4
IL	8/8	9/9	8/8	8/8	8/8	8/8
DSR	17:15:15	17:15:15	19:15:15	-	-	-
HL	44.00	48.44	47.72	69.12	46.22	59.54
HW	25.14	25.92	28.24	36.08	34.88	44.70
HD	9.66	-	-	15.30	21.00	27.38
ED	7.48	6.10	6.66	8.00	6.70	7.58
ND	-	-	-	6.300	3.64	5.24
S-N	-	-	-	7.94	6.32	7.44
S-E	13.50	15.72	14.12	20.12	15.68	20.40
N-E	6.36	5.60	6.28	9.00	6.24	8.48
RW	-	-	-	15.30	11.54	9.00
RH	-	-	-	6.80	5.40	5.96
INS	-	-	-	16.88	12.72	11.90
IOS	-	-	-	27.94	20.98	27.00
INL	-	-	-	9.40	7.68	9.72
INW	-	-	-	7.94	6.00	7.54
PFL	-	-	-	11.12	9.56	11.74
PFW	-	-	-	9.18	7.30	8.40
FL	-	-	-	15.72	11.14	14.68
FW	-	-	-	11.58	9.08	9.10
PL	-	-	-	24.00	16.64	22.56
PW	-	-	-	15.46	12.90	15.32
SVL	1860	1924	1732	-	-	-
TaL	320	386	364	-	-	-
PrO	1/1	1/1	1/1	1/1	1/1	1/1
PoO	3/2	3/3	3/3	3/3	3/3	3/3
Tem	2+3/2+3	2+2/2+2	*/2+2	2+1/2+1	2+1/2+1	2+1/2+1
OCL	-	-	-	15.08	-	-
OCW	-	-	-	13.52	-	-
As	1	1	1	-	-	-

Table 4.8. Continued.

Characters	Head 4	Head 5	Head 6	Head 7
Sex	-	-	-	-
Ve	-	-	-	-
Sc	-	-	-	-
USc	-	-	-	-
SL	7/7	7/7	7/7	7/7
SLe	3-4	3-4	3-4	3-4
IL	-	-	-	-
DSR	-	-	-	-
HL	64.24	68.30	90.90	70.76
HW	40.80	45.12	50.50	52.50
HD	25.64	26.30	44.20	37.32
ED	6.86	7.96	9.56	9.98
ND	5.62	5.78	7.10	6.20
S-N	7.80	6.30	9.50	6.20
S-E	20.40	18.56	26.04	10.60
N-E	9.22	10.10	13.36	22.94
RW	14.40	15.80	18.70	16.54
RH	6.42	6.30	12.24	11.66
INS	15.74	17.90	21.30	24.60
IOS	25.84	28.78	34.40	29.54
INL	9.00	10.14	13.00	11.76
INW	7.50	7.94	10.14	9.00
PFL	12.26	11.80	15.66	13.66
PFW	8.74	8.80	11.90	10.20
FL	9.98	17.36	19.00	16.26
FW	11.34	12.14	14.26	11.74
PL	21.42	23.36	26.70	21.82
PW	12.50	15.40	19.70	16.94
SVL	-	-	-	-
TaL	-	-	-	-
PrO	1/1	1/1	1/1	1/1
PoO	3/3	3/3	3/3	3/3
Tem	2+1/2+1	2+1/2+1	2+2/2+2	2+2/2+2
OCL	-	-	-	-
OCW	-	-	-	-
As	-	-	-	-

Sexual dimorphism

For testing sexual dimorphism, the mensural data were firstly adjusted against SVL using the equation $10^{**}(\text{LG10}(\text{Character})+(\text{LG10}(500)-\text{LG10}(1998))*\text{Regression coefficient})$, where 1998 is the grand mean of SVL. The characters tested between male (n=15) and female (n=12) showed significant dimorphism in the following characters: Ve ($p<0.01$), Sc ($p<0.01$), USc ($p<0.01$), TaL ($p<0.01$), HL ($p<0.05$), HW ($p<0.001$); in juvenile (n=16), HD ($p<0.01$), ND ($p<0.01$), INS ($p<0.05$), FW ($p<0.01$), and PW ($p<0.05$) (Fig. 4.8; Table 4.8). PCA is performed for the male and female specimens of *O. hannah* population from Mizoram using the standardised meristics (Ve, Sc, USc) and allometric adjusted mensurals (TaL, HL, HWHD, ND, INS, FW, and PW). The first two components are extracted based on eigen value and accounted for 74% of the total variation of the data, with PC1 and PC2 representing 56% and 18%, respectively. The loadings of Ve, HL, HW, HD, ND, INS, FW, and PW are high on the first axis with Ve loads negatively on both axes, while Sc and USc load considerably highly on the second axis. The representation of the first two components showed the discrete clustering of male and female along the first and second principal components Fig. 4.9; Table 4.9).

Table 4.9. Information on Principal Component Analysis (PCA) and loadings for *Ophiophagus hannah* population in Mizoram, northeastern India between the adult male and female specimens.

Variables	PC1	PC2
Zscore (Ve)	-0.675	-0.378
Zscore (Sc)	0.040	0.834
Zscore (USc)	0.446	0.795
adj_HL	0.759	-0.504
adj_HW	0.806	0.138
adj_HD	0.895	-0.235
adj_ND	0.767	0.198
adj_INS	0.674	-0.107
adj_FW	0.923	-0.143
adj_PW	0.890	-0.310
adj_TaL	0.899	0.186

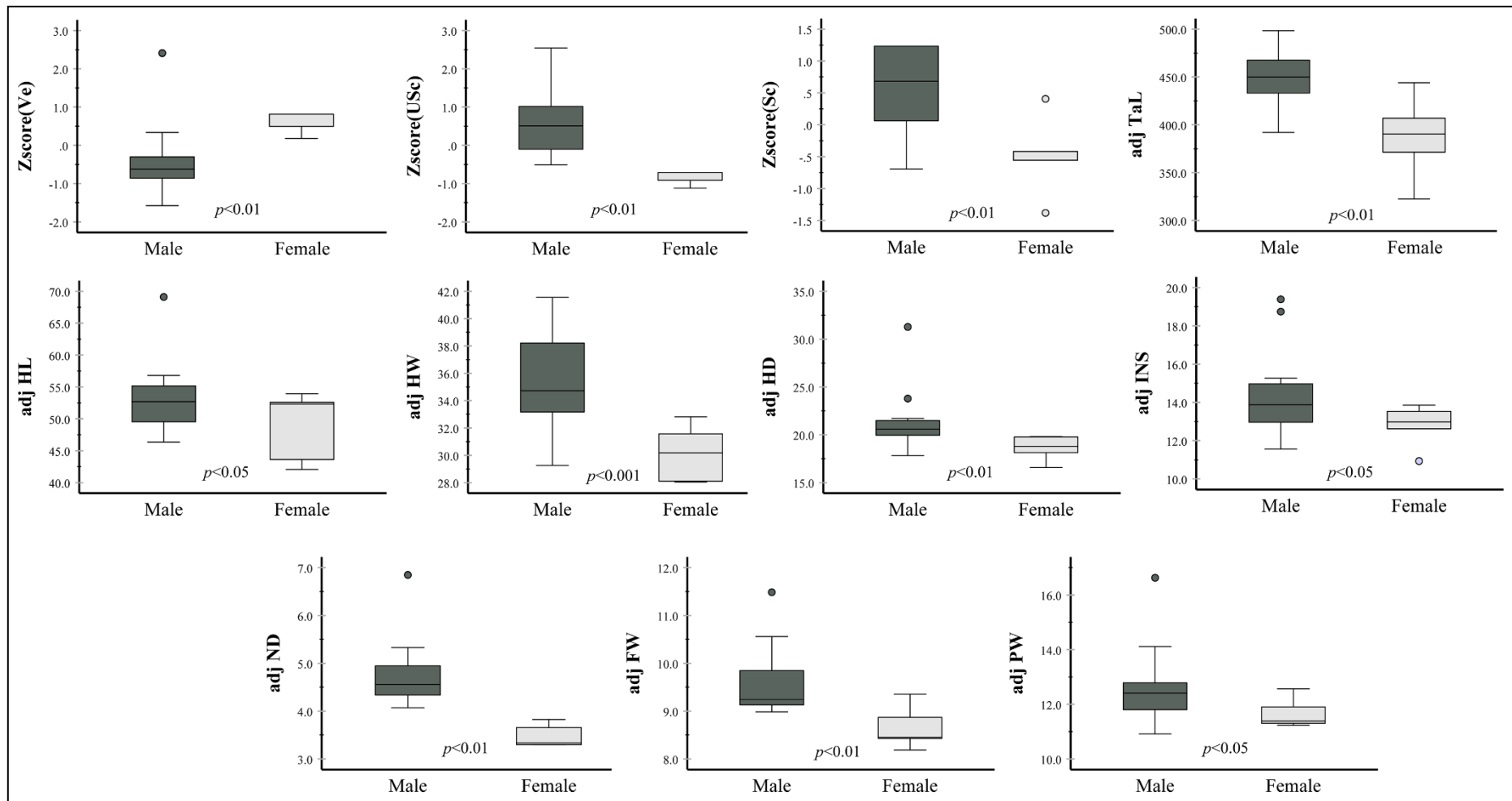


Figure 4.8. Box plot showing the median, interquartile range, range (minimum to maximum), and outliers of the standardised (Z score) meristic and adjusted (adj) mensurals that differed between sexes of *O. hannah* population in Mizoram. Significance at the alpha level of 0.05 are given at each plot.

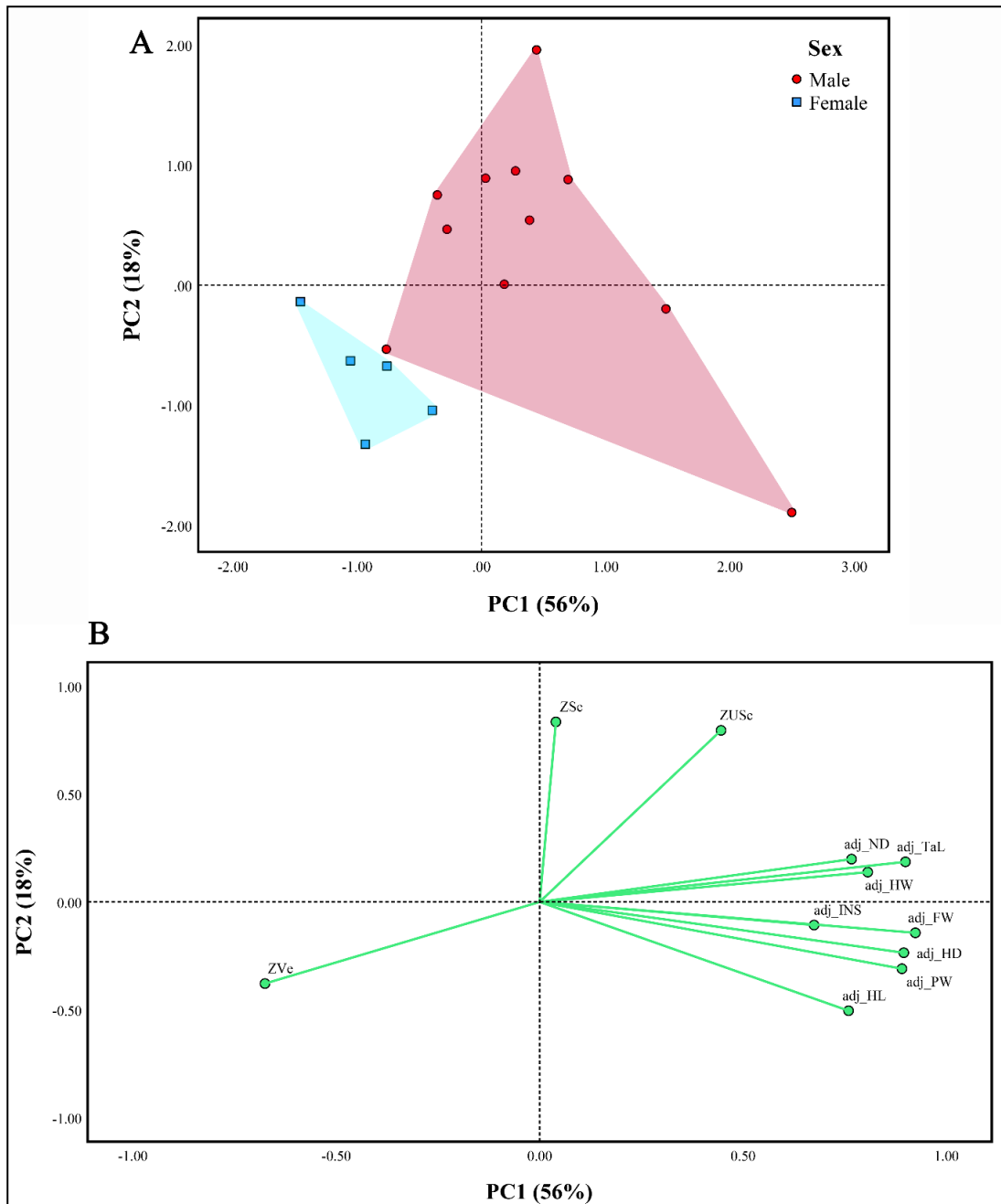


Figure 4.9. (A) Ordination of male and female specimens of *O. hannah* population from Mizoram along the first two principal components based on a PCA of the standardised meristics (ventrals, undivided subcaudals, subcaudals) and allometric adjusted mensurals (tail length, head length, head width, head depth, nostril diameter, internarial space, frontal width, parietal width). (B) PCA loading plot showing the distribution of the analysed variables along the first two principal components.

Comparative test for the systematic position of Mizoram population

Comparative meristic data originated from this study along with other populations from published taxonomic literature is given in Table 4.10. Statistical analysis was performed for Mizoram population against the pre-defined four distinct lineages recovered in Shankar et al. (2021) through one-way ANOVA with population/lineage as the factor. By assigning Mizoram specimens in separate group, this test showed statistically significant difference across the populations/lineages in the Ve ($p < 0.001$), Sc ($p < 0.001$) and ADSR ($p < 0.05$) (Table 4.10; Fig. 4.10). Multiple comparison through Bonferroni Pos hoc test further showed the absence of statistically significant difference between Mizoram specimens against the pre-defined Indo-Chinese specimens, while a similar case is seen between Mizoram and Western Ghats specimens which may be due to insufficient characters and/or sample for the Western Ghats. However, statistically significant differences are seen in the Ve ($p < 0.001$) and ADSR ($p < 0.001$) between Mizoram and Indo-Malayan, and in the ADSR ($p < 0.05$) between Mizoram and Luzon Island specimens (Table 4.11). Ordination of the standardised meristics (Ve, Sc, ADSR) in along the first two principal components in PCA also disclosed that the *O. hannah* population of Mizoram forms an overlapping cluster with respect to the pre-defined samples of Indo-Chinese lineage, while these two samples are altogether forming discrete clustering with respect to the other three lineages (Western Ghats, Indo-Malayan and Luzon Island) (Fig. 4.11). The variables Ve and Sc are loaded positively and have more effect in the first principal component, while only ADSR is loaded positively and have more effect in the second principal component (Table 4.12).

Table 4.10. Test for intraspecific difference (sex pooled) on the standardized meristics of *O. hannah* through one-way ANOVA with population/lineage as the factor. Analysis was performed for Mizoram population against the pre-defined four distinct lineages recovered by Shankar et al. (2021). Significant variations at the alpha level of 0.05 are shown in boldface. Characters tested using Brown-Forsythe test is indicated with octothorpe (#).

Characters	Mizoram (n=27)		Indo-Chinese (n=18)		Western Ghats (n=2)		Indo-Malayan (n=23)		Luzon Island (n=3)		Inter population difference	
	Mean±SD	Range	Mean±SD	Range	Mean±SD	Range	Mean±SD	Range	Mean±SD	Range		
Ve	245.89±6.27	236–261	243.00±3.07	238–251	251	251	255.74±7.29	236–265	249.67±2.52	247–252	F _{3,52} =26.413	p <0.001#
Sc	85.04±7.27	70–94	86.39±6.71	72–99	86.50±0.71	86–87	110±5.05	99–117	98.00±2.65	95–100	F _{4,65} =57.274	p <0.001
ADSR	17.96±0.94	17–19	18.11±1.23	17–21	20.00±1.41	19–21	18.96±1.72	15–23	19	19	F _{4,68} =2.935	p <0.05

Table 4.11. Bonferroni Post hoc test between Mizoram population and the four lineages recovered by Shankar et al. (2021).

Characters	Mizoram vs. Indo-Chinese	Mizoram vs. Western Ghats	Mizoram vs. Indo-Malayan	Mizoram vs. Luzon Island
Ve	p =1.000	NA	p <0.001	p =0.742
Sc	p =1.000	p =0.562	p =0.433	p =1.000
ADSR	p =1.000	p =1.000	p <0.001	p <0.05

Table 4.12. Information on Principal Component Analysis (PCA) and loadings across populations of *O. hannah* using the characters Ve, Sc and ADSR.

Variables	PC1	PC2
Zscore (Ve)	0.736	-0.486
Zscore (Sc)	0.776	-0.161
Zscore (ADSR)	0.681	0.709

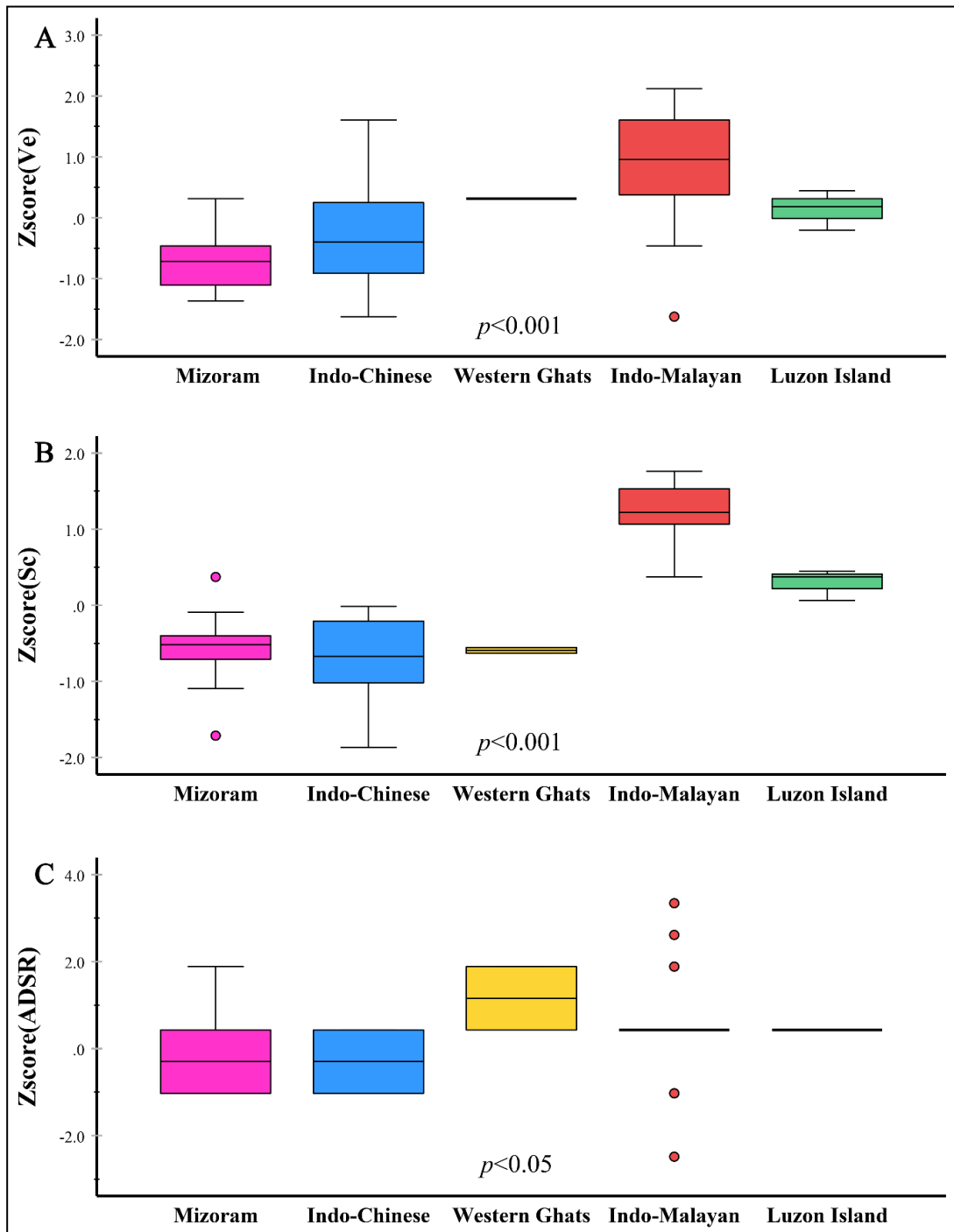


Figure 4.10. Box plot showing the median, interquartile range, range (minimum to maximum), and outliers of the standardised (Z score) Ve (A), Sc (B), and ADSR (C) that differed among *O. hannah* populations/lineages. Significance at the alpha level of 0.05 are given at each plot.

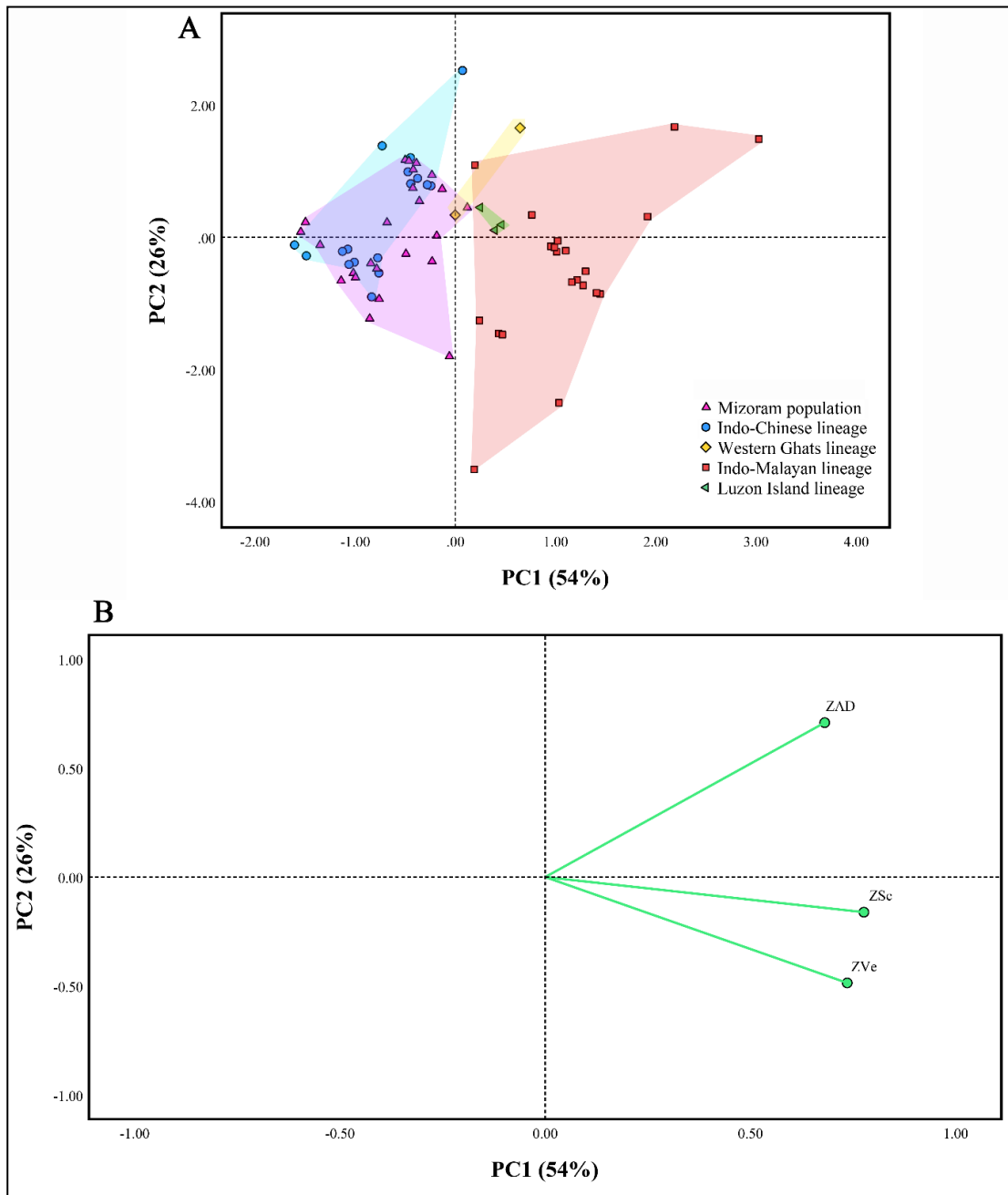


Figure 4.11. (A) Ordination of *O. hannah* populations to see the clustering of Mizoram samples with respect to the pre-defined four lineages (Indo-Chinese, Western Ghats, Indo-Malayan and Luzon Island) along the first two principal components based on a PCA of the standardised meristics (ventrals, subcaudals, anterior dorsal scale rows). (B) PCA loading plot showing the distribution of the analysed variables along the first two principal components.

Distribution and Natural history

The distributional records of the species are mainly based on the documentation of nest attending females during this study. A total of 18 new king cobra nesting sites are documented at elevations ranging from 400–1,450 m a.s.l. in addition to the 23 sites previously reported from Mizoram. These new records are represented by five sampling sites from Aizawl District (Tanhril, Samlukhai, Sailam, Hualngo and Muthi), five sites from Serchhip District (Chhingchhip, and four nests in Thenzawl), four sites from Champhai District (North Khawbung, Tlangsam, and two nests in Zote), two sites from Khawzawl District (two nests in Khawzawl), one site from Lunglei District (Chhipphir), and one site from Mamit District (Dampa Tiger Reserve). Among the overall 18 nests visited, a total of 15 nests comprising a total of 338 eggs are threatened and translocated to laboratory for incubation of the eggs while three nests from Dampa Tiger Reserve, Tlangsam and Zote (nest II) were left untouched because no potential threat is known for them. Moreover, a total of 12 nest attending females were also relocated due to local threat, while one nest attending female from Muthi was already killed at the nest while it was visited, and the nests from Thenzawl (nest IV) and Chhingchhip were deserted by the female probably due to the nest being threatened. The presently documented clutch size of the species ranges from 17 to 31 eggs per clutch (\bar{x} 22.53±3.93), and out of which a total of 310 eggs were hatched under captive incubation in the laboratory using the original nesting materials with the hatching rate of 91.7%. The captive incubation of eggs was conducted during the months of June to August with the room temperature and humidity of 26–30°C and 80–90%, respectively. The hatchlings and the captured females were subsequently relocated to closest forest reserve to original nest site at the distance of 1.1 to 5.6 km (\bar{x} 3.77±1.29 km) (Fig. 4.12; Table 4.13).

Table 4.13. Details of the king cobra nests documented in this study from Mizoram, Northeast India. Abbreviations used: CRF - Community Reserved Forest; RF - Reserved Forest; RRA - Riverine Reserved Area; WLS - Wildlife Sanctuary.

Time of relocation/visit	Place	Grid reference	Elevation (m a.s.l.)	Clutch size	Hatching date	No. hatched	Release sites & distance from original nest
Nest and female relocated due to local threat, hatchling successfully incubated, hatchlings and female relocated to closest forest reserve to original nest site							
14/7/2017	Thenzawl I, Serchhip District	23.268670° N; 92.781702° E	755	21	13/8/2017	20	Zongaw RF; ca. 4.7 km N
14/7/2017	Thenzawl II, Serchhip District	23.262204° N; 92.787157° E	805	26	25/7/2017	24	Zongaw RF; ca. 4.0 km NW
21/6/2020	Thenzawl III, Serchhip District	23.260624° N; 92.776938° E	810	19	5/8/2020	19	Mualthum RF; ca. 3.5 km SW
20/6/2018	Tanhri, Aizawl District	23.754210° N; 92.653862° E	530	28	17/8/2018	24	Tlawng RRA; ca. 2.2 km W
17/6/2019	Samlukhai, Aizawl District	23.403828° N; 92.736597° E	1,029	20	5/8/2019	20	Hmuifang CRF; ca. 3.3 km NE
18/7/2020	Sailam, Aizawl District	23.320818° N; 92.787175° E	531	18	27/7/2020	18	Zongaw RF; ca. 2.9 km NW
11/6/2021	Khawzawl I, Khawzawl District	23.520152° N; 93.176974° E	1,050	25	14/8/2021	20	Murlen NP; ca. 5.6 km NE
25/7/2021	Khawzawl II, Khawzawl District	23.547479° N; 93.183416° E	1,200	23	23/7/2021	18	Murlen NP; ca. 4.8 km NE
24/6/2021	Chhipphir, Lunglei District	23.156045° N; 92.77155° E	504	17	4/8/2021	16	Mualthum RF; ca. 2.3 km S
12/6/2021	N. Khawbung, Champhai District	23.540085° N; 93.316805° E	1,450	18	3/8/2021	16	Murlen NP; ca. 3.2 km N
2/7/2021	Hualngo, Aizawl District	23.663056° N; 92.723056° E	831	25	2/8/2021	25	Tuirial RRA; ca. 5.6 km E
10/8/2021	Zote I, Champhai District	23.494535° N; 93.356810° E	1,323	31	24/8/2021	31	Ngur RF; ca 3.5 km NE
Nest threatened and female killed, nest relocated and eggs incubated successfully, hatchlings relocated to closest forest reserve to original nest site							
6/7/2019	Muthi, Aizawl District	23.765977° N; 92.757833° E	1,130	25	8/8/2019	17	Muthi RF; ca. 1.1 km NW
Nest threatened but deserted by female, hatchlings found and released in the closest forest reserve to original nest site							
3/8/2021	Thenzawl IV, Serchhip District	23.271944° N; 92.783333° E	759	20	NA	20	Zongaw RF; ca. 5.3 km N
24/8/2020	Chhingchhip, Serchhip District	23.481681° N; 92.874639° E	780	22	NA	22	Tawi WLS; 4.6 km W
No obvious threats so this nest was not relocated							
3/7/2017	Dampa Tiger Reserve, Mamit District	23.715076° N; 92.416273° E	400	NA	NA	NA	NA
Female found killed and nest destroyed							
19/7/2021	Tlamsam, Champhai District	23.464739° N; 93.372802° E	1,150	NA	NA	NA	NA
10/8/2021	Zote II, Champhai District	23.491386° N; 93.389895° E	1,005	NA	NA	NA	NA

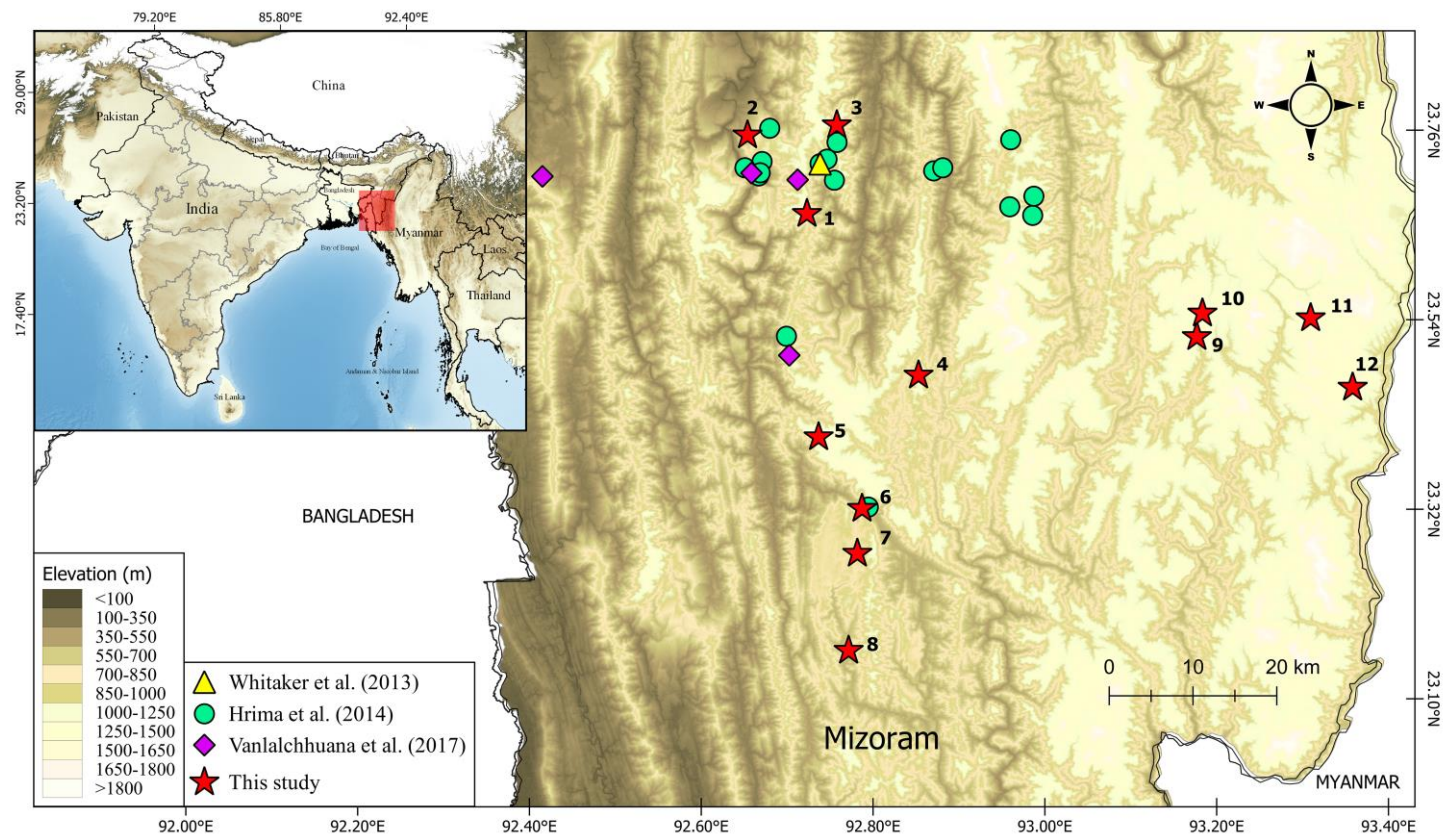


Figure 4.12. Map showing king cobra nesting sites in Mizoram, north-east India from both previous studies and the current conservation programme (red stars, some red stars refer to more than one nesting site) - 1. Hualngo, 2. Tanhril, 3. Muthi, 4. Dampa Tiger Reserve, 5. Chhingchhip, 6. Samlukhai, 7. Sailam, 8. Thenzawl I–IV, 9. Chhipphir, 10. Khawzawl I, 11. Khawzawl II, 12. N. Khawbung, 13. Tlamsam, 14. Zote I, 15. Zote II.



Figure 4.13. *Ophiophagus hannah* in Mizoram, north-east India: A. Deserted nest at Thenzawl IV, B. Deserted hatchlings uncovered inside the nest at Chhingchhip, C. Completely destroyed nest and eggs with the freshly killed female from Tlangsam, D. Female coiling above its nest in Dampa Tiger Reserve, E. Hatching of the incubated eggs, F. Releasing hatchlings at Zongaw Reserved Forests. Photo credits: H.T. Lalremsanga (A, B, E, F), Zakhuma (D), anonymous (C).

Discussion

Distribution and natural history. The elevational range of the species documented in this work (400–1,450 m a.s.l.) is within the known range i.e 60–2,700 m a.s.l. (Ahmed et al. 2009). Although the present work did not record the nesting site of the species from the other north and northeastern Districts (Kolasib and Saitual) as well as the southern Districts (Lawngtlai, Siaha, and Hnahthial) which is plausibly due to insufficient surveys, earlier workers considered the species to be widely distributed throughout the State at the elevations of 40–1,500 m a.s.l. (Lalremsanga et al. 2011). Moreover, the presently recorded clutch size of 17–31 eggs is also within the known range i.e 14–53 eggs in a single clutch (Das 2012; Hrima et al. 2014; Burchfield 1977). Nesting materials from those recorded in Champhai District comprised various leaves of plants such as *Pinus kesiye*, *Quercus griffithii*, *Q. serrata*, *Heteropanax fragrans*, *Lithocarpus pachyphyllus* etc., which are mainly found in the Assam Subtropical Pine Forest (9/C2) (see Fig. 4.13C), while the remainder of documented nests were constructed of bamboo leaves such as *Melocanna baccifera*, *Dendrocalamus hamiltonii*, *Bambusa tulda* etc., which are found in Secondary Moist Bamboo Brakes (2/2S1) (Figs. 4.13A, B & D) (Champion and Seth 1968). As of now, translocation can be considered the only available option for the conservation of threatened nests and nest attending females in the region, a more effective long-term conservation management strategy like intensive awareness campaigns is needed for better management of human-king cobra conflicts, imprinting the ecological roles of snakes among locals, and to mitigate the negative perspective of snakes by and large as suggested by Biakzuala et al. (2022).

Systematics. The phylogenetic trees showed the clustering of Mizoram population of king cobra within the clade of Indo-Chinese lineage thereby corroborating the proposed systematic position of Mizoram population by Shankar et al. (2021). The bPTP species delimitation partitioned Mizoram population and Indo-Chinese as single species; this test also detected the Western Ghats and Indo-Chinese lineages as single species, while the Indo-Malayan and Luzon Island lineages are distinctly partitioned as also recovered by Shankar et al. (2021). In *I6s*, Indo-Chinese lineage comprises of three haplotypes, Indo-Malayan comprises of two haplotypes, while the

Western Ghats and Luzon Island lineages accommodated into single haplotype each. The four lineages are also forming separate haplotype clustering. In *cox1*, only samples from the Indo-Chinese lineage are available thereby a total of six haplotypes are seen within the lineage. In *cytb*, the Indo-Chinese lineage comprises of six haplotypes, seven haplotypes in Indo-Malayan lineage, and single haplotype each in Western Ghats and Luzon Island lineages. The four lineages are also forming disparate haplotype clusters. So, the haplotype networks also support the lineage diversification from the phylogenetic inferences in this work, and corroborate the notions as postulated by Shankar et al. (2021).

However, this work carried out the first-time morphological analysis to test the systematic position of Mizoram king cobra population with respect to the other lineages seen by Shankar et al. (2021). Morphologically, univariate tests do not provide significant difference in the selected characters between the study population and Indo-Chinese as well as with the Western Ghats lineage; while differences are seen with regards to Indo-Malayan and Luzon Island lineages. This may be due to a smaller number of representative specimens from the Western Ghats lineage (i.e only 2 specimens). However, the multivariate PCA showed Mizoram and the predefined specimens of Indo-Chinese lineage clustering together while a marginal separation of Western Ghats lineage is also seen with respect to both Indo-Chinese and Mizoram population. The present systematic reassessment affirms that the study population is a member of the Indo-Chinese lineage, while further assessment on the Western Ghats lineage with more morphological data is warranted. As the conservation status of an evolutionary lineage constituting a distinct conservational unit is largely depends upon regional factors, the present systematic data enrichment will aid in future conservational implications of the study population as well as for the Indo-Chinese lineage altogether.

CHAPTER 5

Sinomicrurus macclellandi (Reinhardt, 1844)

Review of literature

Coral snakes are venomous elapids which were previously categorized into four groups based on the anatomy of the corner of the mouth sensu McDowell (1986, 1987). The first group accommodates the New World coral snake genera, namely *Leptomicrurus* (Schmidt, 1937), *Micrurus* Wagler, 1824 and *Micruroides* Schmidt, 1928; the Temperate Asia coral snake genera *Sinomicrurus* Slowinski, Boundy & Lawson, 2001, and *Hemibungarus* Peters, 1872. The second group is represented by the two species under the genus *Calliophis* Gray, 1834, namely *C. melanurus* (Shaw, 1802) and *C. bibroni* (Jan, 1858) found in the Indian subcontinent. The long-glanded coral snake genus *Maticora* (Gray, 1834) from Sundaland, the Indian endemic *C. nigrescens* (Günther, 1862) as well as the Indochinese *C. maculiceps* (Günther, 1858) comprised the third group. The fourth group accommodates *C. gracilis* Gray, 1834 from north Sumatra and the Malay Peninsula. But, several lines of evidence derived from phylogenetic inferences and hemipenial morphology suggested that coral snakes should be confined under the clades Hemibungarini and Calliophini, where members of the Asian coral snake genus *Hemibungarus* along with other elapid genera (Afro-Asian kraits, mambas, king cobra and cobras) are nested within the former, while the rest of the coral snake genera (Asian and New World) nested within the later clade (see Castoe et al. 2007; Slowinski and Keogh 2000; Slowinski et al. 1997, 2001). According to divergence time estimation, the lineage of the Asian/New World coral snakes is hypothesized to have diverged early in the evolutionary history of elapids, and they emerged approximately 35.6 to 26.9 million years ago (Mya) from the Oriental region, followed by its lineage diversification soon afterwards about 29 Mya (32.5–24.7 Mya) (Kelly et al. 2009).

The Asian coral snake genus *Sinomicrurus* was erected by Slowinski et al. (2001) based on the mitochondrial *cytb* fragment and morphology for all the Asian coral snakes that shared common ancestry with *S. macclellandi*, thereby the genus accommodates five species, namely *S. macclellandi* (Reinhardt, 1844), *S. hatori*

(Takahashi, 1930), *S. japonicus* (Günther, 1868), *S. kelloggi* (Pope, 1928), and *S. sauteri* (Steindachner, 1913). Apart from the traditionally recognized subspecies within the taxon *S. macclellandi* such as *S. macclellandi macclellandi* (Reinhardt, 1844), *S. macclellandi iwasakii* (Maki, 1935), *S. macclellandi swinhoei* (Van Denburgh, 1912), and *S. macclellandi univirgatus* (Günther, 1858); there are also historically recognized six different geographical varieties, subspecies, or synonyms such as *S. personatus* (Blyth, 1854), a junior synonym of *S. macclellandi macclellandi* from Assam, India; *S. macclellandi annularis* (Günther, 1864), solely represented by a single known specimen from southern China; *S. macclellandi nigriventer* (Wall, 1909), erected based on a single type specimen originated from Kasauli in Himachal Pradesh (India); *S. macclellandi gorei* (or *gori*) (Wall, 1910), regarded to be found in Assam and Manipur in India, and also in upper Myanmar; *S. macclellandi concolor* (Wall, 1925a), known from two specimens in Myanmar; and a disputable *S. macclellandi nepalensis* (Shrestha and Majupuria, 1977) from Nepal (David and Ineich 1999; Smart et al. 2021). Mirza et al. (2020) proposed to revalidate the nomen '*nigriventer*' and recognize it as a distinct species based on museum material and molecular data for a freshly collected specimen from Himachal Pradesh, India. However, Smart et al. (2021) provided a broad review of the systematics of *Sinomicrurus* species, and they subsequently elevated *S. iwasakii* and *S. swinhoei* to full species level, resurrected *S. annularis* (Günther, 1864); while sinking *S. hatori* into *S. sauteri*, and *S. nigriventer* into *S. macclellandii* sensu stricto based on the evidence they derived from molecular data, morphometrics and comparative anatomy. Therefore, a total of nine species are currently recognized in the genus fide Smart et al. (2021), namely *S. kelloggi*, *S. japonicus*, *S. boettgeri* (Fritze, 1894), *S. sauteri*, *S. iwasakii*, *S. peinani* Liu, Yan, Hou, Wang, Nguyen, Murphy, Che and Guo, 2020, *S. macclellandi*, *S. annularis*, and *S. swinhoei* which are distributed across India, China, Indochina, and East Asia.

Furthermore, the distribution range for the subspecies or varieties of *S. macclellandi* was well reviewed by Smart et al. (2021), and they affirmed that *S. macclellandi* var. *typica* (fide Wall, 1910) is to be found so far in Mizoram, Arunachal Pradesh and Assam States in India, and also in Myanmar, Thailand and

Cambodia; *S. macclellandi* var. *nigriventer* in Himachal Pradesh (India); *S. macclellandi* var. *concolor* in Myanmar; *S. macclellandi* var. *univirgatus* in Nepal, through the eastern Himalayas up to Sikkim; and *S. macclellandi* var. *gorei* (Wall, 1910) in Assam, Manipur and Mizoram. Particularly in Mizoram, Mathew (2007) recorded *S. macclellandi* for the first time, and the author depicted the specimen of *S. macclellandi* var. *typica*; later, the occurrence of three morphological varieties of *S. macclellandi* has also been noted from the region (Lalremsanga and Zothansiana 2015) namely “Type I” with a regular transverse band corresponding to *S. macclellandi* var. *typica*, “Type II” with vertebral spots corresponding to *S. macclellandi* var. *gorei* and “Type III” with a completely plain morph that does not concur with any of the remaining described varieties such as *S. macclellandi* var. *nigriventer* and *S. macclellandi* var. *concolor*. Later, no variety or subspecies was assigned for the population of *S. macclellandi* from Mizoram (See 119 pp. in Lalremsanga and Lalronunga 2017). However, Smart et al. (2021) provided a comprehensive systematic framework for *Sinomicrurus* species, and they hypothesized the colour variants traditionally considered varieties or subspecies did not exhibit independent lineage in their statistical and molecular analyses. Henceforth, the varieties reported by Lalremsanga and Zothansiana (2015) as well as *S. macclellandi* var. *gorei*, *S. macclellandi* var. *concolor*, *S. macclellandi* var. *nigriventer*, and *S. macclellandi* var. *univirgatus* are considered as mutable chromatic patterns depicting intraspecific variation; and a provisional taxonomy for these variants are provided until more supporting evidence is conceived (see Smart et al. 2021). The recent systematic studies of Asian coral snakes (eg. Castoe et al. 2007; Lalremsanga and Zothansiana 2015; Mirza et al. 2020; Slowinski et al. 2001; Smart et al. 2021), lack extensive genetic data for *S. macclellandi* from northeastern India, especially the type locality and the whole Indian subcontinent. Thus, these studies largely serve as a hindrance to the reappraisal of the putative synonyms of *S. macclellandi* which may be distinct and deserve recognition to highlight their evolutionary importance. In this regard, it is imperative to undertake a robust reappraisal of the systematics of the Northeast Indian *S. macclellandi* based on more genetic markers, representative specimens and populations.

Material and methods

Sampling

A total of 21 preserved specimens of *S. maccllellandi* housed in the collections of the Departmental Museum of Zoology, Mizoram University, India (MZMU) were examined; specimens (n=4) vouchered in the Arunachal Pradesh Regional Centre (APRC), Zoological Survey of India. Fresh specimens were also collected and examined from Meghalaya (n=2) and Mizoram (n=15) after obtaining a herpetological specimen collection permit within Meghalaya State (Permit No. FWC/G/173/Pt-V/2377-87) and Mizoram State (Permit Nos. A.33011/2/99-CWLW/225 and B.19060/5/2020-CWLW/20-26). The live specimens were euthanized using MS-222 following the standardized protocol of Conroy et al. (2009) in compliance with the American Veterinary Medical Association (AMVA) guidelines and approved by the Institutional Animal Ethics Committee (IAEC) (Permission No. MZU-IAEC/2018/12). Then, the liver tissues were dissected and stored them in 95% ethanol for genetic analysis. After dissecting the liver tissues, the freshly euthanized specimens were stored in 70% ethanol and deposited at the reptile section of MZMU, while the other examined museum materials were under preservation in formalin. The sampling sites' geographical coordinates and elevations were recorded using Garmin Montana-650 GPS unit, and a map was prepared using QGIS version 3.16.2.

Genetic data processing

Using the liver tissue, the Genomic DNA was extracted using QIAamp DNA Mini Kit following the manufacturer's protocol (DNeasy® Blood & Tissue Handbook 2023). The fragments of the mitochondrial 16S rRNA (*16s*), cytochrome c oxidase subunit 1 (*cox1*), cytochrome b (*cytb*), NADH dehydrogenase subunit 4 (*nd4*) and nuclear neurotrophin-3 (*nt3*) genes were amplified through Polymerase Chain Reaction (Mullis et al. 1986) based on the thermal conditions given in Table 5.1. The amplified products were purified and sequenced using Sanger's dideoxy method at Barcode BioSciences, Bangalore, India. The gathered datasets consisted of the newly generated sequences of *16s* (OR528021–24), *cox1* (OR527442–47), *cytb* (OR574836–39), *nd4* (OR574840–42), and *nt3* (OR574843–44) along with the

congeneric sequences and the outgroup (*Micrurus fulvius*) obtained from the NCBI GenBank database (Benson et al. 2017). The datasets for each gene were aligned using the MUSCLE algorithm (Edgar 2004) with default parameters in MEGA 11 (Tamura et al. 2021). The uncorrected p-distance was estimation based on complete deletion for gaps/missing data in MEGA 11 (Tamura et al. 2021). For estimating the p-distance using the concatenated mitochondrial and nuclear genes, the dataset was refined to match with the assembled dataset of Smart et al. (2021); the two p-distance matrices were subsequently standardized and ordinated separately in Principal Coordinate Analysis (PCoA) (Gower 1966) to visualize the genetic differentiation across the different taxa in PAST v4.13 (Hammer et al. 2001).

Phylogenetic inferences

Concatenation of the aligned datasets was performed in SequenceMatrix v1.7.8 (Vaidya et al. 2011), and partitioned them by gene and by codon positions. PartitionFinder v2 (Lanfear et al. 2017) was utilized for selecting the best partitioning schemes and for evolutionary model searching under Bayesian Information Criterion. The concatenated, partitioned Bayesian inference (BI) phylogeny and Maximum Likelihood (ML) phylogeny were conducted in Mr.Bayes v3.2.5 (Ronquist et al. 2012) and IQ-TREE (Nguyen et al. 2015), respectively. The BI analysis was conducted by four independent runs with one cold and three hot chains for 20 million generations and sampled every 5000 generations. Tracer v1.7 (Rambaut et al. 2018) was utilized to examine the trace plots generated by the MCMC runs and determine the percentage of burnin cut-off. For the BI analysis, the Bayesian posterior probability (PP) values are interpreted as the nodal supports. The ML analysis was performed using the best partitioning schemes selected by the PartitionFinder v2 (Lanfear et al. 2017) with the models selected under BIC scores by ModelFinder (Kalyaanamoorthy et al. 2017) implemented in IQ-TREE (Nguyen et al. 2015) with 10,000 Ultrafast Bootstrap replicates (UFB) (Minh et al. 2013). In addition, a single locus-based Bayesian Poisson Tree Processes (bPTP) species delimitation method (Zhang et al. 2013) was employed separately for the *cox1*, *cytb* and *nd4* genes partitioned by codon positions. For the input file of bPTP, a non-ultrametric tree was generated in IQ-TREE webserver (Nguyen et al. 2015) with

10,000 Ultrafast Bootstrap replicates (UFB) (Minh et al. 2013) using the nucleotide substitution models selected for each gene based on the lowest BIC score by ModelFinder (Kalyaanamoorthy et al. 2017).

For species tree inference, *BEAST v2.6.7, a package implemented in BEAST v2.6.7 (Bouckaert et al. 2019) was utilized. For this analysis, the reduced dataset concordant with the gathered dataset of Smart et al. (2021) was adopted. Species for every individual was assigned in the taxa selection option following the species delineation in Smart et al. (2021). Furthermore, the nucleotide substitution model was unlinked for each site, and the best models obtained based on the BIC values in JModeltest2 (Dariba et al. 2012) were subsequently implemented through the Standard Nucleotide Substitution Models (SSM), a package coming with BEAST v2.6.7 (Bouckaert et al. 2019). Given that the dataset for the multispecies coalescent tree is mainly based on the assembled dataset of Smart et al. (2021) which assumed molecular clock in their BPP analysis, for that reason the strict clock model which relies on the so-called “Molecular Clock” (Fourment and Darling 2018) was utilized. The tree model for the mitochondrial and the nuclear genes were unlinked to set them as distinct loci. The Yule model and the default values for the other tree priors were used. The Ploidy was set for the nuclear gene tree to autosomal nuclear, and Y or mitochondrial for the mitochondrial gene tree. Using the output .xml file, the MCMC was run for two billion generations by sampling every 200,000 generations with random seeds. The resulting log file from the species tree was visualized in Tracer v1.7 (Rambaut et al. 2018). Then, TreeAnnotator v2.6.4. (Bouckaert et al. 2019) was utilized for summarizing the Bayesian information into a phylogenetic tree based on maximum clade credibility by discarding the first 10% of trees as burn-in. The resulting tree file from the concatenated mitochondrial genes is also annotated in the TreeAnnotator v2.6.4. (Bouckaert et al. 2019), and DensiTree v2.2.7 (Bouckaert 2010) was employed to come by the different topologies in the sets of mitochondrial gene trees.

Morphological data

The snout-to-vent length (SVL) and tail length (TaL) were measured to the nearest millimetre using a measuring tape. A dial calliper accurate to 0.02 mm

(Mitutoyo 505–671) was used for measuring other linear measurements (Fig. 5.1): length of head from tip of snout to angle of jaw (HL); maximum width of head (HW); width of head at level of eye (HWE); HD, depth of head (HD); width of snout at level of nostril (SW); horizontal eye diameter (ED); eye to snout distance (E-S); eye to nostril distance (E-N); distance between the nostrils i.e internarial space (INS); distance between the orbits i.e interorbital space (IOS); width of internarial scale (INW); width of prefrontal scale (PFW); length of frontal scale (FL); length of parietal scale (PL); nuchal band width in scale (NBW); width of white inter-band on head at level of supraocular in measurement (WBH); transverse body band, only that covers more than five dorsal scales (BB); body spots, that covers less than five dorsal scales (BS); transverse bands on tail reaching down the Sc (BT). The meristic data are also obtained from dorsal scale rows (DSR); ventral scales (Ve); subcaudal scales (Sc); condition of anal shield (As); supralabials (SL); infralabials (IF); supralabials contacting the eye (SLe); anterior genials (AG); posterior genials (PG); infralabials touching anterior genial (IL-AG); infralabials touching posterior labials (IL-PG); temporal scales (Tem); preoculars (PrO); postoculars (PoO); and supraocular (SpO). We followed Dowling (1951) for counting Ve, and counted the DSR at one head length posterior to the neck, at the midpoint of snout-vent length, and at one head length anterior to the As. The terminal scute was excluded while counting the Sc. The sex of the specimens was identified by examining everted hemipenes or by ventral tail dissection. The values for bilateral head characters were provided in left/right order. Keogh (1999) was followed for hemipenis terminology.

Osteology

Micro-CT scans were generated for a male specimen of each *S. macclellandi* sensu stricto and *S. macclellandi* var. *gorei* using a Bruker® Skyscan 1272 (Bruker BioSpin Corporation, Billerica, Massachusetts, USA). The head of the specimen was scanned for 210 min at 3 µm resolution, recording data for every 0.4° of rotation with an aluminium 1 mm filter, source voltage 65 kV, and source current 153 uA. Volume rendering was performed with the scan's CTVOX (Bruker BioSpin Corporation, Billerica, Massachusetts, USA) software, and images were edited in

Adobe Photoshop. The osteological description follows the terminology of Heatwole (2009).

Statistical analyses

A priori grouping was made by pooling those specimens which are having two or less than two BS as well as completely plain morph into *S. macclellandi* var. *gorei* group, while those having BB more than two to *S. macclellandi* var. *typica* group. Prior to performing the statistical analyses, the meristic data (Ve, Sc, NBW, BB, BS, and BT) were standardized to their zero mean and standard deviation. Firstly, the meristics data were tested for sexual dimorphism as well as difference between the varieties simultaneously using two-way analysis of variance (ANOVA) using sex and group as the factors. Levene's test (Levene 1961) was performed for testing the homogeneity of variances. In case, the assumption of the two-way ANOVA was violated, either separate one-way ANOVA or Brown-Forsythe test (Brown & Forsythe 1974) were employed as an alternative approach. For mensural data (TaL, HL, HW, HD, ED, ND, E-S, N-S, N-E, RH, RW, INS, IOS, INW, PFW, FL, PL, PW, and WBH), to make a linear relationship with body size and avoid the effect of allometric growth, the best allometric adjustment model was determined through regression analysis (Thorpe 1975). The allometric adjustment was carried out using the equation: $\text{character} + (427.88 - \text{SVL}) * \text{regression coefficient}$, where 427.88 is the grand mean across the groups. Then, the adjusted mensurals were utilized to screen the difference between sex and varieties using a two-way analysis of covariance (ANCOVA) with snout-vent length (SVL) as a covariate, and sex and variety as the factors.

Multivariate Principal Component Analysis (PCA) was employed a to determine the clustering of the studied varieties of *S. macclellandi* based on the identified characters that differ between the groups excluding the sexually dimorphic characters. The specimens which fall short of the selected characters are excluded from the test. The correlation matrices between all pairs of the morphological variables, the variance explained by each eigenvalue, and the PCA loadings for the first two components were also extracted. All statistical analyses and graphical

representations were performed using free access statistical packages viz. PAST 4.13 (Hammer et al. 2001) and PSPP v.1.6.2 (GNU Project 2015).

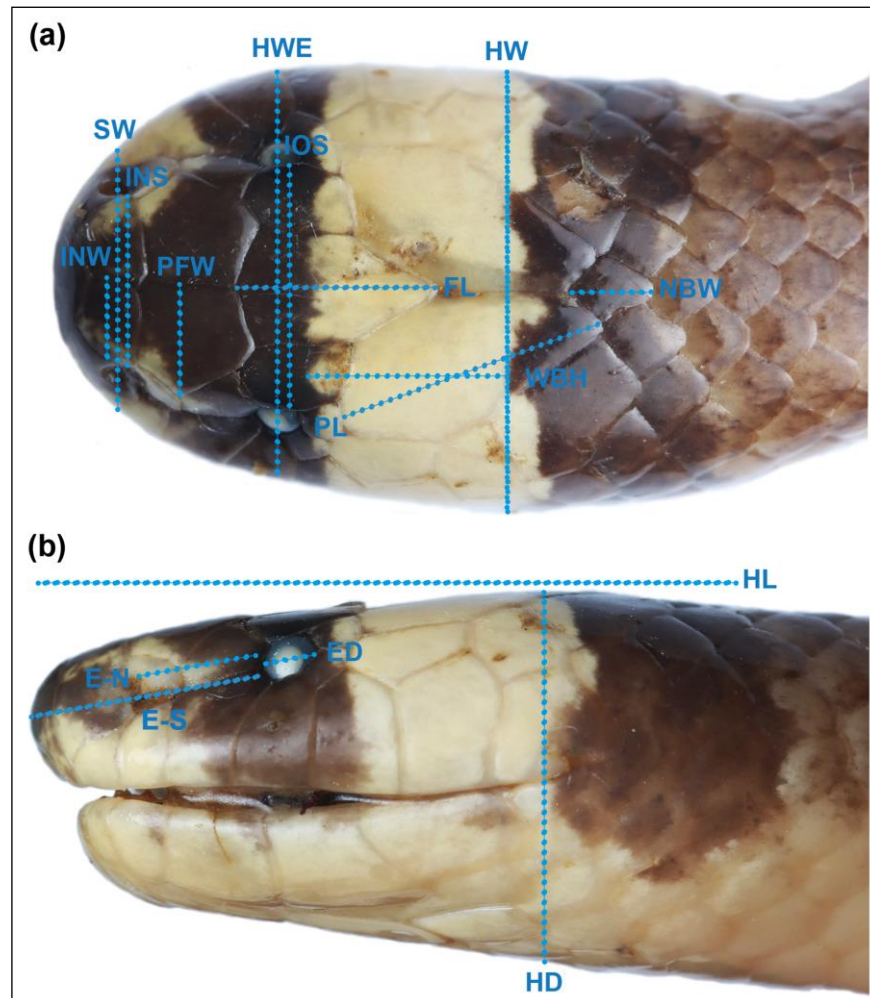


Figure 5.1. Description of head morphometrics used in this chapter: (a) maximum width of head (HW), width of head at level of eye (HWE), width of snout at level of nostril (SW), distance between the nostrils i.e., internarial space (INS), distance between the orbits i.e., interorbital space (IOS), width of internarial scale (INW), width of prefrontal scale (PFW), length of frontal scale (FL), length of parietal scale (PL), width of white inter-band on head at level of supraocular in measurement (WBH); (b) length of head from tip of snout to angle of jaw (HL), depth of head (HD), horizontal eye diameter (ED), eye to snout distance (E-S), eye to nostril distance (E-N); and the meristics nuchal band width in scale (NBW) is also depicted where the NBW is one in this case.

Table 5.1. Detailed information on the primer pairs and PCR thermal conditions used in the amplification of four mitochondrial genes and one nuclear gene of *Sinomicrurus* species.

Target mt gene	Primer pairs	Primer sequences	Primer references	Initial denaturation	Repeated steps (35 cycles)			Final extension	Cooling
					Denaturation	Annealing	Extension		
<i>16s</i>	L02510 (Forward); H03063 (Reverse)	Forward: 5'-CGCCTGTTTATCAAAAACAT-3' Reverse : 5'-CTCCGGTTTGAAGTCAGATC-3'	Palumbi 1996; Rassmann1 997	95°C for 5 min	95°C for 1 min	50.3°C for 30 sec	72°C for 1 min	72°C for 5 min	
<i>cox1</i>	LCO Forward); HCO (Reverse)	Forward: 5'-TAATACGACTCACTATAGGGGGTCAACAAA TCATAAAGATATTGG-3' Reverse : 5'-ATTAACCCTCACTAAAGTAAACTTCAGGGT GACCAAAAAATC-3'	Folmer et al. 1994	94°C for 3 min	94°C for 30 sec	50°C for 40 sec	72°C for 45 sec	72°C for 5 min	
<i>nd4</i>	ND4 (Forward); ND4 LEU (Reverse)	Forward: 5'-CACCTATGACTACCAAAAAGCTCATGTAGAA GC-3' Reverse : 5'-CATTACTTTTACTTGGATTTGCACCA-3'	Arévalo et al. 1994	94°C for 3 min	94°C for 30 sec	52°C for 45 sec	72°C for 1 min	72°C for 5 min	4°C for 15 min
<i>cytb</i>	L14910 (Forward); H16064 (Reverse)	Forward: 5'-GACCTGTGATMTGAAAAACCAAYCGTTGT-3' Reverse : 5'-CTTTGGTTTACAAGAACAATGCTTTA-3'	Burbrink et al. 2000	94°C for 3 min	94°C for 30 sec	49°C for 40 sec	72°C for 30 sec	72°C for 5 min	
Target nu gene					Repeated steps (40 cycles)				
<i>nt3</i>	NT3-F3 Forward); NT3-R4 (Reverse)	Forward: 5'-ATATTTCTGGCTTTTCTCTGTGGC-3' Reverse : 5'-GCGTTTCATAAAAATATTGTTGACCGG-3'	Noonan & Chippindale 2006	94°C for 3 min	94°C for 30 sec	56°C for 50 sec	72°C for 50 sec	72°C for 5 min	

Table 5.2. Details of mitochondrial and nuclear genes utilized for *Sinomicrurus* species with *Micrurus fulvius* as outgroups.

Species	Vouchers	MOTUs (bPTP)	<i>cox1</i>	<i>cytb</i>	<i>16s</i>	<i>nd4</i>	<i>nt3</i>	Locality	References
<i>S. gorei</i> comb. nov.	MZMU1727	A	OR527443	OR574837	OR528022	OR574840	OR574843	Mizoram, India	This study
<i>S. gorei</i> comb. nov.	MZMU1926	A	OR527442	OR574836	OR528023	-	-	Mizoram, India	This study
<i>S. gorei</i> comb. nov.	MZMU2034	A	OR527444	OR574838	OR528024	OR574841	OR574844	Mizoram, India	This study
<i>S. macclellandi</i> var. <i>typica</i>	MZMU2588	B	OR527447	OR574839	OR528021	OR574842	-	Mizoram, India	This study
<i>S. macclellandi</i> var. <i>typica</i>	YSR006A	B	OR527445	-	-	-	-	Meghalaya, India	This study
<i>S. macclellandi</i> var. <i>typica</i>	YSR006B	B	OR527446	-	-	-	-	Meghalaya, India	This study
<i>S. macclellandi</i> var. <i>typica</i>	MZMU272	B	-	MW788935	-	MW788953	MW788968	Mizoram, India	Smart et al. 2021
<i>S. macclellandi</i>	BWS OPAS8	B	-	MW788930	-	MW788949	MW788965	Mongar Dist., Bhutan	Smart et al. 2021
<i>S. macclellandi</i>	CIBHN04	B	MF522833	MF489754	-	MF489758	-	NA	Chen et al. 2017
<i>S. macclellandi</i>	CAS 221494	B	-	MW788923	-	MW788941	MW788960	Kachin, Myanmar	Smart et al. 2021
<i>S. macclellandi</i>	NCBS NRC-AA-0005	C	MT521708	MW788940	-	MT248291	-	Himachal Pradesh, India	Mirza et al. 2020; Smart et al. 2021
<i>S. peinani</i>	KU 311567	D	-	MW788932	-	MW788950	MW788966	Guangxi, China	Smart et al. 2021
<i>S. peinani</i>	CHS643	D	MK064794	MK201448	MK194117	-	-	China	Li et al. 2020
<i>S. cf. peinani</i>	NA	E	MZ230594	MZ230594	MZ230594	MZ230594	-	China	Zhou 2021
<i>S. cf. peinani</i>	YBU16054	F	MN685879	-	-	-	-	Guangxi, China	Liu et al. 2020
<i>S. cf. peinani</i>	YBU16067	F	MN685881	-	-	-	-	Guangxi, China	Liu et al. 2020

Table 5.2. Continued.

Species	Vouchers	MOTUs (bPTP)	<i>cox1</i>	<i>cytb</i>	<i>16s</i>	<i>nd4</i>	<i>nt3</i>	Locality	References
<i>S. cf. peinani</i>	YPX9246	F	MN685895	-	-	-	-	Vinh Phuc, Vietnam	Liu et al. 2020
<i>S. cf. peinani</i>	YBU16086	F	MN685882	-	-	-	-	Guangxi, China	Liu et al. 2020
<i>S. cf. peinani</i>	YBU16054	F	MN685879	-	-	-	-	Guangxi, China	Liu et al. 2020
<i>S. cf. peinani</i>	YPX9247	F	MN685896	-	-	-	-	Vinh Phuc, Vietnam	Liu et al. 2020
<i>S. cf. peinani</i>	YPX9245	G	MN685894	-	-	-	-	Cao Bằng, Vietnam	Liu et al. 2020
<i>S. cf. peinani</i>	YBU16066	H	MN685880	-	-	-	-	Guangxi, China	Liu et al. 2020
<i>S. peinani</i>	ROM 35245	I	-	EF137418	-	EF137410	MW788959	Cao Bằng, Vietnam	Castoe et al. 2007; Smart et al.2021
<i>S. cf. peinani</i>	YPX9244	I	MN685893	-	-	-	-	Cao Bằng, Vietnam	Liu et al. 2020
<i>S. cf. peinani</i>	YPX590/ROM 31157	I	MN685888	KX694853	KX694666	-	KX695049	NA	Liu et al. 2020; Alencar et al. 2016
<i>S. cf. peinani</i>	CHS859	J	MK06492	MK201574	MK194273	-	-	China	Li et al. 2020
<i>S. swinhoei</i>	NMNS 17522	K	-	MW788927	-	MW788945	MW788961	Nantou, Taiwan	Smart et al. 2021
<i>S.cf. swinhoei</i>	CHS853	K	MK064917	MK201569	MK194267	-	-	China	Li et al. 2020
<i>S.cf. swinhoei</i>	CHS718	K	MK064834	MK201485	MK194168	-	-	China	Li et al. 2020
<i>S.cf. swinhoei</i>	CHS032	K	MK064600	MK201248	MK193897	-	-	China	Li et al. 2020
<i>S.cf. swinhoei</i>	CIBSC07	K	MG653600	MG653604	-	MG653608	-	NA	Chen et al. 2017
<i>S.cf. swinhoei</i>	CIBHN05	K	MG653598	MG653602	-	MG653606	-	NA	Chen et al. 2017
<i>S.cf. swinhoei</i>	GP1059	K	MN685873	-	-	-	-	Hainan, China	Liu et al. 2020
<i>S.cf. swinhoei</i>	GP2742	K	MN685877	-	-	-	-	China	Liu et al. 2020

Table 5.2. Continued.

Species	Vouchers	MOTUs (bPTP)	<i>cox1</i>	<i>cytb</i>	<i>16s</i>	<i>nd4</i>	<i>nt3</i>	Locality	References
<i>S.cf. swinhoi</i>	GP1060	K	MN685874	-	-	-	-	NA	Liu et al. 2020
<i>S.cf. swinhoi</i>	GP3360	K	MN685878	-	-	-	-	Sichuan, China	Liu et al. 2020
<i>S.cf. swinhoi</i>	GP5500	K	MN685885	-	-	-	-	Sichuan, China	Liu et al. 2020
<i>S.cf. swinhoi</i>	CIBHN06	K	MG653599	MG653603	-	MG653607	-	NA	Chen et al. 2017
<i>S.cf. swinhoi</i>	ZSHS01	K	MG788982	-	-	-	-	China	Chen et al. 2017
<i>S.cf. swinhoi</i>	KIZ011981	K	MN685886	-	-	-	-	China	Liu et al. 2020
<i>S.cf. swinhoi</i>	ROM37110	K	MN685891	-	-	-	-	Tuyen Quang, Vietnam	Liu et al. 2020
<i>S.cf. swinhoi</i>	YPX9241	K	MN685890	-	-	-	-	Bac Thai, Vietnam	Liu et al. 2020
<i>S.cf. swinhoi</i>	KIZ011601	K	MN685887	-	-	-	-	Phu Tho, Vietnam	Liu et al. 2020
<i>S.cf. swinhoi</i>	ROM31159	K	MN685892	-	-	-	-	Tuyen Quang, Vietnam	Liu et al. 2020
<i>S.cf. swinhoi</i>	RN0749	K	KP749813	-	-	-	-	Taiwan, China	Chen & Lin 2015
<i>S.cf. swinhoi</i>	RN0658	K	KP749808	-	-	-	-	Taiwan, China	Chen & Lin 2015
<i>S.cf. swinhoi</i>	RN0611	K	KP749807	-	-	-	-	Taiwan, China	Chen & Lin 2015
<i>S.cf. swinhoi</i>	RN1024	K	KP749817	-	-	-	-	Taiwan, China	Chen & Lin 2015
<i>S.cf. swinhoi</i>	CIBHN01	K	-	MF489751	-	MF489755	-	NA	Chen et al. 2017
<i>S.cf. swinhoi</i>	CIBHN02	K	-	MF489752	-	MF489756	-	NA	Chen et al. 2017
<i>S.cf. swinhoi</i>	CIBHN03	K	-	MF489753	-	MF489757	-	NA	Chen et al. 2017
<i>S.cf. annularis</i>	KU 312170	K	-	MW788934	-	MW788952	MW788967	Guizhou, China	Smart et al. 2021
<i>S. kelloggi</i>	CHS033	L	MK064601	MK201249	MK193898	-	-	China	Li et al. 2020
<i>S. kelloggi</i>	ROM 37080	M	-	EF137417	-	EF137409	MW788958	Hai Duong, Vietnam	Castoe et al. 2007; Smart et al.2021

Table 5.2. Continued.

Species	Vouchers	MOTUs (bPTP)	<i>cox1</i>	<i>cytb</i>	<i>16s</i>	<i>nd4</i>	<i>nt3</i>	Locality	References
<i>S. kelloggi</i>	GP2193	M	MN685875	-	-	-	-	Hainan, China	Liu et al. 2020
<i>S. kelloggi</i>	GP4643	M	MN685883	-	-	-	-	Hainan, China	Liu et al. 2020
<i>S. kelloggi</i>	ROM37079	M	MN685889	-	-	-	-	Hia Duong, Vietnam	Liu et al. 2020
<i>S. kelloggi</i>	CHS854	M	MK064918	MK201570	MK194268	-	-	China	Li et al. 2020
<i>S. kelloggi</i>	GP1046	M	MN685872	-	-	-	-	NA	Liu et al. 2020
<i>S.cf. kelloggi</i>	GP4839	N	MN685884	-	-	-	-	Guangxi, China	Liu et al. 2020
<i>S.cf. kelloggi</i>	CHS031	O	MK064599	MK201247	MK193896	-	-	China	Li et al. 2020
<i>S.cf. kelloggi</i>	GP2194	O	MN685876	-	-	-	-	Guangdong, China	Liu et al. 2020
<i>S.cf. kelloggi</i>	FJHSHS01	O	MG788980	-	-	-	-	China	Chen et al. 2017
<i>S.cf. peinani</i>	CIBYN08	P	MG653601	MG653605	-	MG653609	-	NA	Chen et al. 2017
<i>S.cf. sauteri</i>	RN1455	Q	KP772310	-	-	-	-	Taiwan, China	Chen & Lin 2015
<i>S.cf. sauteri</i>	RN1270	Q	KP749822	-	-	-	-	Taiwan, China	Chen & Lin 2015
<i>S.cf. sauteri</i>	RN1013	Q	KP749816	-	-	-	-	Taiwan, China	Chen & Lin 2015
<i>S.cf. sauteri</i>	RN0743	Q	KP749811	-	-	-	-	Taiwan, China	Chen & Lin 2015
<i>S.cf. sauteri</i>	RN0035	Q	KP749803	-	-	-	-	Taiwan, China	Chen & Lin 2015
<i>S.cf. sauteri</i>	RN0697	Q	KP749809	-	-	-	-	Taiwan, China	Chen & Lin 2015
<i>S.cf. sauteri</i>	RN0285	Q	KP749804	-	-	-	-	Taiwan, China	Chen & Lin 2015
<i>S.cf. sauteri</i>	RN0726	Q	KP749810	-	-	-	-	Taiwan, China	Chen & Lin 2015
<i>S.cf. sauteri</i>	RN0745	Q	KP749812	-	-	-	-	Taiwan, China	Chen & Lin 2015
<i>S.cf. sauteri</i>	RN1581	Q	KP749827	-	-	-	-	Taiwan, China	Chen & Lin 2015
<i>S. j. japonicus</i>	KUZ<JPN>:R72606	S	-	LC094076	-	-	LC094140	Japan	Kaito et al. 2017
<i>S. j. japonicus</i>	KUZ<JPN>:R72609	S	-	LC094075	-	-	LC094139	Japan	Kaito et al. 2017

Table 5.2. Continued.

Species	Vouchers	MOTUs (bPTP)	<i>cox1</i>	<i>cytb</i>	<i>16s</i>	<i>nd4</i>	<i>nt3</i>	Locality	References
<i>S. j. boettgeri</i>	KUZ<JPN>:R71597	S	-	LC094074	-	-	LC094138	Japan	Kaito et al. 2017
<i>S. j. boettgeri</i>	KUZ<JPN>:R52588	S	-	LC094073	-	-	LC094137	Japan	Kaito et al. 2017
<i>S. j. takarai</i>	KUZ<JPN>:R34196	T	-	LC094049	-	-	LC094126	Japan	Kaito et al. 2017
<i>S.cf. swinhoei</i>	CIBHN03	K	-	MF489753	-	MF489757	-	NA	Chen et al. 2017
<i>S.cf. swinhoei</i>	CIBHN02	K	-	MF489752	-	MF489756	-	NA	Chen et al. 2017
<i>S.cf. swinhoei</i>	CIBHN01	K	-	MF489751	-	MF489755	-	NA	Chen et al. 2017
<i>S. cf. annularis</i>	KU 312170	K	-	MW788934	-	MW788952	MW788967	Guizhou, China	Smart et al. 2021
<i>S. m. swinhoei</i>	NMNS 17522	K	-	MW788927	-	MW788945	MW788961	Nantou, Taiwan	Smart et al. 2021
<i>S.m. iwasaki</i>	KUZ R-48123	U	-	MW788939	-	MW788957	MW788972	Ishigaki Island, Japan	Smart et al. 2021
<i>S. kelloggi</i>	ROM 37080	M	-	EF137417	-	EF137409	MW788958	Hai Duong, Vietnam	Castoe et al. 2007; Smart et al.2021
<i>S. sauteri</i>	NTNUB NA	R	-	MW788928	-	MW788947	MW788964	Nantou, Taiwan	Smart et al. 2021
<i>S. hatori</i>	TESRI 132	R	-	MW788926	-	MW788944		Yilan, Taiwan	Smart et al. 2021
<i>S. j. japonicus</i>	KUZ R-33074	S	-	MW788936	-	MW788954	MW788969	Amami Oshima Island, Japan	Smart et al. 2021
<i>S. j. takarai</i>	KUZ R-34195	T	-	MW788938	-	MW788938	MW788971	Kume Island, japan	Smart et al. 2021
<i>S. j. boettgeri</i>	KUZ R-33165	T	-	MW788937	-	MW788955	MW788970	Okinawa Island, japan	Smart et al. 2021
<i>Micrurus fulvius</i>	ENS10807	V	-	JX398643	-	JX398492	JX398763	Texas, USA	Sheehy 2012
<i>Micrurus fulvius</i>	CAS 214347	V	-	KU754355	-	KU754444	-	Florida, USA	Streicher et al. 2016

Results

Phylogenetic relationships

The combined matrix of *16s* (1,344 bp), *cox1* (716 bp), *cytb* (1,125 bp), *nd4* (875 bp), and *nt3* (641 bp) contained a total of 4,701 bp aligned characters. A largely similar BI (Fig. 5.2) and ML (Fig.5.3) tree topologies were recovered. The BI and ML phylogenies based on the concatenated dataset depicted a lineage diversification among the newly generated sequences of *S. maccllelandi* populations from Mizoram and Meghalaya in India. It was conceived that the Mizoram samples of *S. maccllelandi* var. *gorei* (MZMU1727, MZMU1926, MZMU2034) are forming a strongly supported sister lineage (PP=1.00; UFB=99) of the clade composed by the *S. maccllelandi* var. *typica* and *S. peinani* lineages. The individuals of *S. maccllelandi* from Mizoram (MZMU2588) and the two DNA sub-samples of the topotypical specimen from Shillong, Meghalaya (YSR006) are nested among the previously affirmed *S. maccllelandi* var. *typica* (fide Smart et al. 2021) from Mizoram (MZMU270), Myanmar (CAS 221494), Bhutan (BWS OPAS8), unreported locality (CBHN04), and *S. maccllelandi* (NCBS NRC-AA-0005) from Himachal Pradesh with a well-supported node (PP=1.00; UFB=100).

Although the specimen of *S. nigriventer* fide Mirza et al. (2020) (NCBS NRC-AA-0005) and *S. maccllelandi* var. *gorei* fide Wall (1910) had recently been sunk under *S. maccllelandi* sensu stricto (Smart et al., 2021), the bPTP analysis partitioned the monophyletic clade consisting *S. maccllelandi* + *S. peinani* into four molecular operational taxonomical units (MOTUs) which were assigned as putative Species A (*S. maccllelandi* var. *typica*), Species B (*S. maccllelandi* var. *gorei*), Species C (*S. maccllelandi* var. *nigriventer*), and Species D (*S. peinani*); for *S. peinani*, by not take into account on the other MOTUs (E–J) recovered in the bPTP species delimitation (see Table S2). Therefore, the specimen of *S. maccllelandi* (NCBS NRC-AA-0005) fide Smart et al. (2021) and the Mizoram specimens (MZMU1727, MZMU1926, MZMU2034) were regarded as distinct MOTUs for genetic divergence estimation. Within the aforementioned clade, the mean values of intra-lineage genetic divergences estimated based on *cox1* gene are 0.9% within *S. maccllelandi* var. *gorei* (among Mizoram specimens), 1.2% within *S. maccllelandi* var. *typica* (MZMU2588,

YSR006, CIBHN04), 4% within *S. peinani*; and the mean inter-lineage genetic divergences are 10.1% (*S. macclellandi* var. *gorei* vs. var. *nigriventer*), 10.7% (*S. macclellandi* var. *gorei* vs. *S. macclellandi* var. *typica*), 11.7% (*S. macclellandi* var. *gorei* vs. *S. peinani*), 6.8% (*S. macclellandi* var. *typica* vs. var. *nigriventer*), 8.4% (*S. macclellandi* var. *typica* vs. *S. peinani*), and 9.3% (var. *nigriventer* vs. *S. peinani*). The mean intra-lineage genetic divergence estimated based on *cytb* gene also showed 0.7% within *S. macclellandi* var. *gorei*, 2% within *S. macclellandi* var. *typica* (MZMU2588, MZMU270, CIBHN04, CAS 221494, BWS OPAS8), 1.1% within *S. peinani*; and the mean inter-lineage genetic divergences are 9.5% (*S. macclellandi* var. *gorei* vs. *S. macclellandi* var. *nigriventer*), 10.4% (*S. macclellandi* var. *gorei* vs. *S. macclellandi* var. *typica*), 10.8% (*S. macclellandi* var. *gorei* vs. *S. peinani*), 6.1% (*S. macclellandi* var. *typica* vs. var. *nigriventer*), 7.6% (*S. macclellandi* var. *typica* vs. *S. peinani*), and 8% (*S. macclellandi* var. *nigriventer* vs. *S. peinani*). The ordination of the genetic divergence in the concatenated four mitochondrial genes (*16s*, *cox1*, *cytb* and *nd4*) (Fig. 5.4a) and one nuclear gene (*nt3*) (Fig. 5.4b) along the first two Principal Coordinate (PCo) axes also disclosed the discrete clustering of the *S. macclellandi* var. *gorei* specimens from *S. macclellandi* sensu stricto and from the other congeneric species as well.

The topology of the species tree concurred well with the reconstructed mitochondrial gene tree, and is also largely concurred with the species tree derived by Smart et al. (2021) (Figs. 5.5a, b). Moreover, the species tree and the mitochondrial gene tree also depicted a distinct lineage formed by the Mizoram samples of *S. macclellandi* var. *gorei* while the samples from Meghalaya grouped with the previously affirmed *S. macclellandi* var. *typica* (fide Smart et al. 2021) from Mizoram (MZMU2588; MZMU270), Myanmar (CAS 221494), Bhutan (BWS OPAS8), and unknown location (CIBHN04). The best nucleotide substitution models utilized for the BI, ML and species tree inferences are given in Table 5.3.

Table 5.3. The best partitioning schemes and nucleotide substitution models selected for the partitioned concatenated matrix, Bayesian Poisson Tree Processes species delimitation, and multispecies coalescent tree in the present study.

Models for partitioned concatenated phylogenies			
Partitions	Sites	For Bayesian Inference (PartitionFinder)	For Maximum Likelihood (ModelFinder)
I	<i>16s</i>	GTR+G	TIM2+F+R2
II	<i>cox1pos1</i>	F81	TPM2+F
III	<i>cox1pos2</i> , <i>nd4pos3</i> , <i>cytbpos3</i>	TRN+I+G	TN+F+I+G4
IV	<i>cox1pos3</i> , <i>nd4pos2</i>	TRNEF+G	TNe+G4
V	<i>cytbpos1</i> , <i>nd4pos1</i>	TRN+G	TN+F+R2
VI	<i>cytbpos2</i>	HKY	HKY+F
VII	<i>nt3pos3</i> , <i>nt3pos2</i> , <i>nt3pos1</i>	K80	K2P
Models for Bayesian Poisson Tree Processes (ModelFinder)			
I	<i>cox1pos1</i>		TPM3+F+I
II	<i>cox1pos2</i>		TN+F+G4
III	<i>cox1pos3</i>		TIM2e+G4
IV	<i>cytbpos1</i>		TPM2+F+G4
V	<i>cytbpos2</i>		TPM3+F+I
VI	<i>cytbpos3</i>		TN+F+G4
VII	<i>nd4pos1</i>		HKY+F+G4
VIII	<i>nd4pos2</i>		HKY+F+G4
IX	<i>nd4pos3</i>		HKY+F+I+G4
Models for Multispecies Coalescent Tree (JModeltest)			
I	<i>16s</i>		HKY
II	<i>cox1</i>		HKY+I
III	<i>cytb</i>		HKY+I+G
IV	<i>nd4</i>		HKY+G
V	<i>nt3</i>		K80

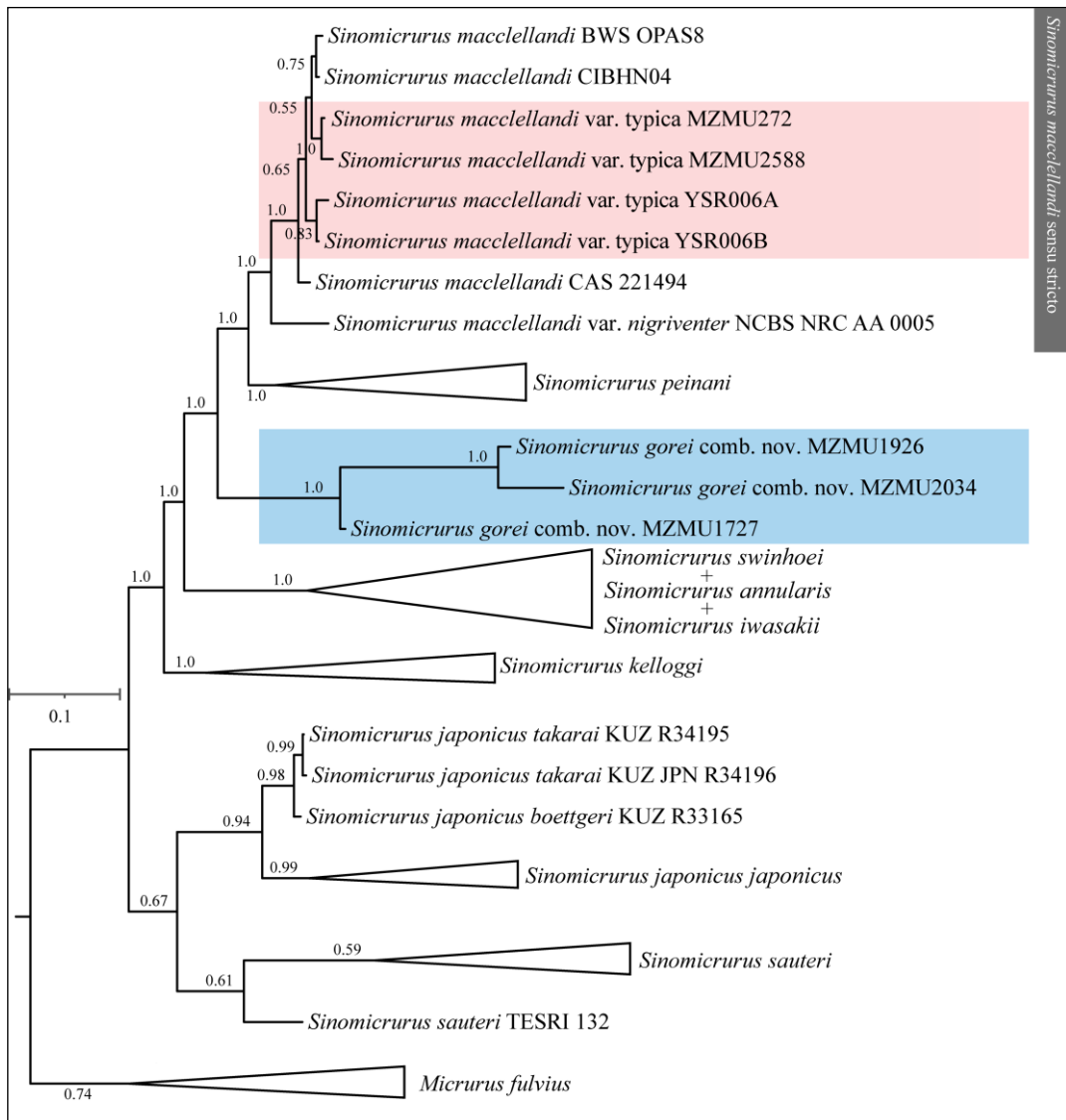


Figure 5.2. Bayesian inference phylogenetic tree constructed using partitioned concatenated sequences of *16s*, *cox1*, *cytb*, *nd4* and *nt3* of *Sinomicrurus* species with *Micrurus fulvius* as outgroup. Numbers at the nodes indicate Bayesian posterior probability and values <0.50 are not shown. The specimens of *S. macclellandi* var. *typica* are shaded in red box, *S. gorei* comb. nov. in blue box, and *S. macclellandi* sensu stricto fide Smart et al. (2021) are indicated in vertical dark-greyish box.

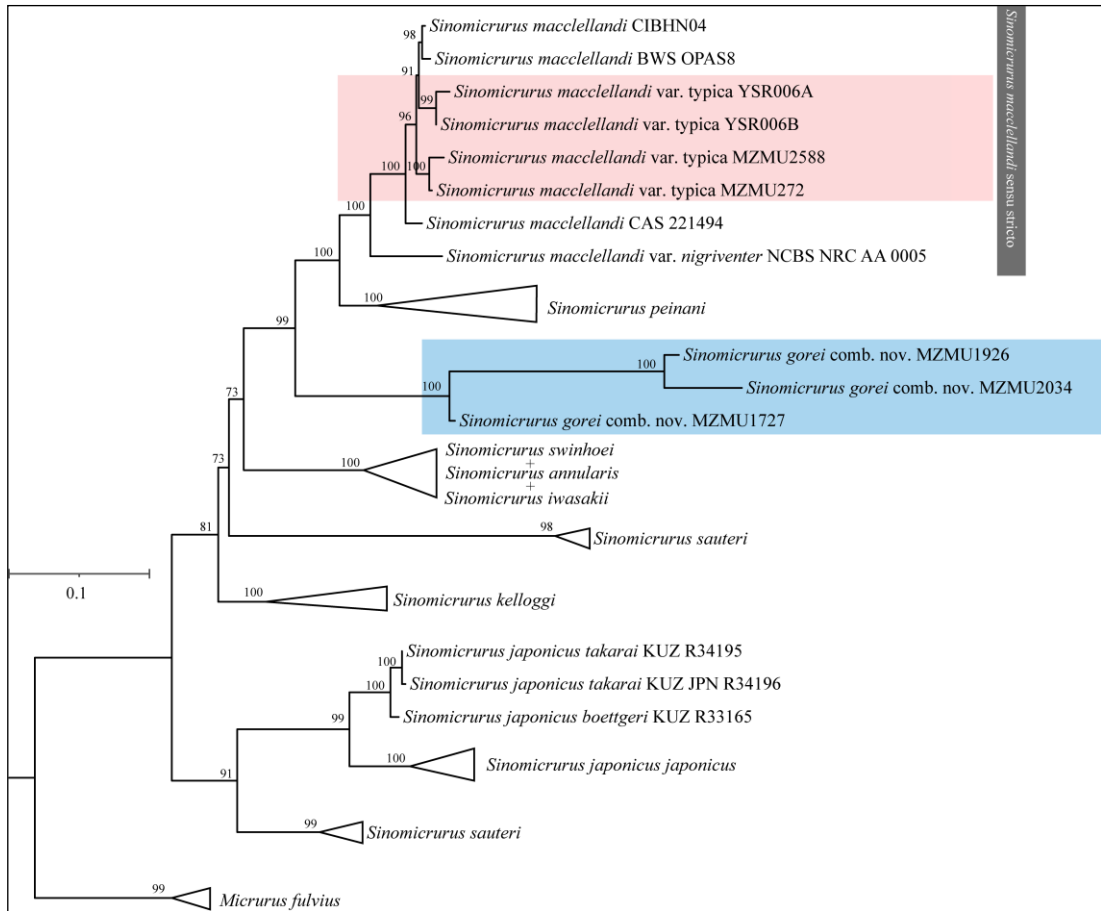


Figure 5.3. Maximum likelihood phylogenetic tree constructed using partitioned concatenated sequences of *16s*, *cox1*, *cytb*, *nd4* and *nt3* of *Sinomicrurus* species with *Micrurus fulvius* as outgroup. Numbers at the nodes indicate ultrafast bootstrap values.

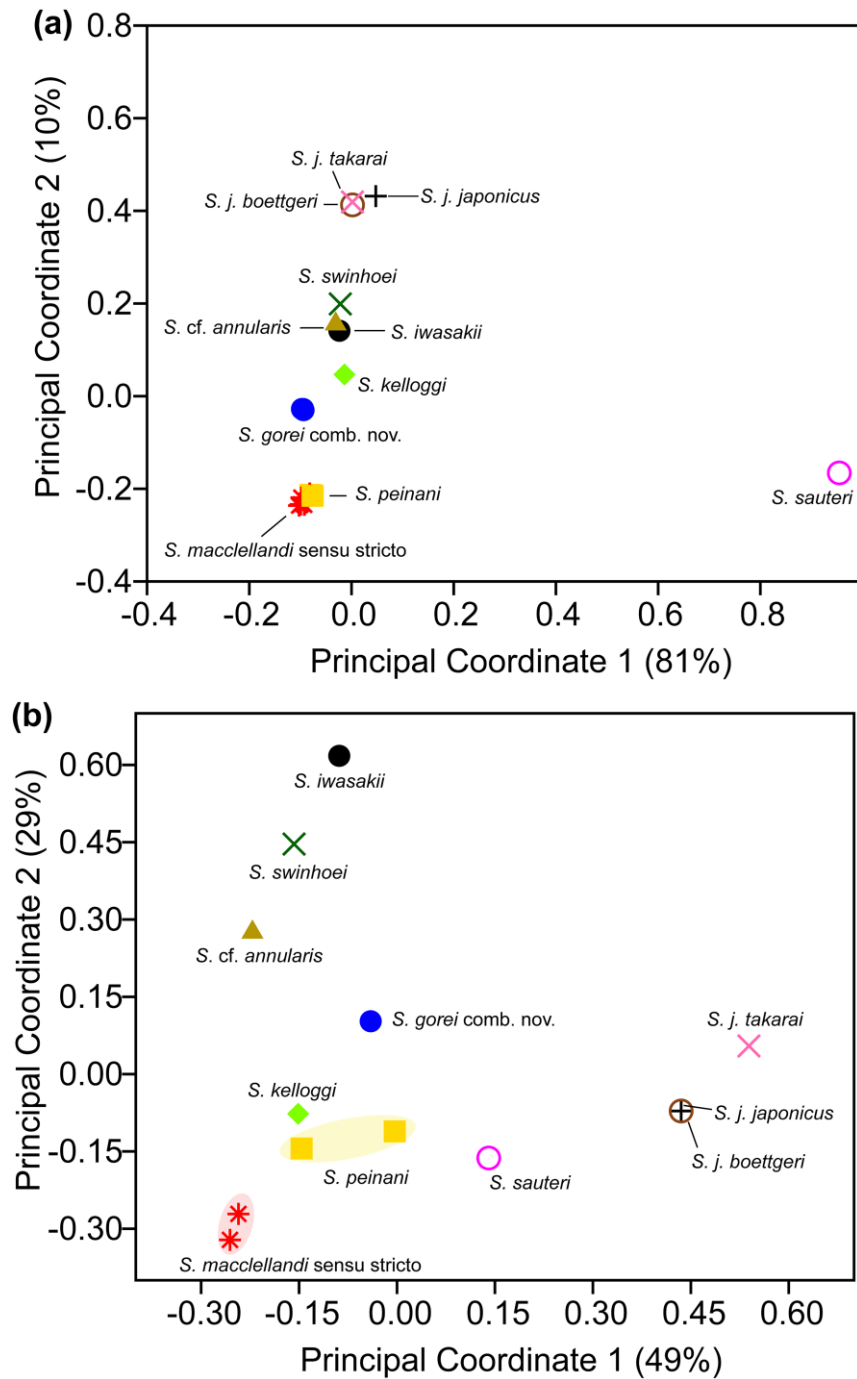


Figure 5.4. Ordination of standardized p-distance estimated from the concatenated mitochondrial 16S, COI, CYTB, ND4 (a) and nuclear NT3 (b) among *Sinomicrurus* species along the first and second principal coordinate (PCo) axes. The total variance captured by PCo1 and PCo2 are given at the x and y axes, respectively.

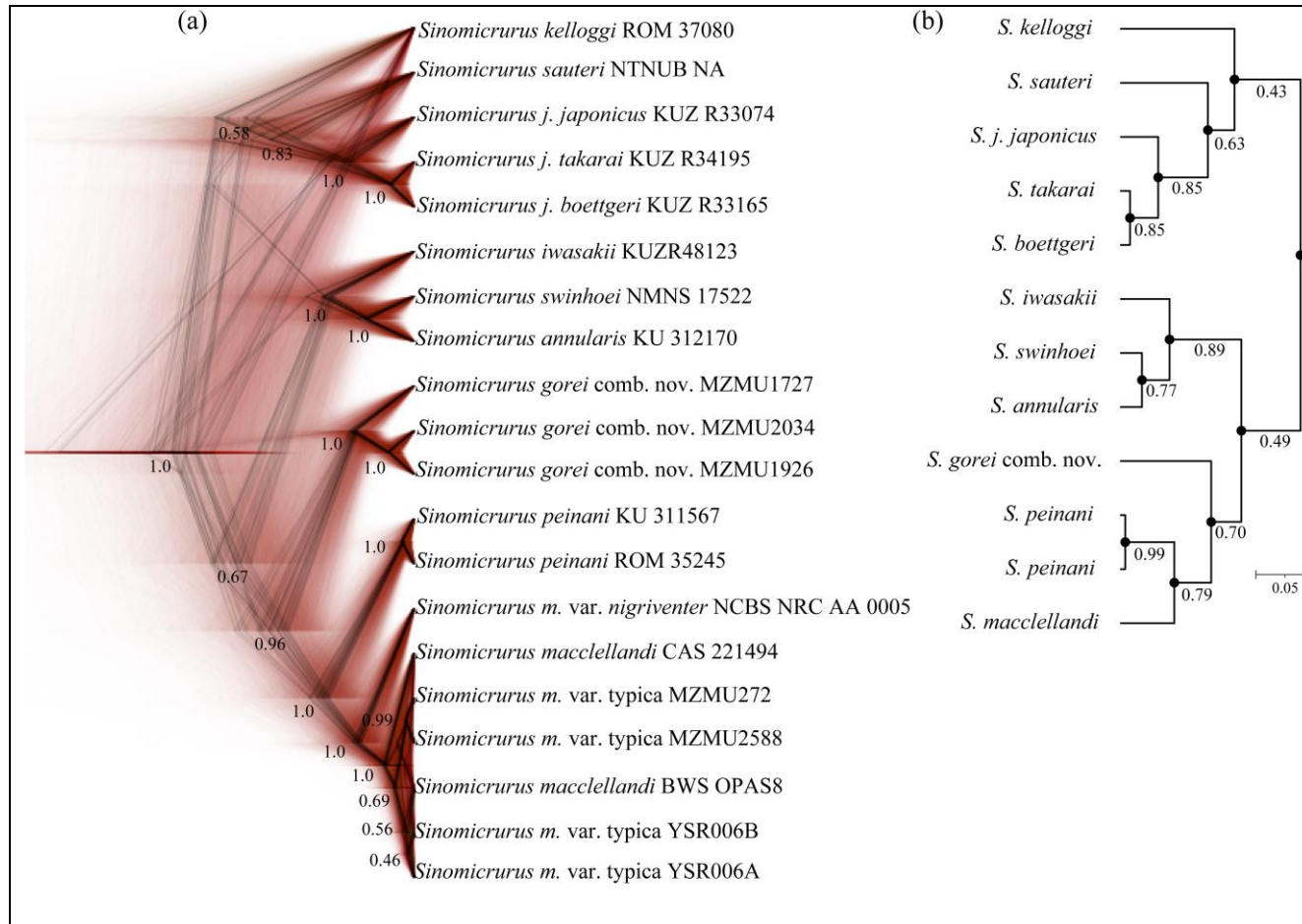


Figure 5.5. DensiTree showing different topologies in the sets of mitochondrial gene trees with posterior probability values at the nodes, and the sets of consensus trees are given in black colour (a), and the species tree of *Sinomicrurus* species summarized using maximum clade credibility (b).

Morphology

A total of 44 individuals of *S. macclellandi* were examined comprising 38 (36 var. *gorei* + 2 var. *typica*) specimens from the Mizoram population, four specimens from Arunachal Pradesh, and two specimens from Meghalaya, Northeast India (Table 5.3). In the analysis, only the adult specimens were included. In addition, the meristics values from published literature were extracted for the type specimens of *S. macclellandi* var. *gorei* from Assam (Wall 1909), the specimen (SGCZM012) from Bangladesh (Rahman et al. 2017); the holotype (ZMUC 65399) data of *S. macclellandi* var. *typica* from Assam (Reinhardt 1844; Smart et al. 2021), and a single specimen from Cambodia (CBC 02885) (Neang et al. 2017).

The test for sexually dimorphic characters using two-way ANOVA for meristics and two-way ANCOVA for mensurals revealed that V_e ($p < 0.01$), TaL ($p < 0.01$), $E-N$ ($p < 0.05$), and $S-E$ ($p < 0.05$) are significantly different between male and female in pooling the two varieties (Fig. 5.6; Table 5.4). Thence, excluding the sexually dimorphic characters, a test between the two groups using two-way ANOVA for meristics, and two-way ANCOVA for mensurals also revealed a statistically significant difference in the BB ($p < 0.001$), BS ($p < 0.001$), BT ($p < 0.001$), NBW ($p < 0.001$), ED ($p < 0.001$), IOS ($p < 0.001$), HL ($p < 0.05$), HW ($p < 0.001$), and HD ($p < 0.001$) (Table 5.4).

For PCA, the standardized values of BB , BS , BT , and NBW ; and the allometric adjusted ED , IOS , HL , HW , and HD were utilized. The first four Principal components ($PC1$, $PC2$, $PC3$ and $PC4$) collectively explained 91% of the variation in the morphometric data matrix ($PC1=63\%$; $PC2=19\%$; $PC3=6\%$; $PC4=4\%$). Ordination of the first two components depicts a clear non-overlapping clustering of *S. macclellandi* var. *typica* and *S. macclellandi* var. *gorei* on the first axis ($PC1$) (Fig. 7a). The loadings of all variables are considerably high on the first axis with only BS having negative loading on $PC1$, while the loading of only HL is considerably high on the second axis with BB , BT , NBW and ED having negative loadings on $PC2$ (Fig. 7b; Table 5.5).

Table 5.4. Morphometry (in mm) and scalation data of *Sinomicrurus* species examined from Mizoram, India. Damaged character that are not feasible to examine is shown in dash (-).

Museum number	MZMU 171	MZMU 242	MZMU 243	MZMU 247	MZMU 269	MZMU 270	MZMU 271	MZMU 272
Sex	Male	Female	Male	Male	Female	Male	Male	Male
SVL	391	416	435	398	639	437	406	595
TaL	41	37	47	44	49	38	38	89
TaL/TL	0.095	0.082	0.098	0.100	0.071	0.080	0.086	0.130
Body bands (cover 5 or more scales)	0	1	1	0	0	0	0	24
Body bands/spots (cover 1-4 scales)	-	-	29	23	0	0	25	-
Tail bands (reaching Sc)	1	4	0	0	0	0	2	4
Nuchal band width (in scales)	2	2	2	2	2	2	2	4
Ventrals	211	222	215	211	230	218	211	196
Subcaudals	33	26	31	30	26	30	28	36
DSR	-	-	13-13-13	13-13-13	13-13-13	13-13-13	13-13-13	-
SL	-	-	7/7	7/7	7/7	7/7	-	-
SL-e	-	-	3-4/3-4	3-4/3-4	3-4/3-4	3-4/3-4	-	-
IF	-	-	6/6	6/6	6/6	6/6	-	-
IF-AG	-	-	1-4/1-4	1-4/1-4	1-4/1-4	1-4/1-4	-	-
IF-PG	-	-	4 th /4 th	4 th /4 th	4 th /4 th	4 th /4 th	-	-
PrO	-	-	1/1	1/1	1/1	1/1	-	-
PoO	-	-	1/1	1/1	1/1	1/1	-	-
SpO	-	-	1/1	1/1	1/1	1/1	-	-
ATem	-	-	1/1	1/1	1/1	1/1	-	-
PTem	-	-	1/1	1/1	1/1	1/1	-	-
ED	-	-	0.8	0.8	1.2	0.8	-	-
E-N	-	-	1.7	1.7	3.0	1.4	-	-
E-SN	-	-	3.1	2.8	5.1	2.8	-	-
IOS	-	-	4.1	3.5	5.6	3.1	-	-
INS	-	-	3.3	2.9	4.6	2.4	-	-
HL	-	-	10.6	9.7	16.4	9.7	-	-
HW	-	-	6.2	5.2	9.4	4.6	-	-
HD	-	-	4.1	3.2	5.8	3.0	-	-
INW	-	-	1.5	1.3	2.0	1.2	-	-
PFL	-	-	2.0	1.9	3.1	1.9	-	-
FL	-	-	3.4	2.8	4.8	2.8	-	-
PL	-	-	4.4	3.9	6.0	3.6	-	-
R visible above	-	-	Y	Y	Y	Y	-	-
HBW at level of SpO	-	-	3.1	2.6	4.7	2.8	-	-

Table 5.4. Continued.

Museum number	MZMU 273	MZMU 284	MZMU 285	MZMU 831	MZMU 832	MZMU 840	MZMU 862	MZMU 894
Sex	Male	Male	Male	Male	Male	Female	Male	Male
SVL	376	375	335	351	326	390	342	372
TailL	39	38	34	38	31	35	28	34
TaL/TL	0.094	0.092	0.092	0.098	0.087	0.082	0.076	0.084
Body bands (cover 5 or more scales)	0	0	1	1	0	0	0	0
Body bands/spots (cover 1-4 scales)	22	21	30	22	22	28	27	23
Tail bands (reaching Sc)	0	0	0	0	1	0	2	0
Nuchal band width (in scales)	2	2	2	2	2	2	3	2
Ventrals	214	220	214	215	208	226	215	226
Subcaudals	30	30	28	29	27	26	30	26
DSR	13-13-13	13-13-13	13-13-13	13-13-13	13-13-13	13-13-13	13-13-13	13-13-13
SL	7/7	7/7	7/7	7/7	7/7	7/7	7/7	7/7
SL-e	3-4/3-4	3-4/3-4	3-4/3-4	3-4/3-4	3-4/3-4	3-4/3-4	3-4/3-4	3-4/3-4
IF	6/6	6/6	6/6	6/6	6/6	6/6	6/6	6/6
IF-AG	1-4/1-4	1-4/1-4	1-4/1-4	1-4/1-4	1-3/1-3	1-4/1-4	1-4/1-4	1-4/1-4
IF-PG	4 th /4 th	4 th /4 th	4 th /4 th	4 th /4 th	4 th /4 th	4 th /4 th	4 th /4 th	4 th /4 th
PrO	1/1	1/1	1/1	1/1	1/1	1/1	1/1	1/1
PoO	1/1	1/1	1/1	1/1	1/1	1/1	1/1	1/1
SpO	1/1	1/1	1/1	1/1	1/1	1/1	1/1	1/1
ATem	1/1	1/1	1/1	1/1	1/1	1/1	1/1	1/1
PTem	1/1	1/1	1/1	2/1	1/1	1/1	1/1	1/1
ED	0.8	0.9	0.7	0.9	0.8	0.8	0.8	0.9
E-N	1.9	1.8	1.7	1.9	1.6	1.7	1.5	1.5
E-SN	3.0	3.1	2.6	2.8	2.7	3.1	2.4	2.6
IOS	3.5	3.3	3.5	3.7	3.3	3.6	2.8	3.3
INS	2.9	3.1	2.5	3.0	2.3	2.8	1.9	2.5
HL	9.7	9.9	8.9	9.6	9.1	9.6	8.5	9.9
HW	5.1	5.6	5.0	5.3	5.0	5.2	4.2	4.9
HD	3.3	3.5	2.7	3.4	2.9	3.4	2.7	3.1
INW	1.3	1.6	1.4	1.4	1.1	1.4	1.2	1.1
PFL	1.9	2.0	1.9	2.1	1.9	2.1	1.8	1.8
FL	3.1	2.6	2.8	2.8	2.5	3.3	2.2	2.6
PL	4.1	3.6	3.6	3.5	3.8	4.3	3.0	3.6
R visible above	Y	Y	Y	Y	Y	Y	Y	Y
HBW at level of SpO	2.3	3.8	2.1	3.5	2.6	3.0	1.9	2.2

Table 5.4. Continued.

Museum number	MZMU 945	MZMU 974	MZMU 977	MZMU 1074	MZMU 1157	MZMU 1214	MZMU 1318	MZMU 1438
Sex	Female	Female	Female	Male	Female	Female	Female	Male
SVL	468	420	401	446	359	435	382	348
TailL	36	36	34	35	28	34	33	36
TaL/TL	0.071	0.079	0.078	0.073	0.072	0.072	0.080	0.094
Body bands (cover 5 or more scales)	0	0	2	0	0	0	0	0
Body bands/spots (cover 1-4 scales)	30	23	29	32	28	32	15	27
Tail bands (reaching Sc)	0	0	0	0	0	4	0	0
Nuchal band width (in scales)	2	2	2	2	2	2	2	2
Ventrals	238	222	231	232	222	236	219	217
Subcaudals	25	29	27	24	24	27	28	30
DSR	13-13-13	13-13-13	13-13-13	13-13-13	13-13-13	13-13-13	13-13-13	13-13-13
SL	7/7	7/7	7/7	-	7/7	7/7	7/7	7/7
SL-e	3-4/3-4	3-4/3-4	3-4/3-4	-	3-4/3-4	3-4/3-4	3-4/3-4	3-4/3-4
IF	6/6	6/6	6/6	-	6/6	6/6	6/6	6/6
IF-AG	1-4/1-4	1-4/1-4	1-4/1-4	-	1-4/1-4	1-4/1-4	1-4/1-4	1-4/1-4
IF-PG	4 th /4 th	4 th /4 th	4 th /4 th	-	4 th /4 th	4 th /4 th	4 th /4 th	4 th /4 th
PrO	1/1	1/1	1/1	1/1	1/1	1/1	1/1	1/1
PoO	1/1	1/1	2/2	-	2/2	2/2	2/2	2/2
SpO	1/1	1/1	1/1	-	1/1	1/1	1/1	1/1
ATem	1/1	1/1	1/1	1/1	1/1	1/1	1/1	1/1
PTem	1/1	1/1	-/1	-	1/1	1/1	1/1	1/1
ED	0.8	0.7	0.7	0.8	0.7	0.8	1.0	0.6
E-N	2.0	2.0	1.8	2.0	1.9	2.1	2.0	1.5
E-SN	3.2	3.2	3.0	2.9	3.2	3.1	3.2	2.9
IOS	3.5	2.5	3.3	-	3.4	2.9	3.8	3.2
INS	2.6	1.9	2.5	2.5	2.6	2.2	3.2	2.9
HL	10.0	9.3	9.2	10.0	10.0	9.6	10.2	9.8
HW	4.9	4.2	4.9	5.2	4.4	5.0	5.5	4.7
HD	3.1	2.6	2.7	3.0	3.2	2.8	3.2	2.9
INW	1.4	1.2	-	-	1.5	1.1	1.8	1.5
PFL	1.8	1.7	-	-	2.0	1.6	2.0	1.8
FL	3.2	2.8	-	-	2.7	2.8	2.9	2.4
PL	3.9	3.2	-	-	3.9	3.3	4.0	3.0
R visible above	Y	Y	Y	Y	Y	Y	Y	Y
HBW at level of SpO	2.6	3.0	2.4	-	2.7	2.5	3.3	2.8

Table 5.4. Continued.

Museum number	MZMU 1444	MZMU 1569	MZMU 1911	MZMU 1913	MZMU 1926	MZMU 2034	MZMU 2035	MZMU 2341
Sex	Femal e	Femal e	Male	Male	Femal e	Fema le	Femal e	Male
SVL	507	473	374	420	674	432	365	388
TailL	44	43	42	41	56	36	34	42
TaL/TL	0.080	0.083	0.10	0.089	0.077	0.077	0.085	0.098
Body bands (cover 5 or more scales)	-	0	2	0	0	2	0	0
Body bands/spots (cover 1-4 scales)	-	35	27	21	27	34	43	32
Tail bands (reaching Sc)	-	1	2	2	0	0	0	0
Nuchal band width (in scales)	2	3	3	2	2	2	2	1
Ventrals	227	230	210	213	232	233	232	220
Subcaudals	27	25	29	31	26	26	28	29
DSR	13-13-13	13-13-13	13-13-13	13-13-13	13-13-13	13-13-13	13-13-13	13-13-13
SL	7/7	7/7	7/7	7/7	7/7	7/7	7/7	7/7
SL-e	3-4/3-4	3-4/3-4	3-4/3-4	3-4/3-4	3-4/3-4	3-4/3-4	3-4/3-4	3-4/3-4
IF	6/6	6/6	6/6	6/6	6/6	6/6	6/6	6/6
IF-AG	1-4/1-4	1-4/1-4	1-4/1-4	1-4/1-4	1-4/1-4	1-4/1-4	1-4/1-4	1-4/1-4
IF-PG	4 th /4 th	4 th /4 th	4 th /4 th	4 th /4 th	4 th /4 th	4 th /4 th	4 th /4 th	4 th /4 th
PrO	1/1	1/1	1/1	1/1	1/1	1/1	1/1	1/1
PoO	2/2	2/2	2/2	2/2	2/2	2/2	2/2	2/2
SpO	1/1	1/1	1/1	1/1	1/1	1/1	1/1	1/1
ATem	1/1	1/1	1/1	1/1	1/1	1/1	1/1	1/1
PTem	1/1	1/1	1/1	1/1	1/1	1/1	1/1	1/1
ED	-	1.0	0.8	0.8	1.2	0.9	0.8	0.8
E-N	-	2.3	2.1	1.4	2.8	2.2	1.9	1.8
E-SN	-	3.7	3.2	3.5	5.8	3.8	3.1	2.9
IOS	-	4.4	3.6	3.1	5.6	4.3	3.4	3.4
INS	-	3.1	3.0	2.4	4.6	3.4	2.9	3.0
HL	-	12.9	9.8	9.8	16.9	10.6	9.7	8.9
HW	-	7.6	4.8	4.3	10.0	6.7	5.0	5.1
HD	-	3.9	3.0	3.0	5.4	4.1	3.0	3.5
INW	-	1.6	1.4	1.4	2.6	1.4	1.2	1.5
PFL	-	2.2	2.0	1.8	2.9	1.9	1.8	2.0
FL	-	3.6	3.2	2.6	4.1	3.0	3.1	2.9
PL	-	4.8	3.8	3.8	6.3	4.8	4.1	3.5
R visible above	-	Y	Y	Y	Y	Y	Y	Y
HBW at level of SpO	-	2.4	2.4	1.9	3.8	2.7	2.6	2.8

Table 5.4. Continued.

Museum number	MZMU 2438	MZMU 2587	MZMU 2588	MZMU 1727	MZMU 2589	MZMU 2590	MZMU N5 1.15 g on 20.10.21	MZMU N6 1.66 g on 20.10.21
Sex	Fema le	Femal e	Female	Femal e	Fema le	Fema le	Male	Female
SVL	345	432	700	380	370	449	161	175
TailL	34	40	77	28	33	41	14	13
TaL/TL	0.090	0.085	0.100	-	0.082	0.084	0.080	0.070
Body bands (cover 5 or more scales)	0	2	28	-	0	0	0	0
Body bands/spots (cover 1-4 scales)	33	23	0	-	29	45	-	-
Tail bands (reaching Sc)	0	3	3	-	1	1	0	0
Nuchal band width (in scales)	2	2	3	2	2	2	2	1
Ventrals	223	235	208	238	236	231	214	238
Subcaudals	30	28	30	26	27	28	29	26
DSR	13-13-13	13-13-13	13-13-13	13-13-13	13-13-13	13-13-13	13-13-13	13-13-13
SL	6/7	7/7	7/7	7/7	7/8	7/7	7/7	7/7
SL-e	2-3/3-4	3-4/3-4	3-4/3-4	3-4/3-4	3-4/4-5	3-4/4-5	3-4/3-4	3-4/3-4
IF	6/6	6/6	6/6	6/6	6/6	6/6	6/6	6/6
IF-AG	1-4/1-4	1-4/1-4	1-3/1-3	1-4/1-4	1-4/1-4	1-4/1-4	1-4/1-4	1-3/1-3
IF-PG	4 th /4 th	4 th /4 th	4 th /4 th	4 th /4 th	4 th /4 th	4 th /4 th	4 th /4 th	4 th /4 th
PrO	1/1	1/1	1/1	1/1	1/1	1/1	1/1	1/1
PoO	2/2	2/2	2/2	2/2	2/2	2/2	2/2	2/2
SpO	1/1	1/1	1/1	1/1	1/1	1/1	1/1	1/1
ATem	1/1	1/1	1/1	1/1	1/1	1/1	1/1	1/1
PTem	1/1	1/1	1/1	1/1	1/1	1/1	1/1	1/1
ED	0.9	1.0	1.7	1.0	0.7	0.9	-	-
E-N	1.6	2.4	2.8	2.6	1.5	2.0	-	-
E-SN	2.8	3.2	5.0	3.7	2.8	3.3	-	-
IOS	3.1	3.6	6.4	-	3.1	3.4	-	-
INS	2.4	2.9	4.7	-	2.0	2.8	-	-
HL	9.9	10.9	17.9	-	8.4	10.8	-	-
HW	4.4	5.6	11.4	-	4.5	5.0	-	-
HD	2.8	3.4	6.2	-	2.7	3.3	-	-
INW	1.4	1.6	2.6	-	1.1	1.4	-	-
PFL	2.0	2.1	3.6	-	1.6	1.8	-	-
FL	2.6	3.0	5.2	-	2.5	3.3	-	-
PL	3.7	3.9	7.1	-	3.5	4.3	-	-
R visible above	Y	Y	Y	Y	Y	Y	Y	Y
HBW at level of SpO	2.5	2.9	6.9	3.9	3.6	2.6	1.9	2.0

Table 5.4. Continued.

Museum number	CBC0 2885	SGCZ M012	ZMUC 65399 Holotype	YSR 006	Gorei type	APRC/ R/91/A	APRC/ R/91/B
Sex	Male	Female	-	Male	Female	Female	Male
SVL	448.3	355	635	415	558.8	400	450
TailL	46.9	32	50.8	45	38.1	41	44
TaL/TL	0.095	0.083	0.074	0.098	0.064	-	-
Body bands (cover 5 or more scales)	29	-	-	-	-	27	18
Body bands/spots (cover 1-4 scales)	-	-	-	-	-	0	0
Tail bands (reaching Sc)	4	-	-	-	-	3	3
Nuchal band width (in scales)	-	-	-	-	-	3	3
Ventrals	201	242	216	195	241	213	193
Subcaudals	30	25	27	31	46	25	30
DSR	13-13-13	13-13-13	13 mid	-	-	13-13-13	13-13-13
SL	7	7	7/7	-	-	7/7	7/7
SL-e	-	3-4	3-4	-	-	3-4/3-4	3-4/3-4
IF	-	6	6/6	-	-	6/6	6/6
IF-AG	-	-	-	-	-	1-3/1-3	1-3/1-3
IF-PG	-	-	-	-	-	4 th /4 th	4 th /4 th
PrO	1	1	1	-	-	1/1	1/1
PoO	2	2	2	-	-	2/2	2/2
SpO	-	-	-	-	-	1/1	1/1
ATem	1	1	1	-	-	1/1	1/1
PTem	1	1	1	-	-	1/2	1/1
ED	-	-	-	-	-	1.06	1.12
E-N	-	-	-	-	-	1.56	1.90
E-SN	-	-	-	-	-	3.34	3.12
IOS	-	-	-	-	-	4.12	4.14
INS	-	-	-	-	-	2.80	3.0
HL	11.9	-	-	-	-	10.12	11.20
HW	-	-	-	-	-	6.52	7.0
HD	-	-	-	-	-	3.90	4.08
INW	-	-	-	-	-	1.30	1.1
PFL	-	-	-	-	-	1.90	1.80
FL	-	-	-	-	-	2.66	3.18
PL	-	-	-	-	-	3.52	4.40
R visible above	-	-	-	-	-	Y	Y
HBW at level of SpO	-	-	-	-	-	2.7	4.56

Table 5.5. Descriptive statistics for sexual dimorphism and difference between *Sinomicrurus maccllellandi* var. *typica* and *S. gorei* comb. nov. based on the examined specimens from the populations of Mizoram, Meghalaya, Arunachal Pradesh, and other published meristic data from Assam, Bangladesh, and Cambodia. Meristics data are analyzed using two-way ANOVA using sex and variety as the factors, or Brown-Forsythe test (indicated in octothorp '#') for meristics; while two-way ANCOVA using sex and variety as the factors with SVL as covariate was used for the mensurals. Statistical significance at the level of alpha 0.05 is indicated by bold. Measurements are given in millimetre.

Characters	Sex	<i>Sinomicrurus gorei</i> comb. nov. (n=38)		<i>Sinomicrurus maccllellandi</i> var. <i>typica</i> (n=10)		Sexual dimorphism		Difference between varieties	
		Mean±SD	Range	Mean±SD	Range				
Ve	Male	216.47±5.97	208.00–232.00	203.83±16.14	193.00–236.00	$F_{1,44} = 11.970$	$p < \mathbf{0.01}$	$F_{1,44} = 33.188$	$p < \mathbf{0.001}$
	Female	230.76±6.65	219.00–242.00	209.75±6.13	202.00–216.00				
Sc	Male	29.12±2.09	24.00–33.00	31.83±3.37	28.00–36.00	$F_{1,46} = 23.561$	$p < \mathbf{0.001}$	$F_{1,46} = 7.055$	$p < \mathbf{0.05}$
	Female	26.62±1.50	24.00–30.00	27.50±2.08	25.00–30.00				
BS	Male	23.94±7.42	0.00–32.00	0	0	$F_{1,38} = 0.559$	$p = 0.459$	$F_{1,38} = 77.641$	$p < \mathbf{0.001}$
	Female	28.38±10.48	0.00–45.00	0	0				
BB	Male	0.29±0.59	0.00–2.00	22.33±3.93	18–29	$F_{1,42} = 0.045$	$p = 0.832$	$F_{1,9,184} = 401.762$	$p < \mathbf{0.001}\#$
	Female	0.41±0.80	0.00–2.00	26.50±1.29	25–28				
BT	Male	0.59±0.87	0.00–2.00	3.50±0.55	3–4	$F_{1,42} = 0.056$	$p = 0.814$	$F_{1,36,861} = 105.988$	$p < \mathbf{0.001}\#$
	Female	0.82±1.42	0–4.00	3.00±0.00	3				
NBW	Male	2.06±0.43	1.00–3.00	3.40±0.55	3.00–4.00	$F_{1,43} = 0.172$	$p = 0.681$	$F_{1,9,962} = 60.632$	$p < \mathbf{0.001}\#$
	Female	2.05±0.23	2.00–3.00	3.38±0.48	3.00–4.00				
TaL	Male	38.00±4.76	28.00–47.00	52.36±18.01	43.00–89.00	$F_{1,43} = 7.964$	$p < \mathbf{0.01}$	$F_{1,43} = 9.318$	$p < \mathbf{0.01}$
	Female	37.20±6.62	28.00–56.00	48.75±21.38	26.20–77.00				

Table 5.5. Continued.

Characters	Sex	<i>Sinomicrurus gorei</i> comb. nov. (n=38)		<i>Sinomicrurus macclellandi</i> var. <i>typica</i> (n=10)		Sexual dimorphism		Difference between varieties	
		Mean±SD	Range	Mean±SD	Range				
ED	Male	0.80±0.08	0.60–0.90	1.24±0.12	1.12–1.40	$F_{1,35} = 0.081$	$p = 0.777$	$F_{1,35} = 46.817$	$p < \mathbf{0.001}$
	Female	0.89±0.16	0.70–1.20	1.18±0.47	0.79–1.70				
E-N	Male	1.70±0.22	1.40–2.10	2.00±0.38	1.50–2.30	$F_{1,34} = 6.315$	$p < \mathbf{0.05}$	$F_{1,34} = 1.107$	$p = 0.300$
	Female	2.11±0.41	1.50–3.00	2.32±0.66	1.56–2.80				
S-E	Male	2.89±0.27	2.40–3.50	3.48±1.03	2.20–4.49	$F_{1,34} = 6.123$	$p < \mathbf{0.05}$	$F_{1,34} = 1.751$	$p = 0.195$
	Female	3.49±0.80	2.80–5.80	3.99±0.89	3.34–5.00				
IOS	Male	3.39±0.31	2.80–4.10	4.79±1.07	3.80–6.18	$F_{1,33} = 1.196$	$p = 0.282$	$F_{1,33} = 23.417$	$p < \mathbf{0.001}$
	Female	3.72±0.87	2.50–5.60	5.23±1.14	4.12–6.40				
INS	Male	2.71±0.38	1.90–3.30	3.17±0.22	3.00–3.42	$F_{1,32} = 1.047$	$p = 0.314$	$F_{1,32} = 1.160$	$p = 0.289$
	Female	2.91±0.78	1.90–4.60	3.47±1.06	2.80–4.70				
HL	Male	9.59±0.53	8.50–10.60	11.45±1.80	9.30–13.48	$F_{1,35} = 3.926$	$p = 0.055$	$F_{1,35} = 4.215$	$p < \mathbf{0.05}$
	Female	10.90±2.45	8.40–16.90	12.63±4.56	9.88–17.90				
HW	Male	5.01±0.49	4.20–6.20	6.78±1.42	4.50–8.40	$F_{1,34} = 4.075$	$p = 0.051$	$F_{1,34} = 15.015$	$p < \mathbf{0.001}$
	Female	5.77±1.77	4.20–10.00	7.85±3.11	5.62–11.40				
HD	Male	3.15±0.36	2.70–4.10	4.56±0.68	3.90–5.60	$F_{1,34} = 0.011$	$p = 0.916$	$F_{1,34} = 25.890$	$p < \mathbf{0.001}$
	Female	3.46±0.94	2.60–5.80	4.50±1.49	3.41–6.20				
INW	Male	1.35±0.16	1.10–1.60	1.41±0.36	1.10–1.90	$F_{1,31} = 3.883$	$p = 0.058$	$F_{1,31} = 0.022$	$p = 0.882$
	Female	1.51±0.39	1.10–2.60	1.73±0.75	1.30–2.60				

Table 5.5. Continued.

Characters	Sex	<i>Sinomicrurus gorei</i> comb. nov. (n=38)		<i>Sinomicrurus maclellandi</i> var. <i>typica</i> (n=10)		Sexual dimorphism		Difference between varieties	
		Mean±SD	Range	Mean±SD	Range				
PFW	Male	1.91±0.09	1.80–2.10	2.16±0.45	1.80–2.80	$F_{1,31} = 2.671$	$p = 0.112$	$F_{1,31} = 3.005$	$p = 0.093$
	Female	2.04±0.43	1.60–3.10	2.50±0.95	1.90–3.60				
FL	Male	2.76±0.32	2.20–3.40	3.25±0.82	2.50–4.40	$F_{1,31} = 2.696$	$p = 0.111$	$F_{1,31} = 0.724$	$p = 0.401$
	Female	3.18±0.61	2.50–4.80	3.52±1.45	2.66–5.20				
PL	Male	3.66±0.37	3.00–4.40	4.51±0.99	3.30–5.70	$F_{1,31} = 0.401$	$p = 0.531$	$F_{1,31} = 0.994$	$p = 0.327$
	Female	4.27±0.89	3.20–6.30	4.64±2.14	3.29–7.10				
WBH	Male	2.63±0.56	1.90–3.80	3.08±0.91	2.60–4.56	$F_{1,34} = 2.835$	$p = 0.101$	$F_{1,34} = 1.434$	$p = 0.239$
	Female	3.01±0.65	2.40–4.70	3.91±2.61	2.13–6.90				

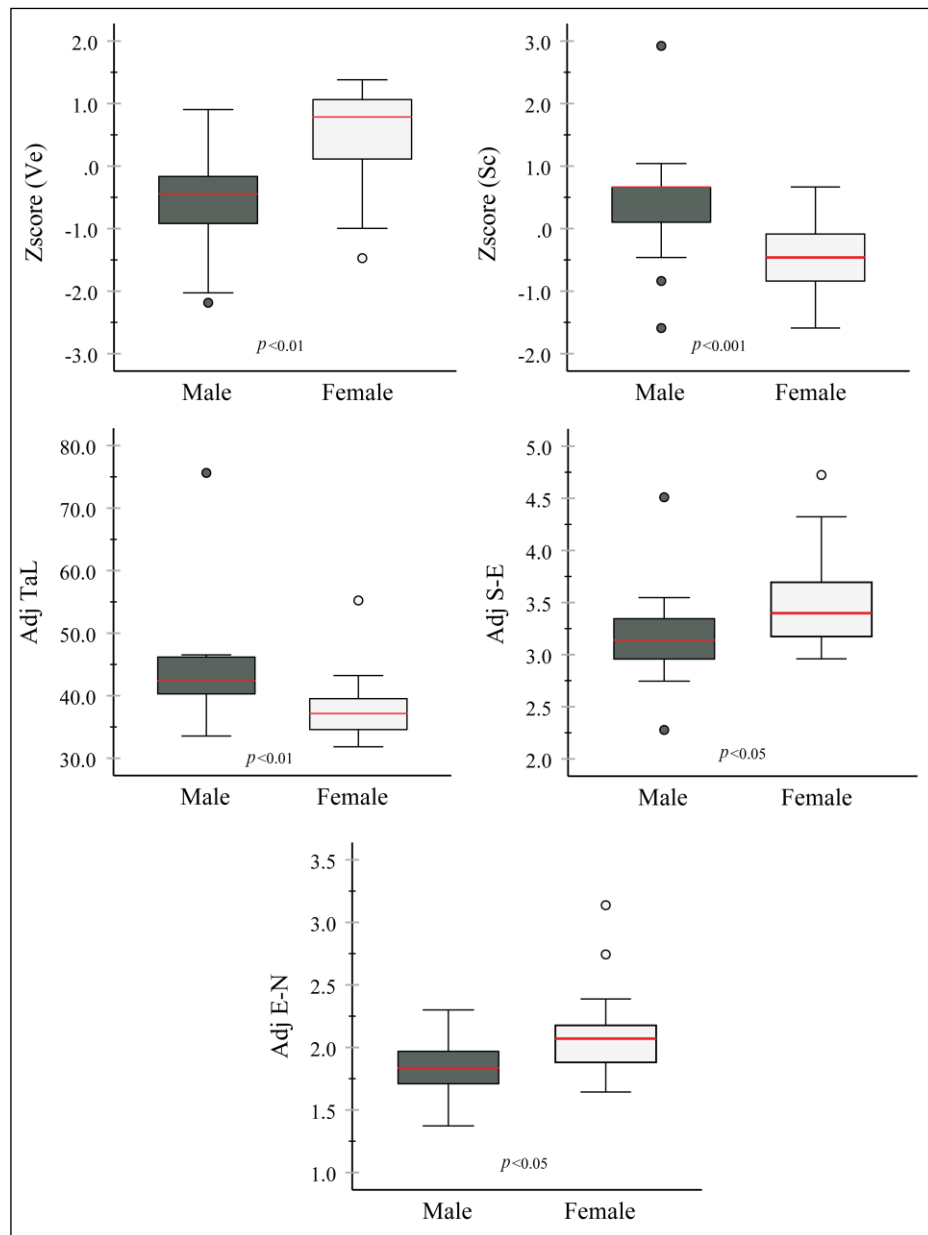


Figure 5.6. Box plot showing median, interquartile range, range (minimum to maximum), and outliers for the statistically significant sexually dimorphic characters among the adult specimens of *Sinomicrurus macclellandi* (in pooling the two varieties) population from Northeast India. The depicted characters are the standardised (Z score) ventrals (Ve) and subcaudals (Sc), and the allometric adjusted (Adj) tail length (TaL) and snout to eye distance (S-E). Significant level (p values) at the alpha level of 0.05 are given at each plot.

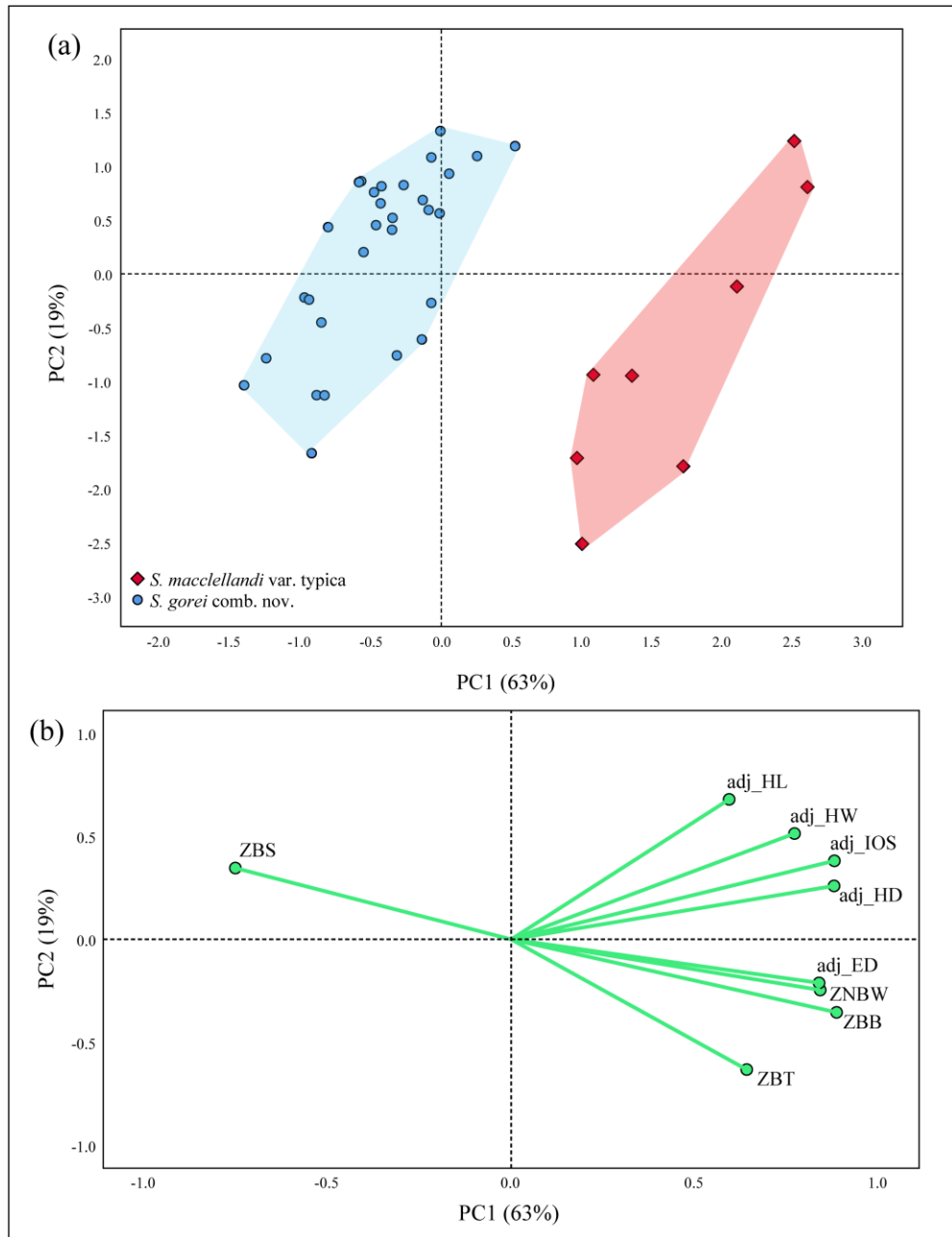


Figure 5.7. (a) PCA score plot of *Sinomicrurus macclellandi* populations from Northeast India along the first two principal components based on a PCA of the standardised meristics such as nuchal band width (NBW), black bands on body (BB), black spots on body (BS), and black bands on tail (BT); and allometric adjusted mensurals such as head length (HL) head width (HW), head depth (HD), interorbital space (IOS), and horizontal eye diameter (ED). Total variance associated with the

PC1 and PC2 are 63% and 19%, respectively; (b) PCA loading plot showing the distribution of the analysed variables along the first two principal components.

Table 5.6. Principal Component (PCA) loadings for *Sinomicrurus maccllellandi* var. *typica* and *Sinomicrurus* var. *gorei* based on the standardized meristics and adjusted mensurals of the examined specimens from the populations of Mizoram, Meghalaya, Arunachal Pradesh, and other published meristic data from Assam, Bangladesh, and Cambodia. Principal components (PC) 1 and 2 collectively explained 82% of variations.

Variables	PC1 (63%)	PC2 (19%)	PC3 (6%)	PC4 (4%)
Zscore(BS)	-0.751	0.346	0.411	0.300
Zscore(BB)	0.886	-0.354	-0.032	-0.021
Zscore(BT)	0.642	-0.632	0.325	0.128
Zscore(NBW)	0.842	-0.246	0.348	-0.213
adj_ED	0.839	-0.211	-0.172	0.411
adj_IOS	0.880	0.381	0.075	-0.113
adj_HL	0.594	0.680	0.199	0.008
adj_HW	0.772	0.514	-0.009	0.051
adj_HD	0.879	0.259	-0.224	0.060

Taxonomy

The evidence derived through morphological analyses, bPTP species delimitation, genetic distance, and phylogenetic analyses strongly suggested that the Northeast Indian specimens examined in this work so far represent two distinct taxonomic entities. Although our genetic analyses suggest *S. nigriventer* (Mirza et al. 2020) as a putative species distinct from *S. maccllellandi*, this study does not primarily focus on the taxonomic status of the species. In consideration of the synonymy of *S. nigriventer* (Mirza et al., 2020) into *S. maccllellandi* fide Smart et al. (2021) as a conservative approach, for the time being, thereby the sub-clade containing the samples of *S. nigriventer* (Mirza et al. 2020) from Himachal Pradesh as well as *S. maccllellandi* var. *typica* from Meghalaya (Fig. 5.7a), Mizoram (Fig. 5.7b), Bhutan, Myanmar and unknown locality were regarded as *S. maccllellandi* sensu stricto fide Smart et al. (2021). On the other hand, the specimens of *S.*

macclellandi var. *typica* and *S. macclellandi* var. *gorei* with the inclusion of an unpatterned morph revealed a statistically significant difference in the univariate analyses as well as a distinct cluster in the PCA. Moreover, the present genetic analyses also corroborated the distinction of the *S. macclellandi* var. *gorei* (Fig. 8c, d) with well supported phylogenetic evidence. The rationale conceived in this work propounded to raise the taxonomical status of *S. macclellandi* var. *gorei* fide Wall (1910) to a full species level, and the species is redescribed herein as:

***Sinomicrurus gorei* Wall, 1908 comb. nov. (Figs. 5.1; 5.7c, d; 5.8a–c; 5.9a–f; 5.10a–c; 5.11a)**

Callophis macclellandi gorei Wall, 1908b: 37 (variety *gorei* mentioned for the first time fide Smart et al., 2021).

Callophis macclellandi gorei Wall, 1910 (formal description in 1909 Part IV published in 1910): 842.

Callophis macclellandi var. *gorei* Wall, 1913: 35; Wall, 1928: 32; Smith, 1943: 424; Sharma, 2003: 195 (in part).

Callophis macclellandi gori Wall, 1918: 629, 631 (in part).

Callophis macclellandi var. *gorei* Wall, 1913b: 639.

Calliophis macclellandi gorei Wall, 1925a: 821; Wall, 1925b: 244; Mahendra, 1984: 327 (populations from Assam, Naga Hills and Manipur).

Calliophis macclellandii gori Bourret, 1936 (Vol. II): 406–409 (in part, Assam).

Sinomicrurus macclellandi macclellandi Lalremsanga & Zothansiam, 2015: 212–221 (in part, population from Mizoram).

Sinomicrurus macclellandii Lalremsanga & Lalronunga, 2017: 119 (in part, population from Mizoram).

Sinomicrurus macclellandi Rahman et al., 2017: 241 (population from Sylhet Division, Bangladesh)

Sinomicrurus macclellandi var. *gorei* Smart et al., 2021: 1–66 (populations for Assam, Manipur and Mizoram).



Figure 5.8. (a) Live specimens of *Sinomicrurus macclellandi* var. *typica* (YSR006) from the type locality in Shillong, Northeast India, (Photo credit: Jayaditya Purkayastha); (b) *S. macclellandi* var. *typica* (MZMU2588) from Mizoram, Northeast India in life (Photo credit: H.T. Lalremsanga); (c) *S. gorei* comb. nov. (MZMU2589) from Mizoram, Northeast India (Photo credit: Vivek Sharma); (d) Unvouchered live specimen of *S. gorei* comb. nov. flattens its posterior body dorsoventrally and elevating the coiled tail, and inset showing its flatten body and tail display in different view from Mizoram, Northeast India.

Comparative material examined. *Sinomicrurus gorei* comb. nov.— 1 syntype from Jaipur, Assam, India (=Jaypor, Dibrugarh District, Assam) (BNHS 2211) collected/catalogued 1908, collector unknown; 36 specimens from Mizoram, India (MZMU171, 242, 243, 247, 269, 270, 271, 273, 284, 285, 831, 832, 840, 862, 894, 945, 947, 977, 1074, 1157, 1214, 1318, 1438, 1444, 1569, 1727, 1911, 1913, 1926, 2034, 2035, 2341, 2438, 2587, 2589, 2590). *Sinomicrurus macclellandi* var. *typica*— the holotype of *Calliophis macclellandi macclellandi* from Assam (now Meghalaya), India (ZMUC R65399); 2 topotypes from Shillong, Meghalaya, India (YSR006 and YSR116); 2 specimens from Assam, India (ZMUC R65401–R65402); 2 specimens from Mizoram, India (MZMU272 and MZMU2588); 2 specimens from Arunachal Pradesh, India (APRC/R/91/A; APRC/R/91/B; APRC/R/121 and APRC/R/126). *Sinomicrurus macclellandi* var. *nigriventer*— the holotype of *Sinomicrurus nigriventer* and 1 specimen from Kasauli, Punjab, India (NHMUK 1948.1.7.7 and NHMUK 1946.1.17.82); 1 specimen from Solan District, Himachal Pradesh, India (NCBS NRC-AA-0005). *Sinomicrurus macclellandi* var. *univirgatus*— 1 specimen from Darjeeling, India (ZMUC R65400). *Sinomicrurus annularis*— the holotype from China (NHMUK 1948.1.18.3); 2 specimens from India (NHMUK 1940.3.4.42 and NHMUK 67.7.22.2) (also see Table S6).

Etymology. The epithet of the specific name was originally derived after Mr. Gore from Jaipur, from whom Frank Wall received the three specimens of this species.

Suggested English Name. Gore's coral snake.

Diagnosis. Based on 38 adult specimens comprised by 36 individuals examined from Mizoram, India (17 males+19 females), and the other meristic data from Assam (syntype) and Bangladesh specimens extracted from literature (Wall, 1910; Rahman et al., 2017; Smart et al., 2021), the species is diagnosable from the other *Sinomicrurus* species based on the following morphological characters: (1) Ve 208–232 (\bar{x} 216.47±5.97) in males, 219–242 (\bar{x} 230.76±6.65) in females; (2) BS 0–32 (\bar{x} 23.94±7.42) in males, 0–45 (\bar{x} 28.38±10.48) in females; (3) BB 0–2 (0.29±0.59) in males, 0–2 (\bar{x} 0.41±0.80) in females; (4) BT 0–2 (\bar{x} 0.59±0.87) in males, 0–4 (\bar{x} 0.82±1.42) in females; (5) NBW 1–3 scales (\bar{x} 2.06±0.43) in males, 2–3 scales (\bar{x}

2.05±0.23) in females; (6) TaL 28–47 mm (\bar{x} 38.00±4.76 mm) in males; 28–56 mm (\bar{x} 37.20±6.62 mm) in females; (7) ED 0.6–0.9 mm (\bar{x} 0.80±0.08 mm) in males, 0.7–1.2 mm (\bar{x} 0.89±0.16 mm) in females; (8) IOS 2.8–4.1 mm (\bar{x} 3.39±0.31 mm) in males, 2.5–5.6 mm (\bar{x} 3.72±0.87 mm) in females; (9) HL 8.50–10.60 mm (\bar{x} 9.59±0.53) in males, 8.40–16.90 mm (\bar{x} 10.90±2.45) in females; (10) HW 4.2–6.2 mm (\bar{x} 5.01±0.49 mm) in males, 4.2–10.0 mm (\bar{x} 5.77±1.77 mm) in females; (11) HD 2.7–4.1 mm (\bar{x} 3.15±0.36 mm) in males, 2.6–5.8 mm (\bar{x} 3.46±0.94) in females (Table 1; Table S4); (12) IL-AG mostly 1–3 (occasionally 1–4); snout hemispherically-blunt with U-like pattern in having SW/HW and SW/HWE ratios of 0.605–0.856 and 0.737–0.900, respectively (Table 2); (13) The pterygoid-palatine arc is parallel to the plane of the skull, and the arc posteriorly converges in its placement. The pterygoid and the palatine are not articulated and are not in contact. The palatine bears 5 functional teeth, and the pterygoid bears 3 teeth anteriorly; (14) Main body of the hemipenis moderately enlarged; 19–22 spines around the main body of the organ.

Comparisons. The species is a medium-sized species with SVL 326–674 mm (sex pooled). For the morphological comparisons, the characters of *S. macclellandi* var. *typica* was depicted to represent *S. macclellandi* sensu stricto. The species is genetically forming sister species to *S. macclellandi* sensu stricto and *S. peinani*. But is clearly distinguished from the genetically closest species *S. macclellandi* sensu stricto by either completely lacking black transverse bands on the dorsum which are instead reduced to cover not more than five dorsal scales or have up to two BB which will be continued by the body spots on the rest of the body (vs. BB 18–29 in sex pooled); anterior edge of black nuchal band usually irregular and straight in orientation, some have minutely pointy edges extending anteriorly or even posteriorly (vs. usually pointed forward, between parietals). It also differs from *S. macclellandi* sensu stricto in the following attributes (values given from sex pooled unless specified): Ve range in females 219–242 (vs. 202–216); NBW 1–3 scales (vs. 3–4 scales); IL-AG 1–3, or occasionally 1–4 (vs. mostly 1–4); BT 0–4 (vs. 3–4); TaL 28–56 mm (vs. 41–89 mm); ED 0.60–1.20 mm (vs. 1.06–1.70 mm); IOS 2.50–5.60 mm (vs. 4.12–6.40 mm); HL 8.40–16.90 (vs. 9.30–17.90); HW 4.20–10.00 mm (vs.

4.50–11.40 mm); HD 2.60–5.80 mm (vs. 3.40–6.20 mm); the snout hemispherically-blunt giving U-like pattern with a SW/HW ratio of 0.605–0.856 and SW/HWE ratio of 0.737–0.900 (vs. the head tapering towards snout tip giving a more V-like or parabolic semi-elliptical shape to the head with lesser SW/HW ratio of 0.465–0.595 and SW/HWE ratio of 0.500–0.718) (Fig. 5.9, 5.10); a distinct diastema between the pterygoid and palatine bones (vs. pterygoid and palatine well-articulated and lack any diastema); pterygoid bears 3 functional teeth (vs. 5–6); palatine with five functional teeth (vs. 6–7) (Fig. 5.11); main body of hemipenis moderately enlarged with spines 19–22 around main body (vs. highly enlarged with 27 spines around the main body) (Fig. 5.12; Tables 5.6, 5.7).

Other comparative data (sex pooled) were extracted from Smart et al. (2021), and the extreme variations in the characters provided by the authors were not taken into account. From *S. peinani*, it differs by having a black rostral band spilling into the frontal (vs. not spilling into frontal); anterior edge of black nuchal band does not curve anteriorly (vs. curved forward); BB 0–4 (vs. 27–35); BT 0–4 (vs. 0–5); NBW 1–3 scales (vs. 1.5–4.5 scales); Ve 219–242 (vs. 209–238); and Sc 24–46 (vs. 26–36). In comparison with the more distantly related lineages among the banded clade (fide Smart et al., 2021), it differs from *S. iwasakii* in the Ve 208–242 (vs. 210–233); Sc 24–46 (vs. 35–40); Tem 1+1, rarely 1+2 (vs. 1+2); BB 0–4 (vs. 26–36); BT 0–4 (vs. 4–6); and NBW 1–3 scales (vs. 3–4 scales). From *S. swinhoei*, it differs in the Ve 208–242 (vs. 207–239); Sc 24–46 (vs. 32–49); BB 0–4 (vs. 26–38); BT 0–4 (vs. 4–7); NBW 1–3 scales (vs. 2–5 scales); and anterior edge of black nuchal band usually irregular and straight in orientation, some have minutely pointy edges extending anteriorly or even posteriorly (vs. straight). From *S. annularis*, it differs in the Ve 219–242 (vs. 194–228); Sc 24–46 (vs. 25–38); BB 0–4 (vs. 0–39); BT 0–4 (vs. 0–6); NBW 1–3 scales (vs. 1–4 scales); and anterior edge of black nuchal band usually irregular and straight in orientation, some have minutely pointy edges extending anteriorly or even posteriorly (vs. straight). To the striped clade (fide Smart et al., 2021), it differs by having DSR 13 (vs. 15 in *S. kelloggi*); mid dorsal and lateral stripe absent (vs. present in *S. boettgeri*, *S. japonicus*, *S. sauteri*); Tem 1+1/1+1, rarely 1+2/1+1 (vs. 1+2 in *S. kelloggi*).

Description. A generalized description of the species is provided based on the meristic features adopted from the type specimens (fide Wall, 1910; Smart et al., 2021) and Bangladesh specimen (fide Rahman et al., 2017), as well as the mensural and meristics data from Mizoram population where plenty of specimens are available. In life, the species is having a reddish or brownish-hued dorsum; the belly is whitish to creamish in colour and interrupted by dark patches after every one to three ventral shields. The adult specimens are characterized by the following linear mensural characters: SVL 326–446 mm (\bar{x} 383.53±36.74 mm) in males, 345–674 mm (\bar{x} 440.51±89.54 mm) in females; TaL 28–47 mm (\bar{x} 38.00±4.76 mm) in males, 28–56 mm (\bar{x} 37.20±6.62 mm) in females; internarials wider than longer with INW 1.10–1.60 mm (\bar{x} 1.35±0.16 mm) in males, 1.10–2.60 mm (\bar{x} 1.51±0.39 mm) in females; prefrontals wider than longer with PFW 1.80–2.10 mm (\bar{x} 1.91±0.09 mm) in males, 1.60–3.10 mm (\bar{x} 2.04±0.43 mm) in females; frontal longer than wider with FL 2.20–3.40 mm (\bar{x} 2.76±0.32 mm) in males, 2.50–4.80 mm (\bar{x} 3.18±0.61 mm) in females; parietals longer than wider with PL 3.00–4.40 mm (\bar{x} 3.66±0.37 mm) in males, 3.20–6.30 mm (\bar{x} 4.27±0.89 mm) in females; WBH 1.90–3.80 mm (\bar{x} 2.63±0.56 mm) in males, 2.40–7.40 mm (\bar{x} 3.01±0.65 mm) in females; ED 0.60–0.90 mm (\bar{x} 0.80±0.08 mm) in males, 0.70–1.20 mm (\bar{x} 0.89±0.16 mm) in females; E-N 1.40–2.10 mm (\bar{x} 1.70±0.22 mm) in males, 1.50–3.00 mm (\bar{x} 2.11±0.41 mm) in females; S-E 2.40–3.50 mm (\bar{x} 2.89±0.27 mm) in males, 2.80–5.80 mm (\bar{x} 3.49±0.80 mm) in females; IOS 2.80–4.10 mm (\bar{x} 3.39±0.31 mm) in males, 2.50–5.60 mm (\bar{x} 3.72±0.87 mm) in females; INS 1.90–3.30 mm (\bar{x} 2.71±0.39 mm) in males, 1.90–4.60 mm (\bar{x} 2.91±0.78 mm) in females; HL 8.50–10.60 mm (\bar{x} 9.56±0.54 mm) in males, 2.40–16.40 mm (\bar{x} 11.01±2.49 mm) in females; HW 4.20–6.20 mm (\bar{x} 5.01±0.49 mm) in males, 4.20–10.00 mm (\bar{x} 5.77±1.77 mm) in females; and HD 2.70–4.10 mm (\bar{x} 3.15±0.36 mm) in males, 2.60–5.80 mm (\bar{x} 3.46±0.94 mm) in females. The species is also characterized by the following meristic characters: Ve 208–232 (\bar{x} 215.88±6.06) in males, 219–242 (\bar{x} 230.76±6.65) in females; Sc 26–33 (\bar{x} 29.12±2.09) in males, 24–46 (\bar{x} 27.62±4.46) in females; DSR 13:13:13; Tem 1+1/1+1, rarely 1+2/1+1; SL 7/7, rarely 6/7 or 7/8; SLe 3rd–4th/3rd–4th, rarely 3rd–4th/4th–5th; IL 6/6; IL-AG 1st–4th/1st–4th, sometimes 1st–3rd/1st–3rd; IL-PG 4th; PrO 1/1; PoO 2/2 or 1/1; SpO 1/1; rostral scale visible from above; NBW 1–3 (\bar{x} 2.06±0.43) in

males, 2–3 (\bar{x} 2.05±0.23) in females; BT 0–4 (\bar{x} 0.59±0.87) in males, 0–4 (\bar{x} 0.82±1.42) in females; BS 0–32 (23.94±7.42) in males, 0–45 (28.38±10.48) in females. Few specimens have one or two dorsal bands that covered more than five dorsal scales (BB) on the anterior part of the body which then continued by the reduced black body spots (BS) viz. a single BB in MZMU242, MZMU243, MZMU231, MZMU285; two BB in MZMU977, MZMU1911, MZMU1926 and MZMU2587.

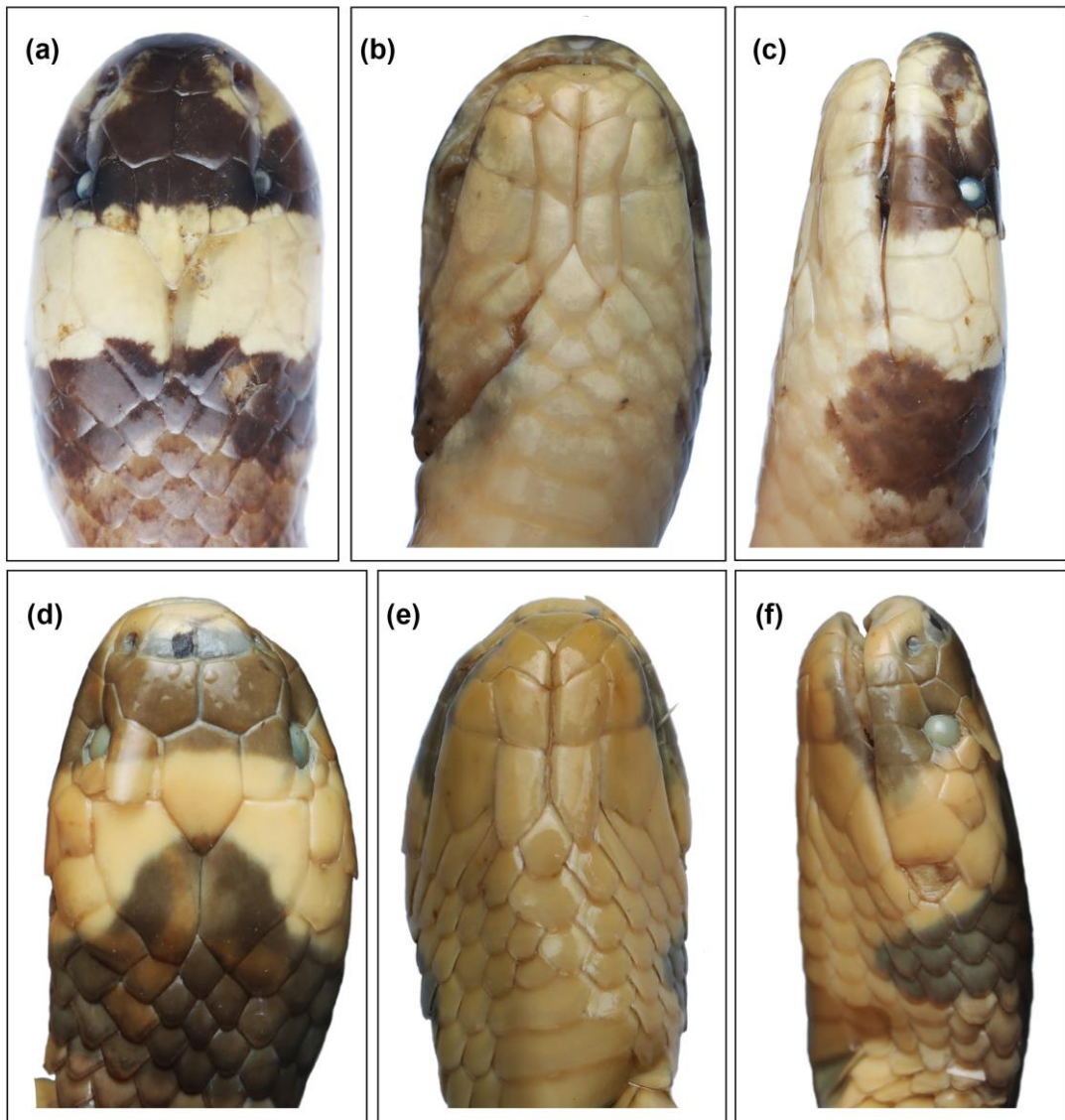


Figure 5.9. Head of *Sinomicrurus gorei* comb. nov. (MZMU2910): (a) dorsal, (b) ventral, and (c) lateral views. Head of *S. macclellandi* var. *typica* (MZMU2588): (d) dorsal, (e) ventral, and (f) lateral views.

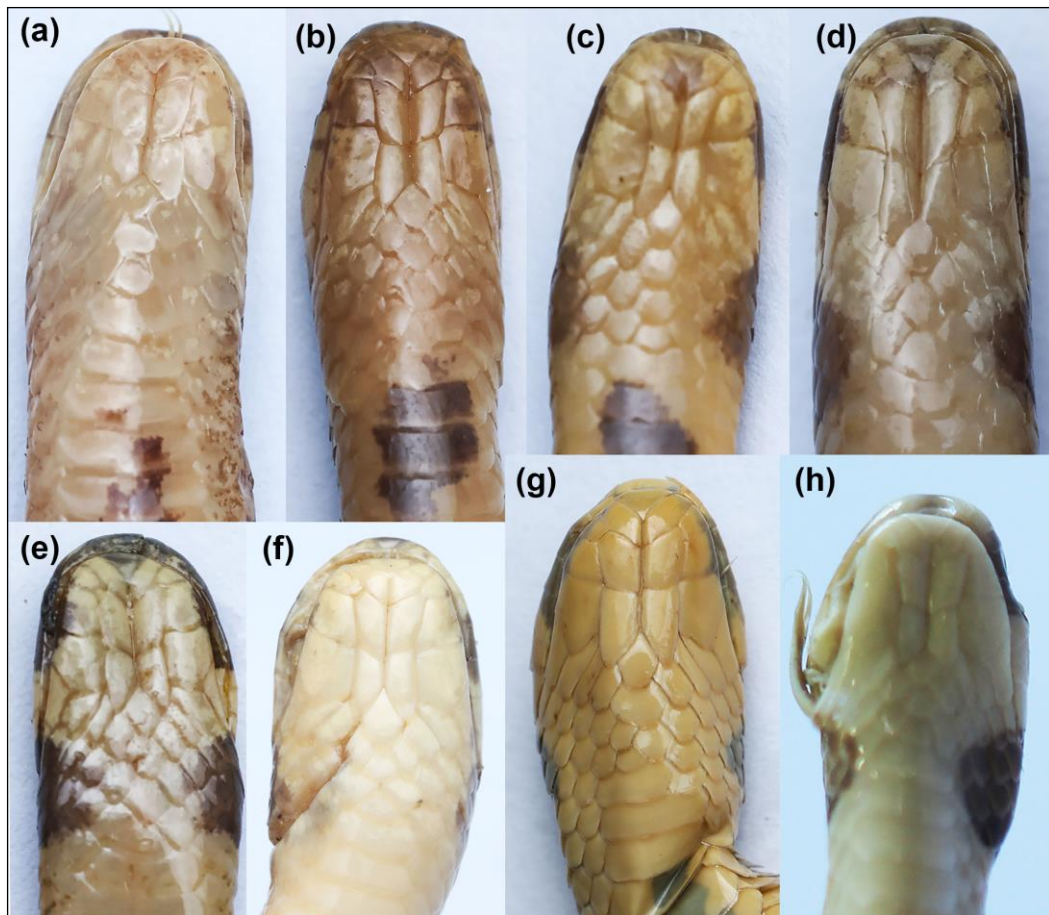


Figure 5.10. Ventral view of the head in *Sinomicrurus gorei* comb. nov.: (a) MZMU831, (b) MZMU840, (c) MZMU945, (d) MZMU1157, (e) MZMU1911, (f) MZMU2910; in *S. maclellandi* var. *typica*: (g) MZMU2588, (h) APRC/R/91/A. Photo credit: Lalmuansanga (a–e).

Osteology. The skull of *S. gorei* (Fig. 5.11) is of a typical coral snake described by Slowinski (1995) and, to an extent, of an elapid (Heatwole 2009). The specimen's skull is well calcified and intact, with no evident signs of damage. The skull is 2.5 times longer than wide (L 11.6 mm, W 4.7 mm). The premaxilla is situated at the anterior border of the nasals and is visible in the dorsal view however, partly concealed from view by the nasals. The nasals are cordiform, broad anteriorly and tapering posteriorly. The frontals are as long as broad, occupying 22% of the length of the skull, broad anteriorly, with subtle tapering towards the posterior end. The parietal, 4.8 mm long, and 2.4 mm wide, occupies 41% of the skull in dorsal view. Quadrate slender, vertically oriented with no lateral expansion visible in dorsal view. The maxilla bears one functional and 3 accessory fangs and not additional teeth. The pterygoid-palatine arc is parallel to the plane of the skull, and the arc posteriorly converges in its placement. The pterygoid and the palatine are not articulated and are not in contact. The palatine bears 5 functional teeth, and the pterygoid bears 3 teeth anteriorly. The pterygoid is 2.3 times the length of the Palatine. The dentary bears 7 functional teeth.

Hemipenis. Based on the processed hemipenis of the specimen MZMU2341, both the organs are slightly forked with two distinctly pointed apical lobes; uniformly arranged spines restricting to the apical half of the organs, and the spines diminished at the basal stalk; sulcus spermaticus at the centre; no complex form of ornamentation is evident; main body moderately enlarged; 19–22 spines around main body of the organ (Fig 5.12a).



Figure 5.11. MicroCT scans of the head of *Sinomicrurus gorei* comb. nov. (a–c) and *S. macclellandi* var. *typica* (d–f); head dorsal view (a & d), head lateral view (b & e) and ventral view of head (c & f). Scale bar 1mm.

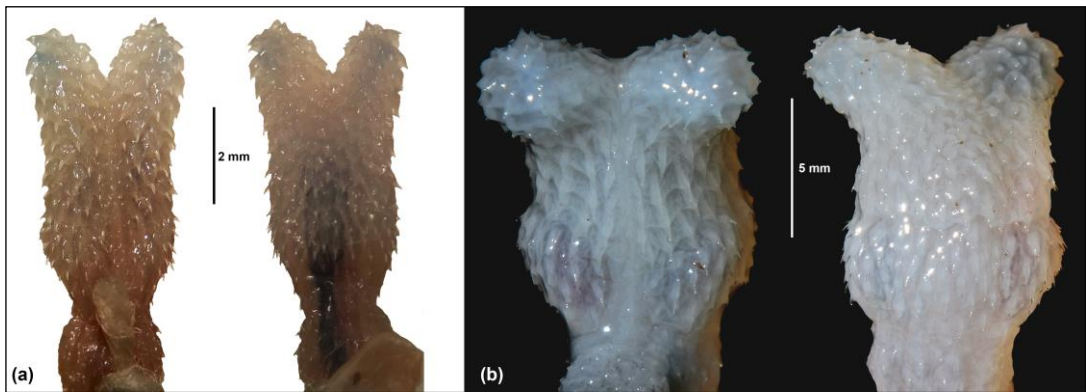


Figure 5.12. Sulcate view (left) and asulcate view (right) of the hemipenis: (a) *S. gorei* comb. nov. (MZMU2341); (b) *S. macclellandi* var. *typica* (YSR006). The organs are slightly forked with two distinctly pointed apical lobes in both species. Main body of hemipenis moderately enlarged with spines 19–22 around main body in *S. gorei* comb. nov. while it is highly enlarged with 27 spines around the main body in *S. macclellandi*. Photo credit: Jayaditya Purkayastha.

Table 5.7. Comparative meristic data between *Sinomicrurus gorei* comb. nov. and *S. macclellandi* var. *typica* from this study and published data.

<i>Sinomicrurus gorei</i> comb. nov.						<i>Sinomicrurus macclellandi</i> var. <i>typica</i>										
Locality	Mizoram, India		Assam, India (Original materials)		Sunam ganj, Bangla desh	Assam, India (Holotype)	Kampot, Cambodia	Meghalaya, India		Arunachal Pradesh, India			Mizoram, India			
Vouchers	MZMU		BMNH 1908.6.23. 92 (Holotype)	-	SGCZM 012	ZMUC 65399	CBC 02885	YSR 00 6	YSR 116	APRC/ R/91/ A	AP RC/ R/9 1/B	APRC /R/ 121	APR C/R/ 126	MZM U 272	MZMU 2588	
Sex	M (n=17)	F (n=19)	F	M	Juv	F	F	M	M	M	F	M	M	F	M	F
Ventrals	208–232 (\bar{x} 215.88±6.06)	219–238 (\bar{x} 229.63±5.91)	241	219	22 3	242	216	201	19 5	203	213	193	199	19 7	196	208
Subcaudals	24–33 (\bar{x} 29.12±2.09)	24–30 (\bar{x} 26.79±1.47)	25	30	3 1	25	27	30	31	36	25	30	28	28	36	30
Black bands on body	0–2 (\bar{x} 0.29±0.59)	0–2 (\bar{x} 0.41±0.80)	0	-	-	-	26	29	22	19	27	18	22	25	24	28
Black spots on body	0–32 (\bar{x} 23.94±7.42)	0–45 (\bar{x} 28.38±10.48)	-	-	-	-	0	0	0	0	0	0	0	0	0	0
Bands on tail	0–2 (\bar{x} 0.59±0.87)	0–4 (\bar{x} 0.82±1.42)	0	-	-	-	3	4	4	3	3	3	3	3	4	3
Nuchal band width (in scale)	1–3 (\bar{x} 2.06±0.43)	2–3 (\bar{x} 2.05±0.23)	2	-	-	-	3.5	-	3	3	3	3	4	4	4	3
Source	This study		Wall 1910; Smart et al. 2021		Rahman et al. 2017	Reinhardt 1844; Smart et al. 2021	Neang et al. 2017	This study								

Table 5.8. Comparative morphometric ratios between *Sinomicrurus gorei* comb. nov. and *S. macclellandi* var. *typica* examined in this study. Interspecific difference in the ratios is analysed using one-way ANOVA using taxa as the factor, and Brown-Forsythe test (indicated in octothorp '#'). Statistical significance at the level of alpha 0.05 is indicated by bold.

Ratios	<i>Sinomicrurus gorei</i> comb. nov. (n=36)		<i>Sinomicrurus macclellandi</i> var. <i>typica</i> (n=8)		Interspecific difference
	Mean±SD	Range	Mean±SD	Range	
HW/HL	0.523±0.049	0.439–0.632	0.606±0.079	0.474–0.731	$F_{1, 6.990} = 5.203$ $p = 0.057^{\#}$
SW/HW	0.716±0.059	0.605–0.856	0.544±0.049	0.465–0.595	$F_{1, 6.879} = 15.723$ $p < \mathbf{0.01}^{\#}$
SW/HWE	0.826±0.044	0.737–0.900	0.621±0.066	0.500–0.718	$F_{1, 7.025} = 49.679$ $p < \mathbf{0.001}^{\#}$
INS/IOS	0.789±0.065	0.645–0.939	0.634±0.089	0.544–0.734	$F_{1, 29} = 18.846$ $p < \mathbf{0.001}$
TaL/TL	0.083±0.009	0.064–0.101	0.096±0.014	0.074–0.130	$F_{1, 32} = 7.254$ $p < \mathbf{0.05}$

Distribution. The distribution range of *S. gorei* is thus far restricted to eastern Assam, Manipur, Mizoram and Nagaland in Northeast India, and Moulvibazar and Sunamganj Districts in northeastern Bangladesh (Rahman et al. 2017; Hakim 2020; Thejavitso Chase, pers. comm.) at elevations between ca. 90 m to 2,000 m above sea level. Prior to this study, previous workers recorded the specimens of *S. gorei* from eight localities in Aizawl and Siahla Districts in Mizoram (Lalremsanga and Zothansiamia 2015). So, this work updated the distributional records of the species from Mizoram based on 16 new localities originating from 28 different sampling sites in Aizawl and Champhai Districts at the elevation range between 150 m to 1,378 m above sea level (Fig. 5.12). Considering the records of the species from Sunamganj College and Kamalganj Upazila in Bangladesh (Rahman et al. 2017; Hakim 2020) situating close to Meghalaya border, the occurrence of *S. gorei* is not unexpected from this State; or perhaps including Tripura, the adjacent State of Mizoram. Additionally, occurrence of the species in the adjoining region of Myanmar is possible as the region share a similar biotope. Detailed distributional records for the Northeast Indian specimens examined are provided in Tables 5.8 and 5.9. The distribution may be summed up as low elevation hills east of the Arakan hill range that is part of the Indo-Burmese biodiversity hotspot.

This work also updated the records of *S. macclellandi* var. *typica* from eight new localities in Aizawl, Champhai, Khawzawl, Mamit and Kolasib Districts in Mizoram at the elevation between 858 m to 1,500 m above sea level in addition to the existing single record from Mualpui in Aizawl District (Lalremsanga and Zothansiamia 2015). The two topotypical specimens of *S. macclellandi* var. *typica* were captured at 2010 h on 20 Aug. 2020 (YSR006) and at 2015 h on 28 Sept. 2022 (YSR116) from Shillong, Meghalaya at the elevation of 980–982 m above sea level; and four examined specimens (APRC/R/91/A; APRC/R/91/B; APRC/R/121; APRC/R/126) plus one unexamined specimen (APRC/R/88) (Kyrti Prosad Nath, pers. comm.) from Arunachal Pradesh were captured at the elevation of 215–523 m above sea level within the campus of Zoological Survey of India, Itanagar and Roing, Lower Dibang valley as per the catalogue of APRC (Fig. 5.13). So, all confirmed

distribution records of *S. gorei* range between ca. 90–1,300 m elevation whereas those of *S. macclellandi* var. *typica* are between 215–1,500 m.

Table 5.9. Detailed specimens collected and/or examined or documented for *Sinomicrurus* species from Mizoram in this work. Voucher acronym: Departmental Museum of Zoology, Mizoram University, India (MZMU). New sampling sites from this work are indicated with bold.

Sl. no	Species	Vouchers	Locality	Latitude	Longitude	Elevation (m a.s.l.)
1	<i>S. macclellandi</i> var. <i>typica</i>	MZMU272	Mualpui, Aizawl District	23.716976°	92.736703°	858
2	<i>S. macclellandi</i> var. <i>typica</i>	MZMU 2588	Hmunhmeltha, Champhai District	23.496264°	93.321225°	1500
3	<i>S. macclellandi</i> var. <i>typica</i>	-	Mamit, Mamit District	23.927002°N	92.493831°	780
4	<i>S. macclellandi</i> var. <i>typica</i>	-	Tawizo, Aizawl District	23.572706°N	92.960630°E	1500
5	<i>S. macclellandi</i> var. <i>typica</i>	-	Kolasib, kolasib District	24.211543°N	92.682050°E	700
6	<i>S. macclellandi</i> var. <i>typica</i>	-	Aizawl, Aizawl District	23.730°N	92.717°E	1000
7	<i>S. macclellandi</i> var. <i>typica</i>	-	Pualreng WLS, Kolasib District	24.235°N	92.8124°E	570
8	<i>S. macclellandi</i> var. <i>typica</i>	-	Khuangpuilam , Kolasib District	24.201736°N	92.687283°	655
9	<i>S. macclellandi</i> var. <i>typica</i>	-	Arro, Khawzawl District	23.531221°N	93.137661°E	1420
1	<i>S. gorei</i> comb. nov.	MZMU 171	Sawlung, Aizawl District	23.981521°	92.931954°	1133
2	<i>S. gorei</i> comb. nov.	MZMU 242	Chawlhmun, Aizawl District	23.747322°	92.690611°	930
3	<i>S. gorei</i> comb. nov.	MZMU 243	College veng, Aizawl District	23.723291°	92.726152°	878
4	<i>S. gorei</i> comb. nov.	MZMU 247	Sairang, Aizawl District	23.807037°	92.654792°	150
5	<i>S. gorei</i> comb. nov.	MZMU 269	MZU Campus, Aizawl District	23.737729°	92.662925°	794

6	<i>S. gorei</i> comb. nov.	MZMU 270	Darlawn, Aizawl District	24.011839°	92.922546°	1100
7	<i>S. gorei</i> comb. nov.	MZMU 271	New Laty, Siaha District	22.376047°	92.923376°	584
8	<i>S. gorei</i> comb. nov.	MZMU 273	College veng, Aizawl District	23.725766°	92.725489°	866
9	<i>S. gorei</i> comb. nov.	MZMU 284	MZU Campus, Aizawl District	23.736067°	92.664851°	822
10	<i>S. gorei</i> comb. nov.	MZMU 285	Falkland, Aizawl District	23.734648°	92.738804°	820
11	<i>S. gorei</i> comb. nov.	MZMU 831	Mission vengthlang, Aizawl District	23.713785°	92.707100°	944
12	<i>S. gorei</i> comb. nov.	MZMU 832	Mission vengthlang, Aizawl District	23.712138°	92.707516°	938
13	<i>S. gorei</i> comb. nov.	MZMU 840	Melthum, Aizawl District	23.692071°	92.719872°	1035
14	<i>S. gorei</i> comb. nov.	MZMU 862	Gosen, Durtlang, Aizawl District	23.790082°	92.731674°	1080
15	<i>S. gorei</i> comb. nov.	MZMU 894	Tlangnuam, Aizawl District	23.704313°	92.715662°	1075
16	<i>S. gorei</i> comb. nov.	MZMU 945	Durtlang north, Aizawl District	23.794934°	92.728339°	1290
17	<i>S. gorei</i> comb. nov.	MZMU 974	Hunthar, Aizawl District	23.745798°	92.716647°	900
18	<i>S. gorei</i> comb. nov.	MZMU 977	Tanhrlil, Aizawl District	23.737970°	92.675536°	970
19	<i>S. gorei</i> comb. nov.	MZMU 1074	Tlangnuam, Aizawl District	23.704319°	92.714506°	1040
20	<i>S. gorei</i> comb. nov.	MZMU 1157	Durtlang, Aizawl District	23.783669°	92.726228°	1220
21	<i>S. gorei</i> comb. nov.	MZMU 1214	Durtlang north, Aizawl District	23.797174°	92.729193°	1260
22	<i>S. gorei</i> comb. nov.	MZMU 1318	Tanhrlil, Aizawl District	23.736250°	92.674736°	967
23	<i>S. gorei</i> comb. nov.	MZMU 1438	Aizawl, Aizawl District	23.747465°	92.732143°	848
24	<i>S. gorei</i> comb. nov.	MZMU 1444	Aizawl, Aizawl District	23.741310°	92.738020°	925
25	<i>S. gorei</i> comb. nov.	MZMU 1569	Mission veng, Aizawl District	23.712930°	92.719557°	1040
26	<i>S. gorei</i> comb. nov.	MZMU 1727	Durtlang Venglai, Aizawl District	23.782105°	92.728342°	1174
27	<i>S. gorei</i> comb. nov.	MZMU 1911	MZU Campus, Aizawl District	23.738798°	92.668488°	870

28	<i>S. gorei</i> comb. nov.	MZMU 1913	Aizawl, Aizawl District	23.732937°	92.722425°	890
29	<i>S. gorei</i> comb. nov.	MZMU 1926	Sialhawk, Champhai District	23.293976°	93.095802°	1300
30	<i>S. gorei</i> comb. nov.	MZMU 2034	Aizawl, Aizawl District	23.739855°	92.728843°	900
31	<i>S. gorei</i> comb. nov.	MZMU 2035	MZU Campus, Aizawl District	23.736209°	92.668979°	873
32	<i>S. gorei</i> comb. nov.	MZMU 2341	Chaltlang, Aizawl District	23.752929°	92.725170°	1106
33	<i>S. gorei</i> comb. nov.	MZMU 2438	ITI veng, Aizawl District	23.719090°	92.731749°	770
34	<i>S. gorei</i> comb. nov.	MZMU 2587	Durtlang, Aizawl District	23.788589°	92.728864°	1205
35	<i>S. gorei</i> comb. nov.	MZMU 2589	Gosen, Durtlang, Aizawl District	23.789950°	92.730811°	1120
36	<i>S. gorei</i> comb. nov.	MZMU 2590	Durtlang Mualveng, Aizawl District	23.785405°	92.725924°	1239
37	<i>S. gorei</i> comb. nov.	uncollected	Murlen National Park, Champhai District	23.661493°	93.285007°	1378

Table 5.10. Detailed specimens collected and/or examined or documented for *Sinomicrurus* species from outside Mizoram. Voucher acronyms: Arunachal Pradesh Regional Centre, Zoological Survey of India (APRC); Collection of Yashpal Singh Rathee (YSR). New sampling sites from this work are indicated with bold.

Sl. no	Species	Vouchers	Locality	Latitude	Longitude	Elevation (m a.s.l.)
1	<i>S. macclellandi</i> var. <i>typica</i>	YSR006	Shillong, Meghalaya	25.692514°	91.935949°	980
2	<i>S. macclellandi</i> var. <i>typica</i>	YSR011	Shillong, Meghalaya	25.691236°	91.935458°	982
3	<i>S. macclellandi</i> var. <i>typica</i>	APRC/R/91/A	ZSI campus, Itanagar, Arunachal Pradesh	27.076°	93.599°	215
4	<i>S. macclellandi</i> var. <i>typica</i>	APRC/R/91/B	ZSI campus, Itanagar, Arunachal Pradesh	27.076°	93.599°	215
5	<i>S. macclellandi</i> var. <i>typica</i>	APRC/R/121	ZSI campus, Itanagar, Arunachal Pradesh	27.076°	93.599°	215
6	<i>S. macclellandi</i> var. <i>typica</i>	APRC/R/126	Roing, Lower Dibang valley, Arunachal Pradesh	28.159°	95.866°	523

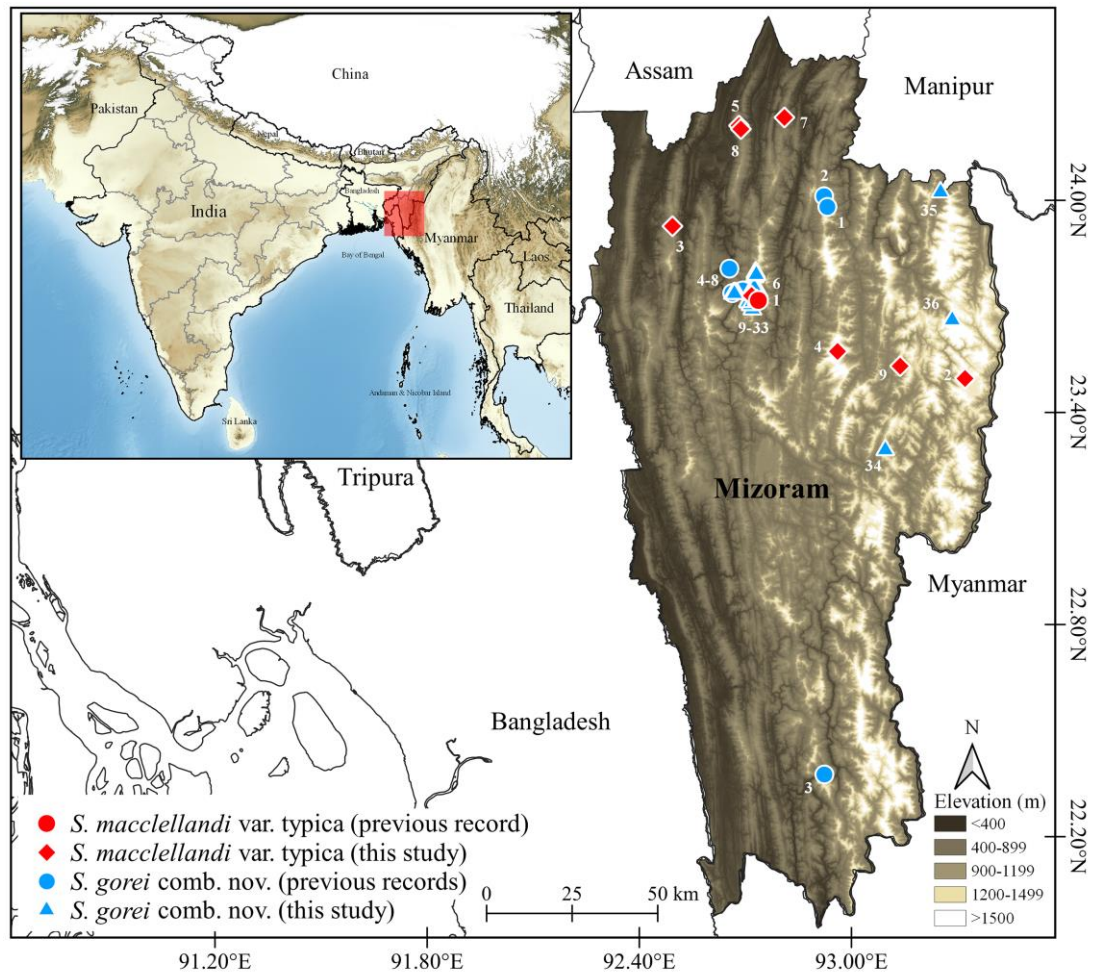


Figure 5.13. Digital elevation map showing the distributional records of *Sinomicrurus macclellandi* var. *typica* and *S. gorei* comb. nov. in Mizoram. The locality numbers are corresponds to the serial number as given in Table 5.9.

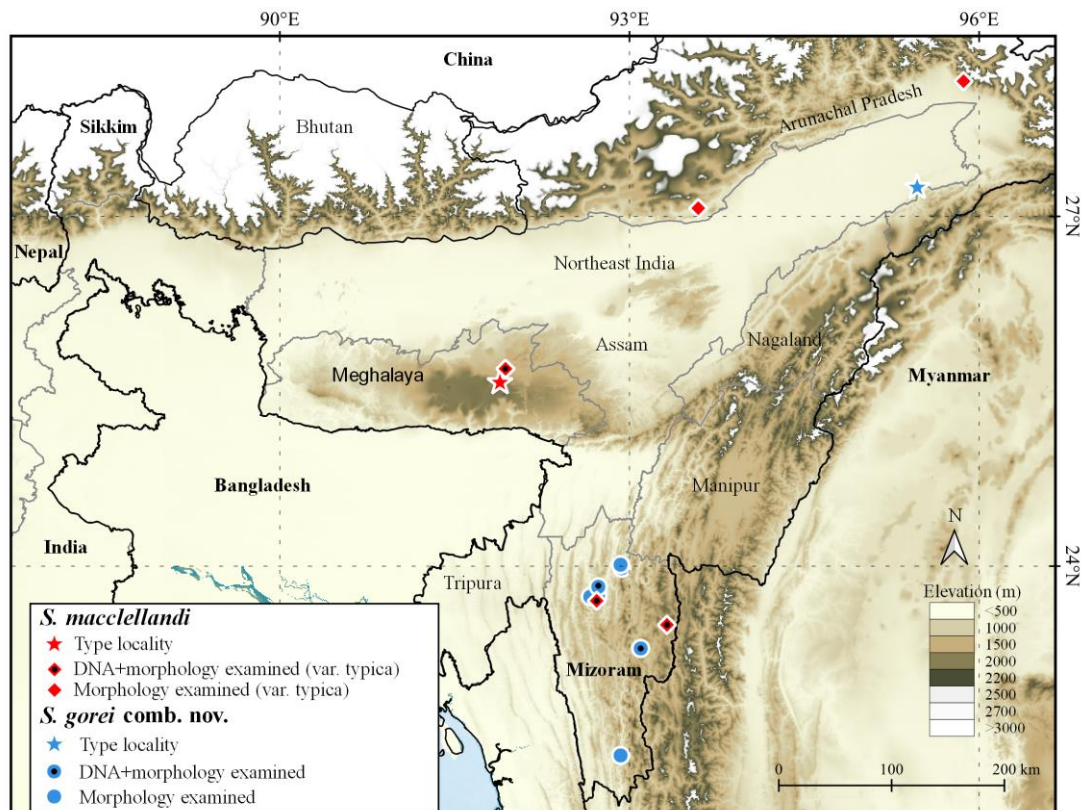


Figure 5.14. Map showing the studied populations of *Sinomicrurus macclellandi* from Northeast India: type locality of *S. macclellandi* from Shillong, Meghalaya (formerly Assam) (in red star); studied populations of *S. macclellandi* var. typica from Meghalaya and Mizoram with DNA+ morphological data (in red diamond with dot), and Arunachal Pradesh with morphological data (in red diamond); type locality of *S. gorei* comb. nov. from Dibrugarh, Assam (in blue star); studied population of *S. gorei* comb. nov. from Mizoram with DNA+morphological data shown in blue circle with dot and with only morphological data shown in blue circle. See the detailed global distributional records of *Sinomicrurus* species in Smart et al. (2021).

Biology. A gravid female (MZMU2590; SVL 449 mm; Weight 8.7 g) was captured on 29th Sept 2021 from Durtlang, Mizoram. The snake was maintained in a natural-like condition and regularly monitored in the facility of the Developmental Biology and Herpetology Laboratory, Department of Zoology, Mizoram University. The female snake was observed laying three eggs (25.8–31.49 mm × 7.05–8.82 mm) on 3rd Sept 2021; and the eggs were immediately separated from the female, took the egg measurements, and subsequently kept in a perforated plastic container with vermiculite as bedding. The room temperature and humidity were recorded once during the day time for every day which fluctuated between 24.7°C to 31.1°C and 70% –90.3%, respectively. The bedding was occasionally changed and kept it damp to maintain humidity. The eggs are also occasionally dusted with antifungal powder to prevent fungal infection. After incubation in the laboratory condition, the two eggs successfully hatched at ca. 1230 h on 3rd Oct 2021 (Fig. 5.14), while one neonate was unable to completely emerge out on its own. So, a longitudinal incision was made on the egg shell and wait for some time, but the neonate was already dead when it was gently taken out with the help of a forceps ca. 1900 h on the same day, which was plausibly due to premature hatching (Fig. 12b). Overall, the clutch produced two male neonates (SVL 105 mm + TaL 15 mm; SVL 151 mm + TaL 15 mm) and one female neonate (SVL 164 mm + TaL 14 mm). Detailed biometric data were provided in Table 5.10. In addition to this observation, another female laying three eggs on 31st Aug 2019 was recorded; unfortunately, the eggs did not hatch which was possibly due to sub-optimal incubation settings.

The presently documented clutch size of *S. gorei* is relatively low compared to those recorded for *S. macclellandi* by Smith (1943) such as six eggs from one specimen in Shillong, Northeast India and 14 eggs recovered from a dead specimen in Maymyo, Myanmar. After the systematic revision of *S. macclellandi* complex (Smart et al. 2021), the clutch size of *S. macclellandi* which was also given as 6–14 by various recent authors (eg. Ahmed et al. 2009; Das 2012; Whitaker and Captain 2008) are difficult to ascertain which variety or species they are based on to provide the data. For instance, the distribution of *S. macclellandi* depicted by Das (2012) was referring to populations of *S. annularis*, *S. macclellandi*, and *S. peinani*; and the

depicted figure was *S. peinani*. Also, Whitaker and Captain (2008) provided the distribution range of *S. macclellandi* which was actually comprised of the range of *S. annularis*, part of *S. macclellandi* and *S. peinani*. Furthermore, Ahmed et al. (2009) did not assign any subspecies (or variants), and the depicted distribution referred to all forms in the species complex (see Smart et al. 2021).

The species has been observed feeding on an earthworm. In captivity, snakes, lizards and frogs were offered as food but none were accepted. Based on its size it may feed on earthworms as observed and may be smaller species of snakes. In addition, a defensive behaviour of the species was also observed in flattening its posterior body dorsoventrally and elevating its coiling tail (Fig. 8c). Such type of defensive strategy has also been documented in other snake genera; for instance, among the New World coral snake genera like *Micrurus* (eg. Brown & Barazowski 2020; Green 1973), and other non-venomous snake genus like *Oligodon* Fitzinger, 1826 (eg. Huang et al. 2011).

Table 5.11. Neonate biometric data (measurements in mm; weights in g) of *Sinomicrurus gorei* comb. nov. (MZMU2590) from Mizoram, Northeast India.

Egg vouchers	MZMU-E5	MZMU-E7	MZMU-E6
Length of eggs	25.8	31.49	27.83
Width of eggs	8.27	8.82	7.05
Weight of eggs	0.5	0.6	0.52
Neonate vouchers	MZMU-N5	MZMU-N6	MZMU-N7
Sex	Male	Female	Male
Eye diameter	0.92	1.08	0.84
Eye-nostril distance	1.48	1.56	1.3
Interorbital distance	1.68	1.86	1.64
Internarial distance	1.21	1.48	1.13
Snout width	1.65	1.74	1.68
Snout length	1.89	2.01	1.73
Head length	5.23	5.65	5.18
Head width	3.23	3.41	3.23
Ventrals	214	238	216
Subcaudals	29	26	28
Dorsal scale rows	13:13:13	13:13:13	13:13:13
Supralabials	07-Jul	07-Jul	07-Jul
Supralabials touching eye	3 rd -4 th	3 rd -4 th	3 rd -4 th
Infralabials	06-Jun	06-Jun	06-Jun
Temporals	1+1/1+1	1+1/1+1	1+1/1+1
Post-oculars	02-Feb	02-Feb	02-Feb
Pre-oculars	01-Jan	01-Jan	01-Jan
SVL (on hatch)	151	164	105
TaL (on hatch)	15	14	15
Relative tail length (on hatch)	0.107	0.125	0.118
Weight (on hatch)	1.46	1.69	1.27



Figure 5.15. (a) Newly hatched neonates of *Sinomicrurus gorei* comb. nov. (MZMU2590) from Mizoram, Northeast India; (b) neonate which was prematurely hatched along with the egg shell.

Discussion

Smart et al. (2021) defined *S. macclellandi* sensu stricto based on molecular data for specimens from Myanmar (CAS 221494), Bhutan (BWS OPAS8) and an unknown location (CIBHN04). Based on molecular data generated in the present study, which represents one topotype from Shillong (YSR006) and, two specimens from Mizoram (MZMU272 & MZMU2588), we confirm Smart et al.'s (2021) definition, which was subsequently used to assess the status of other populations in the region. This chapter also impart additional insight to the morphological disparity based on the meristic data of Smart et al. (2021); for this, the other variants were excluded and regarded the specimens having $BB < 8$ as *S. gorei* and $BB > 16$ as *S. macclellandi* var. *typica*. Statistical analyses using one-way ANOVA and Brown-Forsythe test also showed statistically significant difference between them in the BB ($p < 0.001$), BT ($p < 0.001$), NBW ($p < 0.001$). A disparate clustering of these two taxa was also visualized by the ordination of these three significantly differed meristics along the first and second PCA axes (Fig. 5.15a) that concurred well to the present finding (see Fig. 5.6). Because two-way ANOVA detected the Ve ($p < 0.001$) and Sc ($p < 0.01$) as sexually dimorphic characters, the one-way ANOVA between *S. macclellandi* var. *typica* and *S. gorei* comb. nov. with analysing male and female data separately revealed statistically significant difference between the two taxa in the Ve of male ($p < 0.001$) and female ($p < 0.01$) (Figs. 5.15b, c). Moreover, the main body of the hemipenis in *S. macclellandi* sensu stricto was described to be moderately to highly enlarged based on the hemipenial description of the specimens BNHS 2755.1/4 and BNHS 2218 (see Figs. 11c, d; 29 pp in Smart et al. 2021); arguably, the moderately enlarged main body of the organ can be assigned to the *S. gorei* specimen (BNHS 2755.1/4; $BB=0$; $BT=3$), while the highly enlarged main body of the organ (BNHS 2218; $BB=18$; $BT=4$) can be assigned to *S. macclellandi* var. *typica* (see File S4 in Smart et al. 2021). Moreover, this chapter propose to justify that the genetic data of *S. macclellandi* var. *typica* (MZMU272) collected from Mualpui locality, Aizawl District, Mizoram was mistakenly designated as *S. macclellandi* var. *gorei* specimen “MZMU270” in Smart et al. (2021); thus, no genetic data is generated for the specimen “MZMU270” as of now. Contrarily, the

two specimens of this morph (MZMU269; MZMU270) cluster with the specimens of *S. gorei* in the present morphological analysis thereby necessitating the taxonomic treatment for this completely plain morph from Mizoram as *S. gorei* until there is confirmatory work from DNA data. Because the specimens from different populations in this work are examined by different persons, they were re-examined and statistically tested to avoid any potential recorder bias following the similar approach in Biakzuala et al. (2023), thereby the one-way ANCOVA test did not detect any statistically significant difference between the two readings ($p>0.05$). Furthermore, the present readings and those from Smart et al. (2021) in the common specimens examined (n=21) were tested for recorder bias. Although minor differences are seen in the range of the meristics such as Ve 208–238 vs. 202–238 in Smart et al. (2021); Sc 24–33 vs. 21–33 in Smart et al. (2021); BB 0–1 vs. 0–4 in Smart et al. (2021); BT 0–4 vs. 0–5 in Smart et al. (2021); the one-way ANCOVA test did not detect any statistically significant difference between the two records ($p>0.05$).

In addition, some of the published sequences of *Sinomicrurus* species either form a sister lineage or clustered with the previously confirmed *S. iwasakii* and *S. cf. annularis* in both the BI and ML phylogenetic trees (see Figs. 5.2, 5.3), but we conferred those sequences to *S. cf. swinhoei* considering their partitioning as a conspecific to *S. swinhoei* in our bPTP species delimitation (see Table 5.2). Moreover, *S. cf. annularis* is not detected as a distinct MOTU from *S. swinhoei*. Thus, the monophyletic clade of *S. iwasakii* + *S. swinhoei* + *S. cf. annularis* warrant a rectification of their taxonomic position.

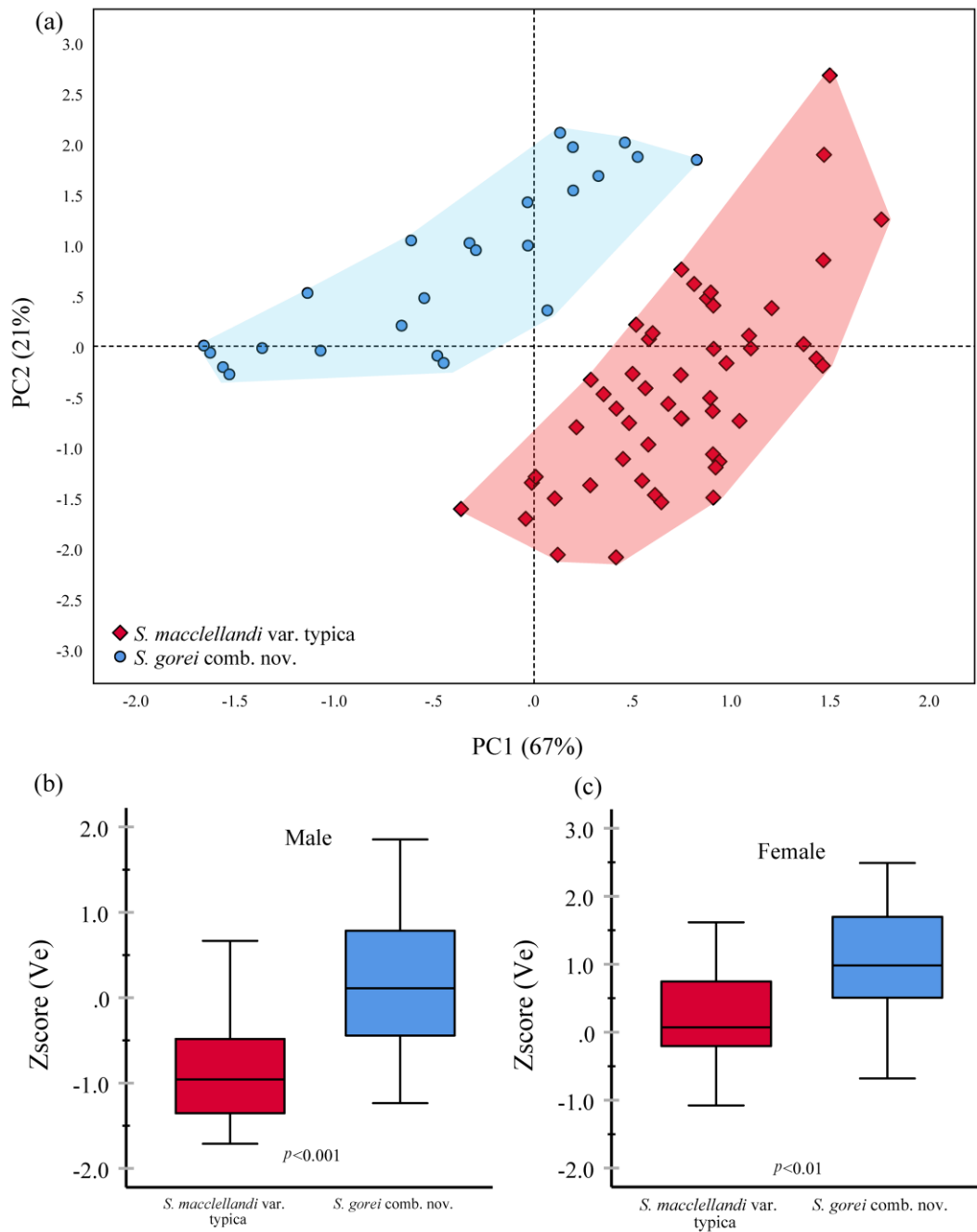


Figure 5.16. (a) Ordination of the standardized meristic characters of body band (BB), tail band (BT), and width of nuchal band (NBW) between *Sinomicrurus maclellandi* var. *typica* and *S. gorei* comb. nov. based on the phenotypic dataset adopted from Smart et al. (2021). Total variance associated with the PC1 and PC2 are 67% and 21%, respectively. Box plot showing median, interquartile range, range (minimum to maximum), and outliers for the statistically significant difference in the

standardized ventral (Ve) among male (b) and female (c) specimens between *S. macclellandi* var. *typica* and *S. gorei* comb. nov. Significant level (p values) at the alpha level of 0.05 given at each plot.

Based on the new and existing distributional records, it is assumable that *S. macclellandi* prefers mid to high elevation forests whereas, *S. gorei* is a low to mid elevation species even in human dominated landscapes. The species elevational ranges largely overlap in the state of Mizoram as the state has a terrain that ranges from low to mid elevation, and the known overlapping occurrence records particularly in Mizoram evince their syntopic existence. Despite the range overlap, the species likely occupy different niche especially in terms of diet as *S. macclellandi* is a fairly large sized species in comparison to *S. gorei*. The former is known to exclusively feed on other snakes (Smith 1943; Whitaker and Captain 2008) whereas the latter likely feeds on earthworms (H.T. Lalremsanga pers. obs.). An individual of *S. gorei* (MZMU243) was dug out from the soil while reconstructing a public springwater tank near Pachhunga University College, Aizawl, Mizoram on 23rd May 2010. This suggested the fossorial behaviour of this species before the rainy season in the region. Nocturnal habits of these snakes make direct observations of these species difficult, and additional sampling throughout the range of the species will be necessary to ascertain whether the two species have a dietary overlap or there actually is resource partitioning between them. Investigating their reproductive biology will also be critical to know the degree of sexual barriers between them which may be of chemical cues, overlapping breeding cycles, or other biological factors (Shine et al. 2002). Furthermore, large scale population genetic studies will be important to investigate the possibility of any hybrid zone between these two taxa within their known range. To the best of our knowledge, existence of hybridization and/or introgression has not been yet noticed across members of this genus in wild population.

Although in the present work, any taxonomic amendments to the other variants were not made, such as *S. macclellandi* var. *nigriventer*, *S. macclellandi* var. *concolor*, and *S. macclellandi* var. *univirgatus*; *S. macclellandi* var. *nigriventer* appears to be a distinct lineage and further investigation would be necessary to

restore it as a valid species. Molecular data for additional specimens of *S. macclellandi* var. *nigriventer*, and *S. macclellandi* var. *univirgatus* would be imperative for stabilizing the taxonomy of the group. By integratively implementing morpho-taxonomy and the phylogenetic species concept that is based on reciprocal monophyly for species recognition (Sokal and Crovello 1970; Baum and Shaw 1995; Luo et al. 2018), the present study elucidated the scientific rationale for considering *S. gorei* to a full species level as it exhibits distinct evolutionary lineage with a considerable genetic divergence and phenetic disparity from the other congeneric species. In contrast, the non-monophyly of the *S. macclellandi* sensu stricto lineages fide Smart et al. (2021) necessitates further reassessment of the systematic status of its current putative synonyms and variants.

Summary

Overall, a total of 179 elapid snake individuals (preserved and live) were examined from Mizoram along with additional data from 29 snake samples housed in other museum collections from Arunachal Pradesh, Meghalaya, West Bengal in India, and Java in Indonesia thereby a total of 208 specimens were examined in this work. Also, a total of 61 DNA sequences of elapid snakes are generated from this study and submitted to NCBI GenBank for acquiring the accession numbers. This study covers the systematics to as far possible as taxonomic works for the elapid snakes from Mizoram State in Northeast India namely *B. fasciatus* (Banded krait), *B. niger* (Greater Black krait), *N. kaouthia* (Monocled cobra), *O. hannah* (King cobra) and *S. macclellandi* (McClelland's coral snake).

In chapter 1, the phylogenetic analyses, based on four mitochondrial genes (this work + GenBank data), reveal the existence of at least three evolutionary lineages within *B. fasciatus*, corresponding to Indo-Myanmar, Sundaic and eastern Asian lineages. At least three taxonomic entities are expected to exist within the nomen *B. fasciatus* and restrict the distribution of *B. fasciatus* sensu stricto to the Indo-Myanmar region. It was also confirmed that populations in eastern India (e.g. Odisha, West Bengal, etc.) and northeastern India (e.g. Mizoram, Assam, etc.) are conspecific. The Indo-Myanmar population (Clade II) was postulated as *B. fasciatus* sensu stricto, while considering the populations from Sundaic region, especially from Greater Sunda Islands (Clade I) and mainland Sundaland including southern China (Clade III) as *B. fasciatus* sensu lato. It was speculated that there might still be cryptic diversity within the eastern Asian lineage (Clade III) due to the high genetic divergence within the clade. In this chapter, a total of 47 localities are presented (40 previous + 7 new) at 49–1,426 m a.s.l. (Fig. 6) while the existing elevation ranged 40–2,300 m a.s.l. (Ahmed et al. 2009; Knierim et al. 2019).

In chapter 2, The present mitochondrial gene-based phylogenetic evidences suggested that the two species of black kraits (*B. niger* and *B. lividus*) are not a sister taxa as they constituted distinct lineages. This contradicted with the morphology-based phylogeny of the genus proposed by Slowinski (1994). *B. niger* is having close

phylogenetic relationship and low inter-specific genetic divergence from the Southeast Asian kraits such as *B. suzhenae* (9.4% in *nd4*), *B. candidus* (2.9–3.6% in *16s*), and *B. wanghaotingi* (8.5–10% in *cytb*). While *B. lividus* is showing close phylogenetic relationship and low inter-specific genetic divergence (in *cytb*) from the kraits of Indian subcontinent such as *B. caeruleus* (11.3%), and *B. ceylonicus* (11.3%). Based on 46 adult specimens, it was uncovered that only the characters of INL and PFL are significantly differed between sexes $p < 0.05$. Anomalous male specimen was collected from Thenzawl locality (MZMU2030) that is characterized by the unusual formula of dorsal scale rows with 17:17:15 while the known value for the taxa is 15:15:15. This anomalous specimen not only represents the longest specimen among the examined specimens, but also divulged the new record of total length for the species i.e 1313 mm (SVL=1175 mm, TaL=138 mm) vs. 1200 mm fide Smith (1943). The meristics on *B. niger* reveal a new lower limit in the Ve range i.e 214–228 vs. 216–231 (Smith 1943). This chapter presents a total of 58 distributional localities (48 previous + 10 new) at 64–1,433 m a.s.l. (Fig. 6) while the known elevation ranged 64–1,433 m a.s.l. fide Lalbiakzuala (2019).

In Chapter 3, the concatenated three mitochondrial genes based phylogenetic analyses depicted a well-supported (PP=0.99; UFB=93) lineage diversification among *N. kaouthia* populations showing two independent lineages, the South Asian Clade containing populations from Northeast India (Mizoram) and Bangladesh; and the Southeastern Asian Clade which accommodates the populations from Myanmar, China, Vietnam, Thailand, and unknown sample locality. This supports the existence of two distinct clades as previously proposed by Shi et al. (2022) based on *cox1* gene. The PCoA ordinations of genetic divergence showed the discrete clustering of *N. kaouthia* from Southeast Asia from the other congeneric samples from South Asia, while a single specimen from China (KIZYPX18216) is seen distant from both South Asia and SE Asian samples. The *N. kaouthia* from China (KIZYPX18216) is also detected as distinct species from both the representative specimens of South Asian and Southeast Asian Clades in the ASAP analysis which warrant further investigation of the taxonomic status of this specimen. The present intra-species analysis accepts the alternative hypothesis which states that the phenotypic variation of hood marking

is having an effect on meristics and morphometrics between the two groups. Owing that *a priori* grouping of the variant accommodated various phenotypic forms; further nesting of significantly different sub-groups within the variant is not unexpected in a larger sampling size. Ascertainment of the probable correlations between the genetic and phenotypic variations within *N. kaouthia* populations remains a crucial challenge. In this study, *N. kaouthia* is recorded from a total of 48 localities in Mizoram at 66–1,470 m a.s.l. (Fig. 6.0) while the known elevation ranged 40–1,500 m a.s.l. (Wallach et al. 2014; Stuart and Wogan 2012; Wüster et al. 1995).

In chapter 4, the phylograms based on *16s*, *cox1* and *cytb* genes also affirmed the nesting of the study population within the clade of Indo-Chinese lineage. Pos-hoc test showed the absence of morphological difference between Mizoram and Indo-Chinese specimens, thereby morphology conforms to the systematic status of Mizoram population as member of Indo-Chinese Lineage. PCA ordination on the standardised meristics (ventrals, subcaudals, anterior dorsal scale rows) also showed an overlapping clustering between Mizoram specimens and the pre-defined specimens of Indo-Chinese Lineage. The present systematic reassessment (morphologically and phylogenetically) affirms that the study population is a member of the Indo-Chinese lineage. Sexual dimorphism in the study population is significant in the ventrals ($p < 0.01$), subcaudals ($p < 0.05$), undivided subcaudals ($p < 0.05$), tail length ($p < 0.001$), head length ($p < 0.05$), head width ($p < 0.0001$), head depth ($p < 0.01$), nostril diameter ($p < 0.05$), internarial space ($p < 0.05$), width of frontals ($p < 0.01$), and width of parietals ($p < 0.05$). In this work, *O. hannah* is documented from 18 localities in Mizoram at the elevation of 400–1,450 m a.s.l. (Fig. 6) while the known elevation ranged 60–2,700 m a.s.l. (Ahmed et al. 2009).

In chapter 5, the BI and ML phylogenies based on the concatenated dataset depicted a lineage diversification among the newly generated sequences of *S. macclellandi* populations from Mizoram and Meghalaya in India. Mizoram samples of *S. macclellandi* var. *gorei* (MZMU1727, MZMU1926, MZMU2034) are forming a strongly supported distinct, and sister lineage (PP=1.00; UFB=99) of the clade composed by the *S. macclellandi* var. *typica* and *S. peinani* lineages. Genetic

divergence-based PCoA disclosed the discrete clustering of the *S. macclellandi* var. *gorei* specimens from *S. macclellandi* sensu stricto and from the other congeneric species as well. Morphologically, two-way ANOVA and ANCOVA also revealed a statistically significant difference in the BB ($p<0.001$), BS ($p<0.001$), BT ($p<0.001$), NBW ($p<0.001$), ED ($p<0.001$), IOS ($p<0.001$), HL ($p<0.05$), HW ($p<0.001$), and HD ($p<0.001$). The presently documented clutch size of *S. gorei* (up to 3 eggs) is relatively low compared to *S. macclellandi* (6-14 eggs). By integratively implementing morpho-taxonomy and phylogenetic species concept that is based on reciprocal monophyly for species recognition, the present study elucidated the scientific rationale for considering *S. gorei* to a full species level as it exhibits distinct evolutionary lineage with a considerable genetic divergence and phenetic disparity from the other congeneric species. *S. macclellandi* is documented from a total of 9 localities in Mizoram (1 previous + 8 new) at the elevation of 858–1,500 m a.s.l. while the overall range is 215–1,500 m a.s.l. On the other hand, *S. gorei* is confirmed from 24 localities in Mizoram (8 previous + 16 new) at the elevation of 150–1,378 m a.s.l. with the overall range of 90–1,378 m a.s.l. (Lalremsanga and Zothansiana 2015; Smart et al. 2021).

In conclusion, this work not only elevates and redescribed *S. gorei* to species level, but also proposed three evolutionary lineages of *B. fasciatus* with redescribing *B. fasciatus* sensu stricto, and enlarges the overall elapid fauna of Mizoram. Considering the nature of the studied species being highly venomous elapid snakes, the findings from this work will be critical for further herpetological studies like reproductive behaviour, natural history, planning conservation strategy, population study and threat assessment, or as far as development of comprehensive snakebite management and *omics* sciences for the deadly venomous snakes of Northeast India.

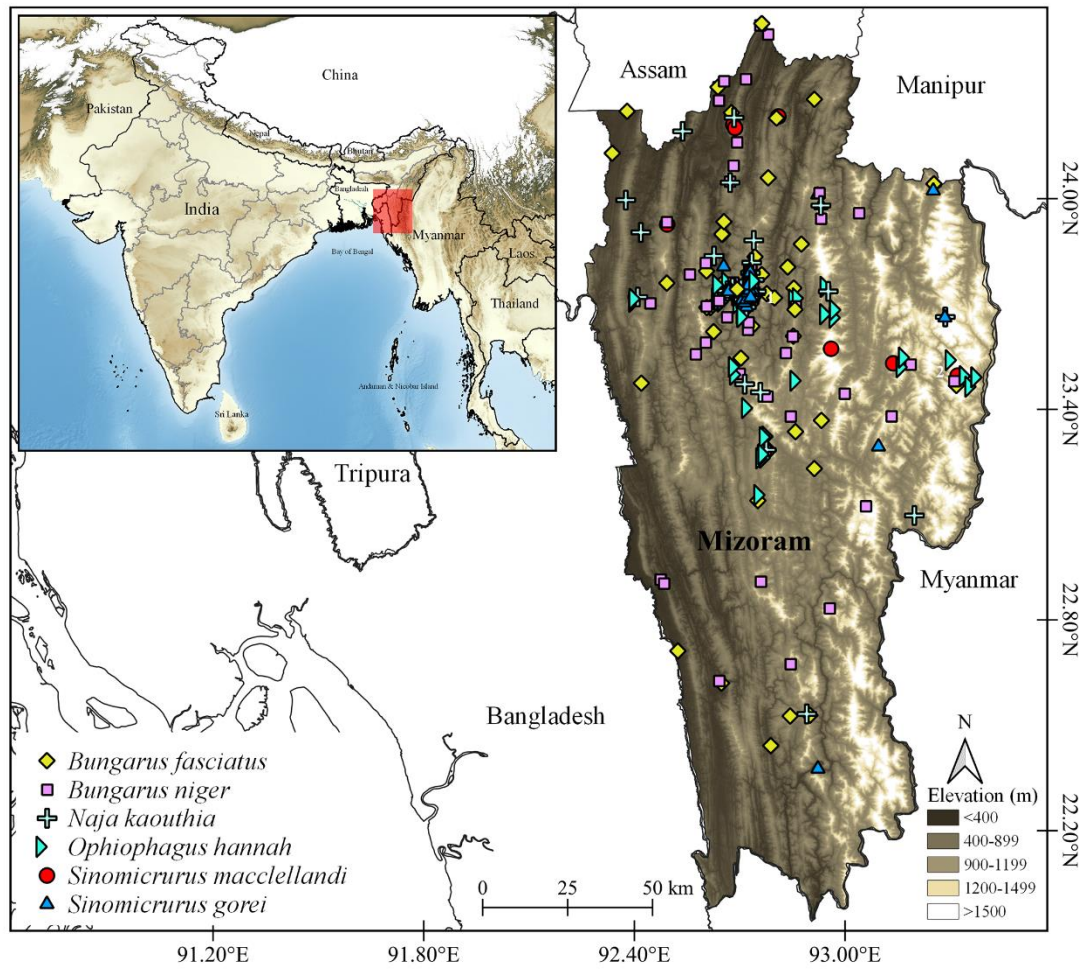


Figure 6.0. Digital elevation map showing the overall distributional records of elapid snakes documented in this study from Mizoram, Northeast India.

References

1. Abtin, E., Nilson, G., Mobaraki, A., Hosseini, A. A., & Dehgannejhad, M. (2014). A new species of krait, *Bungarus* (Reptilia, Elapidae, Bungarinae) and the first record of that genus in Iran. *Russian Journal of Herpetology*, *21*, 243–250.
2. Aengals, R., Kumar, V. S., Palot, M. J., & Ganesh, S.R. (2018). *A checklist of reptiles of India*. Zoological Survey of India, Kolkata.
3. Ahmed, M. F., Das, A., & Dutta, S. K. (2009). *Amphibians and Reptiles of Northeast India. A Photographic Guide*. Aaranyak, India.
4. Ahmed, S. M., Ahmed, M., Nadeem, A., Mahajan, J., Choudhary, A., & Pal, J. (2008). Emergency treatment of a snake bite: Pearls from literature. *Journal of Emergencies, Trauma and Shock*, *1*, 97–105.
5. Ahsan, M. F., & Rahman, M. M. (2017). Status, distribution and threats of kraits (Squamata: Elapidae: *Bungarus*) in Bangladesh. *Journal of Threatened Taxa*, *9*, 9903–9910.
6. Aksornneam, A., Rujirawan, A., Yodthong, S., Sung, Y. H., & Aowphol, A., (2024). A new species of krait of the genus *Bungarus* (Squamata, Elapidae) from Ratchaburi Province, western Thailand. *Zoosystematics and Evolution*, *100*, 141–154.
7. Alencar, L. R., Quental, T. B., Graziotin, F. G., Alfaro, M. L., Martins, M., Venzon, M., & Zaher, H. (2016). Diversification in vipers: Phylogenetic relationships, time of divergence and shifts in speciation rates. *Molecular Phylogenetics and Evolution*, *105*, 50–62.
8. Alfaro, M. E., Karns, D. R., Voris, H. K., Abernathy, E., & Sellins, S. L. (2004). Phylogeny of *Cerberus* (Serpentes: Homalopsinae) and phylogeography of *Cerberus rynchops*: diversification of a coastal marine snake in Southeast Asia. *Journal of Biogeography*, *31*, 1277–1292.
9. Ali, W., Javid, A., Chabber, A.L., Hemmatzadeh, F., Hussain, A., & Bukhari, S.M. (2019). NCBI GenBank direct submission.

10. Amat, F., & Escoriza, D. (2022). Biogeographic Inferences on the Evolutionary History of the King Cobra (*Ophiophagus hannah*, Cantor 1836) Species Complex. *Zoological Studies*, 61, 28.
11. Anwar, M. (2012). First record of banded krait (*Bungarus fasciatus*) from Pilibhit District, Uttar Pradesh-India. *Taprobanica*, 3, 102–103.
12. Arnold, E. N. (1986). Why copulatory organs provide so many useful taxonomic characters: the origin and maintenance of hemipenial differences in lacertid lizards (Reptilia: Lacertidae). *Biological Journal of the Linnean Society*, 29, 263–281.
13. Ashraf, M. R., Nadeem, A., Smith, E. N., Javed, M., Smart, U., Yaqub, T., Hashmi, A. S., & Thammachoti, P. (2019). Phylogenetic analysis of the Common Krait (*Bungarus caeruleus*) in Pakistan based on mitochondrial and nuclear protein coding genes. *Amphibian and Reptile Conservation*, 13, 203–211.
14. Ballard, J. W. O., & Kreitman, M. (1995). Is mitochondrial DNA a strictly neutral marker? *Trends in Ecology and Evolution*, 10, 485–488.
15. Bandelt, H., & Forster, P., Röhl, A. (1999). Median-joining networks for inferring intraspecific phylogenies. *Molecular Biology and Evolution*, 16, 37–48.
16. Bauer, A. M. (1989). Reptiles and the biogeographic interpretation of New Caledonia. *Tuatara*, 30, 39–50.
17. Bauer, A. M., & Lavilla, E. O. (2021). J. G. Schneider's *Historiae Amphibiorum*: Herpetology at the Dawn of the 19th Century. SSAR.
18. Bauer, A. M., Vogel, G., & Campbell, P. D. (2015). A preliminary consideration of the dry snake skin specimens of Patrick Russell. *Hamadryad*, 37, 73–84.
19. Baum D. A., & Shaw K. L. (1995). Genealogical perspectives on the species problem. In Hoch P.C., Stephenson A.G. (Eds.), *Experimental and molecular approaches to plant biosystematics* (pp. 289–303). Missouri Botanical Garden.

20. Benson, D. A., Cavanaugh, M., Clark, K., Karsch-Mizrachi, I., Lipman, D. J., Ostell, J., & Sayers, E.W. (2017). GenBank. *Nucleic Acids Research*, 45, D37.
21. Bhandarkar, W. R., Paliwal, G. T., Bhandarkar, S. V., & Kali, A. A. (2012). Herpetofaunal diversity at navegaon national park, Distt. Gondia Maharashtra. *International Journal of Environmental Rehabilitation and Conservation*, 3, 42–49.
22. Bharos, A. M. (2013). Banded Krait *Bungarus fasciatus* feeding on common Krait *Bungarus caeruleus*. *Journal of the Bombay Natural History Society*, 110, 155–156.
23. Biakzuala, L., Lalrinsanga, Lalremsanga, H. T., Romalsawma, Vanlalhrima, & Laltlanchhuaha, H. (2019). *Bungarus fasciatus* (Banded Krait). Diet. *Herpetological Review*, 50, 797–798.
24. Biakzuala, L., Purkayastha, J., Rathee, Y. S., & Lalremsanga, H.T. (2021). New data on the distribution, morphology, and molecular systematics of two venomous snakes, *Bungarus niger* and *Bungarus lividus* (Serpentes: Elapidae), from north-east India. *Salamandra*, 57, 219–228.
25. Biakzuala, L., Rinsanga, L., Lianzela, S., Romalsawma, Muansanga, L., Decemson, Ht., Vanlalchhuana, M., Tochwawng, L., Laltlanchhuaha, H., & Lalremsanga, H.T. (2022). Collection of vulnerable nests with eggs for the captive incubation of king cobra *Ophiophagus hannah* as a conservation strategy in Mizoram north-east India. *The Herpetological Bulletin*, 159, 18–20.
26. Biakzuala, L., Lalremsanga, H. T., Santra, V., Dhara, A., Ahmed, M. T., Mallick, Z. B., Kuttalam, S., Amarasinghe, A. T., & Malhotra, A. (2023). Molecular phylogeny reveals distinct evolutionary lineages of the banded krait, *Bungarus fasciatus* (Squamata, Elapidae) in Asia. *Scientific Reports*, 13, 2061.
27. Blyth, E. (1854). Report of curator, Zoological Department, for September meeting. *Proceedings of the Asiatic Society of Bengal (Natural History)*, 23, 729–740.

28. Bocage, J. V. B. (1866). Reptiles nouveaux ou peu connus recueillis dans les possessions portugaises de l'Afrique occidentale, qui se trouvent au Muséum de Lisbonne. *Jornal de Sciencias Mathematicas Physicas e Naturales, Academia Real das Sciencias de Lisboa, 1*, 57–78.
29. Boie, F. (1827) Bemerkungen über Merrem's Versuch eines Systems der Amphibien. Marburg. 1820. Erste Lieferung: Ophidier. *Isis von Oken, 20*, 508–566.
30. Bolnick, D. I., Amarasekare, P., Araújo, M. S., Bürger, R., Levine, J. M., Novak, M., Rudolf, V. H. W., Schreiber, S. J., Urbah, M. C., & Vasseur, D. (2011). Why intraspecific trait variation matters in community ecology. *Trends in Ecology and Evolution, 26*, 183–192.
31. Borang, A., Bhatt, B. B., Chaudhury, S. B., Borkotoki, A., & Bhutia, P. T. (2005). Checklist of the snakes of Arunachal Pradesh, northeast India. *Journal of the Bombay Natural History Society, 102*, 19–26.
32. Boruah, B., Das, G. N., Payra, A., Dash, S. K., Pal, N. S., Das, U. P., Kar, N. B., Sethy, J., Palei, H. S., Nandi, D., & Mishra, R. K. (2016). Diversity of herpetofauna and their conservation in and around North Orissa University Campus, Odisha, India. *NeBIO, 7*, 138–145.
33. Bouckaert, R. R. (2010). DensiTree: Making sense of sets of phylogenetic trees. *Bioinformatics, 26*, 1372–1373.
34. Bouckaert, R., Vaughan, T. G., Barido-Sottani, J., Duchene, S., Fourment, M., Gavryushkina, A., Heled, J., Jones, G., Kuhnert, D., De Maio, N., Matschiner, M., Mendes, F. K., Muller, N. F., Ogilvie, H. A., Du Plessis, L., Popinga, A., Rambaut, A., Rasmussen, D., Siveroni, I., ... Drummond, A. J. (2019). BEAST 2.5: An advanced software platform for Bayesian evolutionary analysis. *PLoS Computational Biology, 15*, e1006650.
35. Brown, M. B., & Forsythe, A. B. (1974). Robust tests for the equality of variances. *Journal of American Statistical Association, 69*, 364–367.
36. Brown, R. M., Smart, U., Leviton, A. E., & Smith, E. N. (2018). A new species of long-glanded coralsnake of the genus *Calliophis* (Squamata: Elapidae) from Dinagat Island, with notes on the biogeography and species

- diversity of Philippine Calliophis and Hemibungarus. *Herpetologica*, 74, 89–104.
37. Brown, T. W., & Barazowski, M. B. (2020). Defensive tailcurling and head-mimicking behavior in a variable coralsnake, *Micrurus diastema* (Squamata: Elapidae) in Cusuco National Park, Honduras. *Reptiles & Amphibians*, 27, 231–232.
 38. Burbrink, F. T., & R. Lawson (2007). How and when did Old World ratsnakes disperse into the New World? *Molecular Phylogenetics and Evolution*, 43: 173–189.
 39. Burchfield, P.M. (1977). Breeding the King cobra *Ophiophagus hannah* at Brownsville Zoo. *International Zoo Yearbook*, 17, 136–140.
 40. Cantor, T.E. (1836). Sketch of undescribed hooded serpent with fangs and maxillar teeth. *Asiatic Researches*, 19, 87–94.
 41. Cantor, T. E. (1839). Spicilegium serpentium indicorum [part 1]. Proceedings of the Zoological Society of London, 1839, 31–34.
 42. Camargo, A., Sinervo, B., & Sites, J. W. (2010). Lizards as model organisms for linking phylogeographic and speciation studies. *Molecular Ecology*, 19, 3243–3488.
 43. Cao, S., Guo, L., Luo, H., Yuan, H., Chen, S., Zheng, J., & Lin, R. (2016). Application of COI barcode sequence for the identification of snake medicine (Zaocys). *Mitochondrial DNA Part A*, 27, 483–489.
 44. Capella-Gutiérrez, S., Silla-Martínez, J. M., & Gabaldón, T. (2009). trimAl: a tool for automated alignment trimming in large-scale phylogenetic analyses. *Bioinformatics*, 25, 1972–1973.
 45. Castoe, T.A., Smith, E.N., Brown, R.M., & Parkinson, C. L. (2007). Higher-level phylogeny of Asian and American coralsnakes, their placement within the Elapidae (Squamata), and the systematic affinities of the enigmatic Asian coralsnake *Hemibungarus calligaster*. *Zoological Journal of the Linnean Society*, 151, 809–831.
 46. Castoe, T. A., Streicher, J. W., Meik, J. M., Ingrasci, M. J., Poole, A. W., de Koning, A. P., Campbell, J. A., Parkinson, C. L., Smith, E. N., & Pollock, D. D. (2012). Thousands of microsatellite loci from the venomous coral snake

- Micrurus fulvius* and variability of select loci across populations and related species. – *Molecular Ecology Resources*, 12, 1105–1113.
47. Champion, H. G., & Seth, S. K. (1968). *A Revised Survey of the Forest Types of India*. Manager of publications, Delhi.
 48. Chandra, K., Raha, A., Majumder, A., Parida, A., & Sarsavan, A. (2013). First Record of Banded Krait, *Bungarus fasciatus* (Schneider, 1801), (Reptilia: Elapidae), from Guru Ghasidas National Park, Koriya District, Chhattisgarh, India. *Records of the Zoological Survey of India*, 113, 77–80.
 49. Chao, Z., & Liao, J. (2011). NCBI GenBank direct submission.
 50. Chao, Z., & Liao, J. (2012). NCBI GenBank direct submission.
 51. Charlton, T. (2018). *King cobra. Natural history and captive management*. Natural History Publications (Borneo). Kota Kinabalu, Malaysia.
 52. Chatrath, S. T., Chapeaurouge, A., Lin, Q., Lim, T. K., Dunstan, N., Mirtschin, P., Kumar, P. P., & Kini, R.M. (2011). Identification of novel proteins from the venom of a cryptic snake *Drysdalia coronoides* by a combined transcriptomics and proteomics approach. *Journal of Proteome Research*, 10, 739–750.
 53. Chattopadhyay, B., Garg, K. M., Doss, D. P. S., Vinothkumar, A. K., Kandula, S., Rheindt, F. E., & Ramakrishnan, U. (2021). Cryptic diversity of *Rhinolophus lepidus* in South Asia and differentiation across a biogeographic barrier. *Frontiers in Biogeography*, 13, e49625.
 54. Chen, J., Gan, S., & Zhou, C. (2017). NCBI GenBank direct submission.
 55. Chen, N., & Fu, X.Y. 2008. NCBI GenBank direct submission.
 56. Chen, N., Zhao, S., & Han, L. (2008). NCBI GenBank direct submission.
 57. Chen, Y.L., & Lin, Y.L. (2015). NCBI GenBank direct submission.
 58. Chen, S., Qing J., Liu Z., Liu Y., Tang M., Murphy R. W., Pu Y., Wang X., Tang, K., Guo, K., Jiang, X., & Liu, S. (2020). Multilocus phylogeny and cryptic diversity of white-toothed shrews (Mammalia, Eulipotyphla, Crocidura) in China. *BMC Evolutionary Biology*, 20, 1–14.
 59. Chen, Z. N., Shi, S. C., Vogel, G., Ding, L., & Shi, J. S. (2021). Multiple lines of evidence reveal a new species of Krait (Squamata, Elapidae,

- Bungarus*) from Southwestern China and Northern Myanmar. *Zookeys*, 1025, 35–71.
60. Chippaux, J. P., Williams, V., & White, J. (1991). Snake venom variability: methods of study, results and interpretation. *Toxicon*, 29, 1279–1303.
 61. Conroy, C. J., Papenfuss, T., Parker, J., & Hahn, N. E. (2009). Use of tricainemethanesulfonate (MS222) for euthanasia of reptiles. *Journal of American Association for Laboratory Animal Science*, 48, 28–32.
 62. Consuegra, S., John, E., Verspoor, E., & de Leaniz, C. G. (2015). Patterns of natural selection acting on the mitochondrial genome of a locally adapted fish species. *Genetics Selection Evolution*, 47, 1–10.
 63. Coyne, J.A. (1994). Ernst Mayr and the origin of species. *Evolution*, 48, 19–30.
 64. Daltry, J. C., Wüster, W., & Thorpe, R. S. (1996). Diet and snake venom evolution. *Nature*, 379, 537–540.
 65. Dang, T. T., Nguyen, G. S., Ho, T. L., & Le, X. C. (2011). NCBI GenBank direct submission.
 66. Daniels, J. C. (2002). *Book of Indian Reptiles and Amphibians*. Oxford University Press, London, United Kingdom.
 67. Darriba, D., Taboada, G. L., Doallo, R., & Posada, D. (2012). jModelTest 2: More models, new heuristics and parallel computing. *Nature Methods*, 9, 772–772.
 68. Das, A. (2018). *Notes on Snakes of the Genus Bungarus (Serpentes: Elapidae) from Northeast India*. Indian Hotspots, Springer.
 69. Das, A., Basu, D., Converse, L., & Suresh, C. C. (2012). Herpetofauna of Katarniaghat Wildlife Sanctuary, Uttar Pradesh, India. *Journal of Threatened Taxa*, 4, 2553–2568.
 70. Das, A., Ghosh, A., Giri, V., & Limbu, K.P. (2022). *Bungarus niger* (amended version of 2021 assessment). The IUCN Red List of Threatened Species 2022: e.T127914430A219117076.
 71. Das, I. (2012). *A Naturalist's Guide to the Snakes of South-East Asia*. Edited and designed by D & N Publishing, Bayton, Wiltshire, UK.

72. Dasgupta, G., & Raha, S. (2006). Fauna of Nagaland. In Director (Ed.), *State Fauna Series 12, Reptilia* (pp. 433–460). Zoological Survey of India, Kolkata.
73. Daudin, F. M. (1803). *Histoire Naturelle, Générale et Particulière des Reptiles; Ouvrage faisant suite aux Œuvres de Leclerc de Buffon, et partie de Cours complete d'Histoire naturelle rédigé par C.S. Sonnini, membre de plusieurs Sociétés savantes. Tome cinquième [Volume 5]*. Paris: F. Dufart.
74. David, P., & Ineich, I. (1999). Les serpents venimeux du monde: Systématique et répartition. *Dumerilia*, 3, 3–499.
75. de Queiroz, K. (2007). Species concepts and species delimitation. *Systematic Biology*, 56, 879–886.
76. Deka, A., Bhatia, S., Santra, V., Bharti, O. K., Lalremsanga, H. T., Martin, G., Wüster, W., Owens, J. B., Graham, S., Doley, R., & Malhotra, A. (2023). Multilevel Comparison of Indian Naja Venoms and Their Cross-Reactivity with Indian Polyvalent Antivenoms. *Toxins*, 15, 258.
77. Deshmukh, R. V., Deshmukh, S. A., Badhekar, S. A., & Naitame, R. Y. (2020). Snakes of Bhandara District, Maharashtra, Central India with notes on natural history. *Reptilia Amphibia*, 27, 10–17.
78. DNeasy® Blood & Tissue Handbook (2023). Qiagen. Available at <https://www.qiagen.com/jp/resources/download.aspx?id=68f29296-5a9f-40fa-8b3d-1c148d0b3030&lang=en>.
79. Dolia, J. (2018). Notes on the distribution and natural history of the King Cobra (*Ophiophagus hannah* Cantor, 1836) from the Kumaon Hills of Uttarakhand, India. *Herpetology Notes*, 11, 217–222.
80. Dowling, H. G. (1951). A proposed standard system of counting ventrals in snakes. *British Journal of Herpetology*, 1, 97–99.
81. Dwivedi, A. K., Gupta, B. K., Singh, R. K., Mohindra, V., Chandra, S., Easawarn, S., Jena, J., & Lal, K. K. (2017). Cryptic diversity in the Indian clade of the catfish family Pangasiidae resolved by the description of a new species. *Hydrobiologia*, 797, 351–370.
82. Edgar, R. C. (2004). MUSCLE: multiple sequence alignment with high accuracy and high throughput. *Nucleic Acids Research*, 32, 1792–1797.

83. Faiz, M. A., Ghose, A., Ahsan, M. F., Rahman, M. R., Amin, M. R., Hassan, M. M. U., Chowdhury, M. A. W., Kuch, U., Rocha, T., Harris, J. B., & Theakston, R. D. G. (2010). The greater black krait (*Bungarus niger*), a newly recognized cause of neuro-myotoxic snake bite envenoming in Bangladesh. *Brain*, *133*, 3181–3193.
84. Flint, W. D., & Harris, R. N. (2005). The efficacy of visual encounter surveys for population monitoring of *Plethodon punctatus* (Caudata: Plethodontidae). *Journal of Herpetology*, *39*, 578–584.
85. Fourment, M., & Darling, A. E. (2018). Local and relaxed clocks: The best of both worlds. *PeerJ*, *6*, e5140.
86. Fritze, A. (1894). Die Fauna der Liu-Kiu-Insel Okinawa. *Zoologische Jahrbücher. Abteilung für Systematik, Geographie und Biologie der Tiere*, *7*, 852–926.
87. Fry, B. G., Winkel, K. D., Wickramaratna, J. C., Hodgson, W. C. & Wüster, W. (2003). Effectiveness of snake antivenom: species and regional venom variation and its clinical impact. *Journal of Toxicology: Toxin Review*, *22*, 23–34.
88. Gan, S., & Chen, J. (2015). NCBI GenBank direct submission.
89. Gascon, C., Loughheed, S.C., & Bogart, J. P. (1996). Genetic and morphological variation in *Vanzolinius discodactylus*: a test of the river hypothesis of speciation. *Biotropica*, *28*, 376–387.
90. Ghosh, A., Basu, S., Khatri, H., & Thakur, M. (2018). NCBI GenBank direct submission.
91. Gilman, C. A., Corl, A., Sinervo, B., & Irschick, D. J. (2018). Genital morphology associated with mating strategy in the polymorphic lizard, *Uta stansburiana*. *Journal of Morphology*, *280*, 184–192.
92. GNU Project (2015). GNU PSPP (Version 0.8.5) [Computer Software]. Free Software Foundation.
93. Goncalves, J. M., & Deutsch, H. F. (1956). Ultracentrifugal and zone electrophoresis studies of some Crotalidae venoms. *Archives of Biochemistry and Biophysics*, *60*, 402–411.

94. Gowande, G., Pal, S., Jablonski, D., Masroor, R., Phansalkar, P. U., Dsouza, P., Jayarajan, A., & Shanker, K. (2021). Molecular phylogenetics and taxonomic reassessment of the widespread agamid lizard *Calotes versicolor* (Daudin, 1802) (Squamata, Agamidae) across South Asia. *Vertebrate Zoology*, *71*, 669–696.
95. Gower, J. C. (1966). Some distance properties of latent root and vector methods used in multivariate analysis. *Biometrika* *53*, 325–338.
96. Gray, J. E. (1834). Illustrations of Indian Zoology, chiefly selected from the collection of Major - General Hardwicke. Vol. 2. London (1833-1834): 263 pp.
97. Greene, H. W. (1973). Defensive tail display by snakes and amphisbaenians. *Journal of Herpetology*, *7*, 143–161.
98. Günther, A. (1858). *Catalogue of Colubrine snakes of the British Museum*. London, I - XVI, 1 – 281.
99. Günther, A. (1862). On new species of snakes in the collection of the British Museum. *The Annals and Magazine of Natural History*, *9*, 124–132
100. Günther, A. (1864). *The Reptiles of British India*. Taylor & Francis, London.
101. Günther, A. (1868). Sixth account of new species of snakes in the collection of the British Museum. *The Annals and Magazine of Natural History*, *1*, 413–429.
102. Guo, P., Liu, Q., Zhong, G., Zhu, F., Yan, F., Tang, T., Xiao, R., Fang, M., Wang, P., & Fu, X. (2015). Cryptic diversity of green pitvipers in Yunnan, South-west China (Squamata, Viperidae). *Amphibia Reptilia*, *36*, 265–276.
103. Hakim, J., Trageser, S. J., Ghose, A., Rashid, S. M. A., & Rahman, S. C. (2020). Amphibians and reptiles from Lawachara National Park in Bangladesh. *Check List*, *16*, 1239.
104. Halasan, L. C., Geraldino, P. J. L., & Lin, H. C. (2021). First Evidence of Cryptic Species Diversity and Population Structuring of *Selaroides leptolepis* in the Tropical Western Pacific. *Frontiers in Marine Science*, *8*: 756163.
105. Hammer, O., David A. T. Harper, & Paul D. R. (2001). PAST: Paleontological statistics software package for education and data analysis. *Palaeontologia Electronica*, *4*, 9.

106. Harrison, R. A., Wüster, W., & Theakston, R. D. G. (2003). The conserved structure of snake venom toxins confers extensive immunological cross-reactivity to toxin-specific antibody. *Toxicon*, *41*, 441–449.
107. Heatwole, H. (2009). Biology of the Reptilia. In Carl Gans, Abbot S. Gaunt, and Kraig Adler (Eds.), *Morphology H, the skull of Lepidosauria* (Vol. 20, 610–611).
108. Heigl, F., Horvath, K., Laaha, G., & Zaller, J. G. (2017). Amphibian and reptile road-kills on tertiary roads in relation to landscape structure: using a citizen science approach with open-access land cover data. *BMC Ecology*, *17*, 1–11.
109. Hia, Y. L., Tan, K. Y., & Tan, C. H. (2020). Comparative venom proteomics of banded krait (*Bungarus fasciatus*) from five geographical locales: Correlation of venom lethality, immunoreactivity and antivenom neutralization. *Acta Tropica*, *207*, 105460.
110. Hillis, D. M. (2019). Species delimitation in herpetology. *Journal of Herpetology*, *53*, 3–12.
111. Hobbs, R. J., Hussey, B. M. J., & Saunder, D. A. (1990). Nature Conservation: the Role of Corridors. *Journal of Environmental Management*, *31*, 93–94.
112. Hohenegger, J. (2014). Species as the basic units in evolution and biodiversity: Recognition of species in the Recent and geological past as exemplified by larger foraminifera. *Gondwana Research*, *25*, 707–728.
113. Hotaling S., Foley M. E., Lawrence N. M., Bocanegra J., Blanco M. B., Rasoloarison R., Kappeler P. M., Barrett M. A., Yoder A. D., & Weisrock D. W. (2016). Species discovery and validation in a cryptic radiation of endangered primates: coalescent-based species delimitation in Madagascar's mouse lemurs. *Molecular Ecology*, *25*, 2029–2045.
114. Hrima, V. L., Sailo, V. H., Fanai, Z., Lalronunga, S., Zothansiana, C. L., & Lalremsanga, H. T. (2014). *Nesting ecology of the king cobra, Ophiophagus hannah (Reptilia: Squamata: Elapidae) in Aizawl District, Mizoram, India*. Issues and Trends of Wild life Conservation in Northeast India.

115. Huang, W. S., Greene, H. W., Chang, T. J., & Shine, R. (2011). Territorial behavior in Taiwanese kukrisnakes (*Oligodon formosanus*). *Proceedings of the National Academy of Sciences of the United States of America*, *108*, 7455–7459.
116. Hussain, A. (2020). New Record of Banded Krait *Bungarus fasciatus* (Schneider, 1801) from Ranchi (Jharkhand) with its Preying on Checkered Keel-Back Snake. *Biological Forum*, *12*, 29–32.
117. Ingle, M. (2011). Herpetofauna of Naglok Region, Jashpur District, Chhattisgarh. *Records of the Zoological Survey of India*, *111*, 99–109 (2011).
118. Islam, N.N., Sajib, A.A., Ahmed, M.S., & Islam, M.S. (2020). NCBI GenBank direct submission.
119. Jirsová, D., Štefka, J., Blažek, R., Malala, J. O., Lotuliakou, D. E., Mahmoud, Z.N., & Jirků, M. (2019). From taxonomic deflation to newly detected cryptic species: Hidden diversity in a widespread African squeaker catfish. *Scientific Reports*, *9*, 15748.
120. Jones, M. D. (2020). The spatial ecology of king cobras (*Ophiophagus hannah*) in the Sakaerat Biosphere Reserve, Northeast Thailand. PhD Thesis, School of Biology Institute of Science Suranaree University of Technology.
121. Jones, M. D., Marshall, B. M., Smith, S. N., Crane, M., Silva, I., Artchawakom, T., Suwanwaree, P., Waengsothorn, S., Wüster, W., Goode, M., & Strine, C. T. (2022). How do King Cobras move across a major highway? Unintentional wildlife crossing structures may facilitate movement. *Ecology and Evolution*, *12*, p.e8691.
122. Joshi, P. S., Charjan, A. P., & Tantarapale, V. T. (2017). A herpetofaunal inventory of Vidarbha region, Maharashtra, India. *Bioscience Discovery*, *8*, 582–587.
123. Kaito, T., Ota, H., & Toda, M. (2017). The evolutionary history and taxonomic reevaluation of the Japanese coral snake, *Sinomicrurus japonicus* (Serpentes, Elapidae), endemic to the Ryukyu Archipelago, Japan, by use of molecular and morphological analyses. *Journal of Zoological Systematics and Evolutionary Research*, *55*, 156–166.

124. Kaliontzopoulou, A., Pinho, C., & Martínez-Freiría, F. (2018). Where does diversity come from? Linking geographical patterns of morphological, genetic, and environmental variation in wall lizards. *BMC Evolutionary Biology*, *18*, 1–13.
125. Kalyaanamoorthy, S., Minh, B. Q., Wong, T. K., Von Haeseler, A., Jermini, L. S. (2017). ModelFinder: fast model selection for accurate phylogenetic estimates. *Nature Methods*, *14*, 587–589.
126. Kannan, R. (1993). Nest-desertion by a king cobra (*Ophiophagus hannah*). *Journal of the Bombay Natural History Society*, *90*, 519–520.
127. Kazandjian, T. D., Petras, D., Robinson, S. D., van Thiel, J., Greene, H. W., Arbuckle, K., Barlow, A., Carter, D. A., Wouters, R. M., Whiteley, G., Wagstaff, S. C., et al. (2021). Convergent evolution of pain-inducing defensive venom components in spitting cobras. *Science*, *371*, 386–390.
128. Kazemi, E., Nazarizadeh, M., Fatemizadeh, F., Khani, A., & Kaboli, M. (2021). The phylogeny, phylogeography, and diversification history of the westernmost Asian cobra (Serpentes: Elapidae: *Naja oxiana*) in the Trans-Caspian region. *Ecology and Evolution*, *11*, 2024–2039.
129. Kekäläinen, J., Kähkönen, J., Kiviniemi, V., & Huuskonen, H. (2010). Morphological variation of perch *Perca fluviatilis* in humic lakes: the effect of predator density, competition and prey abundance. *Journal of Fish Biology*, *76*, 787–799.
130. Kelly, C. M., Barker, N. P., Villet, M. H., & Broadley, D. G. (2009). Phylogeny, biogeography and classification of the snake superfamily Elapoidea: a rapid radiation in the late Eocene. *Cladistics*, *25*, 38–63.
131. Keogh, J. S. (1999). Evolutionary implications of hemipenial morphology in the terrestrial Australian elapid snakes. *Zoological Journal of the Linnean Society*, *125*, 239–278.
132. Keogh, J. S. (1998). Molecular phylogeny of elapid snakes and a consideration of their biogeographic history. *Biological Journal of the Linnean Society*, **63**, 177–203.
133. Kinghorn, J. R. (1923). A New Genus of Elapine Snake from Northern Australia. *Records of the Australian Museum*, *14*, 42–45.

134. Kinnear, N. B. (1913). Banded Krait (*Bungarus fasciatus*) in Hyderabad State. *Journal of Bombay Natural History Society*, 22, 635–636.
135. Klaczko, J., Ingram, T., & Losos, J. (2015). Genitals evolve faster than other traits in *Anolis* lizards. *Journal of Zoology*, 295, 44–48.
136. Knierim, T. K., Strine, C. T., Suwanwaree, P., & Hill III, J. G. (2019). Spatial ecology study reveals nest attendance and habitat preference of banded kraits (*Bungarus fasciatus*). *The Herpetological Bulletin*, 150, 6–13.
137. Koirala, B. K., & Tshering, D. (2021). Distribution, habitat use, and nesting behavior of the King Cobra (*Ophiophagus hannah*) in the Trashigang Forest Division, Eastern Bhutan. *Reptiles & Amphibians*, 28, 397–403.
138. Krefft, G. (1869). *The Snakes of Australia; An Illustrated and Descriptive Catalogue of All the Known Species*. Thomas Richards, Government Printer, Sydney.
139. Kuch, U., & Mebs, D. (2007). The identity of the Javan Krait, *Bungarus javanicus* Kopstein, 1932 (Squamata: Elapidae): evidence from mitochondrial and nuclear DNA sequence analyses and morphology. *Zootaxa*, 1426, 1–26.
140. Kuch, U., Kizirian, D., Truong, N.Q., Lawson, R., Donnelly, M. A., & Mebs, D. (2005). A new species of krait (Squamata: Elapidae) from the Red River system of northern Vietnam. *Copeia*, 2005, 818–833.
141. Kundu, S., Lalremsanga, H. T., Tyagi, K., Biakzuala, L., Kumar, V., & Chandra, K. (2020a). Mitochondrial DNA discriminates distinct population of two deadly snakes (Reptilia: Elapidae) in Northeast India. *Mitochondrial DNA Part B: Resources*, 5, 1530–1534.
142. Kundu, S., Lalremsanga, H. T., Rahman, M. M., Ahsan, M. F., Biakzuala, L., Kumar, V., Chandra, K., & Siddiki, A. Z. (2020b). DNA barcoding elucidates the population genetic diversity of venomous cobra species (Reptilia: Elapidae) in Indo-Bangladesh region. *Mitochondrial DNA B: Resources*, 5, 2525–2530.
143. Lalbiakzuala (2019). Study on the morphology, Distribution and Phylogenetic Status of the Genus *Bungarus* (Reptilia: Serpentes: Elapidae) in Mizoram, India. M.Phil Dissertation, Department of Zoology, Mizoram University.

144. Lalremsanga, H. T., & Lalronunga, S. (2017). Mizoram rul chanchin. Bhabani Offset PVT. LTD.
145. Lalremsanga, H. T., Sailo, S., & Chinliansiamia, H. (2011). Diversity of Snakes (Reptilia: Squamata) and role of environmental factors in their distribution in Mizoram, Northeast India. *Advances in Environmental Chemistry*, *64*, 265–269.
146. Lalremsanga, H. T., & Zothansiamia (2015). Morphological variations in *Sinomicrurus macclellandi macclellandi* (Serpentes: Elapidae), the only coral snake species in northeast India. *Science Vision*, *15*, 212–221.
147. Laltanpuia, T. C., Lalrinchhana, C., Lalnunsanga, Lalrotluanga, Hmingthansanga, R., Kumari, A., Vanlalsawmi, R., Lalrintluangi, S., & Lalremsanga, H. T. (2008). Snakes (Reptilia: Serpentes) of Mizoram University Campus, Tanhril, Aizawl with notes on their identification keys [in Mizo]. *Science Vision*, *8*, 112–127.
148. Lanfear, R., Frandsen, P. B., Wright, A. M., Senfeld, T., & Calcott, B. (2017). PartitionFinder 2: new methods for selecting partitioned models of evolution for molecular and morphological phylogenetic analyses. *Molecular Biology and Evolution*, *34*, 772–773.
149. Laopichienpong, N., Muangmai, N., Supikamolseini, A., Twilprawat, P., Chanhom, L., Suntrarachun, S., Peyachoknagul, S., & Srikulnath, K. (2016). Assessment of snake DNA barcodes based on mitochondrial COI and Cytb genes revealed multiple putative cryptic species in Thailand. *Gene*, *594*, 238–247.
150. Laurance, W. F., Goosem, M., & Laurance, S. G. (2009). Impacts of roads and linear clearings on tropical forests. *Trends in Ecology and Evolution*, *24*, 659–669.
151. Laurenti, J. N. (1768). *Specimen medicum, exhibens synopsis reptilium emendatam cum experimentis circa venena et antidota reptilium austracorum, quod auctoritate et consensu*. Joan, Thomae, Vienna.
152. Laxme, S. R. R., Attarde, S., Khochare, S., Suranse, V., Martin, G., Casewell, N.R., Whitaker, R., & Sunagar, K. (2021). Biogeographical venom variation in the Indian spectacled cobra (*Naja naja*) underscores the pressing need for

- pan-India efficacious snakebite therapy. *PLOS Neglected Tropical Diseases*, *15*, e0009150.
153. Lee, M. S., Sanders, K. L., King, B., & Palci, A. (2016). Diversification rates and phenotypic evolution in venomous snakes (Elapidae). *Royal Society Open Science*, *3*, 150277.
 154. Leigh, J. W., Bryant, D. (2015). POPART: full-feature software for haplotype network construction. *Methods in Ecology and Evolution*, *6*, 1110–1116.
 155. Letunic I, & Bork, P. (2021). Interactive Tree Of Life (iTOL) v5: an online tool for phylogenetic tree display and annotation. *Nucleic Acids Research*, *49*, W293–W296.
 156. Lesson, R. P. (1831). Catalogue des Reptiles qui font partie d'une Collection zoologique recueillie dans l'Inde continentale ou en Afrique, et apportée en France par M. Lamare-Piquot. *Bulletin des Sciences Naturelles et de Géologie, Paris*, *25*, 119–123.
 157. Levene, H. (1961). Robust tests for equality of variances. In Olkin I et al. (Eds.), *Contributions to probability and statistics. Essays in honor of Harold Hotelling* (pp. 279–292). Stanford University Press, California.
 158. Leviton, A. E., Zug, G. R., Vindum, J. V., & Wogan, G. O. (2008). *Handbook to the dangerously venomous snakes of Myanmar*. California Academy of Sciences, San Francisco.
 159. Li, J. N., Liang, D., Wang, Y. Y., Guo, P., Huang, S., & Zhang, P. (2020). A large-scale systematic framework of Chinese snakes based on a unified multilocus marker system. *Molecular Phylogenetics and Evolution*, *148*, 106807.
 160. Lim, K. K., Leong, T. M., & Lim, F. L. (2011). The king cobra, *Ophiophagus hannah* (Cantor) in Singapore (Reptilia: Squamata: Elapidae). *Nature in Singapore*, *4*, 143–156.
 161. Limbu, K. P., Ghosh, A., Das, A., & Giri, V. (2022). *Bungarus lividus* (amended version of 2021 assessment). The IUCN Red List of Threatened Species 2022: e.T127914543A219117279.
 162. Liu, Q., Yan, J.-W., Hou, S.-B., Wang, P., Nguyen, S. N., Murphy, R. W., Che, J., & Guo, P. (2020). A new species of the genus *Sinomicrurus*

- (Serpentes: Elapidae) from China and Vietnam. *Zoological Research*, 41, 1–5.
163. Lo, T. B., & Lu, H. S. (1978). Studies on *Bungarus fasciatus* venom. *Toxins*, 1978, 161–181.
 164. Lohman, D. J., Ingram, K. K., Prawiradilaga D. M., Winker, K., Sheldon, F. H., Moyle, R. G., Ng, P. K. L., Ong, P. S., Wang, L. K., Braile, T. M., Astuti, D., & Meier, R. (2010). Cryptic genetic diversity in “widespread” Southeast Asian bird species suggests that Philippine avian endemism is gravely underestimated. *Biological Conservation*, 143, 1885–1890.
 165. Loveridge, A. (1946). *Reptiles of Pacific World*. Macmillan company, New York.
 166. Lu, J., Yang, H., Yu, H., Gao, W., Lai, R., Liu, J., & Liang, X. (2008). A novel serine protease inhibitor from *Bungarus fasciatus* venom. *Peptides*, 29, 369–374.
 167. Lukoschek, V., Scott Keogh, J., & Avise, J.C. (2012). Evaluating fossil calibrations for dating phylogenies in light of rates of molecular evolution: a comparison of three approaches. *Systematic Biology*, 61, 22.
 168. Luo, A., Ling, C., Ho, S. Y., & Zhu, C. D. (2018). Comparison of methods for molecular species delimitation across a range of speciation scenarios. *Systematic Biology*, 67, 830–846.
 169. Majumder, J., Bhattacharjee, P. P., Majumdar, K., Debnath, C. & Agarwala, B. K. (2012). Documentation of herpetofaunal species richness in Tripura, northeast India. *NeBio*, 3, 60–70.
 170. Maki, M. (1935). A new poisonous snake (*Calliophis iwasakii*) from Loo-Choo. *Transactions of the Natural History Society of Formosa, Taihoku*, 25, 216–219.
 171. Malhotra, A., Dawson, K., Guo, P., & Thorpe, R. S. (2011). Phylogenetic structure and species boundaries in the mountain pitviper *Ovophis monticola* (Serpentes: Viperidae: Crotalinae) in Asia. *Molecular Phylogenetics and Evolution*, 59, 444–457.
 172. Mallik, A. K., Srikanthan, A. N., Pal, S. P., D’souza, P. M., Shanker, K., & Ganesh, S.R. (2020). Disentangling vines: a study of morphological crypsis

- and genetic divergence in vine snakes (Squamata: Colubridae: *Ahaetulla*) with the description of five new species from Peninsular India. *Zootaxa*, 4874, 1–62.
173. Marshall, B. M., Strine, C. T., Jones, M. D., Artchawakom, T., Silva, I., Suwanwaree, P., & Goode, M. (2019). Space fit for a king: spatial ecology of king cobras (*Ophiophagus hannah*) in Sakaerat Biosphere Reserve, Northeastern Thailand. *Amphibia Reptilia*, 40, 163–178.
 174. Mason, V. C., Li, G., Minx, P., Schmitz, J., Churakov, G., Doronina, L., Melin, A. D., Dominy, N. J., Lim, N. T., Springer, M. S., Wilson, R. K., Warren, W. C., Helgen, K. M., & Murphy, W. J. (2016). Genomic analysis reveals hidden biodiversity within colugos, the sister group to primates. *Science Advances*, 2, e1600633.
 175. Masson, J. (1930). The distribution of the Banded Krait (*Bungarus fasciatus*). *Journal of Bombay Natural History Society*, 34, 256–257.
 176. Mathew, R. (1983). On a collection of snakes from North-east India (Reptilia: Serpentes). *Records of the Zoological Survey of India*, 80, 449–458.
 177. Mathew, R. (1995). Fauna of Meghalaya, Part I. In Director (Ed.), *State Fauna Series 4, Reptilia* (pp. 379–454). Zoological Survey of India, Kolkata.
 178. Matthew, R. (2007). Fauna of Mizoram. In Director (Ed.), *State Fauna Series No. 14, Reptilia* (pp. 545–577). Zoological Survey of India, Kolkata.
 179. Mayr, E. (1942). *Systematics and the origin of species*. Columbia University Press, New York.
 180. McCarthy, C.J. (1985). Monophyly of elapid snakes (Serpentes: Elapidae). An assessment of the evidence. *Zoological Journal of the Linnean Society*, 83, 79–93.
 181. McDowell, S. B. (1986). The architecture of the corner of the mouth of colubroid snakes. *Journal of Herpetology*, 353–407.
 182. McDowell, S. B. (1987). *Systematics. Snakes: Ecology and evolutionary biology*. Macmillan Publ. Co.
 183. Melaun, C., & Kuch, U. (2010). NCBI GenBank direct submission.
 184. Midtgaard, R. (2022). Repfocus, a Survey of the Reptiles of the World <http://repfocus.dk/Bungarus.html>.

185. Miles, D. B., Snell, H. L., & Snell, H. M. (2001). Intrapopulation variation in endurance of Galapagos lava lizards (*Microlophus albemarlensis*): evidence for an interaction between natural and sexual selection. *Evolutionary Ecology Research*, 3, 795–804.
186. Minh, B. Q., Nguyen, M. A. T., & von Haeseler, A. (2013) Ultrafast approximation for phylogenetic bootstrap. *Molecular Biology and Evolution*, 30, 1188–1195.
187. Mirza, Z. A., Varma, V., & Campbell, P. D. (2020). On the systematic status of *Calliophis macclellandi nigriventer* Wall, 1908 (Reptilia: Serpentes: Elapidae). *Zootaxa*, 4821, 105–120.
188. Mohapatra, P. P., Ray, S., Sarkar, S., Deuti, K., Palot, M. J., Sethy, P. G. S., & Bahuguna, A. (2024). *Checklist of Fauna of India: Chordata: Reptilia. Online version 1.0.* Zoological Survey of India. Kolkatta.
189. Mukherjee, A. K., & Mackessy, S. P. (2021). Prevention and improvement of clinical management of snakebite in Southern Asian countries: a proposed road map. *Toxicon*, 200, 140–152.
190. Mullis, K., Faloona, F., Scharf, S., Saiki, R., Horn, G., & Erlich, H. (1986). *Specific enzymatic amplification of DNA in vitro: the polymerase chain reaction.* In Cold Spring Harbor symposia on quantitative biology (Vol. 51, pp. 263–273). Cold Spring Harbor Laboratory Press, New York.
191. Myers, C. W., & McDowell, S. B. (2014). New Taxa and Cryptic Species of Neotropical Snakes (Xenodontinae), with Commentary on Hemipenes as Generic and Specific Characters. *Bulletin of the American Museum of Natural History*, 385, 1–112.
192. Nagy, Z. T., Joger, U., Wink, M., Glaw, F., & Vences, M. (2003). Multiple colonization of Madagascar and Socotra by colubrid snakes: evidence from nuclear and mitochondrial gene phylogenies. *Proceedings of the Royal Society of London. Series B: Biological Sciences*, 270, 2613–2621.
193. Nater, A., Mattle-Greminger, M. P., Nurcahyo, A., Nowak, M. G., De Manuel, M., Desai, T., Groves, C., Pybus, M., Sonay, T. B., Roos, C., & Lameira, A.R. (2017). Morphometric, behavioral, and genomic evidence for a new orangutan species. *Current Biology*, 27, 3487–3498.

194. Neang, T., Chan, S., Chhin, S., Samorn, V., Poyarkov, N. A., Stephens, J., Daltry, J. C., & Stuart, B. L. (2017). First records of three snake species from Cambodia. *Cambodian Journal of Natural History*, 2, 142–146.
195. Nguyen, L. T., Schmidt, H. A., von Haeseler, A., Minh, B. Q. (2015). IQ-TREE: A fast and effective stochastic algorithm for estimating maximum likelihood phylogenies. *Molecular Biology and Evolution*, 32, 268–274.
196. Nguyen, S. N., Nguyen, V. D. H., Nguyen, T. Q., Le, N. T. T., Nguyen, L. T., Vo, B. D., Vindum, J. V., Murphy, R. W., Che, J., & Zhang, Y. P. (2017). A new color pattern of the *Bungarus candidus* complex (Squamata: Elapidae) from Vietnam based on morphological and molecular data. *Zootaxa*, 4268, 563–572.
197. Niemiller, M. L., Davis, M., Tan, M., Apodaca, J. J., Dooley, K. E., Cucalón, R. V., Benito, J. B., Niemiller, K., Hardman, R. H., Istvanko, D., & Thames, D. (2022). Mitochondrial DNA and Population Genomics Reveal Additional Cryptic Diversity in the Green Salamander (Subgenus *Castaneides*) Species Complex. *Frontiers in Conservation Science*, 3, 890859.
198. Nishikawa, K., Matsui, M., Yong, H. S., Ahmad, N., Yambun, P., Belabut, D. M., Sudin, A., Hamidy, A., Orlov, N. L., Ota, H., & Yoshikawa, N. (2012). Molecular phylogeny and biogeography of caecilians from Southeast Asia (Amphibia, Gymnophiona, Ichthyophiidae), with special reference to high cryptic species diversity in Sundaland. *Molecular Phylogenetics and Evolution*, 63, 714–723.
199. Nunes, P. M. S., Fouquet, A., Curcio, F. F., Kok, P. J. R., & Rodrigues, M. T. (2012). Cryptic species in *Iphisa elegans* Gray, 1851 (Squamata: Gymnophthalmidae) revealed by hemipenial morphology and molecular data. *Zoological Journal of the Linnean Society*, 166, 361–376.
200. Orgogozo, V., Morizot, B., & Martin, A. (2015). The differential view of genotype phenotype relationships. *Frontiers in Genetics*, 6, 179.
201. Outlaw, D. C., & Voelker, G. (2008). Pliocene climatic change in insular Southeast Asia as an engine of diversification in *Ficedula* flycatchers. *Journal of Biogeography*, 35, 739–752.

202. Pandey, D. P., Sharma, S. K., Alirol, E., Chappuis, F., & Kuch, U. (2016). Fatal neurotoxic envenomation following the bite of a greater black krait (*Bungarus niger*) in Nepal: a case report. *Journal of Venomous Animals and Toxins including Tropical Diseases*, 22, 19.
203. Pawar, S., & Birand, A. (2001). *A survey of amphibians, reptiles, and birds in Northeast India*. Centre for Ecological Research and Conservation, India.
204. Pe, T., Myint, T., Htut, A., Htut, T., Myint, A. A., & Aung, N.N. (1997). Envenoming by Chinese krait (*Bungarus multicinctus*) and banded krait (*B. fasciatus*) in Myanmar. *Transactions of the Royal Society of Tropical Medicine and Hygiene*, 91, 686–688.
205. Peng, L., Wang, L., Ding, L., Zhu, Y., Luo, J., Yang, D., Huang, R., Lu, S., & Huang, S. (2018). A new species of the genus *Sinomicrurus* Slowinski, Boundy and Lawson, 2001 (Squamata: Elapidae) from Hainan Province, China. *Asian Herpetological Research*, 9, 65–73.
206. Peters, W.C.H. (1872). *Über drei neue Schlangenarten (Calamaria bitorques, Stenognathus brevirostris und Hemibungarus gemianulis) von den Philippinen*. *Monatsber. königl. Akad, Wiss, Berlin*.
207. Pfenninger, M., & Schwenk, K. (2007). Cryptic animal species are homogeneously distributed among taxa and biogeographical regions. *BMC Evolutionary Biology*, 7, 121–127.
208. Pook, C. E., Joger, U., Stümpel, N., & Wüster, W. (2009). When continents collide: phylogeny, historical biogeography and systematics of the medically important viper genus *Echis* (Squamata: Serpentes: Viperidae). *Molecular Phylogenetics and Evolution*, 53, 792–807.
209. Pope, C. H. (1928). Seven new reptiles from Fukien Province, China. *American Museum Novitates*, 320, 1–6.
210. Puillandre, N., Brouillet, S., & Achaz, G. (2021). ASAP: assemble species by automatic partitioning. *Molecular Ecology Resources*, 21, 609–620.
211. Puinongpo, W., Singchat, W., Petpradub, S., Kraichak, E., Nunome, M., Laopichienpong, N., Thongchum, R., Intarasorn, T., Sillapaprayoon, S., Indananda, C., & Muangmai, N. (2020). Existence of Bov-B LINE

- retrotransposons in snake lineages reveals recent multiple horizontal gene transfers with copy number variation. *Genes*, *11*, 1241.
212. Puerto, G., da Graça Salomão, M., Theakston, R. D. G., Thorpe, R. S., Warrell, D. A., & Wüster, W. (2001). Combining mitochondrial DNA sequences and morphological data to infer species boundaries: phylogeography of lanceheaded pitvipers in the Brazilian Atlantic Forest, and the status of *Bothrops pradoi* (Squamata: Serpentes: Viperidae). *Journal of Evolutionary Biology*, *14*, 527–538.
 213. Purkayastha, J., Das, M., & Sengupta, S. (2011). Urban herpetofauna: a case study in Guwahati City of Assam, India. *Herpetology Notes*, *4*, 195–202.
 214. Pyron, R. A., Kandambi, H. D., Hendry, C. R., Pushpamal, V., Burbrink, F. T., & Somaweera, R. (2013a). Genus-level phylogeny of snakes reveals the origins of species richness in Sri Lanka. *Molecular Phylogenetics and Evolution*, *66*, 969–978.
 215. Pyron, R. A., Burbrink, F. T., & Wiens, J. J. (2013b). A phylogeny and revised classification of Squamata, including 4161 species of lizards and snakes. *BMC Evolutionary Biology*, *13*, 1–53.
 216. Rahman, M. M., Ahsan, M. F., Bhuiya, B. A., & Kundu, S. (2014). NCBI GenBank direct submission.
 217. Rahman, M., Ahsan, F., Al Haidar, I. K., & Islam, A. (2017). First confirmed record of the Maclelland's Coral Snake *Sinomicrurus maclellandi* (Reinhardt, 1844) from Bangladesh. *Russian Journal of Herpetology*, *24*, 241–244.
 218. Rambaut, A., Drummond, A. J., Xie, D., Baele, G., & Suchard, M. A. (2018). Posterior summarization in Bayesian phylogenetics using Tracer 1.7. *Systematic Biology*, *67*: 901–904.
 219. Ramesh, V., Vijayakumar, S. P., Gopalakrishna, T., Jayarajan, A., & Shanker, K. (2020). Determining levels of cryptic diversity within the endemic frog genera, *Indirana* and *Walkerana*, of the Western Ghats, India. *Plos One*. *15*, e0237431.
 220. Ratnarathorn, N., Harnyuttanakorn, P., Chanhom, L., Evans, S. E., Day, J. J. (2019). Geographical differentiation and cryptic diversity in the monocled

- cobra, *Naja kaouthia* (Elapidae), from Thailand. *Zoologica Scripta*, 48, 711–726.
221. Raveendran, D. K., Deepak, V., Smith, E. N., & Smart, U. (2017). A new colour morph of *Calliophis bibroni* (Squamata: Elapidae) and evidence for Müllerian mimicry in Tropical Indian coralsnakes. *Herpetology Notes*, 10, 209–217.
222. Reinhardt, J. T. (1844). Description of a new species of venomous snake, *Elaps macclellandi*. *Calcutta Journal of Natural History*, 4, 532–534.
223. Rheindt, F. E., Wu, M. Y., Movin, N., & Jønsson, K. A. (2022). Cryptic species-level diversity in Dark-throated Oriole *Oriolus xanthonotus*. *Bulletin of the British Ornithologists' Club*, 142, 254–267.
224. Ronquist, F., Teslenko, M., Van Der Mark, P., Ayres, D. L., Darling, A., Höhna, S., Larget, B., Liu, L., Suchard, M. A., & Huelsenbeck, J. P. (2012). MrBayes 3.2: efficient Bayesian phylogenetic inference and model choice across a large model space. *Systematic Biology*, 61, 539–542.
225. Rozas, J., Ferrer-Mata, A., Sánchez-DelBarrio, J. C., Guirao-Rico, S., Librado, P., Ramos-Onsins, S. E., & Sánchez-Gracia, A. (2017). DnaSP 6: DNA sequence polymorphism analysis of large data sets. *Molecular Biology and Evolution*, 34, 3299–3302.
226. Rusmili, M. R. A., Yee, T. T., Mustafa, M. R., Hodgson, W. C., & Othman, I. (2014). Proteomic characterization and comparison of Malaysian *Bungarus candidus* and *Bungarus fasciatus* venoms. *Journal of Proteomics*, 110, 129–144.
227. Russell, P. (1796). *An Account of Indian Serpents, collected on the Coast of Coromandel: Containing Descriptions and Drawings of Each Species; Together with Experiments and Remarks on Their Several Poisons*. W. Bulmer and Co.
228. Ryabinin, V. V., Ziganshin, R. H., Starkov, V. G., Tsetlin, V. I., Utkin, Y. N. (2019). Intraspecific variability in the composition of the venom from Monocled cobra (*Naja kaouthia*). *Russian Journal of Bioorganic Chemistry*, 45, 107–121.

229. Rytwinski, T., & Fahrig, L. (2015). *The impacts of roads and traffic on terrestrial animal populations. Handbook road ecology. 1st Edition.* Wiley, West Sussex.
230. Sanders, K. L., Lee, M. S. Y. (2008). Molecular evidence for a rapid late-Miocene radiation of Australasian venomous snakes. *Molecular Phylogenetics and Evolution*, *46*, 1165–1173.
231. Sanders, K. L., Lee, M. S., Leys, R., Foster, R., & Keogh, J. S. (2008). Molecular phylogeny and divergence dates for Australasian elapids and sea snakes (Hydrophiinae): evidence from seven genes for rapid evolutionary radiations. *Journal of Evolutionary Biology*, *21*, 682–695.
232. Santra, V., Owens, J. B., Graham, S., Wüster, W., Kuttalam, S. R., Bharti, O., Selvan, M., Mukherjee, N., & Malhotra, A. (2019). Confirmation of *Naja oxiana* in Himachal Pradesh, India. *The Herpetological Bulletin*, *150*, 26–28.
233. Savage, J. M. (1995). Systematics and the biodiversity crisis. *BioScience*, *45*, 673–679.
234. Schlegel, H. (1848). Over *Elaps jamesonii* Traillust. *Bijdragen tot de Dierkunde*, *1*, 5.
235. Schmidt, K. P. (1928). Notes on American coral snakes. *Bulletin of the Antivenin Institute of America*, *2*, 63–64
236. Schmidt, K. P. (1937). The history of *Elaps collaris* SCHLEGEL 1837-1937. *Field Museum of Natural History*, *20*, 361-364
237. Schmidt, K. P., & Inger, R. F. (1957). *Living Reptiles of the World*. Hanover House. Garden City, New York.
238. Schneider, J. G. (1801). *Historiae Amphibiorum Naturalis et Literariae. Fasciculus Secundus Continens Crocodilos, Scincos, Chamaesauras, Boas. Pseudoboas, Elapes, Angues. Amphisbaenas et Caecilias.* Frommanni, Germany.
239. Shankar, P. G., Swamy, P., Williams, R. C., Ganesh, S. R., Moss, M., Höglund, J., Das, I., Sahoo, G., Vijayakumar, S. P., Shanker, K., & Wüster, W. (2021). King or royal family? Testing for species boundaries in the King Cobra, *Ophiophagus hannah* (Cantor, 1836), using morphology and

- multilocus DNA analyses. *Molecular Phylogenetics and Evolution*, 165, 107300.
240. Sharma, R. C. (2007). *The fauna of India and the adjacent countries, Vol. 3, Reptilia (Serpentes)*. Zoological Survey of India, Kolkata.
241. Sheehy, C. M. (2012). Phylogenetic relationships of neotropical snail-eating snakes. PhD Thesis. University of Texas at Arlington.
242. Shi, S. C., Vogel, G., Ding, L., Rao, D. Q., Liu, S., Zhang, L., Wu, Z.J., & Chen, Z. N. (2022). Description of a New Cobra (*Naja Laurenti*, 1768; Squamata, Elapidae) from China with Designation of a Neotype for *Naja atra*. *Animals*, 12, 3481.
243. Shine, R. (1982). Ecology of the Australian elapid snake *Echiopsis curta*. *Journal of Herpetology*, 16, 388–393.
244. Shine, R., Reed, R. N., Shetty, S., Lemaster, M., & Mason, R. T. (2002). Reproductive isolating mechanisms between two sympatric sibling species of sea snakes. *Evolution; International Journal of Organic Evolution*, 56, 1655–1662.
245. Shrestha, J., & Majupuria, T. C. (1977). Redescription of *Calliophis maccllellandi* from Kathmandu. *Journal of Natural History Museum (Nepal)*, 1, 103–112.
246. Simoes, B. F., Sampaio, F. L., Douglas, R. H., Kodandaramaiah, U., Casewell, N. R., Harrison, R. A., Hart, N. S., Partridge, J. C., Hunt, D. M., & Gower, D.J. (2016). Visual pigments, ocular filters and the evolution of snake vision. *Molecular Biology and Evolution*, 33, 2483–2495.
247. Singchat, W., Areesirisuk, P., Sillapaprayoon, S., Muangmai, N., Baicharoen, S., Suntrarachun, S., Chanhom, L., Peyachoknagul, S., & Srikulnath, K. (2019). Complete mitochondrial genome of Siamese cobra (*Naja kaouthia*) determined using next-generation sequencing. *Mitochondrial DNA Part B: Resources*, 4, 577–578.
248. Singh, S. (1995). On a collection of reptiles and amphibians of Manipur. *Geobios New Reports*, 14, 135–145.
249. Siqueira-Silva, T., de Lima, L. A. G., Chaves-Silveira, J., Amado, T. F., Naipauer, J., Riul, P., & Martinez, P. A. (2021). Ecological and

- biogeographic processes drive the proteome evolution of snake venom. *Global Ecology and Biogeography*, 30, 1978–1989.
250. Slowinski, J. B. (1994). A phylogenetic analysis of *Bungarus* (Elapidae) based on morphological characters. *Journal of Herpetology*, 28, 440–446.
 251. Slowinski, J. B., & Keogh, J. S. (2000). Phylogenetic relationships of elapid snakes based on cytochrome b mtDNA sequences. *Molecular Phylogenetics and Evolution*, 15, 157–164.
 252. Slowinski, J. B., & Wüster, W. (2000). A new cobra (Elapidae: *Naja*) from Myanmar (Burma). *Herpetologica*, 56, 257–270.
 253. Slowinski, J. B., Knight, A., & Rooney, A. P. (1997). Inferring species trees from gene trees: a phylogenetic analysis of the Elapidae (Serpentes) based on the amino acid sequences of venom proteins. *Molecular Phylogenetics and Evolution*, 8, 349–362.
 254. Slowinski, J. B., Boundy, J., & Lawson, R. (2001). The phylogenetic relationships of Asian coral snakes (Elapidae: *Calliophis* and *Maticora*) based on morphological and molecular characters. *Herpetologica*, 233–245.
 255. Smart, U., Ingrasci, M. J., Sarker, G. C., Lalremsanga, H., Murphy, R. W., Ota, H., Tu, M. C., Shouche, Y., Orlov, N. L., & Smith, E. N. (2021). A comprehensive appraisal of evolutionary diversity in venomous Asian coralsnakes of the genus *Sinomicrurus* (Serpentes: Elapidae) using Bayesian coalescent inference and supervised machine learning. *Journal of Zoological Systematics and Evolutionary Research*, 59, 2212–2277.
 256. Smith, M. A. (1940). The amphibians and reptiles obtained by Mr. Ronald Kaulback in Upper Burma. *Records of the Zoological Survey of India*, 43, 465–486.
 257. Smith, M. A. (1943). *The fauna of British India, Ceylon and Burma. Reptilia and Amphibia, Volume 3. Serpentes*. Taylor & Francis, London.
 258. Smith, O. A. (1911). Large common and banded krait. *Journal of Bombay Natural History Society*, 21, 283–284.
 259. Sodhi, N. S., & Brook B. W. (2006). *Southeast Asian Biodiversity in Crisis*. Cambridge University Press, Cambridge.

260. Sokal, R. R., & Crovello, T. J. (1970). The biological species concept: a critical evaluation. *American Naturalist*, *104*, 127–153.
261. Sonnini de Manoncourt, C. S., & Latreille, P. A. (1801). Histoire Naturelle des Reptiles, avec Figures Dessinees d'Apres Nature. 3. Librairie encyclopédique de Roret, Paris.
262. Soto, J. G., Perez, J. C., & Minton, S. A. (1988). Proteolytic, hemorrhagic and hemolytic activities of snake venoms. *Toxicon*, *26*, 875–882.
263. Soubrier, J., Steel, M., Lee, M. S., Der Sarkissian, C., Guindon, S., Ho, S. Y., & Cooper, A. (2012). The influence of rate heterogeneity among sites on the time dependence of molecular rates. *Molecular Biology and Evolution*, *29*, 3345–3358.
264. Srinivasulu, C., Venkateshwarlu, D., & Seetharamaraju, M. (2009). Rediscovery of the Banded Krait *Bungarus fasciatus* (Schneider 1801) (Serpentes: Elapidae) from Warangal District, Andhra Pradesh, India. *Journal of Threatened Taxa*, *1*, 353–354.
265. Steindachner, F. (1913). Über zwei neue Schlangenarten aus Formosa. *Denkschriften der Kaiserlichen Akademie der Wissenschaften / Mathematisch-Naturwissenschaftliche Classe*, *50*, 218–220.
266. Streicher, J. W., McEntee, J. P., Drzich, L. C., Card, D. C., Schield, D. R., Smart, U., Parkinson, C. L., Jezkova, T., Smith, E. N., & Castoe, T. A. (2016). Genetic surfing, not allopatric divergence, explains spatial sorting of mitochondrial haplotypes in venomous coralsnakes. *Evolution*, *70*, 1435–1449.
267. Stuart, B., & Wogan, G. (2012). *Naja kaouthia*. The IUCN Red List of Threatened Species 2012: e.T177487A1488122.
268. Stuart, B., Nguyen, T. Q., Thy, N., Vogel, G., Wogan, G., Srinivasulu, C., Srinivasulu, B., Das, A., Thakur, S., & Mohapatra, P. (2013). *Bungarus fasciatus*. The IUCN Red List of Threatened Species 2013: e.T192063A2034956.
269. Stuart, B., Wogan, G., Grismer, L., Auliya, M., Inger, R. F., Lilley, R., Chandard, T., Thy, N., Nguyen, T. Q., Srinivasulu, C., & Jelić, D. (2012).

- Ophiophagus hannah*. The IUCN Red List of Threatened Species 2012: e.T177540A1491874.
270. Stuart, B. L., Inger, R. F., & Voris, H. K. (2006). High level of cryptic species diversity revealed by sympatric lineages of Southeast Asian Forest frogs. *Biology Letters*, *2*, 470–474.
 271. Subba, A., Luitel, S., Rai, T. P., & Limbu, K.P. (2023). Bizarre record: Banded Krait, (*Bungarus fasciatus*) (Schneider 1801), feeding on other krait species. *Reptiles & Amphibians*, *30*, e18661.
 272. Suntrarachun, S., Chanhom, L., Thaveekarn, W., & Tirawatnpong, T. (2011). NCBI GenBank direct submission.
 273. Suntrarachun, S., Chanhom, L., & Sumontha, M. (2014). Phylogenetic analysis of the king cobra, *Ophiophagus hannah* in Thailand based on mitochondrial DNA sequences. *Asian Biomedicine*, *8*, 269–274
 274. Supikamolse, A., Ngaoburanawit, N., Sumontha, M., Chanhom, L., Suntrarachun, S., Peyachoknagul, S., & Srikulnath, K. (2015). Molecular barcoding of venomous snakes and species-specific multiplex PCR assay to identify snake groups for which antivenom is available in Thailand. *Genetics and Molecular Research*, *14*, 13981–13997.
 275. Tajima, F. (1993). Simple methods for testing molecular clock hypothesis. *Genetics*, *135*, 599–607.
 276. Takahashi, S. (1930). *Synopsis of the terrestrial snakes of Japan*. Shuny ô-do. (in Japanese).
 277. Talukdar, A., Malhotra, A., Lalremsanga, H. T., Santra, V., & Doley, R. (2023). *Bungarus fasciatus* venom from eastern and north-east India: venom variation and immune cross-reactivity with Indian polyvalent antivenoms. *Journal of Proteins and Proteomics*, *14*, 61–76.
 278. Tamura, K., Stecher, G., & Kumar, S. (2021). MEGA11: molecular evolutionary genetics analysis version 11. *Molecular Biology and Evolution*, *38*, 3022–3027.
 279. Tan, K. Y., Tan, C. H., Sim, S. M., Fung, S. Y., & Tan, N.H. (2016). Geographical venom variations of the Southeast Asian monocled cobra (*Naja kaouthia*): venom-induced neuromuscular depression and antivenom

- neutralization. *Comparative Biochemistry and Physiology Part C: Toxicology & Pharmacology*, 185, 77–86.
280. Tan, K. Y., Ng, T. S., Bourges, A., Ismail, A. K., Maharani, T., Khomvilai, S., Sitprija, V., Tan, N. H., & Tan, C.H. (2020). Geographical variations in king cobra (*Ophiophagus hannah*) venom from Thailand, Malaysia, Indonesia and China: On venom lethality, antivenom immunoreactivity and in vivo neutralization. *Acta Tropica*, 203, 105311.
281. Tan, N. H., & Ponnudurai, G. (1990). A comparative study of the biological properties of krait (genus *Bungarus*) venoms. *Comparative Biochemistry and Physiology Part C: Toxicology & Pharmacology*, 95, 105–109.
282. Tarroux, A., Bety, J., Gauthier, G., & Berteaux, D. (2012). The marine side of a terrestrial carnivore: intra-population variation in use of allochthonous resources by Arctic foxes. *Plos One*, 7, e42427.
283. Thorpe, R. S. (1975). Quantitative handling of characters useful in snake systematics with particular reference to intraspecific variation in the ringed snake *Natrix natrix* (L.). *Biological Journal of the Linnean Society*, 7, 27–43.
284. Thorpe, R. S., Pook, C. E., & Malhotra, A. (2007). Phylogeography of Russell's viper (*Daboia russelii*) complex in relation to variation in the colour pattern and symptoms of envenoming. *Herpetological Journal*, 10, 209–218.
285. Tongpoo, A., Sriapha, C., Pradoo, A., Udomsubpayakul, U., Srisuma, S., Wananukul, W., & Trakulsrichai, S. (2018). Krait envenomation in Thailand. *Therapeutics and clinical risk management*, 1711–1717.
286. Tsai, I. H., Tsai, H. Y., Saha, A., & Gomes, A. (2007). Sequences, geographic variations and molecular phylogeny of venom phospholipases and threefinger toxins of eastern India *Bungarus fasciatus* and kinetic analyses of its Pro31 phospholipases A2. *The FEBS Journal*, 274, 512–525.
287. Tu, A. T., James, G. P., & Chua, A. (1965). Some biochemical evidence in support of the classification of venomous snakes. *Toxicon*, 3, 5–8.
288. Turelli, M., Barton, N. H., & Coyne, J. A. (2001). Theory and speciation discuss recent examples of progress in each of these areas. *Trends in Ecology and Evolution*, 16, 330–343.

289. Uetz, P., Freed, P., & Hošek, J. (2024). The Reptile Database. <http://www.reptile-database.org>. Accessed 07 May 2024.
290. Vaidya, G., Lohman, D. J., & Meier R. (2011). SequenceMatrix: concatenation software for the fast assembly of multi-gene datasets with character set and codon information. *Cladistics*, 27, 1716–180.
291. Van Denburgh, J. (1912). Concerning certain species of reptiles and amphibians from China, Japan, the Loo Choo Islands, and Formosa. *Proceedings of the California Academy of Sciences (Series 4)*, 3, 187–258.
292. van Thiel, J., Khan, M. A., Wouters, R. M., Harris, R. J., Casewell, N. R., Fry, B. G., Kini, R. M., Mackessy, S. P., Vonk, F. J., Wüster, W., & Richardson, M. K. (2022). Convergent evolution of toxin resistance in animals. *Biological Reviews*, 97, 1823–1843.
293. Vanlalchhuana, M., Lalrinsanga, Lalbiakzuala, Lalengliana, H. C., Zothanga, Lalremsanga, H. T., Romalsawma, Lianzela, S., Vanlalhrima, V. Sailo, V. Vanchhawng, Pachuau, P., Laltlanchhuaha, H., Lalneihsanga, D., Lallawmkima, Lalsiamkima, Lalnunzira, J., & Lalremruata, H. (2016). The nesting ecology and hatchlings of the King cobra *Ophiophagus hannah* (Reptilia: Squamata: Elapidae) in Mizoram, Northeast India. In Zothanzama J., and Lalremsanga H.T. (Eds.), *Science and Technology for Shaping the Future of Mizoram* (pp. 325–330 pp).
294. Vences, M., Miralles, A., Brouillet, S., Ducasse, J., Fedosov, A., Kharchev, V., Kostadinov, I., Kumari, S., Patmanidis, S., Scherz, M.D., Puillandre, N., & Renner, S. S. (2021). iTaxoTools 0.1: Kickstarting a specimen-based software toolkit for taxonomists. *Megataxa*, 6, 77–92.
295. Vodá, R., Dapporto, L., Dincă, V., & Vila, R. (2014). Cryptic matters: Overlooked species generate most butterfly beta-diversity. *Ecography*, 38, 405–409.
296. Voris, K., & Harold (1966). Fish Eggs as the Apparent Sole Food Item for a Genus of Sea Snake, *Emydocephalus* (Krefft). *The Ecological Society of America*, 47, 152–154.

297. Wagler, J. (1824). *Serpentum Brasiliensium species novae, ou histoire naturelle des espèces nouvelles de serpens*. In Jean de Spix, *Animalia nova sive species novae*. Monachii [Munich], Typis F.S. Höbschmanni, Brazil.
298. Wagner, P., Ihlow, F., Hartmann, T., Flecks, M., Schmitz, A., & Böhme, W. (2021). Integrative approach to resolve the *Calotes mystaceus* Duméril & Bibron, 1837 species complex (Squamata: Agamidae). *Bonn Zoological Bulletin*, 70, 141–171.
299. Wall, F. (1908). A popular treatise of the common Indian snakes. Part VIII. *Journal of the Bombay Natural History Society*, 18, 711–735.
300. Wall, F. (1909). Notes on snakes from the neighbourhood of Darjeeling. *Journal of the Bombay Natural History Society*, 19, 337–357.
301. Wall, F. (1910). Notes on snakes collected in Upper Assam. Part II. *Journal of the Bombay Natural History Society*, 19, 825–845.
302. Wall, F. (1912). A popular treatise on the common Indian snakes. Part 15. *Bungarus fasciatus* and *Lycodon striatus*. *Journal of the Bombay Natural History Society*, 20, 933–953.
303. Wall, F. (1923). Notes on a collection of snakes from Sinlum Kaba. *Journal of the Bombay Natural History Society*, 29, 466–468.
304. Wall, F. (1925a). Notes on snakes collected in Burma in 1924. *Journal of the Bombay Natural History Society*, 30, 805–821.
305. Wall, F. (1925b). A hand-list of the snakes of the Indian empire. Part V. *Journal of the Bombay Natural History Society*, 30, 242–252.
306. Wallach, V., Williams, K. L., & Boundy, J. (2014). *Snakes of the world: a catalogue of living and extinct species*. CRC press, Boca Raton.
307. Wallach, V., Wüster, W., & Broadley, D. G. (2009). In praise of subgenera: taxonomic status of cobras of the genus *Naja* Laurenti (Serpentes: Elapidae). *Zootaxa*, 2236, 26–36.
308. Westerberg, K., Brown, R., Eagle, G., & Votier, S. C. (2019). Intra-population variation in the diet of an avian top predator: generalist and specialist foraging in great black-backed gulls *Larus marinus*. *Bird Study*, 66, 390–397.

309. Whitaker, R., & Captain, A. (2008). *Snakes of India: The Field Guide*. Draco Books.
310. Whitaker, R., & Martin, G. (2014). Diversity and distribution of medically important snakes of India. *Clinical Toxinology in Asia Pacific and Africa*, 115–136.
311. Whitaker, N., Shankar, P.G., & Whitaker, R. (2013). Nesting ecology of the King Cobra (*Ophiophagus hannah*) in India. *Hamadryad*, 36, 101–107.
312. Williams, H. F., Layfield, H. J., Vallance, T., Patel, K., Bicknell, A. B., Trim, S. A., & Vaiyapuri, S. (2019). The urgent need to develop novel strategies for the diagnosis and treatment of snakebites. *Toxins*, 11, 363.
313. World Health Organization. (2022). Snakebite Information and Data Platform. https://www.who.int/teams/control-of-neglected-tropical-diseases/snakebite-envenoming/snakebite-information-and-data-platform/overview#tab=tab_1.
314. Wüster, W. (1996). Taxonomic changes and toxinology: systematic revisions of the Asiatic cobras (*Naja naja* species complex). *Toxicon*, 34, 399–406.
315. Wüster, W., & Thorpe, R. S. (1992). Asiatic cobras: population systematics of the *Naja naja* species complex (Serpentes: Elapidae) in India and Central Asia. *Herpetologica*, 48, 69–85.
316. Wüster, W., & Thorpe, R. S. (1994). *Naja siamensis*, a cryptic species of venomous snake revealed by mtDNA sequencing. *Experientia*, 50, 75–79.
317. Wüster, W., & Broadley, D. G. (2003). A new species of spitting cobra from northeastern Africa (Serpentes: Elapidae: *Naja*). *Journal of Zoology*, 259, 345–359.
318. Wüster, W., & Broadley, D. G. (2007). Get an eyeful of this: a new species of giant spitting cobra from eastern and north-eastern Africa (Squamata: Serpentes: Elapidae: *Naja*). *Zootaxa*, 1532, 51–68.
319. Wüster, W., & Kaiser, H. (2023). Bungled *Bungarus*: lessons from a venomous snake complex illustrate why taxonomic decisions belong in taxonomy-competent journals. *Zootaxa*, 5297, 139–143.

320. Wüster, W., Otsuka, S., Malhotra, A., & Thorpe, R. S. (1992). Population systematics of Russell's viper: a multivariate study. *Biological Journal of the Linnean Society*, *47*, 97–113.
321. Wüster, W., Thorpe, R. S., Cox, M. J., Jintakune, P., & Nabhitabhata, J. (1995). Population systematics of the snake genus *Naja* (Reptilia: Serpentes: Elapidae) in Indochina: multivariate morphometrics and comparative mitochondrial DNA sequencing (cytochrome oxidase I). *Journal of Evolutionary Biology*, *8*, 493–510.
322. Wüster, W., Crookes, S., Ineich, I., Mané, Y., Pook, C. E., Trape, J. F., & Broadley, D. G. (2007). The phylogeny of cobras inferred from mitochondrial DNA sequences: evolution of venom spitting and the phylogeography of the African spitting cobras (Serpentes: Elapidae: *Naja nigricollis* complex). *Molecular Phylogenetics and Evolution*, *45*, 437–453.
323. Wüster, W., Chirio, L., Trape, J. F., Ineich, I., Jackson, K., Greenbaum, E., Barron, C., Kusamba, C., Nagy, Z. T., Storey, R., & Hall, C. (2018). Integration of nuclear and mitochondrial gene sequences and morphology reveals unexpected diversity in the forest cobra (*Naja melanoleuca*) species complex in Central and West Africa (Serpentes: Elapidae). *Zootaxa*, *4455*, 68–98.
324. Xie, Y. L., Wang, P., Zhong, G. H., Zhu, F., Liu, Q., Shi, L., & Guo, P. (2017). NCBI GenBank direct submission.
325. Xu, W., Dong, W. J., Fu, T. T., Gao, W., Lu, C. Q., Yan, F., Wu, Y. H., Jiang, K., Jin, J. Q., Chen, H. M., & Zhang, Y. P. (2021). Herpetological phylogeographic analyses support a Miocene focal point of Himalayan uplift and biological diversification. *National Science Review*, *8*, a263.
326. Yan, J., Li, H., & Zhou, K. (2008). Evolution of the mitochondrial genome in snakes: gene rearrangements and phylogenetic relationships. *BMC Genomics*, *9*, 1–7.
327. Yang, D. T., & Rao, D. Q. (2008). *Amphibia and Reptilia of Yunnan*. Yunnan Science and Technology Press, China.
328. Yang, D., Wang, D., & Huang, S. (2016). NCBI GenBank direct submission.

329. Yang, Z. (1995). A space-time process model for the evolution of DNA sequences. *Genetics*, *139*, 993–1005.
330. Zhang, H., Chen, S. L., Cui, L. N., Du, H., & Yao, H. (2011). NCBI GenBank direct submission.
331. Zhang, J., Kapli, P., Pavlidis, P., & Stamatakis, A. (2013). A general species delimitation method with applications to phylogenetic placements. *Bioinformatics* *29*, 2869–2876.
332. Zhou, S. (2021). NCBI GenBank direct submission.
333. Zhou, C., Gan, S., Zhang, J., Fan, Y., Li, B., Wan, L., Nie, J., Wang, X., & Chen, J. (2022). Application of DNA Barcoding for the Identification of Snake Gallbladders as a Traditional Chinese Medicine. *Revista Brasileira de Farmacognosia*, *32*, 663–668.
334. Ziganshin, R. H., Kovalchuk, S. I., Arapidi, G. P., Starkov, V. G., Hoang, A. N., Nguyen, T. T. T., Nguyen, K. C., Shoibonov, B. B., Tsetlin, V. I., & Utkin, Y.N. (2015). Quantitative proteomic analysis of Vietnamese krait venoms: Neurotoxins are the major components in *Bungarus multicinctus* and phospholipases A2 in *Bungarus fasciatus*. *Toxicon*, *107*, 197–209.
335. Zug, G., Brown, H., Schulte, J., & Vindum, J. (2007). Systematics of the Garden Lizards, *Calotes versicolor* Group (Reptilia, Squamata, Agamidae), in Myanmar: Central Dry Zone Populations. *Proceedings of the California Academy of Sciences*, *57*, 35–68.

BRIEF BIO-DATA OF THE CANDIDATE

Name: Lalbiakzuala

Father's name: Lalmangaihzuala

Date of Birth: 8th April 1994

Marital Status: Married

Nationality: Indian

Religion: Christianity

Contact: +919774901952

Email ID: bzachawngthu123@gmail.com

Permanent Address: D-42, Durtlang Mualveng, Aizawl, Mizoram-796014

Educational qualifications:

Exams	Board	Subject	Percentage	Division	Year
HSLC	MBSE	General	68%	I	2010
HSSLC	MBSE	Science	59%	II	2012
B.Sc	MZU	Zoology	81.33%	Distinction	2015
M.Sc	MZU	Zoology	70%	I	2017
M.Phil	MZU	Zoology	81.67%	Distinction	2020

CERTIFICATE ON PLAGIARISM CHECK

Name of Research Scholar/Student	Lalbiakzuala	
Ph.D registration Number	MZU/Ph.D./1384 of 16.03.2020	
Title of Ph.D thesis	Taxonomic study on the elapid snakes of Mizoram, India (Reptilia: Serpentes: Elapidae)	
Name & Institutional Address of the Supervisor	Prof. H.T. Lalremsanga Department of Zoology Mizoram University Aizawl-796004, India	
Name of the Department and School	Department of Zoology, School of Life Sciences	
Date of submission		
Date of plagiarism check	12.06.2024	
Name of the software used	Turnitin	
Percentage of the similarity detected by the Turnitin software	Core Areas	4%
	Non-Core areas	6%
Percentage of similarity permissible under MZU regulations	Core Areas	a common knowledge or coincidental terms and/or up to fourteen (14) consecutive words, if option is available in the software.
	Non-Core areas	Up to 10%

I hereby declare/certify that the Ph.D thesis submitted by me is complete in all respect, as per the guidelines of the Mizoram University (MZU) for this purpose. I also certify that the Dissertation (soft copy and print version) has been checked for plagiarism using TURNITIN similarity check software. Copy of the Report generated by the Turnitin software is also enclosed.

Place: Aizawl, Mizoram

Date: 12.06.2024

(LALBIAKZUALA)

(Prof. H.T. LALREMSANGA)

Supervisor

(Prof. H.T. LALREMSANGA)

Head

PLAGIARISM VERIFICATION CERTIFICATE

This is to certify that the plagiarism check has been performed for Ph.D thesis “**Taxonomic study on the elapid snakes of Mizoram, India (Reptilia: Serpentes: Elapidae)**” submitted by Mr. Lalbiakzuala, under the supervision of Prof. H.T. Lalremsanga, Department of Zoology, School of Life Sciences, Mizoram University. The check performed by the Scholar/Student is found correct/adheres to MZU regulations and authentic software **Turnitin** has been used for the similarity check.

(Prof. G. GURUSUBRAMANIAN)

Dean

School of Life Sciences

PAPER NAME

Core Area.doc

AUTHOR

Lalbiakzuala

WORD COUNT

20188 Words

CHARACTER COUNT

110231 Characters

PAGE COUNT

49 Pages

FILE SIZE

206.5KB

SUBMISSION DATE

Jun 12, 2024 12:00 PM GMT+5:30

REPORT DATE

Jun 12, 2024 12:01 PM GMT+5:30

● 4% Overall Similarity

The combined total of all matches, including overlapping sources, for each database.

- 3% Internet database
- 3% Publications database
- Crossref database
- Crossref Posted Content database
- 1% Submitted Works database

● Excluded from Similarity Report

- Small Matches (Less than 15 words)
- Manually excluded sources

Summary

PAPER NAME
Non-core.doc

AUTHOR
Lalbiakzuala

WORD COUNT
10451 Words

CHARACTER COUNT
58479 Characters

PAGE COUNT
26 Pages

FILE SIZE
124.0KB

SUBMISSION DATE
Jun 12, 2024 12:00 PM GMT+5:30

REPORT DATE
Jun 12, 2024 12:01 PM GMT+5:30

● 6% Overall Similarity

The combined total of all matches, including overlapping sources, for each database.

- 5% Internet database
- 4% Publications database
- Crossref database
- Crossref Posted Content database
- 2% Submitted Works database

● Excluded from Similarity Report

- Manually excluded sources

Publications (chronological order).

Title of the publications originated from this thesis work are indicated in bold.

Accumulative Impact factor- 33 (Journal Citation Report 2024).

Sl. No.	Authors	Title	Journal	Year, volume (issue): pages	Impact Factor (JCR 2024)	Index	Publisher & Country
1.	Lal Biakzuala , Hmar Tlawmte Lalremsanga, J. Ramhermawia, H. Lalrinkima, C. Malsawmtluangi, Lalramliana & K. Lalchhandama	Natural History Notes: <i>Ophiophagus hannah</i> (Endoparasite)	<i>Herpetological Review</i>	2020, 51(1): 151-152	-	SCOPUS	Society for the Study of Amphibians and Reptiles: U.S.A
2.	Lalmuansanga, Gospel Zothanmawia Hmar, Lal Biakzuala , Lalrinsanga & Hmar Tlawmte Lalremsanga	Notes on Geographic Distribution: <i>Theلودerma nagalandensis</i> (A new state record for Mizoram)	<i>Herpetological Review</i>	2020, 51(2): 270	-	SCOPUS	Society for the Study of Amphibians and Reptiles: U.S.A
3.	Gospel Zothanmawia Hmar, Lalmuansanga, Lal Biakzuala , Hmar Tlawmte Lalremsanga & V.L. Mawia	New geographical distribution of Asiatic Softshell Turtle from Mizoram, India	<i>Zoos' Print Journal</i>	2020, 35(5):107-110	-	SCI	Zoo Outreach Organisation: India
4.	Vanlalsiammawii, Remruatpuii, Van Lal Malsawmhriatzuali, Lalmuansanga, Gospel Zothanmawia Hmar, Saisangpuia Sailo, Ht. Decemson, Lal Biakzuala & Hmar Tlawmte Lalremsanga	An additional record of the Tamdil leaf litter frog <i>Leptobrachella tamdil</i> (Sengupta et al, 2010) from Dampa Tiger Reserve, Mizoram, India	<i>Journal of Threatened Taxa</i>	2020, 12(8):15951 - 15954	-	SCOPUS	Wildlife Information & Liaison Development Society: India
5.	Remruatpuii, Lal Biakzuala & Hmar Tlawmte Lalremsanga	Natural History Notes: <i>Smithophis atemporalis</i> (Reproduction)	<i>Herpetological Review</i>	2020, 51(1): 156-157	-	SCOPUS	Society for the Study of Amphibians and Reptiles: U.S.A

Sl. No.	Authors	Title	Journal	Year, volume (issue): pages	Impact Factor (JCR 2024)	Index	Publisher & Country
6.	Lal Lawmsanga, Vanlal Hrima, Lal Biakzuala & Hmar Tlawmte Lalremsanga	First Record of Dicephalism in a Red-tailed Bamboo Pitviper, <i>Trimeresurus erythrurus</i> (Cantor 1839)	Reptiles & Amphibians	2020, 27(2): 262-263	-	SCI	International Reptile Conservation Foundation (IRCF): U.S.A
7.	Lalmuansanga, Lal Biakzuala , Lalrinsanga, Michael Vanlalchhuana, Gospel Zothanmawia Hmar & Hmar Tlawmte Lalremsanga	Natural History Notes: <i>Naja kaouthia</i> (Diet and feeding behavior)	<i>Herpetological Review</i>	2020, 50(2): 355-356	-	SCOPUS	Society for the Study of Amphibians and Reptiles: U.S.A
8.	Hmar Tlawmte Lalremsanga, Lal Biakzuala , Lalrinsanga, Michael Vanlalchhuana, Andrew Vanlallawma & Hrahse Laltlanchhuaha	Natural History Notes: <i>Trimeresurus erythrurus</i> (Reproduction)	<i>Herpetological Review</i>	2020, 51(1): 158-159	-	SCOPUS	Society for the Study of Amphibians and Reptiles: U.S.A
9.	Ht. Decemson, Lal Biakzuala , Ghan Shyam Solanki, Binoy Kumar Barman & Hmar Tlawmte Lalremsanga	The Twin-spotted Treefrog (<i>Rhacophorus bipunctatus</i> Ahl 1927) in Mizoram, India	<i>Reptiles & Amphibians</i>	2020, 27(2): 242-244	-	SCI	International Reptile Conservation Foundation (IRCF): U.S.A
10.	Hmar Tlawmte Lalremsanga, Lal Muansanga, Mathipi Vabeiryureilai, Lal Biakzuala , Lal Rinsanga, John Zothanzama, Nachimuthu Senthil Kumar & Jayaditya Purkayastha	First Record of the Nagaland Montane Torrent Toad, <i>Duttaphrynus chandai</i> Das, Chetia, Dutta, and Sengupta 2013 (Anura: Bufonidae), from Mizoram, India, with Comments on Phylogenetic Relationships	<i>Reptiles & Amphibians</i>	2020, 27(3): 467-471	-	SCI	International Reptile Conservation Foundation (IRCF): U.S.A

Sl. No.	Authors	Title	Journal	Year, volume (issue): pages	Impact Factor (JCR 2024)	Index	Publisher & Country
11.	Tbc. Lalhruaitluangi, Ro Malsawma, Lal Biakzuala , Lal Muansanga, Ht. Decemson, Mathipi Vabeiryureilai, Lal Rinsanga & Hmar Tlawmte Lalremsanga	Notes on the Diet and Feeding Behavior of the Khumhzi Striped Ichthyophis, <i>Ichthyophis khumhzi</i> Kamei, Wilkinson, Gower, and Biju 2009 (Amphibia: Gymnophiona: Ichthyophiidae), from Mizoram in Northeastern India	<i>Reptiles & Amphibians</i>	2020, 27(3): 464-466	-	SCI	International Reptile Conservation Foundation (IRCF): U.S.A
12.	Lal Muansanga, Ht. Decemson, Lal Biakzuala , Gospel Zothanmawia Hmar, Hmar Tlawmte Lalremsanga, Madhurima Das & Jayaditya Purkayastha	First Record of the Jampui Bent-toed Gecko, <i>Cyrtodactylus montanus</i> Agarwal, Mahony, Giri, Chaitanya, and Bauer 2018 (Squamata: Gekkonidae), from Mizoram, India	<i>Reptiles & Amphibians</i>	2020, 27(2): 267-268	-	SCI	International Reptile Conservation Foundation (IRCF): U.S.A
13.	Lal Biakzuala , Vanlalhrima, Binoy Kumar barman & Hmar Tlawmte Lalremsanga	Rediscovery and updated distribution of <i>Lycodon septentrionalis</i> from Mizoram state, north-east India	Herpetological Bulletin	2020, 152: 24-25	-	SCOPUS	British Herpetological Society: United Kingdom
14.	Ht. Decemson, Lal Biakzuala & Hmar Tlawmte Lalremsanga	Interspecific amplexus between two sympatric species, <i>Ammirana nicobariensis</i> (Stoliczka, 1870) and <i>Microhyla berdmorei</i> (Blyth, 1856) at Tuitun stream, Mizoram, India	<i>Herpetology Notes</i>	2020, 13: 433-434	-	SCOPUS	Societas Europaea Herpetologica: Germany
15.	Lal Lawmsanga, Vanlal Hrima, Lal Biakzuala & Hmar Tlawmte Lalremsanga	First Record of Dicephalism in a Red-tailed Bamboo Pitviper, <i>Trimeresurus erythrurus</i> (Cantor 1839)	Reptiles & Amphibians	2020, 27(2): 262-263	-	SCI	International Reptile Conservation Foundation (IRCF): U.S.A
16.	Hmar Tlawmte Lalremsanga, Lal Biakzuala , Lalrinsanga, Michael Vanlalchhuana, Andrew Vanlallawma & Hrahse Lalanchhuaha	Natural History Notes: <i>Trimeresurus erythrurus</i> (Reproduction)	<i>Herpetological Review</i>	2020, 51(1): 158-159	-	SCOPUS	Society for the Study of Amphibians and Reptiles: U.S.A

Sl. No.	Authors	Title	Journal	Year, volume (issue): pages	Impact Factor (JCR 2024)	Index	Publisher & Country
17.	Ht. Decemson, Lal Biakzuala & Hmar Tlawmte Lalremsanga	Interspecific amplexus between two sympatric species, <i>Amnirana nicobariensis</i> (Stoliczka, 1870) and <i>Microhyla berdmorei</i> (Blyth, 1856) at Tuitun stream, Mizoram, India	<i>Herpetology Notes</i>	2020, 13: 433-434	-	SCOPUS	Societas Europaea Herpetologica: Germany
18.	Gospel Zothanmawia Hmar, Lalmuansanga, Lal Biakzuala , Lalruatthara, Lalrinsanga & Hmar Tlawmte Lalremsanga.	Inventory Survey on the Ophidian Fauna of Reiek Community Reserved Forest, Mamit District, Mizoram, India	<i>Journal of Environmental Biology</i>	2020, 41: 821-826	0.6	SCOPUS	Triveni Enterprises: India
19.	Van Lal Malsawmhriatzuali, Lal Biakzuala , Gospel Zothanmawia Hmar, Lalmuansanga, Lalrinsanga & Hmar Tlawmte Lalremsanga	A new state report of two striped <i>Ichthyophis</i> Fitzinger (Amphibia: Gymnophiona: Ichthyophiidae) from Mizoram, Northeast India	<i>Journal of Environmental Biology</i>	2020, 41: 827–831	0.6	SCOPUS	Triveni Enterprises: India
20.	Shantanu Kundu, Hmar Tlawmte Lalremsanga, Kaomud Tyagi, Lal Biakzuala , Vikas Kumar & Kailash Chandra	Mitochondrial DNA discriminates distinct population of two deadly snakes (Reptilia:Elapidae) in Northeast India	<i>Mitochondrial DNA Part B: Resources</i>	2020, 5(2): 1530-1534	0.5	SCOPUS	Taylor & Francis Ltd.: United Kingdom
21.	Shantanu Kundu, Hmar Tlawmte Lalremsanga, Md. Mizanur Rahman, Md.Farid Ahsan, Lal Biakzuala , Vikas Kumar, Kailash Chandra & A. M. A. M.Zonaed Siddiki	DNA barcoding elucidates the population genetic diversity of venomous cobra species (Reptilia: Elapidae) in Indo-Bangladesh region	<i>Mitochondrial DNA Part B: Resources</i>	2020, 5(3): 2525-2530	0.5	SCOPUS	Taylor & Francis Ltd.: United Kingdom
22.	Shantanu Kundu, Hmar Tlawmte Lalremsanga, Jayaditya Purkayastha, Lal Biakzuala , Kailash Chandra & Vikas Kumar	DNA barcoding elucidates the new altitude record and range-extension of lesser-known bullfrog (<i>Hoplobatrachus litoralis</i>) in northeast India	<i>Mitochondrial DNA Part B: Resources</i>	2020, 5(3): 2668-2672	0.5	SCOPUS	Taylor & Francis Ltd.: United Kingdom

Sl. No.	Authors	Title	Journal	Year, volume (issue): pages	Impact Factor (JCR 2024)	Index	Publisher & Country
23.	Lal Biakzuala, Hmar Tlawmte Lalremsanga, Lal Tlanchhuaha & Binoy Kumar Barman	Observations on the oviposition of <i>Blythia reticulata</i> (Blyth, 1854) with new distributional records from Mizoram State, NE India	<i>Herpetozoa</i>	2020, 33(1): 53-57	0.8	SCOPUS	Pensoft Publishers: Austria
24.	Lal Biakzuala, Vanlal Hrima, Michael Vanlalchhuana, Andrew Vanlallawma, Mathipi Vabeiryureilai, Lal Muansanga, Sarathbabu Subarayan, Nachimuthu Senthil Kumar & Hmar Tlawmte Lalremsanga	Contributions to <i>Lycodon zawi</i> , a little-known colubrid snake (Reptilia: Serpentes: Colubridae)	<i>Herpetological Journal</i>	2020, 30(4): 234-237	1.1	SCOPUS	British Herpetological Society: United Kingdom
25.	Gernot Vogel, Tan Van Nguyen, Hmar Tlawmte Lalremsanga, Lal Biakzuala, Vanlal Hrima & Nikolay A. Poyarkov	Taxonomic reassessment of the <i>Pareas margaritophorus-macularius</i> species complex (Squamata, Pareidae)	<i>Vertebrate Zoology</i>	2020, 70(4): 547-569	2.4	SCOPUS	Senckenberg Gesellschaft für Naturforschung : Germany
26.	Lal Biakzuala & Hmar Tlawmte Lalremsanga	Rediscovery of <i>Oligodon catenatus</i> (Blyth, 1854) (Squamata: Colubridae) from India	<i>Amphibian & Reptile Conservation</i>	2020, 14(3): 226-230	1.3	SCOPUS	Amphibian & Reptile Conservation: U.S.A
27.	Gospel Zothanmawia Hmar, Lal Biakzuala, Lalmuansanga, Dadina Zote, Vanlalhruaia, Hmar Betlu Ramengmawii, Kulendra Chandra Das & Hmar Tlawmte Lalremsanga	A first distribution record of the Indian Peacock Softshell Turtle <i>Nilssonina hurum</i> (Gray, 1830) (Reptilia: Testudines: Trionychidae) from Mizoram, India	<i>Journal of Threatened Taxa</i>	2021, 12(14): 17036 - 17040	-	SCOPUS	Wildlife Information & Liaison Development Society: India
28.	Ht. Decemson, Vanlalsiammawii, Lal Biakzuala, Mathipi Vabeiryureilai, Fanai Malsawmdawngliana & H.T. Lalremsanga	Occurrence of Tamdil Leaf-litter Frog <i>Leptobrachella tamdil</i> (Sengupta et al., 2010) (Amphibia: Megophryidae) from Manipur, India and its phylogenetic position	<i>Journal of Threatened Taxa</i>	2021, 13(6): 18624–18630	-	SCOPUS	Wildlife Information & Liaison Development Society: India

Sl. No.	Authors	Title	Journal	Year, volume (issue): pages	Impact Factor (JCR 2024)	Index	Publisher & Country
29.	Lal Muansanga, Malnica Vanlal Malsawmtluangi, Gospel Zothanmawia Hmar, Lal Biakzuala , Vanlal Siammawii, Vabeiryureilai Mathipi and Hmar Tlawmte Lalremsanga	The first record of <i>Kurixalus yangi</i> Yu, Hui, Rao and Yang, 2018 (Anura: Rhacophoridae) from Mizoram State, India, with a reassessment of previous records of its congeners from Mizoram	<i>Journal of Animal Diversity</i>	2021, 3 (2): 9–17	-	SCI	Lorestan University Press: Iran
30.	Lalmuansanga, Lal Biakzuala , Lalrinsanga, Michael Vanlalchhuana, Gospel Zothanmawia Hmar, Ht. Decemson, Romalsawma & H.T. Lalremsanga	Natural History Notes: <i>Rhabdophis subminiatus</i> (Red-necked keelback). Reproduction	<i>Herpetological Review</i>	2021, 52(1): 170	-	SCOPUS	Society for the Study of Amphibians and Reptiles: U.S.A
31.	Lalmuansanga, Lal Biakzuala , Gospel Zothanmawia Hmar, R.L. Kima, John Zothanzama & H.T. Lalremsanga	Natural History Notes. <i>Duttaphrynus melanostictus</i> (Common Asian Toad). Diet and feeding behaviour.	<i>Herpetological Review</i>	2021, 52(1): 114	-	SCOPUS	Society for the Study of Amphibians and Reptiles: U.S.A
32.	Lal Muansanga, Saisangpuia Sailo, Lal Biakzuala , Gospel Z. Hmar, John Zothanzama, Ht. Decemson & H.T. Lalremsanga	Interspecific Amplexus of a Male Terai Treefrog, <i>Polypedates teraiensis</i> (Dubois 1897), and a Female Cope's Assam Frog, <i>Hydrophylax leptoglossa</i> (Cope 1868), at Pualreng Wildlife Sanctuary in Mizoram, India	<i>Reptiles & Amphibians</i>	2021, 28(1): 84–85	-	SCI	International Reptile Conservation Foundation (IRCF): U.S.A

Sl. No.	Authors	Title	Journal	Year, volume (issue): pages	Impact Factor (JCR 2024)	Index	Publisher & Country
33.	Lal Muansanga, Lizia Vanlalhriatpuii Hlondo, Lal Biakzuala , Gospel Zothanmawia Hmar & Hmar Tlawmte Lalremsanga,	Interspecific amplexus between two rhacophorids (Anura: Rhacophoridae), <i>Polypedates teraiensis</i> (Dubois, 1897) and <i>P. braueri</i> (Vogt, 1911), at the Pualreng Wildlife Sanctuary, Mizoram, India	<i>Herpetology Notes</i>	2021, 14: 585–587	-	SCOPUS	Societas Europaea Herpetologica: Germany
34.	Lal Muansanga, L.H. Laltlanhlui, Lal Biakzuala , Yash Singh Rathee & H.T. Lalremsanga	Observations of Feeding Behavior and a Note on Clutch Size in Wall's Keelback, <i>Herpetoreas xenura</i> (Wall 1907) (Squamata: Natricidae)	<i>Reptiles & Amphibians</i>	2021, 28(1):82–83	-	SCI	International Reptile Conservation Foundation (IRCF): U.S.A
35.	Gospel Zothanmawia Hmar, Lal Biakzuala , Lalmuansanga, Dadina Zote, Vanlalhruaia, H.B. Ramengmawii, Ht. Decemson, K.C. Das & H.T. Lalremsanga	First Record of the Exotic Red-eared Slider, <i>Trachemys scripta elegans</i> (Wied 1838) (Emydidae), from Mizoram, India	<i>Reptiles & Amphibians</i>	2021, 28(1): 52–53	-	SCI	International Reptile Conservation Foundation (IRCF): U.S.A
36.	Lal Muansanga, Lal Duhzuali, Lal Biakzuala , Vabeiryureilai Mathipi, Saisangpuia Sailo & H.T. Lalremsanga	Rediscovery of Doria's Foam-nesting Treefrog, <i>Chirixalus doriae</i> Boulenger 1893 (Anura: Rhacophoridae), from India	<i>Reptiles & Amphibians</i>	2021, 28(1): 79–81	-	SCI	International Reptile Conservation Foundation (IRCF): U.S.A
37.	Fanai Malsawmdawngliana, Mathipi Vabeiryureilai, Tara Malsawmdawngzuali, Lal Biakzuala , Lalengzuala Tochwawng & Hmar Tlawmte Lalremsanga	A new record of <i>Liocheles australasiae</i> (Fabricius, 1775) (Scorpiones: Hormuridae) from the state of Mizoram, India	<i>Journal of Animal Diversity</i>	2021, 3(1):11–17	-	SCI	Lorestan University Press: Iran

Sl. No.	Authors	Title	Journal	Year, volume (issue): pages	Impact Factor (JCR 2024)	Index	Publisher & Country
38.	Ht. Decemson, Sushanto Gouda, Lal Biakzuala , Lalmuansanga, Gospel Zothanmawia Hmar, Mathipi Vabeiryureilai & H.T. Lalremsanga	An annotated checklist of amphibians in and around Dampa Tiger Reserve, Mizoram, India	<i>Journal of Threatened Taxa</i>	2021, 13(3): 17918–17929	-	SCOPUS	Wildlife Information & Liaison Development Society: India
39.	Vanlal Siammawii, Malnica Vanlal Malsawmtluangi, Lal Muansanga, Lal Biakzuala & Hmar Tlawmte Lalremsanga	Adactyly in a Mawphlang Odorous Frog, <i>Odorrana mawphlangensis</i> (Pillai and Chanda 1977) (Ranidae), from Mizoram, India	<i>Reptiles & Amphibians</i>	2021, 28(2): 324–325	-	SCI	International Reptile Conservation Foundation (IRCF): U.S.A
40.	Lal Muansanga, Vanlal Siammawii, Gospel Zothanmawia Hmar, F. Malsawmdawngliana, Lal Biakzuala , Ht. Decemson1, Zothan Sangi & H.T. Lalremsanga	New elevation and locality records and notes on the natural history of the Tamdil Leaf-Litter Frog, <i>Leptobranchella tamdil</i> (Sengupta, Sailo, Lalremsanga, Das, and Das, 2010) (Megophryidae), in Mizoram, India	<i>Reptiles & Amphibians</i>	2021, 28(2): 295–297	-	SCI	International Reptile Conservation Foundation (IRCF): U.S.A
41.	Ht. Decemson, Vabeiryureilai Mathipi, Vanlalsiammawii, Lal Biakzuala , Saipari Sailo & Hmar Tlawmte Lalremsanga	A new record of the Banladeshi Cricket Frog, <i>Minervarya asmati</i> (Howlader, 2011), from Manipur State, with comments on the occurrence of the Paddy Frog, <i>Fejervarya multistriata</i> (Hallowell, 1861) (Anura: Dicroglossidae), in Mizoram, India	<i>Reptiles & Amphibians</i>	2021, 28(2): 250–254	-	SCI	International Reptile Conservation Foundation (IRCF): U.S.A

Sl. No.	Authors	Title	Journal	Year, volume (issue): pages	Impact Factor (JCR 2024)	Index	Publisher & Country
42.	Vanlal Siammawii, Malnica Vanlal Malsawmtluangi, Lal Muansanga, Lal Biakzuala & Hmar Tlawmte Lalremsanga	Brachyphalangy in a Tamenglong Horned Frog, <i>Xenophrys numhumaeng</i> (Mahony, Kamei, Teeling, and Biju 2020) (Megophryidae), from Mizoram, India	<i>Reptiles & Amphibians</i>	2021, 28(2): 322–323	-	SCI	International Reptile Conservation Foundation (IRCF): U.S.A
43.	Lal Muansanga, Ht Decemson, Lal Biakzuala , LH Laltlanhlui, Fanai Malsawmdawngliana, Gospel Zothanmawia Hmar, Mathipi Vabeiryureilai, Nachimuthu Senthil Kumar & Hmar Tlawmte Lalremsanga	On the Phylogenetic Relationships of the Indian Gliding Frog, <i>Pterorana khare</i> Kiyasetuo and Khare 1986 (Anura: Ranidae), with New Distributional Records from Mizoram, India	<i>Reptiles & Amphibians</i>	2021, 28(2): 205–212	-	SCI	International Reptile Conservation Foundation (IRCF): U.S.A
44.	Girish Choure, Shubham Adhikari, Pallavi Choure, Ajinkya Unawane, Lal Biakzuala & Hmar Tlawmte Lalremsanga	First Record of a Leucistic Indian Ratsnake, <i>Ptyas mucosa</i> (Linnaeus 1758) from India	<i>Reptiles & Amphibians</i>	2021, 28(2): 240–241	-	SCI	International Reptile Conservation Foundation (IRCF): U.S.A
45.	Lalmuansanga, Lal Biakzuala , Lalnunkima & H.T. Lalremsanga	Natural History Notes. <i>Euphlyctis cyanophytis</i> (Indian Skipping Frog). Diet	<i>Herpetological Review</i>	2021, 52(2): 371	-	SCOPUS	Society for the Study of Amphibians and Reptiles: U.S.A
46.	Vanlal Siammawii, Lal Biakzuala & H.T. Lalremsanga	Natural History Notes. <i>Duttaphrynus chandai</i> (Nagaland Montane Torrent Toad). Hindlimb malformation.	<i>Herpetological Review</i>	2021, 52(4): 823	-	SCOPUS	Society for the Study of Amphibians and Reptiles: U.S.A

Sl. No.	Authors	Title	Journal	Year, volume (issue): pages	Impact Factor (JCR 2024)	Index	Publisher & Country
47.	Khan Ashaharraza, Lal Biakzuala & Hmar Tlawmte Lalremsanga	A Leucistic Checkered Keelback, <i>Fowlea piscator</i> (Serpentes: Natricidae), from Mizoram, India	<i>Reptiles & Amphibians</i>	2020, 27(1): 42-43	-	SCI	International Reptile Conservation Foundation (IRCF): U.S.A
48.	Ht. Decemson, Lal Biakzuala , Gospel Zothanmawia Hmar, Lalmuansanga, Fanai Malsawmdawngliana, Mathipi Vabeiryureilai & H.T. lalremsanga	Natural History Note: <i>Calotes versicolor</i> (Indian Garden Lizard). Ectoparasite	<i>Herpetological Review</i>	2021, 52(3): 646	-	SCOPUS	Society for the Study of Amphibians and Reptiles: U.S.A
49.	Lal Biakzuala , H.T. Lalremsanga, Lalrinsanga, Lalmuansanga, Mathipi Vabeiryureilai & Romalsawma	DNA barcoding reveals intra-species genetic diversity of <i>Amphiesma stolatum</i> (Linnaeus, 1758) in Indo-Malayan region	<i>Science and Technology Journal</i>	2021, 9(2): 134-140	-	-	Mizoram University: India
50.	Pallavi Choure, Girish Choure, Shubham Adhikari, Ajinkya Unawane, Lal Biakzuala & Hmar Tlawmte Lalremsanga	Chromatic aberrations: Cases of piebaldism, hypomelanism, albinism, and melanism in <i>Bungarus caeruleus</i> (Serpentes: Elapidae) from India	<i>Sauria</i>	2021, 43(3): 73-77	-	SCI	Terrariengemeinschaft Berlin: Germany
51.	Hmar Tlawmte Lalremsanga, Lal Muansanga, Ht. Decemson & Lal Biakzuala *	Interspecific amplexus by a male Terai Tree Frog, <i>Polypedates teraiensis</i> (Dubois 1987) (Anura: Racophoridae), and female Serchhip Horned Frog, <i>Xenophrys serchhipii</i> (Mathew and Sen 2007) (Anura: Megophryidae), from Mizoram State, India	<i>Reptiles & Amphibians</i>	2021, 28(2): 278-279	-	SCI	International Reptile Conservation Foundation (IRCF): U.S.A

Sl. No.	Authors	Title	Journal	Year, volume (issue): pages	Impact Factor (JCR 2024)	Index	Publisher & Country
52.	Ht. Decemson, Vanlal Siammawii, Vabeiryureilai Mathipi, Lal Biakzuala & Hmar Tlawmte Lalremsanga	First record of <i>Duttaphrynus chandai</i> (Anura: Bufonidae) from Manipur State, northeastern India, with updated information on its distribution and natural history	<i>Herpetology Notes</i>	14: 1219–1223	-	SCOPUS	Societas Europaea Herpetologica: Germany
53.	Gospel Zothanmawia Hmar, Hmar Betlu Ramengmawii, Lal Biakzuala , Dadina Zote, Vanlal Hruaia, Tlau Liana, Hmar Tlawmte Lalremsanga & Kulendra Chandra Das	New records of the endangered Southeast Asian Box Turtle, <i>Cuora amboinensis</i> (Testudines, Geoemydidae), from Mizoram, northeast India	<i>Herpetology Notes</i>	2021, 14: 1177–1180	-	SCOPUS	Societas Europaea Herpetologica: Germany
54.	Shantanu Kundu, Hmar Tlawmte Lalremsanga, Lal Biakzuala , Ht. Decemson, Lal Muansanga, Kaomud Tyagi, Chandra Kailash & Vikas Kumar	Genetic diversity of the Pegu Rice Frog, <i>Microhyla berdmorei</i> (Anura: Microhylidae) based on mitochondrial DNA	<i>Mitochondrial DNA Part B: Resources</i>	2021, 6(5): 1586–1591	0.5	SCOPUS	Taylor & Francis Ltd.: United Kingdom
55.	Lal Biakzuala , Hmar Tlawmte Lalremsanga, Vishal Santra, Joseph Ramhermawia, Chenkual Malsawmtluangi & Hmar Lalrinkima	Intestinal obstruction associated with helminth parasitic infection in a wild-caught Pope's Green Pitviper, <i>Trimeresurus popeiorum</i> Smith 1937	<i>Reptiles & Amphibian</i>	2021, 28(2): 224–226	-	SCI	International Reptile Conservation Foundation (IRCF): U.S.A
56.	Ht. Decemson, Mathipi Vabeiryureilai, Lal Biakzuala & Hmar Tlawmte Lalremsanga	Confirmation on the occurrence of <i>Calotes geissleri</i> Wagner, Ihlow, Hartman, Flecks, Schmitz and Böhme, 2021 (Sauria: Agamidae) in Chandel, Manipur, India with comments on its phylogenetic position	<i>Journal of Animal Diversity</i>	2021, 4(3): 14–19	-	SCI	Lorestan University Press: Iran

Sl. No.	Authors	Title	Journal	Year, volume (issue): pages	Impact Factor (JCR 2024)	Index	Publisher & Country
57.	Jayaditya purkayastha, Hmar Tlawmte Lalremsanga, Sanath Chandra Bohra, Lal Biakzuala , Ht. Decemson, Lal muansanga, Mathipi Vabeiryureilai, Suraj Chauhan & Yashpal Singh Rathee	Four new Bent-toed geckos (<i>Cyrtodactylus</i> Gray: Squamata: Gekkonidae) from northeast India	<i>Zootaxa</i>	2021, 4980 (1): 451–489	0.8	SCOPUS	Magnolia Press: New Zealand
58.	Lalbiakzuala , Vanlal Hruaia, Lal Biakhlui & Hmar Tlawmte Lalremsanga	Second observation of the reproductive biology of <i>Blythia reticulata</i> (Blyth, 1854) (Reptilia, Squamata, Colubridae)	<i>Herpetozoa</i>	2021, 34: 121-124	0.8	SCOPUS	Pensoft Publishers: Austria
59.	Hmar Tlawmte Lalremsanga, Jayaditya Purkayastha, Mathipi Vabeiryureilai, Lal Muansanga, Ht Decemson & Lal Biakzuala *	Range extension of <i>Ichthyophis multicolor</i> Wilkinson et al., 2014 to India and first molecular identification of <i>Ichthyophis moustakius</i> Kamei et al., 2009	<i>Check List</i>	2021, 17(4):1021–2029	0.6	SCOPUS	Centro de Referencia em Informacao Ambiental: Brazil
60.	Mathipi, Vabeiryureilai, L. H. Laltlanhlui, Lal Biakzuala , Fanai Malsawmdawngliana, Lal Muansanga, and H. T. Lalremsanga	On the Phylogeny of the Suffry Red-webbed Treefrog, <i>Zhangixalus suffry</i> (Bordoloi, Bortamuli, and Ohler 2007), with Notes on Distribution and Comparisons with the Giant Treefrog, <i>Zhangixalus smaragdinus</i> (Blyth 1852), and Other Closely Related Species in Mizoram	<i>Reptiles & Amphibian</i>	2021, 28(3): 475–479	-	SCI	International Reptile Conservation Foundation (IRCF): U.S.A
61.	Lal Biakzuala , Ht. Decemson, Gospel Zothanmawia Hmar, Lalmuansanga, Lalrinsanga, H.T. Lalremsanga, Lalrengpuii Sailo et al.	Natural History Notes: <i>Leptobrachium smithi</i> (Southern Bicolor-eyed Toadfrog) and <i>Polypedates teraiensis</i> (Perching Frog). Interspecific amplexus.	<i>Herpetological Review</i>	2021, 52(4): 829	-	SCOPUS	Society for the Study of Amphibians and Reptiles: U.S.A

Sl. No.	Authors	Title	Journal	Year, volume (issue): pages	Impact Factor (JCR 2024)	Index	Publisher & Country
62.	Malnica Vanlal Malsawmtluangi, Lalmuansanga, Lal Biakzuala & H.T. Lalremsanga	Natural History Notes: <i>Kurixalus yangi</i> . Diet	<i>Herpetological Review</i>	2021, 52(4): 829	-	SCOPUS	Society for the Study of Amphibians and Reptiles: U.S.A
63.	Hmar Tlawmte Lalremsanga, Jayaditya Purkayastha, Lal Biakzuala *, Mathipi Vabeiryureilai, Lal Muansanga & Gospel Zothanmawia Hmar	A new striped species of <i>Ichthyophis</i> Fitzinger, 1826 (Amphibia: Gymnophiona: Ichthyophiidae) from Mizoram, northeast India	<i>Amphibian & Reptile Conservation</i>	2021, 15(2): 198–209	1.3	SCOPUS	Amphibian & Reptile Conservation: U.S.A
64.	Lal Biakzuala , Jayaditya Purkayastha, Yashpal Singh Rathee & Hmar Tlawmte Lalremsanga	New data on the distribution, morphology, and molecular systematics of two venomous snakes, <i>Bungarus niger</i> and <i>Bungarus lividus</i> (Serpentes: Elapidae), from north-east India	<i>Salamandra</i>	2021, 57(2): 219–228	1.3	SCOPUS	Deutsche Gesellschaft fur Herpetologie und Terrarienkunde: Germany
65.	Ronald Rohluosang Sinate, Ht. Decemson, Lal Biakzuala & Hmar Tlawmte Lalremsanga	Geographic Distribution Notes: <i>Bungarus niger</i> (New state report for Manipur)	<i>Herpetological Review</i>	2021, 52(4): 797	-	SCOPUS	Society for the Study of Amphibians and Reptiles: U.S.A
66.	Ht. Decemson, Ronald Rohluosang Sinate, Lal Biakzuala & Hmar Tlawmte Lalremsanga	Geographic Distribution Notes: <i>Sylvirana lacrima</i> (New state report for Manipur)	<i>Herpetological Review</i>	2021, 53(2): 260	-	SCOPUS	Society for the Study of Amphibians and Reptiles: U.S.A
67.	Chinliansiam, Hmar Tlawmte Lalremsanga & Lal Biakzuala	Natural History Notes: <i>Smithophis bicolor</i> . Reproduction	<i>Herpetological Review</i>	2021, 53(3): 520	-	SCOPUS	Society for the Study of Amphibians and Reptiles: U.S.A

Sl. No.	Authors	Title	Journal	Year, volume (issue): pages	Impact Factor (JCR 2024)	Index	Publisher & Country
68.	Vabeiryureilai Mathipi, Ht. Decemson, Lal Biakzuala & Hmar Tlawmte Lalremsanga	Natural History Notes: <i>Coelognathus radiatus</i> . Predation	<i>Herpetological Review</i>	2021, 53(3): 520	-	SCOPUS	Society for the Study of Amphibians and Reptiles: U.S.A
69.	Siammawii, V., Ht, D., Fanai, M., Muansanga, L., Biakzuala, L. , Mathipi, V. and Tlawmte, L.H.	DNA barcoding elucidates the range-extension of the Bangladesh Skittering Frog, <i>Euphlyctis kalasgramensis</i> (Dicroglossidae), in northeast India	<i>Reptiles & Amphibian</i>	2022, 29: 321–325	-	SCI	International Reptile Conservation Foundation (IRCF): U.S.A
70.	Shantanu Kundu, Hmar Tlawmte Lalremsanga, Lal Biakzuala , Kaomud Tyagi, Kailash Chandra & Vikas Kumar	Mitochondrial DNA illuminates the genetic diversity of mimetic mock viper (<i>Psammodynastes pulverulentus</i>) from Northeast India	<i>Records of the Zoological Survey of India</i>	2021, 121(4): 521–526	-	SCI	Zoological Survey of India: India
71.	Lal Biakzuala , Lal Muansanga, Ht Decemson, Gospel Zothanmawia Hmar, Fanai Malsawmdawngliana, Vabeiryureilai Mathipi, and H. T. Lalremsanga.	New distributional records of the Baibung Small Treefrog, <i>Theloderma baibungense</i> (Jiang, Fei, and Huang 2009) (Anura: Rhacophoridae), from Mizoram, India with comments on taxonomy, natural history and conservation status.	<i>Reptiles & Amphibian</i>	2022, 29: 66–70	-	SCI	International Reptile Conservation Foundation (IRCF): U.S.A
72.	Hmar Tlawmte Lalremsanga, Amit Kumar Bal, Gernot Vogel & Lal Biakzuala *	Molecular phylogenetic analysis of the lesser known colubrid snakes reveals a new species of <i>Herpetoreas</i> (Squamata: Colubridae: Natricinae), and new insights to the systematics of <i>Gongylosoma scriptum</i> and its allied colubrine snakes from Northeast India.	<i>Salamandra</i>	2022, 58(2): 101–115	1.3	SCOPUS	Deutsche Gesellschaft für Herpetologie und Terrarienkunde: Germany

Sl. No.	Authors	Title	Journal	Year, volume (issue): pages	Impact Factor (JCR 2024)	Index	Publisher & Country
73.	Hmar Tlawmte Lalremsanga, Hauzel Chinliansiam, Sanath Chandra Bohra, Lal Biakzuala , Mathipi Vabeiryureilai, Lalmuansanga, Fanai Malsawmdawngliana, Gospel Zothanmawia Hmar, Ht Decemson & Jayaditya Purkayastha	A new Bent-toed geckos (<i>Cyrtodactylus</i> Gray: Squamata: Gekkonidae) from the state of Mizoram, India	<i>Zootaxa</i>	2022, 5093(4): 465–482	0.8	SCOPUS	Magnolia Press: New Zealand
74.	Jayaditya Purkayastha, Hmar Tlawmte Lalremsanga, Beirathie Litho, Yashpal Singh Rathee, Sanath Chandra Bohra, Vabeiryureilai Mathipi, Lal Biakzuala & Lalmuansanga	Two new bent-toed gecko (<i>Cyrtodactylus</i> Gray: Squamata: Gekkonidae) from Northeast India.	<i>European Journal of Taxonomy</i>	2022, 794(1): 111–139	1.1	SCOPUS	National Museum of Natural History: France
75.	Lal Biakzuala , Hmar Tlawmte Lalremsanga, Angshuman Das, Mathipi Vabeiryureilai, Lalmuansanga, Vanlal Hrima, Vikas Kumar, Shantanu Kundu, Jayaditya Purkayastha & Gernot Vogel	A contribution to the taxonomic status of Asian Bronzeback Snakes (Colubridae, Ahaetuliinae, <i>Dendrelaphis</i>) from Northeast India.	<i>Zoosystema</i>	2022, 44(7): 177–196	0.9	SCOPUS	National Museum of Natural History: France
76.	Ronald Rohluosang Sinate, Ht. Decemson, Lal Biakzuala & H.T. Lalremsanga	Geographic Distribution Notes: <i>Boiga quincuiciata</i> (New State report for Manipur).	<i>Herpetological Review</i>	2022, 53(1): 78	-	SCOPUS	Society for the Study of Amphibians and Reptiles: U.S.A

Sl. No.	Authors	Title	Journal	Year, volume (issue): pages	Impact Factor (JCR 2024)	Index	Publisher & Country
77.	Ht. Decemson, Vanlal Siammawii, Vabeiryureilai Mathipi, Lal Biakzuala & H.T. Lalremsanga	Geographic Distribution Notes: <i>Amolops indoburmanensis</i> (New State report for Manipur).	<i>Herpetological Review</i>	2022, 53(1): 69	-	SCOPUS	Society for the Study of Amphibians and Reptiles: U.S.A
78.	Hmar Tlawmte Lalremsanga, Lalremmawia Rokhum, Mathipi Vabeiryureilai & Lal Biakzuala	Birth and neonate colouration of <i>Ahaetulla prasina</i> in north-east India	<i>Herpetological Bulletin</i>	2022, 160: 43–44	-	SCOPUS	British Herpetological Society: United Kingdom
79.	Lal Biakzuala , Lalrinsanga, Samuel Lianzela, Ro Malsawma, Lalmuansanga, Ht. Decemson, Michael Vanlalchhuana, Lalengzuala Tochhawng, Hrahsel Laltlanchhuaha & Hmar Tlawmte Lalremsanga	Collection and captive incubation of King Cobra (<i>Ophiophagus hannah</i> Cantor, 1836) from vulnerable nests as a conservation strategy in Mizoram north-east India	<i>Herpetological Bulletin</i>	2022, 159: 18–20	-	SCOPUS	British Herpetological Society: United Kingdom
80.	Lalremsanga, H.T., Muansanga, L., Biakzuala, L. , Decemson, H., Malsawmdawngliana, F., Rinsanga, L., Colney, Z. and Vabeiryureilai, M.	An updated distribution map and a new elevational record of the Coastal Bullfrog (<i>Hoplobatrachus litoralis</i>).	<i>Reptiles & Amphibian</i>	2022, 29: 237–240	-	SCI	International Reptile Conservation Foundation (IRCF): U.S.A
81.	Hmar Tlawmte Lalremsanga, Ht Decemson, Mathipi Vabeiryureilai, Fanai Malsawmdawngliana, Van Lahlhimpua & Lal Biakzuala *	Phylogenetic position of <i>Tropidophorus assamensis</i> Annandale, 1912 with updated morphological data and distributional records	<i>Herpetological Journal</i>	2022, 32(1): 1–4	1.1	SCOPUS	British Herpetological Society: United Kingdom

Sl. No.	Authors	Title	Journal	Year, volume (issue): pages	Impact Factor (JCR 2024)	Index	Publisher & Country
82.	Lal Biakzuala, Malsawmtluanga & H.T. Lalremsanga	Ophiophagy by banded krait (<i>Bungarus fasciatus</i>) exposed by a road kill	<i>Taprobanica: The Journal of Asian Biodiversity</i>	2021, 10(2): 127	-	SCI	Research Center for Climate Change (RCCC) and the Faculty of Mathematics & Natural Sciences (FMIPA) - University of Indonesia: Indonesia
83.	Malsawmdawngliana, Fanai, Lal Muansanga, Ro Malsawma, Mathipi Vabeiryureilai, Hmar Tlawmte Lalremsanga & Lal Biakzuala*	Systematics and Ecological Data Enrichment for the Recently Described Lushai Hills Dragon Snake, <i>Stoliczka vanhnuailianai</i> Lalronunga, Lalhmangaiha, Zosangliana, Lalhmingliani, Gower, Das & Deepak, 2021 (Squamata: Xenodermidae) from Northeast India	<i>Current Herpetology</i>	2022, 41(2): 163–171	0.6	SCOPUS	The Herpetological Society of Japan: Japan
84.	Rathee, Y.S., Purkayastha, J., Lalremsanga, H.T., Dalal, S., Biakzuala, L. , Muansanga, L. and Mirza, Z.A.	A new cryptic species of green pit viper of the genus <i>Trimeresurus</i> Lacépède, 1804 (Serpentes, Viperidae) from northeast India	<i>Plos One</i>	2022, 17(5): e0268402	2.9	SCOPUS	Public Library of Science: USA
85.	Remruatpuii, Lal Biakzuala , Vishal Santra & Hmar Tlawmte Lalremsanga	Additional notes on morphology and distributional records of the snake genus <i>Smithophis</i> (Squamata: Serpentes: Natricidae) from north-east India	<i>Russian Journal of Herpetology</i>	2022, 29(6): 331–340	0.9	SCOPUS	Folium Publishing Company: Russian Federation

Sl. No.	Authors	Title	Journal	Year, volume (issue): pages	Impact Factor (JCR 2024)	Index	Publisher & Country
86.	Bohra, S.C., Zonunsanga, H.T., Das, M., Purkayastha, J., Biakzuala, L. and Lalremsanga, H.T.	Morphological and molecular phylogenetic data reveal another new species of bent-toed gecko (<i>Cyrtodactylus</i> Gray: Squamata: Gekkonidae) from Mizoram, India	<i>Journal of Natural History</i>	2022, 56(41–44): 1585–1608	0.8	SCOPUS	Taylor & Francis Ltd.: United Kingdom
87.	Premjit Singh Elangbam, Ht. Decemson, Lal Biakzuala , H.T. Lalremsanga	Geographic Distribution Notes: <i>Lycodon jara</i>	<i>Herpetological Review</i>	2022, 53(4): 631–632	-	SCOPUS	Society for the Study of Amphibians and Reptiles: U.S.A
88.	Angshuman Das Tariang, Fanai Malsawmdawngliana, Lal Biakzuala , Ht Decemson, Lal Muansanga, Lal Rinsanga, Mathipi Vabeiryureilai and Hmar Tlawmte Lalremsanga	Confirmation on the occurrence of <i>Calotes irawadi</i> Zug, Brown, Schulte & Vindum 2006 (Squamata: Agamidae) in Mizoram, Northeast India	<i>Hamadryad</i>	2023, 39(1&2): 88–94	-	SCOPUS	Centre for Herpetology, Madras Crocodile Bank Trust: India
89.	Lalrinsanga, Hmar Tlawmte Lalremsanga, Ht. Decemson, Vabeiryureilai Mathipi, Lal Tanpuii, Lal Muansanga, Lal Biakzuala*	Contributions to the morphology and molecular phylogenetics of <i>Gonyosoma prasinum</i> (Blyth, 1854) (Reptilia: Squamata: Colubridae) from Mizoram, India	<i>Hamadryad</i>	2023, 39(1&2): 96–103	-	SCOPUS	Centre for Herpetology, Madras Crocodile Bank Trust: India
90.	Lal Biakzuala , Hmar T. Lalremsanga, Vishal Santra, Arindam Dharab, Molla T. Ahmed, Ziniya B. Mallick, Sourish Kuttalam, Anita Malhotra	Molecular phylogeny reveals distinct evolutionary lineages of the Banded Krait, <i>Bungarus fasciatus</i> (Squamata: Elapidae) in Asia	<i>Scientific Reports</i>	2023, 13: 2061	3.8	SCOPUS	Nature Publishing Group: United Kingdom

Sl. No.	Authors	Title	Journal	Year, volume (issue): pages	Impact Factor (JCR 2024)	Index	Publisher & Country
91.	Ht Decemson, Ronald Rohluosang Sinate, Lal Biakzuala , Mathipi Vabeiryureilai and Hmar Tlawmte Lalremsanga	Confirmation on Irawadi Forest Lizard <i>Calotes irawadi</i> Zug, Brown, Schulte and Vindum 2006 (Squamata: Agamidae) from Manipur, Northeast India	<i>Reptiles & Amphibians</i>	2023, 30: e1704	-	SCI	International Reptile Conservation Foundation (IRCF): U.S.A
92.	Amarasinghe, A. A. Thasun, Rafaqat Masroor, H. T. Lalremsanga, Sanjaya Weerakkody, Natalia B. Ananjeva, Patrick D. Campbell, Stevie R. Kennedy-Gold, Sanjaya K. Bandara, Andrey M. Bragin, Atthanagoda K. A. Gayan, Vivek R. Sharma, Amit Sayyed, Lal Biakzuala , Andradige S.Kanishka, et al.	Integrative approach resolves the systematics of barred wolf snakes in the <i>Lycodon striatus</i> complex (Reptilia, Colubridae)	<i>Zoologica Scripta</i>	2023, 00: 1–24	2.3	SCOPUS	Wiley-Blackwell Publishing Ltd.: United Kingdom
93.	Amit Kumar Bal, Lal Biakzuala , Hmar Tlawmte Lalremsanga	Natural History Notes: <i>Hebius vemingi</i> (Diet)	<i>Herpetological Review</i>	2023, 54(1): 137	-	SCOPUS	Society for the Study of Amphibians and Reptiles: U.S.A
94.	Hmar Tlawmte Lalremsanga, Ht Decemson, Sushanto Gouda, Romalsawma Hmar, Gospel Zothanmawia Hmar, Lal Biakzuala , R. Zonunsanga, Paul Lalnuntluanga	Natural History Notes: <i>Lycodon zawi</i> (Diet)	<i>Herpetological Review</i>	2023, 54(1): 139	-	SCOPUS	Society for the Study of Amphibians and Reptiles: U.S.A

Sl. No.	Authors	Title	Journal	Year, volume (issue): pages	Impact Factor (JCR 2024)	Index	Publisher & Country
95.	Vanlal Siammawii, Fanai Malsawmdawngliana, Lal Biakzuala , Lal Muansanga, Hmar Tlawmte Lalremsanga	Natural History Notes: <i>Odorrana mawphlangensis</i> (Parasite)	<i>Herpetological Review</i>	2023, 54(1): 103–104	-	SCOPUS	Society for the Study of Amphibians and Reptiles: U.S.A
96.	Lal Biakzuala , Ht Decemson, Hmar Tlawmte Lalremsanga, Lal Hmunmawia, Paul Lalnuntluanga	Natural History Notes: <i>Oligodon cf. cyclurus</i> (Diet)	<i>Herpetological Review</i>	2023, 54(1): 141–142	-	SCOPUS	Society for the Study of Amphibians and Reptiles: U.S.A
97.	Vanlalhrauaia, Lalengzuala Tochwawng, H. Laltlanchhuaha, Ht Decemson, Lal Biakzuala , Hmar Tlawmte Lalremsanga	Natural History Notes: <i>Bungarus niger</i> (Diet)	<i>Herpetological Review</i>	2023, 54(1): 131–132	-	SCOPUS	Society for the Study of Amphibians and Reptiles: U.S.A
98.	Premjit Singh Elangbam, Lal Biakzuala , Parag Shinde, Ht. Decemson, Mathipi Vabeiryureilai, Hmar Tlawmte Lalremsanga	Addition of four new records of pit vipers (Squamata: Crotalinae) to Manipur, India	<i>Journal of Threatened Taxa</i>	2023, 15(6): 23315–23326	-	SCOPUS	Wildlife Information & Liaison Development Society: India
99.	Lal Biakzuala , Zeeshan A. Mirza, Harshil Patel, Yashpal Singh Rathee, Hmar Tlawmte Lalremsanga	Reappraisal of the systematics of two sympatric coral snakes (Reptilia, Elapidae) from Northeast India	<i>Systematics and Biodiversity</i>	2024, 21(1): 2289150	1.8	SCOPUS	Taylor and Francis: UK
100.	Tan Van Nguyen, Hmar Tlawmte Lalremsanga, Lal Biakzuala , Gernot Vogel	Taxonomic reassessment of the <i>Herpetoreas xenura</i> (Wall, 1907) (Squamata: Serpentes: Natricidae) from Myanmar with description of a new species	<i>European Journal of Taxonomy</i>	2024, 932: 158–203	1.1	SCOPUS	Museum National d'Histoire Naturelle: France

Sl. No.	Authors	Title	Journal	Year, volume (issue): pages	Impact Factor (JCR 2024)	Index	Publisher & Country
101.	Lal Biakzuala, Lal Muansanga, Fanai Malsawmdawngliana, Lalrinnunga Hmar, Hmar Tlawmte Lalremsanga	New country record of <i>Trimeresurus uetzi</i> Vogel, Nguyen & David, 2023 (Reptilia: Squamata: Viperidae) from India	<i>Journal of Threatened Taxa</i>	2024, 16(5): 25268-25272	-	SCOPUS	Wildlife Information & Liaison Development Society: India
102.	Hmar Tlawmte Lalremsanga, Annie Malsawmkimi, Mathipi Vabeiryureilai, Lal Muansanga, Fanai Malsawmdawngliana, Lal Biakzuala, Olivier, S.G. Pauwels	Molecular identification of python species (Squamata: Pythonidae) from Mizoram, Northeast India, with comments on wildlife trafficking	<i>Taprobanica: The Journal of Asian Biodiversity</i>	2024, 13(1): 16–24	-	SCI	Research Center for Climate Change (RCCC) and the Faculty of Mathematics & Natural Sciences (FMIPA) - University of Indonesia: Indonesia

Grant Award

Name of Grant: First Rufford Small Grants.

Name of Project: Educating Young Minds for Snakebite Management and Conservation of Snakes in Mizoram, India.

Amount: £5,410 (=Rs. 5,47,391.915/- on 8 Feb. 2022).

Funding Agency: Rufford Foundation, United Kingdom.

Current Status: Completed

Project Leader: Mr. Lalbiakzuala

Team Members: Prof. H. T. Lalremsanga, Dr. Sushanto Gouda, Mr. Vishal Santra.

Paper presented/attended on conference/seminar/workshop/training:

I. Invited Speech				
	Title of presentation	Conference/Seminar/Symposium/ Workshop/Training	Type	Date
1.	Snake Bite and its Management	“Training of Nurses” under the Central Sector scheme of “Development of Nursing Services: organized by Mizoram Nursing Council	Oral	13 Jul. 2022
2.	Snake Bite and its Management	“Training of Nurses” under the Central Sector scheme of “Development of Nursing Services: organized by Mizoram Nursing Council	Oral	28 Jul. 2022
3.	Snake Bite and its Management	One-Day Workshop on Maintaining the Ecosystem: A Study of Snakes of Mizoram: organized by Govt. Mamit College	Oral	22 Sep. 2022
II. Paper presented				
1.	Review on the systematic status of king cobra, <i>Ophiophagus hannah</i> (Cantor, 1836) (Squamata: Elapidae) population in Mizoram, Northeast India.	National Seminar on Biotechnology for Sustainable Biosphere: organized by Department of Biotechnology, School of Life Sciences, Mizoram University	Oral	30 Jun.–1 Jul. 2023
2.	Taxonomical insight on <i>Sinomicrurus macclellandi</i> (Reinhardt, 1844) (Squamata: Elapidae) population of Mizoram, Northeast India	National Webinar on Herpetology- Indian scenario: organized by National Science Association, Department of Zoology, St. Joseph’s College	Oral	26–27 Nov. 2021
3.	DNA barcoding reveals intra-species genetic diversity of <i>Amphiesma stolatum</i> (Linnaeus, 1758) in Indo-Malayan region	International Seminar on Recent Advances in Science and Technology (ISRAST): organized by North-east India Academy of Science & Technology and Mizoram University	Oral	16–18 Nov. 2020
III. Participations				
1.	Applications of Molecular Phylogenetics: four days online workshop organized by BIOLOGIA LIFE SCIENCE LLP, India		Attended	9–12 Aug. 2021
2.	Basics of Bioinformatics and Phylogenetics: three days online workshop organized by BIOLOGIA LIFE SCIENCE LLP, India		Attended	1–3 Jul. 2021
3.	An insight into the lizards of Assam: a webinar organized by Help Earth, Guwahati, India		Attended	13 Jun. 2021
4.	Introduction to Herpetology: online two days workshop organized by NIDUS and Anala Outdoors, India		Attended	28–29 Aug. 2020
5.	Spider-Ant Symbionts: International e-Conference organized by BioLogic, India		Attended	23 Aug. 2020
6.	Geographic Information System (GIS) using QGIS- Basics and Application in Zoogeographical Research: hands-on workshop organized by Developmental Biology and Herpetology Laboratory, Department of Zoology, Mizoram University		Attended	31 Mar. 2020
7.	Amphibians and Reptiles of Indian Peninsula: webinar organized by Nature Club of Rajapalayam Rajus’ College and Wildlife Association of Rajapalayam (WAR)		Attended	25 May. 2020



Lal Biakzuala

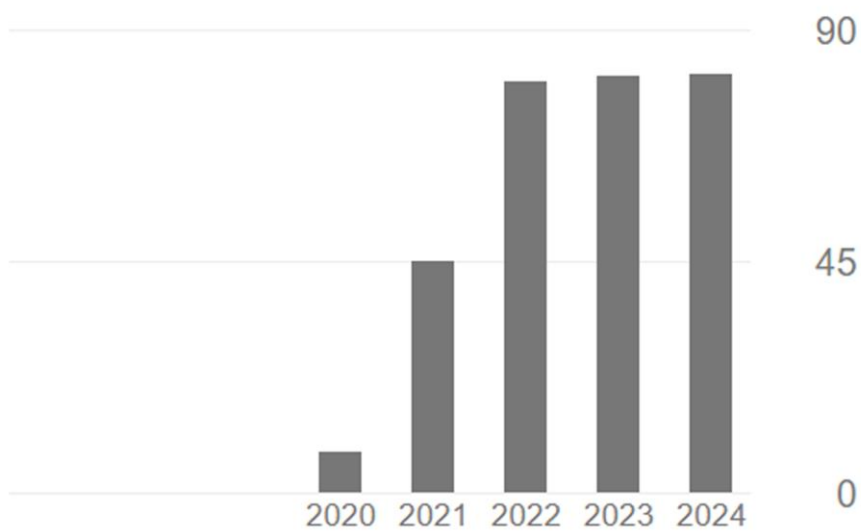
Research Scholar

Verified email at mail.mzu.edu.in - [Homepage](#)

Herpetology

Cited by

	All	Since 2019
Citations	301	301
h-index	9	9
i10-index	8	8



PARTICULARS OF THE CANDIDATE

NAME OF THE CANDIDATE: LALBIAKZUALA
DEGREE: DOCTOR OF PHILOSOPHY
DEPARTMENT: ZOOLOGY

TITLE OF THE THESIS: Taxonomic study on the elapid snakes of Mizoram, India (Reptilia: Serpentes: Elapidae)

DATE OF ADMISSION: 16.03.2020

APPROVAL OF RESEARCH PROPOSAL:

B.O.S: 02.06.2020
SCHOOL BOARD: 12.06.2020
MZU REGISTRATION NO. 2189 of 2012
Ph.D. REGISTRATION NO. & DATE: MZU/Ph.D./1384 of 16.03.2020
EXTENSION: NA

(Prof. H.T. LALREMSANGA)

Head

Department of Zoology

Mizoram University

ABSTRACT

**TAXONOMIC STUDY ON THE ELAPID SNAKES OF MIZORAM,
INDIA (REPTILIA: SERPENTES: ELAPIDAE)**

**A THESIS SUBMITTED IN PARTIAL FULFILLMENT OF THE
REQUIREMENTS FOR THE DEGREE OF DOCTOR OF PHILOSOPHY**

LALBIAKZUALA

MZU REGN NO.: 2189 OF 2012

PH.D REGN NO.: MZU/PH.D./1384 OF 16.03.2020



DEPARTMENT OF ZOOLOGY

SCHOOL OF LIFE SCIENCES

NOVEMBER, 2024

Taxonomic study on the elapid snakes of Mizoram, India
(Reptilia: Serpentes: Elapidae)

BY

LALBIAKZUALA

Department of Zoology

Name of Supervisor

Professor H.T. Lalremsanga

Submitted

In partial fulfillment of the requirement of the Degree of Doctor of Philosophy in
Zoology of Mizoram University, Aizawl.

ABSTRACT

The present thesis focuses on the systematics and taxonomic study for the elapid snake family which is one of the several families accommodating under the caenophidian snake lineage. Species of this family are having a well-developed venom delivery system with a non-movable pair of venom delivering fangs at the anterior end of the upper dentition except the genus *Emydocephalus* Krefft, 1869, the only known non-venomous elapid snake genus. Elapid snakes are estimated to emerged less than 40 million years ago and showed high rates of diversification among reptiles. The family accommodates over 60 genera (more than 300 nominal species) distributing worldwide in the tropical and subtropical regions including the terrestrial genera. In the study area i.e Mizoram state of northeastern India, previous workers have documented a total of five species under the family Elapidae namely *B. fasciatus* (Schneider, 1801), *B. niger* Wall, 1908, *N. kaouthia* Lesson, 1831, *O. hannah* (Cantor, 1836), and *S. maccllellandi* (Reinhardt, 1844). However, the existing literature underrepresented elapid specimens in their studies, and limited data is available at morphological and molecular level from Mizoram particularly for *O. hannah*, *S. maccllellandi*, *B. fasciatus* and *B. niger*; while there is no existing taxonomic or systematic framework for *N. kaouthia* from the area so far. Accurate determination of intra-specific variations and inter-specific boundaries among the deadly venomous elapid snakes is imperative for accurate biodiversity assessment as well as for developing efficient snakebite management particularly in Mizoram as well as for the whole Northeast Indian region. This study aims to establish taxonomic framework for the elapid snakes in Mizoram for the better understanding of their respective species distribution and the true diversity of the family in the area. The following objectives were proposed for this study:

1. To survey and document the distribution of species belonging to the family Elapidae in Mizoram.
2. To analyze the morphological and meristic variations among different species of the family Elapidae.

3. To analyze the genetic data and phylogenetic status of different species under the family Elapidae using mitochondrial *16s*, *cox1*, and *cytb*.

In this work, integrated taxonomic approach is applied by implementing descriptive morphology, morphometric analyses and phylogenetic inferences. The combination of morpho-taxonomy and the phylogenetic species concept that is based on reciprocal monophyly were successfully implemented for species recognition in this work.

Bungarus fasciatus, despite its wide distributional range, most of the existing studies have hitherto dealt onto its possible medical significance, ecology, or venomics. Although the molecular systematics of *B. fasciatus* has never been deeply studied, several previous DNA barcoding research have dictated the existence of intra-specific or geographical variations. Establishment of accurate species boundary is critical in considering the variability in snake venom composition and its possible consequence to the antivenom effectiveness. Most of the published literature on *Bungarus* taxonomy and systematics have apparently underestimated the diversity of *B. fasciatus* at the intraspecies level. The present thesis work enhances the inherent knowledge gaps for the species through comparative morphological analyses and molecular phylogenetic inferences using mitochondrial genes. A total of 15 individuals are examined from Mizoram (MZ), and other morphological data were outsourced from Java (JV) (n=15) and West Bengal (WB) (n=8). Analyses on the morphological characters revealed that tail length ($p<0.001$), head width ($p<0.05$) and head length ($p<0.05$) showed significant dimorphism between males and females within JV and MZ populations. Inter-population differences were statistically significant ($p<0.001$) for Ve (MZ vs. JV), BB, BT, and NBW (the latter three characters are tested among three populations), all of which showed a higher number in the MZ population; for mensural characters, inter-population differences were also statistically significant for TaL ($p<0.05$) and HL ($p<0.001$). Post-hoc tests conducted among the three populations for BB, BT, and NBW showed that, except for BT between MZ and WB populations ($p>0.05$), significant differences are seen for all characters: BB

($p < 0.001$ across all the populations), NBW ($p < 0.001$ in MZ vs. WB, and JV vs. WB; $p < 0.05$ in MZ vs. JV), and BT ($p < 0.001$ in MZ vs. JV; $p < 0.01$ in JV vs. WB). The representation of the first two components depicts substantial separation of the Javanese and the Indian populations on the first axis (PC1), and marginal separation of the WB and MZ populations on the second axis (PC2). Based on the present study, the existence of at least three different taxonomic entities was postulated within the nomen *B. fasciatus*, and also confirm that populations in eastern India (e.g. Odisha, West Bengal, etc.) and northeastern India (e.g. Mizoram, Assam, etc.) are conspecific. The Indo-Myanmar population (Clade II) was postulated as *B. fasciatus* sensu stricto, while considering the populations from Sundaic region, especially from Greater Sunda Islands (Clade I) and mainland Sundaland including southern China (Clade III) as *B. fasciatus* sensu lato. Consequently, *B. fasciatus* sensu stricto was redescribed in this chapter, including hemipenial morphology, based on MZ population, from where a large number of samples are available. The species is documented in Mizoram from total of 47 localities in this work (40 previous + 7 new) at 49–1,426 m a.s.l.

For *B. niger*, limited study and data is available for the species especially from Mizoram, and there even exist insubstantial number of genetic data in the public access genetic data repository like GenBank, and the only available data were also originated from Nepal and unspecified locality from India. Considering the fact that the species can be medically important due to its venom lethality and few existing records of deadly envenomation, appraising the regional and overall distributional records of this species will be crucial for mapping and better understanding of the taxon's geographical range. Based on an integrated taxonomic approach, this chapter attempts to provide the systematic status of the species among the congeneric species especially with respect to the morphologically alike species (*B. lividus*) for the first time. Thus, this work is crucial for enriching the knowledge paucity, particularly on the morpho-taxonomy, molecular systematics and distribution of this poorly studied deadly venomous species. A total of 46 adults and 3 juvenile specimens housed in the collections of the Departmental Museum of Zoology, Mizoram University (MZMU) were examined. In both the phylogenetic

trees, the samples of *B. niger* from Mizoram were clustered together (PP=0.96; UFB=87) and formed a distinct lineage along with the conspecific samples from Nepal and unspecified locality from India (PP=1.0; UFB=100). Our analyses also clearly nested *B. lividus* among the kraits of Indian subcontinent such as *B. sindanus*, *B. caeruleus* and *B. ceylonicus* with a high branch support (PP=1.0; UFB=100), whereas *B. niger* formed a highly-supported sister lineage to the Southeast Asian endemic kraits such as *B. suzhenae* and *B. multicinctus* + *B. candidus* + *B. wanghaotingi* clade (PP=1.0; UFB=94). The ASAP species delimitation was conducted for the three mitochondrial genes separately and produced 10 distinct species partitions each and accurately detected *B. niger* as distinct species. Among the examined specimens, a peculiar nape colouration was observed in a juvenile specimen (MZMU 1809); it was mottled with light patches at both sides from the rim of posterior temporals up to part of the first dorsal scale. Moreover, a peculiar male specimen was collected from Thenzawl locality (MZMU2030) which was characterized by the unusual formula of dorsal scale rows with 17:17:15 while the known feature for the species is 15:15:15. Based on the statistical analyses, it was uncovered that only the characters of internarial length and prefrontal length are statistically significant ($p < 0.05$). This work documented *B. niger* from a total of 58 distributional localities (48 previous + 10 new) at 64–1,433 m a.s.l.

N. kaouthia have been included in the multiple phylogenetic studies of elapid snakes, but only a few studies on venomics and systematic studies suggested intra-specific or geographical variability among *N. kaouthia* populations. Although Shi et al. (2022) proposed two distinct clades of *N. kaouthia* based on *cox1* gene which is partly based on the DNA sequences generated in this work from Mizoram viz. the South Asian clade which is represented by populations from Northeast India (based on Mizoram specimens), Nepal, Bhutan, Tibet (China), and Bangladesh; while the Southeastern Asian clade is represented by the populations from Southern Myanmar, central and southern part of Thailand, Cambodia, central and southern part of Laos, southern part of Vietnam, and the Malay Peninsula. Prompted by the limited availability of biological samples and systematic studies of *N. kaouthia* populations

from Northeast (NE) India especially from Mizoram, this chapter aims to reassess the systematic status of *N. kaouthia* population from Mizoram, NE India. a total of 28 adult and 16 juvenile specimens were examined. Of these, 33 are preserved specimens housed in the collections of MZMU. the concatenated three mitochondrial genes based phylogenetic analyses depicted a well-supported (PP=0.99; UFB=93) lineage diversification among *N. kaouthia* populations showing two independent lineages, the South Asian Clade containing populations from Northeast India (Mizoram) and Bangladesh; and the Southeastern Asian Clade which accommodates the populations from Myanmar, China, Vietnam, Thailand, and unknown sample locality. This supports the existence of two distinct clades as previously proposed by Shi et al. (2022) based on *cox1* gene. The PCoA ordinations of genetic divergence showed the discrete clustering of *N. kaouthia* from Southeast Asia from the other congeneric samples from South Asia, while a single specimen from China (KIZYPX18216) is seen distant from both South Asia and SE Asian samples. The *N. kaouthia* from China (KIZYPX18216) is also detected as distinct species from both the representative specimens of South Asian and Southeast Asian Clades in the ASAP analysis which warrant further investigation of the taxonomic status of this specimen. The present intra-species analysis accepts the alternative hypothesis which states that the phenotypic variation of hood marking is having an effect on meristics and morphometrics between the two groups. Owing that *a priori* grouping of the variant accommodated various phenotypic forms; further nesting of significantly different sub-groups within the variant is not unexpected in a larger sampling size. Ascertainment of the probable correlations between the genetic and phenotypic variations within *N. kaouthia* populations remains a crucial challenge. In this study, *N. kaouthia* is recorded from a total of 48 localities in Mizoram at 66–1,470 m a.s.l.

The evidence of many potential biogeographical barriers across the range of the king cobra (*O. hannah*) populations propounded cryptic diversity within the species. Concerning this, four distinctly evolving lineages representing four candidate species have been detected such as the Indo-Chinese, Western Ghats, Indo-Malayan and Luzon Island lineages where the northeastern Indian populations including samples from Mizoram found to be nested within the foremost lineage.

Moreover, biogeographical analyses and niche modeling of the species determined that the distribution of the species across its range is highly influenced by the presence of humid climatic condition. Although the occurrence of the species in Mizoram was recorded in earlier faunal inventory works from the state, while other literature on the species from Mizoram predominantly focused on the breeding ecology and natural history. A limited number of specimens from Mizoram has been included in the previous molecular studies, and not much assessment of the morphological data has been done from this population. Mizoram king cobra samples were also lacking in the morphological analyses of Shankar et al. (2021). Therefore, this thesis aims to provide additional information on the systematics of king cobra population in Mizoram based on morphological analyses and mitochondrial genes inferences. A total of 27 adult individuals represented by 14 preserved and 13 live individuals were examined. The molecular analyses affirmed the nesting of the study population within the clade of Indo-Chinese lineage. Pos-hoc test showed the absence of morphological difference between Mizoram and Indo-Chinese specimens, thereby morphology conforms to the systematic status of Mizoram population as member of Indo-Chinese Lineage. PCA ordination on the standardised meristics (ventrals, subcaudals, anterior dorsal scale rows) also showed an overlapping clustering between Mizoram specimens and the pre-defined specimens of Indo-Chinese Lineage. The present systematic reassessment (morphologically and phylogenetically) affirms that the study population is a member of the Indo-Chinese lineage. Sexual dimorphism in the study population is significant in the ventrals ($p < 0.01$), subcaudals ($p < 0.05$), undivided subcaudals ($p < 0.05$), tail length ($p < 0.001$), head length ($p < 0.05$), head width ($p < 0.0001$), head depth ($p < 0.01$), nostril diameter ($p < 0.05$), internarial space ($p < 0.05$), width of frontals ($p < 0.01$), and width of parietals ($p < 0.05$). In this work, *O. hannah* is documented from 18 localities in Mizoram at the elevation of 400–1,450 m a.s.l.

For *S. maccllellandi*, the distribution range for the subspecies or varieties was well reviewed by Smart et al. (2021), and they affirmed that *S. maccllellandi* var. *typica* is to be found so far in Mizoram, Arunachal Pradesh and Assam States in India, and also in Myanmar, Thailand and Cambodia; *S. maccllellandi* var. *nigriventer*

in Himachal Pradesh (India); *S. maccllelandi* var. *concolor* in Myanmar; *S. maccllelandi* var. *univirgatus* in Nepal, through the eastern Himalayas up to Sikkim; and *S. maccllelandi* var. *gorei* (Wall, 1910) in Assam, Manipur and Mizoram. Smart et al. (2021) provided a comprehensive systematic framework for *Sinomicrurus* species, and they hypothesized the colour variants traditionally considered varieties or subspecies did not exhibit independent lineage in their statistical and molecular analyses. Henceforth, the varieties reported by Lalremsanga & Zothansiyama (2015) as well as *S. maccllelandi* var. *gorei*, *S. maccllelandi* var. *concolor*, *S. maccllelandi* var. *nigriventer*, and *S. maccllelandi* var. *univirgatus* are considered as mutable chromatic patterns depicting intraspecific variation; and a provisional taxonomy for these variants are provided until more supporting evidence is conceived. The recent systematic studies of Asian coral snakes, lack extensive genetic data for *S. maccllelandi* from northeastern India, especially the type locality and the whole Indian subcontinent. Thus, these studies largely serve as a hindrance to the reappraisal of the putative synonyms of *S. maccllelandi* which may be distinct and deserve recognition to highlight their evolutionary importance. In this regard, it is imperative to undertake a robust reappraisal of the systematics of the Northeast Indian *S. maccllelandi* based on more genetic markers, representative specimens and populations. Specimens examined are comprised by a total of 21 preserved specimens of *S. maccllelandi* housed in the collections of MZMU as well as specimens (n=4) vouchered in the Arunachal Pradesh Regional Centre (APRC), Zoological Survey of India were. Fresh specimens were also collected and examined from Meghalaya (n=2) and Mizoram (n=15). The BI and ML phylogenies based on the concatenated dataset depicted a lineage diversification among the newly generated sequences of *S. maccllelandi* populations from Mizoram and Meghalaya in India. Mizoram samples of *S. maccllelandi* var. *gorei* (MZMU1727, MZMU1926, MZMU2034) are forming a strongly supported distinct, and sister lineage (PP=1.00; UFB=99) of the clade composed by the *S. maccllelandi* var. *typica* and *S. peinani* lineages. Genetic divergence-based PCoA disclosed the discrete clustering of the *S. maccllelandi* var. *gorei* specimens from *S. maccllelandi* sensu stricto and from the other congeneric species as well. Morphologically, two-way ANOVA and ANCOVA

also revealed a statistically significant difference in the BB ($p<0.001$), BS ($p<0.001$), BT ($p<0.001$), NBW ($p<0.001$), ED ($p<0.001$), IOS ($p<0.001$), HL ($p<0.05$), HW ($p<0.001$), and HD ($p<0.001$). The presently documented clutch size of *S. gorei* (up to 3 eggs) is relatively low compared to *S. macclellandi* (6–14 eggs). By integratively implementing morpho-taxonomy and phylogenetic species concept that is based on reciprocal monophyly for species recognition, the present study elucidated the scientific rationale for considering *S. gorei* to a full species level as it exhibits distinct evolutionary lineage with a considerable genetic divergence and phenetic disparity from the other congeneric species. *S. macclellandi* is documented from a total of 9 localities in Mizoram (1 previous + 8 new) at the elevation of 858–1,500 m a.s.l. while the overall range is 215–1,500 m a.s.l. On the other hand, *S. gorei* is confirmed from 24 localities in Mizoram (8 previous + 16 new) at the elevation of 150–1,378 m a.s.l. with the overall range of 90–1,378 m a.s.l.

Except for *S. macclellandi*, the studied four elapid species are confirmed deadly venomous species that are capable of inflicting severe clinical or even lethal envenomation upon humans; but, the distribution and other status of the deadly venomous snakes beyond the “Big Four” are poorly known across pan India. Correspondingly, not only the lethal dose and lethality period of snake venoms differed across species, but ecological and environmental factors are also known to have suggested variation in venom composition across populations of a similar species. Due to this intraspecies venom variability, the efficacy of snakebite treatment can be compromised because anti snake venom (ASV) prepared against the venom of a particular snake population may fail to neutralize the envenomation from disparate snake population. In fact, cryptic diversity occurs in most animal species groups, and the failure to determine cryptic diversity can result to imprecise estimation of the true degrees of biodiversity. Henceforth, this work not only elevates and redescribed *S. gorei* to species level, but also proposed three evolutionary lineages of *B. fasciatus* with redescribing *B. fasciatus* sensu stricto, and enlarges the overall elapid fauna of Mizoram. Considering the nature of the studied species being highly venomous elapid snakes, the findings from this work will be critical for further herpetological studies like reproductive behaviour, natural history, planning

conservation strategy, population study and threat assessment, or as far as development of comprehensive snakebite management and *omics* sciences for the deadly venomous snakes of Northeast India.